

N-19333.2

new
B
80

N69-21581-591

MINUTES OF THE TENTH CONFERENCE OF THE
INTERNATIONAL COMMITTEE ON AERONAUTICAL
FATIGUE - HELD IN MELBOURNE, MAY 1967

J. Y. Mann

February 1968

LIBRARY
USA GEOSTRAT. ANAL. & TECH. KAN.

No. in file
Title Author
(Aug 68)

ACCESSION NO. _____
PO REGISTR. _____

DISTRIBUTION STATEMENT A
Approved for Public Release
Distribution Unlimited

20050906 081

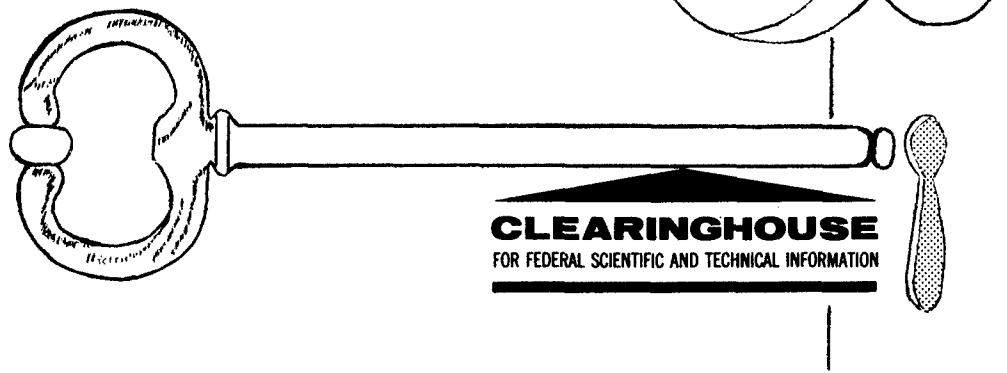
Best Available Copy

DISTRIBUTED BY:

CLEARINGHOUSE
FOR FEDERAL SCIENTIFIC AND TECHNICAL INFORMATION

U. S. DEPARTMENT OF COMMERCE / NATIONAL BUREAU OF STANDARDS / INSTITUTE FOR APPLIED TECHNOLOGY

YOUR KEY...



to scientific and technical advancement

Mr. Scientist. . . Engineer. . . Businessman. . . the Clearinghouse for Scientific and Technical Information can serve as your key to progress in research and development. Each year, some 40,000 unclassified documents from more than 125 Government agencies enter our collection. The Clearinghouse announces, reproduces and sells these reports to the public at a nominal cost. To make this wealth of scientific and technical information readily available, we have tailored our services to meet the needs of the highly selective customer as well as the general user. Some of these services are listed below.

U.S. GOVERNMENT RESEARCH AND DEVELOPMENT REPORTS (USGRDR). This semimonthly journal abstracts approximately 40,000 new Government-sponsored reports and translations annually. Features a quick-scan format, cross references, edge index to subject fields, and a report locator list.

U. S. GOVERNMENT RESEARCH AND DEVELOPMENT REPORTS INDEX (USGRDR-I). Published concurrently with the USGRDR to index each issue by subject, personal author, corporate source, contract number and accession/report number. Quarterly Indexes and an Annual Cumulative also are available.

CLEARINGHOUSE ANNOUNCEMENTS IN SCIENCE AND TECHNOLOGY. A semimonthly current awareness announcement service in 46 separate categories representing complete coverage of all documents announced by the Clearinghouse. Highlights special interest reports.

FAST ANNOUNCEMENT SERVICE (FAS). Selective announcement service emphasizing commercial applications of report information. Covers approximately 10 percent of Clearinghouse document input. Compiled and mailed in 57 categories.

SELECTIVE DISSEMINATION OF MICROFICHE (SDM). Automatic distribution twice monthly of Government research and development reports on microfiche. Economical and highly selective. Several hundred categories from which to choose.

ADDITIONAL INFORMATION concerning these and other Clearinghouse services is available by writing to:

Customer Services
Clearinghouse
U.S. Department of Commerce
Springfield, Virginia 22151

70-492DB

I.C.A.F. Doc. No. 412

COMMONWEALTH



OF AUSTRALIA

DEPARTMENT OF SUPPLY

AUSTRALIAN DEFENCE SCIENTIFIC SERVICE

AERONAUTICAL RESEARCH LABORATORIES

Minutes Of The Tenth Conference

OF THE

International Committee On Aeronautical Fatigue

HELD IN MELBOURNE, MAY 1967

Edited by

J. Y. MANN

69-21581 N 69-21591

(ACCESSION NUMBER)

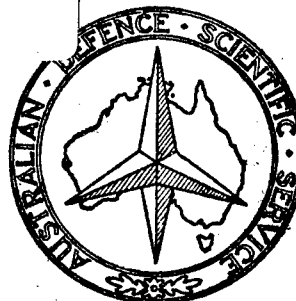
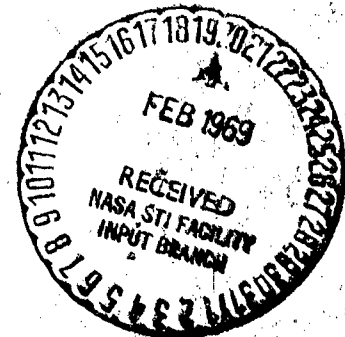
(THRU)

(PAGES)

(CODE)

(FOR Tenth OR AD NUMBER)

(CATEGORY)



February, 1968

MELBOURNE

FEB 26 '70

COMMONWEALTH



OF AUSTRALIA

DEPARTMENT OF SUPPLY
AUSTRALIAN DEFENCE SCIENTIFIC SERVICE
AERONAUTICAL RESEARCH LABORATORIES

Minutes Of The Tenth Conference
OF THE
International Committee On Aeronautical Fatigue

HELD IN MELBOURNE, MAY 1967

Edited by

J. Y. MANN



February, 1968

MELBOURNE

CONTENTS

1.	<u>LIST OF PARTICIPANTS AT THE 10TH I.C.A.F. CONFERENCE</u>	3
2.	<u>CONFERENCE PROGRAMME</u>	7
3.	<u>ICAF REVIEW OF THE PERIOD JUNE 1965 TO MAY 1967</u>	9
4.	<u>REVIEW OF SOME INVESTIGATIONS ON FATIGUE IN THE NETHERLANDS</u>	21 ✓
1.	Introduction	24
2.	Full scale fatigue tests on 7075-T6 tension skins	24
3.	Fatigue strength of riveted, bolted and adhesive- bonded aluminium alloy specimens	25
4.	Fatigue strength of aluminium alloy lugs	29
5.	Fatigue strength of modern aluminium alloys (2024-T81 and 7178-T6)	30
6.	Fatigue crack propagation in aluminium alloy specimens	32
7.	Residual static strength of aluminium alloy specimens	38
8.	Some remarks of future research	40
9.	References	41
5.	<u>A REVIEW OF SWISS INVESTIGATIONS ON AERONAUTICAL FATIGUE DURING THE PERIOD JUNE 1965 TO APRIL 1967</u>	55 ✓
1.	Gust investigation	58
2.	Statistics of fatigue loads	59
3.	Test facilities	62
4.	Test programmata	66
5.	Damage detection	70
6.	Fatigue tests	74
7.	Service experiences	97
8.	Conclusions	98
9.	Future research	99
10.	References	100
11.	Figures	102
12.	Tables	104
13.	Annexes	104

6.	<u>A REVIEW OF THE WORK IN THE UNITED KINGDOM ON THE FATIGUE OF AIRCRAFT STRUCTURES DURING THE PERIOD MAY 1965 - APRIL 1967</u>	137 ✓
1.	Introduction	140
2.	Concord programme	140
3.	Fatigue loading actions	148
4.	Fatigue research	152
5.	Design data on materials and structural elements	161
6.	Full scale testing	163
7.	Acoustic fatigue	165
7.	<u>REVIEW OF INVESTIGATIONS ON AERONAUTICAL FATIGUE IN THE FEDERAL REPUBLIC OF GERMANY. PERIOD OF REVIEW MAY 1965 TO MARCH 1967</u>	175 ✓
	Section I - Laboratorium für Betriebsfestigkeit	179 ✓
1.	Improving the fatigue life by the use of Taper-Lok fasteners	180
2.	Selection of the appropriate method of analysis for a statistical evaluation of random loads	183
3.	Constant amplitude tests on double-shear joints	187
4.	Fatigue strength of various heats of 18/7/5 Ni Co Mo maraging steel	189
5.	Fatigue strength of aluminium alloys	193
6.	Influence of the spectrum shape on the fatigue strength of an aluminium alloy	197
7.	Fatigue strength of electron-beam welded sheet of a maraging steel	199
8.	Comparative investigation on the fatigue strength of chemically etched and mechanically milled test specimens	203
9.	Investigations in progress or in an advanced stage of preparation	207
	<u>Section II</u> - Hamburger Flugzeugbau GmbH, Hamburg - Vereinigte Flugtechnische Werke GmbH, Bremen	209
1.	Influence of galvanic Cadmium plating on the fatigue strength of 1.6604.6 (AICMA FE PL 74) steel lugs - HFB	210
2.	Investigation on the effect of various types of rivets - VFW	213

3.	Comparative tests on butt welded and notched specimens of 1.7734.5 (AICMA FE PL 52S) steel material - VFW	216
	<u>Section III</u>	218
1.	Technical Notes (TM) published by Laboratorium für Betriebsfestigkeit, Darmstadt-Eberstadt, during the present Period of Review (May 1965 to March 1967)	219
2.	ICAF-Documents by German Authors, distributed during the present Period of Review (May 1965 to March 1967)	220
8.	<u>REVIEW OF SOME BELGIAN WORKS ON FATIGUE DURING THE PERIOD MAY 1965 - APRIL 1967</u>	223 ✓
1.	<u>S.T.A.é. Works</u>	226
1.1	Modified (swing tail) Douglas DC-4 fuselage tests	226
1.2	Fatigue pressurization tests	232
1.3	Fatigue test on detailed part	233
1.4	Specimens	234
1.5	Residual strength	234
2.	<u>Some investigations carried out at the C.N.R.M. (Centre National de recherches métallurgiques)</u>	235
2.1	Cumulative damage on aluminium alloy 24 S.T.	235
2.2	Effect of "Low cycle fatigue" damage in low alloy heat-treated steel	235
9.	<u>A REVIEW OF RESEARCH ON AERONAUTICAL FATIGUE IN THE UNITED STATES 1965 - 1967</u>	243 ✓
I.	<u>NASA Langley Research Center</u>	247
A.	Supersonic transport considerations	247
B.	Fatigue crack propagation and fracture	247
C.	Plastic behavior at notches	250
D.	Development of test facilities	250
E.	Contract research	250
F.	Definition of load environment	251
II.	<u>NASA Lewis Research Center</u>	252
A.	Crack initiation and propagation	252
B.	Cumulative damage	252
C.	High-temperature low-cycle fatigue	252

III.	<u>U.S. Air Force Flight Dynamics Laboratory</u>	252
	A. Fatigue damage indicator (S-N Gage)	252
	B. Optimization of ordered load spectra in full-scale structural fatigue tests	253
	C. Fracture mechanics - crack propagation	253
	D. Time compression in elevated temperature fatigue testing	253
	E. Fatigue strength design and analysis of aircraft structures	254
	F. F-100 program	255
	G. Sonic fatigue	267
IV.	<u>U.S. Air Force Materials Laboratory</u>	255
	A. Mechanical-metallurgical aspects of the fatigue process	255
	B. Crack propagation and notch effects	256
	C. Structural reliability	258
	D. Mechanism of stress corrosion cracking	259
	E. Work hardening	260
	F. Surface effects	261
V.	<u>U.S. Navy Aeronautical Structures Laboratory</u>	262
	A. Structural fatigue research	262
	B. Environments research	263
VI.	<u>Federal Aviation Agency</u>	264
VII.	<u>Institute for the Study of Fatigue and Reliability - Columbia University</u>	265
VIII.	<u>Northrop Norair</u>	265
IX.	<u>Lockheed-California Company</u>	265
	<u>Appendix</u> - Fatigue of structural materials suitable for the supersonic transport	275
10.	<u>A REVIEW OF RECENT FATIGUE WORK IN ITALY (1965 - 1967)</u>	295 ✓
	1. Basic and general investigations	300
	2. Flight loads	301
	3. Materials, structural components and joints	301
	4. Testing of complete airframe and full-scale structure	301
	<u>Appendix 1</u> - Costarmaereo	303
	<u>Appendix 2</u> - Recent activities in the field of fatigue at Istituto Sperimentale dei Metalli Leggeri, Novara-Milano	309

<u>Appendix 3</u>	- Report on Fiat activities in the fatigue field 1965 - 1967	328
<u>Appendix 4</u>	- Piaggio activity in the aeronautical fatigue field (years 1965 + 1967)	334
<u>Appendix 5</u>	- Activity of the Societa' Aeronautica Macchi in the field of aeronautical fatigue during the period 1965/1967	336
11.	<u>A REVIEW OF FRENCH WORK ON FATIGUE FOR THE PERIOD 1964 - 1966</u>	339 ✓
A.	<u>Work at the "Centre d'Essais Aeronautique de Toulouse"</u>	342
A. 1	Specifications of current tests for characterization of metals	342
A. 2	Toughness bending tests on square bar specimens	345
A. 3	Fatigue tests on smooth and notched specimens	360
B.	<u>Miscellaneous tests</u>	371
B. 1	Tests by aircraft manufacturers	371
B. 2	O.E.C.D. work on fatigue damage	376
12.	<u>REVIEW OF SOME SWEDISH INVESTIGATIONS ON FATIGUE DURING THE PERIOD JUNE 1965 TO MARCH 1967</u>	381 ✓
1.	Study of the fatigue properties of high-strength steels	384
2.	The effect of cold-working on the fatigue strength of high strength steels	385
3.	The effect of shot-peening on the fatigue strength of material Nimonic 90 at elevated temperatures	387
4.	Fatigue tests with riveted joints	388
5.	Fatigue strength of lugs	389
	Planned fatigue research for the near future	392
13.	<u>A REVIEW OF AUSTRALIAN INVESTIGATIONS ON AERONAUTICAL FATIGUE DURING THE PERIOD APRIL 1965 TO MARCH 1967</u>	407 ✓
1.	Investigations on materials	411
2.	Fatigue of joints	415
3.	Fatigue of components and structures	417
4.	Reliability and residual strength	418

5. Kinetic heating	419
6. Flight loads	420
7. Fatigue life assessment	422
8. Fatigue problems in service	422
9. Miscellaneous, equipment, testing techniques, etc.	424
10. Proposed fatigue research	424
11. Acknowledgements	425
12. Publications	426
14. <u>CLOSED TECHNICAL MEETING</u>	429
1. List of participants	431
2. Review of Munich research recommendations	433
3. Topics proposed for discussion at the Melbourne meeting	437
4. Recommendation session	443
<u>APPENDIX I</u> - Programme of the 5th I.C.A.F. Symposium	446
<u>APPENDIX II</u> - List of participants at the 5th I.C.A.F. Symposium	448

10TH ICAF CONFERENCE

MELBOURNE

May 16 - 17, 1967

1. LIST OF PARTICIPANTS AT THE 10TH I.C.A.F. CONFERENCE

The 10th ICAF Conference was held in the Theatrette of the National Mutual Centre, Collins Street, Melbourne, on 16th - 17th May, 1967. It was attended by the following persons.

AUSTRALIA

MANN, J.Y.	National Delegate. Aeronautical Research Laboratories, Department of Supply, Melbourne
DANCE, J.B.	A.R.L.*
FINNEY, J.M.	A.R.L.
FODEN, F.J.	A.R.L.
GORNALL, W.J.	Commonwealth Aircraft Corporation Pty. Ltd., Melbourne
GRACE, W.G.	Repco Research Pty. Ltd., Dandenong
GRANDAGE, J.M.	A.R.L.
HOOKE, F.H.	A.R.L.
HOOPER, D.R.	Government Aircraft Factories, Department of Supply, Melbourne
JOHNSTONE, W.W.	A.R.L.
KENTWELL, J.A.C.	Commonwealth Aircraft Corporation Pty. Ltd., Melbourne
LAWRENCE, T.F.C.	A.R.L.
MACNAUGHTAN, J.	Department of Air, Canberra
MILLIGAN, I.S.	Department of Civil Aviation, Melbourne
O'BRIEN, K.R.A.	Department of Civil Aviation, Melbourne
PATCHING, C.A.	A.R.L.
PAYNE, A.O.	A.R.L.
RIDER, C.K.	A.R.L.
SCOLES, B.A.J.	Department of Civil Aviation, Melbourne

* A.R.L. - Aeronautical Research Laboratories, Department of Supply, Melbourne

SNOWDEN, K.

Broken Hill Smelters Pty. Ltd.,
Melbourne

STEVENS, R.H.

Qantas, Sydney

WESTON, M.R.

Department of Civil Aviation,
Melbourne

WILLS, H.A.

Department of Supply, Melbourne

WOOD, F.J.P.

Department of Air, Melbourne

FRANCE

BARROIS, W.

National Delegate. Service Technique
de l'Aeronautique, Paris

GERMANY

BUXBAUM, O.

National Delegate. Laboratorium
für Betriebsfestigkeit, Darmstadt

KRÄMER, D.E.

Deutsche Lufthansa, Hamburg

ITALY

IALLI, D.

National Delegate. I.A.M. R.Piaggio
S.p.A., Finale Ligure

NETHERLANDS

van BEEK, E.J.

National Delegate. Royal
Netherlands Aircraft Factories
"Fokker", Amsterdam

NEW ZEALAND

LABETT, E.T.

Department of Civil Aviation,
Wellington

SWEDEN

EGGWERTZ, S.

National Delegate. Flytekniska
Försöksanstalten, Bromma

JARFALL, L.E.

Flytekniska Försöksanstalten,
Bromma

SWITZERLAND

BRANGER, J.

National Delegate. Eidgenössische
Flugzeugwerk, Emmen

WEIBEL, J.P.

Eidgenössische Flugzeugwerk,
EmmenUNITED KINGDOM

RIPLEY, E.L.

National Delegate. Royal Aircraft
Establishment, Farnborough

LAMBERT, J.A.B.

Hawker Siddeley Aviation Ltd.,
Hatfield

PHILLIPS, C.E.

National Engineering Laboratory,
East Kilbride

TROUGHTON, A.J.

Hawker Siddeley Aviation Ltd.,
WoodfordUNITED STATES OF AMERICA

HARDRATH, H.F.

National Delegate. NASA Langley
Research Centre, Hampton

DONELY, P.

NASA Langley Research Centre,
Hampton

FORNEY, D.M.

Air Force Material Laboratory,
Dayton

JENSEN, H.T.

Sikorsky Aircraft, Stratford

2. CONFERENCE PROGRAMME

Tuesday, 16th May, 1967

Morning Session (Chairmen: T.F.C. Lawrence; J.Y. Mann, Australia)

- Opening address by Mr. H.A. Wills, Chief Scientist, Department of Supply
- E.J. van Beek: Review of the period June 1965 to May 1967
- A. Hartman: Review of some investigations on fatigue in the Netherlands (presented by E.J. van Beek)
- J. Branger: A review of the Swiss investigations on aeronautical fatigue during the period June 1965 to April 1967

Afternoon Session (Chairman: H.F. Hardrath, U.S.A.)

- P.D. Adams and E.L. Ripley: A review of the work in the United Kingdom on the fatigue of aircraft structures during the period May 1965 - April 1967 (presented by E.L. Ripley)
- E. Gassner: Review of investigations on aeronautical fatigue in the Federal Republic of Germany (presented by O. Buxbaum)

Wednesday, 17th May, 1967

Morning Session (Chairmen: E.L. Ripley, U.K. and E.J. van Beek, Netherlands)

- H.F. Hardrath: A review of research on aeronautical fatigue in the United States 1965 - 1967
- V. Villa: A review of recent fatigue work in Italy (1965-1967) (presented by D. Lalli)
- W. Barrois: A review of French work on fatigue for the period 1964 - 1966.

Afternoon Session (Chairman: I.S. Milligan, Australia)

- G. Wallgren: Review of some Swedish investigations on fatigue during the period June 1965 to March 1967 (presented by S. Eggwertz)
- J.Y. Mann: A review of Australian investigations on aeronautical fatigue during the period April 1965 to March 1967

INTERNATIONAL COMMITTEE ON AERONAUTICAL FATIGUE
(ICAF)

Review of the period June 1965 to May 1967

Prepared by

J. Schijve and J. Branger

1. Introduction

The activities of the period under review are overshadowed by the sudden death of our secretary, Dr. F.J. Plantema. On a Sunday morning, 13 November 1966, he was stricken by a heart attack. Of course this blow was most heavily felt by his family. At the NLR everybody of his department was startled and overcome with great sadness. Citing an NLR letter: "We at the Structures and Materials Department of NLR lost our chief, a man we have known as very modest and as somebody who never put himself in the foreground. He was very mindful of good human relations and proved to be a good friend to all of us. He was capable of taking the right decisions, and he always took them with great care. We lost an amiable man, who was a beloved and dedicated chief".

Similar words apply to the feelings in ICAF. We lost our secretary. In May 1951 Dr. Plantema took the initiative for the foundation of the International Committee on Aeronautical Fatigue and until his death he was the only official of ICAF, co-ordinating and stimulating its activities. The technical aspects of his work will be reported in the Dr. F.J. Plantema Memorial Lecture, that will be presented by Mr. Branger during the Symposium next week and this need not be repeated here.

In passing it may be noted that Dr. Plantema prepared 38 Quarterly Bulletins and the Secretary's Review as well as the Minutes of the Business Meetings of 9 conferences. In addition he did a lot of work by correspondence. All this work he performed in the most careful and conscientious manner that was characteristic to him. The personal satisfaction he gained from the secretarial work was the knowledge that ICAF was generally appreciated as a useful organisation and also as a circle of sincere friends.

For ICAF the death of Dr. Plantema is a closure to a period that has been marked by his personal pursuance of good ICAF-relations. He has left us a sound organisation and it is up to us to carry on his valuable work.

2. Activities in the period June 1965 to May 1967

The membership of ICAF as shown in Appendix A did not change during the period under review. Applications for membership have been received from two countries. They will be discussed during the Business Meeting in Melbourne.

The ninth ICAF Conference and the fourth ICAF Symposium (June 1965) organized by the German Centre under the direction of Professor Gassner were generally felt to have been very successful. During the Conference we had for the first time a Closed Technical Session. This originated from the idea that we should have an opportunity to discuss fatigue problems of mutual interest in a smaller group of participants. The discussion during the Closed Technical

Session touched upon a variety of subjects and was characterized by a lively exchange of opinions. It was therefore decided in Munich to continue this type of activity during the Australian meeting.

The size of the Munich meeting can be illustrated by the following data :

Symposium,	3 days,	15 papers,	179 participants.
Conference,	2 days,	10 reviews,	74 participants.
Closed Technical Meeting,	1 day,	discussions only,	31 participants.

One technical excursion and one social tour.

It is hardly imaginable that an ICAF meeting could be further intensified.

The National Reviews on aeronautical fatigue investigations as well as a summary of the discussion during the Closed Technical Meeting were published in the Minutes of the Ninth Conference prepared by the German Centre. This well edited report is considered to be a most valuable document. Unfortunately the publication of the symposium book has met with unforeseen difficulties. It is hoped, however, that this problem can be overcome since the collection of papers presented at the symposium will certainly become a frequently consulted source of references.

With respect to ICAF's relations to AGARD it may be repeated that there was no collaboration on an official basis during the period under review. However, through the personal relations between AGARD fatigue specialists and ICAF delegates (who in some cases were the same persons) the AGARD activities on aeronautical fatigue could be reported in the Quarterly Bulletins as before.

3. Preparation of present meeting

Already in 1961 an initial Australian invitation for holding an ICAF meeting in Australia had been received. The possibilities to attract a sufficient number of overseas attendees were explored in 1964, which justified the decision taken at Munich to accept the Australian invitation for holding the 1967 meeting in Melbourne. Since then Mr. Mann and his group have vigorously been working on the organisation of the meeting, which will encompass the Tenth Conference with a closed technical session and the Fifth Symposium.

The title of the symposium is "Aircraft Fatigue - Design, Operational and Economic Aspects". The organising committee succeeded in collecting a series of promising papers. 20 papers were accepted, the last list of them was distributed on February 1967 (preliminary lists were sent to the delegates in September and October 1966). They embraced the following subjects: Loading conditions, design and certification, fatigue testing, and economic and operational aspects.

Programs of the whole meeting were sent in March 1966, August 1966 and November 1966 in more and more elaborated form, the final program being dispatched in April 1967.

This and all the further preparations caused a lot of work that was done with great enthusiasm and thoroughness. All persons who devoted much time and efforts to the organisation

of the meeting, especially the organizing committee (Mr. Lawrence, Mr. Mann, Mr. Gornall, Mr. Hooper and Mr. Scoles) deserve the great appreciation of ICAF.

The meeting will certainly be a high success and this will be the well-deserved reward of the team.

The organising committee has considered the suggestion that a special lecture in honour of the late Dr. Plantema be instituted as part of the ICAF bi-annual meetings. This idea has received full support from all delegates. Mr. Branger, who has been ICAF delegate since the first ICAF conference, was invited to present this lecture during the Melbourne symposium. This lecture will be given at the evening of 22nd May.

4. ICAF-Secretary

During the present period the secretary Dr. Plantema suddenly passed away as reported in the introduction to this review. In the period from November 1966 until May 1967 Dr. Schijve acted as a secretary ad interim.

At the preliminary Business Meeting held on 17th May in Melbourne it was formally moved and agreed that Mr. Branger be elected to the position of ICAF Secretary, as the successor to Dr. Plantema. It was agreed that the general policy of ICAF would be to elect a Secretary for a period of two years, but that after such period the Secretary should be eligible for re-election. If he felt unable to continue in this position he should notify the other delegates six month in advance.

5. Some information on new ICAF Documents

In the period reviewed the number of ICAF documents has grown from 305 to 357. A list of these documents will be issued separately as ICAF Doc. 361.

Taking also into consideration the papers presented at the Munich symposium a few general remarks will be made on the subjects dealt with in the various documents.

The first impression is that the list of subjects is of an unusually large variety. Nevertheless a few general issues can be mentioned, namely: Full-scale testing, crack propagation and residual strength. The same remark was made in the Secretary's Review presented two years ago in Munich. Apparently we are still struggling with the same problems.

Aspects related to full-scale testing discussed in the papers were testing procedures, airworthiness criteria, apparatus for simulating service loads, scatter, economy of testing, relation to service life. In addition design aspects were considered in some papers with special attention to the failsafe philosophy. Only a few papers were dealing with service loads.

In some fifteen papers crack propagation and residual strength were investigated. Empirical results were mainly restricted to aluminium alloys. Theoretical treatments of predicting crack rates and strength in cracked condition were presented in some papers.

The prediction of fatigue life under variable-amplitude loading including random loading was studied in a small number of papers. The assessment of allowable design stresses is a related topic studied in another paper.

Reports on fatigue testing of materials and components partly had an ad-hoc nature. There were four papers on the fatigue strength of lugs, indicating that lugs are still an important structural element for which fatigue life is a problem of major concern.

Subjects of other papers to be mentioned are: Cyclic plastic stresses at a notch root, poor detail design features, fatigue life in service of motor car components, fatigue life under non-sinusoidal loading, low-cycle fatigue embrittlement of steel.

In conclusion it may be said that the variety of subjects in the specialized field of aeronautical fatigue may appear to be somewhat remarkable to an outsider. For the insider, however, the variety is well known and to him it implies that an exchange of knowledge, data and opinions is highly necessary. This exchange is the basic reason for the existence of ICAF.

Presented at the 10th ICAF Conference
MELBOURNE, 16th May 1967.

APPENDIX A

ICAF Secretary J. Branger, c/o Eidg. Flugzeugwerk
CH 6032 Emmen (Luzern), Switzerland

List of ICAF National Centres (May 1967)

Australia	Mr. J.Y. Mann, ICAF Representative, Structures Division, Aeronautical Research Laboratories, Box 4331, G.P.O., Melbourne 3001
Belgium	Administration de l'Aéronautique Matériel Volant, Aérodrome de Haren, Hangar 7, Brussels 13 Attention: Mr. J. van Laer
France	Service Technique Aéronautique Bureau Etudes Générales 4, Av. de la Porte d'Issy, Paris XV Attention: l'Ingénieur Principal en l'Air, W. Barrois
Germany (Fed. Republic)	Laboratorium für Betriebsfestigkeit Mühltalstr. 55-57, Darmstadt-Eberstadt - 61 Attention: Prof. Dr. Ing. E. Gassner
Italy	Ministero Difesa - Aeronautica Direzione Generale Costruzioni, Rome Viale dell'Università Attention: Col. Dr. Ing. Vittorio Villa
Netherlands	Nationaal Lucht- en Ruimtevaartlaboratorium (NLR) (National Aerospace Laboratory NLR) Voorsterweg 31, Post Emmeloord, NOP Attention: Dr. J. Schijve
Sweden	Flygtekniska Försöksanstalten Post box 11021, Bromma 11 Attention: Mr. G. Wällgren
Switzerland	Eidg. Flugzeugwerk CH 6032 Emmen (Luzern) Attention: Mr. J.P. Weibel
United Kingdom	Royal Aircraft Establishment, Structures Department, South Farnborough, Hants., Attention: Mr. E.L. Ripley
United States	NASA Langley Research Center Fatigue Branch, Mailstop 129 Langley Station, Hampton, Va. 23365 Attention: Mr. Herbert F. Hardrath

N 69-21582

REVIEW OF SOME INVESTIGATIONS ON FATIGUE
IN THE NETHERLANDS

Compiled by
A. Hartman
Nationaal Lucht- en Ruimtevaartlaboratorium
Amsterdam

(NLR Report MP.249)

Note: Reprints from this publication may be made on condition that full credit be given to the Nationaal Lucht- en Ruimtevaartlaboratorium (Nat. Aero- and Astronautical Res. Inst.) and the Author(s)

CONTENTS

1. Introduction
2. Full scale fatigue tests on 7075-T6 tension skins
3. Fatigue strength of riveted, bolted and adhesive-bonded aluminium alloy specimens
4. Fatigue strength of aluminium alloy lugs
5. Fatigue strength of modern aluminium alloys (2024-T3 and 7178-T6)
6. Fatigue crack propagation in aluminium alloy specimens
 - (1) Application of the stress intensity factor to the growth of micro-cracks
 - (2) The effect on crack propagation of testing indoors and outdoors.
 - (3) The effect on crack propagation of environment and loading frequency
 - (4) Crack propagation rates in 2024-T3 alclad sheet from different manufacturers
7. Residual static strength of aluminium alloy specimens
8. Some remarks on future research
9. References

1 Introduction.

The review of some investigations on fatigue in The Netherlands compiled for this tenth ICAF conference covers the research in the period since the meeting in Munich in June 1965 till about the first of January of this year. In the sections 2-7 a summary will be given of investigations which in this period of about one and a half year have been completed or have reached an advanced stage. Section 8 gives some concluding remarks which are chiefly related to investigations planned for the near future or which are still in their initial stage.

In 1966 the Materials and Structures Department of the NLR has moved from the Main Laboratory in Amsterdam to the Branch Laboratory in the North East Polder into a new building with some new equipment and superior possibilities for utilization of machinery and apparatus. A great variety of preparatory studies related to the static and fatigue testing at the NLR of the wings and other sections of the Fokker F-28 Fellowship have delayed the progress of other investigations.

2 Full scale fatigue tests on 7075-T6 tension skins.

Although the tests described in the review presented in Munich were almost completed at that time, a full analysis and a study of the consequences for designing load sequences for testing new aircraft were made during the period now being reviewed. The amount of data that came available from the 13 tests was very large, due to a great variety of different cracks being found, and in addition the observations made on crack propagation and residual strength. A survey of relevant literature has been included.

It is impossible to recapitulate all conclusions of the final report here (see ref.9), but some of them will be briefly indicated.

1. The picture of fatigue sensitive components in the structure was different for the variable-amplitude tests and the constant-amplitude tests. The main cause was thought to be related to the maximum load applied in the test.
2. The picture of fatigue sensitive components and the fatigue lives obtained was not very much different for the programme tests and the random tests.
3. The fatigue life was reduced to 50 % by the GTAC.
4. Values of $\sum n/N$ ranged from 1.4 to 2.5.
5. Crack propagation mainly occurred at the load cycles with the higher amplitudes.

6. The average standard deviation for similar failures in one structure was $\bar{G}_{\log N} = 0.085$. This value may be larger for similar failures in a fleet of aircraft.
7. Open holes, free sheet edges and empty rivet holes were locations prone to fatigue crack nucleation.
8. With the present knowledge it cannot be expected that a method of programming load sequences could be outlined that would guarantee a reasonably accurate equivalence with random service loads.
9. The Palmgren-Miner rule is inadequate for judging whether a certain type of fatigue loading has to be applied or can be omitted in full-scale testing.
10. Fatigue loads with small amplitudes can be damaging if they imply an increase of load ranges pertaining to other types of loading.
11. A realistic load-time history for a full-scale test should be a flight by flight simulation. The GTAC should not be applied in batches.
12. The selection of the maximum load to be applied in a full-scale test is a delicate problem (see conclusions 1 and 5 above). It is proposed to adopt the load level that on the average is equalled or exceeded 10 times in the target life.

3 Fatigue strength of riveted, bolted and adhesive-bonded aluminium alloy specimens.

In the previous review some data were given of a comparative investigation on double row single lap joints in 2024-T3 alclad and 7075-T6 clad sheet material with different types of rivets and bolts. The fatigue tests with fluctuating tensile loading were of two types viz. the standard constant load amplitude tests to determine the S-N curves of the joints and programme fatigue tests comprising six stress amplitudes applied alternately in increasing and decreasing order. The number of cycles at each of the six stress amplitudes was based on a gust spectrum using the conversion factor $1 \text{ ft/sec} = 0.33 \text{ kg/mm}^2$. In both types of tests the mean gross stress in the sheet was 7 kg/mm^2 .

The investigation has now been completed and the results were published (ref.1). Conclusions from the report are:

- (1) As regards fatigue strength of the aluminium alloy joint, snap rivets of 2117 Al-alloy riveted in the aged condition and snap rivets of 2017 and of 2024 Al-alloy riveted in the quenched condition were almost equivalent. The same was found for snap rivets of 2017 Al-alloy and Huck bolts (patented special bolt manufactured by Huck Manufacturing Company) of equal static shear strength. Replacement of the snap rivets by Avdel blind rivets without any further change of the rivet pattern resulted in lower fatigue strength properties. In the programme tests this replacement resulted in a decrease of the fatigue life with a factor of about 4.
- (2) In 11 out of 13 series of riveted specimens the magnitude of $\sum \frac{n}{N}$ at fracture was above unity. This confirms the experience of the NLR that with fluctuating fatigue loading ($R > 0$) a fatigue life estimate of riveted lap joints with the Palmgren-Miner rule $\sum \frac{n}{N} = 1$ will usually be conservative.
- (3) The rating orders of the 13 series of riveted lap joints as determined from the results of the constant load amplitude tests and those of the programme fatigue tests showed only moderate agreement.
- (4) The programme tests and the constant amplitude tests showed good agreement as regards the effect of the type of rivet and grain direction of the sheet on the fatigue properties of the joint. The programme test indicated a greater effect of the sheet material used in the manufacture of the joint.

The number of factors which can affect the fatigue strength of riveted joints is large and many of them are influenced by the manufacturing procedure and in all probability are not accurately reproducible.

Considering the above a study of the effect of the manufacturing procedure on the fatigue strength of riveted joints has been started. The specimen is a single lap joint of 2024-T3 alclad sheet of 1.0 mm thickness with two rows of eight 2024 aluminium alloy snap rivets of 3.2 mm shank diameter with a row and rivet pitch of 20 mm. The fatigue tests are constant stress amplitude tests and programme tests with a mean gross stress in the sheet of 7.0 kg/mm^2 . Variables of the manufacturing process to be studied are:

- (1) different riveting procedures: pneumatic, hydraulic, manual.
- (2) different surface treatments of the metal prior to the riveting:
no surface treatment, anodizing, painting.
- (3) application of a post temperature cycle corresponding to the curing cycle of the Redux metal adhesive.

Programme fatigue tests have not yet been made and only some results of constant stress amplitude tests can be given at this meeting. Fig.1 gives three mean S-N curves, viz. of

specimens A: no surface treatment of the sheets, diameter of hydraulically made closing head of rivet 1.5 times shank diameter;

specimens B: as specimens A except chromic acid anodized and painted contact surface;

specimens C: as specimens B except ratio of 1.7 between diameters of closing head and shank.

A comparison of the S-N curves A and B indicates that anodizing and painting of the contact surface had a small deteriorating effect on the fatigue strength of the riveted specimens. An increase in the ratio of the diameter of the closing head to the diameter of the shank of the rivet from 1.5 to 1.7 had a notably favourable effect, indicating that the "amount" of riveting is indeed important.

The investigation on the fatigue properties of the riveted-adhesive bonded construction as applied in the pressure cabin of the Fokker F-28 aircraft has been continued and could be completed recently. A publication on this investigation will be issued before long (ref.2). The scope of the investigation included a study of the effects on the fatigue strength of low (-55°C) and elevated temperature ($+50^{\circ}\text{C}$), frequency of loading, artificial ageing of the adhesive, anodizing process prior to bonding and a comparison with specimens of the same dimensions but riveted only or adhesive-bonded only. The type of specimen used is a single lap joint in 2024-T3 alclad sheet material of 0.8 mm thickness, width 160 mm, with three rows of countersunk 2024 aluminium alloy rivets with a diameter of 3.2 mm and a pitch of 20 mm. The adhesives, EC 2216 manufactured by the 3-M company and AW 106 manufactured by CIBA, are both room temperature curing thermosetting two component adhesives of the epoxy type. The fatigue tests were constant stress amplitude tests with a stress ratio $R = 0.1$.

The investigation led to the following conclusions:

Comparison of
riveted, adhesive bonded
and riveted-adhesive bonded
2024-T3 alclad specimens.

The test data indicate that in respect of
fatigue strength at +20 and +50°C the adhe-
sive bonded specimens and the riveted-adhe-
sive bonded specimens were almost equivalent.
Both had a notable higher fatigue strength
at these temperatures than the merely rive-
ted specimens (see fig.2).

Effects on the fatigue strength of riveted adhesive-bonded specimens of:

Temperature of testing
Range -55°C to +50°C

- (1) With EC 2216 as adhesive the fatigue strength decreased continuously with increasing temperature.
- (2) With AW 106 as adhesive the fatigue strength showed an optimum around room-temperature.
- (3) With increasing temperature the relative frequency of failure of the specimens by fracture in the metal at the edge of the overlap decreased while that by fracture in the metal through the rivet holes increased.

Adhesive

AW 106 or EC 2216

The two adhesives were almost equivalent in the temperature range from room-temperature to +50°C. EC 2216 has to be preferred to AW 106 for applications at -55°C.

Frequency of loading

In the range of 6-4000 cycles/minute the frequency of loading had only a slight effect. The effect was more pronounced at elevated temperature (50°C) than at room temperature or at low temperature (-55°C).

Artificial ageing

4 weeks at 70°C,
98-100 % R.H.

- (1) Both with AW 106 and EC 2216 as adhesive the artificial ageing reduced the fatigue life of the specimens. The reduction in fatigue life which ranged from 0-50 % depended on the adhesive used and on the temperature of testing.

Pretreatment of the metal

Chromic acid anodizing

Sulfuric acid anodizing

- (1) The two anodizing processes yielded equal fatigue strength of the EC 2216 specimens at -55°C .
- (2) On the average anodizing by the chromic acid process resulted in a slightly higher fatigue life (factor appr. 1.4) in the tests at 20 and 50°C .

4 Fatigue strength of aluminium alloy lugs.

The tests on lugs reported in the previous review were continued on lugs with a 3 % expanded hole. The nominal dimensions of the lugs were: width 30 mm, pin diameter 10 mm, head distance 20 mm, resulting in $K_t = 3.5$. This is the same type of lug as used before. Various methods for expanding the hole were explored but none of them was superior to the method used before, that means drawing a tapered pin through a thin-walled steel bush in the hole and removing the bush afterwards. More attention was paid now to a good alignment, while in addition reaming of the hole was applied. Programme tests were carried out on lugs of 2024-T3 and 7075-T6 material. The mean stress was 8 kg/mm^2 instead of $S_m = 12.5$ in the previous investigation. The increase of the fatigue life as compared with the standard lug was in the order of 30 times for the 2024 specimens which is a much better result than obtained in the preceding test series (approximately 3 times). The 7075 lugs with expanded hole had extremely long endurance and tests were stopped before failure occurred. The improvement of the fatigue life due to the expansion of the hole exceeded a factor of 200 times. For lugs with a normal hole the programme life of the 7075 lugs was about 4 times shorter than for the 2024 lugs. After expansion of the hole the former lugs were superior, however. This confirms the observation that a low-ductility material may get a larger benefit with respect to fatigue from a treatment that introduces residual compressive stresses.

5 Fatigue strength of modern aluminium alloys (2024-T81 and 7178-T6).

Sheet of the type 2024 aluminium alloy is mostly used in the T3 temper (naturally aged). However, in the T8 temper (artificially aged) the material has a higher yield strength and a higher tensile strength. On the other hand it is likely that due to lower ductility the alloy in the T8 temper will have reduced fatigue and residual strength properties. In view of obtaining quantitative information on the latter issue comparative fatigue tests, crack propagation tests and residual strength tests have been performed on 2024 sheet specimens in both tempers T3 and T8.

In the fatigue tests five types of specimens have been used, one unnotched and four notched. The four types of notched specimens, viz. a specimen with a central hole $K_t = 2.43$, a specimen with two unloaded rivets, a specimen with an adhesive bonded doubler and a specimen with 2 rows of loaded rivets, have been used to obtain information on a range of notches which have proved to be representative for aircraft structures. Fig.3 gives information on shape and dimensions of the specimens. For each type of specimen the S-N curve for a certain value of the mean stress was determined with about 15 to 20 specimens. Supplementary to the constant load amplitude test 3-5 programme tests were carried out at the same mean stress, the programmed loading having been derived from a gust spectrum.

A comparison of the test data of the specimens in the T8 and in the T3 temper showed a shorter fatigue life of the T8 specimens both in the constant load and in the programme tests for all five types of specimens. As for the constant load amplitude tests this is illustrated for the specimens with unloaded and loaded rivets in the figures 4 and 5. The comparison of the S-N curves for the same temper of the alloy shows a significantly higher fatigue strength of an unloaded rivet with respect to a loaded one. Partly this has to be attributed to the excentricity of the single lap joints used for the specimens with loaded holes which introduced bending stresses.

The superiority of the 2024-T3 alclad material to the 2024-T8 alclad material in the programme tests appears from the figures in the table below. For both tempers $\sum \frac{n}{N}$ had a mean value of about 1.

Type of specimen see fig.3	Number of periods in the programme tests		$\sum \frac{n}{N}$	
	2024-T8.1	2024-T3	2024-T8.1	2024-T3
A	13	19	0.98	1.22
B	6	14	0.67	0.85
C	8	16	1.24	1.24
D	38	61	1.23	0.87
E	30	60	0.94	0.91

Comparative fatigue crack propagation tests and residual strength tests at room temperature on clad 2024-T3 and 2024-T8 sheet material indicated that crack propagation rates in the T8 material were about a factor 2 larger than in the T3 material (ref.19). The residual strength of the T8 material was lower, see fig.6.

It can be concluded from the fatigue, the crack propagation and the residual strength tests, that for applications at room temperature T3 material should be preferred above T8 material. The 2024-T8 material has superior properties at elevated temperatures (150°C).

The investigation on the 7178 material was of a more, exploratory nature than that on the 2024 alloy. It has been restricted to specimens type A and B of fig.3. The specimens which were cut from hat stringers (extruded material), exhibited a large scatter in fatigue life both in the constant load amplitude and in the programme tests. The fatigue life of the specimens at the same stress amplitude or under programme loading was significantly higher than that of clad 2024-T3 or T8 sheet material!

6 Fatigue crack propagation in aluminium alloy specimens.

The study at the NLR of fatigue crack propagation in aluminium alloy specimens was continued. In this review a brief discussion will be given of the following aspects.

- (1) Application of the stress intensity factor to the growth of micro-cracks.
- (2) The effect on crack propagation of testing indoors and outdoors.
- (3) The effect on crack propagation of environment and loading frequency.
- (4) Crack propagation rates in 2024-T3 alclad sheet from different manufacturers.

The effects on crack propagation of ground-to-air cycles and the width of the specimen are omitted from the discussion. Typical results were already presented at the ICAF Conference in Munich. Since then these investigations have been completed and full data can be found in the published reports (refs 3 and 4).

(1) Application of the stress intensity factor to the growth of micro-cracks.

Paris and collaborators (ref.5) have introduced the stress intensity factor in equations for the crack propagation rate in fatigue tests. They proposed the simple equation

$$\text{crack rate } \frac{d\ell}{dn} = f(K) \quad (1) \quad K = \text{stress intensity factor.}$$

The validity of this crack rate equation has been verified for macro fatigue cracks, notably by the group of Paris (refs 5 and 6). A good correlation has been found between crack rate and K-value particularly with aluminium alloys. Our test results, however, showed the relation in equation (1) to be dependent on the stress ratio R (see ref.7). Schijve has applied his data on the growth of micro-cracks in fatigue tests on plain and notched aluminium alloy specimens of different size to verify the applicability of equation (1) for the growth of fatigue cracks in the micro-stage (ref.7). The dimensions of the specimens which Schijve has used in his investigation are given in fig.7. The fatigue tests were performed on specimens of bare 2024-T3 aluminium alloy sheet of 2 mm thickness with $S_{\min} = 0$ (stress ratio $R = 0$). The crack growth started at the corners of the minimum section. This corner cracks had the shape of a quarter of a circle and the crack length ℓ was measured from the edge of the hole or the edge of the unnotched specimen along the specimen surface. The crack rate has been plotted as a function of the stress intensity factor K in fig.8. The results plotted were obtained at different stress

levels, tabulated in fig.8 with the corresponding fatigue lives, and at three values of the crack length, viz. $l = 0.2, 0.5$ and 1 mm. The graph in fig.8 demonstrates a surprisingly good correlation of the growth of the corner cracks in the three specimens with the stress intensity factor. After the corner cracks had completely penetrated the sheet thickness, the crack front was perpendicular to the sheet surface. For these larger edge cracks ($l > 2$ mm) the crack rate has also been plotted versus the stress intensity factor. The three average curves are reproduced in fig.9. Although there are some differences between the results for the three types of specimens, these differences are small. The curve for the corner cracks in fig.8 has been replotted in fig.9 and a comparison with those of the edge cracks shows that the crack rate of a corner crack is much smaller than the crack rate of an edge crack. It is clear that it must be smaller in view of the restraint on crack opening. Schijve assumed that the ratio between the stress intensity factors for corner cracks and edge cracks is the same as the ratio between the K-values for a central (through) crack and a circular crack in an infinite body. This ratio is $2/\pi$ and application led to a satisfactory agreement between the $dl/dn-K$ plots for the small corner cracks and the larger edge cracks (see fig.9).

The consequence of the above agreement is that this crack rate, and hence the crack life, for crack growth from $l = 0.1$ mm onwards can be predicted if equation (1) has been empirically determined. Unfortunately attempts to predict the fatigue life of the notched specimens in fig.7 from the unnotched specimen data were unsuccessful (ref.7). It was thought that this might be due to the effect of inclusions on crack nucleation.

(2) The effect on crack propagation of testing indoors and outdoors.

The different behaviour of the two aluminium alloys 2024-T3 alclad and 7075-T6 clad in a comparative investigation on crack growth in an indoor and in an outdoor environment has been reported at the previous meeting. The sheet specimens, width 100 mm, thickness 2 mm, were provided with five small central notches spaced about 230 mm along the axis of the specimen. The tests were conducted in two test rigs, one located indoors and the other one outdoors (rural environment, about 85 km from the salt water of the North Sea). The crack propagation tests were run concurrently with full scale fatigue tests on tension skins and the same random and programmed load sequences, representing a severe gust spectrum, were employed. Tests with and without ground-to-air cycles (GTAC) were performed. The frequencies of loading were in the order of 20 cycles per minute. For more details on the specimens, the environment, the test set up etc. the reader is referred to refs 8 and 9.

A summary of the results is given in table 1. The data in the last column of this table show only small differences between the crack rates in the 2024 alloy tested indoors and outdoors, thus indicating almost the same fatigue crack propagation in both environments. However, the data for the 7075 material indicate in all tests a significantly faster crack propagation outdoors than indoors. An acceleration of the crack rate due to the "outdoor" environment should be considered when applying crack propagation data of 7075 material indoors for an estimation of the crack propagation in an actual aircraft. This counts the more because the rural outdoor environment used in the tests can not be considered as aggressive.

(3) The effect on crack propagation of environment and loading frequency.

The normal environments for aircraft are air and water. Depending on the temperature and the relative humidity air contains small quantities of water vapour and small concentrations of impurities like SO_2 , CO_2 etc. The aim of the first investigation of the NLR on the effect of air on crack propagation in aluminium alloys was to determine firstly whether air has an effect and secondly which of the components are responsible for this effect (refs 10 and 11). The crack growth tests were made on 2024-T3 alclad specimens with a high frequency of loading (appr. 3600 c/min). The results showed that normal air affects the crack propagation in aluminium alloys and that the dominant factor is not the concentration of oxygen in the air but the concentration of water vapour. The number of load cycles for the same extension of the crack length in wet 99,998 % pure argon gas was almost the same as in wet pure oxygen or wet air but significantly shorter than in pure but dry oxygen.

The study on the effect of environment has been continued by three series of tests (not yet published).

- (1) Crack propagation tests with a high frequency of loading on 7075-T6 clad specimens were carried out in air with a range of water vapour concentrations. The purpose of the tests was to see whether the water vapour would have the same effect as for the 2024-alloy.
- (2) Crack propagation tests with a high frequency of loading on 2024-T3 alclad specimens were also conducted with liquid water or a water displacing oil as environment. The purpose of the former tests was to observe whether liquid water (rain) would have a different effect than wet air of 100 % R.H. and of the latter whether wetting of the surface with a water displacing oil would increase the fatigue life.

- (3) Crack propagation tests on 2024-T3 alclad specimens in wet (100 % R.H.) and in dry (20 p.p.m. H_2O ; p.p.m. = parts per million) air with different frequencies of loading. The effect of the environment on a metal is time dependent. In a fatigue test with high frequency of loading the time available for a reaction between the metal and the environment during one cycle is shorter than in tests with low frequency of loading. If a reaction between the metal and the environment occurs it is likely that the effect of the environment on the fatigue crack growth will be frequency dependent.

Some results of the tests on the 7075-T6 clad specimens are given in the figures 10 and 11. Fig.10 gives the data and the mean S-N curves for crack growth from a cracklength $l = 1.5$ mm until $l = 25$ mm in dry and in wet air and with a high loading frequency. It shows that the scatter in fatigue life was small and that the fatigue life in dry air was significantly longer than in wet air. The ratio between the two fatigue lives increased from a value of about three at the high stress amplitude of 7.5 kg/mm^2 to a value of about ten at the low stress amplitude of 3 kg/mm^2 . To facilitate a comparison of these results with those for the previously tested 2024-T3 alclad aluminium alloy, the mean S-N curves for crack growth in the latter alloy have also been plotted in fig.10. Comparison at the same stress level and the same environment shows that the crack growth in the 7075 material was noticeably faster but that the two aluminium alloys showed a similar behaviour with respect to the effect of water vapour.

Fig.11 gives the data and the mean curve of the fatigue life for crack growth from $l = 1.5$ mm to $l = 25$ mm versus the concentration of the water vapour in the air for a stress amplitude of 3 kg/mm^2 . The data show that like with the 2024 alloy (see refs 10 and 11) there is a transition range where small changes in the concentration of the water vapour have a rather large effect on the fatigue growth. Outside this range the effect of the concentration of the water vapour is only slight. The critical range of the concentration of the water vapour (appr. 200-20 p.p.m. = R.H. 0.5 - 0.05 %) lies far below the normal relative humidity of air which varies approximately between 30 and 100 %.

The next figure, number 12, reproduces data for crack growth of 2024-T3' alclad specimens immersed in distilled water or wetted with a water displacing low viscosity oil. A comparison of these data with the mean S-N curve for crack growth in wet air which has also been reproduced in the figure shows that:

- (1) the rate of crack growth in liquid water was only slightly faster than in wet air.
- (2) wetting of the metal with the water displacing oil had an unfavourable rather than a favourable effect on the crack growth.

The importance of the loading frequency for the water vapour effect on the crack growth is illustrated by figures 13 and 14. The first figure shows a small effect of the humidity on the growth rate at the low frequency (30 cycles/min) and a much larger effect at the high frequency (3600 cycles/min), the ratio between the fatigue lives in dry and in wet air being only appr. 1.3 in the first case but 4.6 in the second case. Fatigue loads on aircraft structures in service generally have a relatively low frequency and moreover variations of the concentration of the water vapour in normal air are small. Consequently the present results underline that in respect of fatigue life of aircraft the humidity of the environment air is not very important.

Fig.14 indicates that the crack growth of 2024-T3 alclad in dry air is much more affected by the frequency of loading than in wet air. An increase of the frequency of loading from 30 cycles/min to 3600 cycles/min in wet air increased the mean number of cycles for crack growth from 1.5 to 25 mm from 28 k.c. to 50 k.c. (i.e. with a factor of 1.8) and in dry air from 42 k.c. to 240 k.c. (i.e. with the much higher factor 5.7). With regard to practical application of laboratory data it is a fortunate result that the frequency effect is not large at the humidity that is normal for a laboratory.

In fig.14 the plotted test data for dry air further show that on double logarithmic paper the relation between fatigue life and frequency of loading is rather well represented by a straight line. The same will probably be valid for tests in wet air.

The above results suggest that the factors humidity of the air and frequency of loading interact and have to be considered jointly. It would be convenient to have a parameter with both factors in order to obtain a master curve for the crack growth of 2024-T3 alclad accounting for different values of humidity of the air and frequency of loading. Simple parameters as

$$\frac{\text{water concentration of the air (p.p.m.)}}{\text{frequency of loading (c/min)}} \quad \text{or} \quad \frac{\log \text{ water concentration of the air}}{\log \text{ frequency of loading}}$$

did not meet with success. This was particularly so with regard to the S-shape of the curve in fig.13 giving the relation between the humidity of the air and the fatigue life with a high frequency of loading. An S-shape of this curve has been assumed in view of the test results obtained at the lower stress am-

plitude $S_a = 4 \text{ kg/mm}^2$ (refs 10 or 11). It is not certain whether the S-shape will be applicable at $S_a = 6.5 \text{ kg/mm}^2$. This will be verified in the near future.

From a fundamental point of view a rather complicated relation between the two factors humidity of the air and frequency of loading does not seem unlikely, if crack growth is considered as conversion of cyclic slip into crack extension in interaction with an oxide film with properties depending on the time per cycle and the humidity of the air. A theory on the effect of frequency and environment needs knowledge of the oxydation at room temperature of aluminium and aluminium alloys in air of different humidities in the relatively short time of a fatigue cycle (0.01 - 10 sec) and knowledge of the interaction of this oxide film with the above mentioned conversion of cyclic slip into crack extension. However, information on these subjects is scarce and continued research will be necessary to arrive at an acceptable explanation of the effect on crack growth of the two factors, frequency of loading and humidity of the air.

(-) Crack propagation rates in 2024-T3 alclad sheet from different manufacturers.

The crack growth tests on 2024-T3 alclad sheet material from seven different manufacturers on specimens with the load parallel to the rolling direction of the sheet have been continued with programme fatigue tests with a low frequency of loading, appr. 10 c/min, on the same type of specimen. Secondly constant load amplitude tests were carried out with a high frequency of loading, appr. 3000 c/min, on specimens with the load perpendicular to the rolling direction (ref.12).

The material quality rating depended on the type of test. The ratios between the fatigue lives for the most superior of the seven materials and the most inferior material were in the order of 2:1 for the constant amplitude tests and in the order of 1.5:1 for the programme tests.

The crack propagation life for the sheet specimens loaded transverse to the grain direction was on the average about 30 % shorter than the life of specimens loaded parallel to the rolling direction. The directionality effect was hardly affected by the stress amplitude, the crack length and the manufacture of the material.

As for materials from two manufacturers crack growth tests have been made on sheets from two different batches. The test data indicate ratios between the crack propagation lives for the two batches in the order of 1.5:1. This

batch effect appeared to be correlated with the ductility of the alloy (see fig.15).

In general the correlation between the crack propagation rates and the ductility of the materials appeared to be rather complicated. Although a low ductility is unfavourable for crack propagation, materials with the same ductility (as determined in a tensile test) can still give noticeably different crack growth rates. It is thought that this is probably associated with differences in the heat treatment of the alloy regarding solution heating, quenching and flattening before ageing. Also the presence of minor quantities of certain elements may be important.

There was no apparent correlation between the crack propagation rates and the grain size, the thickness of the cladding layer or the electrical conductivity. Fractographic observations suggest that inclusions had little effect on the propagation that occurs according to the tensile mode of fracture. Inclusions are believed to be important for fast fatigue crack propagation and residual strength (see also section 7).

7 Residual static strength of aluminium alloy specimens.

Apart from information on the fatigue crack propagation properties the fail safe design philosophy requires knowledge on the effect of cracks on the residual static strength. Supplementary to the crack growth tests discussed in the preceding section systematic investigations have been carried out at the NLR to study the various factors which affect the residual strength of cracked sheet. A summary will be given of the data on the effects of the following parameters: width and thickness of the sheet, loading rate and manufacture.

(1) Manufacture. Five out of seven 2024-T3 alclad sheet materials of different manufactures which have been used to determine the effect of manufacture on fatigue crack propagation (see section 5) have been compared in residual strength tests (ref.13).

Small but systematic differences between the residual strength properties of the five materials were found. The difference in residual strength between the best and the worst material was in the order of 10 %. Comparison of the residual strength and the fatigue crack propagation properties of the five materials showed that high residual strength did not correlate with good fatigue crack propagation properties. It indicates that static crack propagation and fatigue crack propagation are probably governed by different factors.

A weak correlation was found with the number of inclusions. A small number of inclusions resulted in a high residual strength. Especially the number of manganese containing constituents appeared to be important. The lower this number the higher was the residual strength. It correlated with the fact that the most inferior material contained about 20 % more manganese than the most superior material.

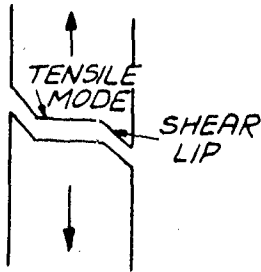
(2) Rate of loading. The effect of the rate of loading has been determined on 2024-T3 clad sheet specimens (thickness 2 mm) with a central transverse saw cut (ref.14). The duration of the tests ranged from about 0.4 sec. to 30 min. It turned out that the stress to initiate slow crack growth decreased slightly at increasing testing speed. In the range of loading rates investigated the residual strength of the specimens was not affected by the testing speed. Since the extreme loading rates in civil aircraft are between the limits applied in the investigation these results support the opinion that results of normal residual strength tests on aluminium alloys are of general applicability in aircraft design.

(3) Width. Residual strength tests on the effect of the width of the specimen have been carried out both on clad 2024-T3 and 7075-T6 sheet material of 2 mm thickness (ref.15). Geometrically similar specimens were used having widths of 150, 300 and 600 mm. The specimens had a central transverse slit made by means of a jeweller's fret saw. The test data indicated that for the same relative crack length (same ratio between crack length and sheet width) a wide sheet has a lower gross fracture stress than a narrow sheet. However, for the same absolute crack length the wide sheet fractured at higher stress. For the 2024-material this trend is illustrated in the figures 16 and 17 by the reversed sequence of the curves giving the fracture stress σ_c of the three types of specimens as a function of the initial crack length l_o in absolute and relative units respectively.

Using an energy criterion for fracture Broek showed in ref.15 that for an infinite sheet the relation between the fracture stress σ_c and the initial crack length l_o is given by

$$\sigma_c l_o^{1/2a} = \text{constant} \quad (2)$$

where a is a constant which has a higher value for a more ductile material. The test data showed that this relation was also met for small cracks in wide sheets ($\frac{l_o}{w} < 0.2$). This means that this relation can be used in most cases where aircraft sheet structures are concerned. The equation is not valid if the stresses are so high that general yielding occurs.



(4) Thickness. The effect of the sheet thickness has been investigated for 2024-T4 and 2014-T4 for sheet thicknesses ranging from 0.5 to 20 mm. The fracture stress as a function of sheet thickness had a maximum (see fig.18). Closely related to this phenomenon was the mode of fracture. Specimens thinner than the optimum thickness had slant fractures, whereas thicker specimens had flat tensile mode fracture at the centre and shear lips at the edges. The residual strength and the fracture mode are related to the state of stress at the crack tip during the test. Broek's explanation of the fracture mode transition in ref.16 is based on the observation that crack growth in static tests is the consequence of initiation, growth and coalescence of microvoids; a conception of crack growth based on electronmicroscopical study of fracture surfaces.

The initiation and growth of the microvoids is governed principally by the shear stresses at the crack tip, the coalescence of the microvoids by the tensile stresses. The planes of maximum shear stress will have the greatest microvoid concentration. These planes of maximum shear stress have different orientations in the case of plane stress (thin sheet) and in the case of plane strain (ref.18). This can explain the different fracture modes in thin sheets and thick plates.

Reference is made to the afore mentioned publication of Broek for details of a tentative explanation of the maximum of the residual strength in fig.18.

8 Some remarks on future research.

Although some of the investigations reviewed in the preceding sections were of special interest with respect to the development of the Fokker F-28 Fellowship aircraft the greater part was concerned with subjects of general technical interest. The latter were designed to fill up gaps in data on fatigue properties of materials and structural elements and to increase our knowledge of the fatigue phenomenon. This policy will be continued.

The list of subjects to be studied in the near future comprises

- (1) The fatigue strength of joints. Continuation of the investigations on lugs, riveted, bolted and adhesive bonded joints.
- (2) The fatigue properties of modern materials that are used in the aircraft industry or may be so in future.
- (3) The fatigue phenomenon. Continuation of investigations on crack growth. Fractographic investigations etc.
- (4) The effect of fatigue cracks on static strength properties. Extension of the residual strength tests to panels built up from sheet and stringers.
- (5) Interaction of fatigue with other phenomena e.g. creep.
- (6) The effect on the fatigue strength of thermal, mechanical and other treatments of the metal, e.g. anodizing.

A large part of our efforts in the near future will concern ad hoc tests and the full scale fatigue testing of the wing of the Fokker F-28 Fellowship aircraft. This testing, which will be carried out in close co-operation between the manufacturer and the NLR, will be a simulation of actual flights, as Mr. Van Beek will discuss in his Symposium paper.

9 References.

1. Hartman, A.
Jacobs, F.A.
van der Vet, W.J.
Constant load amplitude and programme fatigue tests on single lap joints in clad 2024-T3 and 7075-T6 aluminium alloy with two rows of rivets or huckbolts.
NLR-TN M.2147 (1965).
2. Hartman, A.
Fatigue tests on single lap joints in clad 2024-T3 aluminium alloy manufactured by a combination of riveting and adhesive bonding.
NLR-TN M.2170 (1967).
3. Schijve, J.
de Rijk, P.
The effect of "ground-to-air cycles" on the fatigue crack propagation in 2024-T3 alclad sheet material.
NLR-TR M.2148 (1966).

4. Schijve, J.
Nederveen, A.
Jacobs, F.A.
The effect of the sheet width on the fatigue crack propagation in 2024-T3 alclad material.
NLR-TR M.2142 (1965).
5. Paris, P.C.
Gomez, M.P.
Anderson, W.E.
A rational analytic theory of fatigue.
The trend in engineering 13 (1961) p.9.
6. Paris, P.C.
Erdogan, F.
A critical analysis of crack propagation laws.
Trans. ASME series D 85 (Dec.1963), p.528.
7. Schijve, J.
The significance of fatigue cracks in the micro-range and the macro-range.
Paper presented at the 69th Annual Meeting of ASTM (1966).
NLR Report MP.243.
8. Schijve, J.
de Rijk, P.
The crack propagation in two aluminium alloys in an indoor and an outdoor environment under random and programmed load sequences.
NLR-TN M.2156 (1965).
9. Schijve, J.
Broek, D.
de Rijk, P.
Nederveen, A.
Sevenhuysen, P.J.
Fatigue tests with random and programmed load sequences with and without ground-to-air cycles.
A comparative study on full-scale wing center sections.
NLR Report S.613 (1965).
10. Hartman, A.
Jacobs, F.A.
An investigation into the effect of oxygen and water vapour on the propagation of fatigue cracks in 2024-T3 alclad sheet.
NLR-TN M.2123 (1964).
11. Hartman, A.
On the effect of oxygen and water vapour on the propagation of fatigue cracks in 2024-T3 alclad sheet.
Intern.Journ.of Fracture Mechanics, volume 1, number 3, pp.167-188 (1965).
12. Schijve, J.
de Rijk, F.
The fatigue crack propagation on 2024-T3 alclad sheet materials from seven different manufacturers.
NLR-TN M.2162 (1966).

13. Broek, D. Static tests on cracked panels of 2024-T3 alclad sheet materials from different manufacturers.
NLR-TN M.2164 (1966).
14. Broek, D. The influence of the loading rate on the residual strength of aluminium alloy sheet specimens.
Nederveen, A. NLR-TN M.2154 (1965).
15. Broek, D. The effect of finite specimen width on the residual strength of light alloy sheet.
NLR-TN M.2152 (1965).
16. Broek, D. The effect of the sheet thickness on the fracture toughness of cracked sheet.
NLR-TN M.2160 (1966).
17. Broek, D. Crack propagation properties of 2024-T8 sheet under static and dynamic loads.
NLR-TN M.2161 (1966).
18. Schijve, J. Analysis of the fatigue phenomenon in aluminium alloys.
NLR-TR M.2122 (1964).
19. Broek, D. Crack propagation properties of 2024-T8 sheet under static and dynamic loads.
NLR-TN M.2161 (1966).

Table 1. Comparison between the crack propagation lives simultaneously obtained in an indoor and an outdoor test rig (results from ref. 8) ($2w = 100$ mm, $t = 2$ mm).

$$\text{Ratio} = \frac{\text{indoor crack-propagation life}}{\text{outdoor crack-propagation life}}$$

MATERIAL	TYPE OF LOADING	CRACK GROWTH FROM $2\ell_a - 2\ell_b$ (mm)	RATIO
2024-T3	RANDOM	5 - 12	1.2
	RANDOM + GTAC	8 - 18	0.9
	PROGRAM	7 - 24	1.1
	PROGRAM + GTAC	6 - 14	1.2
7075-T6	RANDOM + GTAC	4 - 28	1.6
	PROGRAM	4 - 9	2.1
	PROGRAM + GTAC	6 - 22	1.5

FIG. 1. Mean S-N curves of single lap riveted joints in 2024 - T3 clad of 1 mm thickness.

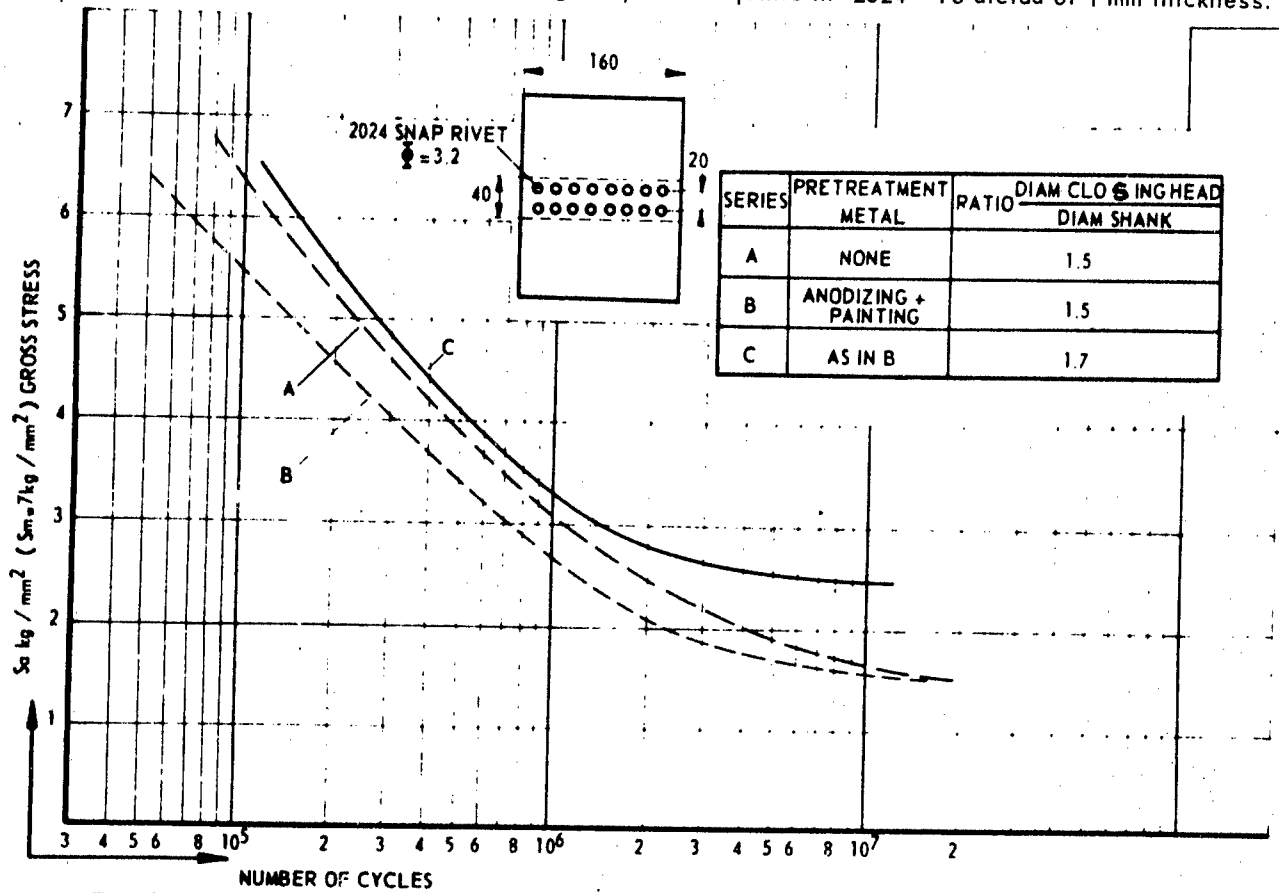


Fig. 2. Mean S-N curves of riveted, EC 2216 adhesive bonded and riveted EC 2216 adhesive bonded specimens. Unaged condition.

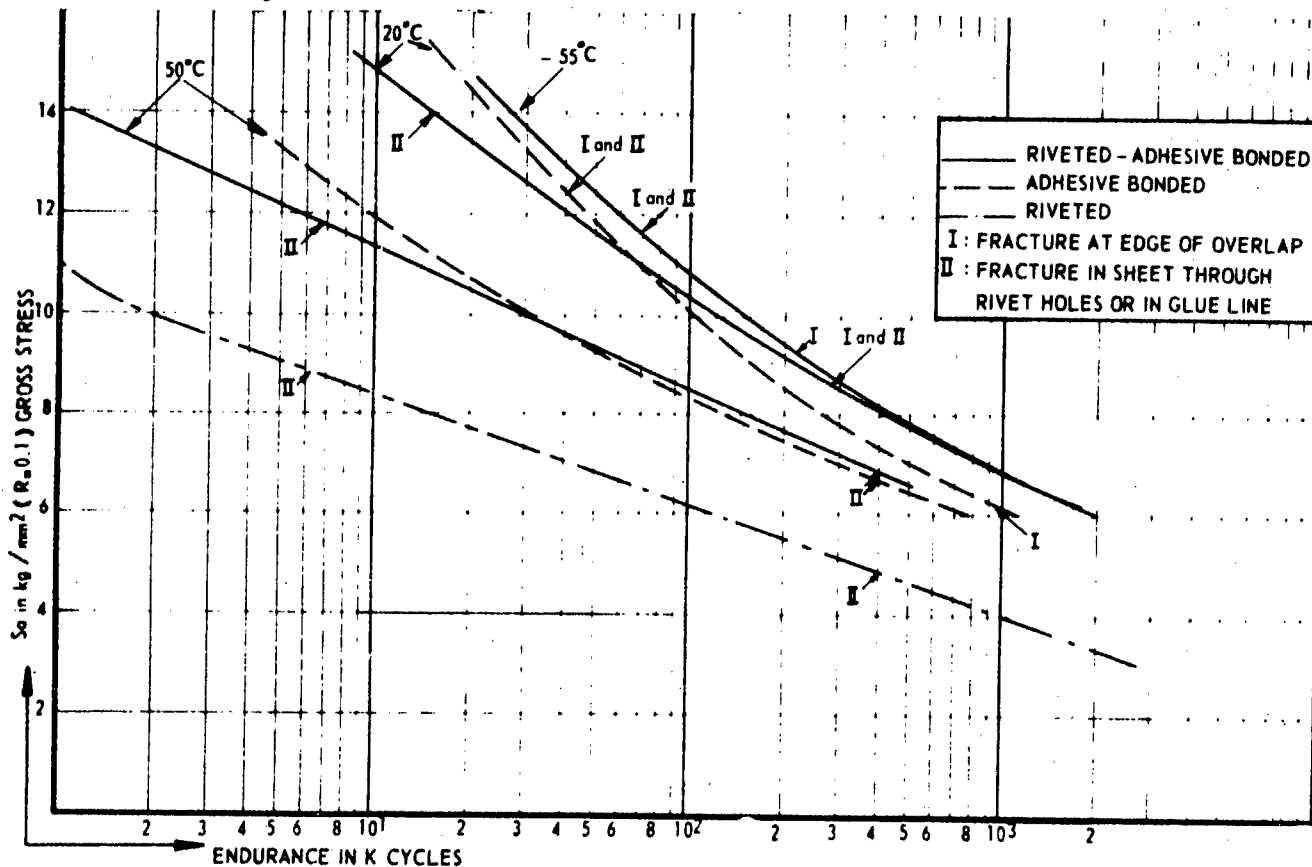


Fig. 3. Dimensions of the specimens.

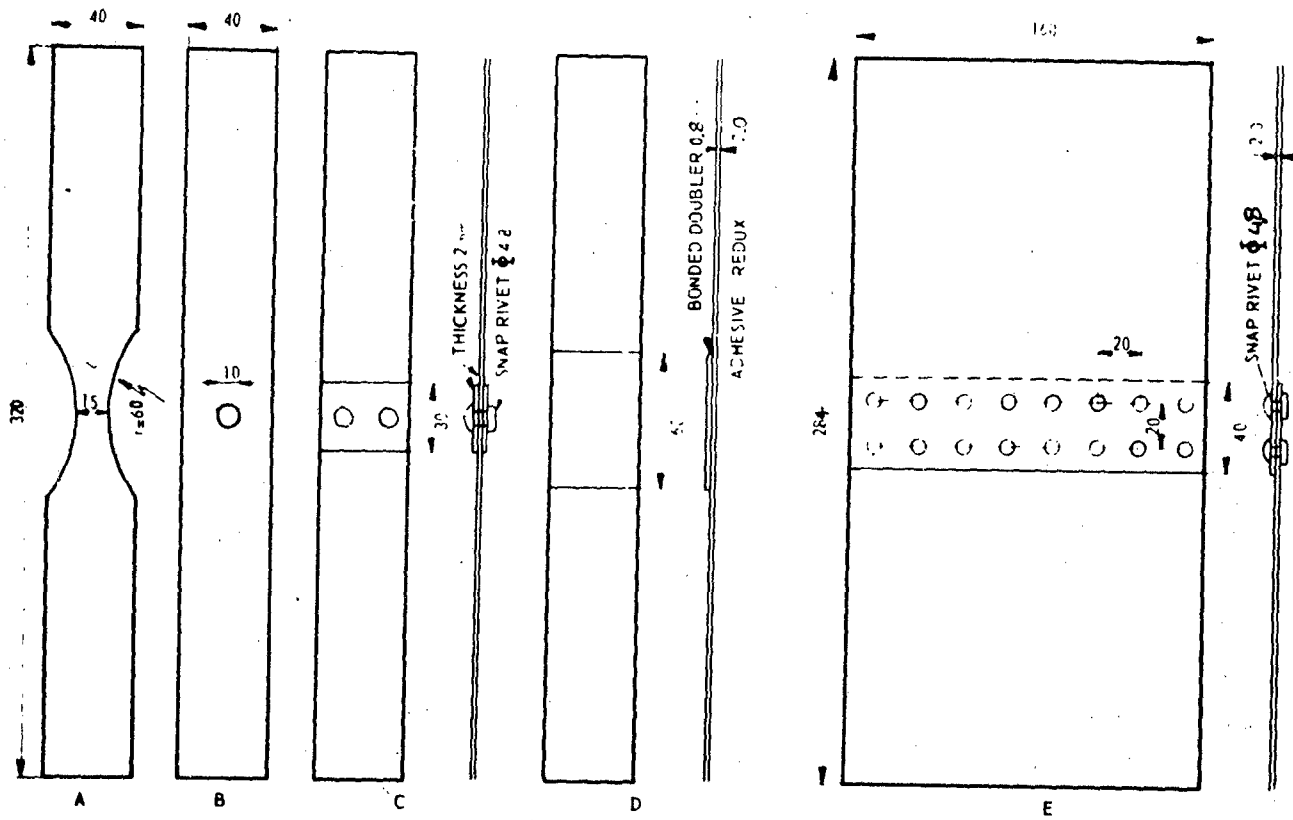


Fig. 4. S-N curves for specimens with unloaded rivets (fig. 3, type C)

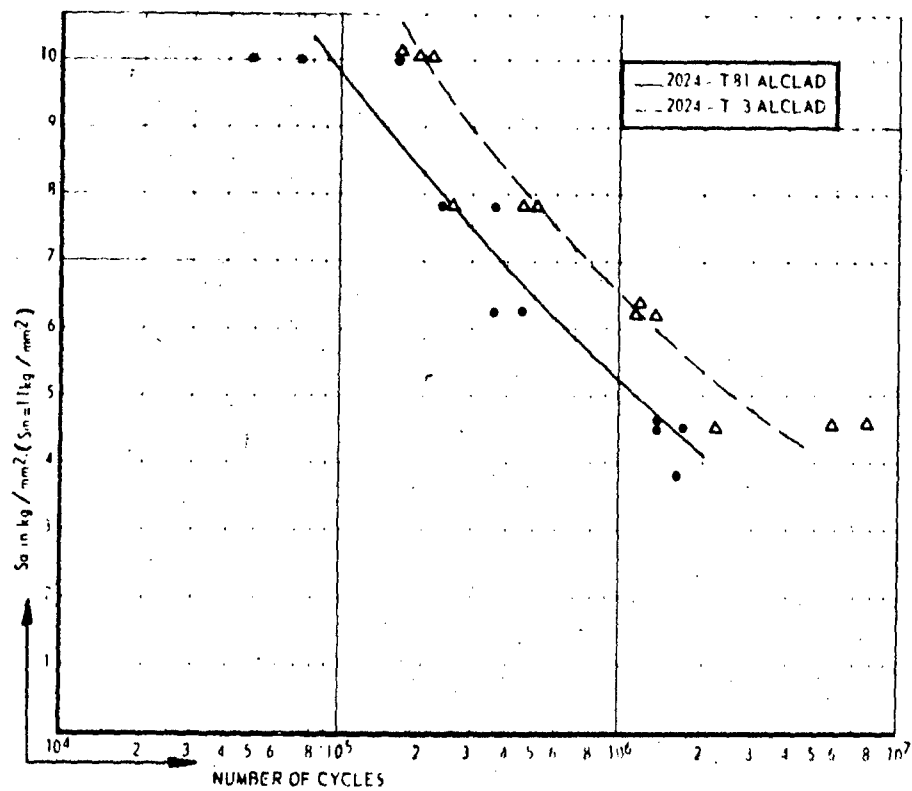


Fig. 5. S-N curves for riveted lap joint specimens (fig. 3, type E).

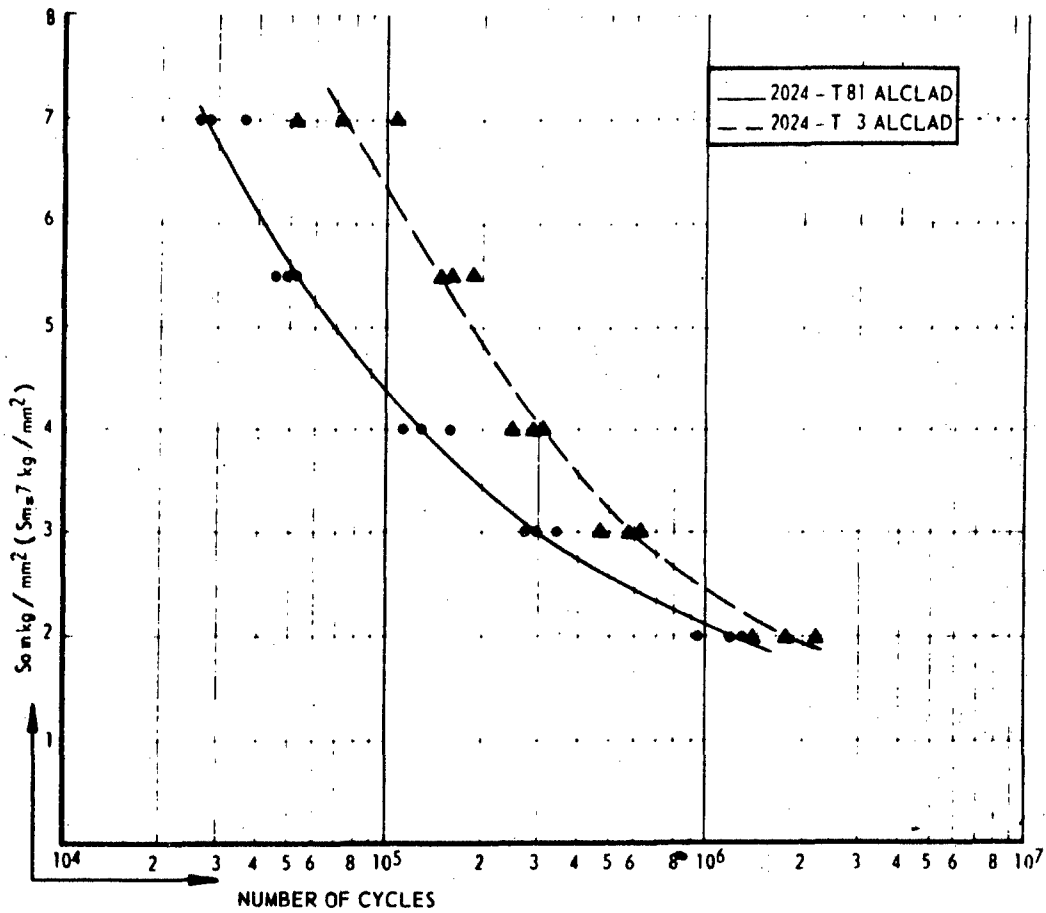
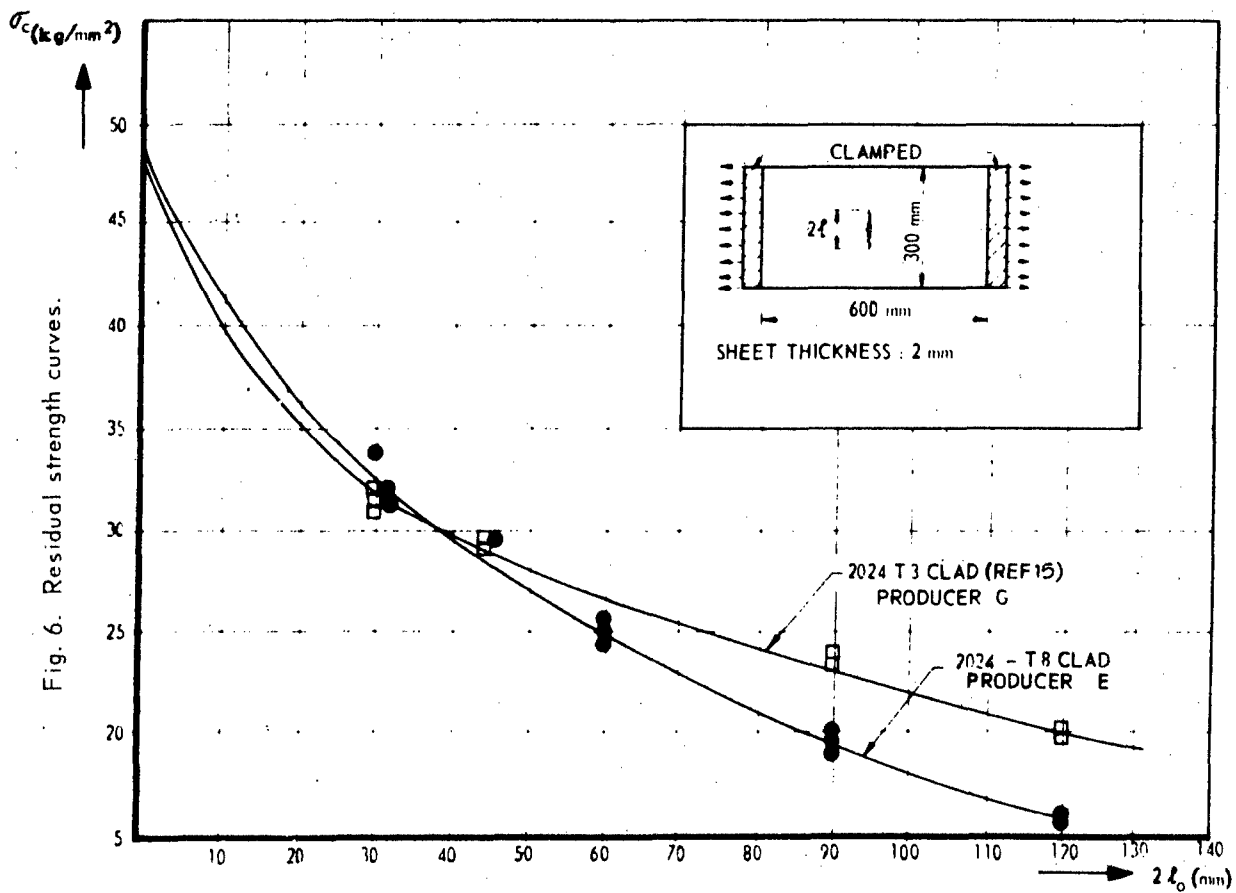


Fig. 6. Residual strength curves.



Specimens (fig 3)	S _{max}	N	S _{max}	N	S _{max}	N	S _{max}	N
■ unnotched	32	70	24	180	18	4000		
□ large notched	32	3	24	14	16	60	12	180
○ small notched	32	7	24	28	18	80	14	350

S_{max} is net stress in kg/mm², k is based on gross stress.

N is fatigue life in kc

NOTCHED SPECIMENS
(K_t = 2.66)

UNNOTCHED SPECIMEN
(K_t = 1.085)

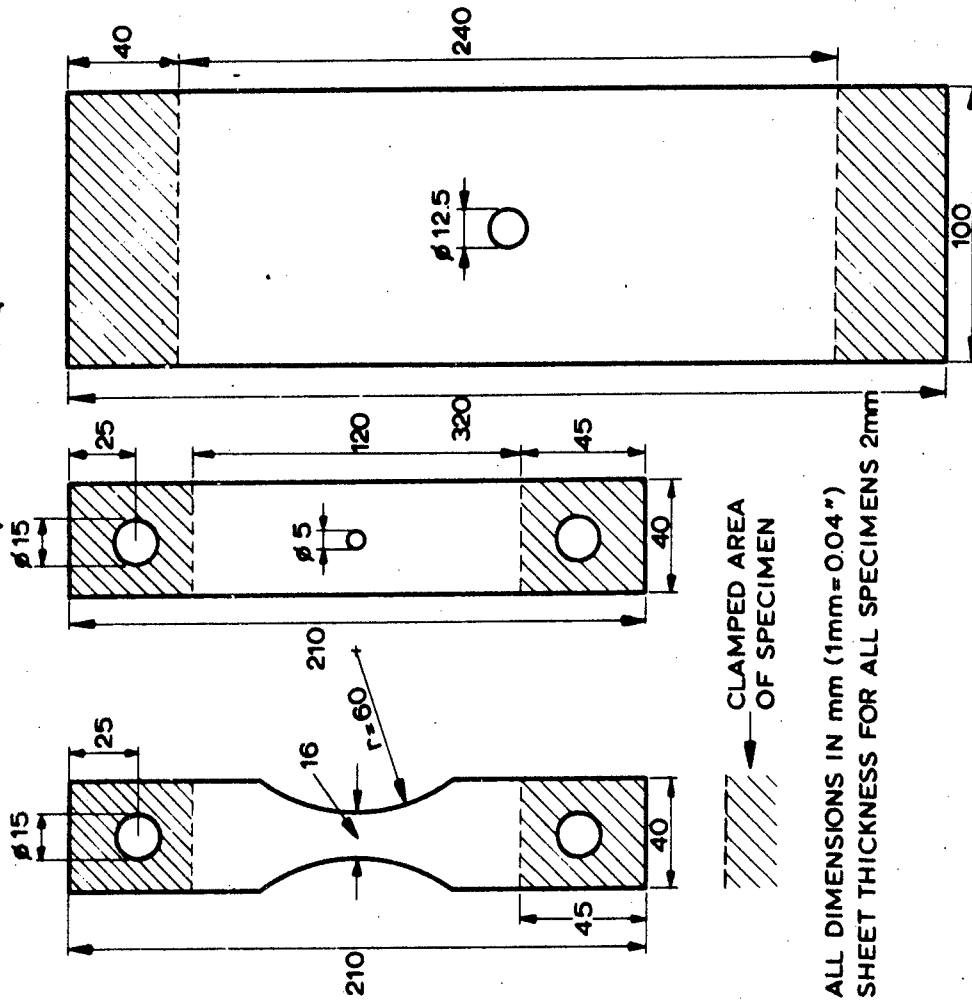


Fig. 7. Unnotched specimen and specimens notched by a hole, cut from bare 2024 - T3 sheet material. Specimens were used for the observation of the growth of very small cracks (ref. 7).

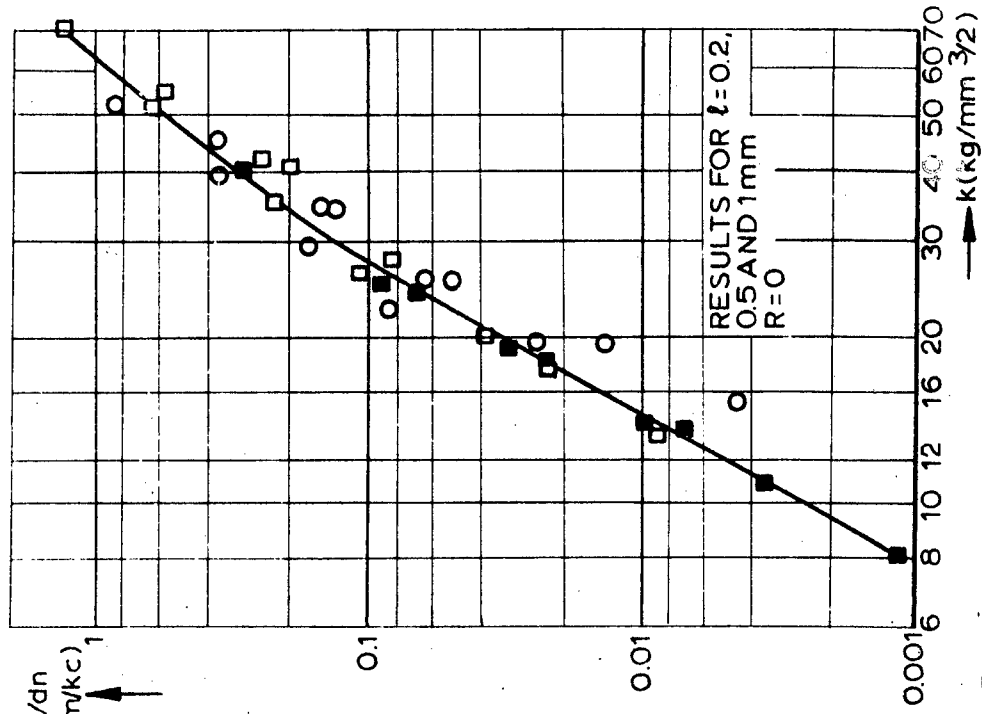


Fig. 8. The crack rate as a function of k for small corner cracks in unnotched and notched 2024 - T3 specimens. (Ref. 7)

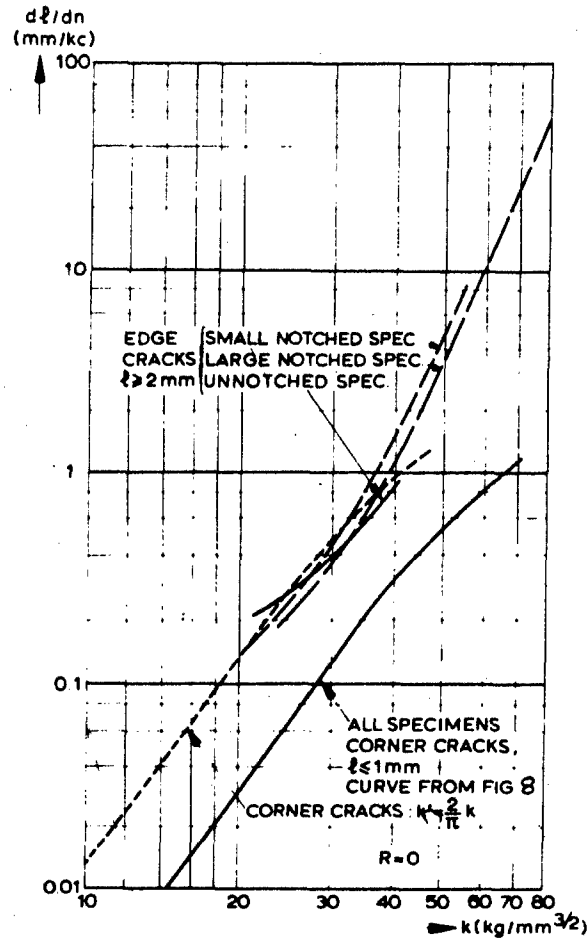


Fig. 9. The crack rate as a function of k for edge cracks in unnotched and notched 2024 - T3 specimens (ref. 7). Comparison with corner cracks.

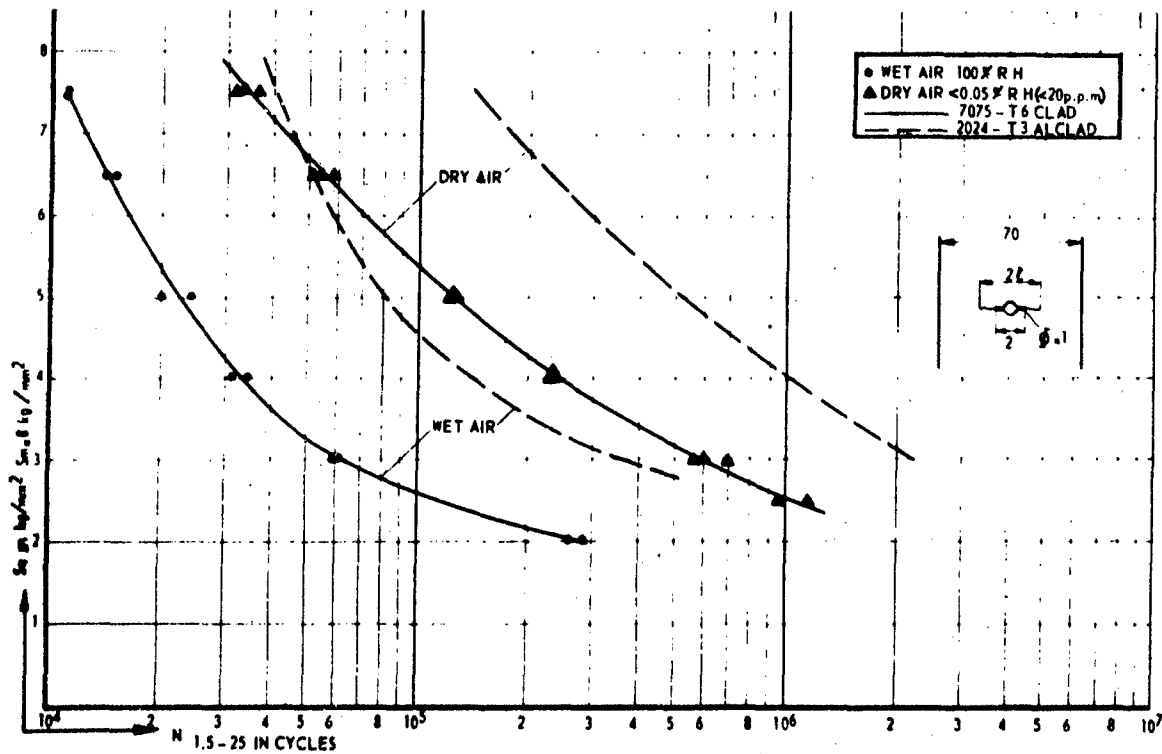


Fig. 10 S-N curves of 7075 - T6 clad for crack growth from 1.5 to 25 mm in dry and wet air. Frequency 35(0 c/minute.

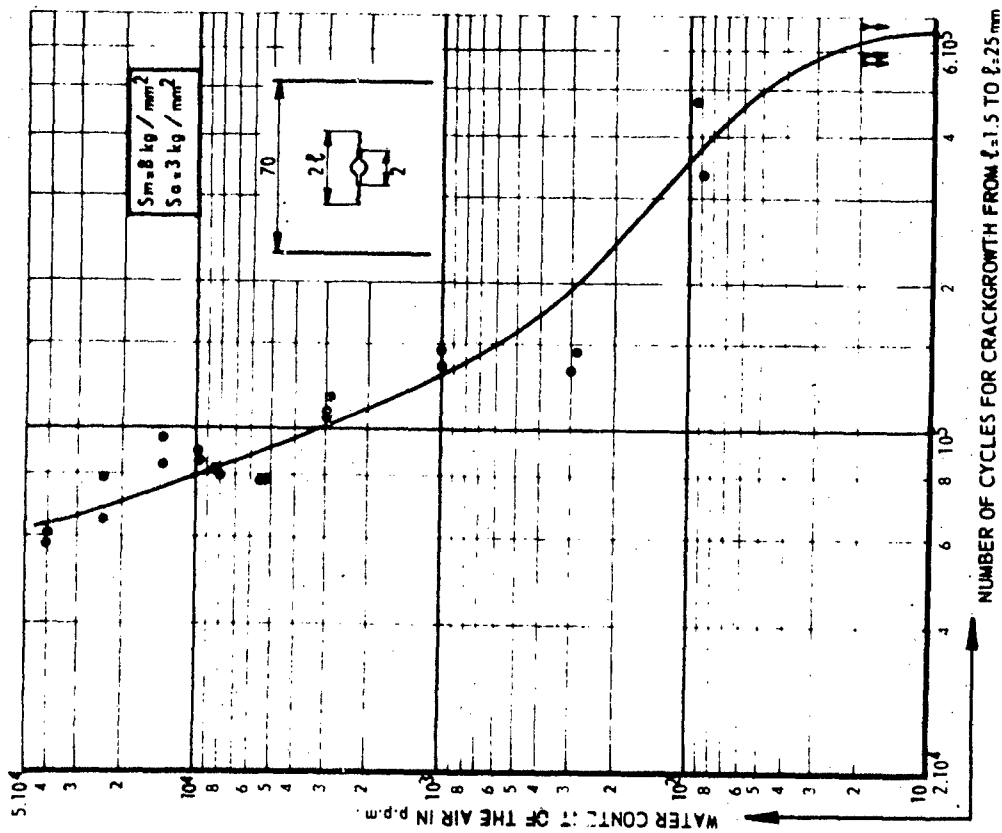


Fig. 11 Effect of the water content of the air on the crack growth of 7075-T6 clad sheet.

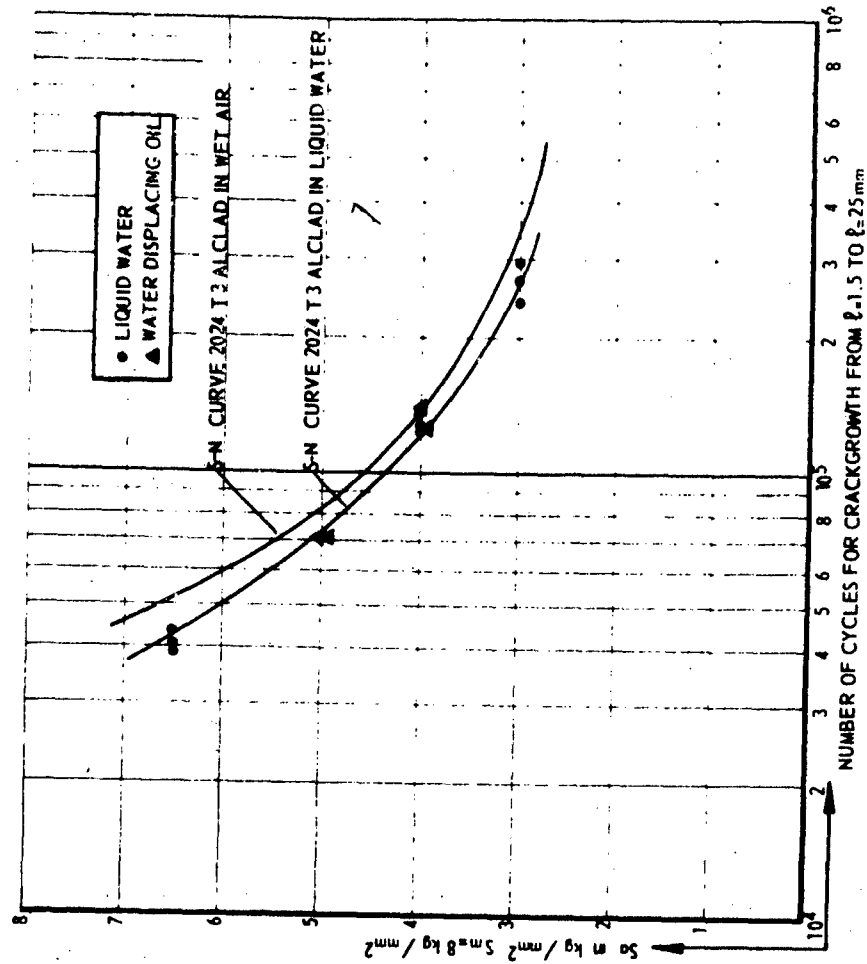


Fig. 12 Comparison of crack growth in 2024-T3 Alclad in wet air and immersed in water or wetted with a water displacing oil.

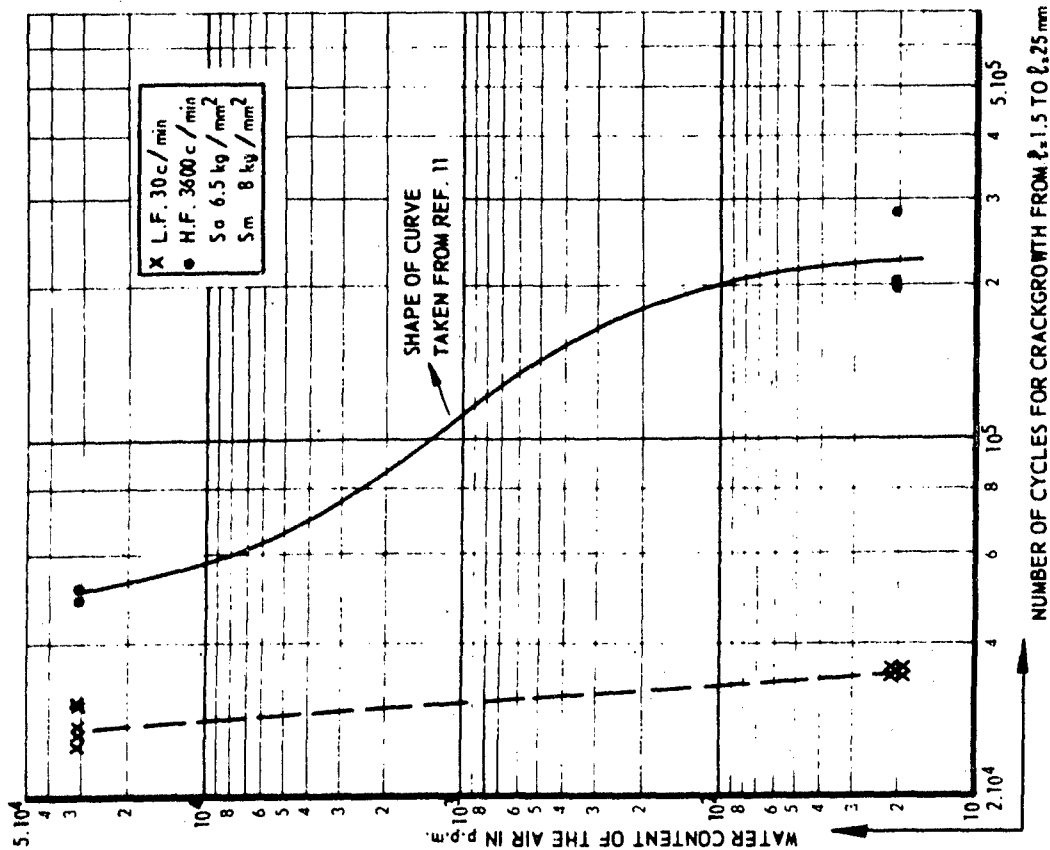


Fig. 13. Crack growth in 2024-T3 alclad versus water content of air low-and with high frequency of loading.

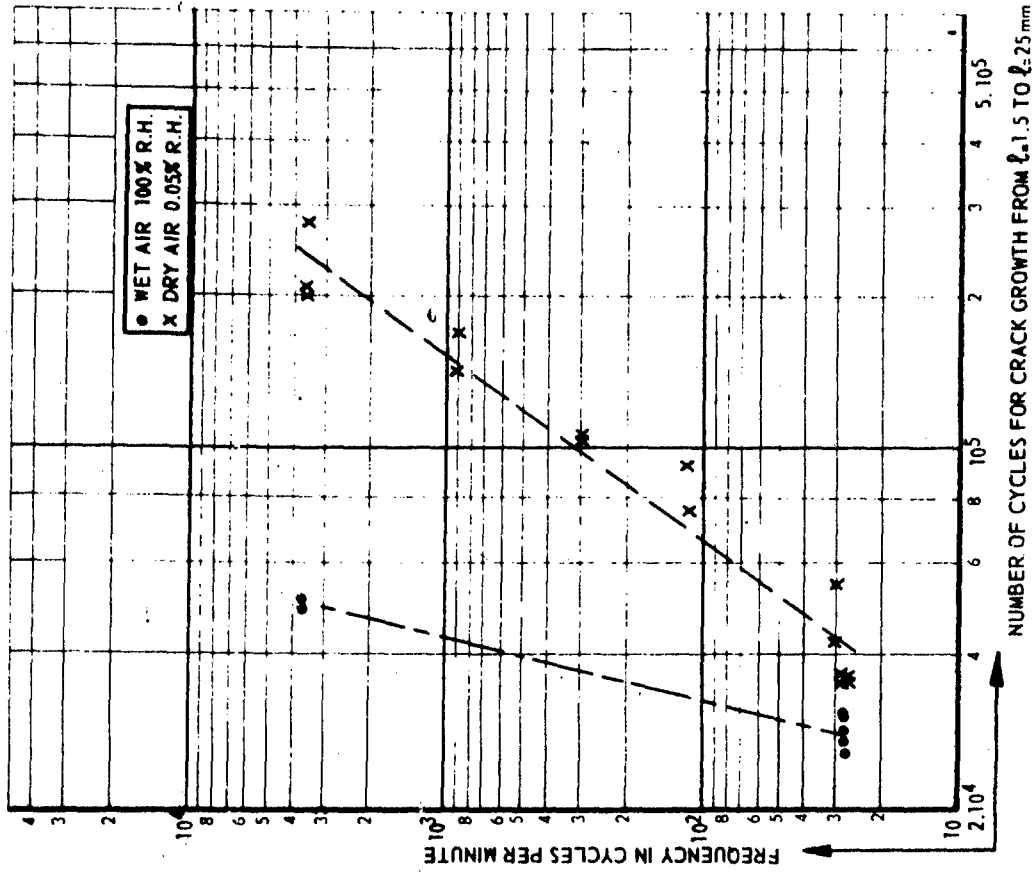
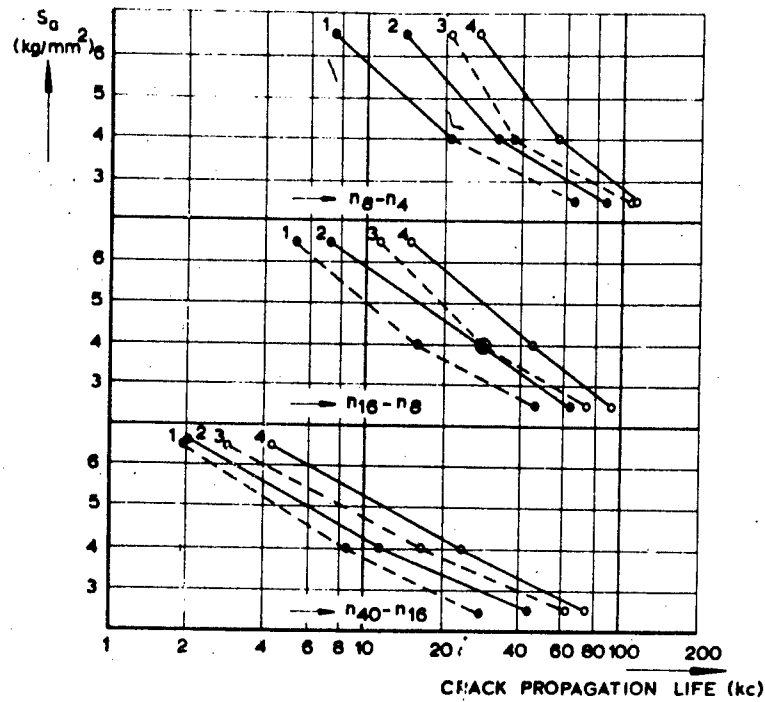


Fig. 14. Crack growth in 2024-T3 alclad versus frequency of loading for tests in wet and in dry air.



TEST SERIES	MANUFACTURER	STATIC PROPERTIES			REFERENCE
		S_u	S_{Q2}	$\delta(2'')$	
1	C	48.5	36.9	16	
2	C	46.9	34.4	23	
3	F	48.3	37.1	19	
4	F	46.3	35.2	22	

2024-T3 ALCLAD SHEET SPECIMENS, WIDTH 160mm, THICKNESS 2mm.

Fig. 15 The crack propagation life for three crack propagation intervals and two batches of manufactures C and F. Data from ref. 12.

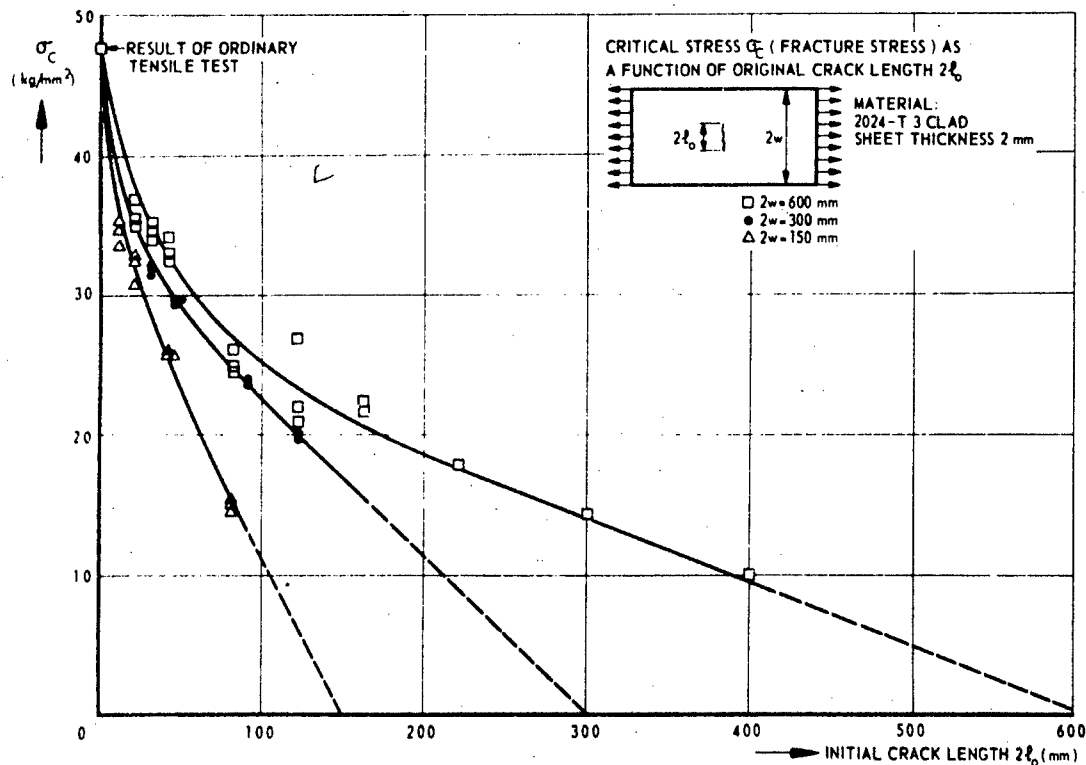


Fig. 16 Residual strength of 2024-T3 specimens.

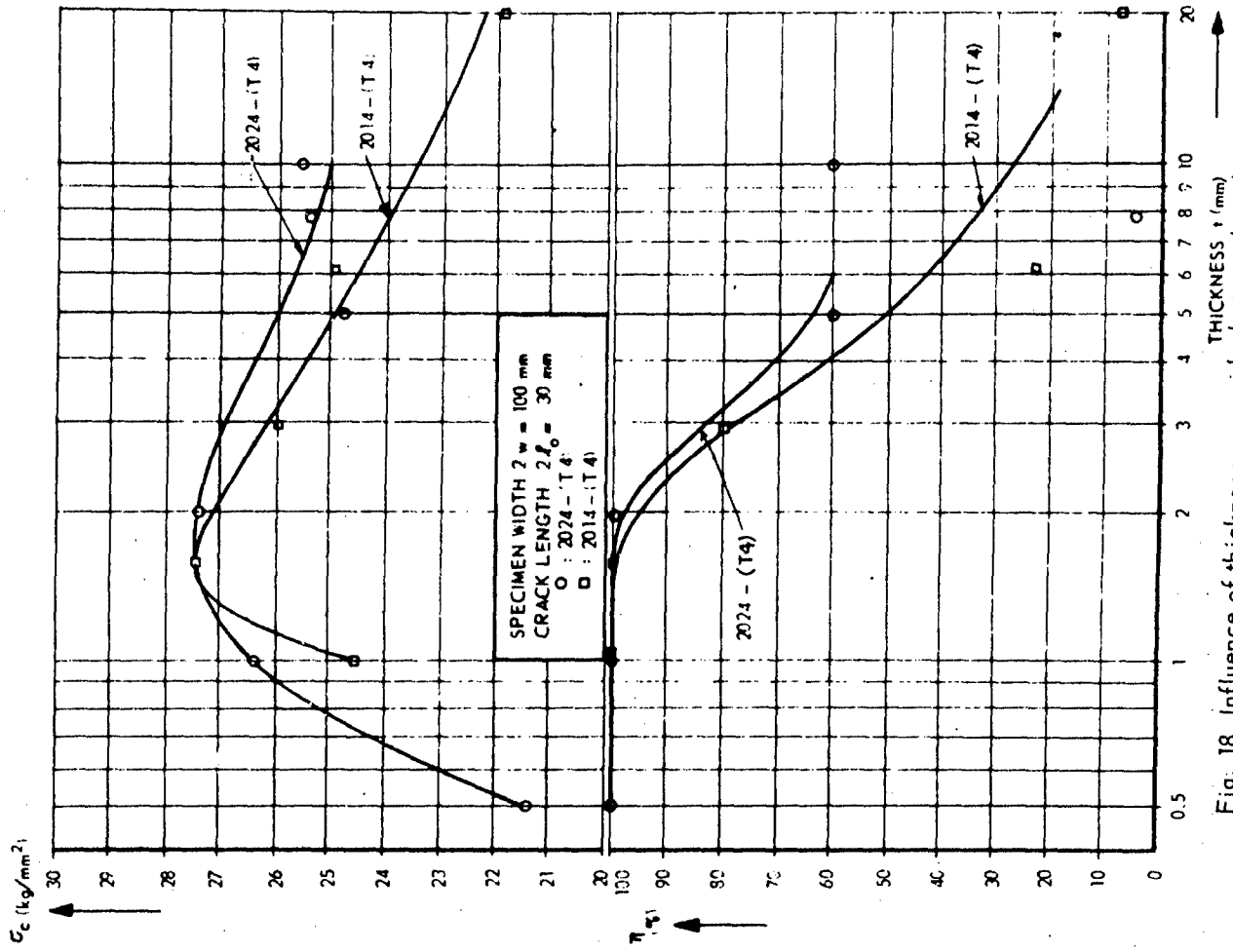


Fig. 18 Influence of thickness on residual strength and fracture mode.

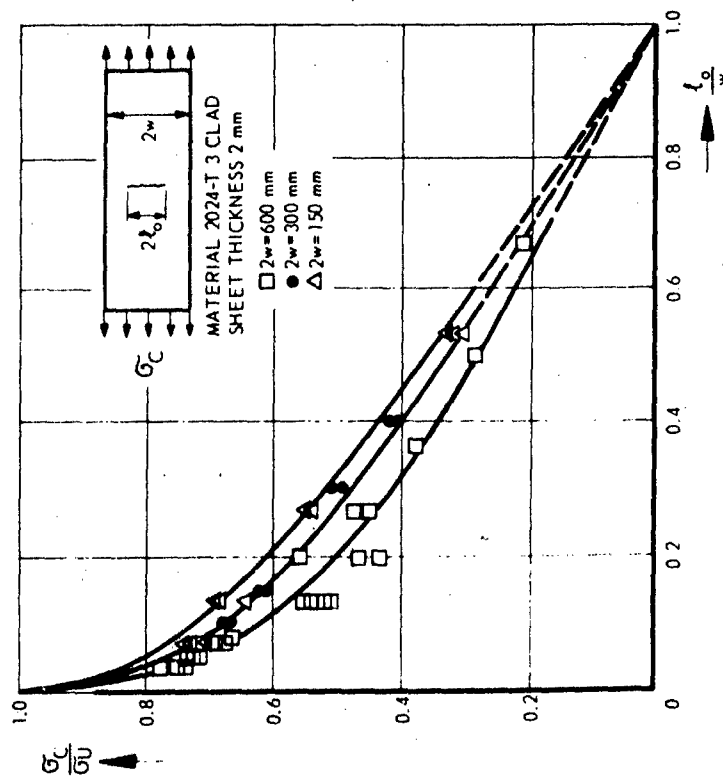


Fig. 17 Relative reduction in strength due to cracks.

PRECEDING PAGE BLANK NOT FILMED.

N 69-21583

A REVIEW OF SWISS INVESTIGATIONS ON AERONAUTICAL FATIGUE

DURING THE PERIOD JUNE 1965 TO APRIL 1967

Compiled by

J. Branger

Eidgenössisches Flugzeugwerk

Emmen

Note: Copyright permission for publication may be
granted subject to written application

PRECEDING PAGE BLANK NOT FILMED.

CONTENTS:

		<u>Page No.:</u>
1.	Gust investigation	58
2.	Statistics of Fatigue Loads	59
3.	Test Facilities	62
4.	Test Programmata	66
5.	Damage Detection	70
6.	Fatigue Tests	74
7.	Service Experiences	97
8.	Conclusions	98
9.	Future Research	99
10.	REFERENCES	100
11.	FIGURES	102
12.	TABLES	104
13.	ANNEXES	104
	TERMINOLOGY = Annex 4	

1. Gust Investigation

The somewhat sophisticated measuring installation in our VENOM test aircraft had been reduced to an extent which renders the evaluation easier. Due to the results from the fully equipped aircraft a reduction was possible without loss of needed information.

Some more flights in very gusty weather for the investigation of gust velocities and of aircraft response over the wing span were made [1].

The calculation of AC-stress-relations to recorded gust-spectra was prepared. The corresponding computer program-mata are actually worked out.

Fig. 1 represents such an investigation of a recent test flight.

At another test flight a MIRAGE III S A.C. recorded heavy clear air gusts:

Date : 9.11.66; Time: 14⁵² to 15²⁵

Altitude : 12'000 m/M (40'000 ft)

AC-speed : Ma 1,84

Calculated vertical gust velocities:

-11 m/sec to +8 m/sec

(= -36 to +26 f.p.s.)

The process of the recorded rotational speeds round the three AC-axes points to an asymmetric transverse gust, the main portion of which was not the vertical component !

Data like this are important not only for fatigue, but also for limit load considerations on passenger aircraft as CONCORDE or SST.

2. Statistics of Fatigue Loads

All fatigue meters and accelerometers mentioned in our previous reviews are still in service. There are

Fatigue meters of the RAE type, produced by MECHANISM Ltd.

type M 1730 A: In 3 DH-100 VAMPIRE A.C.

In 2 DH-112 VENOM

type M 1967: In 3 PILATUS P3

In 6 A.S. HUNTER Mk.58

In all MIRAGE III S

PERAVIA - Accelerometers with trailing pointer

in all DH-100 VAMPIRE A.C.

in all DH-112 VENOM

in all A.S. HUNTER Mk.58

in all PILATUS P3

in all MIRAGE III S

In civil transport aircraft of Swiss carriers there are still neither fatigue meters nor other such recording instruments installed.

The load spectra of the mentioned military AC, calculated with the readings and records on the 1st march 1967 are given in the following Table 1:

Table 1

Number of C.G.-accelerations $n \times g$ equalled or exceeded
per 1000 hours:

	VAMPIRE DH-100	VENOM DH-112	HUNTER Mk. 58	PILATUS P3	MIRAGE III S
+10,5			0,024		
+10,0			0,049		
+ 9,5			0,073		
+ 9,0			0,122		
+ 8,5	0,024	0	0,341		
+ 8,0	0,132	0,0266	1,095		
+ 7,6			1,655		
+ 7,5	0,264	0,195		0	
+ 7,0	0,743	0,719	4,4	0	18,1
+ 6,6	1,066	1,554			
+ 6,5				0,0287	
+ 6,0	18,9	12,7		0,0574	
+ 5,5				0	
+ 5,0	375,9	483,2	1322		141,6
+ 4,5				68,4	
+ 4,0	3386	4352			
+ 3,5			11247	1042,7	1786
+ 2,5	18416	22079	25960	2668,9	4238
+ 1,75			39377	6599,4	14389
+ 0,25			3478	1384,6	692,8
- 0,5	80,5	159,3	124,2	75,2	54,2
- 1,0	13,3	28,8			
- 1,5			13,2	2,28	0
- 3,1	0,024	0,240			
- 3,0				0	
- 3,5	0	0,115		0	
- 3,8			0,122		
- 4,0			0,122		
- 4,5			0,073		
- 5,0			0,049		

It is our policy to provide all new AC of some importance, for which a long service time can be foreseen, with fatigue meters right from their first flight. Thus their individual fatigue story can be supervised during the whole service life.

The Swiss Army is still flying some 40 C-3603 aircraft of our own design, built during the war. They serve as target towing AC and target AC for Anti-Aircraft-Training. The HISPANO-engines are by now expired, while the structure is still safe for at least 1500 hours. So probably we shall install in these aircraft new engines, and on this occasion we shall certainly install also fatigue meters too as a very long service time must be considered.

Continuous records are moreover running in one VENOM and in one MIRAGE III S. Further continuous records were made in a FAIRY GANNET and in one of the mentioned C-3603 for the establishment of this target-mission's spectra, and in a PILATUS PORTER P6 for the establishment of the ground load story of these light STOL-Transport-Aircraft. On this you will be informed by Mr. Weibel's lecture [2].

By a special action which is still running we get statistics of side loads on undercarriages during taxiing.

3. Test Facilities

3.1 Our full-scale Fatigue History Simulator is still doing his work. Visitors of our Establishment are always impressed by the genuine sequence of the loads, the flight by flight simulation with it's representation and especially by the realistic simulation of the landing impact with the effect of the wheel spin up force. The Simulator has up to-day simulated more than 60'000 flights with more than 5 Mio quasicycles in about 6 years [3].

3.2 The twin-chain test rig for 36 test rods also is still running, controlled by the same unit as the History Simulator. It has now reached a running time of about 24'000 hours representing 120 periods each consisting of 350 flights [4].

3.3 The well known AMSLER-Works at Schaffhausen designed two new devices as a complement to existing standard test machines. The so called "Function Pulsator" introduces thus a pulsating capability of 0,5 dm³ (0,1 gallon) at 200 kp/cm² (2850 psi) up to 120 cycles per minute with different program shapes, while the so called "Hydro-Pacer" applies a control possibility for slow cycling (max. 10 c.p.m.) or non linear pacing to existing static test machines [3].

3.4 Another Swiss firm, RUSSENBERGER + MUELLER, also at Schaffhausen, specialists in vibration testing and testing equipment designed a new small high speed fatigue machine for single amplitude tests for loads up to 500 kp (1100 lb), called MICROTRON 657. It works on the resonance principle (50 - 200 Hz), is electromagnetic driven and an electronic closed loop control system keeps the system always under it's natural frequency, see Fig. 2 [5].

For S.T.M. a special adaption of this machine (Microtron 654) was designed by RUSSENBERGER specially for fatigue testing of jet engine rotor blades under reverse bending.

The blade is fixed with its root in a very hard spring. The deflexion of the latter can be neglected with respect to the deflexion of the blade under test. Therefore, the blade vibrates in its true natural frequency. The excitation of the blade is done electromagnetically in connection with an amplifier and a feed back system. For counting the number of cycles an electronic two-decade-system with a mechanical preset counter has been used. To stop the machine if a crack occurs on the blade, two amplitude sensitive relays are incorporated in the machine.

For measuring the amplitude of the blade, an optical readout system is adapted to the machine, which gives a quick and precise reading of the maximum amplitude of the blade.

Fig. 3 shows the complete machine with the mounting table, the fixation for the blade, the optical readout and the amplifier with the different control units.

Fig. 4 has been taken on a vibrating blade, exposed over several cycles.

For maintaining a constant amplitude on the blade, a special automatic control system is incorporated in the electronic circuit. It consists of a proportional-integral regulator which allows to maintain the amplitude as good as $\pm 1\%$ or less, even over long periods of time.

- 3.5 In the last years we developed, designed and built in our works a new fatigue test bed which works on a quite different principle. It is the so called "Six-Rod-Fatigue-Test-Bed" Fig. 5 as there are 6 identical test rods, arranged rotation-symmetrical to a main axis and parallel to it and to each other.

Each rod gets its axial loading by a hydraulic jack, but all 6 jacks are controlled by the same and only hydraulic device which is situated in the centre of the machine, so that all 6 jacks are loaded by exactly the same pressure in each instant. The hydraulic control device is, by means of electro-hydraulic valves, connected to an electronic control, similar to that of the full-scale History Simulator. As that one, this facility too is not working on a resonance principle, but with distinct hydraulic pressures, which follow in any desired sequence. 80 loads can be chosen out of 127 available load levels to form a loading program. The 127 load levels are separated by steps of equal magnitude, all levels are thus fixed to a constant ratio. The basic level amount can be set at will.

It is evident that we designed this test facility to be able to run history loadings simultaneously on 6 test rods, thus getting the scatterband in one run, eliminating scatter by program-deviations. Its performance is, for each rod, maximum 8 tons axial tension load, same for compression load (this one evidentially limited by buckling) at a speed of minimum 1,0 cycles per Min. up to a maximum of 5 cycles per second, or 300 cpm. It follows that the same history program can be run on this test bed as on the History Simulator, but up to about 50 times faster.

The length-limits of the punched tape which contains the loading program are: Minimum 1 1/2 feet (180 orders), maximum 1000 feet (120'000 orders). Long tapes on spool are automatically reset after it has passed through. Each rod has its own counter, a seventh counter counts the tape passings. After a break the jack of the broken test rod is automatically switched off.

To enable undisturbed electronic measurements on the test rods, this test facility is also situated in the same big Faraday cage as the History Simulator.

As the Fatigue History Simulator, also the 6-specimen fatigue test machine is running fully automatically, unmanned, 24 hours a day, 7 days a week.

Any failure of the facility stops the machine automatically and a signal points to the failed group. Even at a frequency of 300 cpm long tapes with periods of 39'000 cycles need 2 h 10 min. plus 5 min. for the automatic reset of the tape. Thus about 10 periods per day are run, and as fatigue history tests need mostly about 100 periods to failure, such a test-run of 6 specimen takes 10 days net.

- 3.6 Another test facility was made last year in our research department by a new control and a modified piping of the existing high altitude test bed for engines: The high altitude test chamber is thus actually working as a fatigue test bed for an entire (e.g. full scale) cockpit of a jet fighter. Air pressure, air temperature and air flow are simulated in their flight by flight sequences.

4. Test Programmata

The full VENOM History Program, called VENOM Program I, will be published soon in a special report [6], see Annex 1 and 2.

The same History Program but tailored for the 6-specimen test bed is called No. II. It differs from No. I by omitting those orders which are specially needed for running a fatigue test of a whole aircraft only. It is self-evident for our philosophy, that the genuine sequence of the loads is strictly observed, as well as the same flight by flight sequence is maintained as that of program I. Program II was then counted by the different methods defined by Schijve [7]. The resulting modified program, in which the genuine load sequence is still followed, is called VENOM Program III, where the meancrossing peak count method is applied to the air loads (mean equal to 1 g in air); Program IV same as II but the ground loads reduced to the highest peak load between landing and take-off, Program V for the combination of III and IV, Program VI for the mean-crossing peak count method, where the mean value is supposed to be the 0 g-level. In Number VII all occurrences of No. II are omitted, which differ only 0,5 g (or 5% of the design ultimate load) from the 1,0 g-level in the air loads and only 0,3 g from the 1,0 g-level in the ground loads. No. IX is similar to VII, but only the small deviations of the air loads are omitted, whilst in No. X the same was done for the ground loads only.

VII, IX and X were made without considering the influence of the weight history (by fuel consumption), whilst Program XIV, XV and XVI do consider this influence, otherwise being the same.

All these programs, schematic represented in Fig. 6, were made for investigation purposes. The only way to submit them to other investigators is by manufacturing copies of the punched tapes, because otherwise the genuine load sequence is lost.

On his request we sent last year such a copy of the 8-hole punched tape of program No. 1 to Dr. Gassner, and during this winter his specialist for test beds came over to our works for making another copy on an analog magnetic tape.

The same ways are obviously open to all ICAF-delegates.

We think that the digital control, e.g. by punched type, is much more versatile. For instance, by modifying the key to the eight-hole code you are able to alter the ratio between air loads and ground loads, or the ratio between the different fuel weights.

The basic key to all VENOM programs is given in the following table 2:

Table 2

Case	c.g.- acceleration n.g	Fuel Weight					Load
		5/5	4/5	3/5	2/5	1/5	
Air	+6,5		A4				Tension
	+6,0		B4				
	+5,5			C3			
	+5,0		D4	D3			
	+4,5		E4	E3			
	+4,0		F4	F3	F2		
	+3,5		G4	G3	G2		
	+3,0		H4	H3	H2		
	+2,5		J4	J3	J2	J1	
	+2,0	K5	K4	K3	K2	K1	
	+1,5	L5	L4	L3	L2	L1	
	+1,0	M5	M4	M3	M2	M1	
	+0,5	N5	N4	N3	N2	N1	
	+0	00	00	00	00	00	
	-0						
	-0,5		Q4	Q3			Compression
	-1,0		R4				
	-1,5		S4				
Ground	0,4	T5	T4	T3	T2	T1	
	0,7	U5	U4	U3	U2	U1	
	1,0	V5	V4	V3	V2	V1	
	1,3	W5	W4	W3	W2	W1	
	1,6	X5	X4	X3	X2	X1	
	1,9			Y3	Y2	Y1	
	2,2			Z3	Z2	Z1	

The ratios between air and ground loads on one hand, and between the different fuel weights on the other hand are easy to calculate for all parts of a given aircraft. Fig. 7 represents these data for the wing of the VENOM AC. With these data the actual figures for the Code-Key to test a distinct part can be calculated. Table 3 gives these figures for stat. B of Fig. 7 in relation to the "1 g air case at full fuel weight", coded M5 in table 2, which figure is reduced to 100 %:

Table 3

Case	c.g.- accelera- tion n·g	Fuel Weight					Load
		5/5	4/5	3/5	2/5	1/5	
Air	+6,5		697				Tension
	+6,0		644				
	+5,5			597			
	+5,0		536	543			
	+4,5		483	489			
	+4,0		429	434	442		
	+3,5		375	380	387		
	+3,0		322	326	332		
	+2,5		268	272	277	281	
	+2,0	+200	215	217	221	225	
	+1,5	+150	161	163	166	169	
	+1,0	+100	107	109	111	113	
	+0,5	+ 50	54	54	55	56	
	0	0	0	0	0	0	
	-0,5	- 50	-54	-54	-55	-56	Compression
	-1,0	-100	-107	-109	-111	-113	
	-1,5	-150	-161	-163	-166	-169	
Ground	0,4	- 53	- 32	- 18	- 17	- 15	
	0,7	- 93	- 56	- 32	- 31	- 26	
	1,0	-132	- 79	- 46	- 44	- 38	
	1,3	-172	-103	- 59	- 57	- 49	
	1,6	-212	-127	- 73	- 70	- 60	
	1,9			- 87	- 83	- 72	
	2,2			-101	- 96	- 83	

Thus the same tape can be used to investigate nearly all parts of an aircraft by history loading. The only thing you need, beside the tape, is the electronic reading unit, which can be bought from special firms for about 3000 dollars (for instance from INFRANOR, Genève).

Further programs we made are:

No. VIII, a single amplitude cycling program, the ratio R between the lower and the upper peak load being free to choose and No. XI, a blocked program consisting of two blocks, each with 50 cycles.

More on ground loading programs you shall find in Mr. Weibel's lecture [2].

For terminology see Annex 4. All history program-tapes (I to VII, IX, X, XIV, a.s.o.) contain one period q .

In annex 3 we try to represent five periods of all ground loads of VENOM program I (1000 hours, or 1750 flights resp.) by a diagram which originates from the range-mean count method [7]. It proves that this presentation is more significant than was Fig. 7 in [4], resp. Fig. 8 in ICAF Doc. 285. The same is possible for the air loads, but that needs chromolithography. In this presentation only the sequence of the loads is lost.

5. Damage Detection

5.1 The crack detector which was developed at Emmen (Fig. 8) 5 years ago [4] [8] seems to be really a damage indicator. As a sample you see in Fig. 9 the fatigue damage story of specimen No. D 75 recorded by the crack detector, or better called damage indicator. Data of this test:

Test bed: 6-rod fatigue test bed Type F+W

Loading program: No. VIII/100, e.g. single amplitude

loading with same Limit Loads as Program No. I:

Upper Load = +5265 kp (= 52% of design ultimate load)

Lower Load = -1600 kp (= 15,8% of design ultimate load)

R = -0,3

Loading frequency: 3,5 cycles per second (10 times slower for the reproduction from the magnetic tape to the Plotter)

Test rod: Fig. 24; Mat. Specification: Table 6

Break at 3247 cycles

First crack (visible by microscope) at about 1250 cycles

Second crack at about 2750 cycles. (e.g. 38,5% of Life time)

The abscisse of the record represents to the right the time or number of cycles; the ordinate represents upward the electric resistance, or downward the conductivity of the surface in the hole of the rod.

The conductivity is obviously influenced by the strain in the hole which itself is produced by the external load forced upon the test rod (+5265 kp is on the upper limit, 1'600 kp on the lower limit): It is decreased by tension, and oscillates with the load amplitude. But a second phenomenon has recorded its vestige in this representation.

Dr. Maria Ronay of the Columbia University interprets it as follows: " Apart from this strain indicating feature the diagram consists of two distinct parts. In the first part the original conductivity decreases from the first cycle on, the rate of decrease being the largest at the beginning, getting smaller in the course of cycling, reaching a steady rate of decrease, similarly to fatigue hardening curves. The appearance of the first crack marks the beginning of the second part of the diagram where the decrease of con-

ductivity due to the increase in length and widening of the crack is of an exponential nature."

It seems that the damage indicator may become a tool in investigation and detection of pre-cracking damage too. If decrease of conductivity can be equalled with some kind of damage, according to our results damage starts from the first cycle on.

Very interesting is the end of the story of specimen No. D 20, told in Fig. 10. Data of this test:

Test bed: Same as for D 75.

Loading program: No. XI/100, e.g. twin-block-program,

- first block consisting of 50 cycles with an upper load of +5265 kp, lower load = 0;
- second block consisting of 50 cycles with an upper load of 0, lower load of -1600 kp.

Loading frequency (

Test rod (same as for No. D 75

Mat. Specification (

Break at 27242 cycles (or at 272,42 block pair)

Second crack at the first cycle (tension) of block-pair

No. 243.

Note: The difference between the two O-Load-Lines on the left of "2.crack" are due to a very small first crack, but mainly to the play in the plotter-mechanism. On the right of "2.crack" this gap is easy to interpret as the increasing width of the second crack, when you know, that the ordinate from the base line is the meter of the electric resistance. During the compression blocks the crack is closed by the load, increasing thus the conductivity. Near the end of the life, the effect of compression increases due to the decreasing stiffness of the partially cracked specimen. Such twin-block programs are good means for distinction of disorder-damage from crack damage.

Beside these recordings the indicator serves as a very accurate prophet of the moment of break. Fig.11 shows a diagram recorded 4 cycles before break. The indicator enabled us to make even moving pictures of fatigue

breaking without consuming too many miles of film.

We finally arrived to take movies at 600 frames per second of the last cycles in a fatigue test running at 4 cycles per second.

We hope to improve the indicator furthermore, thus a new one is actually being built.

- 5.2 Another development was not so successful. It is the automatic electronic inspection of test specimen by isolated copper-loops bonded to the critical surfaces of the specimen, which I mentioned in Munich. Further tests proved that the problem is not at all solved. Neither copper, stainless steel, silver, nor thin bands or thin wires stood the tests in history loadings. Either the indicator cracked too early or too late.

It would be an enormous help in testing and in aircraft servicing when an automatic inspection system was available. Thus I would like to call all members to work on this important problem.

Perhaps the system developed by BOEING, will fill the gap. Unfortunately we have not got details yet.

- 5.3 Another method for detecting cracks in the inner structure of an aircraft would be inspection by x-ray.

Up to the last ICAF-Conference we were not really successful in x-raying although we consulted the best specialists available.

Anyhow, some months ago, when we looked for a damage in a wing of the VENOM test - in a case where we were quite sure that there was a damage - we finally tried to x-ray the wing when it was loaded by a positive 3 g - airload. That was the solution: On the developed pictures we found a classic fatigue crack, which, by further x-ray pictures, turned out to have a length of some feet! Since that discovery more than 100 aircraft were x-rayed on which we applied simultaneously a positive 3 g - load on the wings. On the pictures of

four of these aircraft, beginning fatigue cracks were detected. Thus the wings could be reinforced before a much more expensive repair was necessary.

5.4 The evaluation of x-ray pictures is very difficult.

Each picture has to be carefully inspected, and that independently by three specialists. Even applying a 3 g - load, beginning fatigue cracks are no more than a hair half an inch long on the x-ray picture.

That's the reason why we looked for an improvement. After a successful demonstration by PHILIPS of the new x-ray-television-chain developed by C.H.F. MUELLER Hamburg, we were allowed to buy this facility which we completed with a convenient adapter and a Motor car to put the facility in. Fig. 12 shows the principle of the chain (more-over a magnetic tape recorder is included), which produces high quality, direct visible, 20 to 30 times enlarged pictures (wires of $\varnothing 25\mu$ can be seen). On Fig. 13 are the x-ray and TV-Units with the adapter, x-raying a VENOM aircraft, represented.

At the mentioned demonstration on the History Simulator we were able to see and to get probably the first movies of a fatigue crack in a wing under increasing and decreasing loading. It was a rather exciting event (Fig.14).

We hope this facility will make the inspection of service aircraft easier, as the adapter can be moved during the inspection, the inspection takes place instantaneously and we don't have to wait for the developing of the pictures. We hope it will be possible to inspect by this device a fleet of fighters regularly, say all 500 or 300 hours towards the end of their life.

To prevent illusions it has to be mentioned here, that this procedure works only in connection with a full scale history fatigue test, because otherwise you don't know where you have to x-ray the aircraft. It is only by the full scale test that you learn the critical zones.

6. Fatigue Tests

6.1 Full Scale Fatigue Test on DH-112 VENOM AC

On the first series of test, which brought three VENOM to about 5000 flight hours each, with one catastrophic failure in a port wing, I reported at the Munich-Review. This series began on the 25.7.62 and ended on the 7.5.65. [8]

The second series began on the 14.10.65 and ended on the 22.7.66. It was a continuation of the test with three of the remaining five wings of the first series. One month earlier, when both wings had 8540 hours, the starbord wing switched off. The investigation was finally sucessful, thanks to the x-ray pictures shot yet under no loading. This wing was then completly disassembled, or better to say, desintegrated, to enable a careful inspection of each single part, as this wing had stood the longest test, and because we had no confidence in other methods to bring to light really all fatigue cracks. We didn't find more, but the crack, which caused the stop of the test and which was detected by x-ray, was so much the better, see Fig. 15. It is about three feet long. The missing pieces were taken for material tests. This part is the butt-joint-strap of the outer and inner bottom skin between the main spar and the false spar, on the inside, between the skin and rib 7. On both sides of this rib are fuel tanks. Thus it is not possible to see the crack otherwise than by x-ray.

The failed wing was replaced by another test-wing, which had at this time 4740 hours. Already 10 hours later it stopped the test too, although the x-ray pictures shot before hadn't shown any crack. But now the idea to x-ray under load was the successful venture. It was from this wing that we took movies. The part was not yet completly broken, there were several cracks, which totalled a length of about 1 1/2 foot. So ended the second series.

Now we reinforce the remaining wings at all zones which had important fatigue cracks on the test wings. With these reinforced wings the third test series began on the 21.12.66.

The first of these tests stopped on the 22.2.67, due to the same catastrophic failure as mentioned in the first series. The failing port wing had at this moment 10'630 hours, of which 8550 hours before the reinforcement.

The last test run, with the only remaining wings, began on the 28th of April. At this time the port wing had 5072 hours (it was just reinforced), while the starbord wing had 7152 hours, of which 5072 hours were run before the reinforcement. The test shall be run up to failure.

The location of all the cracks which were found on the whole VENOM test, are indicated in Fig. 16, while Fig. 17 represents the reinforcements made before the beginning of the third series. These same are now being introduced on the whole fleet of service aircraft.

6.2 Endurance Test of Oxygen-bottles

Light alloy bottles filled with compressed Oxygen-gas are very dangerous, if they are struck by a gun shot or an ack-ack fragment, because they explode like a bomb, if the pressure was higher than about 40 kp/cm² (or 600 psi). Thus we had to replace these bottles on our new MIRAGE fighters by special designed steel bottles. In type-testing 2 bottles were fatigue tested up to failure.

Data of the test:

- Test bed: Facility at the EMPA for bursting tests, adapted for repeated loading.
- Test program: Single amplitude cycling by water pressure;
upper limit = 138 kp/cm² (1970 psi);
lower limit = 0; frequency = 3 cycles per Minute.

- Test specimen: Steel bottle; capacity 7.7 dm³
(~1.7 UK gallons or ~2 US gallons);
weight 11 kg; diameter \varnothing 145 mm (shape designed for
interchangeableness with the light alloy bottle);
wall thickness 4 mm.
- Steel: Weldable Cr-Mo-V-alloy
(C 0.1 - 0.16; Cr 1.25 - 1.5; Mo 0.8 - 1.0; V 0.2 - 0.3;
Mn 0.8 - 1.1; S_{max} 0.02; P_{max} 0.03; S_{max} 0.03)
strenght after welding: 100 kp/mm²
- Service pressure (specified) = 125 kp/cm²
- Max. service pressure by temperature increase of 30°C
(54°F) = 138 kp/cm²
- Proof pressure (specified) = 187 kp/cm²
- Burst pressure (specified) = 312 kp/cm²
actual burst pressure = 400 kp/cm²
- Safe life (specified) : 3000 cycles

In the fatigue tests one bottle failed at 21'000 cycles (fig. 18), the other at 17'000 cycles [9]. Thus these bottles are admit for at least 5000 cycles (e.g. 5000 flights) although the stress office had not **considered fatigue** in designing the bottle. Obviously the mentioned steel is very suitable for the purpose. It should be added that the replaced light alloy bottle had a weight of 8 kp and a capacity of 6.7 dm³.

6.3 Fatigue tests on flexible metallic hoses

On the ATAR-jet-engine of the MIRAGE fighter (built under Licence in Switzerland) there are flexible metallic hoses designed and manufactured by the firm BOA A.G. at Lucerne. As there are different designs available, fatigue test had to be made with the purpose of finding the best suited design.

Test data:

- Test bed:

Facilities at F+W and EMPA for hydraulic tests, adapted for repeated loading.

- Test program:

Single amplitude cycling by Kerosene pressure; upper limit = 70 kp/m² (1000 psi); lower limit = 0; frequency = 51 cycles per minute.

- Test specimen:

Flexible hose fitted with connectors (straight and elbow); length 400 mm (16"), inner diameter \varnothing 16 mm (5/8"); different designs of the flexible wall.





- Service pressure: 70 kp/cm²

Proof pressure: 160 kp/cm² (2280 psi)

Burst pressure: Not specified

- Fatigue-test results: Table 4.

Table 4

Type	Design	Mat. Spec.	Nr.of test specimen	N cycles up to first leak	Notes
Boa Supra		AISI 321	S1	22100	1) [14000]
			S2	26962	1) [14000]
			S3	13960	1) [14000]
			S4	16273	1) [14000] L
			S5	16644	1) [14000] L
			S6	21008	1) [14000] L
			S7	5808	2)
			S8	4680	2)
Boa Parallel		AISI 321	P1	79162	1) [14000]
			P2	61800	1) [14000]
			P3	58990	1) [14000]
			P4	45046	1) [14000] L
			P5	47552	1) [14000] L
			P6	60504	1) [14000] L
Boa Duo		AISI 321	D1	73830	1) [14000]
			D2	75854	1) [14000]
			D3	74876	1) [14000]
			D4	100624	1) [14000] L
			D5	105820	1) [14000] L
			D6	53896	1) [14000] L
			D7	144400	1) [18000]
			D8	140400	1) [12000]
			D9	92280	1) [12000]
			D10	97340	1) [18000]
			D11	78200	1) [12000]
			D12	69600	1) [12000]
Spring-tube		AISI 304	F1	158000	no leak
			F2	50000	1) [14000]
			F3	138722	1) [14000]
			F4	114500	1) [14000] L
			F5	158000	no leak
			F6	150000	1) [14000] L

- 1) first 14000 cycles without torsion,
following cycles with additional torsion load on.
- 2) All cycles with additional torsion load on
- L One end elbow-connector

Fig. 19 shows fatigue-cracks at their beginning, 200 times enlarged, of a Boa Supra and a Boa Duo flexible hose [10].

6.4 Fatigue tests on compressor blades

Some blades of each production lot of the first stage compressor blades of a jet engine have to be tested in fatigue. The test is a comparing test, it doesn't simulate the service conditions. It is done as a routine test on the Microtron 654 test bed mentioned earlier, see section 3.4. In addition to this requirement this fatigue machine was recently used by EMPA (on order of STM) to compare the influence of different surface treatments of these blades on their fatigue behaviour.

The tests were not carried out up to failure but only up to the moment where the machine switched automatically off due to a certain deviation of the vibration-amplitude. This was the case about 10'000 cycles after the first fatigue crack started, what can be heard by ear. In the following table 5 the figure N gives the number of cycles up to this beginning of a crack.

The blade is a forging which needs a machining operation on the aerofoil as well as on the root section. The material is an austenitic stainless steel of the following composition (approximately):

Carbon	0,17	%
Nickel	2	%
Chromium	13	%
Tungsten	3	%

The dimensions of the blade are: About 200 mm (8 inches) long and 50 mm (2 inches) wide. The first mod flexion frequency is about 135 cycles/sec.

The surface was initially smoothed by an electropolishing process; later on this was replaced by a Bright Shot treatment followed by applying a protective layer of a heat treated lacquer.

The full amplitude was chosen to such a value, that cracks began from 10^5 to 10^6 cycles. The stresses are proportional to the amplitude.

Up to now 142 blades of 12 different treatments were tested. In table 5 only the mean values are given (in 10^6 cycles).

To form a mean value, for each amplitude level only that half of all specimen were considered which cracked the first.

The table indicates that:

- Brightshot has a favourable effect (ref. 1 to 3 or 5)
- Brightshot must be of standard quality (ref. 2 to 3)
- Electropolishing seems not to be favourable (ref. 7 to 8)
- Varnish coating seems to be unfavourable (ref. 7 to 3), perhaps due to the coating process, but
- ref. 11 (to 7, resp. did not confirm this supposition)
- An unsuited remover has an unfavourable effect (ref. 12)

The metallographic investigation did not indicate that the scatter was influenced by the texture (Fig. 20) [11].

But an interesting crack initiator could be investigated at a routine blade test, see Fig. 21:

21 a represents the surface, showing a corrosion nest crossed by the crack.

21 b and 21 c are showing the opened crack, with the mentioned corrosion point indicated. It is 0,1 mm deep and crosses the Brightshot layer. Cut rectangularly, not etched, shows 20 d (white is material, the cut crack surface is on the right bord of the picture, the blade surface on the upper bord). By the way, this blade was not intended for use.

To prevent misunderstanding it must be mentioned here, that these blades are fixed in a floating manner on the rotor, thus they do not vibrate in service. The vibrating tests described are comparing quality tests.

Table 5

	Full amplitude in mm (at the top of the blade)									32	34	36	38	40
1	4.01	B	●							0.32	0.247	0.129		
2	4.41	B	●	B								0.379	0.149	0.192
3	4.42	B	●		B								0,48 ³⁾	0,332
4	4.08	B	●		B			●			1.90		0.170	
5	4.02	B	●		A								0.63	0.251
6	4.03	A			A							2.808	0.194	0.154
7	4.07	B	●		B	●	●				0.514	0.174	0.186	
8	4.92	B			B	●	●					>1.0		
9	4.91	B			B		●					0.77		
10	4.05	B	●		B		●							0.114 ³⁾
11	4.10	B	●		B		● ●	●1)				1.64		
12	4.06	B	●		B		●	●2)			0.100	0.105 ³⁾		
Reference No.	Test series No.	Manufacturer of the blades	at first electropolished	Bright shot, light	Bright shot, standard qual.	Cleaned by Trichlor	Varnish coated at 200°C	Varnish removed	Beginning corrosion before shot treatment	Number of cycles x 10 ⁶ up to first crack (appearing at about 40 mm to 75 mm from the root)				
										1) Varnish removed by Turco 5061, and blade re-coated 2) Varnish removed by another medium 3) One of two specimens only				
										Fatigue tests on compressor blades, carried out on Microtron 654.				

6.5 Fatigue test on a Canopy

On a high altitude flight of a VENOM AC the cockpit canopy had burst without any sign of an outer cause. Thus fatigue was supposed, and therefore we got an order to test the canopy.

In the first test we pulsed the canopy, which is put on an old fuselage, by pressure only. Minimum pressure difference 0, Maximum pressure difference 0,210 kp/cm² (3 psi), e.g. same as in a AC. Pressure was given by air.

To minimize the burst effect the cockpit was filled with plastic foam blocks up to about 90%.

After 20'000 cycles of this single amplitude fatigue test no failure occurred. This represents 20'000 altitude flights or 60'000 flights in all. Thus we decided to repeat the test but including the other main parameter, the temperature change. To simulate all conditions as good as possible the test is made in the high altitude test chamber of the research department, in which we can simulate simultaneously

air pressure outside the cockpit

air temperature outside the cockpit

air speed outside the cockpit

air pressure inside the cockpit

air temperature inside the cockpit

The full program is represented on Fig. 22. The ratio of high altitude flights to low altitude flights (< 5000 m or 15'000 ft) is about 1 : 3, this is considered in the outlined manner. The frequency must not be faster, as otherwise the Skin-temperature would not follow.

Fig. 23 gives an idea of the test installation. The test is still running, up to now we have 600 complete periods without failure.

6.6 ICAF-Rod fatigue tests

The so called ICAF - test rod, which we mentioned the first time in Rome [4] is represented in Fig. 24. The characteristic data of the tested materials are presented in the following

table 6

Property	Unit	SNV-L Spec. 755.6 (design)	D 2, D 11, D 20 (actual)	VENOM Wing spar booms Group 2 (actual)
Tensile strength	kp/mm2 p.s.i. t.s.i.	Min. 60 85000 38	60,8 to 67.1	66,0 to 66.5
0.2 Yield strength	kp/mm2 p.s.i. t.s.i.	Min. 52 74000 33	54.6 to 62.3	61.0 to 62.4
Composition	Zn Mg Cu Mn Cr Fe Si Ti Al	5,5 - 7,0 2,0 - 3,0 1,0 - 2,5 0,2 - 1,0 0,1 - 0,4 0,6 0,6 0,3 rest	6,30 2,30 1,60 0,30 0,15 0,20 0,20 0,05 rest	6.15 2.20 1.65 0.18 0.15 0.15 0.15 > 0.05 rest
Ultimate Load	kp lb	10135 (22300)	12700 (28000)	12280 (27000)
Limit Load of test rod	kp lb	6757 (14900)		

Corresponding specifications: USA 75 S, UK DTD 5074, France A-Z6 GU
Germany 3.4364

6.6.1 The 36 ICAF-testrods on the twin-chain test rig mentioned at the Rome-Conference are still running, parallel to the VENOM test on the History Simulator, e.g. with VENOM program I/100. They had fulfilled in March (1967) 120 periods without failure. The last findings of the damage indicator (Fig. 8) of the involved holes are indicated in table 7.

Table 7

Group	Material Spec.	No. of all holes	Finding at No. of periods	% of holes with:		
				almost no damage	evident damage	visible crack
0	755.6	12	90	67	33	
			115	33	59	8
			120	25	67	8
1	755.6	14	90	43	57	
			115	29	57	14
			120	22	64	14
2	755.6	14	90	22	78	
			115		50	50
			120		50	50
3	C 77 S	12	90	50	50	
			115	33	42	25
			120	8	67	25
4	DTD 363	8	90	12	88	
			115		88	12
			120		88	12
5	DTD 363	12	90	42	58	
			115	33	67	
			120	25	75	

The specimen of group 5 seem to have the longest life, while in group 2 probably the first failures will occur.

6.6.2 The new 6-specimen fatigue test bed began its work by testing different unnotched test rods, mainly to enable us to find and to eliminate the weak points of the new machine. The tests itself are not interesting here as they confirmed solely known facts.

For the testing of the ICAF-test rod Fig. 24 on the new machine a comprehensive plan was set up to run the history programs outlined in section 4 of this review.

In all VENOM programs one period represents 350 flights or 200 flying hours. The highest peak load (tension) occurs once in one period. It is coded A4 in table 2. In program I (see paragraph 6.6.1 before) the ICAF - rod gets a load of +5265 kp (tension), when the AC is loaded to its design limit load on the History Simulator. Point A4 is used as criterion of the load level of a program (all other levels being always proportional to it). We call the level at the limit load "100" (%), thus a program is called I/100, II/100. a.s.o. if A4 is getting +5265 kp.

Station B of Fig. 7 (which is represented by the ICAF-test rod on the twin-chain test rig) suffers the lowest peak load, compression, in case X5 (table 2), which is a ground case happening during take-off runs at full fuel weight 59 times in one period of 350 flights. In a program I/100 (or II/100) the test rod gets a compression load of -1600 kp. in case X5. The ratio between the lowest and the highest peak load at station B of Fig. 7 (Undercarriage attachment to the wing and wing spar-boom-kink) in the VENOM-programs is thus

$$R = \frac{-1600}{+5265} = -0,3$$

This same ratio was chosen for the single amplitude program VIII, as well as for the twin-block program XI. Thus the program VIII/100 could be interpreted as a

most simplified program II/100.

The following reasoning was leading for the construction of program XI: In one period of the history program II there are 397 Zero-crossings, 350 of them originating from the 350 flights, e.g. from the ground to air cycles, and 47 from negative accelerations in the air. In the same time, e.g. in one period, there are 20'208 quasi-cycles on the airborne AC and 18'690 quasi-cycles on groundtaxying, or
 $20'208 - 47 = 20'161$ tension fluctuations and
 $18'690 + 47 = 18'737$ compression fluctuations.

The ratio of fluctuations to Zero-crossings is thus

$$\frac{20'161}{397} = 53 \quad \text{and} \quad \frac{18'737}{397} = 47$$

respectively, the average value being about 50 : 1. Fifty fluctuations happen after each Zero-crossing, alternating on the positive and the negative loadside. In program XI the ratio between both sides was chosen to $R = -0,3$, permitting comparisons with program VIII. Additionally we found by chance, as mentioned in the note of paragraph 5.1, that program XI is a help for distinction between crack indication and disorder indication. The comparison of program VIII and XI is represented in Fig. 25. The difference of the life-time is 1 : 2,3. It proves that it is not allowed to shift two opposite fluctuation cycles together and to form one alternating cycle with them. The demolition of this assumption which was widely accepted will have important consequences although the result was on the conservative side.

Program XIII/100 is the same as XI/100, but the minimum load is -657 kp (instead of -1600 kp) with $R = -0,125$ (instead of -0,3), what is representativ for a station near A in Fig. 7 (instead of station B), e.g. for a part located inside of the main under-carriage. The maximum load is +5265 kp (same as for program XI/100). The specimen of program XIII/100 had a life 1,4 times longer than those of program XI/100.

Table 8 gives a survey of the single amplitude and block-program tests, table 9 of the history fatigue tests, all run on the new 6-specimen fatigue test machine (see paragraph 3.5), all with the so-called ICAF-test rod Fig. 24, and all manufactured from "Perunal 755.6" bars (similar to 75 S or DTD 5074), from which also the VENOM wing spar booms and the 36 rods on the twin-chain test bed are manufactured, see table 7.

Glossary of terms used in table 8 and 9
(see also annex 3, scheme of History loading):

a	=	Number of specimen tested by the same program
N _i	=	Number of cycles or periods to failure of rod i
\bar{N}	=	$\frac{\sum N_i}{a}$ = mean value of Number N _i to failure
e _i	=	$\bar{N} - N_i$ = deviation to mean value
\bar{e}	=	$\sqrt{\frac{\sum e_i^2}{a}}$ = root mean square of deviations
\bar{e}_r	=	$\frac{\bar{e}}{\bar{N}} \cdot 100$ = "relative scatter" (%) *
L _u	=	Upper Load in a single amplitude test
L _L	=	Lower Load in a single amplitude test
L _q	=	Highest peak load in one period q
L _d	=	Lowest peak load in one period q

* The relative scatter is the root mean square of deviations related to the mean value of numbers to failure, given in percent.

Table 8

test run number	1	2	3	4	7	5a	5b	6	12	11
program number	VIII/152	VIII/132	VIII/115	VIII/100	VIII/100	VIII/87	VIII/87	VIII/100	XI/100	XIII/100
axial load	+ 8000	+ 6959	+ 6053	+ 5265	+ 5265	+ 4580	+ 4600	+ 5265	+ 5265	+ 5265
	- 2420	- 2115	- 1840	- 1600	- 1600	- 1385	- 1400	- 1600	- 1600	- 657
frequency, cpm	180	180	180	180	210	180	125	180	210	210
number of specimen a	6	6	6	6	5	6	6	6	6	6
specimen number	D 41-46	D 55-60	D 61-66	D 67-72	D 73-78	D 35-40	D 47-52	D 29-34	D 17-22	D 23-28
anodised, thickness in μ	6	6	6	6	6/20 ¹⁾	20	20	20	20	20
cycles to failure	N 1	1085	1800	5508	2868	9109	6800	5638	28407	34835
	N 2	661	1649	5307	3267	8777	9000	6202	22309	39143
	N 3	689	1688	5601	3247	9239	9000	4954	28207	42140
	N 4	689	1812	5383	2)	7931	8900	5608	27242	37527
	N 5	623	1440	3934	2744	8050	8200	6173	26531	39201
	N 6	677	1449	5530	2715	8432	7400	6172	29038	33110
$\bar{N} = \frac{\sum N_i}{a}$	655,5	1126	1640	5210	2968	8590	8217	5791	26956	37659
$\bar{e}_T = \frac{\bar{e}}{\bar{N}} \cdot 100 (\%)$	5,42	3,6	9,1	11,1	8,1	5,8	10,4	7,8	8,3	7,9

1) anodised - de-anodised - re-anodised

2) corrosion by surface treatment

3) run on Amsler 15 T-Pulsator by EMPA

Table 9

test run No.	15	17	16	10	14	13	9	20	19	21
history program No.	II/127	II/109	II/102	II/100	III/100	III'/100	VI/100	XIV/102	XV/102	XVI/102
No of orders in one period	air pos.	39428	39428	39428	38468	38468	988	17722	17722	39428
	air neg.	638	638	638	638	638	638	638	638	638
	ground	37029	37029	37029	37029	37029	350	6811	37029	6811
axial loads	L _q kp	+ 6700	+ 5740	+ 5370	+ 5265	+ 5265	+ 5265	+ 5370	+ 5370	+ 5370
	L _d kp	- 2032	- 1744	- 1632	- 1600	- 1600 (1x - 3000)	- 1600	- 1632	- 1632	- 1632
frequency, cpm	240	240	240	240	240	240	240	240	240	240
number of specimen a	6	6	6	6	6	5	6			
specimen number	D 103-108	D 121-126	D 109-114	D 91-96	D 115-120	D 97-102	D 85-90	D 139-144	D 133-138	D 145-150
periods q to failure	N 1	18,418	32,840	76,405	61,197	58,353	131,272	77,837	68,044	67,727
	N 2	19,149	43,077	83,023	103,5 ²⁾	59,989	157,753	92,866	82,726	79,235
	N 3	17,320	25,320	83,999	87,354	62,962	269,416	80,503	81,930	68,609
	N 4	14,951	39,042	97,404 ¹⁾	103,215	(38,932) ³⁾	188,844	65,134	45,335	59,258
	N 5	18,935	31,751	86,212	78,843	54,874	166,018	60,989	68,836	47,410
	N 6	20,839	41,750	93,317 ¹⁾	63,826	58,551	120,302	76,797	97,266	76,779
$\bar{N} = \frac{\sum N}{6}$	18,352	35,630	86,227	91,254	71,847	58,946	167,268	75,688	74,023	66,503
$\bar{e}_r = \frac{\bar{e}}{\bar{N}} \cdot 100 (\%)$	9,7	17,5	8,0	18,8	25,0	4,4	29,0	13,8	21,8	16,1

All specimen mentioned on table 9 were
anodised to a thickness of 6μ

- 1) failure of lug (fretting) - D 112 and D 114
2) stopped at 102 periods, failure point estimated (D 116)
3) failed by buckling at -3000 kp; not considered for \bar{N}

Test run 5 b, compared with 4 and 6, demonstrates the unfavourable effect of de-anodising, halving the life.

Test 5b was run by EMPA on AMSLER Vibrophore to compare these two completely different test machines. If the small load differences in run 5a are taken in account the two mean values (of the 6 specimen on each test bed) coincide very well. The scatter on the new facility is smaller, which was expected.

The influence of the thickness of the anodised layer is contrary as expected, see test 4 and 6.

Probably this ostensible discrepancy will be explicated later on by the different manufacturing methods.

The relative scatter figures \bar{e}_r are rather small for all 10 test runs of table 8, 3,6 to 11,1 %.

Opposite to that the scatter of the 7 fatigue history tests on table 9 ist very different, \bar{e}_r having values from 4,4 up to 29 %.

Obviously it is not admissible to simplify program II by applying the mean-crossing peak count method [7], where the mean value is the 0 g - level, because the resulting program VI almost doubled the life (run 10 and 9).

In test run 13, after 38.932 periods a ground load of -3000 kp was applied, representing a 3 g touch down with full fuel weight, as it may happen in an emergency landing just after take-off. One rod failed by buckling at this load. The other five were run up to fatigue failure. Their life was reduced to 82% of value of test run 14, where this single load was not applied.

Test run 19 with program XV/102 (all increments of $\pm 0,5$ g from the $+1,0$ g level in air loads omitted) shows a shorter life than the corresponding test run 16 with the full fatigue history program II/102. Already test run 18 seemed to point to this phenomenon, but was not considered because there was a program failure on the beginning of the run. Now, test run 20 with program XIV/102 (all increments of $\pm 0,5$ g from the $+1,0$ g level in air and all increments of $0,3$ from the $1,0$ g level on ground omitted) which was terminated the 6th May confirms this trend. Test run 21 with program XVI/102 shall tell us if omitting the small tension deviations (XV), or omitting the small compression deviations (XVI) or both are responsible for this very interesting phenomenon. Those of my colleagues which were at the Rome meeting 4 years ago may remember that I told a funny idea: What, if material recreates itself, e.g. by small load fluctuations as nature recreates itself in Spring ?! As a result of our increased knowledge of fatigue since, today I would compare this effect to a good afternoon nap, - quite relaxing for all the strains accumulated during forenoon.

To explain this phenomenon I would like to present the views of our metallurgist who works with us within the framework of an exchange program with Columbia University.

It is generally believed that fatigue damage is caused by the concentration and accumulation of irreversible displacements. At very low amplitudes the deformation is reversible and dispersed: Failure does not occur. Using the nomenclature of Wood [12], in the F range (Fatigue range) of an S/N curve, that range which tends to parallelism with the N axis, deformation concentrates in the slip planes which later open up to fissures, and this is where damage occurs. In the H range (Hardening) of the S/N curve, the range which descends rapidly towards the N axis, subgrains develop, the deformation and damage concentrating in subgrain and grain boundaries, where later cracking occurs.

The size of the subgrains decreases with the number of elapsed strain cycles and as hardening saturates after prolonged cycling, it reaches a limiting size [13]. This limiting subgrainsize depends on amplitude, the larger the amplitude the smaller the subgrainsize, reaching a limiting size with respect to amplitude too [14]. It had been recently found that the subgrainsize would adjust to the saturation stress even if the saturation stress was changed during the test in fatigue [15].

As fatigue damage was believed to be due to the abnormal concentration of deformation in slip planes, subgrain and grain boundaries, there had been attempts to disperse fatigue deformation and thus increase fatigue life. Successful attempts of Wood used a few initial large amplitudes [16] or a few cycles at elevated temperature [17] in order to avoid concentration of deformation in slip bands at the subsequent F range cycling. While these attempts use one kind of single amplitude cycling followed by an other kind of single amplitude cycling, it seems that a history program would provide a still better possibility to disperse fatigue deformation.

While under single amplitude cycling the material hardens, slip concentrates or a limiting subgrainsize develops with maximum misorientation, later in course of cycling after the structure reached a steady, cyclic state, the material has no other means to find relief from accumulating infinitesimal irreversibilities, but cracking.

Under conditions of history program loading with the amplitude continuously changing it is very likely that no well defined cellstructure can develop, but the substructure is in a continuous change thus more able to adjust to accumulating microstrains.

A good proof of the lesser extent of precracking damage under history program versus single amplitude cycling is that the conductivity hardly increases in this range during history program and the ratio of precrack life to crack propagation life is 10/1, versus 1/3, of the single amplitude cycling.

We intend to do mechanical hysteresis loops to investigate the hardening and/or softening under history program loading also to investigate the substructure that develops due to history program loading by means of electronmicroscopy.

It is possible that no well defined subgrains nor slip bands can develop and the substructure may resemble that produced by cycling under the endurance limit.

As single amplitude cycling produces a certain trend of damage in the material while history program loading most likely means a continuous change, a redoing of what former cycles caused, intuitively a greater scatter of precrack life is expected under history program, the precrack life itself being much longer. It would be quite important to do some separate crack propagation tests under history program cycling. As our tests indicate the crack propagation stage is shorter under history program than at single amplitude cycling, this stage showing very little scatter, most of the scatter originating in the precracking stage.

All these relief mechanisms, the continuous change of the structure of the material, or better to say the prevention of the concentration of deformation and damage into certain zones, the prevention of the development of a fatigue structure are the intuitively felt beneficial effects of history program cycling against single amplitude cycling in general.

To turn to the beneficial effect of some period of low amplitude cycling (taxying) within a history program one should mention that Weissmann [18] increased single amplitude fatigue life by inserting a period of lower amplitude cycling. He found an increase in cell size well defined cell walls and a decreased dislocation density in the interior of the subgrains resulting from the lower amplitude cycling. This recovery of substructure due to cycling with lowered strain amplitude is attributed to a mechanism involving dislocation climb, made possible by the increased vacancy generation and decreased dislocation generation and multiplication during low amplitude cycling.

How this applies to history program loading further research must show, but the increase of conductivity during a period of low amplitude cycling within the history program implies a recovery of structure and stress relief.

Rod D 112 which failed at 97.404 periods by lug failure (obviously due to fretting), was tested to its residual ultimate load. This was 10'900 kp, still higher than the design ultimate load, and compared with the actual ultimate load of rod D 112 (non fatigued) of 12'000 kp not very much lower, standing still 91%. But the fracture differs substantially: It is brittle instead of ductile as on new specimen. Fig. 26 shows the two diagrams of the ultimate load test. Even more significant is the aspect of the two fracture surfaces.

A similar difference exists between fractures of fatigue tests of the low and the high cycling mode. Fig. 27 shows in "a" specimen D 42, tested at run 1, e.g. by a low cycling mode, which failed in a ductile manner, whereas specimen D 95 in "c", tested at run 10, e.g. by history loading, failed in quite a brittle manner. D 69 in "b" (test 4) shows a transition between "a" and "c".

These very different aspects of fracture point to that Miner-Palmgrens hypothesis doesn't have any base in metallurgy.

The test runs of the 6-specimen fatigue test machine are surveied at any time by an oscilloscope screen and by continuous records. Fig. 28 gives an enlarged view of program VIII and a survey of the block program XI, Fig. 29 a survey of program III, some short flights (in the sense of fatigue) and the begin of a flight in gusty weather. Please note the ground loads before and after refueling; the third short flight was without refueling. On Fig. 29 the upper trace is the strain gage record, the lower trace the recording of the damage indicator. Same in Fig. 30, but extended.

Fig. 31 represents the whole damage story of specimen D 18, loaded by program XI (twin blocks), recorded by the damage indicator. All 223 block-pairs are visible. During pair number 224 at cycle number 9 (tension) the failure occurred. On the left side of the picture the upper hole was indicated. Then, as a first crack appeared on the lower hole of the rod, the indicator was moved to this one. Note the play in the plotter mechanism on the left side, the gap due to the first crack on your right and the disorder damage indicated by the increasing limits.

Fig. 32 finally represents the end of the life of specimen D 99. From the left bord of the picture to the right one, where the failure occurred, are the last 48'656 cycles recorded by the damage indicator. 50 mm from the left bord is a small interruption: That is the automatic resetting of the spool with its tape (which has a length of 196 Meter or 644 ft). Then the last period begins, number 63: Failure occurred at 0.9624 of the period length. Each flight is visible (there are 391), that's the reason for the irregular aspect, besides the disturbance produced by the fatigue damage.

Although the 6-specimen fatigue test machine can be run up to a frequency of 300 cpm, this had to be reduced to the frequencies given in table 8 and 9, since at higher frequencies the specimen would be warmed slowly.

7. Service Experiences

Observations of fatigue damages on service aircraft are now so numerous that we intend to prepare a special report as a base for reliability considerations, although it is not a scientific reason why we are surveying these damages:

Our establishment is responsible for advertising the maintenance people in time on fatigue risks. Thus safety considerations are forcing us. It is our chance or our pain (as you wish) that a big portion of our air force consists of VENOM A.C. which is designed almost entirely with DTD 687 (similar to 75 S), e.g. the light alloy which is rather ill reputed for fatigue safety.

Thus, our task is an interesting one for research in fatigue, but less nice in relation to the responsibility for safety.

May I outline shortly our to-day's guidelines for the setting up of instructions to our maintenance people of aircraft in service:

1. Fatigue damage is beginning by the very first loadings, although there is nothing to see.
2. Once a fatigue crack is appearing so much damage has already happened that it can not be stopped definitively by holes or reinforcements (if it was really a fatigue crack).
3. The part involved has to be replaced or bridged over or, if that is not possible, its admissible life has to be restricted to an amount which considers the rate of crack propagation. This part has to be inspected at corresponding short intervals on the whole fleet.

8. Conclusions

Some work has been done in the field of the ICAF research recommendations No. 1, 2, 3, 4 and 7, which were stated following the Munich closed technical meeting 1965.

More than ever we are convinced that the Miner-Palmgren hypothesis is not applicable in aeronautical fatigue.

More, we think that the hypothesis is dangerous for aircraft designers and airworthiness authorities, because it serves as an indolent mean for narcotizing their bad conscience.

It's results are worse than an estimate based on experience.

We believe that - except in some special cases - neither single amplitude cycling nor program loading nor random loading are giving the answers to the designer's problems, and that only fatigue history loading will produce reliable results, history loading, which simulates the genuine sequence of the loadings and which does not neglect the smaller load variations, neither in the air nor on the ground.

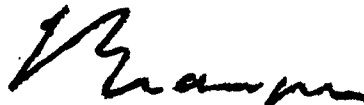
And we think, that the first appearance of a crack is more important than the cycles to failure why more research should be devoted to the pre-crack phase.

And that we should try to find or develop alloys which are good-natured: Which become by this pre-crack phase as little as possible brittle and sensitive to notches in case of very fast loading rates.

9. Future Research

- 9.1 Gust investigation (continuation)
- 9.2 Flight load statistics (continuation)
- 9.3 Full-scale fatigue test VENOM (termination) and prepare the MIRAGE test.
- 9.4 Fatigue test of PORTER strut attachment.
- 9.5 Fatigue history loading on the 6-specimen test bed: Light alloys and high strength steels.
- 9.6 Damage indicator, further development; search for an automatic crack announcer.
- 9.7 x-raying service aircraft.
- 9.8 Publications: The VENOM program; the VENOM test; Fatigue damage on service AC.

FABRIQUE FEDERALE D'AVIONS
Chief designer:



10. REFERENCES

- | | | | |
|------|---|----------------------------|---|
| [1] | F+W FO-782 | GIROD, | Böenuntersuchung-Auswertung von Flugmessungen, 1965 (not yet published) |
| [2] | F+W S-194 | WEIBEL, | Undercarriage Loadings of Three Aircraft: PORTER PC-6, VENOM DH-112 and MIRAGE III S |
| [3] | Schweizer Archiv,
No.8,
August 1966 | ERISMANN, | Allgemeine Entwicklungstendenzen der statischen und dynamischen Prüfmaschinen |
| | do.
(ICAF-Doc. 337) | BRANGER, | Ein Simulator der Ermüdungsgeschichte für Grossobjekte (Fatigue History Simulator F+W) |
| [4] | ICAF-Doc. 271 | VILLA, | Minutes of the eight ICAF-Conference at Rome (Sect. 5), 1963 |
| [5] | Schweizerische Technische Zeitschrift,
No.30, 28.7.66. | RUSSENBERGER, | Neue Entwicklungen auf dem Gebiete elektromechanischer Resonatoren für die Materialprüfung |
| [6] | F+W S-197 | BRANGER, | The VENOM-Program (not yet published) |
| [7] | ICAF-Doc. 178 | SCHIJVE, | The anaysis of random load-time histories with relation to fatigue test and life calculations |
| [8] | ICAF-Doc. 338 | GASSNER, | Minutes of the ninth ICAF-Conference at Munich (Sect.10) 1965 |
| [9] | EMPA 37993 | STEINER, | Pulsation von Sauerstoff-Flaschen 1967 (not published) |
| [10] | EMPA 33194/1+2 | STEINER, | Acht Los-Prüfungsschläuche, 1966 (not published) |
| [11] | EMPA 34516/1 | STAFFELBACH
und FISCHER | Kompressor-Laufschaukeln Stufe 1, 1965 (not published) |

- [12] W.A. WOOD Acta Met Vol. 11 (1963) 643
- [13] J.C. GROSSKREUTZ J.Appl. Physics Vol.34 (1963) 372
- [14] J.C. GROSSKREUTZ Acta Met Vol. 11 (1963) 717
and P. WALDOW
- [15] J.E. PRATT J. Materials Vol. 1 (1966) 77
- [16] W.A. WOOD and Some direct Observations of Cumu-
W.H. REIMANN lative Fatigue Damage in Metals.
Institute for the Study of Fatigue
and Reliability, Columbia University
Technical Report No. 11, Oct. 1964.
- [17] H.D. NINE and On Improvement of Fatigue Life by
W.A. WOOD Dispersal of Cyclic Strain,
Institute for the Study of Fatigue
and Reliability, Columbia University
Technical Report No. 36, July 1966.
- [18] S. WEISSMANN, Transactions of the ASME,
A. Shrier and Vol. 59, (1966) 709
V. GREENHUT

11. FIGURES

- Fig. 1a,b Gust investigation
- Fig. 2 Working principle of the electronically controlled fatigue machine MICROTRON
- Fig. 3 MICROTRON 654 blade fatigue test machine
- Fig. 4 Vibrating blade, exposed over several cycles
- Fig. 5a-d Six-Rod-Fatigue Test Bed for History Loading
- Fig. 6 VENOM Programmata, Schematic Presentation
- Fig. 7 VENOM AC: Ratio of Air-to-Ground - Loads and Ratio between the different Fuel weights
- Fig. 8 Damage Indicator type F+W
- Fig. 9 Damage story of Specimen D 75
- Fig. 10 Damage story of Specimen D 20
- Fig. 11 Conductivity in a cracked hole
- Fig. 12a-d X-ray-television chain (picture amplifier and TV-chain)
- Fig. 13a-d Wing of VENOM AC x-rayed by TV-chain
- Fig. 14a-h Fatigue crack in the butt-joint strap at rib 7 of wing No. 068, at 4750 hours, taken by the X-Ray TV-Chain during history loading.
- Fig. 15 Cracked butt-joint strap at rib 7 of wing No. 166, at 8540 hours.
- Fig. 16 Location of the fatigue cracks
- Fig. 17 Reinforcements of the endangered parts
- Fig. 18a-c O₂ - Bottle
- Fig. 19a,b Boa Supra and Boa Duo
- Fig. 20a,b Fatigue cracks in compressor blades
- Fig. 21a-d Corrosion as initiator of a fatigue crack
- Fig. 22 Canopy fatigue test program

- Fig. 23a-c Canopy fatigue test installation
- Fig. 24 ICAF-test rod
- Fig. 25 Comparison of program VIII to XI
- Fig. 26 Ultimate load diagram of a new and a fatigued test specimen
- Fig. 27a-c Fractures of different fatigue tests
- Fig. 28a,b Program VIII and XI on the oscilloscope screen
- Fig. 29a,b Program III strain-gage and damage indicator on the oscillocop screen, short and long flights
- Fig. 30a,b Same enlarged
- Fig. 31 D 18 damage story
- Fig. 32 The end of D 99 by history loading

12. TABLES

Page:

Table 1	Fatigue spectra of 5 AC	60
Table 2	Basic key to the VENOM-Program	67
Table 3	Specific loads on the VENOM tests	68
Table 4	Flexible metallic hoses	78
Table 5	Compressor blade fatigue tests	81
Table 6	Static properties and composition of test rod material	83
Table 7	Damage survey of 36 test rods	84
Table 8	Single amplitude and block program tests	88
Table 9	History fatigue tests	89

13. ANNEXES

Annex 1	Gust and manoeuvre loads	} VENOM program I or II, represented by the range-mean count method [7], which shall be pub- lished in [6].
Annex 2	Ground loads	
Annex 3	Diagram of ground loads	
Annex 4	Scheme of History Loading	

NOTES to Fig. 1a and 1bMain data:

Date : 16.11.66; 1510 to 1520

AC : VENOM No. J-1712; Pilot: M. Brennwald

Fig. 1 represents the records recorded from 30,5 seconds to 51 sec. after switching on the recorder, e.g. during 20,5 seconds of flight at a flying speed of 520 km/h = 280 kn = 145 m/sec over a distance of 3000 m (10'000 ft), at an altitude of 1400 m (= 4600 ft) above sea level, or 964 m (= 3200 ft) above level of the lake (same point approximatly as described in ICAF-Doc. 216).

Records:

F = strain gage on main undercarriage

S = strain gage on main spar (steel tube crossing the fuselage, station A of Fig.7)

nSP = vertical acceleration of Center of Gravity, in g.

nL' = vertical acceleration at station C, port wing

nL = vertical acceleration at station D, port wing

nR' = vertical acceleration at station C, starboard wing

nR = vertical acceleration at station D, starboard wing

Evaluation by computer:

Δv = vertical component of gust speed in meter per second.

Remarkable peak values of these gusts:

Max. vert.speed upwards (positive) +10,2 m/sec = +33,5 fps

Max. vert.speed downwards (neg.) - 5,0 m/sec = -16,4 fps

Increment of vert.speed: +0,82 m/sec on 1 m distance

-0,64 m/sec on 1 m distance

at $n_{sp} = 3,5$ g (34 m/sec²) the stress in the crossing tube was 32,5 kp/mm² (46'000 psi), while in a steady acceleration of 3,5 g this stress would be 20 kp/mm².

At point 47,7 sec even a stress of 34,0 kp/mm² at only 3,3 g is recorded, what would be 18,9 kp/mm² in steady acceleration, of what a dynamic factor of 1,8 results !

Distance from a +10,2 m/sec gust to a -3,8 m/sec gust = 110 Meter (+33,5 fps to -12,5 fps on 360 ft).

Distance from a +5,5 m/sec to a -5,0 m/sec and to a +4,1 m/sec gust = 110 Meter (+18,1 fps to -16,4 fps to +13,5 fps on 360 ft).

Loading rate: 5,65 kp/mm² per 0,01 sec, or 8000 psi per 0,01 sec.

(a value which is comparable to the loading speed in notch impact tests, which are still about 100 times faster), in steel ($\sigma_{Br} = 120$ kp/mm²)

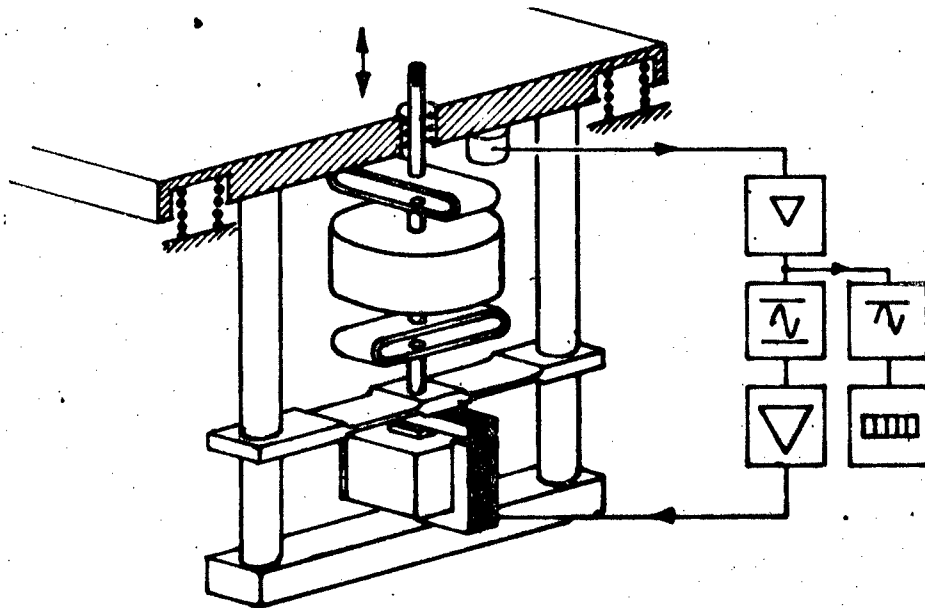


Fig. 2
Working principle of the
electronically controlled
fatigue machine MICROTRON

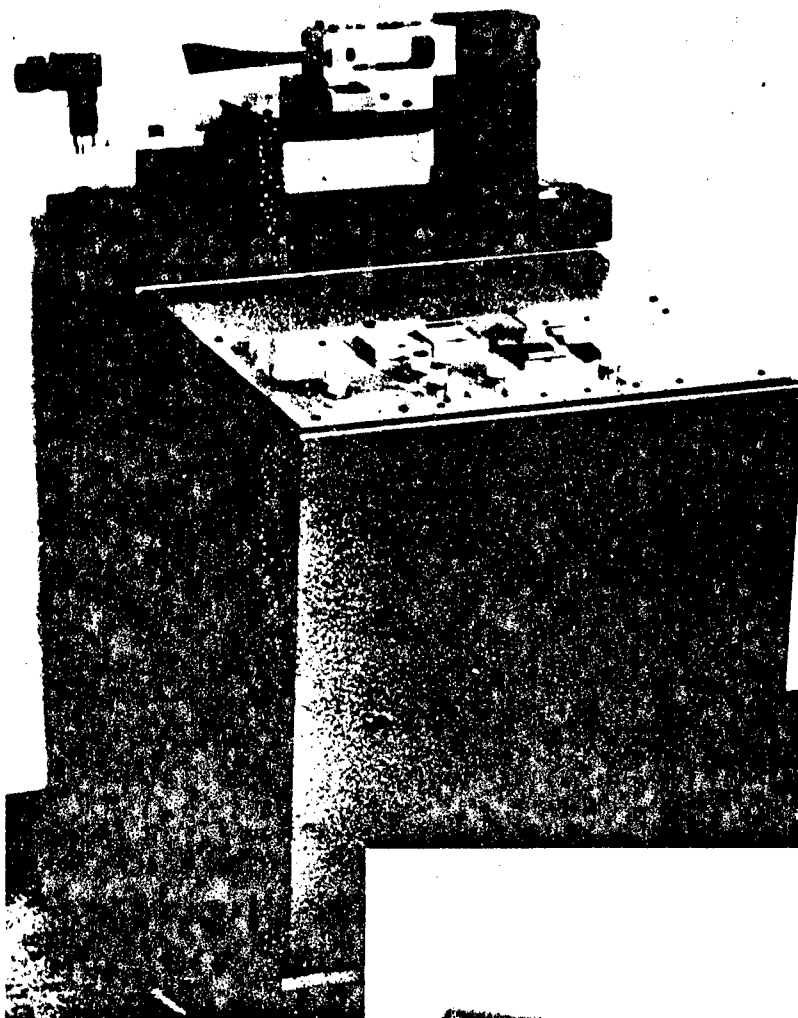
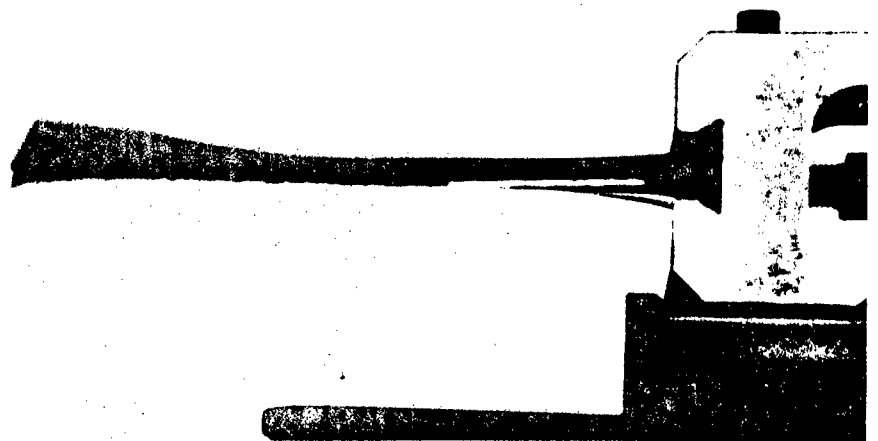


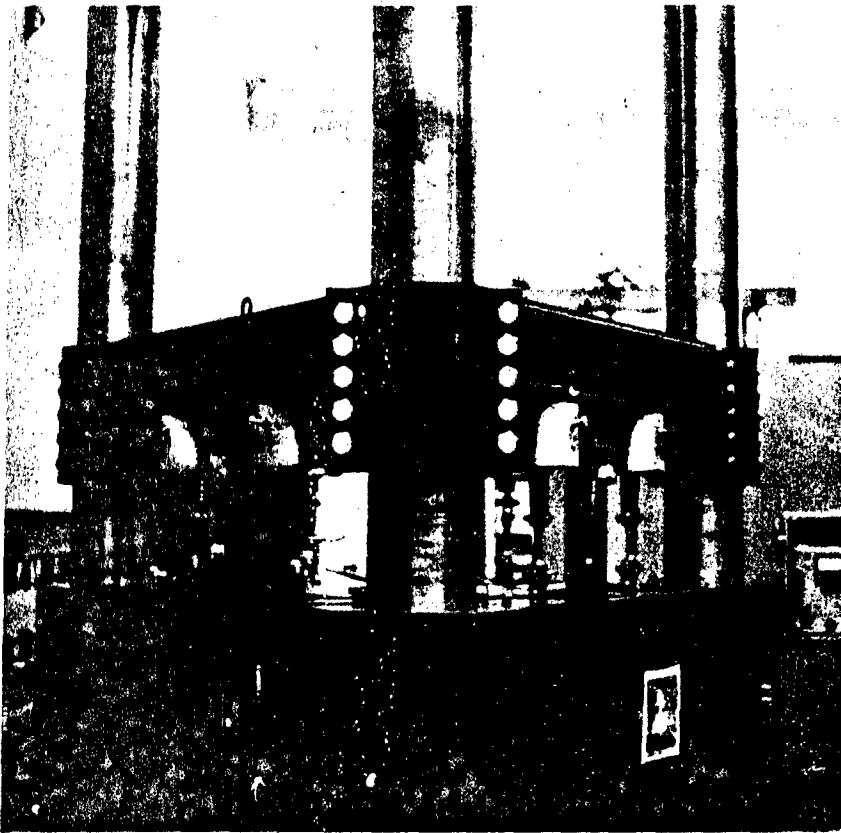
Fig. 3
Microtron 654 blade
fatigue test machine

Fig. 4
Vibrating blade, exposed
over several cycles

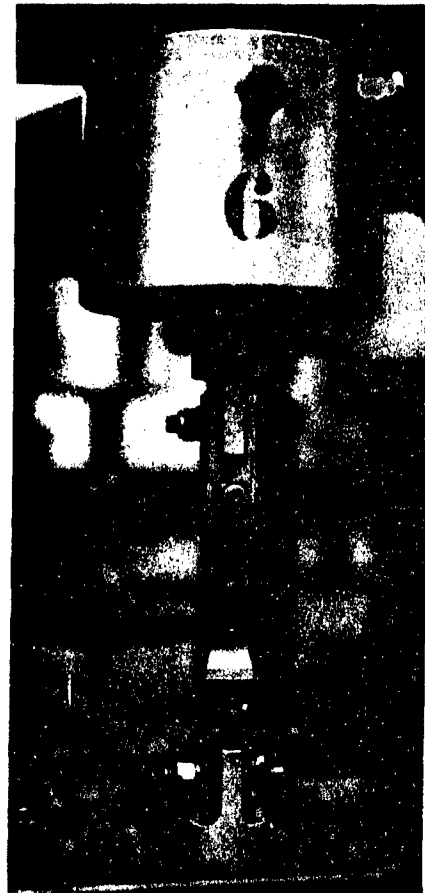


Six - Rod - Fatigue Test Bed for History Loading

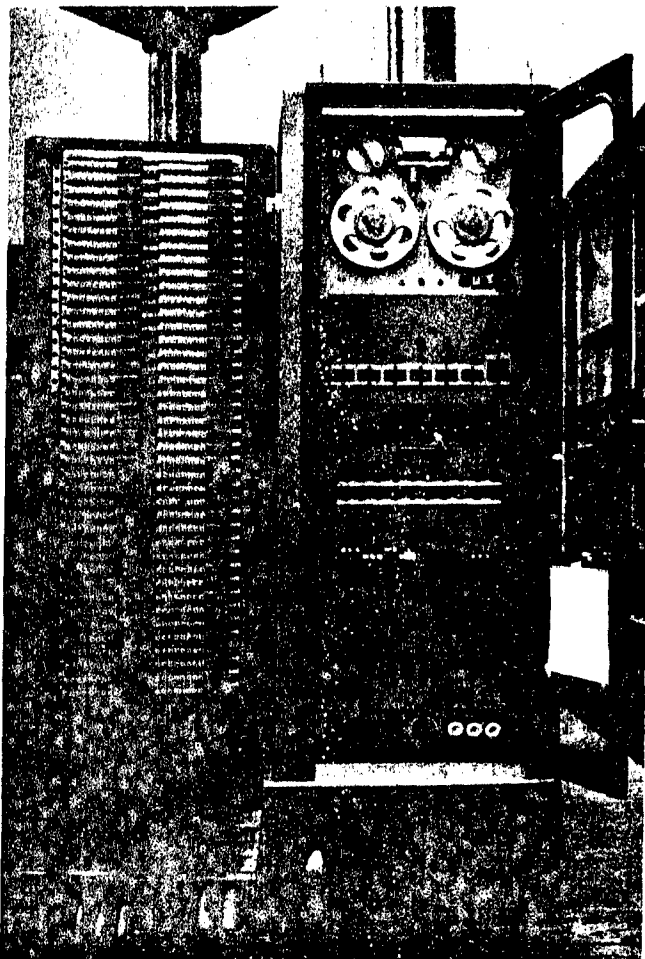
a



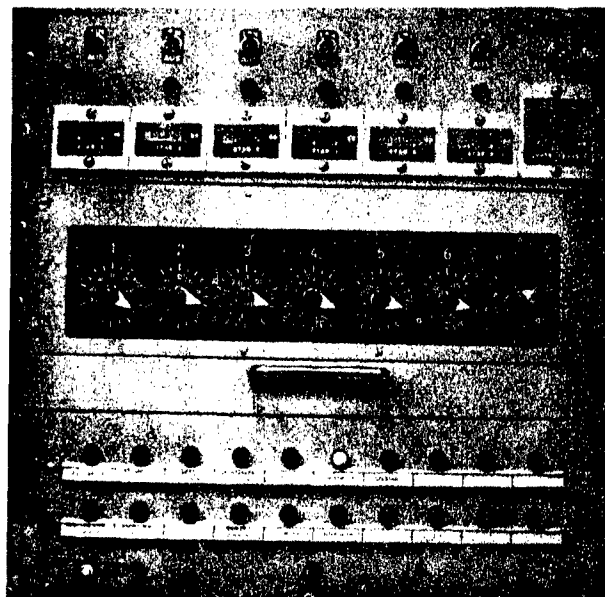
b



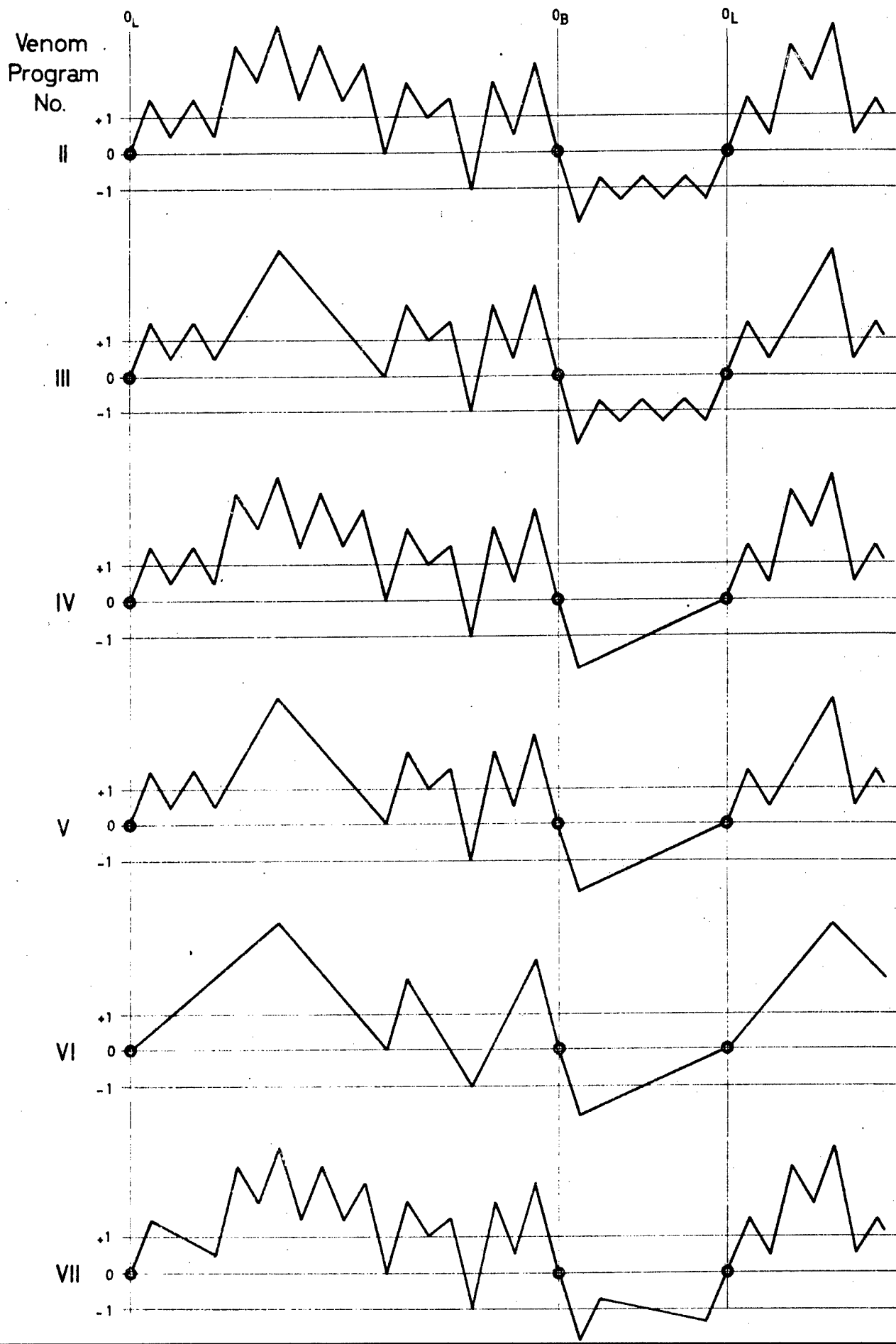
c



d

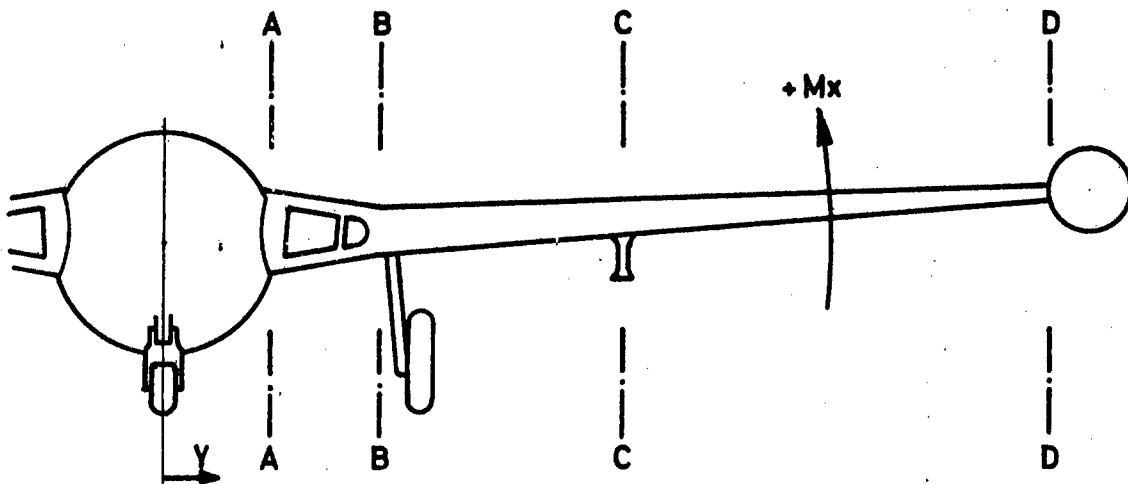


Schematic Presentation of different counting methods



VENOM: Ratio of Air to Ground Loads

Ratio between different Fuel Weights

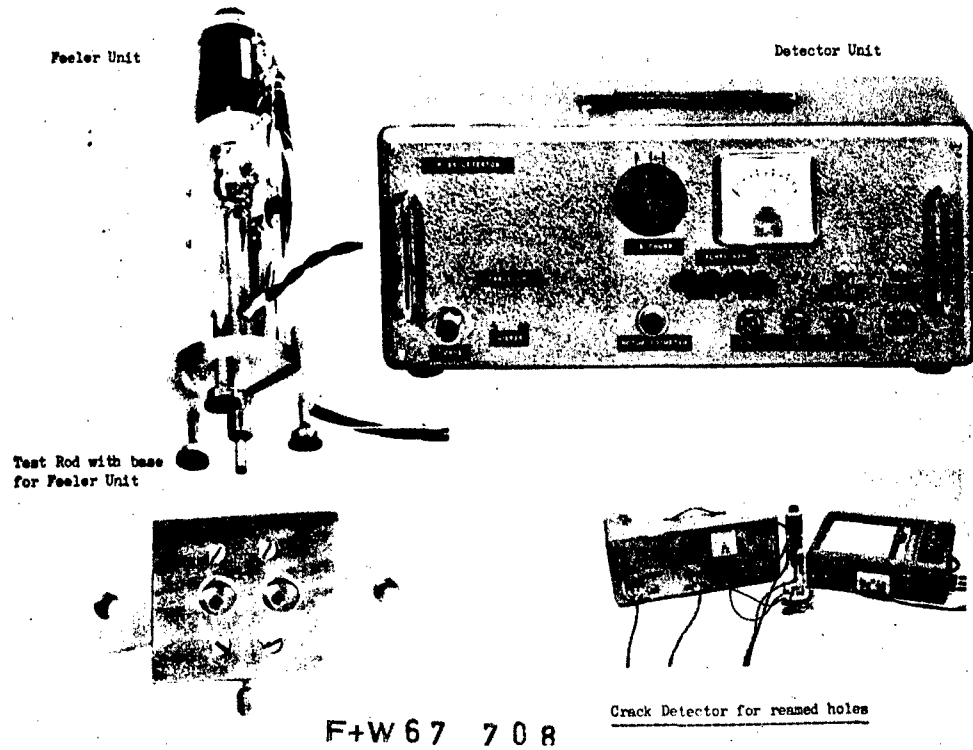


The figures in the table represent the Moment M_x due to air loads at the 1 g - level airborne, which is reduced to 100 (%) for full fuel weight (5/5), and due to the 1 g - level on the ground, all that for different wing stations (A to D), in %.

		Fuel weight				
Wing station	Case	5/5	4/5	3/5	2/5	1/5
A	Air	+100	+118	+134	+127	+123
	Ground	- 16	+ 10	+ 31	+ 31	+ 35
B	Air	+100	+125	+146	+139	+132
	Ground	-132	- 93	- 61	- 55	- 45
C	Air	+100	+189	+263	+247	+227
	Ground	-293	-179	- 89	- 80	- 73
D	Air	-100	- 37	+ 14	+ 12	+ 10
	Ground	-133	- 67	- 15	- 15	- 15

Damage Indicator type F+W

Fig. 8



Conductivity in a cracked hole

Fig. 11.

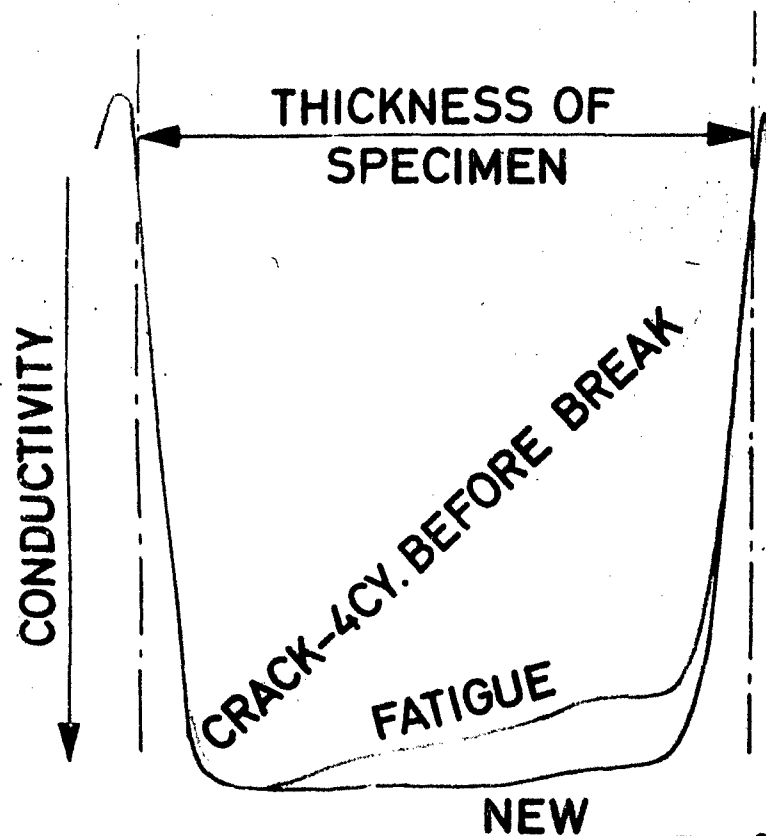


Fig. 9

Fig. 9+10

Damage Story of Specimen Nr. D75
Single Amplitude Loading,
 $R = -0,3$ (VIII/100)

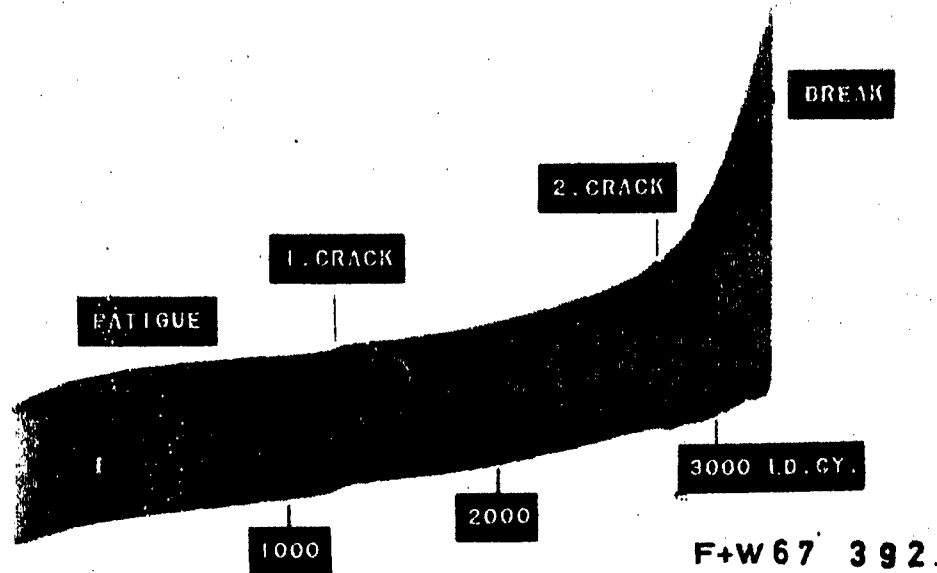
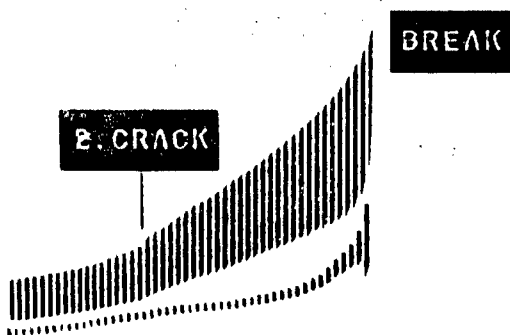
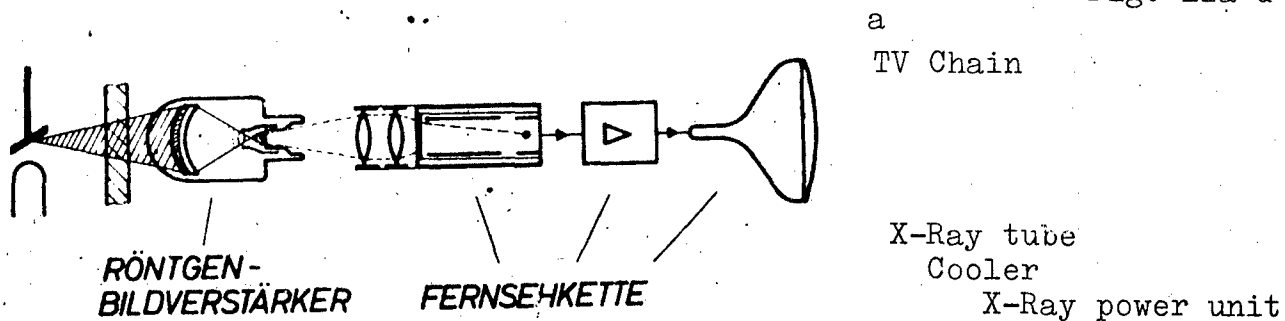


Fig. 10

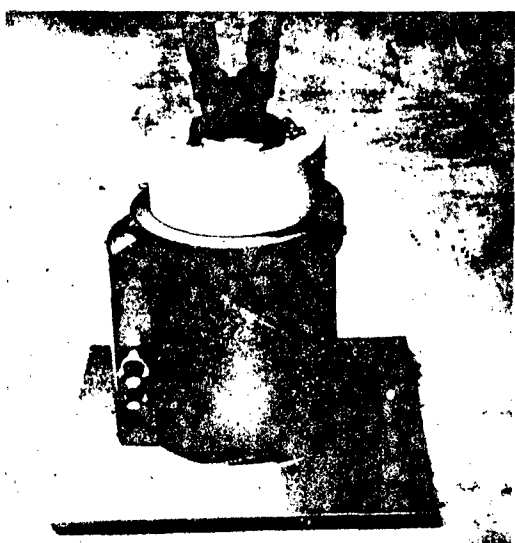
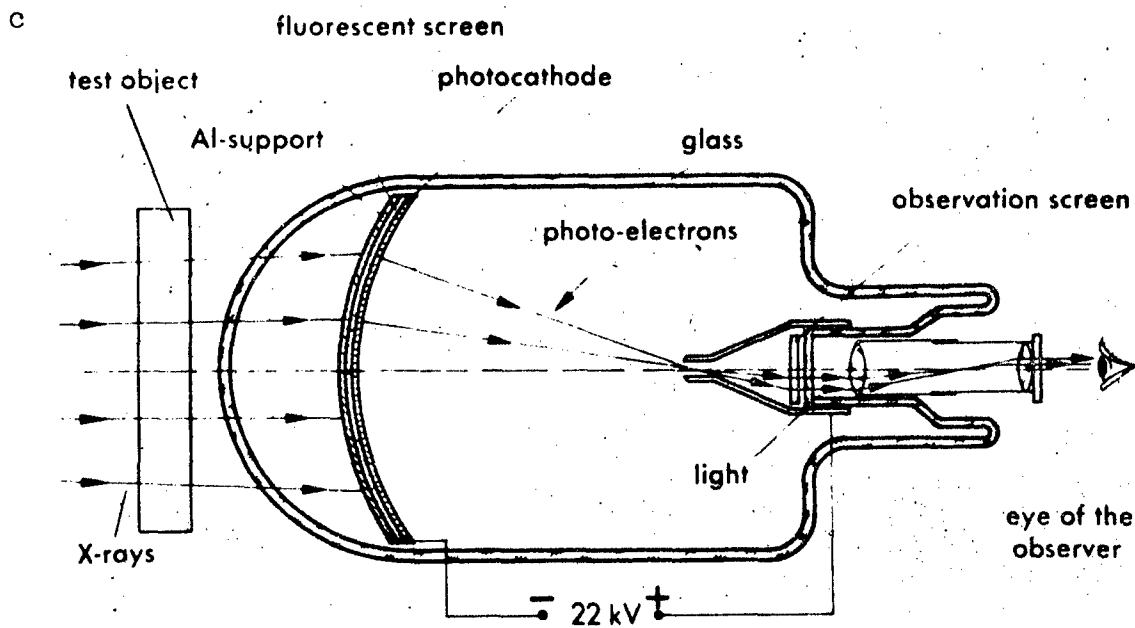
Damage Story of Specimen Nr. D 20
Program Loading, $R = 0/\infty/-0,3$ (XI/100)



F+W 67 391



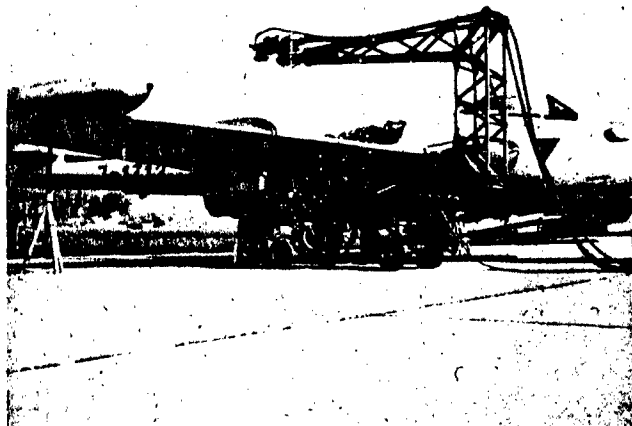
X-Ray Picture amplifier



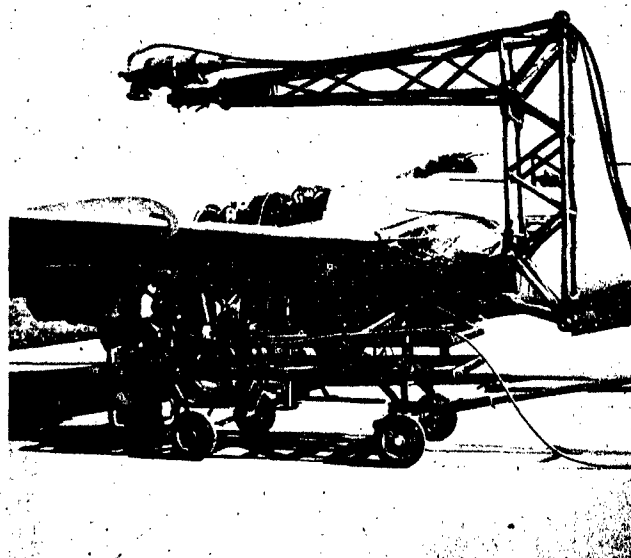
X-Ray picture amplifier:
principle of function

Wing of Venom AC x-rayed by TV-chain

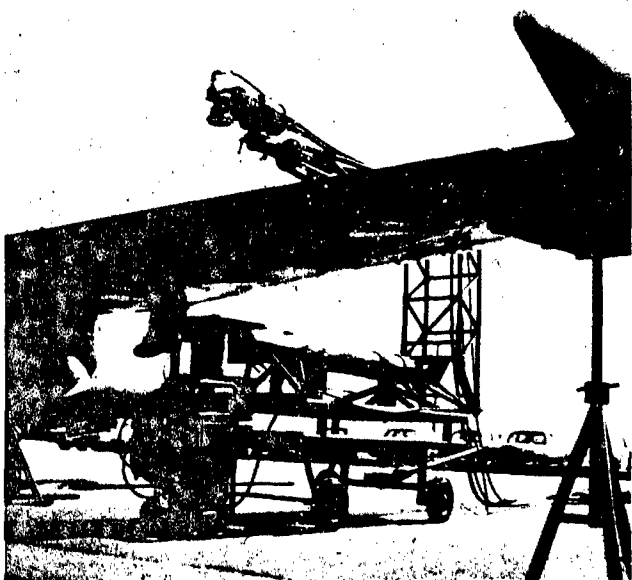
a



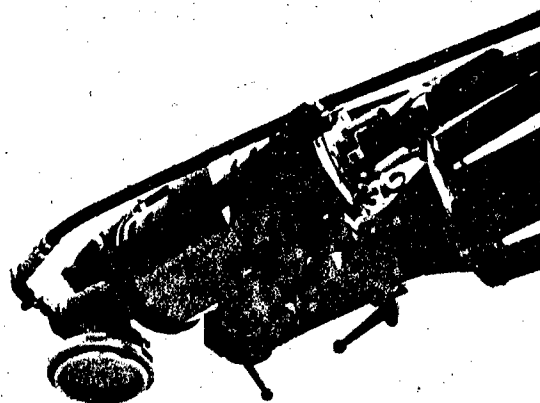
b



c



d

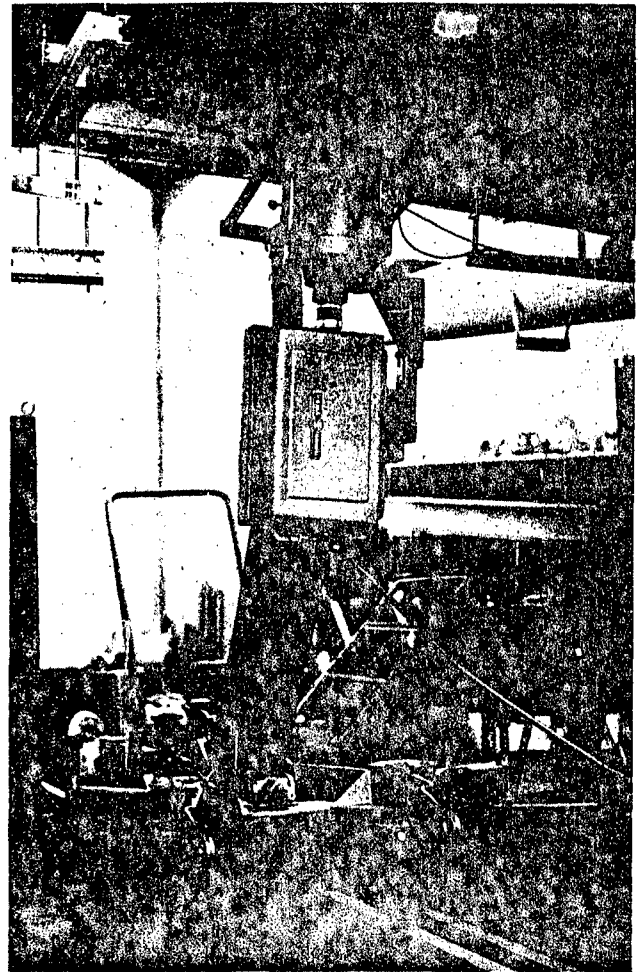


X - ray TV - chain taking a movie film of a fatigue crack during history loading.

a



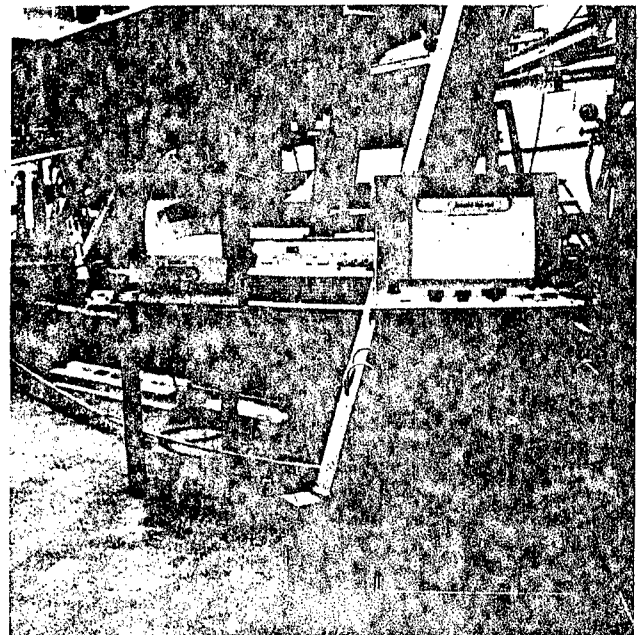
b



c

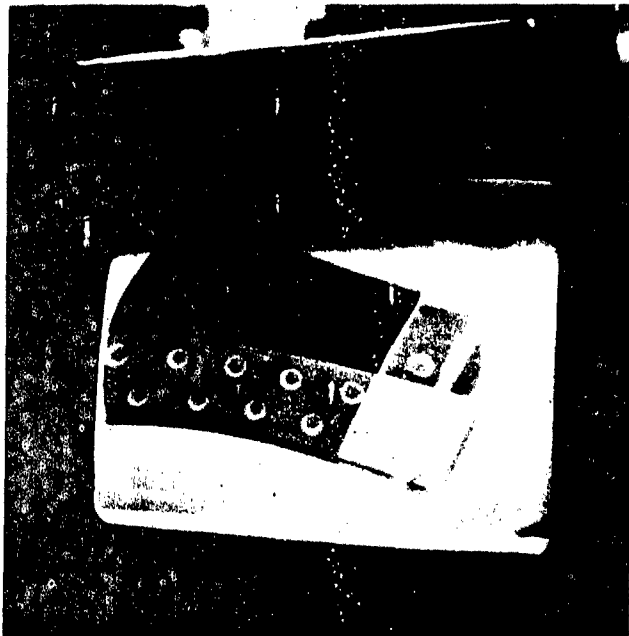


d



fatigue crack in the butt-joint strap at rib 7 of wing Nr.068
at 4750 hours, taken by the X-ray TV-chain during history loading

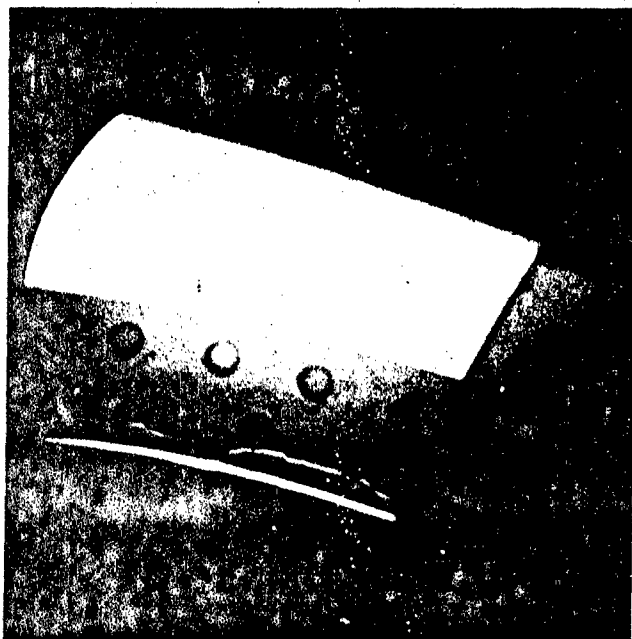
e



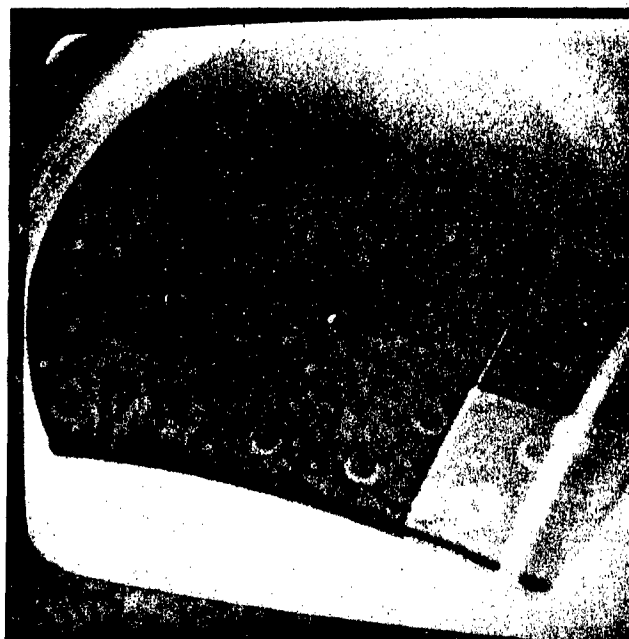
f

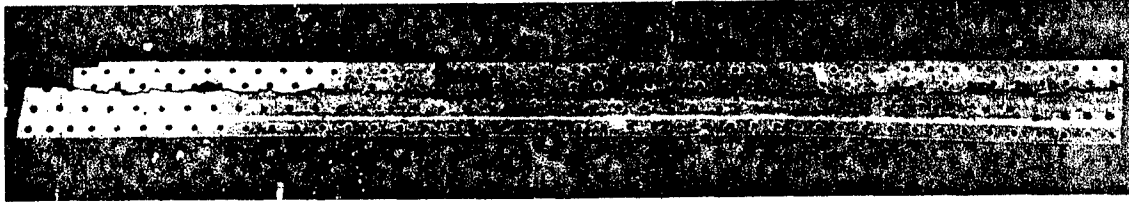


g

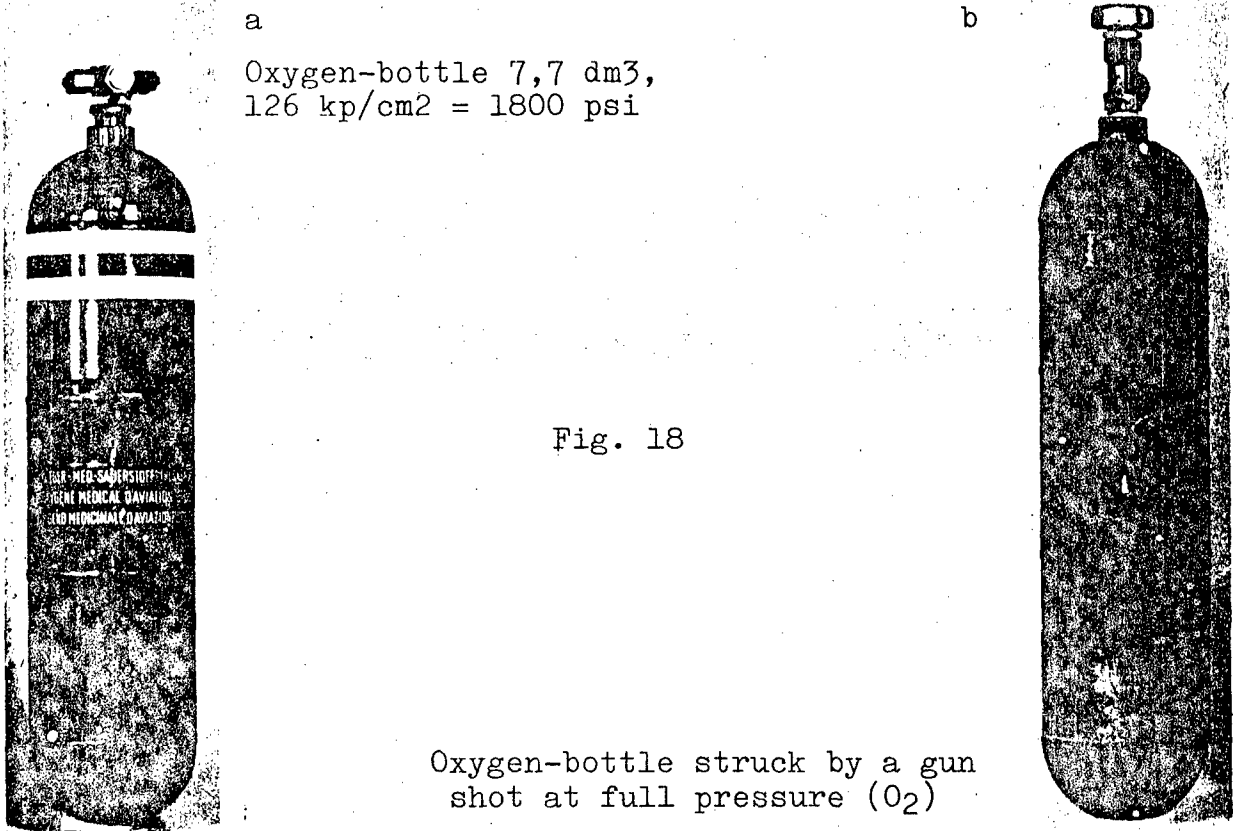


h





Cracked butt - joint strap at rib 7 of wing Nr.166, at 8540 hours



a
Oxygen-bottle 7,7 dm³,
126 kp/cm² = 1800 psi

Fig. 18

Oxygen-bottle struck by a gun
shot at full pressure (O₂)



c

Fatigue - crack of Oxygen-
bottle after 21000 cycles
of full pressure cycling.

Fig. 16

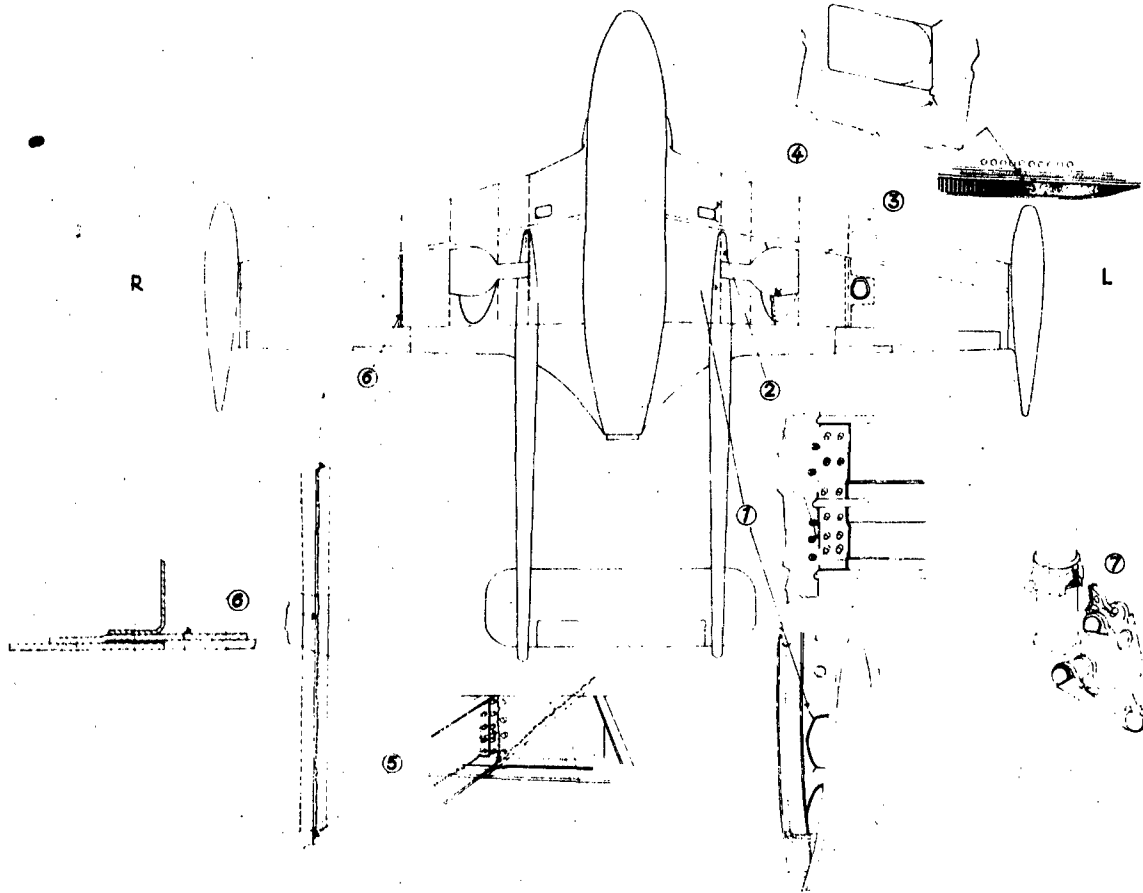


Fig. 17

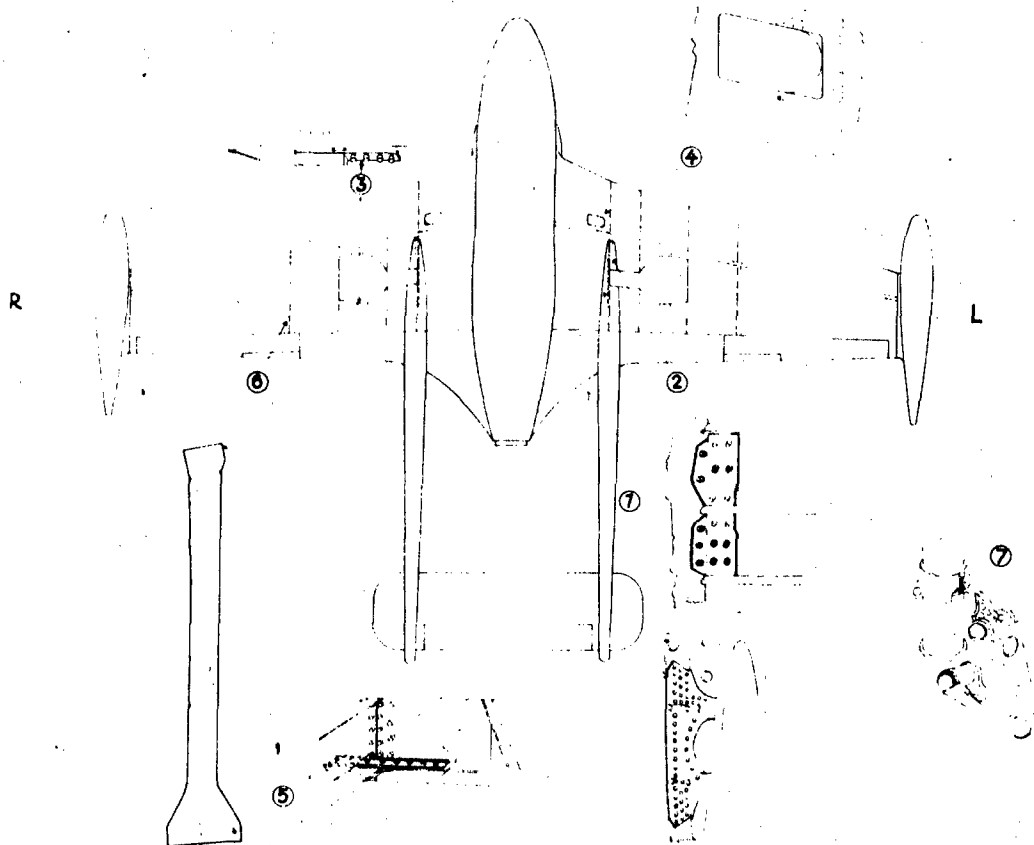


Fig. 19a+b

Fatigue cracks in flexible metallic hoses

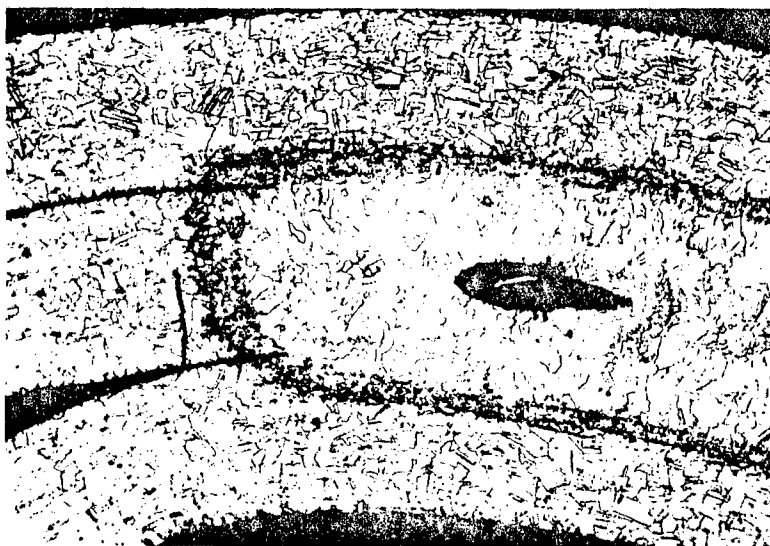
a

x200



type Boa Supra

b



type Boa Duo

Fig. 20a+b

Fatigue cracks in compressor blades

a

x200 x200

b

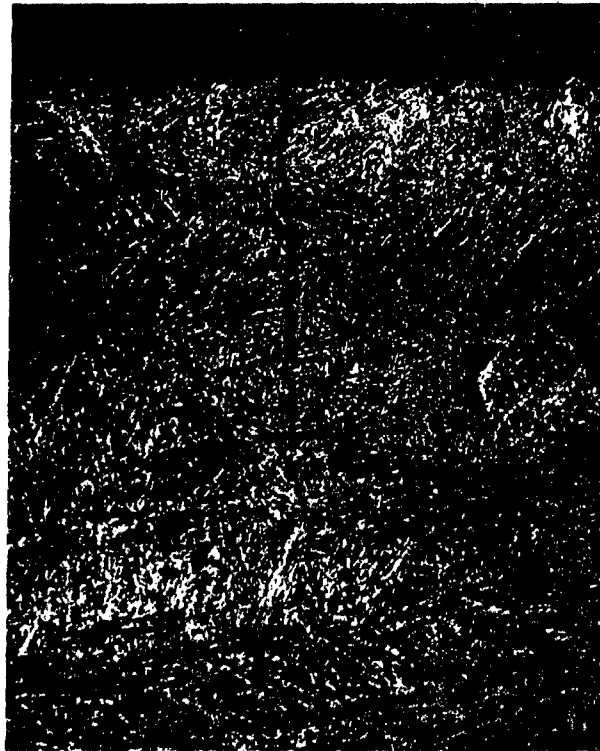
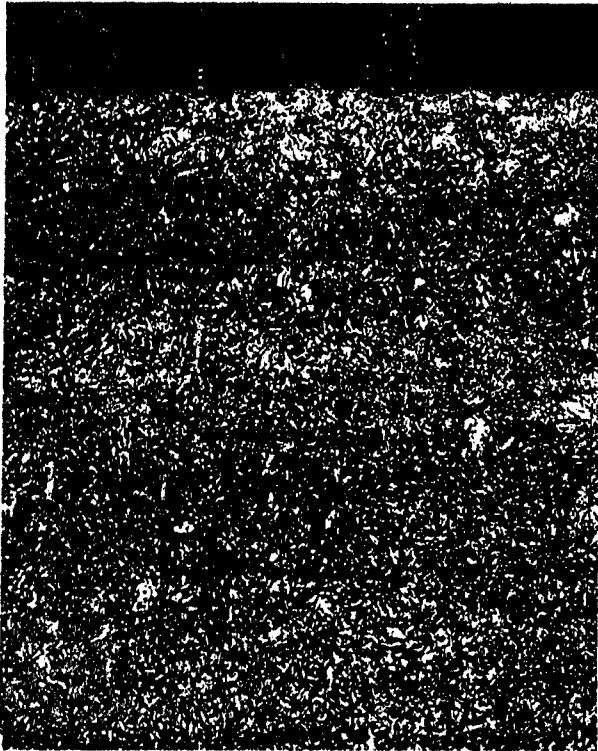
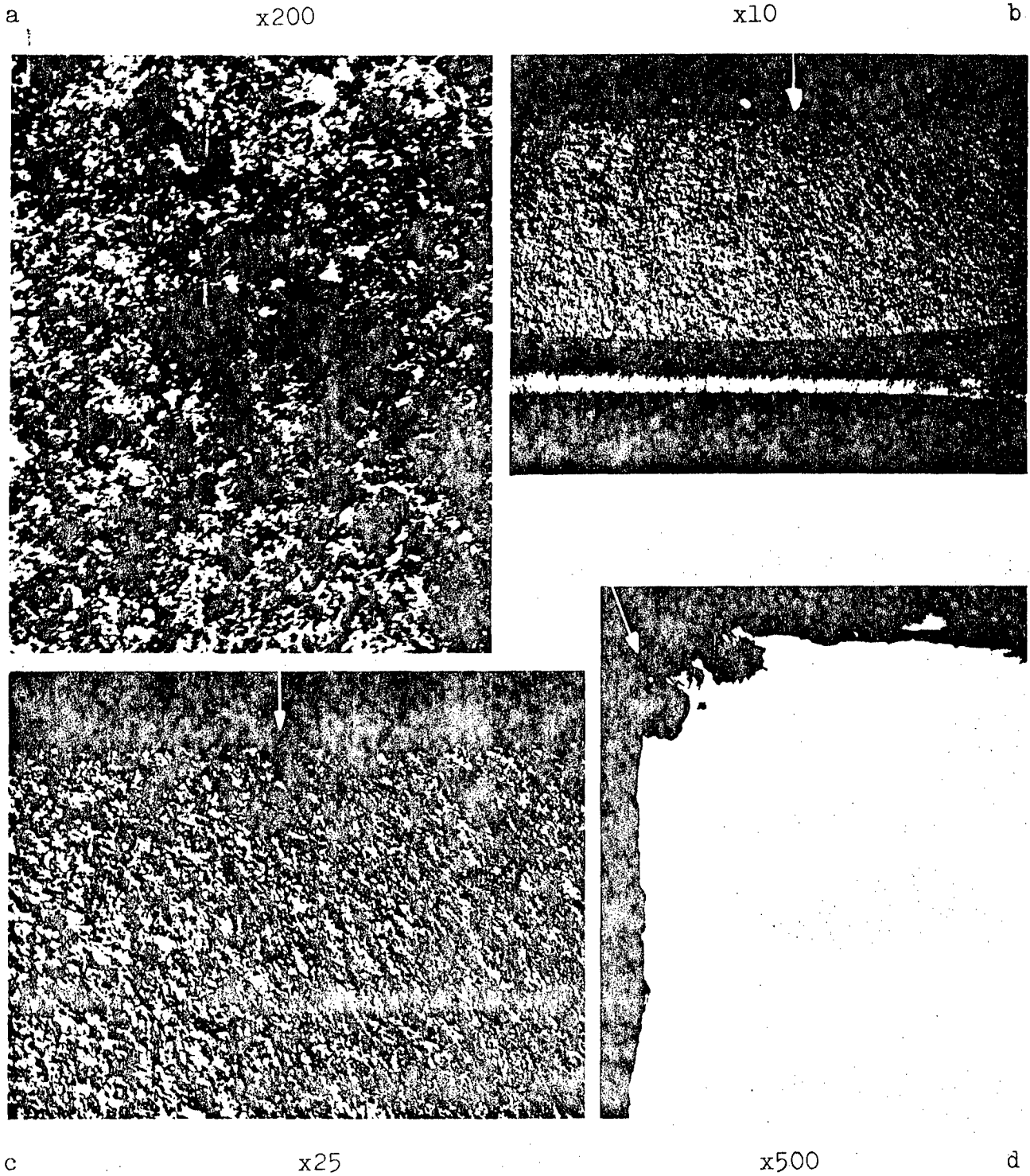
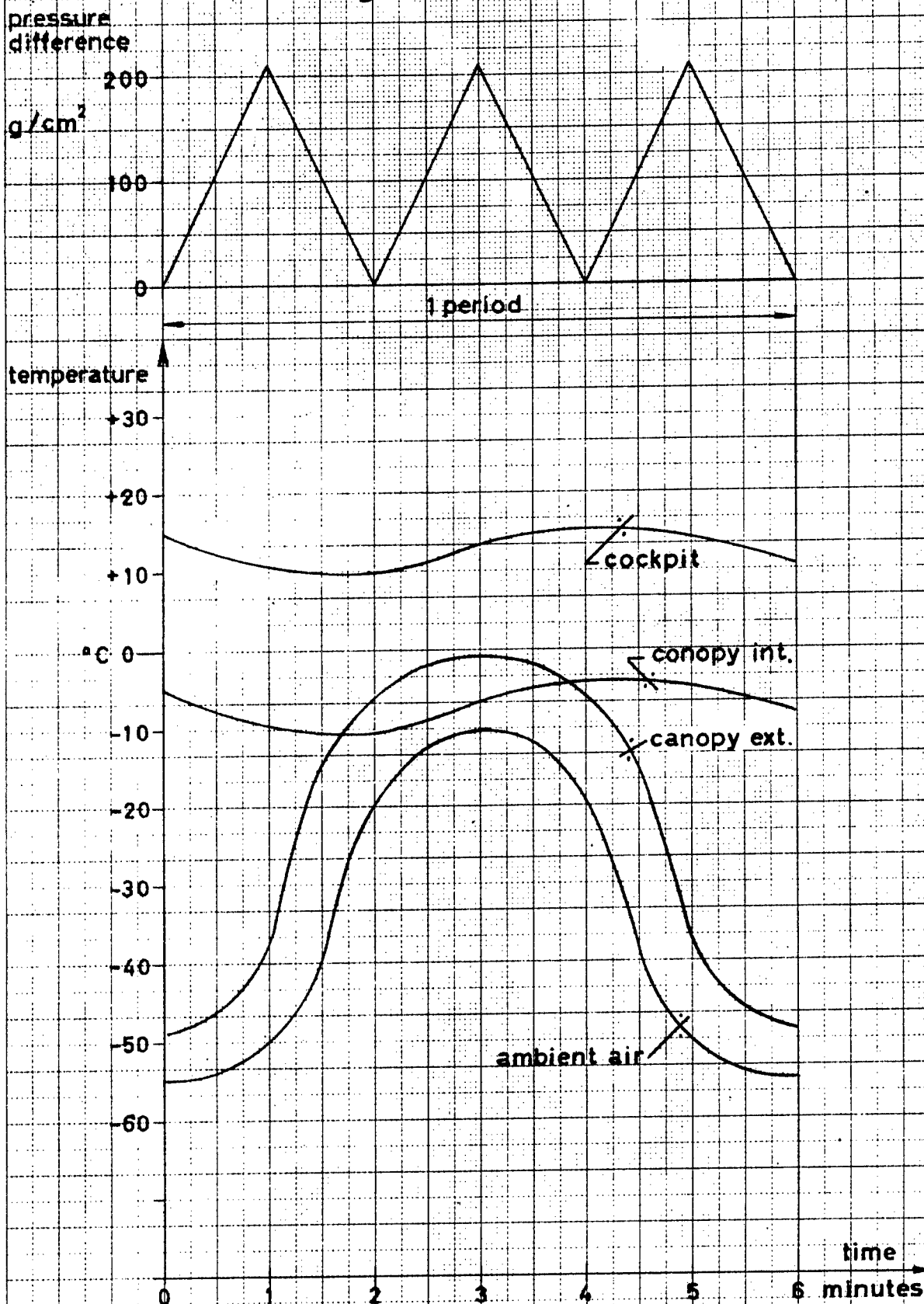


Fig. 21a-d

Corrosion as initiator of a fatigue
crack of a compressor blade (No. 158)

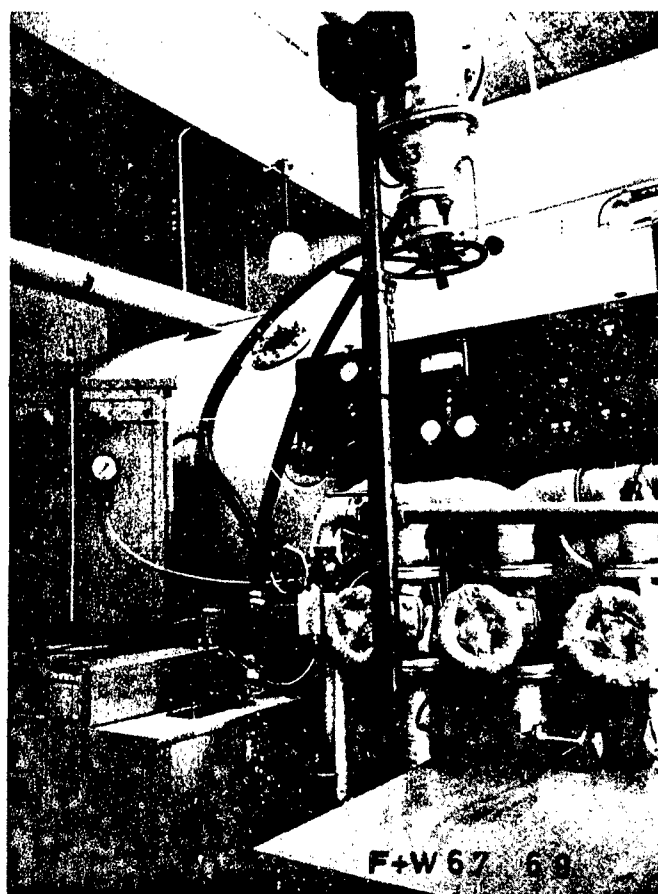


VENOM CANOPY Fatigue Test Program

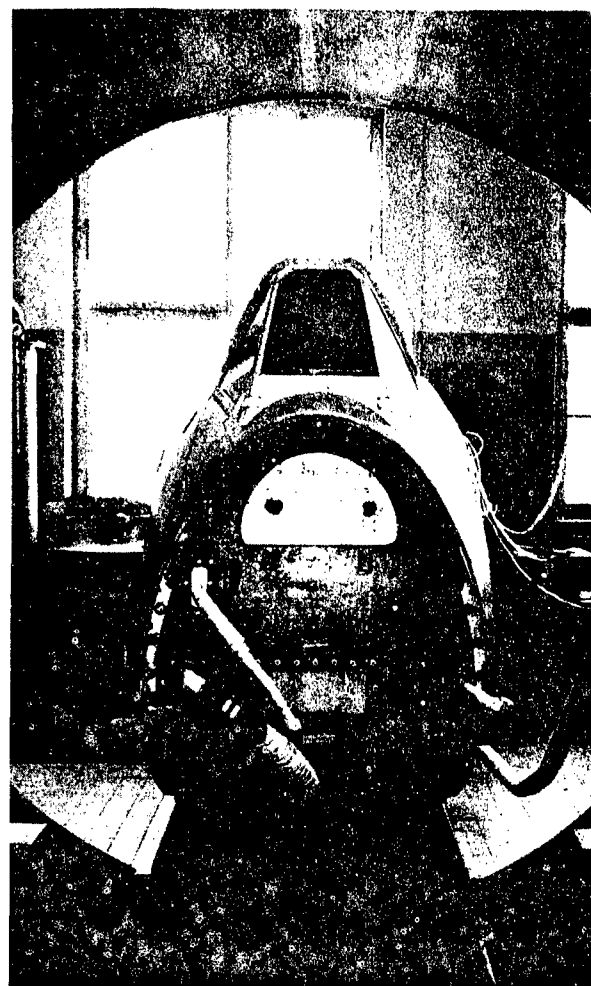


Canopy fatigue test installation

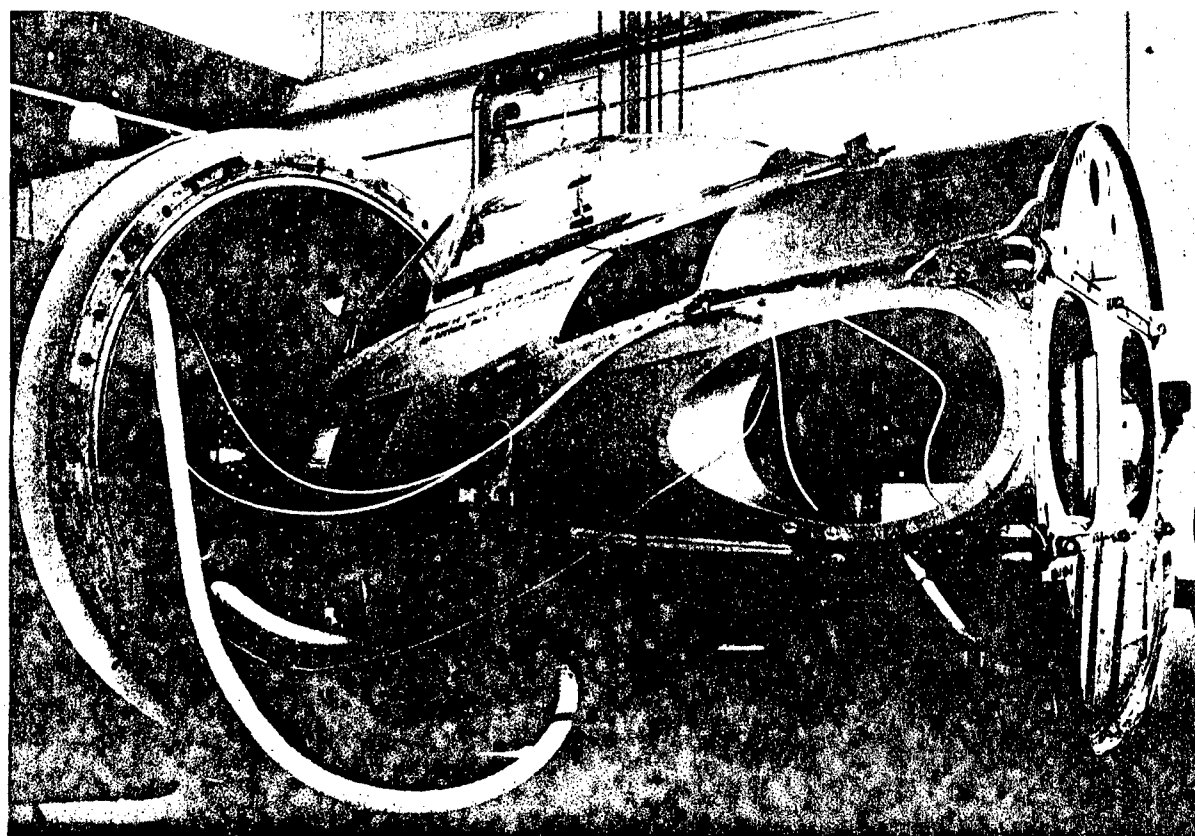
a



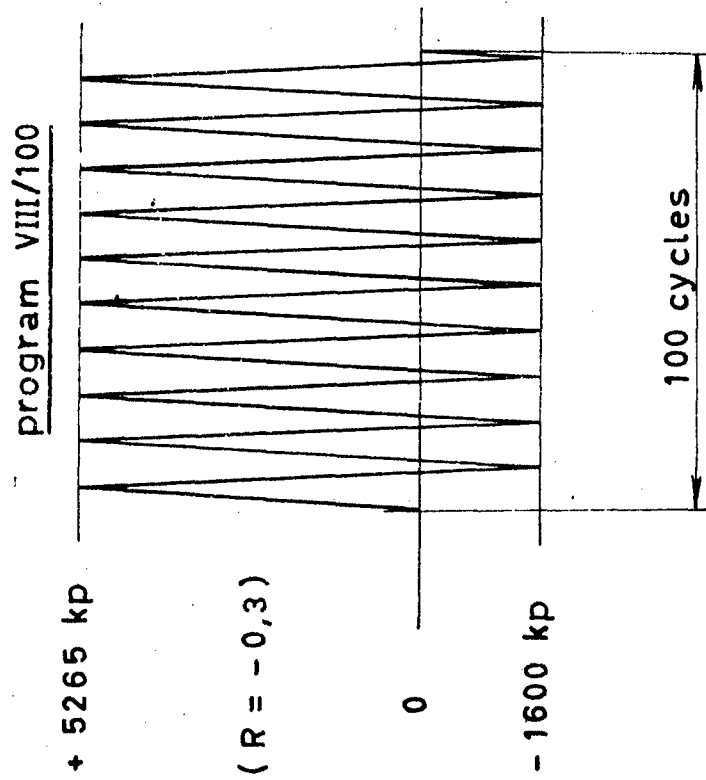
b



c



TEST SPECIMEN : ICAF - Test rod Fig. 24



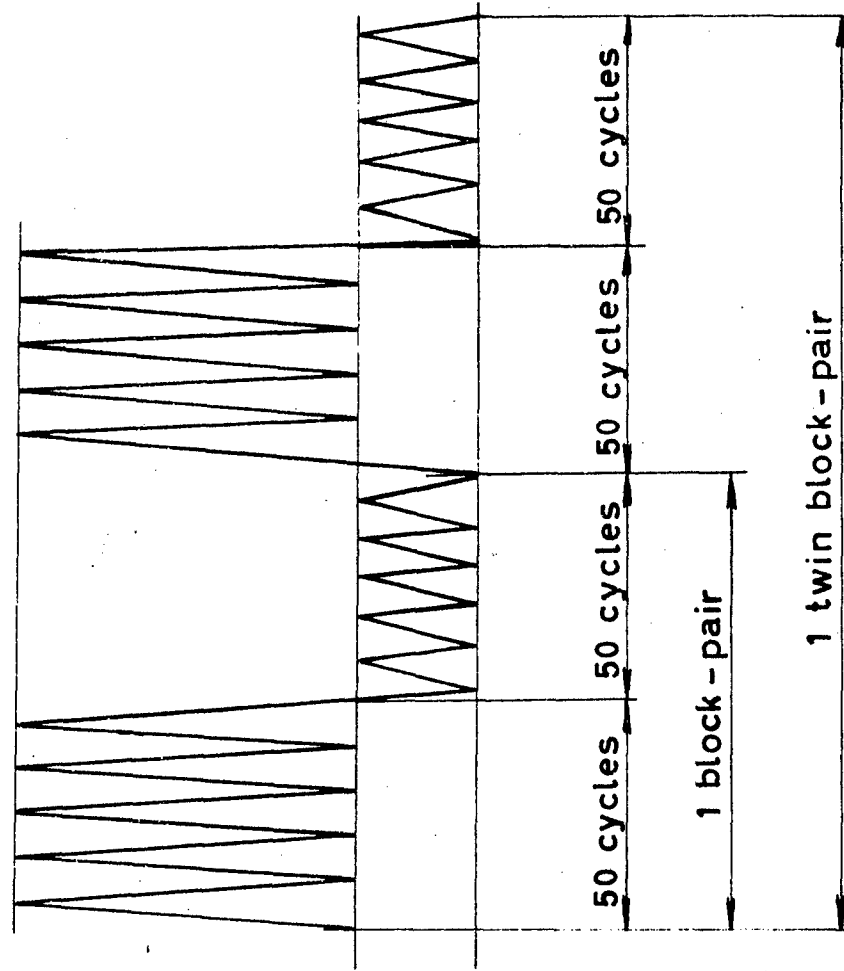
Mean value of 6 specimen,
No of 100 cycles or twin
block - pairs resp., up to
failure.

$$\bar{N}_{100c} = 57,91$$

specific scatter.

$$\bar{e}_r = 7,8\%$$

program XI/100



$$\bar{N}_{t.b.p.} = 134,78$$

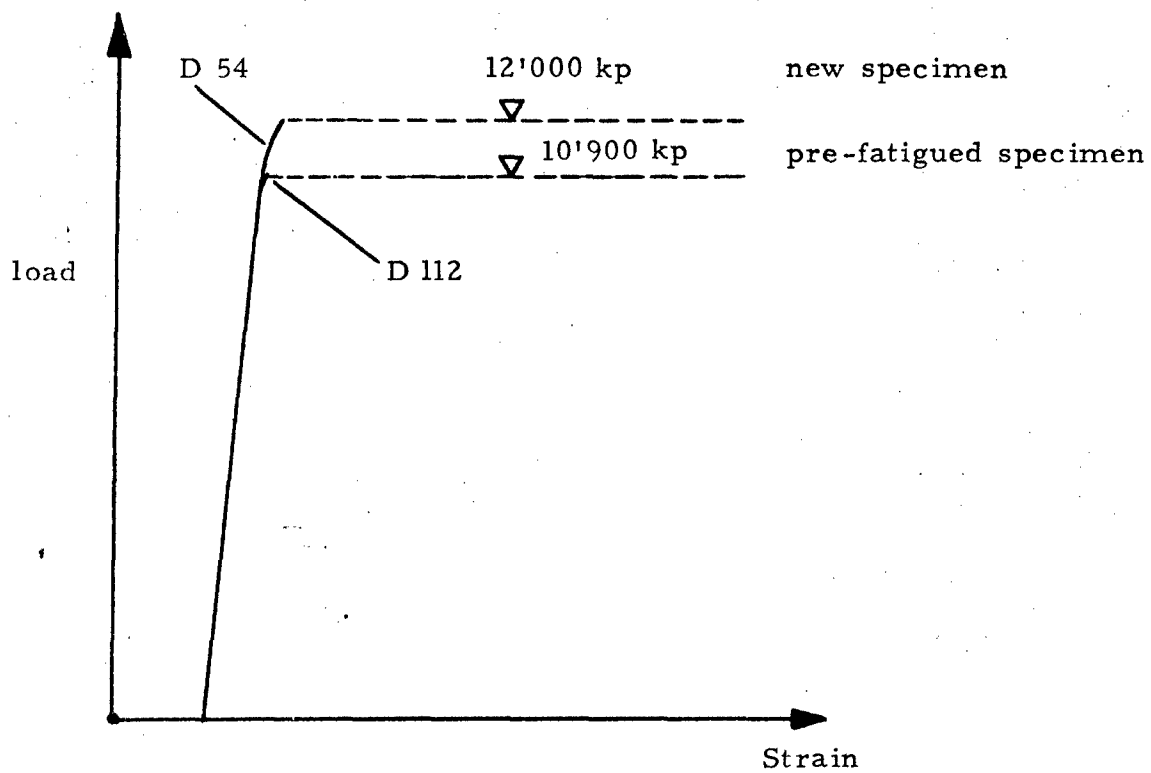
$$\bar{e}_r = 8,3\%$$

Fig. 25

Fig. 26

Ultimate Load-Strain Diagram

of a new specimen and
of a pre-fatigued specimen



D 112 pre-fatigued by
97.404 periods of
history program 11/102

Fig. 27

a



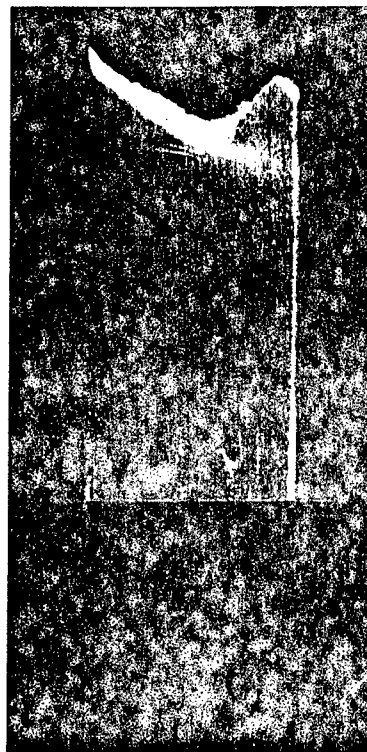
b



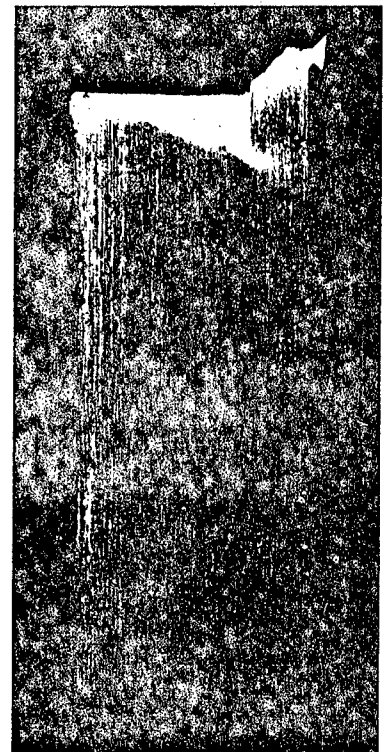
c



D 42
661 C



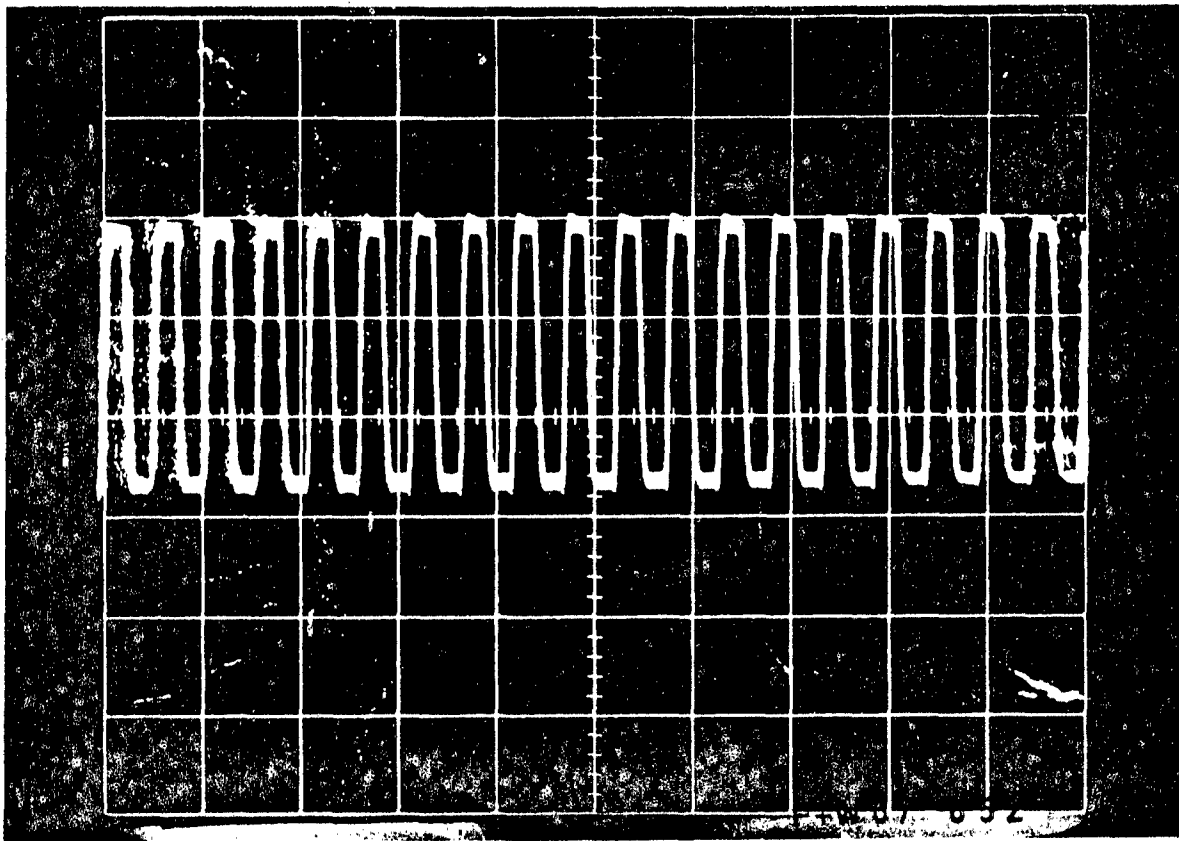
D 69
5601 C



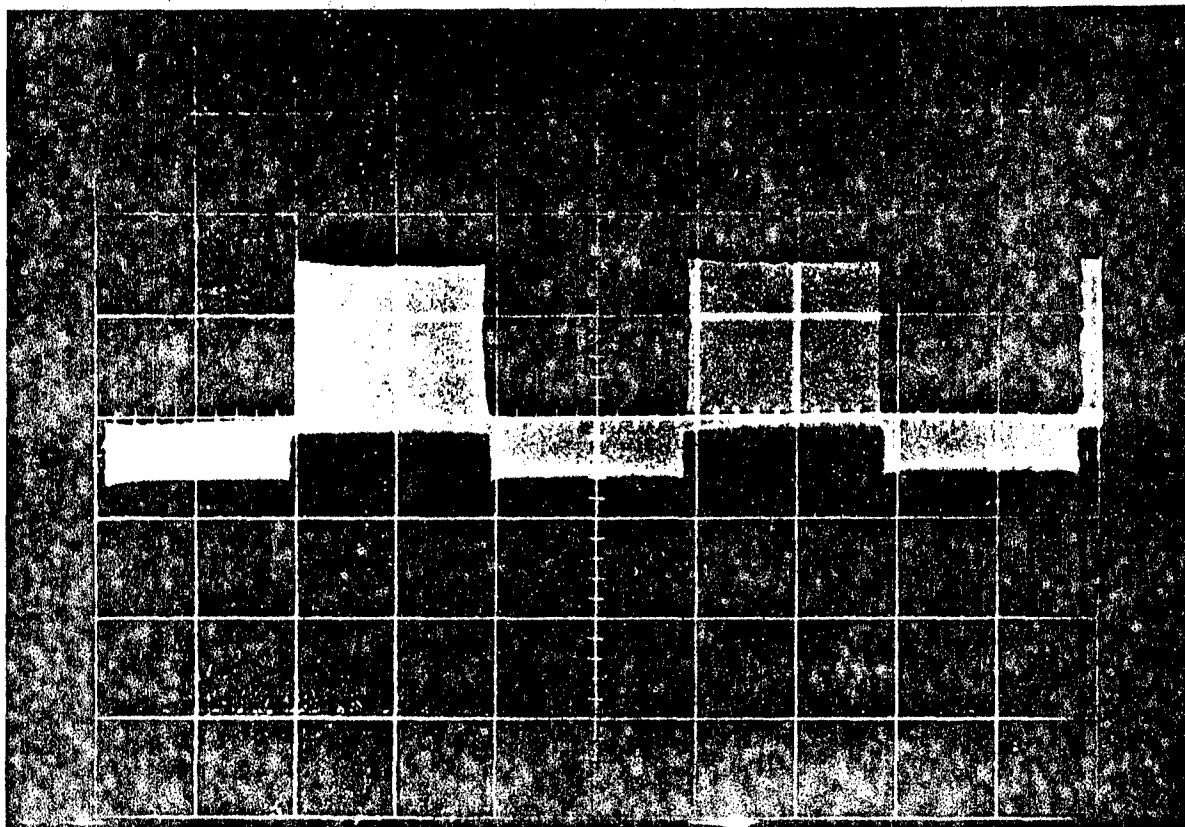
D 95
78,843 q

fractures of different fatigue test specimen

Program VIII



Program XI



on the oscilloscope screen of the 6 - specimen fatigue test machine

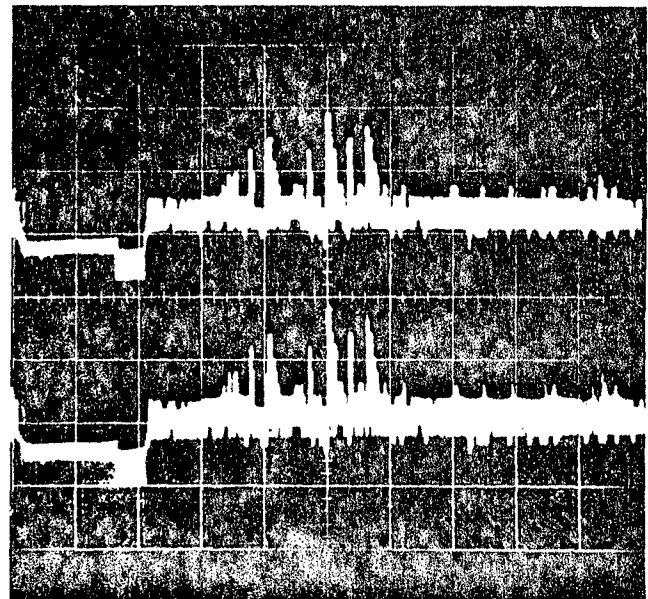
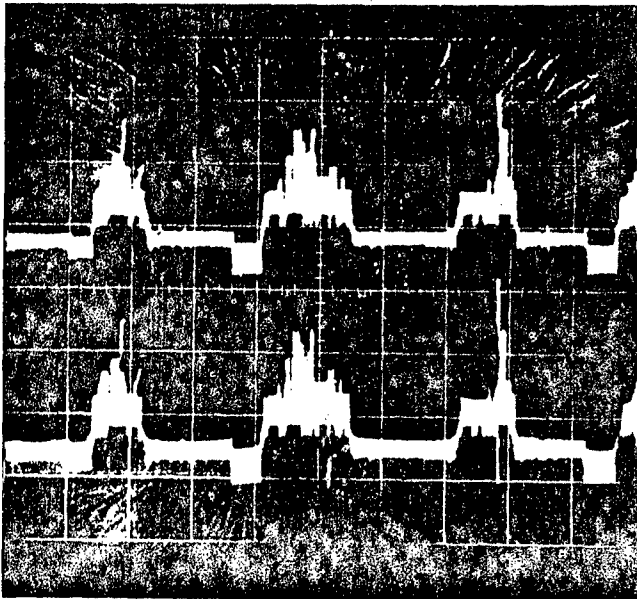
Program III on the screen:

strain gage (upper trace) and damage indicator (lower trace) records

a

b

Fig. 29



same, extended

a

b

Fig. 30

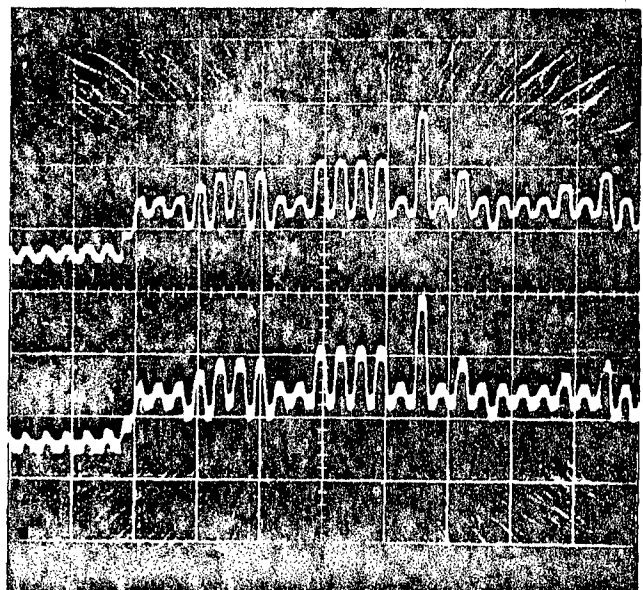
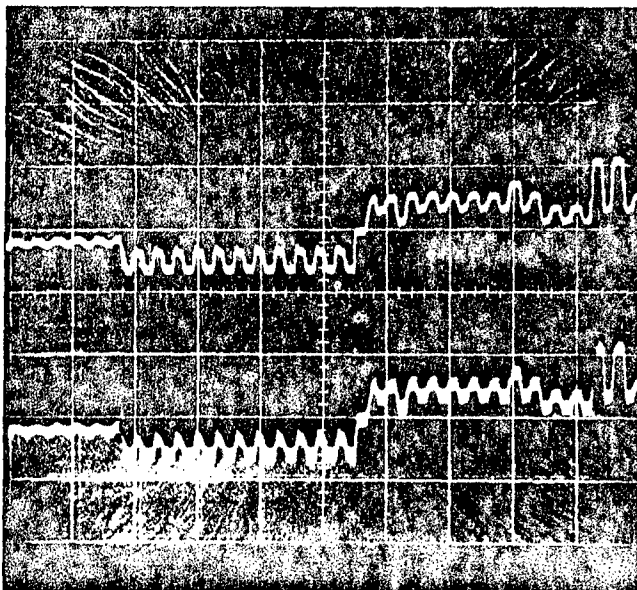


Fig. 31

Damage Story of Specimen Nr. D18 Program Loading, $R = 0/\infty/-0,3$ (XI/100)

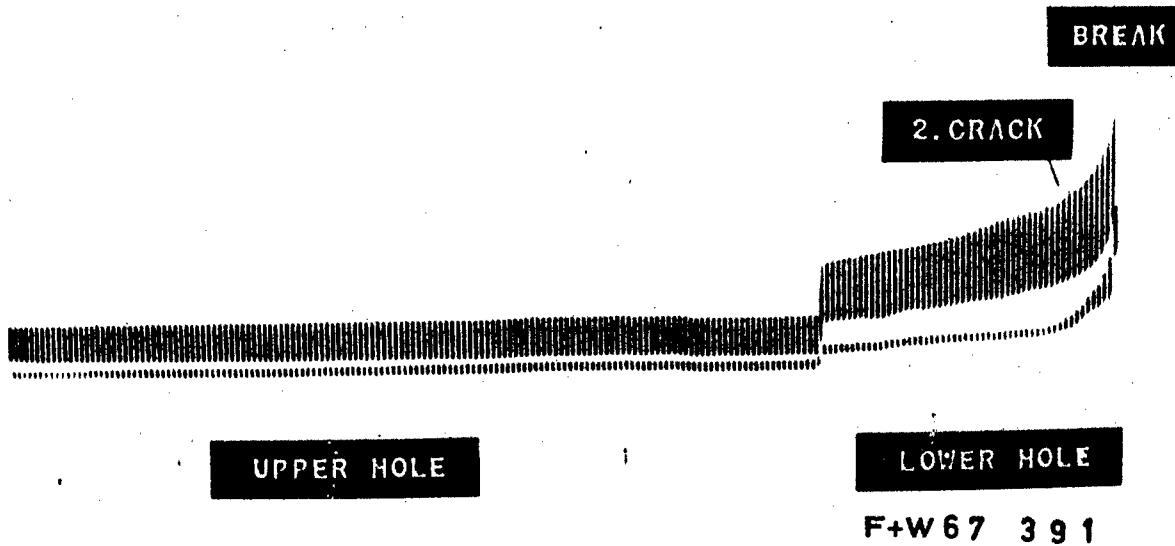
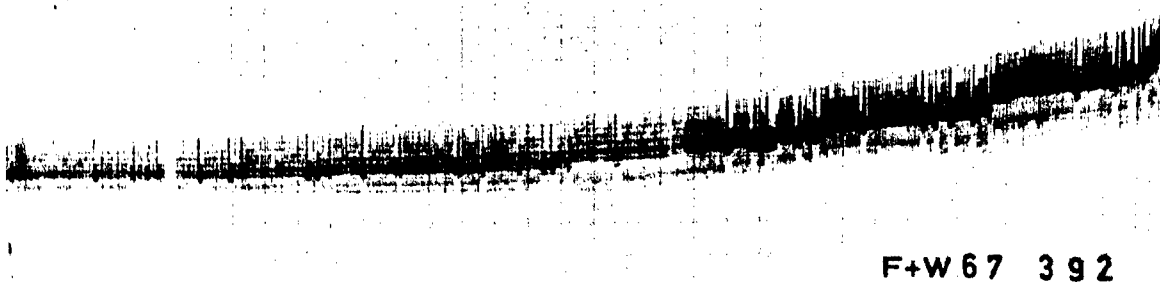


Fig. 32

Damage Story of Specimen Nr. D99 History Loading (III/100)

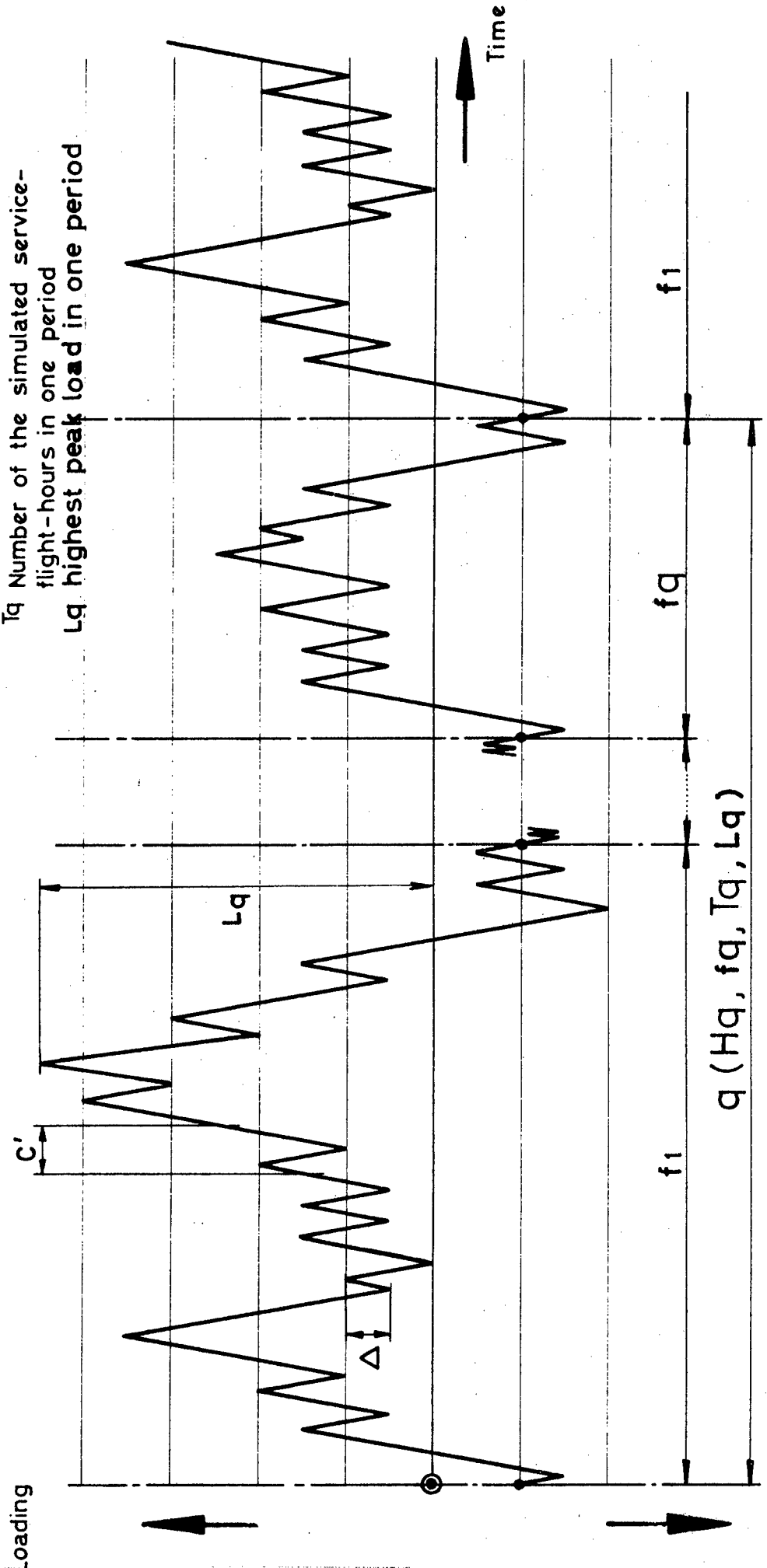


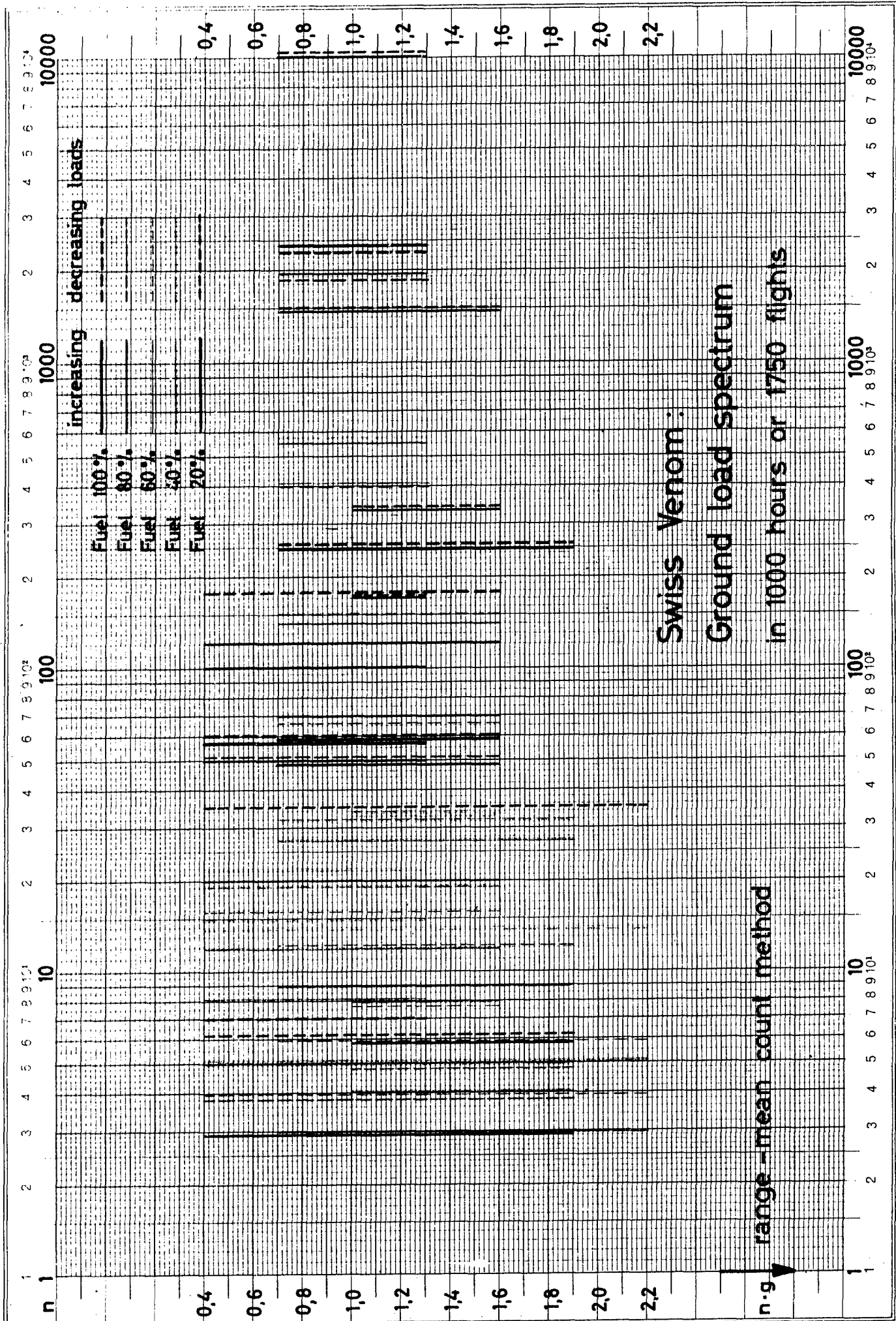
Ground-Loading Spectrum Table, counted and represented by the
Range-Mean Count Method [7]

Fuel	mean load of range (g)	Range (g), increasing load						Range (g), decreasing load						mean load of range (g)	Fuel
		0,3	0,6	0,9	1,2	1,5	1,8	1,8	1,5	1,2	0,9	0,6	0,3		
100 %	0.85			59										0.85	100 %
	1.00		2432									2302		1.00	
	1.15			59										1.15	
80 %	0.85			50										0.85	80 %
	1.00		1925									1825		1.00	
	1.15			50										1.15	
60 %	0.85			8										0.85	60 %
	1.00		406		12							403		1.00	
	1.15			71									67	1.15	
	1.30		8		9			4		12		8		1.30	
	1.45					3			6					1.45	
40 %	0.85			22							15			0.85	40 %
	1.00		561		21					20		568		1.00	
	1.15			142		5			4		152			1.15	
	1.30		33		28		5	14		32	5	32		1.30	
	1.45			4										1.45	
20 %	0.85			100							7			0.85	20 %
	1.00		9978		120					176		10265		1.00	
	1.15			1470		3			6		1493		170	1.15	
	1.30	170	333		247			34		256		339		1.30	
	1.45			6										1.45	

Scheme of History Loading

- C' quasi-cycle
- Δ lowest considered load step
- f flight type
- q period
- Hq Number of quasi-cycles of a period
- fq Number of flight types of a period (different or uniform)
- Tq Number of the simulated service-flight-hours in one period
- Lq highest peak load in one period





N 69-21584

A REVIEW OF THE WORK IN THE UNITED KINGDOM

ON THE FATIGUE OF AIRCRAFT STRUCTURES

DURING THE PERIOD MAY 1965 - APRIL 1967

Compiled by

P.D. Adams and E.L. Ripley, O.B.E.

of the

Royal Aircraft Establishment

Farnborough

(R.A.E. Reference: Tech. Memo. No. Structures 691, March 1967)

CONTENTS

	<u>Page</u>
1 INTRODUCTION	140
2 CONCORD PROGRAMME	140
2.1 Creep and overageing	142
2.2 Room temperature fatigue	144
2.3 Interaction of creep and overageing on fatigue properties	144
2.3.1 Notched sheet specimens	144
2.3.2 Small structural elements	145
2.3.3 Box beam tests	146
2.4 Interaction of creep, overageing, and thermal stress on fatigue properties	146
2.5 Testing of major structural components	147
3 FATIGUE LOADING ACTIONS	148
3.1 Data on atmospheric turbulence	148
3.2 Flight load measurements	149
3.3 The Civil Aircraft Airworthiness Data Recording Programme (CAADRP)	150
4 FATIGUE RESEARCH	152
4.1 Crack propagation	152
4.2 Residual strength and fracture toughness investigations	154
4.3 Fatigue of pressure vessels	156
4.4 Cumulative damage studies	156
4.5 Monitoring of fatigue damage	157
4.6 Fatigue of bolts	158
4.7 Fatigue properties of a new Al-Zn-Mg alloy	159
4.8 Fretting-fatigue	159
4.9 Basic mechanisms	159
5 DESIGN DATA ON MATERIALS AND STRUCTURAL ELEMENTS	161
6 FULL SCALE TESTING	163
7 ACOUSTIC FATIGUE	165
7.1 Loading actions	165
7.2 Response of structures to acoustic excitation	166
7.3 Acoustic fatigue testing	166
Acknowledgements	167
References	168

1 INTRODUCTION

In the past two years considerable fatigue research has centred round the Concord Project and good progress has been made in understanding the special conditions arising from the thermal cycle. The work has covered many facets. Important among these has been the basic research on creep, overageing and fatigue and on the interactions one with another; also on the structural effects of thermal stress cycles and their combination with mechanical stress cycles. In addition confidence has been gained in the ability to represent the aircraft service environment in the test laboratory. New testing techniques have been developed and demonstrated in tests on major components.

During this period, however, the other more familiar research programmes have not been neglected and it is proposed to review the major topics as well as the Concord research programme in the following order:-

- (a) Concord programme.
- (b) Fatigue loading actions.
- (c) Fatigue research.
- (d) Design data on materials and structural elements.
- (e) Full scale testing.
- (f) Acoustic fatigue.

This follows broadly the pattern of the previous review¹.

The present review has been compiled from the authors' knowledge of the work aided by contributions from research laboratories in the R.A.E., N.E.L. and the aircraft industry. It has been made as complete as possible within the information available and it is believed that the more important items have been covered. Inevitably something will have been missed and this is regretted. The source of the information used has not normally been identified directly in the text, but where a paper has been prepared the reference is given and this provides a useful bibliography.

2 CONCORD PROGRAMME

Before discussing the detailed Concord test programme it is worthwhile to first outline a typical flight profile so that an understanding of the complete environment and loading actions can be obtained.

Immediately after take off the aircraft will climb subsonically until it is clear of populated areas and then, still climbing, accelerate to its cruising

speed of Mach 2.2. After the cruise phase has been completed the aircraft will decelerate to subsonic speeds at altitude and then descend to its destination.

In the initial climb at subsonic speeds the external surfaces of the structure will cool a little and then heat up in the acceleration phase, reaching a temperature of about 120°C which will be maintained during the cruise. During deceleration and descent the external structural temperature will drop to about -20°C rising again to ambient temperature on landing. The temperature of the internal structure will lag behind that of the surface structure due to the time it takes for heat to be conducted to it. Thus on the climb the external structure will be hotter than the internal structure and this will set up thermal stresses due to the different amounts of expansion. During the cruise the internal structural temperature will gradually approach that of the external structure and the thermal stresses will decay. The reverse effect takes place during descent and recovery giving thermal stresses of opposite sign, which together make a complete fatigue cycle.

The aircraft will also be subjected to the normal pattern of fatigue loads - taxiing loads, ground-air-ground cycle, gust and manoeuvre loads, cabin pressurisation etc. Almost all of these will occur while the aircraft is on the ground or flying subsonically. The exception is clear air turbulence which will be encountered while the aircraft is flying supersonically but this produces only a small proportion of the total fatigue damage. Thus almost all of the fatigue damage due to external loadings occurs while the structure is at ambient temperature before the acceleration phase or is approaching ambient temperature after the deceleration phase. This is a great simplification both in representation in full scale tests and also in the research programmes.

One effect of the thermal cycle has already been mentioned, namely thermal stress. Also to be considered are creep and overageing. All of the structure will suffer overageing and much of it will suffer creep. There are notable exceptions, such as the fin, where the creep effects will be less than in those areas, such as the wing, which are subject to steady loads throughout flight.

Thus the structure is subjected to externally applied fatigue loads, interspersed with periods of creep and overageing, interspersed with fatigue cycles of thermal stress and the task of the designer and test engineer is indeed complex to understand and interpret all of these effects and their interactions.

The task has been tackled by breaking the problem down and studying smaller parts separately, gradually bringing them together as knowledge is gained. The story of the work so far is in the following sections.

In addition to the aircraft design and development aspects of this work, this research programme has a very important bearing on the fatigue approval test programme. Because it is necessary to allow the heat to be conducted naturally through the structure so that the appropriate thermal stresses are generated, it is extremely difficult to shorten the thermal cycle. Some gain can be obtained by forcing the thermal conditions after the peak thermal stress has been reached so that the structure more quickly attains the equilibrium conditions at the end of cruise and after landing. While ideally this is possible on a simple specimen and in fact is being used for some of the tests, it would be very complex on a major structural component. Thus at present there seems little hope of making the test cycle shorter than a flight cycle if thermal stresses are to be represented adequately. If the problem was only that of simulating creep and overageing it is thought that adequate representation could be obtained by employing a higher temperature for a shorter time.

As it is necessary that the fatigue approval test shall be ahead of the flight aircraft by a suitable factor to ensure safety in service and as it does not appear possible to shorten appreciably the thermal cycle in the test, the only remaining possibility is to make each test cycle represent several flights - i.e. to accelerate the test so that more fatigue damage is done in each test cycle than in a real flight. Techniques to do this are being sought in the research programme described in the following sections. Once a technique has been chosen, reliance will have to be placed on results of the test programme to interpret the failures on the approval test specimens. Thus a great deal of confidence has to be established since the natural reaction is to explain an unexpected premature failure as a fault in the test rather than a fault in the design.

A full description of the whole of the Concord test programme, including work in both France and the United Kingdom is given in a paper² to be presented to the Fifth I.C.A.F. Symposium in Melbourne in May 1967.

2.1 Creep and overageing

A great deal of basic material creep test data has been obtained from tests on aluminium alloys DTD.5070A, 2024-T.81 and L.73. Short term accelerated

test data were correlated using the Fisher-Dorn parameter $\phi = -\frac{Q}{RT}$ and recently acquired long term test data (of order 30000 hr) agree well with the extrapolations made from the short term results.

From the results of material tests it is expected that the gross creep deformation of the Concord structure will be very small. However work on the effects of creep around stress concentrations has indicated that although relatively small creep strain occurs away from the notch very high local strains accumulate at the edge of the notch leading eventually to the initiation of small cracks. These local strain measurements have been made by engraving a squared grid, (approximately 0.050 inch square) on the specimen surface adjacent to the notch and then evaluating the magnitude of the local strains from measurements of the deformation of these squares at regular intervals during the test.

Creep bending experiments on box beam specimens has also revealed incidents of creep cracking initiating from cut outs and rivets adjacent to the cut outs. This work is to be extended to test panels with various cut out geometries and also to box beam structures to be loaded in combined bending and torsion.

Creep cracking has also been observed in the head of aluminium alloy rivets in lap joints. These joint tests form part of a large scale research investigation into the efficiency of riveted joints as a function of joint geometry and sealants.

Further joint tests of one particular geometry are being conducted to investigate time-temperature correlation of creep deformation. Initial results indicate that such a correlation is likely to be found although considerable scatter in the data exists due, it is thought, to variability in the properties of the sealants used and also variability in the setting of the individual rivets in the joints.

Creep deformation, being a non linear function of stress, results in stress redistribution within a structure exposed to time at temperature under an applied load. Before theoretical studies of structural problems can be investigated an equation of state requires to be found that will successfully interpret the creep behaviour of materials under changing stress conditions.

The research on creep under variable stress has shown that creep in commercial aluminium alloys consists of at least two components, one being

recoverable and the other permanent. The recoverable or transient component appears to have a Poisson's Ratio close to the elastic value while the permanent component is purely plastic with a Poisson's Ratio of 0.5. The rate of accumulation of the permanent creep strain appears to depend on the transient component. Work is in hand to evaluate possible techniques for measuring separately the two components with a view to determining more precisely the time/temperature/stress/strain relationships of each component.

2.2 Room temperature fatigue

Extensive room temperature fatigue testing has been conducted both to evaluate the basic material properties of various aluminium alloys and also to investigate the fatigue properties of various types of riveted construction as a function of the high temperature sealants used.

2.3 Interaction of creep and overageing on fatigue properties

2.3.1 Notched sheet specimens

An initial series of highly accelerated tests, with respect to the Concord environment, have been conducted on aluminium alloy DTD 5070A. The test programme consisted of periods of cold fatigue loading of the $P \pm p$ type interspersed with periods of exposure to elevated temperature with an applied stress. The results indicated that there was a reduction in endurance relative to the fatigue life at room temperature.

A more detailed programme on an RR 58 alloy is in progress and the results, in general, support those of the earlier investigation. It has been shown that periods of heating with zero applied stress (overageing) interspersed with fatigue at room temperature reduced the fatigue life. The interspersed tests with a mean stress applied during the hot period showed a smaller reduction in endurance, indicating that a beneficial effect may be derived from creep deformation. This is thought to result from a favourable stress redistribution at the notch during the creep period. It appears, therefore, that the net effect on fatigue endurance is very much a compromise between the damaging effect of overageing and the beneficial effect of creep. However, the results show that the balance between the two effects is very critical and appears to be sensitive to the local stress distribution.

The metallurgical processes which result in the loss in fatigue strength are not known but detailed metallurgical studies are being planned to investigate these effects.

2.3.2 Small structural elements

Work is proceeding on investigations to discover the effects on resultant endurance of inserting one period of overageing and/or creep at different stages during the fatigue life. The main investigations are concentrating on aluminium alloys RR 58, HID 54, L65 and 2024-T81. The tests on HID 54 have been completed and the results are to be published shortly³.

The tests have shown that if a period of temperature soak under zero load was applied during the crack nucleation stage there was a reduction in the resulting fatigue life as compared with uninterrupted fatigue test results. This effect was shown to be greater for notched specimens than for lugs and joints. It is now believed, however, that the HID 54 material was not fully aged in the as received condition and that the observed reduction in endurance was due to the material rising to peak hardness during the heating period. However, it was possible to show that overall creep strains of the order of 0.02% tended to oppose the effect of ageing and resulted in an improved endurance at low stress amplitudes.

It was also shown that the effect of overageing and creep had little effect on the residual tensile strength of cracked lug specimens.

Results from RR 58 specimens show that the test material is approximately fully aged and reductions in endurance due to ageing are smaller than those measured with HID 54 specimens. The beneficial effect of tensile creep strain has again been demonstrated with RR 58 and, in addition, it has been shown that compressive creep strain is detrimental.

Further work will include the effects of temperature cycling, the influence of the fatigue loading frequency and the effect of heating during crack propagation. A comparison will be made of heating effects under constant and variable amplitude loading.

Two riveted joint test programmes have been initiated to study overageing and creep-fatigue interaction effects. One is on 3 inch and the other on 6 inch wide 3 row joints with countersunk rivets.

Periods of heating during which either zero or a tensile mean load is applied were interspersed with fatigue loadings of the $P \pm p$ type.

The general results confirm the findings of the notched sheet investigations. It has been shown that interspersed periods of overageing alone produce

a greater loss of endurance than interspersed periods of creep and overageing. Some tests showed that there was an improvement in life as a result of creep and overageing interspersions.

Some room temperature fatigue tests have been conducted on the joints during which either zero or constant load dwell periods were introduced during the course of the test, each dwell period corresponding to the duration of the hot periods of the interspersed tests. The object of these tests was to establish whether the reduction in endurance observed from the interspersed tests resulted from the insertion of hot periods or whether it was simply due to interrupting the room temperature fatigue test. The test results gave substantially the same fatigue life as continuously run room temperature fatigue tests establishing, therefore, that the reduction in endurance observed from the interspersed tests is entirely a function of the 'hot' interspersions.

2.3.3 Box beam tests

A series of tests are in progress on aluminium alloy box beam specimens 6 ft x 20 inch x 6 inch deep. These boxes have deliberately been made shallow to minimise the effects of thermal stress. All of these tests, except the room temperature control fatigue tests, have been conducted by interspersing periods of high temperature, during which a mean stress is applied, with room temperature fatigue loading cycles of the $P \pm p$ type.

The results indicated that, in general, there was an improvement in the fatigue endurance as compared to the datum room temperature fatigue life and not a reduction in life as was expected from the notched specimen results. It is possible, however, that the improvement in fatigue performance may have resulted from the release of built in stress due to creep induced stress redistribution during the heating periods. Further tests are being planned to investigate the effect of zero stress during the high temperature interspersions.

2.4 Interaction of creep, overageing, and thermal stress on fatigue properties

Box beam structures 10 ft x 16 inch x 16 inch deep are being tested under simulated Concord conditions. These boxes have deliberately been made deep so that thermal stresses are induced. The upper and lower surfaces are convectively heated initially to produce the thermal stress pattern after which the whole structure is force heated to isothermal conditions. Thermal stresses of the opposite sign are then applied by cooling of the upper and

lower box surfaces using air cooled with liquid nitrogen. The whole box is then force cooled to reach an isothermal condition at room temperature. At this stage mechanical fatigue loadings are applied and the thermal cycle then repeated.

The initial investigations will be conducted with only a minimum dwell time at the peak temperature thus minimising the extent of any creep and overageing effect. This test result will then be compared with the endurance achieved by a box tested with mechanical fatigue cycles only and further tests conducted during which the ratio of mechanical to thermal cycles will be varied and also the magnitude of the time at peak temperature will be increased, thus introducing the effects of creep and overageing.

2.5 Testing of major structural components

The first major test in the United Kingdom part of the Concord programme has been a test on a 15 ft long section of fuselage at Filton. Convective heating and cooling has been used, based on a method developed at R.A.E. The specimen is in a totally enclosed duct which may be operated as a closed or open circuit. Heat exchangers, fired by town gas, heat the air and cooling is initially by ambient air, followed by injection of liquid nitrogen into the air stream. The loading on this specimen is only internal pressure. Automatic control of the entire cycle is obtained from a punched tape input. The specimen is being used to obtain design development information and at present the rig is running under accelerated conditions - i.e. each test cycle is more damaging than a real aircraft flight.

At R.A.E. preparations are well advanced for tests on a 65 ft long specimen of the forward fuselage, on a complete engine nacelle and on a complete airframe. These tests will be extremely complex and will simulate all the loading actions encountered during typical airline operations - these will include, as appropriate, taxiing loads, ground to air loads, gust and manoeuvre loads, cabin pressurisation and air conditioning and transfer of fuel as well as the thermal cycling. Heating and cooling will be primarily by convective methods, but some additional heating by radiation may be necessary in critical areas.

One of the major problems of a test programme of this nature is to ensure reliability of the test rig so that testing can continue twenty-four hours a day, seven days a week, except for the necessary breaks for inspection and maintenance. To meet this need a special control system has been developed

which is capable of controlling the tests on the forward fuselage and nacelle and has capacity also for controlling a test on the rear fuselage if it is decided to remove this from the complete airframe and test it separately. Essentially the system comprises two small on-line computers. One of these provides the step by step instructions for the test and completely controls every phase. The other computer generates independently a similar control programme and checks that the test has followed it. Small deviations are reported and large deviations cause the rig to shut down. Thus very extensive recording and subsequent analysis is avoided. Manual control of all operations is possible so that special tests and calibrations can easily be done. Provision has been made for the computers to generate a system of random loadings and a large store is available so that this can be examined and approved before it is applied. It is expected that a similar control system will be used on the test of the complete airframe.

3 FATIGUE LOADING ACTIONS

One of the major problems in fatigue life estimation is that of defining accurately the relevant load spectrum for an aircraft or component⁴. It is therefore important that statistical data on the environmental loads should be accumulated as well as an understanding obtained of the dynamic responses of the structure under these applied loads.

Considerable effort in the past two years has been directed to defining more closely the turbulence spectra, in particular for very high and very low altitudes. An increasing number of flight load measurement investigations have been initiated and particular emphasis is being placed on fins, tailplanes and undercarriages as well as the wing structure.

3.1 Data on atmospheric turbulence

Counting accelerometers continue to be carried on a number of passenger aircraft and provide the main statistical source of information on loads due to atmospheric turbulence. A large sample of flight records from aircraft not fitted with cloud warning radar have been analysed and the derived gust frequencies studied⁵.

Analysis of gust loads below altitudes of one thousand feet has also been made⁶. The sources of information were varied and a comparison was drawn between the passenger transport sources and the data acquired during special investigation. The study concluded that the evaluated gust data gave reliable

average figures for passenger transport operations. However, owing to the wide variation of gust frequencies with ground topography and weather conditions it was concluded that for military aircraft flying at low altitudes a more detailed knowledge of operating conditions was necessary before reliable estimates of gust frequencies could be made.

To extend the knowledge on low level conditions a special flight research programme has been initiated to compare low level turbulence over land and sea in and around the United Kingdom. The programme will also delineate between turbulence encountered in coastal waters and out to sea.

The turbulence encountered by shorthaul transport aircraft has been analysed on a flight by flight basis⁷. It was found that the magnitude and distribution of gusts within a flight is dependent on the total number of gusts in the flight but that the correlation between successive flights was low.

Analysis of the results from the investigation of clear air turbulence in Australia in 1963 (TOPCAT) has been completed and a summary paper detailing meteorological observations and flight plans and the measurements of wind, temperature and turbulence has been published⁸. The turbulence data have been analysed⁹ in the form of power spectra and indicate that at short wavelengths the spectra agree well with a $-5/3$ power law and that the energy densities of the three components (ug, vg, wg) were similar. In some respects, however, particularly at long wavelengths, the spectra were found to be dissimilar to those found for low level turbulence and there were some indications that the turbulence was anisotropic.

A theoretical study on the response of a slender wing aircraft to atmospheric turbulence has been completed. The aircraft was represented by two rigid and three flexible normal deformation modes and a particular study was made of the vibrational environment in the cockpit. The responses showed some sign of the resonance reported earlier¹⁰ on more slender aircraft, but it was not so marked. It was also shown that more response was due to the higher frequency elastic modes than had been indicated by previous calculations.

3.2 Flight load measurements

A better understanding of the fatigue of aircraft structures in service should accrue from the load measurement programmes¹¹ now in progress on several military and civil aircraft. These are primarily concerned with the measurement

of the internal loads in wing, fin and tailplane structures during flight in turbulent air, manoeuvres, loading and taxiing conditions¹². The measured loads will be correlated with accelerations measured at the centre of gravity and with control surface positions. The strain gauge responses will be interpreted in terms of a load calibration applied to the flight aircraft or by reference to strain gauges similarly positioned in the fatigue test specimens.

The specific problems of undercarriage load measurement are being investigated in separate programmes and these should provide data on rough runway operation.

The use of fatigue load meters continues to provide data on the severity of loading experienced by individual aircraft and the average load spectra to be expected in various roles. This information is invaluable in providing the anticipated spectra for new military aircraft. Fatigue load meters having a working temperature range of -50 to 150°C are in production. Facilities are available for 3 extra banks of 6 counters each, to be added to the basic fatigue load meter, any bank of which can be operated in a selected aircraft regime, e.g. at high Mach number or certain sweep angles.

3.3 The Civil Aircraft Airworthiness Data Recording Programme (CAADRP)

The loads encountered by an aircraft in flight are the resultants of the individual effects of the environment, the aircraft's characteristics and the practical expertise of the pilot.

Most in-flight recorders, such as the V-g recorder, the counting accelerometer and the fatigue load meter measure the resultant effect of these individual parameters. It might be argued that this is the effect that is required to be measured since the structural performance of the aircraft depends directly on the magnitudes that are measured. However, such measurements can never explain the origin of these loads; they can never delineate, for example, between loads induced by manoeuvres and turbulence induced loads. Similarly there are a host of other circumstances in which the interaction of pilot, aircraft and environment play a vital role in the determination of the resultant loads in the structure. Only when the individual causes and effects are broken down is it possible, to determine whether the present accepted requirements and standards will be applicable to future aircraft types.

The realisation that a great void existed in the knowledge of aircraft operating procedure led, in 1962, to the initiation of the CAADRP investigations¹³. The basic aims of the programme were to study:-

- (i) the effect of environment and operational usage on the aircraft,
- (ii) the efficiency with which the aircraft is operated within the bounds of its flight limitations,
- (iii) the unusual occurrences caused by environment, operational usage or malfunction of some part of the aeroplane.

In order to acquire the data to achieve these basic aims, continuous trace recorders were fitted to several aircraft in normal airline service and have provided data on indicated airspeed, normal acceleration, barometric height, outside air temperature, control surface movement, aircraft heading, autopilot mode and flap usage. The scope of the recording has recently been extended to include pitch, roll, Mach number, throttle setting and a number of other parameters, such as radio height, and deviation from ILS glide path, specifically chosen to make detailed studies of landings. At present data are accumulating at the rate of 10000 hr per year and have thus enabled a variety of investigations to be made. Unusual occurrences (Special Events)^{14,15} have been examined in a manner not possible with earlier recording methods; these have assisted in accident investigation and have indicated the causes of some aircraft handling problems. The observance of speed and acceleration limitations and compliance with flying instructions have been analysed and a number of pilot instructions have been modified as a result of these analyses.

Data on take off and landings has also been forthcoming and have shown that multiple bounces on landing and heaving oscillations during high speed taxiing are significant contributions to loading problems. Theoretical research on undercarriage damping¹⁶ is now to be co-ordinated with this operational information with the aim of specifying new requirements. Methods of analysing the structural severity of a landing are being developed using centre of gravity acceleration and radio altitude information.

The recorded data have enabled manoeuvre and gust loads to be separated by using control surface information thus allowing detailed study of the effects of turbulence. A special study of turbulence¹⁷ has been conducted on an acceleration trace from 3284 flying hours. From these data, the peak counts from twenty-four patches of turbulence containing the larger loads have been extracted and the statistical properties compared with power-spectral predictions.

Another area of interest that is being investigated is the degree of warning available when encountering severe turbulence. Many aircraft have a

maximum rough airspeed which is below the cruising speed and are required to slow down in turbulence. The continuous records have made it possible to estimate the frequency with which the pilot was able to slow down before encountering the largest acceleration in the patch of turbulence. Initial results indicate that some action was taken by the pilot in 60% of the occurrences analysed.

4 FATIGUE RESEARCH

4.1 Crack propagation

A series of crack propagation tests on 10 inch wide sheet panels of aluminium alloy 2024-T3 with length-width ratios of 1, 2, 3 and 4 has been completed¹⁸. These tests examined the variation in crack propagation rates with panel width under nominally the same mean and cyclic stresses. The results indicated that at the highest nominal stress $10000 \pm 8000 \text{ lb/in}^2$, the measured crack growth rates varied with length-width ratio. The highest rate recorded was on the 1 : 1 panel with the 2 : 1 and 3 : 1 panels some 40% lower. Strain gauge examination of the strain field at the test section indicated that a correlation existed between the crack growth rate and the measured static strain distribution. It was recommended that a length-wide ratio of 2 : 1 should be adopted as a standard crack propagation test piece. This avoids the higher strains at the test section recorded in the 1 : 1 panel which were thought to be caused by end effects and also it avoids the possibility of panel resonance effects if longer panels are used.

A test programme to investigate one aspect of the influence of stringer geometry on crack propagation in stiffened L72 sheet has been completed¹⁹. For these tests stiffeners were Araldite bonded to the sheet, transversely to the axis of loading and the crack propagated between and parallel to the stiffeners. Two types of stiffener were tested, both providing similar restraint in the plane of the sheet but one presenting much greater lateral stiffness to sheet bowing. It was found that both types of stiffener reduced crack propagation rate to a similar and marked extent once the crack had exceeded about 20% of critical crack length. It was deduced that the crack growth rate depends on the restraint provided in the plane of the sheet and that the ability of a stiffener to prevent bowing or buckling is of little consequence in flat specimens under uniaxial loading.

As part of a programme of tests at room temperature on mill annealed and duplex annealed American manufactures Tl-8 Al-1 Mo-1V alloy sheets, fluctuating

tension fatigue tests have been made on plain and holed test pieces²⁰. Fatigue crack propagation, residual strength and fracture toughness tests have also been conducted. The results indicated that the duplex annealed material had superior toughness and at low stress levels an improved fatigue crack propagation performance, compared with mill annealed material. These improvements were gained at a small, approximately 5%, drop in tensile strength.

The effects of environment and test frequency on crack propagation in aluminium alloys are being studied. Tests of aluminium alloy RR 58 in wet air, dry air, water vapour and oxygen and vacuo have been completed²¹ and the results indicate that for this alloy the observed frequency effects are likely to be due to environmental corrosion.

A bend method of measuring the crack propagation characteristics of thick sections has recently been developed²² at the R.A.E. The apparatus consists essentially of a cantilever beam 22 inches long with a test piece 6 inches \times $\frac{1}{2}$ inch \times 1 inch forming the centre section of the beam and having a $\frac{1}{8}$ inch deep crack starting notch. The cantilever is rigidly clamped at one end and oscillated through a known amplitude at the free end by means of an eccentric driven by an electric motor. The throw of the eccentric can be varied in fixed steps to set the stress in the test piece at the start of the test. Since the bending moment will reduce as the crack propagates a strain gauge system has been developed to monitor the change in bending moment with crack propagation rate. The cycling frequency can readily be changed by using a variable speed driving motor.

Tests have been conducted on a number of materials, including a 65 tons/in² EN24 steel. The results from these tests indicate good agreement with similar crack propagation tests in tension. Some tests have been conducted at 100°C with the same apparatus and, for these tests a special remote measuring electric resistance method of measuring crack length has been developed²³. Further elevated temperature tests are planned extending up to 300°C. Results are presented in terms of a crack rate versus crack tip stress (or strain) intensity factor and a general law for fatigue crack propagation based on crack tip strain has been proposed²⁴.

The results of work on crack propagation at the National Engineering Laboratory, East Kilbride has revealed a different approach to the problem of determining the conditions for fatigue crack propagation. A report²⁵ has been

prepared discussing the effects of a tensile mean stress on the value of the cyclic stress necessary just to cause an edge-crack of length ℓ to grow in a mild steel plate. The results follow the same general pattern of behaviour as was found under completely reversed loading cycles, that is, whether or not a crack grows depends on the value of the parameter $\sigma^3 \ell$; if $\sigma^3 \ell > C$ (an experimental constant) a crack will grow, if $\sigma^3 \ell < C$ a crack remains dormant. However, the value of C when a tensile mean stress is present cannot be predicted simply from the corresponding zero mean load value, since as the tensile mean stress increases it appears to approach the value of $\sigma^3 \ell$, derived from the crack growth rate relationship for mild steel, i.e. $dc/dn = 0.09 \times 10^{-6} \sigma^3 \ell$, assuming that a crack will remain dormant if its growth rate is less than one atomic spacing per cycle.

Rotating bending tests on sharply notched specimens (in which the whole life is spent in propagating a crack through the specimen cross-section) have been carried out in oil, water and brine to study the effects of either keeping the atmosphere away from the crack tip or of a corrosive environment on the crack growth rate characteristics. A paper has been written²⁶ discussing the results obtained on mild steel and aluminium alloy specimens.

Tests on the crack growth rate characteristics²⁷ of various aluminium alloys show that the pronounced mean stress dependence of these alloys is related to their fast fracture characteristics. A paper²⁸ has also been written proposing a theory of fatigue crack growth based on the assumption that the crack length increases each cycle an amount proportional to the change in length of that part of the crack tip profile which is subjected to tensile stresses. Experimental work has started to determine the rate of crack growth at low frequencies (approx. 10 c/min) and high stress levels in order to check the validity over a wide range of conditions of the previous crack-growth data accumulated at high testing frequencies and relatively low stress levels. An infra-red photographic technique for monitoring crack growth rate of high temperature crack propagation tests is being developed²⁹. Preliminary results indicate that the crack tip is defined accurately thus allowing accurate measurements to be made.

4.2 Residual strength and fracture toughness investigations

During the past two years there has been increasing interest in fracture mechanics and more facilities for fracture toughness testing have been made available.

A great deal of data on the value of the fracture toughness parameter in the three principal directions is being accumulated for both aluminium and titanium alloys. The effects of testing techniques, such as the speed and form of loading, the level of the fatigue stress for crack formation and the size and design of the specimen, on the measured value of the parameter are being investigated. Alloy composition variations are being tried to give optimum fracture toughness values without excessive reduction in other important properties such as U.T.S., fatigue resistance and stress corrosion resistance. The heat treatment and position of the specimen from within a forging are variables being studied.

It is generally acknowledged that the fracture toughness parameter K_{1C} is of value at the design stage when assessing the various properties of the candidate materials but it is not so certain to what extent K_{1C} can be used quantitatively in a service problem. The difficulty appears to lie in the complex stress analysis problem which so often obtains in the vicinity of cracks which occur in "solid" structural components. As a first step some fifteen problems have been listed (e.g. loaded hole with asymmetrical corner crack) which typify, in a simplified form, the types of problem that have arisen. Theoretical stress analysis solutions exist for two or three only of these problems and a programme of work is being considered aimed at approximate solutions to be checked by experiment for the other cases. If this work is fruitful, it may be possible to relate the service problem, for which adequate theoretical analysis may be impossible in the time available, to one of the simplified cases and thus to obtain quickly at least some quantitative appreciation of the problem.

Static strength tests on plates and sheets of steels of differing strengths and ductilities containing fatigue cracks of different lengths have been carried out to determine values of the fracture mechanics parameter K_{1C} . The results³⁰ obtained, together with data taken from the literature, show that there is a correlation between K_{1C} and the reduction of area measured in a conventional tensile test. Tests to determine the fatigue crack growth characteristics and K_{1C} for beryllium copper sheets heat treated to various ductilities have also been carried out. Results³¹ so far, together with some test results for perspex suggest that for a constant reduction of area, K_{1C} is proportional to the square root of Young's modulus. As part of a collaborative research programme, tests to determine K_{1C} have been started on fatigue cracked high strength steel specimens.

The residual strength of L65 joint specimens cracked in fatigue was discussed in a previous review paper¹. A report covering the full details of the test programmes and results has now been formally issued³².

As an extension to a fatigue substantiation exercise, twenty D.T.D. 683 spar booms have been statically tested after allowing fatigue cracks to propagate to varying depths within the spars. The results³³ confirmed that a large reduction in static strength results from a very small fatigue cracked area, for example a 10% loss of area due to a fatigue crack reduced the static strength of the spar by 70%.

4.3 Fatigue of pressure vessels

The test programme in an internal-pressure combined-stress fatigue machine has now commenced; the first stage, viz. the determination of the stress/endurance curve for cylinders of diameter ratios $K = 1.20$ and 2.0 subjected to pulsating internal pressure only is nearing completion. A complementary programme of similar tests on thin walled cylinders of larger diameter i.e. $K = 1.015$ has also been commenced, using new 2 ton/in^2 capacity pulsating pressure equipment.

4.4 Cumulative damage studies

Initial investigations on cumulative damage studies being conducted at the Royal Aircraft Establishment were reported at the 1965 I.C.A.F. Conference¹.

This work is continuing; the object being the development of a method of life prediction based on the use of data obtained under random loading conditions. The results of tests on aluminium alloy specimens showed Miner's Rule to underestimate fatigue life, when using data obtained under sinusoidal loading conditions, by a factor which increased with value of maximum stress in the stress-time history. This also applied to the rule based on random loading data, but the life factor ($\sum n/N$) was not as great as for Miner's Rule, indicating some improvement in prediction for the new rule. It is believed that these results can be explained by consideration of the beneficial effects of residual stresses, at stress concentrations, which result from plastic deformation under high loads in the stress-time history; as a result of the plastic deformation the mean stress is effectively reduced at the point of fatigue initiation. Such considerations can also explain the increase in $\sum n/N$ with mean stress³⁴. Work is now in progress on a programme using L65 and RR58 lug specimens, investigating the effect of mean and peak stress on fatigue

life prediction. The first part of this work, the effect of mean stress, is well advanced, the results so far showing the expected increase in $\Sigma n/N$ with both mean and peak stress. The next stage in the work will be to test the cumulative damage behaviour of lug specimens under narrow band random loading conditions, first with initial residual stresses due to preloading, and subsequently with high tensile and/or air-ground-air cycles at various stages in the fatigue life.

In support of the main cumulative damage effort which is using only narrow band random loading to represent the variable amplitude loading condition, a programme has just been started to assess the effect of power spectrum shape on the fatigue behaviour of L65 lug specimens under stationary and variable rms random loading conditions. Tests will be carried out using narrow band, wider band single hump, bimodal and low pass filter power spectrum shapes, together with comparative block programmed tests.

The effect of loading waveform is to be investigated on aluminium alloy notched specimens. First tests will use a trapezoidal waveform and will explore the effects of varying frequency, loading rate, and the period of dwell at peak loads in order to assess the relative importance of these parameters to fatigue endurance.

The National Engineering Laboratory have also initiated a research programme on cumulative damage. A large number of direct-stress³⁵ and rotating-bending tests³⁶ on plain and sharply-notched specimens of mild steel, aluminium alloy and brass have been carried out, using various load programmes, to obtain a general background knowledge of the effects of varying-amplitude stresses on fatigue life and to establish the shortcomings of existing methods of endurance prediction. Most recent work has been concentrated on more accurate simulation of service conditions using two random-loading rigs³⁷ which apply a Rayleigh distribution of random stress amplitudes and a new machine with which the stress can be programmed on seven levels in a regular or random manner by means of a punched tape input.

4.5 Monitoring of fatigue damage

Two new methods which may give a measure of the relative severity of fatigue loadings in aircraft structural members are at present being assessed, using structural elements.

In the first method, which was developed in the United States, a "fatigue life gauge" is bonded to the element. The gauge undergoes a progressive change of resistance under strain cycling and this resistance change may be used as a measure of the overall severity of the loading action. Preliminary tests at R.A.E. and in Industry have confirmed however, that the change of resistance of the gauge is proportional to the work done in strain hardening the gauge material and is not affected by load sequence effects which may in fact greatly influence the fatigue life of the parent member, i.e. the gauge is carrying out a process more or less analogous to the Palmgren-Miner cumulative damage sum. The comparatively high threshold sensitivity of the gauge, somewhat above 1000 micro strain, causes difficulty in application and work is in progress in Industry to develop a simple strain multiplying device to overcome this problem. Notwithstanding the limitation of the gauge in the present state of development, work is going ahead on possible applications to service problems.

In the second method, a thin sheet coupon containing a small fatigue crack is attached to the element so that it undergoes a strain history corresponding to that experienced by the element. The consequent growth of the crack in the coupon may give an adequate measure of the amount of fatigue damage suffered by the element. It is hoped that this type of coupon will prove to be more satisfactory than the notched coupons tried previously in that it should give a continuous indication of the accumulation of fatigue damage without the scatter associated with nucleation in the notched coupons.

4.6 Fatigue of bolts

An investigation³⁸ has been made of the fatigue performance of a bolt when the seating of the nut is inclined to the axis of the bolt. For these tests $\frac{5}{8}$ inch S. & W. steel bolts were used having $\frac{5}{8}$ inch B.S.F. machined threads. The steel bolts were tested in fluctuating axial tension for inclinations of nut seating in the range 0° to 4° .

It was found that there was a progressive reduction in endurance with inclination, the highest rate of reduction occurring at an inclination between 1° and 2° . The reduction in endurance also varied with stress level, being most marked at low stress amplitudes. The corresponding reductions in fatigue strength for a given endurance are significant. For example, 1° inclination can reduce fatigue strength at 10^7 cycles by 40%.

4.7 Fatigue properties of a new Al-Zn-Mg alloy

Tests have been commenced on a new Al Mg Zn alloy which, in plain specimen form, has shown considerably better fatigue performance than the commonly-used Cu and Zn aluminium alloys. Lug and joint specimens in the new alloy and in L65 are being tested comparatively under constant amplitude and variable amplitude loading.

4.8 Fretting-fatigue

A Report³⁹ has been prepared on the effect of mean stress, range of slip and clamping conditions on the fretting-fatigue strength of a 67 ton/in² En 26 alloy steel. Similar work on L65 aluminium alloy has proceeded; the original programme employing $\frac{1}{2}$ ton/in² contact pressure is being supplemented by further tests under 2 ton/in² contact pressure. Comparative tests on a 100 ton/in² En 30B steel have been completed and a report is being prepared.

The fretting-fatigue strength under zero mean stress of rough-machined specimens (200 micro-inch C.L.A.) of the En 26 steel was about double that of polished specimens (4 micro-inch C.L.A.); a similar but less pronounced effect of rough-machining was observed for the L65 aluminium alloy. In the case of the En 26, tests have also been carried out on rough-machined specimens stress-relieved in vacuo before the fretting-fatigue test. These indicated that the higher fretting-fatigue strength of the rough-machined specimens was chiefly due to favourable machining stresses.

Anti-fretting treatments investigated recently have included a copper-bearing grease, locking liquids and cold polymerising resins (with reinforcements including a commercial mica-iron oxide mixture), glass beads and a single fabric layer. When incorporated into a bonded layer of epoxy resin, the latter was very effective on the L65 under 2 ton/in² contact pressure at moderate slips, but wore through in a million cycles at a slip range of 2×10^{-3} in. Commercially bonded coatings of molybdenum disulphide increased the fretting-fatigue strength of the En 26 by 50 per cent under zero mean stress but had no effect under mean stresses of 25 ton/in² and above. A similar treatment applied to the L65 had little effect on its fretting-fatigue strength.

4.9 Basic mechanisms

Some metallographic studies on shear mode fatigue fractures in aluminium alloys Al-7.5 Zn-2.5 Mg and Al-2.5 Cu-1.5 Mg have been conducted⁴⁰. It has been

demonstrated using optical and transmission electron metallography that damage zones are produced by reversed slip ahead of shear mode fatigue cracks. Examination of shear mode fatigue fractures using fractography, optical metallography and the Laue back reflection technique, has shown that shear modes fracture occurs on $\{111\}$ planes.

A comparison has been made of the fatigue behaviour of two aluminium-zinc-magnesium alloys⁴¹. The torsional fatigue deformation of two aluminium alloys, Al-7.5 Zn-2.5 Mg and Al-4 Zn-5 Mg, has been examined in various conditions of heat treatment. Two well defined deformation modes were observed, one in which localised trans-crystalline slip produced narrow zones of precipitate re-solution, and another in which localised deformation occurred in the precipitate depleted zones at the grain boundaries. An attempt was made to correlate the torsional deformation modes of the two alloys with the fracture modes observed on rotating bending corrosion fatigue test pieces. It was found that test pieces of the Al-7.5 Zn-2.5 Mg alloy, subjected to torsional fatigue in certain conditions of heat treatment, exhibited localised trans-crystalline deformation and precipitate re-solution, and that rotating bending test pieces in these same conditions of heat treatment exhibited extensive shear mode crack growth when fatigued in aqueous 3% NaCl solution. In the Al-4 Zn-5 Mg alloy there was no correlation between localised trans-crystalline torsional fatigue deformation and shear mode failure on rotating bending corrosion fatigue test pieces. In the latter alloy the grain boundaries exhibited a high corrosion susceptibility and the initial shear mode growth stage was replaced by intercrystalline crack growth.

Further work⁴² has been done in comparing the fatigue behaviour and microstructural damage that occurs in two aluminium alloy compositions, Al-7.5 Zn-2.5 Mg and Al-4 Zn-5 Mg. Particular emphasis has been placed on the relation between corrosion fatigue and stress corrosion in these two compositions. It can be shown that the former alloy in the fully age hardened condition fails in a trans-crystalline mode in both air and 3% NaCl solution whereas changing the environment with the second alloy changes the mode of fracture encouraging inter-crystalline crack growth. Furthermore this inter-crystalline fatigue crack growth is similar in mechanism to stress corrosion failure in this alloy.

A detailed study⁴³ of the corrosion fatigue and stress corrosion cracking of the Al-4 Zn-5 Mg alloy has also been conducted in two conditions of heat-treatment, i.e. aged to peak hardness at 120°C and at 150°C. The frequency

used for most of the fatigue tests was 20 c/min, but comparisons have been made at frequencies of 180 and 1500 c/min. The $s/\log n$ curve at 20 c/min showed a clearly defined "knee" and fatigue limit. Progressively lower fatigue lives were obtained at the higher test frequencies. All crack paths were inter-crystalline under both corrosion fatigue and stress corrosion conditions, although air fatigue cracks in this material are mainly trans-crystalline. The effect of both anodic and cathodic polarization have been studied. Marked changes in crack growth rate were observed when a fatigue specimen was alternately made anodic and cathodic in a 3% NaCl solution against either a platinum or aluminium electrode with an externally impressed current. Similar changes in crack growth rate could be obtained with impressed currents under steady stress corrosion conditions. Stress corrosion crack growth rates have been shown to be dependent on the chloride ion concentration of electrolytes used, suggesting a metal dissolution mechanism of stress corrosion in this material.

5 DESIGN DATA ON MATERIALS AND STRUCTURAL ELEMENTS

Whilst the basic research work described in the preceding sections provides for a greater understanding of particular phenomena, it can never provide information in sufficient depth for the aircraft designer. Therefore extensive test programmes are initiated to evaluate the properties of various forms of engineering materials. These investigations cover batch-to-batch variations of material from various sources. From these the overall average properties of the material can be evaluated, as well as the relevant scatter information. A probability method can then be used to determine safe design values.

The basic fatigue properties of materials at room temperature form a large proportion of the work done in this field and examples of recent work reported are the fatigue strengths of pre-forged RR 58 plate⁴⁴ of extruded DTD 5014 bar⁴⁵ and of extruded DTD 5014 sections⁴⁶.

As previously mentioned the Concord project has inevitably demanded information on creep-fatigue interaction on various materials. The design data tests so far implemented include fatigue tests without creep periods, fatigue tests with creep and simple creep tests without fatigue. The fatigue cycles O-P-O and $P \pm p$ are both used considerably but consideration is being given to a Gassner type of loading with a Rayleigh distribution of peak loads. A report⁴⁷ covering recent work on 2024-T81 material has been prepared.

In addition to the above mentioned work on materials, a large amount of work is being done on the fatigue of hydraulic tubes and tests covering the temperature range -40°C to 225°C have recently been concluded⁴⁸.

Publication of the above work is sometimes done in official documents and sometimes in Data Sheets issued by the Royal Aeronautical Society. In particular the Technical Department of the R.Ae.S. under the guidance of its Fatigue Committee has published Data Sheets on the following subjects in the last two years:-

- | | |
|--|---|
| Supplementary notes on the fatigue strength of aluminium alloys. | - Information on effects of type of loading, surface treatments and surface condition. |
| Effect of mean stress on endurance of aluminium alloys. | - Typical S-N curves for 3 groups of aluminium alloys. |
| Fatigue limit of steels. | - Correlated experimental data. |
| Brief specification of axial loading fatigue testing machines. | - Tabular summary of machine capacities. |
| Estimation of endurance of pin joints. | - Semi-empirical method for single or multi-pin joints with or without interference (revision). |
| Fatigue crack propagation rates. | - Correlated data for DTD 5070A aluminium alloy. |
| Stress concentration data. | - Revised and extended data on a wide range of bar, tube and plate geometries. |
| Introduction to design information on acoustic fatigue. | - Outline of design/analysis procedure. |
| Definitions of terms for acoustic fatigue analysis. | - |
| Short bibliography on acoustic fatigue. | - |
| General principles for design of acoustically excited structure. | - Brief summary of good design practice. |
| Bandwidth correction. | - Conversion curves. |
| Combination of levels in dB. | - |

- | | |
|---|---|
| The relation between sound pressure level and rms fluctuating pressure. | - Conversion curves. |
| Natural frequencies of uniform flat plates. | - Theoretical curves. |
| Natural frequencies of flat sandwich panels. | - Theoretical curves and Algol program. |
| Estimation of rms stress in skin panels under acoustic loading. | - Approximate theoretical method. |
| Endurance of riveted skin-rib flange connections. | - Experimental data. |

The Committee is currently considering the following items:

- | | |
|--|---|
| Endurance of bolts. | - Revision and extension of data, in conjunction with I.Mech.E. Committee. |
| Endurance of steels. | - Correlated data. |
| Endurance of cylinders, under internal pressure. | - Correlated data. |
| Statistical methods in fatigue analysis. | - Extension of existing information to include extreme value/Weibull distributions. |

6 FULL SCALE TESTING

The policy of doing full side testing on all major projects has been maintained and there is a growing tendency for these tests to be more complex. In one major test which is now almost finished, the loading sequence within each simulated flight was randomised. Each flight was divided basically into three levels of gusts and three levels of manoeuvres with a predetermined number of cycles of each level within each flight. An additional high level manoeuvre load was applied at each hundredth flight. In each flight, the gust loads were applied first and were followed by the manoeuvre loads. This was necessary to allow for a change in loading condition between the two sets of loads. The gust loads were broken down into three positive half cycles relative to the 1 g flight condition and three negative half cycles. The order in which these were applied was determined by random selection, but once the total number of cycles of a given level for a particular flight had been applied, any

further selections of that level were ignored for the remainder of that flight. A similar system of selection was used for the three manoeuvre load levels each cycle of which consisted of an excursion from 1 g to the positive level chosen, down to an associated level below 1 g and return to 1 g. No difficulties have been experienced in running this system. Another major test, about to start in the near future, will also use a randomised sequence on a flight by flight basis. In this case however, no restriction will be made on the number of loads at a given level within a particular flight but reliance will be placed on defining the overall proportions of the various load levels, so that in a reasonably long sample the numbers of loads at each level will approximate closely to that required. Since the programme will be predetermined and stored on tape, the actual numbers of cycles at any level at any time will be known accurately. In this system, although gust loads have again been broken down into positive and negative half cycles a restriction will be imposed to ensure that a positive half cycle is always followed by a negative half cycle but not necessarily of the same magnitude. Mention was made in section 2.5 that for the Concord component tests provision is made for pre-randomized load sequences controlled and monitored by computers.

The ground to air load cycle has been a significant part of major tests for some time and the ground phase of tests has been extended by applying ground taxiing loads. The need for these ground loads has been emphasised by instances of upper wing surface fatigue cracks outboard of undercarriage stations. It is considered that these fatigue cracks are the direct consequence of tensile load oscillations during taxiing. It is worthwhile noting that in this respect aircraft having undercarriages attached only to the fuselage would appear to be particularly vulnerable to this type of failure.

During the period of this report several civil aircraft types have been fatigue tested: in particular the H.S.A. Trident and the B.A.C. V.C.10 and 111 aircraft. The particular feature of the Trident and V.C.10 test programme was the use of a single full scale test specimen to cover both the static and fatigue clearance of the aircraft.

In the case of the Trident, the fatigue programme was sub-divided into flights of three basic severities each containing multi-amplitude gust loads as well as ground to air cycles and taxi loads. The specimen was initially loaded to 50% of ultimate to check stress calculations and then fatigue cycled for 10000 test fatigue cycles before static proof loading to 66.6% of ultimate.

This type of testing, with fatigue cycles regularly interspersed with static load applications continued successfully to 60000 test flights. At 40000 test flights artificial cracks (saw cuts) were introduced into one wing in order to study crack propagation rates and residual strength characteristics. It is now planned to continue the testing on to 100 000 flights.

The V.C.10 test, however, concentrated most of the static tests prior to the fatigue load application although no static loads were applied in excess of proof loading. The fatigue loads were applied flight by flight in block programme form with ground to air cycles and taxi loads. The pressure cabin was not fatigue cycled since the hoop stresses due to pressurization were small. However a proof load test was conducted on the fuselage using air as the pressurization medium; the cabin being filled with foam plastic to reduce the explosion risk.

The B.A.C.111 aircraft was tested in a more conventional manner; there being a complete static strength specimen as well as a separate fatigue test specimen. The fatigue test is being conducted in a water-tank under block programme loading with six gust levels, ground to air cycles and taxi loads.

7 ACOUSTIC FATIGUE

7.1 Loading actions

Work to acquire more data on certain 'acoustic' load inputs has continued. Flight measurements of the spectral density of pressure fluctuations in thick boundary layers have been completed⁴⁹, and indicate that Strouhal number based upon boundary layer displacement thickness provides an adequate frequency parameter even at low frequencies. The results also showed that the root mean square level of the pressure fluctuations is still better related to kinetic pressure q rather than wall stress as suggested by some workers, although in both cases there is Mach number dependancy. Preparations are in hand to measure pressure spectra and spacial correlation at $M = 2.2$, in flight, to substantiate present estimates of the level likely on Concord.

Interest also continues in the pressure fluctuations beneath leading edge vortices on slender delta planforms. Early measurements indicated a potential fatigue hazard. Flight measurements have been taken on an HP.115 aircraft⁵⁰, and these confirm the early measurements taken in wind tunnels and on free-flight tests on models. The spectral density under the vortex shows a

two-humped form, the lower hump being attributed to the low-frequency content of the vortex, and the upper one to the boundary layer contribution, which has an enhanced level when compared with the free-stream boundary layer.

Present indications suggest that this form of loading action may contribute to fatigue damage only at the comparatively high angles of incidence associated with climb and descent, and also if appreciable sideslip is experienced. Further flight measurements of pressure fluctuations are being taken beneath the vortex of the B.A.C.221 'ogee' delta at more representative Reynolds numbers, and measurements of structural response are also being taken as a check on estimates of the generalised forces associated with Concord wing panel response.

In the past two years a special form of jet-efflux noise has arisen during flight and has come to be known as shock-cell noise. It is associated primarily with highly-choked engines, and is particularly strong on engines having convergent-divergent nozzles. It takes the form of relatively narrow-band noise, of high spectral density, the centre frequency changing with altitude. Structural damage from this cause has taken place on two types of civil aircraft. Full scale flight tests are being conducted by industry, and scale model research is being done by N.G.T.E. and Industry aimed at reducing the intensity of the noise at source.

7.2 Response of structures to acoustic excitation

By far the most important development in calculating the response of a structure to random excitation is the use of a new analytical approach using a quasi-statistical method based upon a modal density concept. Preliminary experiments indicate a high degree of correlation with theory provided a large number of modes are present. Experiments are now in hand to measure the response of typical aircraft structures where errors might result from the presence of highly preferred modes. The method also holds out hope for predicting the sound radiated from aircraft structures excited by wide band noise and a flight programme is being carried out, using a Comet aircraft, to measure structurally radiated sound, and to relate this to the estimated value based upon this new method of response prediction.

7.3 Acoustic fatigue testing

The acquisition of design data for simple structural elements using direct excitation from an electrodynamic exciter continues. Some results have

been published in R.Ae.S Design data sheets for riveted skin stringer intersections under random loading and tests are currently in progress on similar types of specimen but incorporating detail design changes e.g. increased thickness of skin along rivet line. Tests are commencing on box specimens tested in a siren facility to check whether the fatigue performance predicted from the data on small elements is achieved in more complex structural assemblies. The work, reported in the 1965 review paper¹, in which an attempt was made to induce the correct stress pattern in a complete tailplane using sinusoidal electrodynamic excitation proved to be successful insofar as stress distributions could be induced in the skin, stringers and ribs which showed relative severities corresponding to those measured in a true noise environment. However it was found impossible to produce fatigue failures in a reasonable time due to limitations on power input. It is hoped to continue this work using random force input and energy levels high enough to induce failures. "Ad hoc" work continues using siren facilities or jet engines to help in design problems and problems which arise in service.

Acknowledgements

The authors wish to acknowledge the valuable assistance given them in the preparation of this paper by their colleagues in Structures Department, R.A.E., Chemistry, Physics and Metallurgy Department, R.A.E., National Engineering Laboratory and the United Kingdom aircraft industry.

REFERENCES

<u>No.</u>	<u>Author</u>	<u>Title, etc.</u>
1	E.L. Ripley R.D.J. Maxwell	A review of work in the United Kingdom on the fatigue of aircraft structures during the period May 1963 - April 1965. R.A.E. Technical Report 65193 (1965)
2	N'Guyen E.L. Ripley	Fatigue design philosophy and testing of the Concord. Paper to be presented to Fifth ICAF Symposium (1967)
3	J.R. Heath Smith F.E. Kiddle	Influence of ageing and creep on fatigue of structural elements in an Al 6% Cu alloy. Unpublished Min. Tech. Report
4		Symposium on aircraft loading actions problems, October, 1966. Unpublished Min. Tech. Report
5	N.I. Bullen	A review of counting accelerometer data on aircraft gust loads. R.A.E. Technical Report 66234 (1966)
6	N.J. Bullen	A review of information on the frequency of gust at low altitude. A.R.C. C.P.873
7	N.I. Bullen	The chance of a rough flight. A.R.C. C.P.836
8	E.W. Wells	Project Topcat. Summary of meteorological observations and aircraft measurements during routine flights in Australian jet stream. R.A.E. Technical Report 66122 (1966)
9	Anne Burns C.K. Rider	Project Topcat. Power spectral measurements of clear air turbulence associated with jet streams. R.A.E. Technical Report 65210 (1965)
10	J.K. Zbrozek	Vertical accelerations due to structural vibrations of a slender aircraft flying in continuous turbulence. R.A.E. Technical Note Aero 2901 (1963)

REFERENCES (Cont'd)

<u>No.</u>	<u>Author</u>	<u>Title, etc.</u>
11	P.B. Hovell	Flight strain measurements and structural integrity of aircraft. Conference on stresses in service Proc. Inst. Civil Engineers (1966)
12	P. Person	Measurement of torsional fatigue loads on an aircraft undercarriage under service condition. Conference on stresses in service Proc. Inst. Civil Engineers (1966)
13		The civil aircraft airworthiness data recording programme. R.A.E. Technical Report 64004 (1964)
14		Civil aircraft airworthiness data recording programme. Special events of a meteorological origin (Nov 1963 - Dec 1964). R.A.E. Technical Report 65243 (1965)
15		Civil aircraft airworthiness data recording programme. Special events of an operational nature (Feb 1964 - Dec 1964). R.A.E. Technical Report 65242 (1965)
16	H. Hall	Some theoretical studies concerning oleo damping characteristics. R.A.E. Technical Report 66312 (1966)
17	G.R. King	Civil aircraft airworthiness data recording programme. Study of severe turbulence encountered by civil aircraft. Unpublished Min. Tech. Report
18	T.F. Carter	Crack propagation tests on 2024-T3 unstiffened aluminium alloy panels of various length width ratios. R.A.E. Technical Report 66366 (1966)

REFERENCES (Cont'd)

<u>No.</u>	<u>Author</u>	<u>Title, etc.</u>
19	P.H. O'Neill	A note on the effect of stringer stiffness on the growth rate of fatigue cracks in flat panels. Unpublished Min. Tech. Report
20	M.S. Binning N.F. Gunn G.I. Lewis	An evaluation of American manufactured Ti - 8 Al - 1 Mo - 1V alloy sheet. R.A.E. Technical Report 66207 (1966)
21	F.J. Bradshaw C. Wheeler	The effect of environment on fatigue crack growth in aluminium and some aluminium alloys. Appl. Met. Res. 5, 112 (1966)
22	S. Pearson	A bend method for measuring fatigue crack propagation in thick materials. R.A.E. Technical Report 66204 (1966)
23	D.M. Gilbey S. Pearson	Measurement of the length of a central or edge crack in a sheet of material by an electrical resistance method. Unpublished Min. Tech. Report
24	S. Pearson	Fatigue crack propagation in metals. Nature 211, 1077-78 (1966)
25	N.E. Frost A. Greenam	The effect of a tensile mean stress on the alternating stress required to cause an edge crack to grow in mild steel. Unpublished N.E.L. Report
26	N.E. Frost A. Greenam	Fatigue tests on sharply notched mild steel and aluminium alloy specimens in various liquid environments. Unpublished N.E.L. Report
27	N.E. Frost K. Denton	Fatigue crack growth characteristics of aluminium alloys. N.E.L. Report 260 (1966)
28	N.E. Frost J.R. Dixon	Fatigue crack propagation in metals. Nature, 212, 1569 (1966)

REFERENCES (Cont'd)

<u>No.</u>	<u>Author</u>	<u>Title, etc.</u>
29		An infra-red photographic technique for high temperature crack propagation rate measurement. Unpublished H.S.A. Ltd. Report
30	L.P. Pook	Correlation of a fracture mechanics parameter with mechanical properties for high strength steels. N.E.L. Report 225 (1966)
31	L.P. Pook	Fracture toughness and fatigue crack growth characteristics of beryllium-copper. Unpublished N.E.L. Report
32	G.R. Eynon W.T. Kirkby	Residual static strength of a bolted joist cracked in fatigue. R.A.E. Technical Report 66111 (1966)
33	-	The residual strength of cracked spar booms. Unpublished H.S.A. Report
34	H. Hardrath	Cumulative damage. <u>Fatigue - an inter disciplinary approach</u> Proc. 10th Sagamore Army Materials Research Conference (1963)
35	K.J. Marsh	Direct stress cumulative fatigue damage tests on mild steel and aluminium alloy specimens. N.E.L. Report 204 (1965)
36	K.J. Marsh	Variable amplitude rotating bending fatigue tests on aluminium alloy, brass and mild steel specimens. N.E.L. Report 263 (1966)
37	K.J. Marsh J.A. Mackinnon	Fatigue under random loading: development of testing rigs and preliminary results. N.E.L. Report 234 (1966)
38	F.E. Kiddle	Variation of bolt fatigue life with inclination of nut seating. Unpublished Min. Tech. Report

REFERENCES (Cont'd)

<u>No.</u>	<u>Author</u>	<u>Title, etc.</u>
39	J.E. Field D.M. Waters	Effect of mean stress, range of slip and clamping conditions on the fretting fatigue strength of EN 26 alloy steel. N.E.L. Report 275 (1967)
40	C.A. Stubbington P.J.E. Forsyth	Some observations on shear mode fatigue fracture in aluminium alloys. R.A.E. Technical Report 65159 (1965)
41	C.A. Stubbington P.J.E. Forsyth	A comparison of the fatigue behaviour of two aluminium-zinc-magnesium alloys. R.A.E. Technical Report 66201 (1966)
42	C.A. Stubbington P.J.E. Forsyth	Further observations on microstructural damage produced by torsional fatigue of an aluminium -7.5% zinc -2.5% magnesium alloy. R.A.E. Technical Report 65025 (1965)
43	P.J.E. Forsyth E.G.F. Sampson	Corrosion fatigue and stress corrosion cracking of an aluminium -5% magnesium -4% zinc alloy totally immersed in 3% NaCl and other corrodents. R.A.E. Technical Report 65158 (1965)
44	M.G. Bader	2nd interim report on fatigue strength of preforged and rolled aluminium alloy to specification HID RR 58. Battersea College of Technology Report B.C.T./MET/33
45	M.G. Bader	Fatigue strength of extruded bar in aluminium alloy to specification DTD 5014 at room temperature and in supersonic aircraft environment. Battersea College of Technology Report B.C.T./MET/34
46	M.G. Bader	Fatigue strength in extruded section in aluminium alloy to specification DTD 5014. Battersea College of Technology Report B.C.T./MET/35

REFERENCES (Cont'd)

<u>No.</u>	<u>Author</u>	<u>Title, etc.</u>
47	M.G. Bader M.J. Morton	The intersection of ageing, creep and fatigue in a high strength aluminium alloy (2024-T81). Battersea College of Technology Report B.C.T./MET/37
48	H. Stott	Fatigue tests on stainless steel hydraulic tubing over the temperature range -40°C to $+250^{\circ}\text{C}$. Electro-Hydraulics Report R1164
49	K.H. Heron	Flight measurements of pressure fluctuations in a turbulent subsonic boundary layer and its relation to wall shear stress. Unpublished Min. Tech. Report
50	B.F. Fairhead K.H. Heron D.R.B. Webb F.L. Hunt	Flight measurements of fluctuating wall pressures and structural strains beneath the vortex in a highly swept wing. Unpublished Min. Tech. Report

N 69-21585

REVIEW OF INVESTIGATIONS ON AERONAUTICAL FATIGUE

IN THE FEDERAL REPUBLIC OF GERMANY

PERIOD OF REVIEW MAY 1965 TO MARCH 1967

Compiled by

E. Gassner

Laboratorium für Betriebsfestigkeit

Darmstadt-Eberstadt

(LBF Report S-73)

Note: Copyright permission for publication may be
granted subject to written application

TABLE OF CONTENTS

	<u>Page</u>
<u>SECTION I</u> - LABORATORIUM FÜR BETRIEBSFESTIGKEIT	
Improving Fatigue Life by the Use of Taper-Lok Fasteners W. Lipp	180
Selection of the Appropriate Method of Analysis for a Statistical Evaluation of Random Loads W. Lipp	183
Constant Amplitude Tests on Double-Shear Joints W. Schütz	187
Fatigue Strength of Various Heats of 18/7/5 Ni Co Mo Maraging Steel W. Schütz	189
Fatigue Strength of Aluminium Alloys W. Schütz	193
Influence of the Spectrum Shape on the Fatigue Strength of an Aluminium Alloy H. Ostermann	197
Fatigue Strength of Electron-Beam Welded Sheet of a Maraging Steel E. Haibach	199
Comparative Investigation on the Fatigue Strength of Chemically Etched and Mechanically Milled Test Specimens D. Schütz	203
Investigations in Progress or in an Advanced Stage of Preparation	207

SECTION II – HAMBURGER FLUGZEUGBAU GMBH, Hamburg

– VEREINIGTE FLUGTECHNISCHE WERKE GMBH, Bremen

Influence of Galvanic Cadmium Plating on the Fatigue Strength of
1.6604.6 (AICMA FE PL 74) Steel Lugs
HFB 210

Investigation on the Effect of Various Types of Rivets
VFW 213

Comparative Tests on Butt Welded and Notched Specimens of
1.7734.5 (AICMA FE PL 52 S) Steel
VFW 216

SECTION III

Technical Notes (TM) published by Laboratorium für Betriebsfestigkeit,
Darmstadt-Eberstadt, during the present Period of Review
(May 1965 to March 1967) 219

ICAF-Documents by German authors, distributed during the present
Period of Review (May 1965 to March 1967) 220

SECTION I

LABORATORIUM FÜR BETRIEBSFESTIGKEIT

Darmstadt-Eberstadt

Improving Fatigue Life by the Use of Taper-Lok Fasteners

Comparative variable amplitude tests employing an LBF Standard Distribution [ref. 1] have been performed on 2024-T3 specimens incorporating

countersunk rivets

and

Taper-Lok Fasteners.

The test results showed that the mean number of cycles-to-failure \bar{N} of the specimens with Taper-Lok Fasteners was 8.5 times that of the specimens with countersunk rivets (see Fig. 1).

Cracking originated at different points for the two types of specimen, viz.: For the countersunk-riveted specimens at the edge of the rivet hole, and for the specimens with Taper-Lok Fasteners in the undisturbed plate near the bearing surface of the nut, or else at points where fretting corrosion occurred between the faying surfaces in the area of the pressure cone (see Fig. 2).

The installation of the 5/16" conical Taper-Lok Fasteners induced an interference of between 0.0965 and 0.122 mm.

The scatter of 1 : 3.5 for a probability of survival between $P_S = 90$ percent and 10 percent was normal for the countersunk-riveted specimens, whereas for the specimens with Taper-Lok Fasteners the scatter of 1 : 14.5, attributable to the scatter inherent in interference fits or induced by different contact pressures, is exceptionally large.

Particulars

Type of loading	: axial
Stress ratio \bar{R} ($= \bar{S}_{\min} / \bar{S}_{\max}$)	: - 0.2
Material	: 2024-T3
Maximum stress amplitude of the load spectrum, \bar{S}_a	: $\pm 17.5 \text{ kp/mm}^2$ on net area
Endurance 1	: 10^6 cycles

W. Lipp

References

- [1] "Verwendung eines Einheits-Kollektivs bei Betriebsfestigkeitsversuchen",
LBF TM Nr. 15/65, Laboratorium für Betriebsfestigkeit, Darmstadt-Eberstadt.

Glossary of Terms used in the FiguresFig. 1

Bezogene Lebensdauer, \bar{N}	- reference endurance, \bar{N}
Probe mit Senknietung	- specimen with countersunk rivet
Probe mit Taper-Lok Fastener	- specimen with Taper-Lok Fastener
P_U	- probability of survival, P_S

Fig. 2

Einspannung	- grips
Bruchlage der Probe mit Senkniet	- fracture surface of the specimen with countersunk rivet
Bruchlage der Probe mit Taper-Lok Fastener	- fracture surface of the specimen with Taper-Lok Fastener

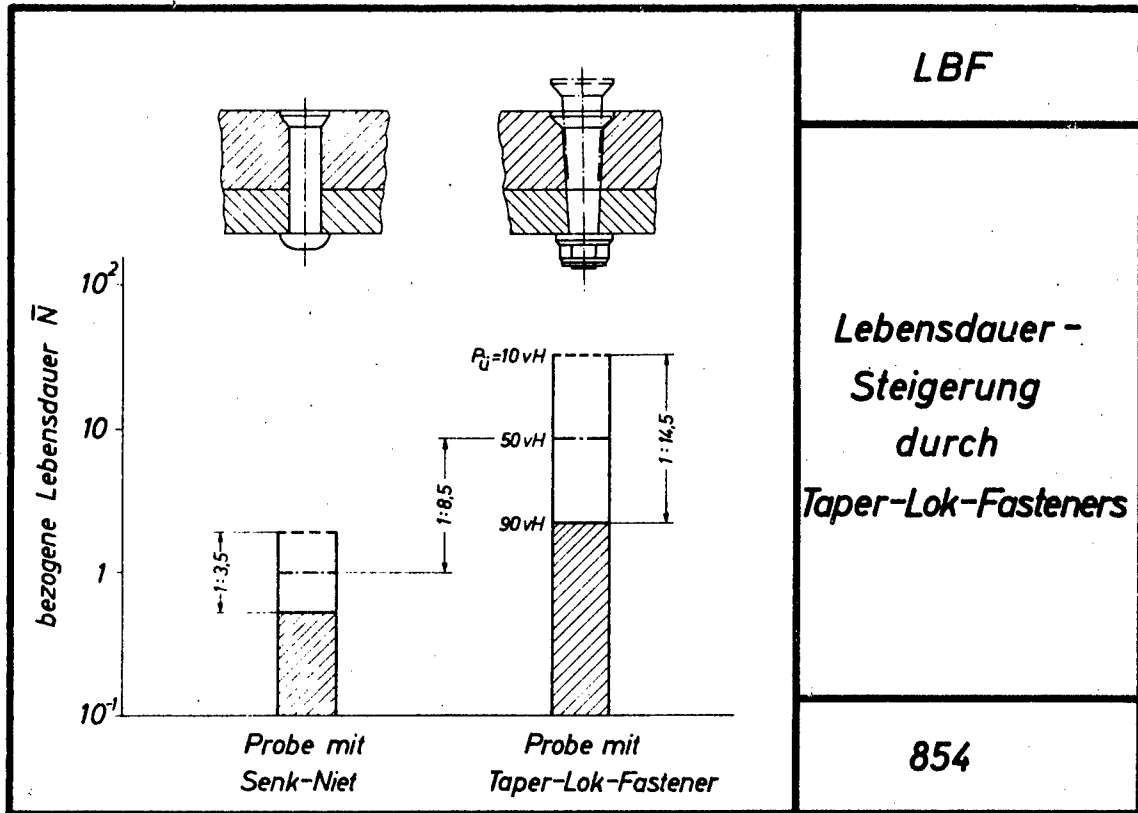


Fig. 1 Improving Fatigue Life by the Use of Taper-Lok Fasteners

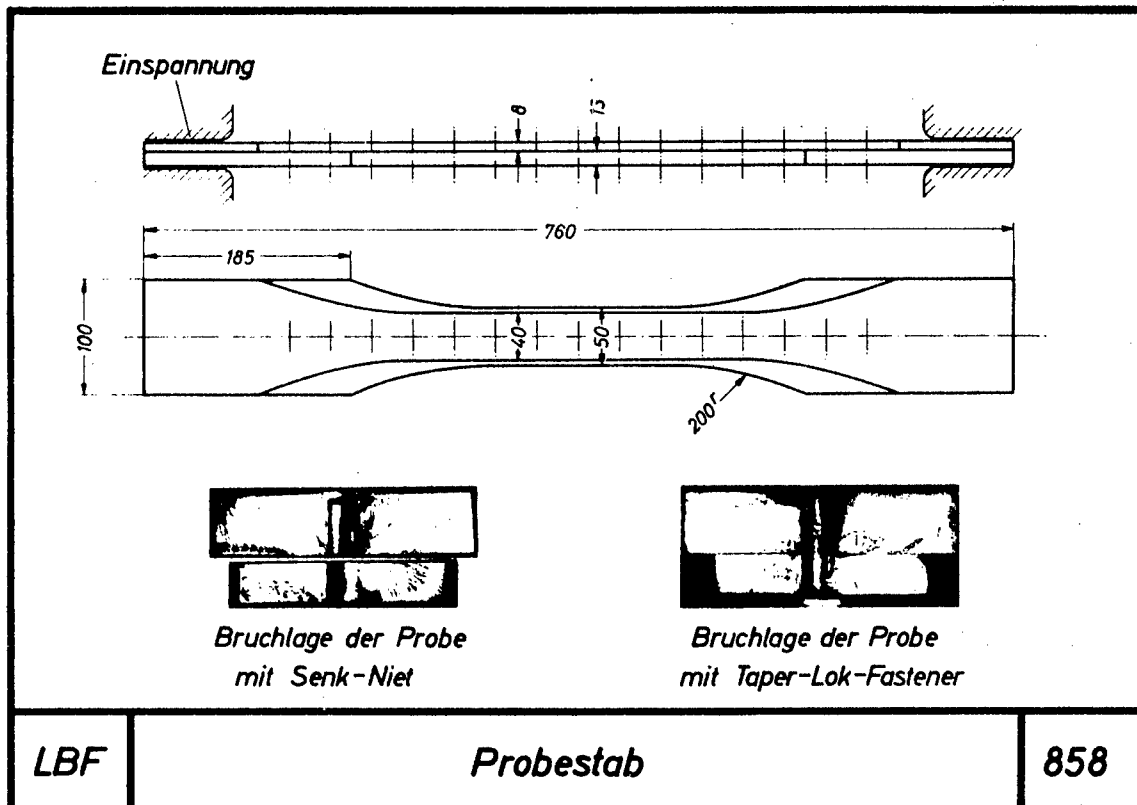


Fig. 2 Test Specimen

Selection of the Appropriate Method of Analysis for a Statistical Evaluation of Random Loads

Among the many methods of analysis presently available, there are two which have been used preferably in recent years, namely those of the cumulative frequency of level-crossings and the cumulative frequency of range-pairs.

These two methods of analysis, however, in most cases render stress spectra differing in shape (see Fig. 1) and, naturally, fatigue tests based on such spectra also yield differing fatigue strength results.

Two particularly characteristic types of actual loading conditions (see Fig. 1):

- A_1 constant amplitude sinusoidal basic oscillations, superimposed by constant amplitude oscillations at a ratio of 1 : 30, and
- A_2 constant amplitude sinusoidal basic oscillations, superimposed by stepwise decreasing constant amplitude oscillations at a ratio of 1 : 30

were analysed using each one of the two methods; with the four spectra achieved, fatigue tests were then performed and the test results recorded numerically.

For loading sequence A_1 , the fatigue lives obtained by employing the two methods of analysis differed by a ratio of 1 : 4; for loading sequence A_2 , the difference was 1 : 6.25 (see Fig. 2). Compared with the random loading sequence, the stress spectrum obtained by the level-crossing method renders conservative results, whereas the spectrum obtained by the range-pair method renders unconservative results.

The lives obtained by applying Miner's hypothesis to the four load spectra A_1/B , A_1/C , and A_2/B , A_2/C (see Fig. 1) show a fairly close agreement with test results.

Particulars

Specimen : solid circular rod with diametral hole
 Material : mild steel St 37
 Type of loading : plane bending
 Stress ratio \bar{R} : - 1

W. Lipp

Glossary of Terms used in the Figures

Fig. 1

Original-Spannungs-Abläufe	- actual loading sequences (A_1 , A_2)
$\bar{\sigma}_o$	- \bar{S}_{\max}
$\bar{\sigma}_u$	- \bar{S}_{\min}
sinusförmige Grundschiwingung	- sinusoidal basic oscillation
30 überlagerte Störschwingungen	- 30 superimposed oscillations
H_1 , H_2 ... = Anzahl der Grundschiwingungen mit jeweils 30 konstant überlagerten Störschwingungen	- H_1 , H_2 ... = number of sinusoidal basic oscillations, on each of which 30 constant amplitude oscillations are superimposed
Zugehörige Amplituden-Kollektive B und C	- associated stress spectra B and C
Häufigkeit H	- frequency, H
Überschreitungs-Häufigkeiten der Spannungs-Grenzen (B) bzw. Spannungs-Bereiche (C)	- cumulative frequency of level-crossings (B), or range-pairs (C), resp.

Fig. 2

bezogene Lebensdauer

A₁ bzw. A₂ = Original-Ablauf

B = Spannungs-Grenzen

C = Spannungs-Bereiche

D = Miner-Rechnung

siehe Bild 852

- relative fatigue life
- actual loading sequences, A₁ and A₂
- level-crossing method, B
- range-pair method, C
- Miner's hypothesis, D
- see Fig. 1

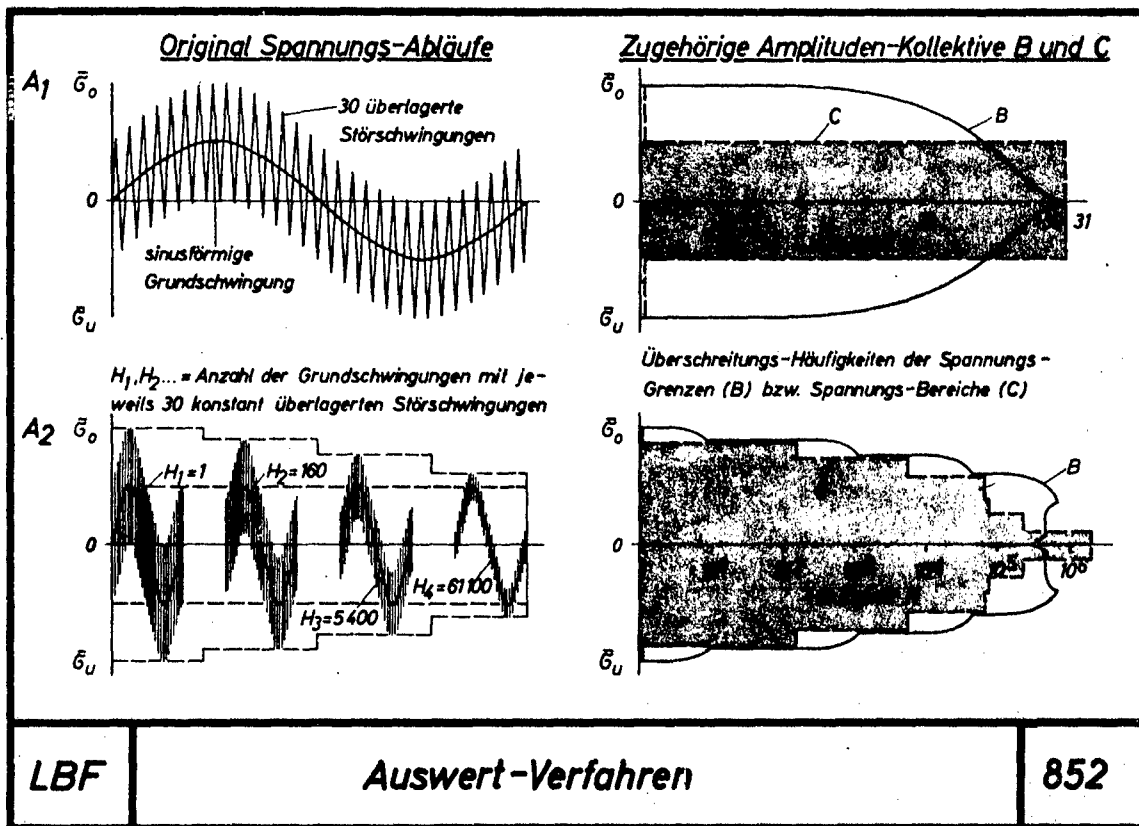


Fig. 1 Methods of Analysis

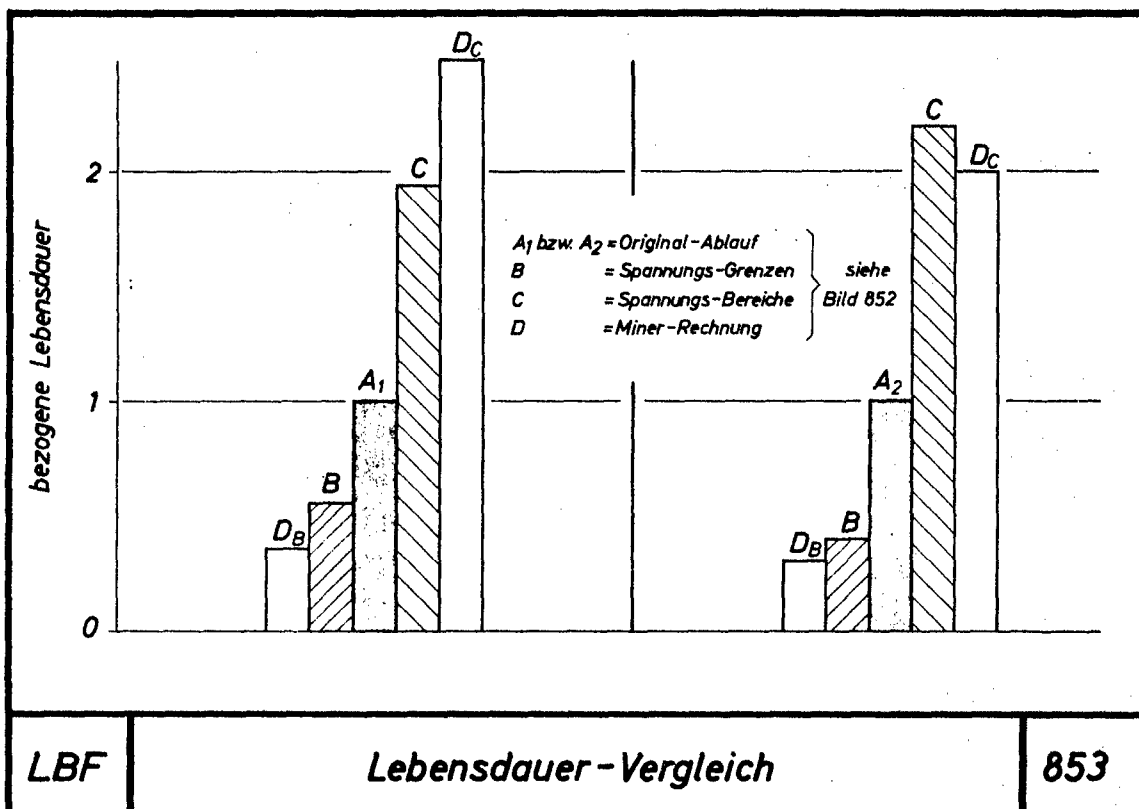


Fig. 2 Fatigue Life Comparison

Constant Amplitude Tests on Double-Shear Joints

Constant amplitude tests carried out on double-shear joints, employing as fasteners prestressed* 10 K steel bolts ($F_{tU} = 100 \text{ kp/mm}^2$), steel Huckbolts, aluminium Huckbolts, aluminium snaphead rivets, and steel pins, indicate that the load transferred by friction between the faying surfaces is the main factor influencing fatigue life. The more the sheets are pressed together, the higher is the fatigue strength of the joint.

With the prestressed* bolted joint, fracture is not induced by the notch effect of the bolt hole but by fretting away from the hole. Reducing or eliminating fretting by the use of PVC interlayers, primer, or Molykote will result in a further increase in fatigue strength, see the Figure. This effect is particularly pronounced for high mean stresses (in the present case, $S_m = + 7.4 \text{ kp/mm}^2$).

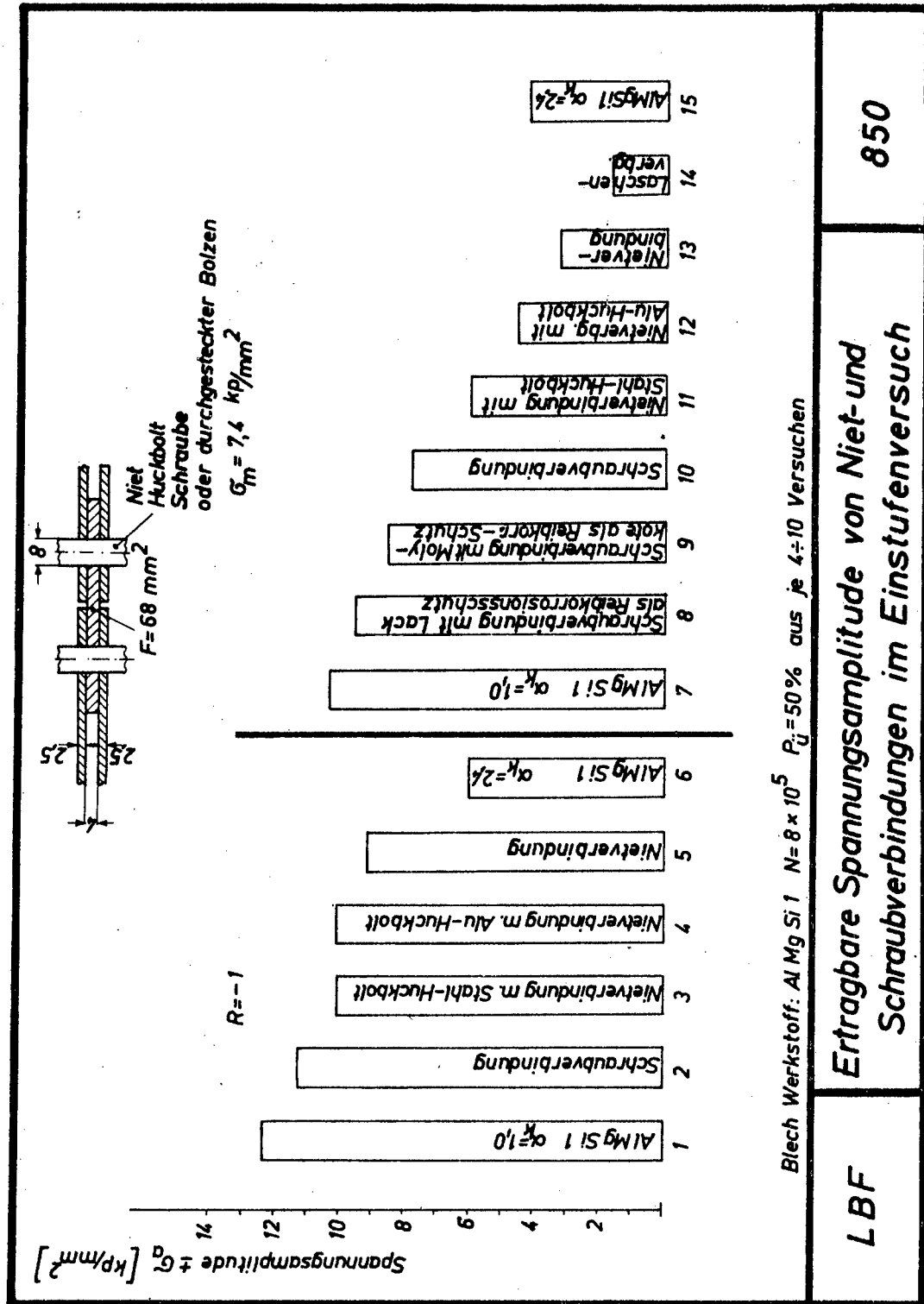
For a prestressed* bolted joint employing anti-fretting measures, finite life at $8 \cdot 10^5$ cycles-to-failure for the above mean stress is approx. $\pm 9.0 \text{ kp/mm}^2$ (based on net area); for a riveted joint it is approx. $\pm 3.0 \text{ kp/mm}^2$. At a stress ratio $R = -1$ the difference is much less.

W. Schütz

Glossary of Terms used in the Figure

Blechwerkstoff: Al Mg Si 1 (W 3355.7)	- sheet material: 6061-T6
$N = 8 \times 10^5$	- endurance $N = 8 \times 10^5$ cycles
$P_U = 50\%$ aus je 4-10 Versuchen	- probability of survival $P_S = 50$ percent established from 4 to 10 tests each
Spannungsamplitude $\pm \sigma_a$	- stress amplitude, $\pm S_a$
Niet/Huckbolt/Schraube/oder durchgesteckter Bolzen	- rivet, Huckbolt, bolt, or through-pin
σ_m	- mean stress, S_m
α_k	- stress concentration factor, K_t
Schraubverbindung	- bolted joint
Nietverbindung m. Stahl-Huckbolt (Alu-Huckbolt)	- riveted joint with steel Huckbolt (aluminium Huckbolt)
Schraubverbindung mit Lack (Molykote) als Reibkorrosionsschutz	- bolted joint using primer (Molykote) for protection against fretting
Laschenverbindung	- joint with through-pin

* We regret that "prestressed" is an erroneous translation in the present context; it should be replaced by "under pretension", with the sentences correspondingly altered.



LBF

Ertragbare Spannungsamplitude von Niet- und Schraubverbindungen im Einstufenversuch

850

Fatigue Strength of Riveted and Bolted Joints Established from Constant Amplitude Tests

Fatigue Strength of Various Heats of 18/7/5 NiCoMo Maraging Steel

There was a general opinion that a particularly large scatter in fatigue strength is inherent in 18/7/5 NiCoMo maraging steel. In order to check this, we have carried out constant amplitude and variable amplitude tests on eight variants of the material. The variants tested are:

Variant	Form	Type of Melting	Grain Direction	Ultimate Tensile Strength $F_{tu}(\text{actual})$ [kp/mm ²]	Manufacturer	Notes
1.	Sheet	Vacuum arc remelted	Longitudinal	180.0	A	Same Heat
2.	Sheet	Vacuum arc remelted	Transverse	180.0	A	
3.	Sheet	Vacuum electron-beam remelted	Longitudinal	187.0	A	
4.	Sheet	Air melted	Longitudinal	188.0	A	
5.	Hand Forging	Vacuum induction melted; Vacuum arc remelted	Longitudinal	175.0	B	Same Heat Same Forging
6.	Hand Forging	Vacuum induction melted; Vacuum arc remelted	Transverse	181.0	B	
7.	Sheet	Vacuum arc remelted	Transverse	195.0	B	
8.	Cast Box Section	Air cast	-	170.0	C	

Variants No. 7 and 8 were studied under other research programs and are incorporated in the table only for completeness.

The present investigation will be continued on three further variants, viz.: Bar steel with low, medium, and high titanium content (which influences ultimate tensile strength).

The results of the S-N tests at a stress concentration factor $K_t = 3.1$ under axial loading are presented in Fig. 1. The hatched scatter bands incorporate the mean S-N curves of variants No. 1 to 7. There are no significant differences in fatigue life for endurance up to $N = 10^5$ cycles.

The cast material, particularly at higher endurance, is much inferior to the forged material.

Contrary to the behaviour under constant amplitude loading, the variants show significant differences in fatigue strength under variable amplitude loading, see Fig. 2.

Some of the above eight variants were studied additionally in the annealed condition ($F_{tu} \approx 100$ to 110 kp/mm^2). Similar to other ultra high-strength steels, at high stress concentration factors and high mean stresses ($K_t = 4.5$; $R = 0$) the fatigue strength of NiCoMo maraging steel in the annealed condition is approximately the same as in the hardened condition (see the following Table). This is due to its high notch sensitivity and high mean stress sensitivity in the hardened condition.

Variant 5

Fatigue Strength (S_a , kp/mm^2) at $K_t = 4.5$ under Constant Amplitude Loading

Endurance, N		$3 \cdot 10^3$	10^4	10^5
R = -1	annealed	46.0	33.5	16.6
	hardened	60.0	43.5	20.0
R = 0	annealed	35.5	26.5	12.6
	hardened	40.0	26.5	12.0

Glossary of Terms used in the Figures

Fig. 1

Formzahl α_k	- stress concentration factor, K_t
Beanspruchungsart: axial	- type of loading: axial
Überlebenswahrscheinlichkeit P_U	- probability of survival, P_S
Lastspielzahl N	- endurance, N
Spannungsamplitude $\pm \sigma_a$	- stress amplitude, $\pm S_a$
Werkstoff	- material
Ni Co Mo	- 18/7/5 Ni Co Mo maraging steel
GS Ni Co Mo	- Ni Co Mo cast maraging steel
Halbzeug	- form
Blech	- sheet
Freiformschmiedestück	- hand forging
Gußkast.-Profil	- cast box section
Erschmelzungsart	- type of melting
vakuumlichtbogenumgeschmolzen	- vacuum arc remelted
vakuumelektronenstrahlungumgeschmolzen	- vacuum electron-beam remelted
an Luft erschmolzen	- air melted
vakuuminduktionserschmolzen	- vacuum induction melted
an Luft vergossen	- air cast
Faserrichtung	- grain direction
längs	- longitudinal
quer	- transverse
σ_B	- ultimate tensile strength, F_{tu}

Fig. 2

Lastkollektiv: LBF-Normverteilung	- stress spectrum: LBF Standard Distribution
$P_U = 50\%$ aus 4 - 8 Vers.	- $P_S = 50\%$ established from 4 to 8 tests each
Variante	- variant

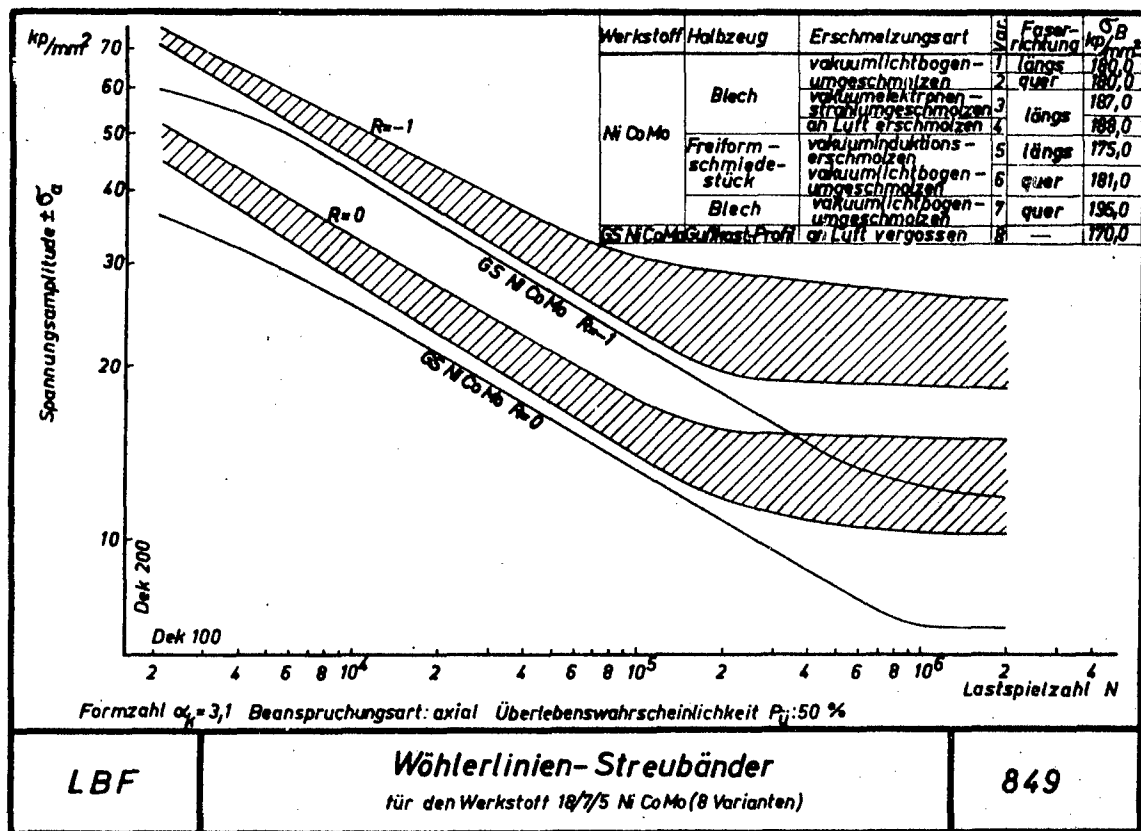


Fig. 1 Scatter Bands for S-N Test Results on 18/7/5 NiCoMo Maraging Steel (8 Variants)

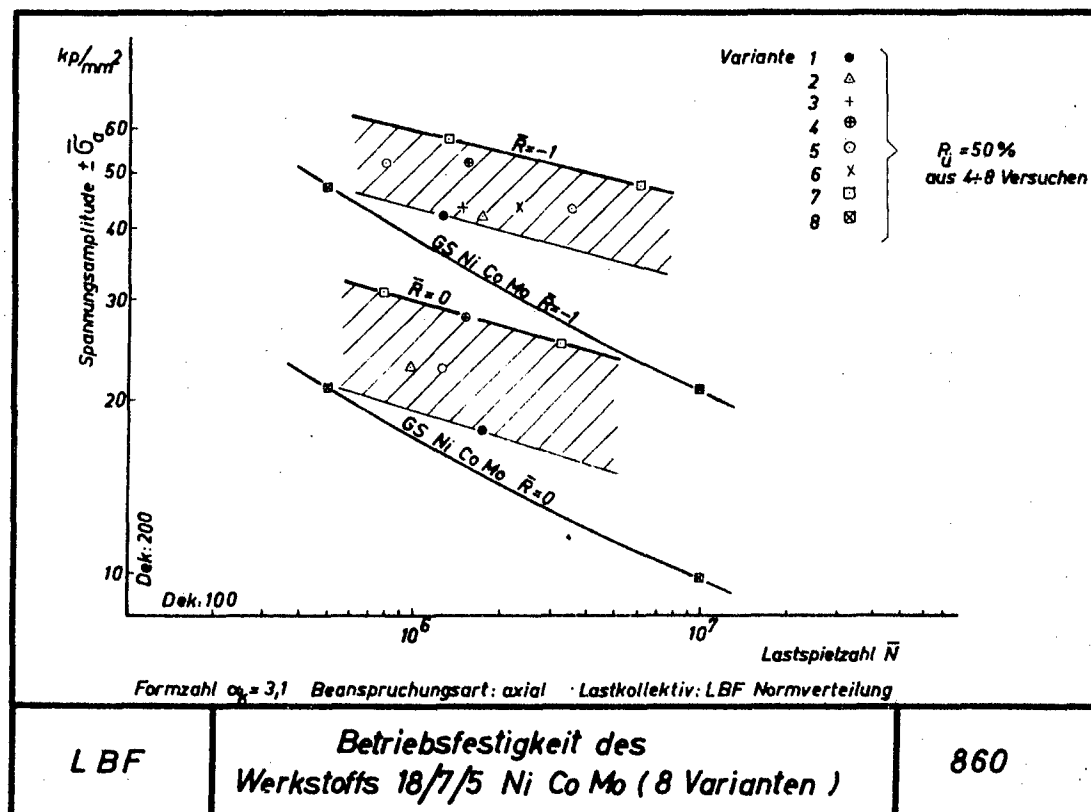


Fig. 2 Strength under Variable Amplitude Loading of 18/7/5 NiCoMo Maraging Steel (8 Variants)

Fatigue Strength of Aluminium Alloys

The fatigue performance of the high-strength silver-bearing aluminium alloy AZ 74 (3.4354.7), of Otto Fuchs, has been investigated in an extensive research program. Some other aluminium alloys were investigated less extensively. Of the AZ 74 alloy, more than 2000 specimens taken from extrusions were tested with stress concentration factors $K_t = 1.0, 1.8, 2.5, 3.1$, and 4.5 , and some 400 specimens, taken from hand forgings in the longitudinal and short transverse direction, with $K_t = 3.1$. The aluminium alloys additionally studied were:-

- W 3425.7 (7079-T6); test specimens taken from hand forgings in the longitudinal and short transverse direction, with $K_t = 3.1$.
- W 3425.7; test specimens taken from extrusions, with $K_t = 3.1$.
- W 3125.5 (2024-T3); test specimens taken from extrusions, with $K_t = 3.1$.

The test results obtained under constant amplitude and under variable amplitude loading are presented in the Figure. This combined presentation allows the following conclusions to be drawn:-

1. At $K_t = 3.1$, the three above materials in the extruded form show rather similar fatigue strengths (for mechanical properties see the Table).
2. Under constant amplitude loading, the specimens taken from hand forgings in the longitudinal direction and the corresponding extruded specimens show but a small difference in fatigue strength; under variable amplitude loading, however, the specimens taken from extrusions are superior.
3. The fatigue strength of the specimens taken from hand forgings in the short transverse direction is -in some cases to a considerable extent- inferior to that of the specimens taken in the longitudinal direction.

The addition of silver to the AZ 74 (3.4354.7) material aims at improving the stress corrosion behaviour of the material as compared to the common zinc-bearing alloys. This objective has been achieved, as shown by test results of Otto Fuchs and other institutions. At the same time it is noted that the addition of silver obviously has no significant effect on the fatigue strength of the alloy.

An analysis of crack propagation and residual strength tests has not been completed yet. However, AZ 74 does not appear to be superior to any marked extent to the other aluminium alloys studied.

Chemical Composition of AZ 74 (3.4354.7)

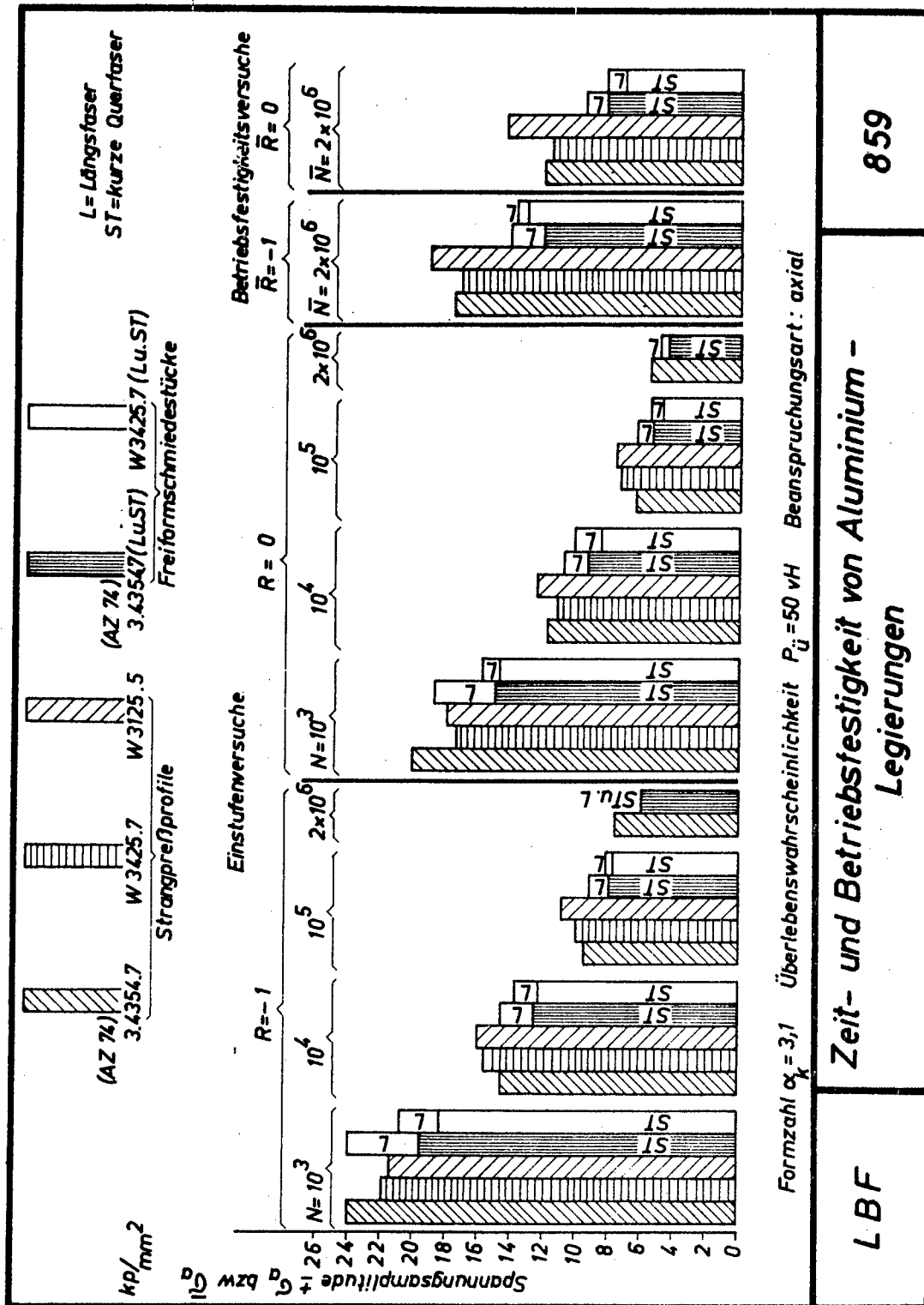
Cu	Mn	Fe	Ag	Zn	Mg	Si	Cr	Ti
0.99	0.07	0.25	0.40	5.90	2.34	0.05	0.22	0.06

Table

Material	Ultimate Tensile Strength F_{tu} [kp/mm ²]	Yield Strength 0.2 % offset [kp/mm ²]	Elongation δ_5 [percent]
<u>AZ 74 (3.4354.7)</u>			
Extrusion	54.7	50.6	10.0
Hand forging; longitudinal direction	51.0	44.8	11.5
Hand forging; transverse direction	49.0	43.1	8.0
<u>W 3425.7 (7079-T6)</u>			
Extrusion	55.6	49.5	11.0
Hand forging; longitudinal direction	56.0	50.1	12.0
Hand forging; transverse direction	53.1	46.5	10.0
<u>W 3125.6 (2024-T3)</u>			
Extrusion	52.2	38.0	15.5

Glossary of Terms used in the Figure

Spannungsamplitude σ_a bzw. $\bar{\sigma}_a$	- stress amplitude S_a or \bar{S}_a , resp.
Formzahl α_k	- stress concentration factor, K_t
Überlebenswahrscheinlichkeit P_0	- probability of survival, P_S
Beanspruchungsart: axial	- type of loading: axial
Einstufenversuche	- constant amplitude tests
Betriebsfestigkeitsversuche	- variable amplitude tests
Strangpreßprofile	- extrusions
Freiformschmiedestücke	- hand forgings
L = Längsfaser	- L = longitudinal grain direction
ST = kurze Quersfaser	- ST = short transverse grain direction



Influence of the Spectrum Shape on the Fatigue Strength of an Aluminium Alloy

Of the investigation already mentioned in the ICAF 1965 German Review, the first part, involving the spectrum shapes characterized by the parameter p (i.e. the "p - parameter spectra"), has been completed.

The investigation was carried out using flat bar specimens of 3.1354.5 (2024-T3) aluminium alloy containing a hole, with a stress concentration factor $K_t = 3.1$. The stress spectra employed as well as the definition of the parameter p characterizing the spectrum shape are presented on the left-hand side of Fig. 1.

The results of the test series covering spectra ranging from the extreme case of the constant amplitude test with $p = 1.00$ to the LBF Standard Distribution with $p = 0.00$ show a marked dependence of the fatigue strength (stress amplitude S_a) from the spectrum shape. As nine to twelve specimens were tested at each stress level, the \bar{S} - \bar{N} curves plotted in Fig. 2 may be regarded as statistically proved; the fatigue limit for $p = 1.00$ was determined using the staircase method. The scatter bands plotted in Fig. 2 incorporate all values between $P_S = 90$ percent and $P_S = 10$ percent probability of survival.

The second part of the investigation, involving the spectrum shapes characterized by the parameter q (see the right-hand side of Fig. 1), will be completed presumably in the course of this year.

H. Ostermann

Glossary of Terms used in the Figures

Fig. 1

p-Wert-Kollektive
Überschreitungshäufigkeit H/\bar{H}
 $p = 0 \hat{=}$ Einstufenversuch
 $p = 1 \hat{=}$ LBF-Normverteilung

- p-parameter spectra
- cumulative frequency of level-crossings
- $p = 0 \hat{=}$ constant amplitude test
- $p = 1 \hat{=}$ LBF Standard Distribution

Fig. 2

Spannungsamplitude $\pm \bar{\sigma}_a$
Lastspielzahl \bar{N}
Werkstoff: 3.1354.5
Flachstab: $\alpha_k = 3.1$
Beanspruchung: axial
 $\bar{R} = \bar{\sigma}_U / \bar{\sigma}_O = -1$

- stress amplitude, $\pm \bar{S}_a$
- endurance, \bar{N}
- material: 2024-T3
- flat bar specimen with $K_t = 3.1$
- type of loading: axial
- $\bar{R} = \bar{S}_{\min} / \bar{S}_{\max} = -1$

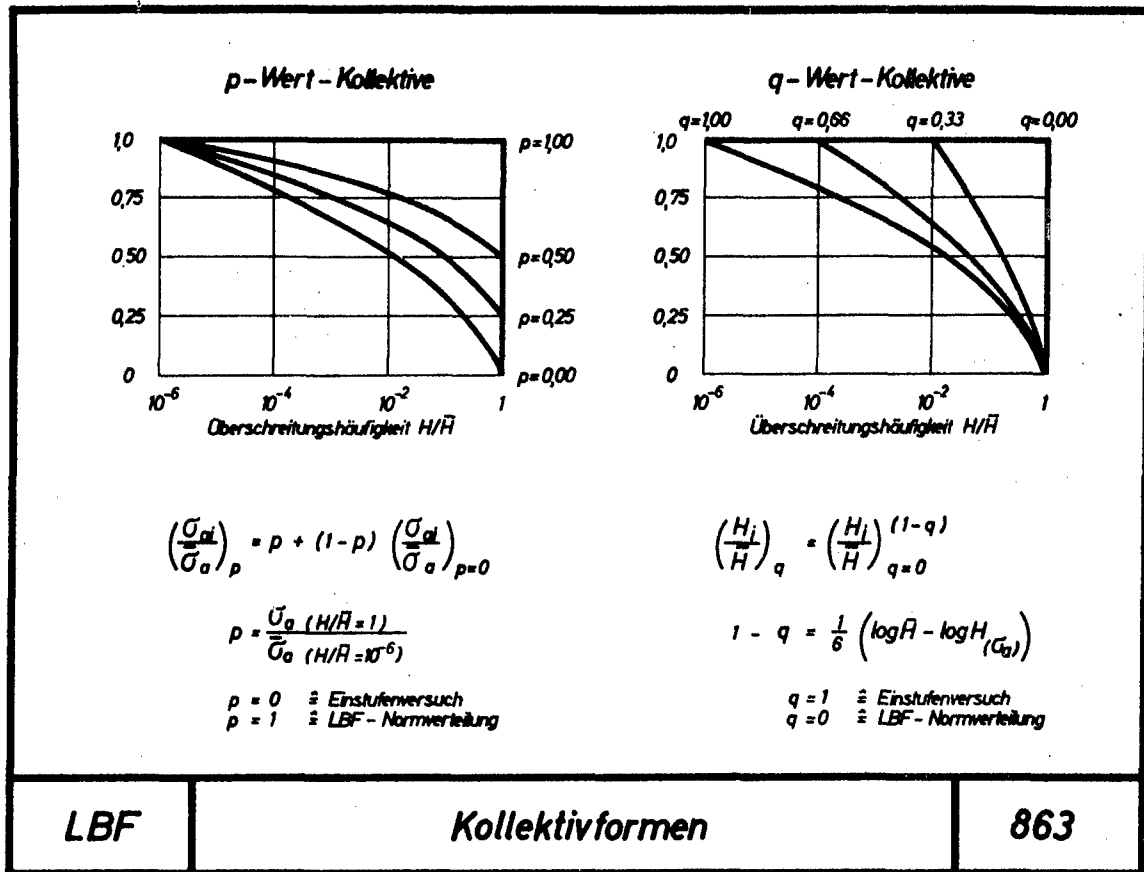


Fig. 1 Spectrum Shapes

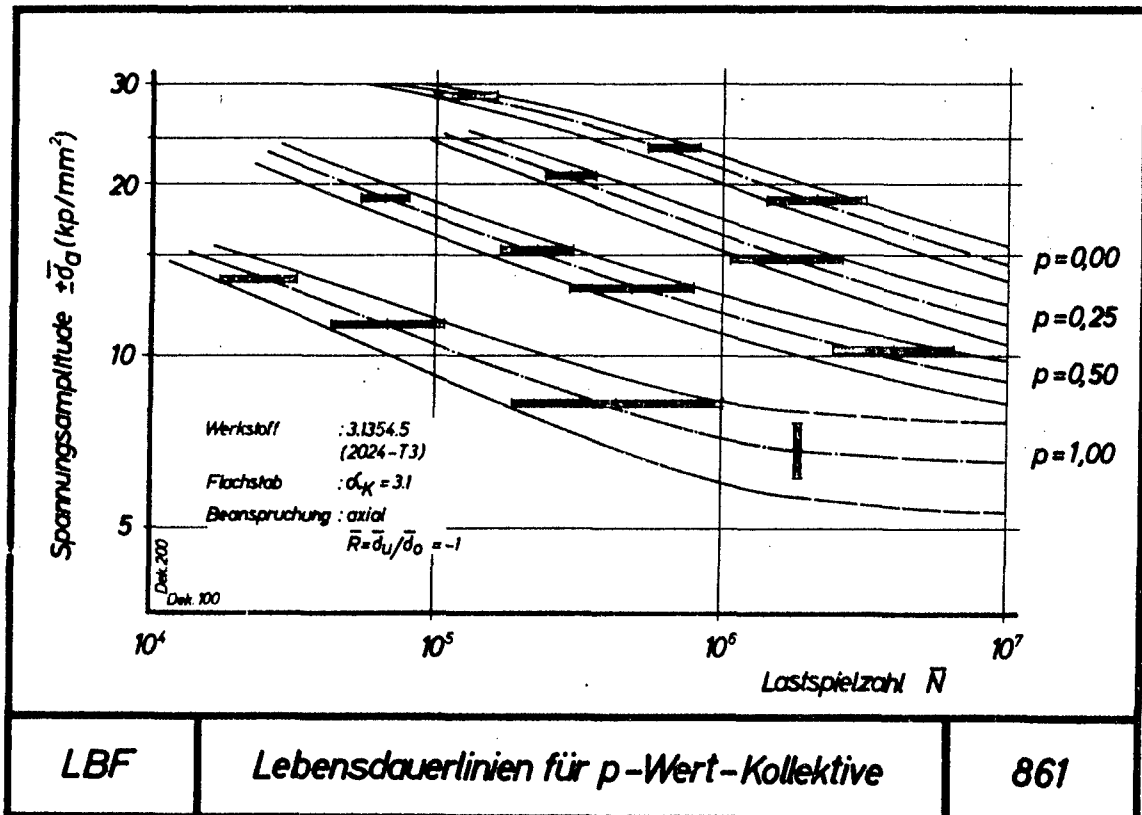


Fig. 2 $\bar{S}-\bar{N}$ Curves (Variable Amplitude Tests)
Established for p-Parameter Spectra

Fatigue Strength of Electron-Beam Welded Sheet of a Maraging Steel

Constant amplitude tests at $R = +0.1$ were carried out on unwelded and electron-beam welded sheet specimens in the range of 10^4 to $2 \cdot 10^6$ cycles.

Details on material, specimen dimensions, and welding conditions are given subsequently to the text.

Basis of the present investigation was a welding speed of 85 mm/sec, i.e. the speed resulting in optimum static strength for welded specimens.

Optimum fatigue strength behaviour, however, was observed for a welding speed of 10 mm/sec; it must be noted, though, that the majority of failures in this test series were clamping failures or sheet failures away from the weld.

A statistical evaluation was practically not possible because of the exceptionally large scatter of test results. The curves plotted in the Figure have therefore been designated as the lower boundaries of the scatter band (disregarding a number of outlying results), and they have been associated more or less arbitrarily with a probability of survival of $P_S = 90$ percent.

The fracture surface indicates that the high welding speed (85 mm/sec) often results in a porous weld; at the low welding speed (5 mm/sec), the decrease in fatigue strength is probably due to an overheating of the repeatedly melted welding area.

Preliminary tests showed that for sheets heat-treated prior to and after welding the difference in fatigue strength performance is practically negligible; thus, in the actual investigation only sheets heat-treated after welding were used.

For further details see E. Haibach, "Beitrag zur Schwingfestigkeit elektronenstrahlgeschweißter Verbindungen", to be published shortly in the volume "Beiträge zum

Elektronenstrahlschweißen", Deutscher Verlag für Schweißtechnik GmbH,
Düsseldorf/Germany.

The present investigation will be continued in order to evaluate systematically the influence of various welding conditions on fatigue strength.

Material: Maraging Ni Co Mo steel "Ultrafort 301", of "Deutsche Edelstahlwerke",
Krefeld/Germany.

Nominal Chemical Composition:

C	Si	Mn	Mo	Ni	Co	Ti
< 0.03	< 0.10	< 0.10	4.8	8.0	18.0	0.45

Nominal Mechanical Properties: (In the heat-treated condition)

Ultimate tensile strength, F_{tu}	=	180 kp/mm ²
Yield strength, 0.2 percent offset	=	165 kp/mm ²
Elongation, δ_5	=	6 percent
Impact strength, a_k	=	3 kp/mm ²

Specimen: (Surface and edges polished, weld bead ground flush)

	welded	unwelded
Dimensions, mm	35 x 2 x 300	30 x 2 x 300
Test section, mm ²	30 x 2	20 x 2
Length of parallel test section, mm	30	30

Welding Conditions:

Butt welded in the annealed condition.

Welding Speed [mm/sec]	Welding Amperage [mA]
5	3.1
10	5.2
85	16.0

Heat-treated after welding.

E. Haibach

Glossary of Terms used in the Figure

Lastspielzahl N

- endurance, N

Spannungsamplitude $\pm \sigma_a$

- stress amplitude, $\pm S_a$

P_U

- probability of survival, P_S

$R = \sigma_U / \sigma_O$

- $R = S_{\min} / S_{\max}$

ES

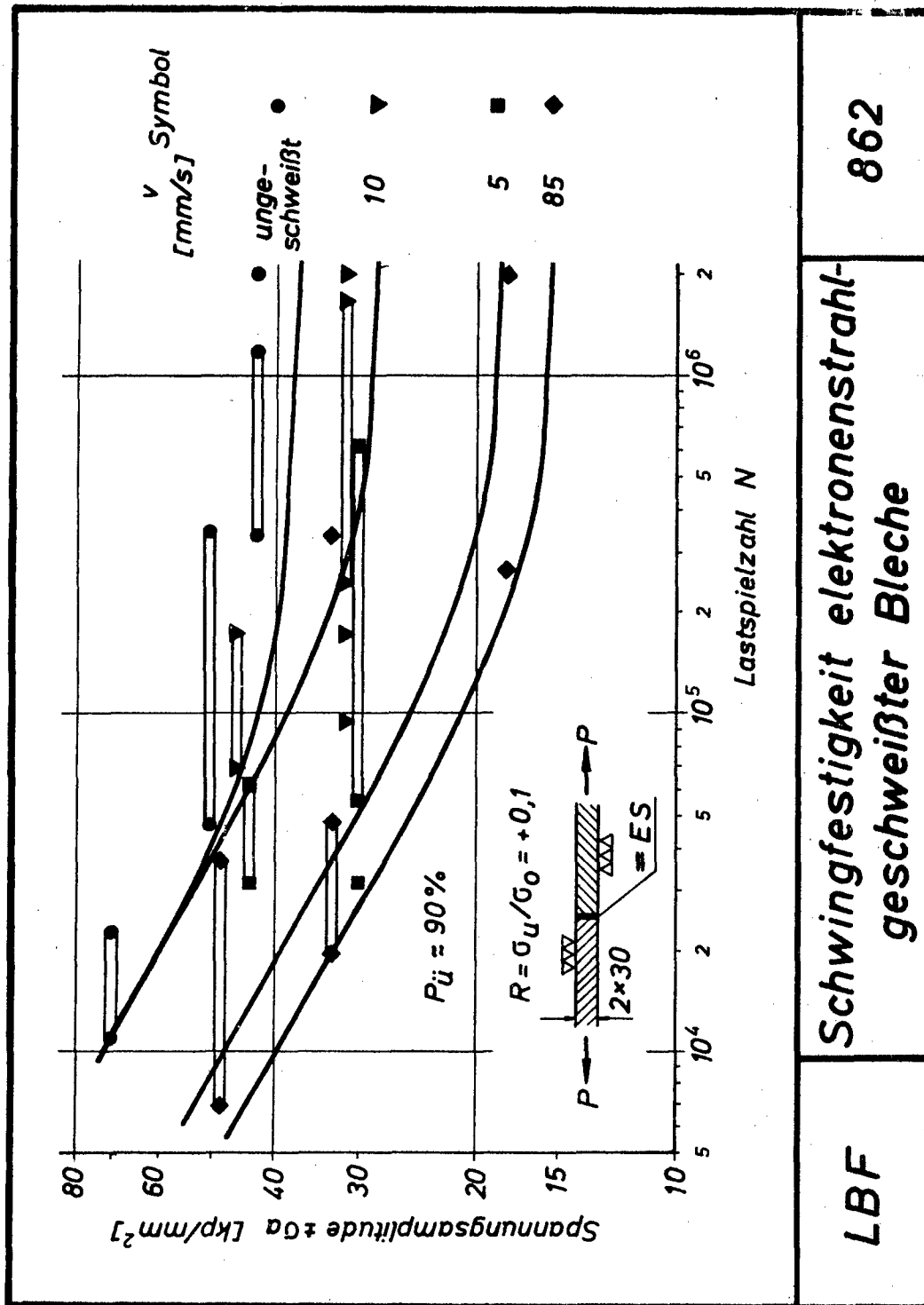
- electron-beam welded

v [mm/s]

- welding speed, v [mm/sec]

ungeschweißt

- unwelded



Fatigue Strength of Electron-Beam Welded Sheet Specimens

Comparative Investigation on the Fatigue Strength of Chemically Etched and Mechanically Milled Test Specimens

Chemical etching of highly stressed structural components is finding increased employment in aircraft engineering. In order to study the fatigue strength performance of chemically etched as compared to mechanically milled components, fatigue tests have been carried out on notched specimens of 2024-T3 aluminium alloy; the test specimens were manufactured with machined notches and with chemically etched notches, resp., see Fig. 1. The notched specimens were loaded in bending. Up to now, constant amplitude tests have been performed in the finite life range at stress ratios $R = -1.0$, -0.5 , and 0 .

It is a fact that in actual structures stresses in transverse grain direction cannot always be avoided. As the effect of chemical etching -in the present paper always compared with mechanical milling- was expected to be most adverse in this case, the chemically etched specimens were taken in transverse grain direction.

The mechanically notched specimens up to now have been studied only in the longitudinal grain direction; thus, a strict comparison of results on mechanically milled and chemically etched specimens is not possible yet. The results hitherto obtained are presented in Fig. 1 and 2. For the above reason, the following inferences are only tentative:-

- The average fatigue life of chemically etched specimens (transverse grain direction) is only 50 percent that of the mechanically milled specimens (longitudinal grain direction).
- The scatter of test results -as expected- is lower for chemically etched than for mechanically milled specimens.

The investigation is to be continued on chemically etched specimens loaded in grain direction and on mechanically milled specimens loaded across the grain direction. Furthermore, it is intended to determine the difference in fatigue strength between chemically etched and mechanically milled specimens also at the fatigue limit.

Another investigation is planned to determine the effect of chemical etching on the fatigue strength of structural components. Service failures indicate that the fatigue strength of chemically etched -as compared to mechanically milled- components is particularly low in thin sheets with high local bending stresses. As this applies for instance to buckling shear panels, such panels were selected to be used as test specimens. Initial test results are already available; because of the small number they are, however, not statistically proved yet.

1. Chemically etched shear panels have a lower endurance than mechanically milled panels.
2. Failures originate at the intersection of folds formed by the buckling skin at loads beyond the critical value.
3. In clad panels, which have also been studied, the cladding has an adverse effect on endurance.
4. Application of a single overload results in a greatly reduced fatigue life.

In the course of the further investigation, constant amplitude tests at various stress ratios shall be performed principally; a number of variable amplitude tests shall be conducted in addition.

D. Schütz

Glossary of Terms used in the Figures

Lastspielzahl N

Spannungsamplitude $\pm \sigma_a$

Kerbe mechanisch geätzt
(Längsfaser)

Kerbe chemisch geätzt
(Querfaser)

Werkstoff 3.1354.5

α_k

r

- endurance, N
- stress amplitude, $\pm \sigma_a$
- notch mechanically milled
(longitudinal grain direction)
- notch chemically etched
(transverse grain direction)
- material 2024-T3
- stress concentration factor, K_t
- radius of the notch

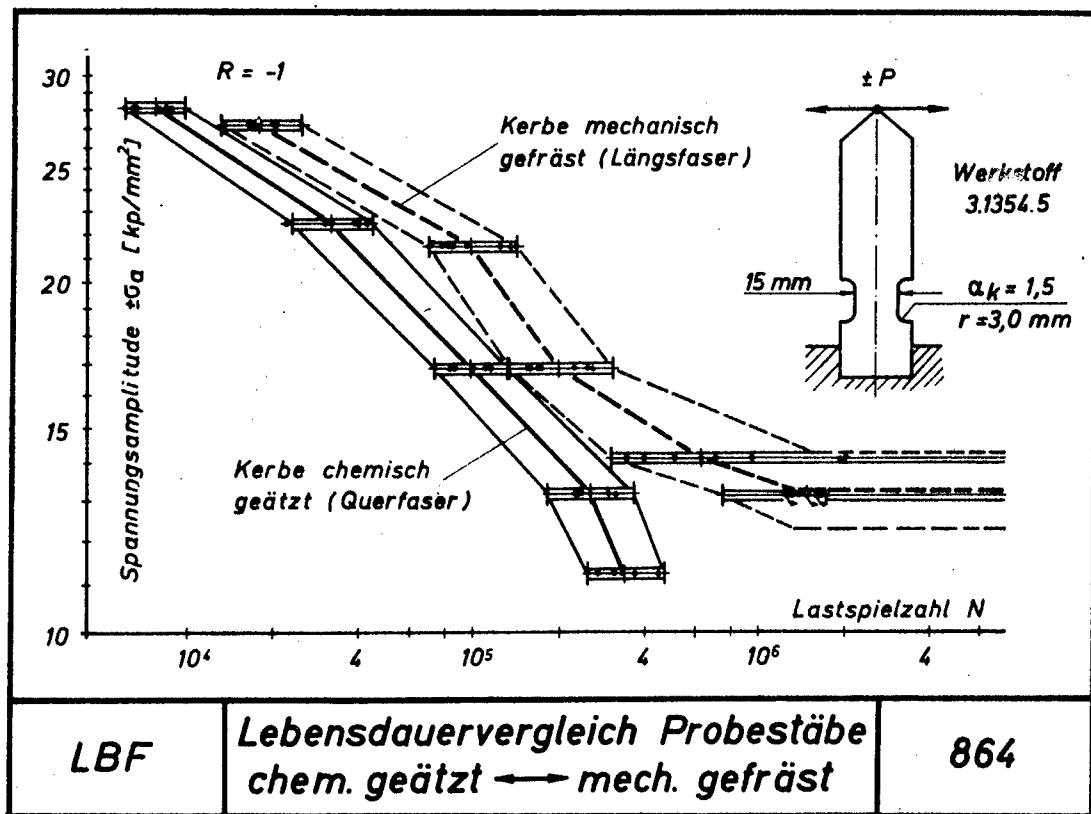


Fig. 1 Fatigue Strength Comparison of Chemically Etched and Mechanically Milled Specimens

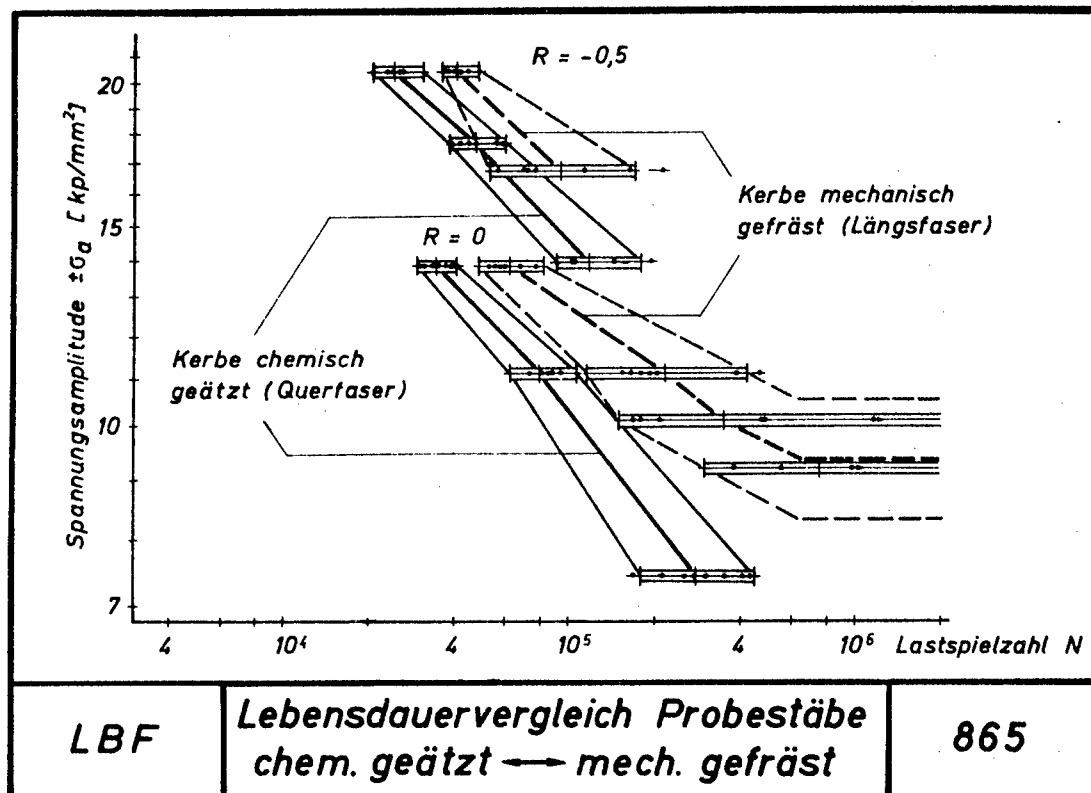


Fig. 2 Fatigue Strength Comparison of Chemically Etched and Mechanically Milled Specimens

Investigations in Progress or in an Advanced Stage of Preparation

Derivation of Reliable Load Frequency Distributions for Airplanes from Flight Measurements

The state of that program is described in the paper by O. Buxbaum and O. Svenson presented at the present Symposium.

O. Buxbaum

Fatigue Load Survey for the F-104 G

Two aircraft are instrumented with strain gages and calibrated for measuring the following parameters:-

- a) Vertical c.g. acceleration, lateral c.g. acceleration, pressure altitude, pressure airspeed, roll rate, and yaw acceleration.
- b) Bending, torsion, and shear at three R/H and one L/H cross section of the wings.
- c) Bending and shear at the fin near the fuselage.
- d) Bending, torsion, and shear of the stabilizer.
- e) Vertical, drag, and side loads at the nose and main landing gears.

These data will be recorded continuously on magnetic tape over about 50 flights.

Besides that program, about 30 airplanes of the German Air-Force are instrumented with vertical c.g. acceleration counters. The data accumulated will be analysed and applied in a full-scale fatigue test.

O. Buxbaum

Constant Amplitude and Variable Amplitude Tests on Ti 6Al 4V, Ti 8Al 1Mo 1V,
and Ti 5Al 2.5Sn

W. Schütz

Influence on Fatigue Strength of the Size of the Individual Programmes in
Eight-Step Variable Amplitude Tests

W. Lipp

The Influence on Fatigue Life of Internal Stresses at the Notch Root Produced by
the Ground-Air-Ground Cycle

It is generally known that the G-A-G cycle -particularly as simulated in the flight-by-flight tests- produces very high damage. This damaging effect is ascribed to unfavourable internal stresses at the notch root, which are induced by the G-A-G cycle.

In order to confirm this, it is intended to conduct a test where the local strains at the notch root ($K_t = 2.5$) of a specimen subjected to a flight-by-flight test program are reproduced in a plain specimen by corresponding loads. The investigation shall be carried out taking into consideration similar tests, reports on which have already been published.

D. Schütz

SECTION II

HAMBURGER FLUGZEUGBAU GMBH

Hamburg-Finkenwerder

VEREINIGTE FLUGTECHNISCHE WERKE GMBH

Bremen

Influence of Galvanic Cadmium Plating on the Fatigue Strength of 1.6604.6
(AICMA FE PL 74) Steel Lugs

The following variants were tested:

1. Unplated
2. Lug and bore fully cadmium plated
3. Lug cadmium plated, with the bore covered during plating.

Results

Variant 2 in the range of 10^5 to 10^6 cycles-to-failure has a fatigue life about twice that of variants 1 and 3 (see the Figure). This probably is attributable to its improved resistance to fretting. It may be assumed that the positive influence of cadmium plating the bore surface, i.e. increased fretting resistance, outweighs the negative influence, i.e. hydrogen embrittlement. The standard deviation $s = 0.27$ for all three specimens studied is relatively large; the tests are therefore being repeated at a higher stress amplitude.

Details on treatment

Cadmium plating according to "Deutsche Luftfahrtnormen" LN 29741/KN 3000;

Baked for three hours at $190 \pm 10^\circ \text{C.}$;

Chromatized by immersion in solutions on the basis of six-valent chromium compounds.

For installation, the pins were lubricated with Molykote C.

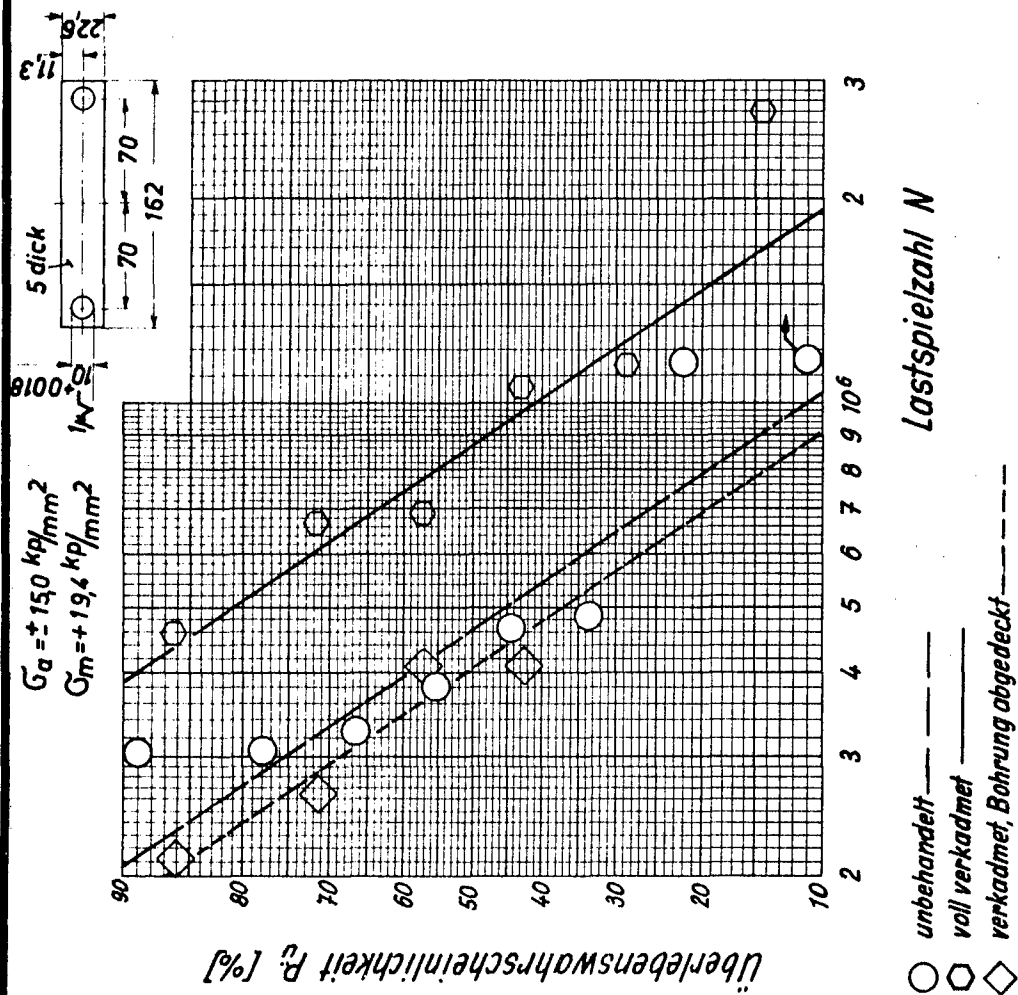
HAMBURGER FLUGZEUGBAU GMBH,
HAMBURG-FINKENWERDER

Glossary of Terms used in the Figure

Lastspielzahl N	- endurance, N
Überlebenswahrscheinlichkeit P_0	- probability of survival, P_S
unbehandelt	- unplated
voll verkadmet	- fully cadmium plated (lug and bore)
verkadmet, Bohrung abgedeckt	- cadmium plated, with bore covered during plating
σ_a	- stress amplitude, $\pm S_a$
σ_m	- mean stress, S_m
5 dick	- thickness of lug 5mm
	all dimensions given in mm

HFB 1967

*Einfluß der galvanischen
Verkadmung auf die
Lebensdauer von
Augenstäben aus Stahl*
(1.6604.6)



Influence of Galvanic Cadmium Plating on the Fatigue Strength of 1.6604.6 Steel Lugs

Investigation on the Effect of Various Types of Rivets

The effect of various rivet types on the fatigue strength of a test specimen as shown in the Figure has been studied in an extensive test program. The joining elements used were snaphead rivets, Taper-Lok Fasteners, Huckbolts, Jo bolts, and Cherrylock rivets; in addition, specimens were tested incorporating snaphead-riveted interference bushes.

The specimen used and the results obtained are presented in the Figure. The results indicate that the specimens incorporating snaphead rivets, Taper-Lok Fasteners, Huckbolts, and riveted interference bushes have fairly similar fatigue strengths, whereas specimens employing Jo bolts and Cherrylock rivets show markedly inferior fatigue characteristics.

It is noted, however, that the two materials used for the specimen part I and part II (see the Figure) were not the same in all cases studied and that the diameters of the fastening elements differed by various degrees (see the Table).

Failure in all specimens tested started from the rivet hole.

VEREINIGTE FLUGTECHNISCHE WERKE

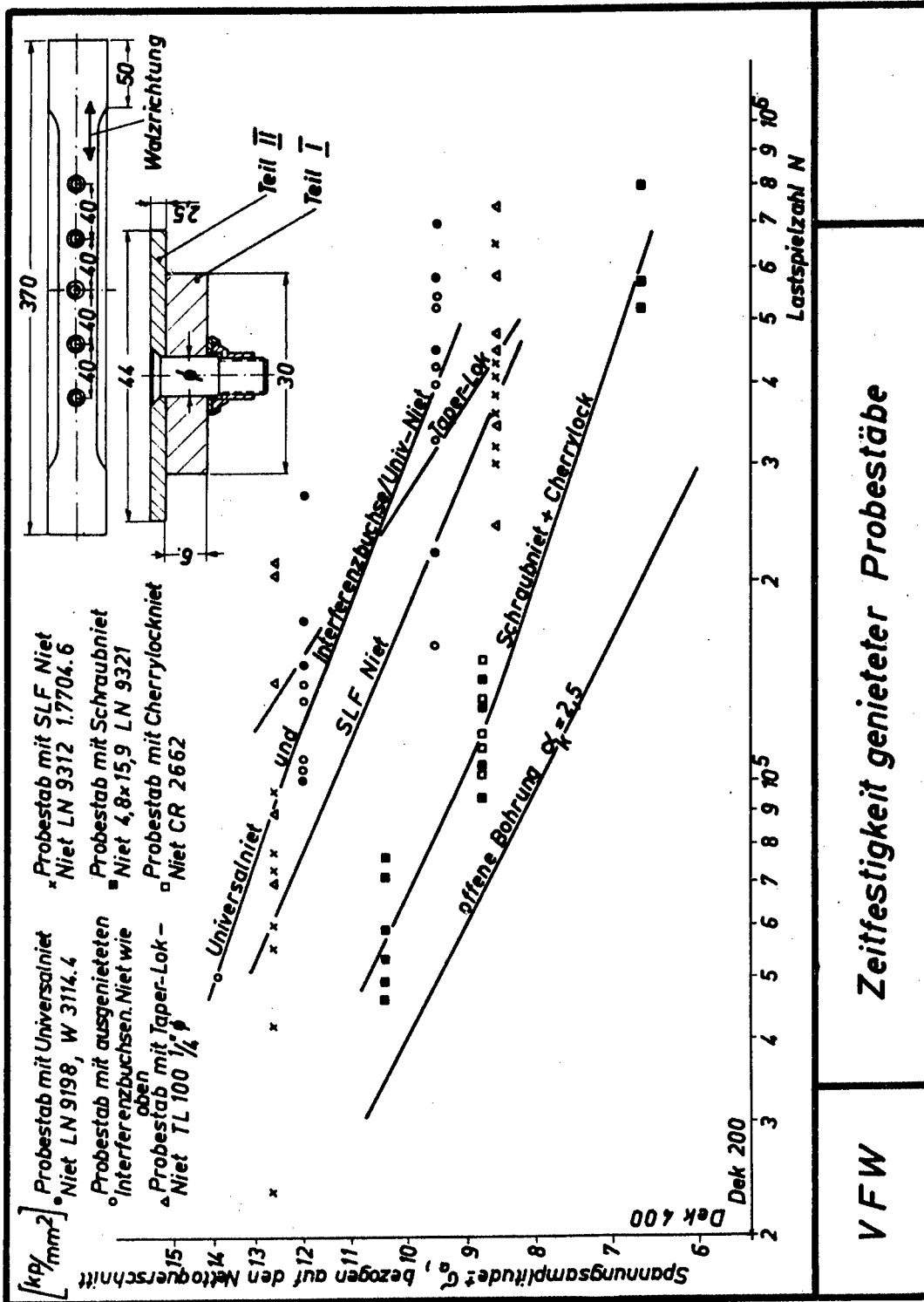
Bremen

Table

Rivet Type	Specimen Materials		Rivet Diameter [mm]	Notes
	Part I	Part II		
Snaphead rivet	W3125.6 (2024-T3)	W3126.5 (2024-T3) alclad	4.00	-
Snaphead-riveted interference bushes	W3125.6	W3126.5	4.00	Interference bush diameter 5.0mm; material: 1.4544.9 (SAE 30321)
Taperlok TL 100	3.4364.7 (7075-T6)	3.1364.5 (2024-T3) alclad	6.25	Installed strictly according to specifications of manufacturer
Huckbolt	W3125.6	3.1364.5	6.00	-
Jo bolt	W3125.6	W3126.5	4.80	-
Cherrylock rivet	W3125.6	W3126.5	4.80	-
(Rivet hole)	(W3125.6)	-	-	(bore diameter 4 mm)

Glossary of Terms used in the Figure

- | | |
|---|---|
| -Lastspielzahl N | - endurance, N |
| -Spannungsamplitude $\pm \sigma_a$, bezogen auf den Nettoquerschnitt | - stress amplitude $\pm \sigma_a$, based on net area |
| -Probestab mit Universalniet. Niet LN9198 W3114.4 | - specimen with snaphead rivet; rivet according to "Deutsche Luftfahrtnormen" LN9198; material: W3114.4 (2024-T4) |
| -Probestab mit ausgenieteten Interferenzbuchsen. Niet wie oben | - specimen with riveted interference bushes. rivet same as above |
| -Probestab mit Taper-Lok Niet. TL 100 1/4" \varnothing | - specimen with Taper-Lok Fastener; TL 100 1/4" diameter |
| -Probestab mit SLF-Niet. Niet LN9312, 1.7704.6 | - specimen with Huckbolt; bolt according to LN 9312; material: 1.7704.6 (SAE 4340) |
| -Probestab mit Schraubniet. Niet LN9321, 4.8 x 15.9 | - specimen with Jo bolt; bolt according to LN 9321; 4.8 x 15.9 mm |
| -Probestab mit Cherrylockniet. Niet CR 2662 | - specimen with Cherrylock rivet CR 2662 |
| -offene Bohrung $\alpha_k = 2,5$ | - specimen with circular hole, $K_t = 2.5$ |



VFW

Zeitfestigkeit genieteter Probestäbe

Fatigue Strength of Riveted Specimens in the Finite Life Range

Comparative Tests on Butt Welded and Notched Specimens of 1.7734.5
(AICMA FE PL 52 S) Steel Material

The fatigue strength of butt welded specimens with both welding surfaces ground flush (root layer ground out) in the range of 10^4 cycles-to-failure was somewhat higher than that of the flat bars with circular holes ($K_t = 2.5$), see the Figure. It is noted, however, that the welded specimens showed a much larger scatter.

In the range of 5×10^5 cycles-to-failure, the test results indicate that the fatigue strengths of the welded specimens and of the flat bar specimens are rather similar.

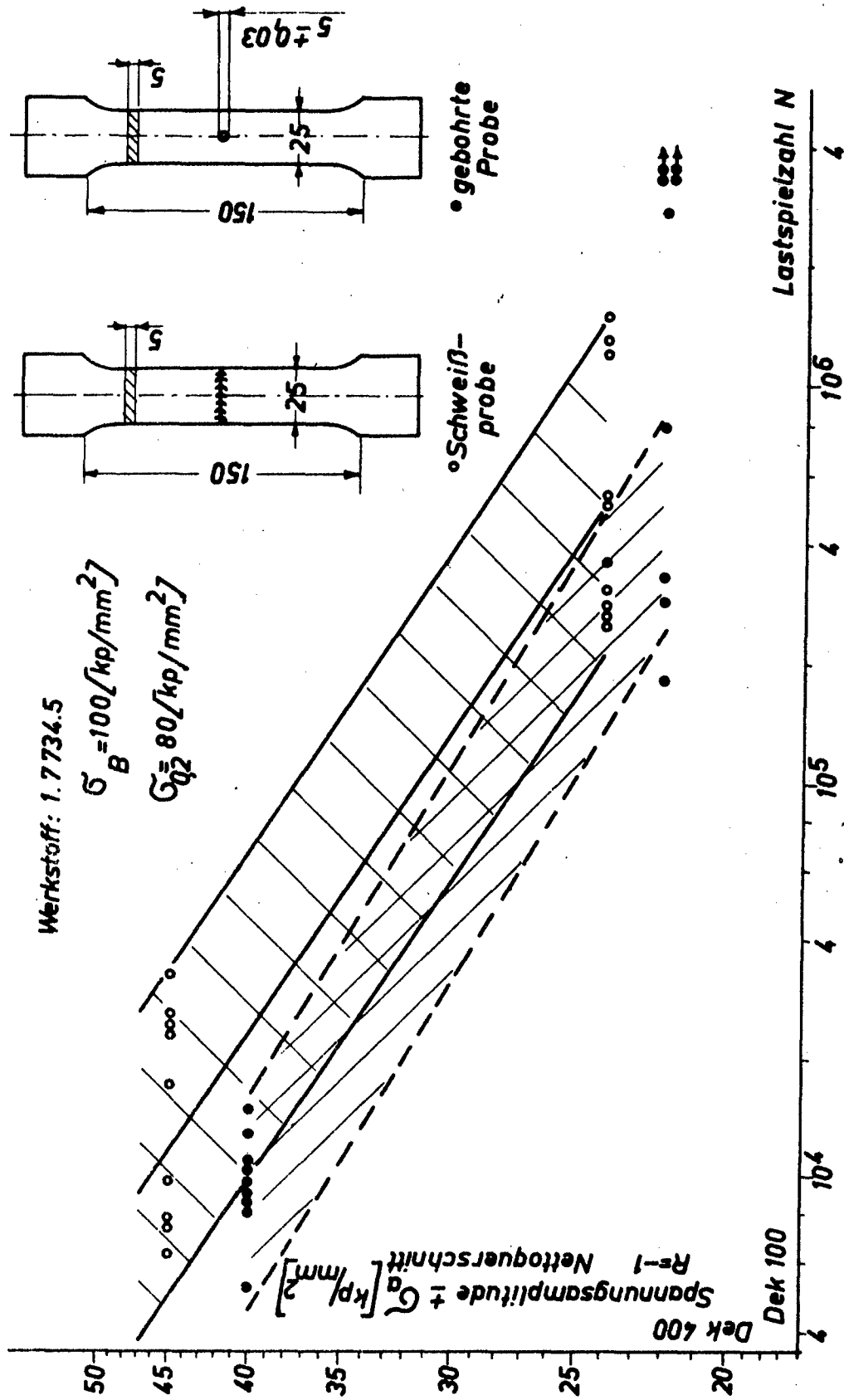
Welding electrodes used

Root layer: Fox CM 2 Kb Electrode 2.5 mm	}	both manufactured by Böhler
Top layer : Fox CM 2 Ti Electrode 3.5 mm		

VEREINIGTE FLUGTECHNISCHE WERKE GMBH
 Bremen

Glossary of Terms used in the Figure

Lastspielzahl N	- endurance, N
Spannungsamplitude $\pm \sigma_a$, bezogen auf den Nettoquerschnitt	- stress amplitude $\pm S_a$, based on net section
Schweißprobe	- welded specimen
gebohrte Probe ($\alpha_k = 2,5$)	- specimen with circular hole ($K_t = 2.5$)
Werkstoff: 1.7734.5	- material: 1.7734.5 (AICMA FE PL 52 S) steel
σ_B	- ultimate tensile strength, F_{tu}
$\sigma_{0.2}$	- yield strength, 0.2 percent offset
P_U	- probability of survival, P_S
5 dick	- thickness of specimen: 5mm
	- all dimensions given are in mm



MFV

Zeitfestigkeit geschweißter und gebohrter Probestäbe

Fatigue Strength of Welded and Notched Specimens in the Finite Life Range

SECTION III

Technical Notes (TM)

published by Laboratorium für Betriebsfestigkeit,
Darmstadt-Eberstadt, during the present Period of Review
(May 1965 to March 1967)

ICAF-Documents

by German authors, distributed during the present
Period of Review (May 1965 to March 1967)

- | | |
|----------|---|
| TM 15/65 | Verwendung eines Einheits-Kollektivs bei Betriebsfestigkeitsversuchen
E. Haibach and W. Lipp |
| TM 16/65 | Betriebsfestigkeit gebohrter Flachstäbe aus Stahl
Ni Co Mo 18/7/5
W. Schütz |
| TM 17/65 | Zeit- und Dauerfestigkeit ungekerbter und gekerbter Flachstäbe aus den Werkstoffen Al Mg Si und Al Mg 5
W. Schütz |
| TM 18/66 | Vergleichende Dauerfestigkeitsversuche mit blanken und vakuumkadierten Schrauben M 16 x 2 aus dem Fließwerkstoff 1.6604.6
H. Ostermann |

ICAF-Documents by German Authors, Distributed during the present Period
of Review (May 1965 to March 1967)

- 307 Technical Notes, Laboratorium für Betriebsfestigkeit, Darmstadt, LBF TM 1-14
- 308 Contributions of German Aircraft Manufacturers to the 9th ICAF-Conference
 E. Gassner
- 311 Review of Investigations on Aeronautical Fatigue in the Federal Republic of
 Germany (LBF Report S-55)
 E. Gassner
- 317 Rißfortschreitung, Schädigung und Dauerbruch in axial belasteten Flachstäben
 mit Querschlitze bei ein- und mehrstufiger Beanspruchung (Fatigue Crack
 Propagation, Damage, and Fatigue Failure in transversally slotted flat plate
 Specimens under Axial Constant and Variable Load Amplitudes)
 K. Klöppel and T. Seeger
- 318 Zeitfestigkeit und Betriebsfestigkeit von Titanwerkstoffen im Vergleich zu
 Stählen und Leichtmetallen (Fatigue Strengths under Constant Amplitude
 and Programme Loading of Titanium-Base Materials compared to those of
 Steels and Light Metals)
 E. Haibach
- 319 Wirklichkeitsgetreue Lebensdauerfunktion für Fahrzeugbauteile (Life Func-
 tion for Automobile Components established from Service Data)
 E. Gassner and W. Lipp
- 320 Zeitfestigkeit gekerbter Proben aus Stahl Ck 35 bei nicht-sinusförmigem
 Beanspruchungsablauf (Finite Fatigue Life of Notched Ck 35 Steel Specimens
 under Non-Sinusoidal Loading)
 E. Gassner and W. Lipp
- 328 Critical Comparison of Modern Fatigue Testing Machines with regard to
 Requirements and Design
 T. Haas and H. Kreiskorte
- 338 Minutes of the Ninth Conference of the International Committee on
 Aeronautical Fatigue, Part I and Part II
 E. Gassner
- 340 Kennzeichnung der Dauerschwingfestigkeit durch Mittelwert und Streuung
 (Determining the Strength under Repeated Loading by Statistical Mean
 and Standard Deviation)
 H. Ostermann

- 341 Betriebsbeanspruchung von Radfelgen (Wheel Rim Loads in Service)
O. Svenson
- 342 Betriebsfestigkeit von Augenstäben aus einer Aluminiumlegierung 3.1254.7
(Fatigue Strength under Program Loading of Aluminium Alloy Lugs of 3.1254.7
(2014-T6) Material)
O. Buxbaum
- 343 Einfluß unterschiedlich hoher und häufiger Vorbelastungen auf die Schwing-
festigkeit gebohrter Flachstäbe aus St 37 (The Effect of Prestresses of Varying
Magnitude and Frequency on the Fatigue Strength of Drilled Flat Bars of Mild
Steel St 37) Teil A: Wöhlerversuche. (Part A: S-N Tests.)
H. Ostermann and W. Schütz
- 345 Fatigue Strength of Notched and Unnotched Al Mg Si 1 and Al Mg 5 Materials
(in German Language)
W. Schütz
- 347 Untersuchung der Möglichkeiten der Verwendung von Aluminium-Knetlegie-
rungen, insbesondere der Gattung Al Zn Mg Cu, für biege- und drehbean-
spruchte Federn (Investigation of the possibilities of using wrought aluminum
alloys, especially of the type Al Zn Mg Cu, for springs subjected to bending
and torsional stresses)
E. Wauschkuhn
- 348 Einfluß unterschiedlich hoher und häufiger Vorbelastungen auf die Schwing-
festigkeit gebohrter Flachstäbe aus St 37. Teil B: Mehrstufen- und Betriebs-
festigkeitsversuche. (Influence of the cyclic ratio on the fatigue strength of
drilled flat bars of St 37 steel material. Part B: Multi-step and program tests.)
E. Gassner and W. Schütz
- 349 Über eine Beziehung zwischen der Lebensdauer bei konstanter und bei veränd-
erlicher Beanspruchungsamplitude und ihre Anwendbarkeit auf die Bemessung
von Flugzeugbauteilen. (The relationship between fatigue life under constant
and under variable stress amplitudes and its utilization for the design of
aircraft structures.)
W. Schütz
- 350 Kennwerte des Spannungskollektives der Flügelunterseite Boeing 727 aus Eich-
und Meßflügen. (Characteristics of the stress frequency distribution of wing
lower surface of model Boeing 727 from flight-measurements)
O. Buxbaum

1 N 69-21586

REVIEW OF SOME BELGIAN WORKS ON FATIGUE

DURING THE PERIOD MAY 1965 - APRIL 1967

Compiled by

J. van Laer

Ministere des Communications

Administration de l'Aeronautique

(Rapport MV. 67-03)

CONTENTS

1. <u>S.T.Aé. Works</u>	226
1.1 Modified (swing tail) Douglas DC-4 fuselage tests	226
1.1.1 Description of the test specimen	226
1.1.2 Loading program	228
1.2 Fatigue pressurization tests	232
1.2.1 Testing equipment	232
1.2.2 Results	233
1.3 Fatigue tests on detailed part	233
Flying controls of the swing tail fuselage	
1.4 Specimens	234
Glass fiber reinforced plastic	
1.5 Residual strength	234
2. <u>Some investigations carried out at the C.N.R.M. (Centre National de recherches métallurgiques)</u>	235
2.1 Cumulative damage on aluminium alloy 24 S.T	235
2.2 Effect of "Low cycle fatigue" damage in low alloy heat-treated steel	235

1. S.T.Aé. Works.

Most of the activity of the belgian S.T.Aé. in the field of the fatigue during the recorded period was devoted to full scale structural tests.

1.1. Modified (swing tail) Douglas DC-4 fuselage tests. (fig.1)

This test was already mentioned in the last ICAF review. The tests began in January 65 and was terminated at the end of February 66 after 28.000 simulated flights.

1.1.1. Description of the test specimen.

The specimen consists of a portion of a Douglas DC-4 fuselage extending from the station 742 to the frame 852 at which the tail structure (vertical and horizontal stabilizer and surfaces) is bolted. The tail part beyond the frame 852 was represented on the specimen by a dummy steel structure bolted to the frame.

The actual modification on the airplane consists to cut a portion of the fuselage from station 780 to 858 and to replace this part by a prefabricated kit (fig.2).

The kit is riveted to the fuselage at its front end and bolted at its rear end to the tail structure. It consists of two parts articulated around a vertical axis situated on the right side; when closed the two parts are jointed together by 11 hydraulic locks distributed along two reinforced frames at the station 800.

The opening is made by means of hydraulic actuators situated on the top of the fuselage.

The structure of the front part is made as seen on the figure (2.) of two heavy box frames on both ends (stations 780 and 800). These box frames are connected by box beams which transmit when the fuselage is closed the load from the hydraulic locks. The hinges are attached to specially reinforced box beams situated at stringers (n°10 to 12) and (n° 22 to 24). The rear part of the kit has a similar structure, but with longer box beams for supporting the rear hinges, these beams going to the heavy frame 858.

1.1.2. Loading program.

It was shown by the structural strength investigation that the higher stresses were induced in the modified part of the fuselage during the opening of the tail and also when opened if wind blows along the longitudinal axis of the aircraft. It was thus necessary to introduce in the fatigue loading program a ground phase which in fact produces the main damage, and to be comprehensive, to add the less important loads which are the flight loads.

The flights loads were assumed those arising from the utilization on a moderately short range (230 NM), low altitude, with an average flight time of 82 minutes. Unhappily the tail load spectrum is complicated, and experimental and statistical data are rather scarce. Some theoretical evaluations have been done with some flight tests to check the estimates. The tail spectrum incorporates several super-imposed effects:

- a) a ground-air cycle which is the variation of the 1g equilibrium load with speed, weight, change of configuration. This load depends much of the C.G. position.
- b) the manoeuvring loads mostly the take-off rotation, and change of configuration.
- c) the vertical and lateral gust loads on the empennages.
- d) the landing and taxiing loads.

Happily the stresses induced in the rear part of the fuselage by the flight loads are rather low and the deficiency in actual data can be compensated by a certain conservatism.

The loading amplitude and the number of occurrences are not easy to choose; in fact these depend of the fatigue limit of the structure which is just what has to be verified by the tests. An assumption must then be made on the fatigue resistance of the structure. In accordance with the theory of Haithby-Eggewertz an amplitude of ± 20 ft/sec gust was chosen for the testing load and the number of repetitions was taken as 3 per flight.

To take into account the manoeuvre and the effect of change of configuration 2 cycles with the same amplitude were added. All these loads were superimposed on a G.A.C. load which was supposed to be of 1750 Kg (down load) (C.G. forward).

The ground loads were taken more easily into consideration because they come mostly from the manoeuvring of the tail. During the opening of the cone, the weight distribution is transferred from the 11 locks to the two hinge points and the stress distribution varies accordingly. When the fuselage is open, the tail may be submitted to wind forces and some additional fatigue damage. The drag force of the wind and its location were obtained by tunnel testing. Stresses induced by the wind higher than 20 Knots are not negligible. An operation limit of 35 Knots is set for the opening of the cone. Fatigue damage must be evaluated for wind between 20 and 35 Knots. Meteorological statistical data exist for wind amplitudes and frequencies and are given on two forms: either mean wind velocity, or maximum wind (gust) velocity.

Mean wind (taken for period of 10 minutes).

For 148.888 measurements

43.336	higher than 11 Kn.	or the cumulative frequency is 0,291
12.431	" " " 17 Kn.	" " " 0,0835
3.673	" " " 22 Kn.	" " " 0,025
0.51	" " " 28 Kn.	" " " 0,004

Gust (the maximum taken during the hour).

For 131.472 hours

17.804	observations higher than 20	- cumulative frequency 0,1354.
7.779	" " " 30	- " " 0,059
1.250	" " " 40	- " " 0,0095

From these data it was decided to choose for the wind loads 7 gusts of an amplitude of 35 Knots per flight.

To sum up, the loading cycle is represented on the figure 3.

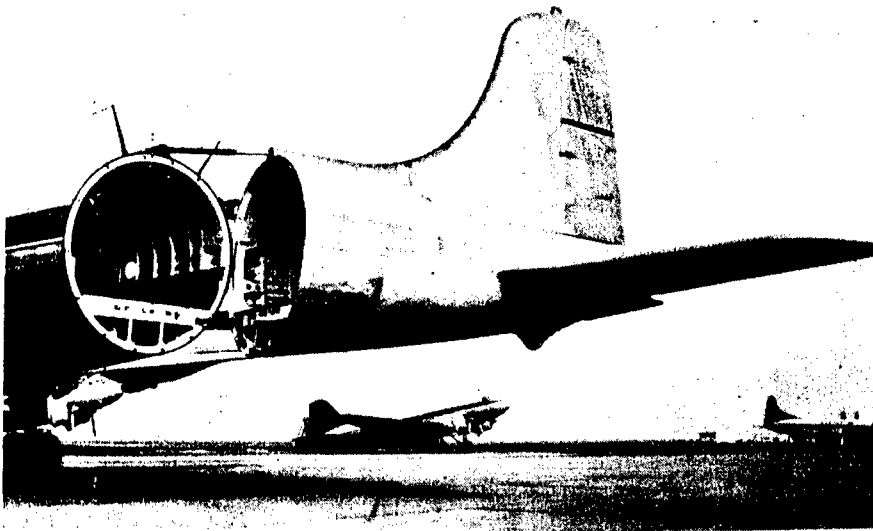


FIG. 1.

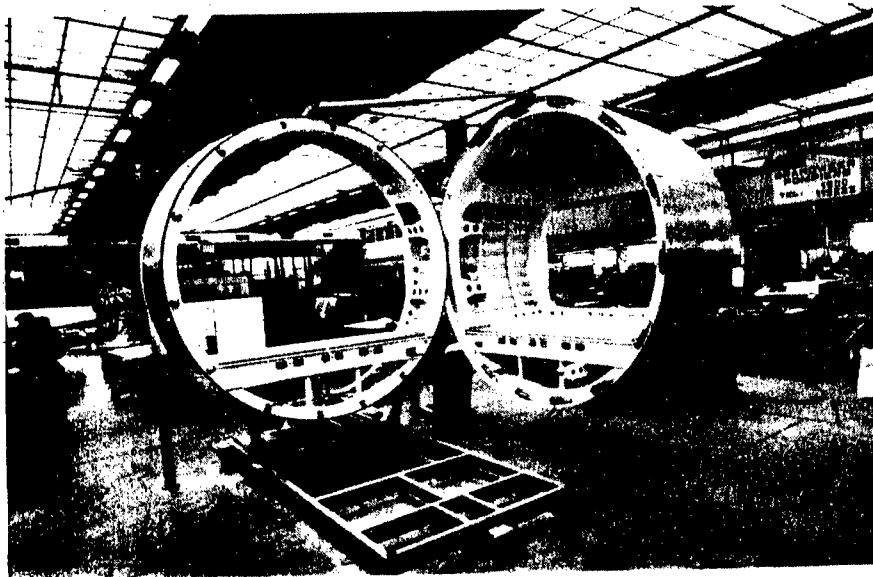


FIG. 2.

TO WEIGHT 64000 Lbs
ZERO FUEL WEIGHT 60600 Lbs

DC-4.- SWING TAIL TYPICAL FLIGHT

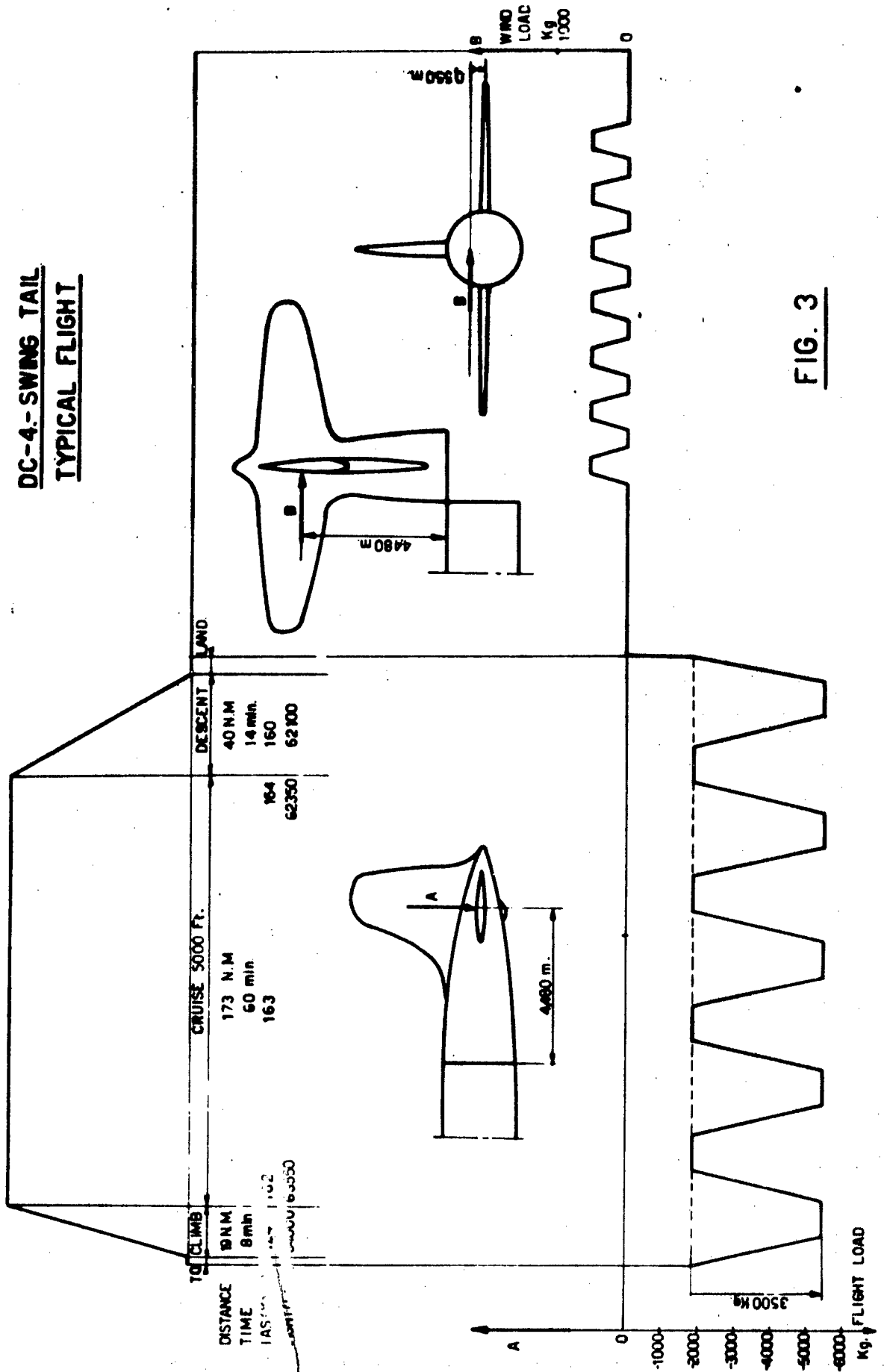


FIG. 3

Testing Equipment.

The test specimen is mounted cantilever in a rigid steel frame; two loading hydraulic actuators are used; one for the flight loads and one for the wind loads on the ground.

The loading sequence is all automatic. Its begins by the flight loads, next the cone opens, after which it is loaded by the wind gust and thereafter closes.

The duration of a complete sequence representing one flight is of about 3 1/2 minutes.

The complete description of the system was given in the last review. The figure (4) shows the cone in the test frame. The figure (5) shows the Program Control panel, on which are mounted the pressure gages, hydraulics valves, load counter and indicating lamps etc... The figure (6) shows the cone open.

Results.

The figure (7) shows the progression of the tests during the period 65-66.

After a few troubles which occurred during the first 10.000 cycles reinforcements were made and no more troubles occurred and the tests progressed steadily.

The first trouble occurred with the upper hinge axle which was found seized. (photo 8). The axle were replaced by a chrome plated axle and in place of the bronze bushing, a ball pivoting joint was installed.

The second important trouble was due to the failure of some bolts fixing the upper forward hinge (photo 9).

The upper hinge was reinforced and rigidified to eliminate the bending of the bolt heads. Reinforcements were also made on the box beam supporting the hinge.

At about 8.000 cycles, it was found by inspection that a crack had developed in the rear upper hinge. (see photo 10). After a long delay the test were resumed and till the end (at about 28.000 cycles) we had only rather minor trouble, as fatigue crack developing through a greasing hole of the eye bolt of the rear hydraulic actuator. A thorough inspection was made after the test but did not disclose any important defect. An airplane was modified at the end of 66 and made test flights and received his certification in February 67.

1.2. Fatigue pressurization tests.

It was envisaged to apply the same modification of a swing tail to Douglas DC-6 and DC-7 airplanes. For the fatigue proof, it was thus necessary to include in the loadings the pressure load of the fuselage. A tank test was not considered practical, because the opening and closing phase was still the most critical part of the loading spectrum. The weight of the movable part was now much higher than in the former case. The only way of doing the pressurization was to air pressure the test specimen. The specimen was made air-tight by means of a rear bulkhead made of steel plates reinforced by vertical channels and of a rubber seal installed in the joint between the rear cone and front part of the fuselage. To have a smaller air volume, to reduce danger in case of explosive decompression, and time necessary to obtain the pressure, the specimen was filled with plastic foam.

The loading program was the same in principle to that used for the DC-4; it includes the flight loads during which the fuselage was pressurized and depressurized; the opening of the fuselage and the application of the wind loads.

As the length of the flight stage was longer the number of applied gusts had been increased to 10; the inside pressure was simultaneously increase to 4,6 psi.

For the ground phase a fewer number of wind gusts (two of 35 Knots intensity) were applied. It was thought that it was the peak to peak range which was important and it was necessary to reduce the number of wind gusts to keep the already long cycle time low.

The duration of one cycle was 4 minutes.

1.2.1. Testing equipment.

The equipment used for the testing of the DC-4 modified was completed by an air compressor, a motorised three way air valve, and a mercury manometer with electrical contacts.

The cycle was automaticly controlled and the figure (12) shows the schematic diagram of the hydraulic and pneumatic systems.

1.2.2. Results.

The tests began in may 66 on the same specimen that have been already submitted to the fatigue loading spectrum of the DC-4 and that had made 27.722 simulated flights without pressurisation. Due to the installation of the rear steel bulkhead the weight of the moving part of the tail cone was increased considerably, but the bending moment was kept equal to this of the DC-7. The shear force was somewhat higher but the resulting effect may be considered to be conservative. The testing progressed steadily and at the end of september 10.000 cycles were accomplished without too much difficulties. Most of the fatigue troubles were caused by the increased weight and were found in the structure around the rear skid mounted below the floor at the station 929. (fig. 13)

1.3. Fatigue tests on detailed part.

Flying controls of the swing tail fuselage.

The flying controls of the swing tail fuselage are made in two sections due to the fuselage break. The continuity of the flying controls (elevator and rudder) must be reestablished automatically when the cone is closed. The first system conceived was not satisfactory and was replaced by a system based on the same principle but of radically other realization. The flying controls of each part are terminated by compression rods; when the fuselage is closed, the compression rods come in contact and the movement of the rods are transmitted to pulleys and cables (see fig. 14).

A fatigue test was made on a set of control which was installed on a Amslerpulsator. (see fig. 15). The load was rather low for the testing machine and therefore was monitored by strain gages.

The results were very satisfactory.

1.4. specimens.

Glass fiber reinforced plastic.

A few tests were made on some glass fiber reinforced polyester specimens.

Some were made on specimens reinforced with an unidirectional roving and other with fabric reinforcement.

The fatigue machine used was the Amsler pulsator.

With the unidirectional roving the fatigue resistance was rather high and the cracks were developing in a direction parallel to the fibers.

The crack is seen by the apparition of a whitish color and there is a local increase in temperature at the extremities of the crack.

The propagation speed was rather low and the crack geometry is complicated. (fig. 16)

1.5. Residual Strength. (fig.17) (fig.18)

A few test were made on nylon fabric specimen with a central slit, to determine the residual strength. The resistance of the unslitted fabric was of 8933 Kg/m (warp) and of 4767 Kg/m (woof).

The results show the same trend found for metallic specimen, yet the deformation of the slit is far from negligible. There exist a critical stress and a slow crack growth stress. The critical stress is a function of the length of the slit and also of the absolute width of the specimen

2. Some investigations carried out at the C.N.R.M. (Centre National de recherches métallurgiques).

2.1. Cumulative damage on Aluminium Alloy 24 S.T.

This work is a co-operative research, sponsored by O.E.C.D. (Organisation of Economic Co-operation and Development) between 9 European, U.S. and Canadian laboratories.

The belgian contribution is made at the C.N.R.M. fatigue laboratory. In the first phase of the investigation, each laboratory involved has had to determine the Wohler curve and the endurance limit of unnotched specimens in rotative bending (3000 cpm) (constant bending machine type).

25 specimens were tested at each of the three stress levels.

(35 Kg/mm², 30 Kg/mm², 25 Kg/mm²)

The endurance limit was determined by the Staircase method on 21 specimens.

If a good correlation was found for the endurance limit ($20 \text{ Kg/mm}^2 \pm 0,5$ at $30 \cdot 10^6$ cycles), greater variability was obtained at the higher stresses.

<u>Stress level.</u>	<u>lowest result cycles.</u>	<u>highest result cycles.</u>
35 Kg/mm ²	50.000	180.000
30 "	215.000	800.000
25 "	$2 \cdot 10^6$	$5 \cdot 10^6$
Endurance limit	$20 \text{ Kg/mm}^2 \pm 0,5.$	

In the second phase of the research, damage for two different cycles ratio ($\frac{n}{W} = 0.15$ or $0,30$) are produced at one or two of the stress levels and the residual life or the endurance limit is investigated; 25 specimens are used for each treatment.

The tests are still in progress, but show already great differences with those obtained in accordance with the Miner rule when applied to mean values.

2.2. Effect of "Low cycle fatigue" damage in Low Alloy heat-treated Steel.

The purpose of the investigation was to determine the effect of "plastic fatigue" on the impact properties of three types of steel: A302-B (Mx, Mo), Dacol W30 (Mn, No, Cr, V), Soudo Tenox S6 (Mn, Mo, Ni, Cr).

2.2.1. The results of the Side Bend Tests on sheet specimens showed that the higher transition temperature obtained were not a regular fonction of the number of cycles nor of the ratio $\frac{n}{N}$.

2.2.2. Charpy tests were executed on specimens extracted from fatigue test pieces which were submitted to alternative tensile - compressive deformations of several amplitudes and for several ratio of $\frac{n}{N}$. The transition temperature curve was drawn and the temperature transition was found to rise with the ratio $\frac{n}{N}$ between the limits 1% - 10% both for fatigue tests made at ambient temperature and at 300°C.

For damage made for a number of cycle ratio lower than 1%, there is a marked softening effect of the first fatigue cycles.

In spite of dispersion, the results were shown to be dependent of the chemical composition of the steel, the best results were obtained with the Ducol W 30.

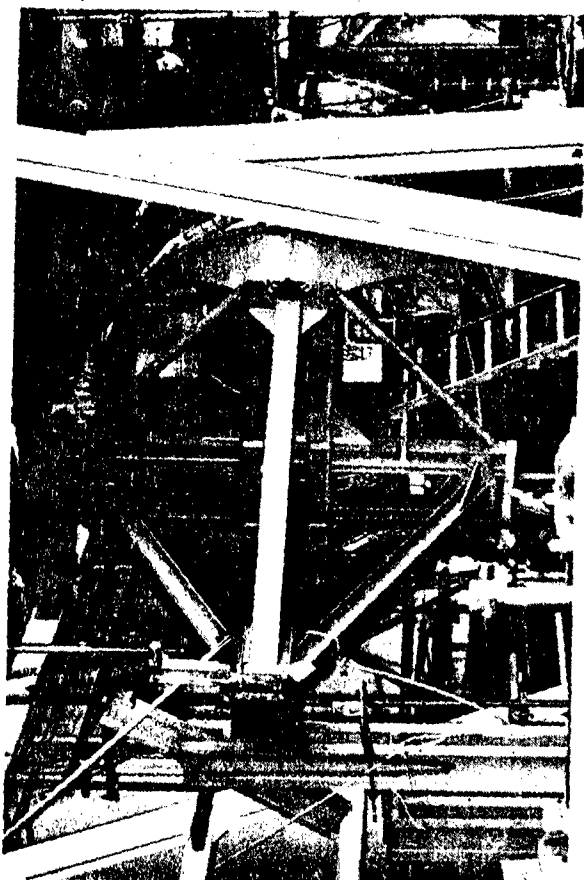


FIG. 4.

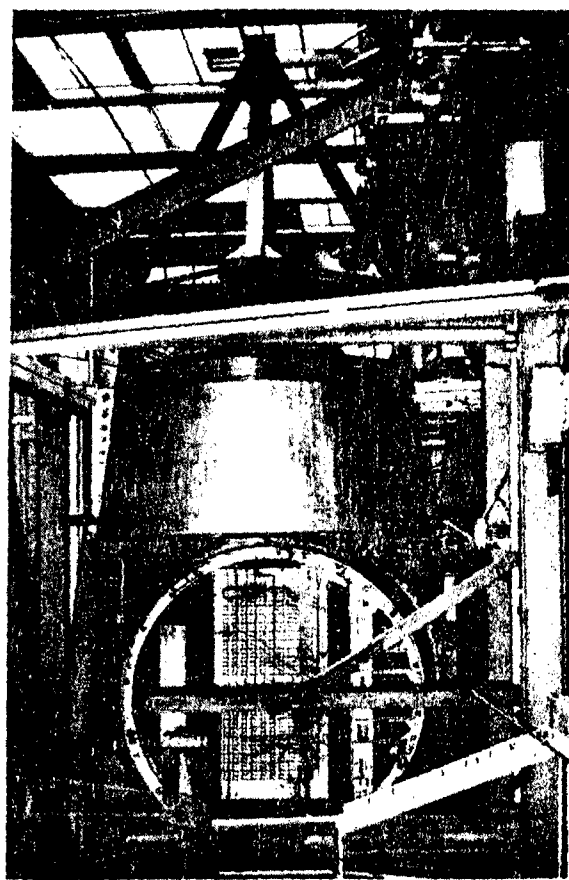


FIG. 6.

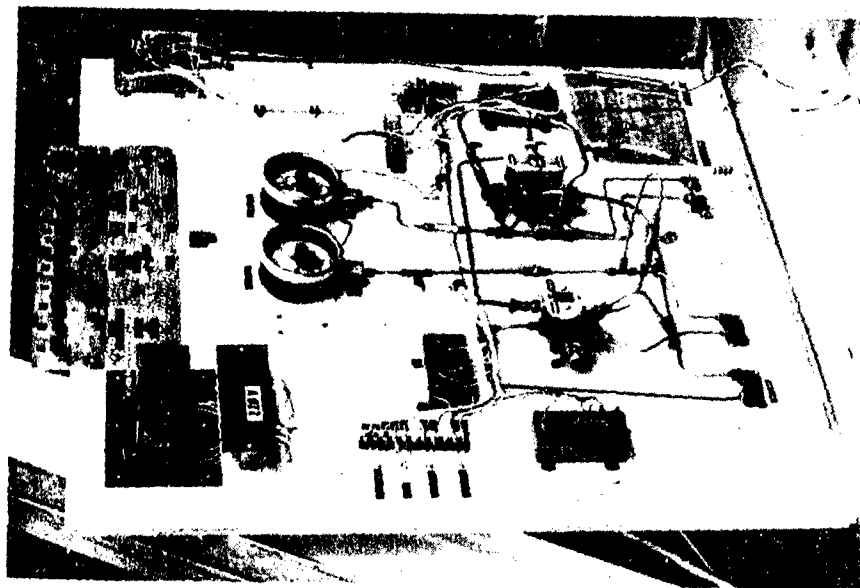
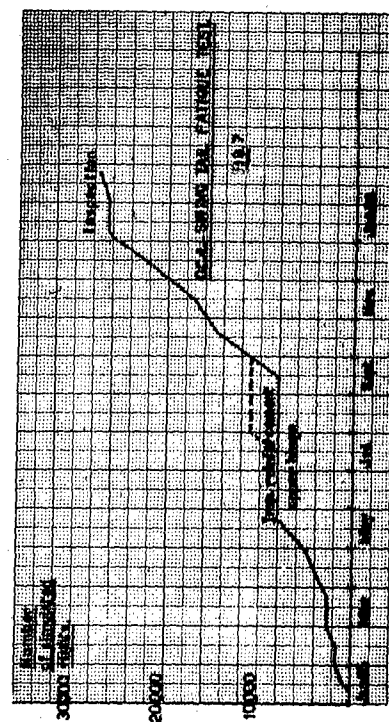


FIG. 5.



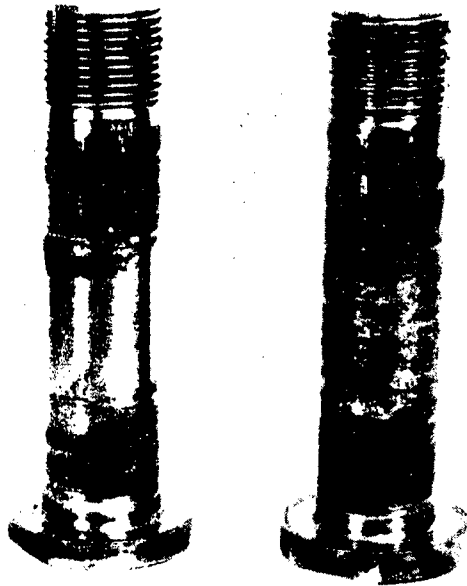


FIG. 8.

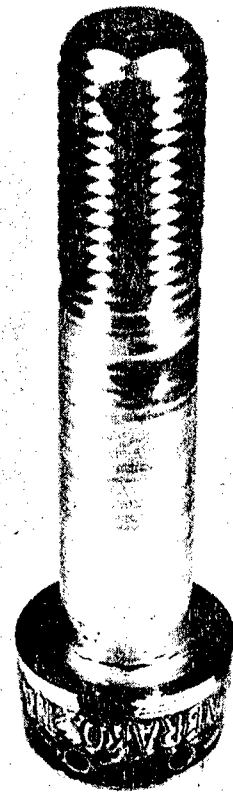


FIG. 9.

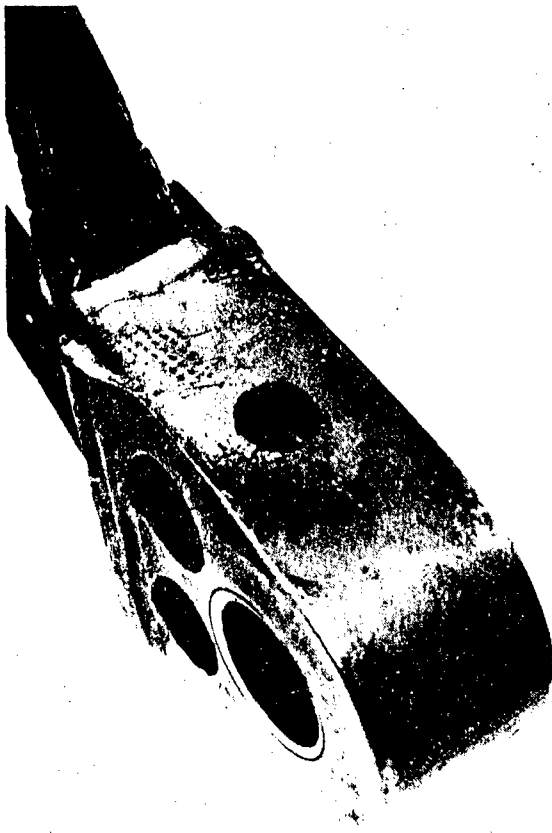


FIG. 10.



FIG. 11.

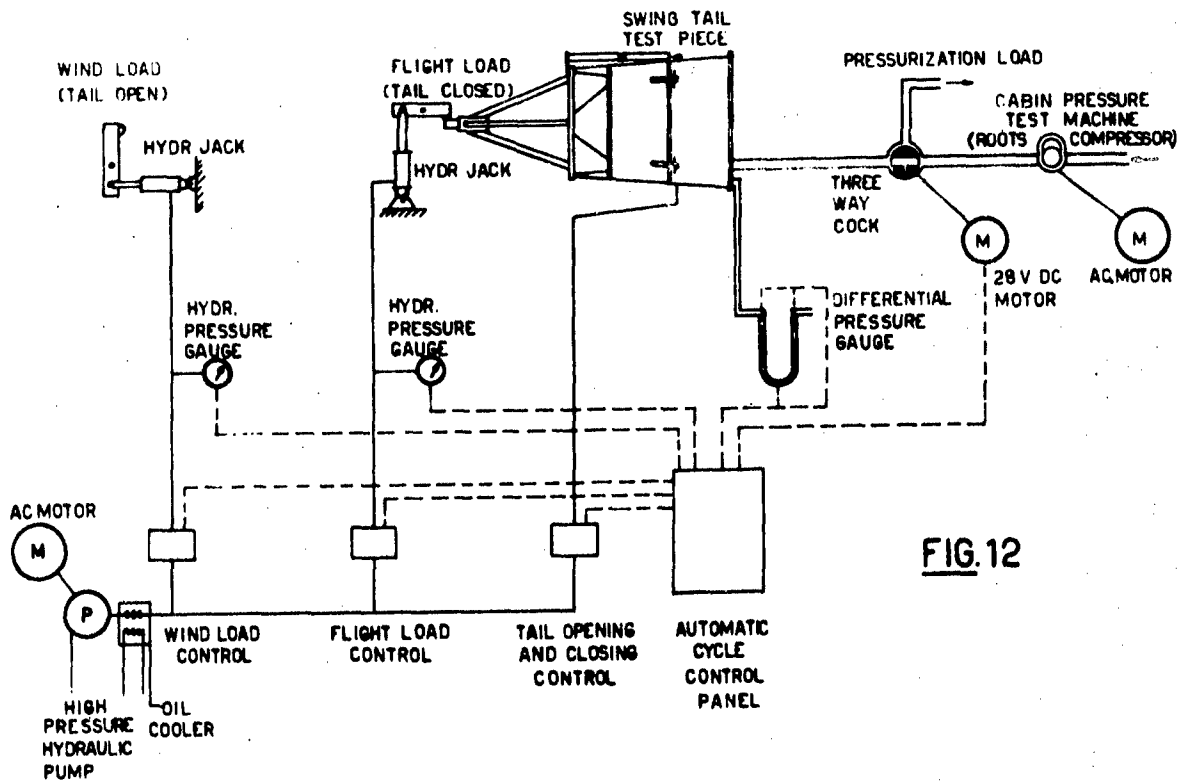


FIG. 12

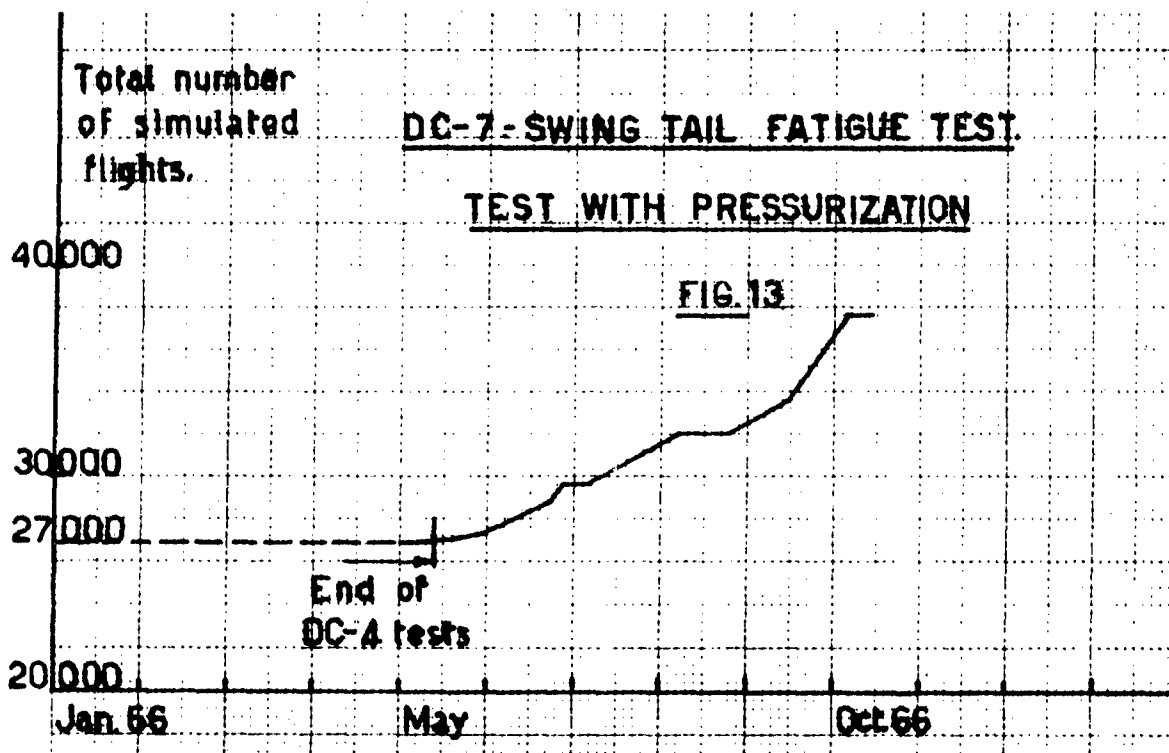
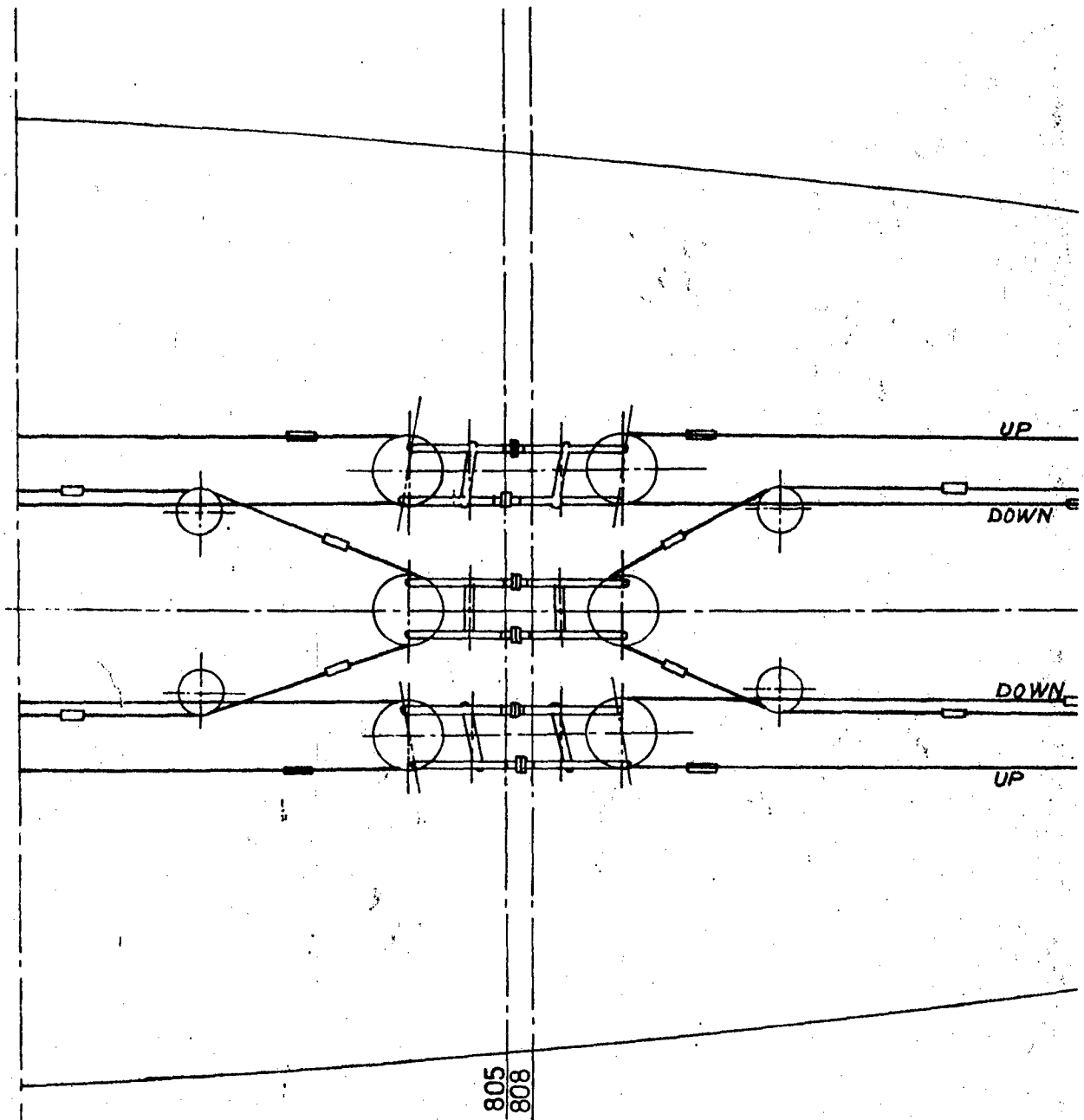


FIG. 13

FIG. 14

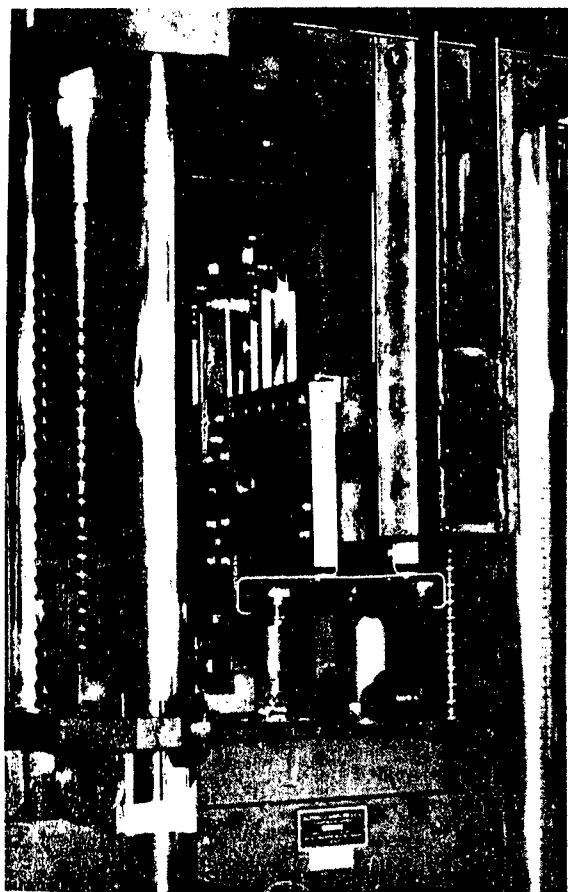


FIG. 15.

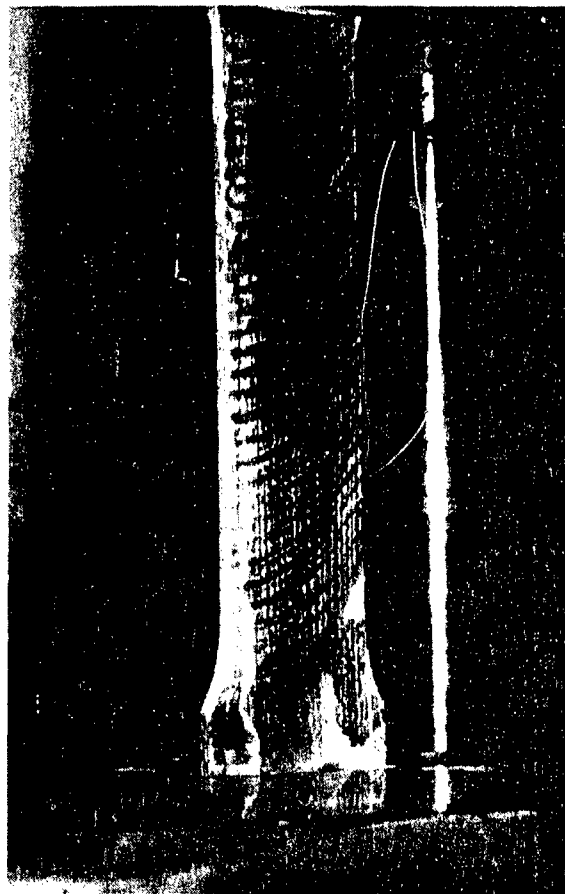


FIG. 16

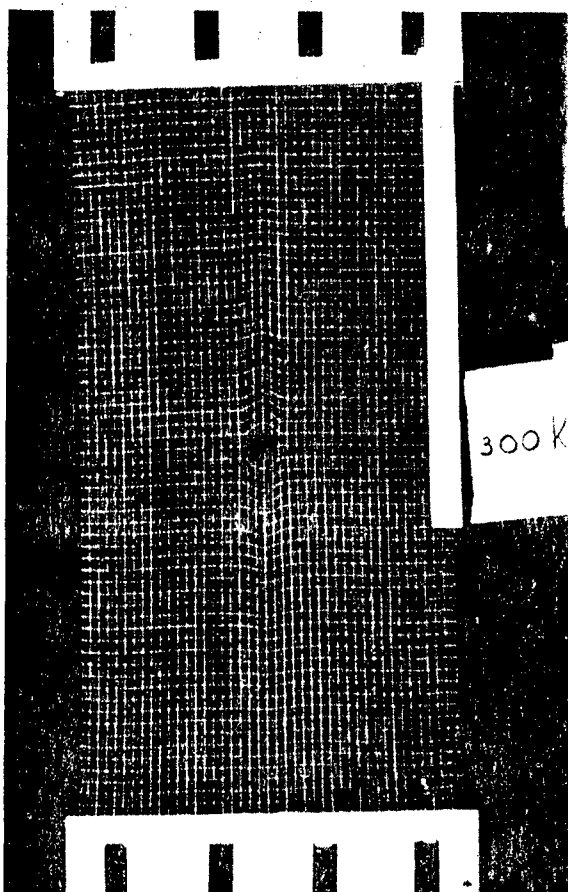


FIG. 17

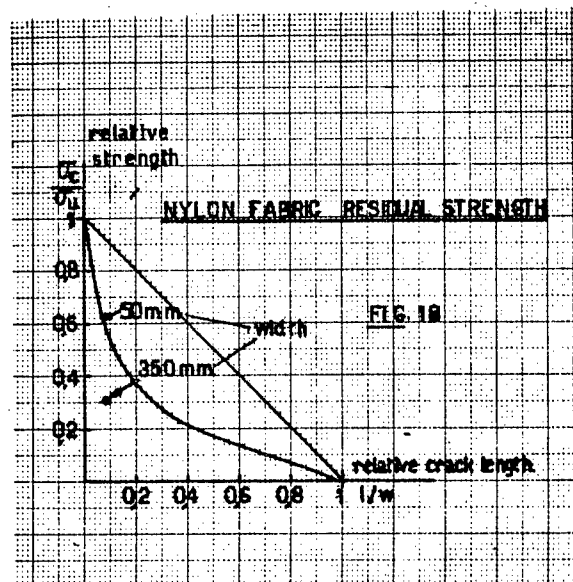
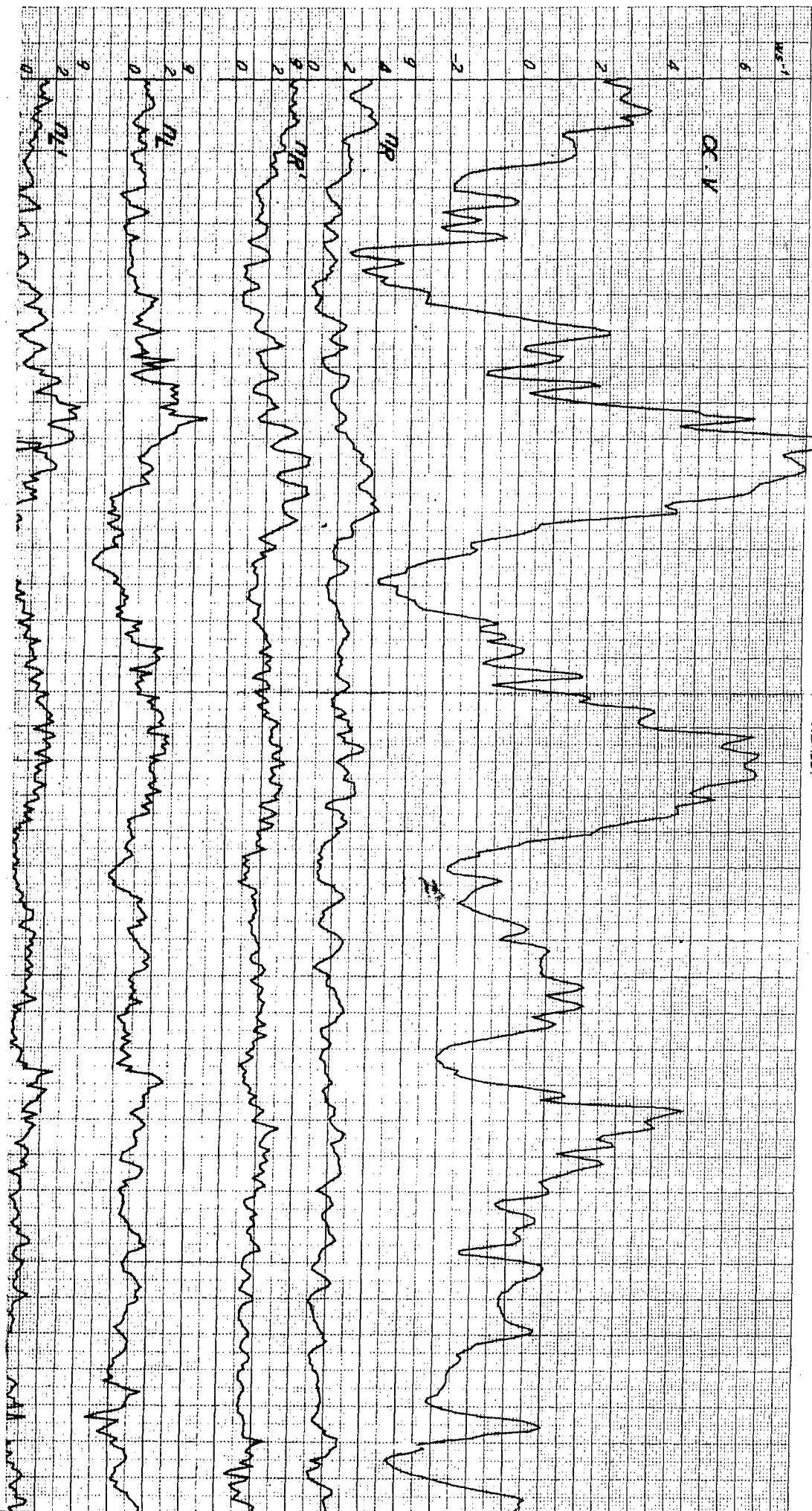


FIG. 18.

max. 10.2m/sec

PRECEDING PAGE BLANK NOT FILMED.

107-13



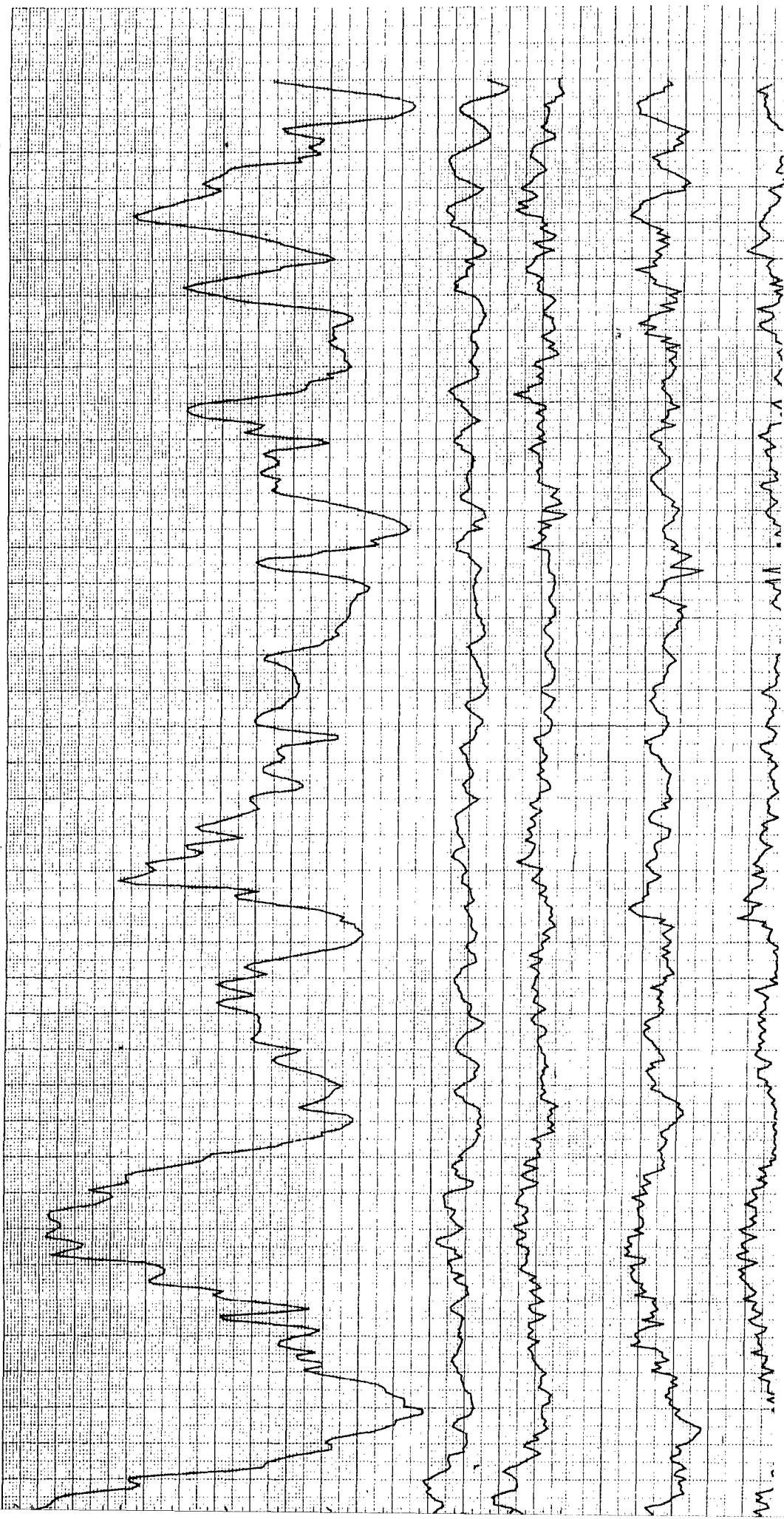
S-196

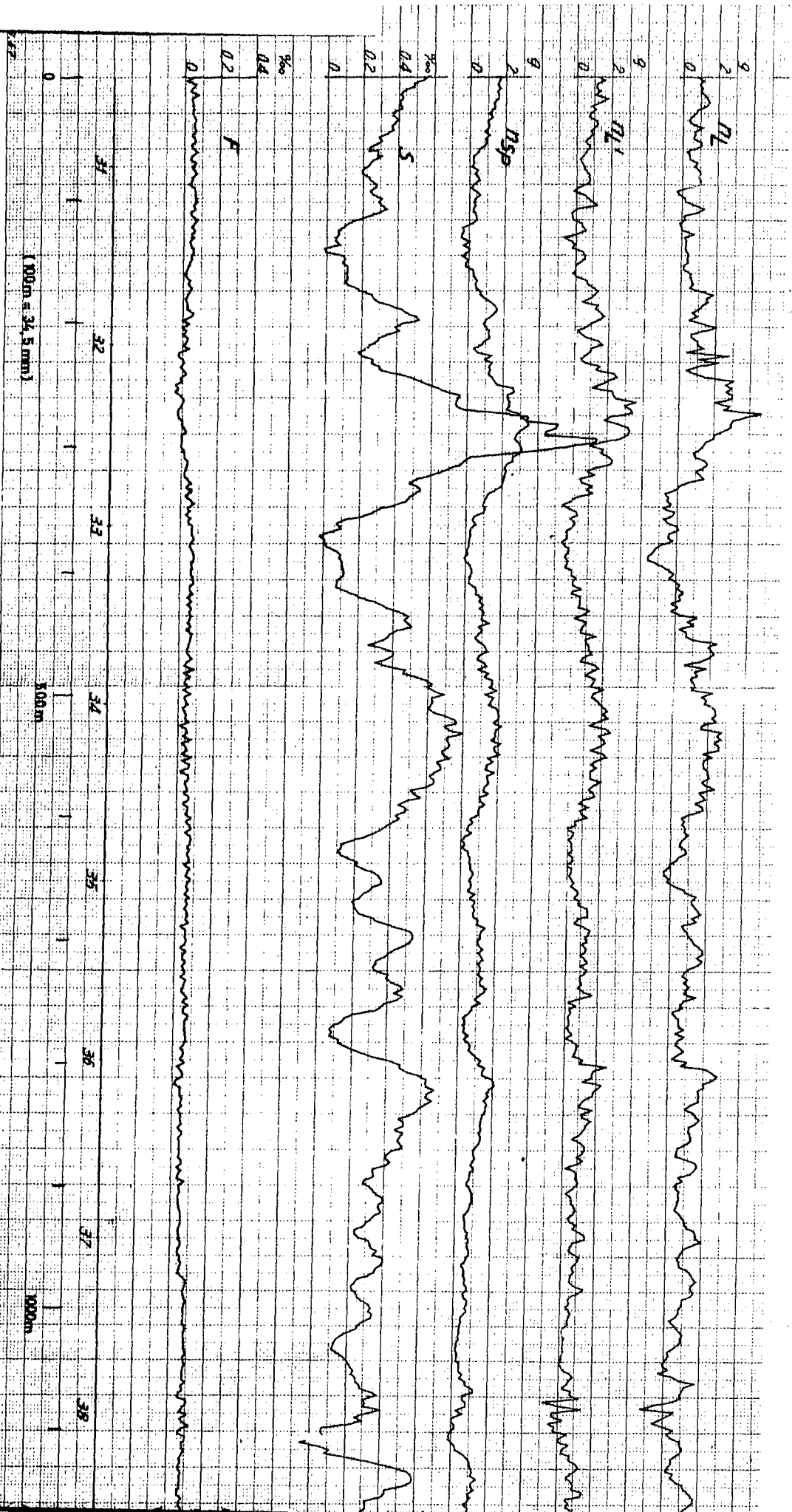
Fig. 1a

107 - C

107-B

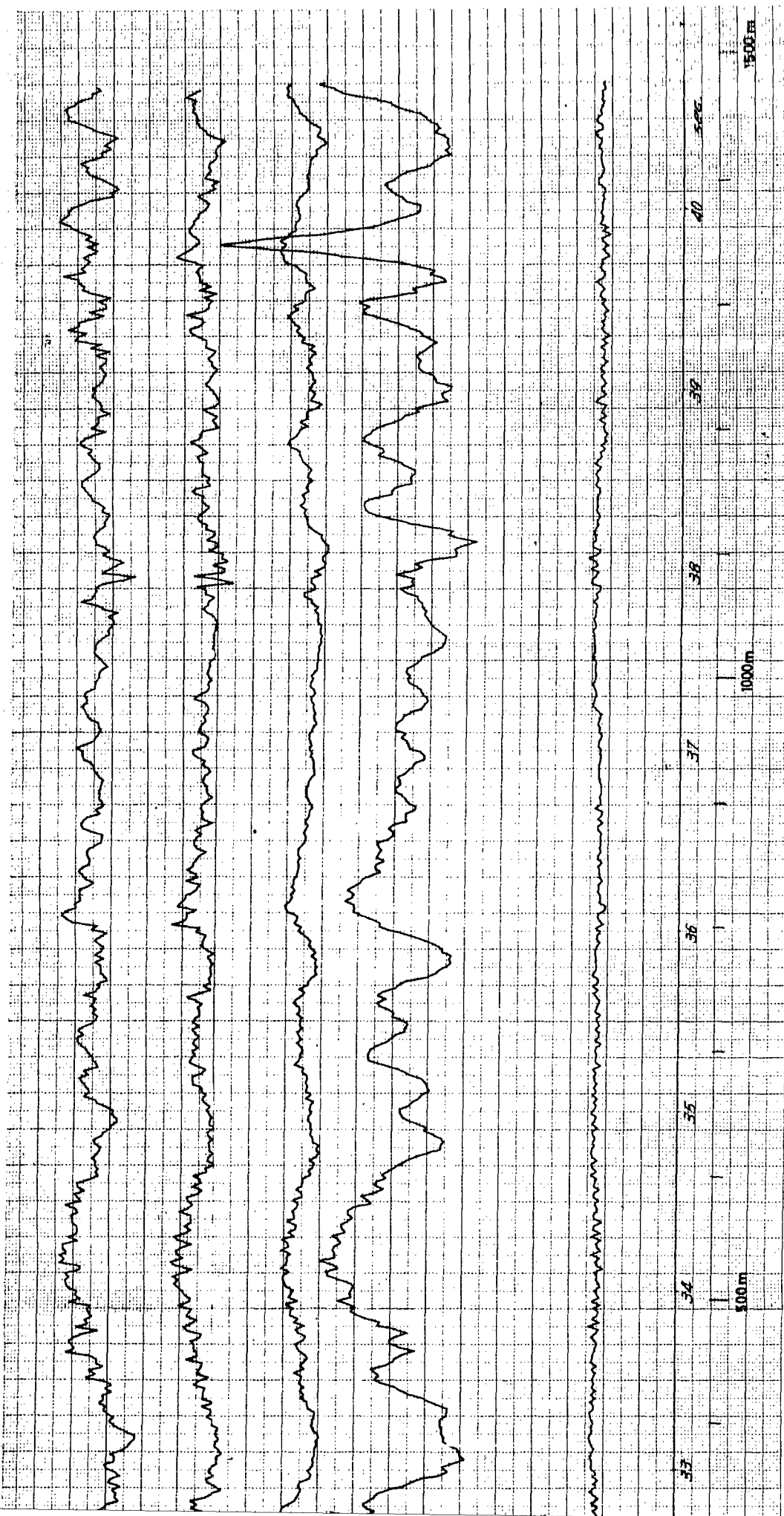
PRECEDING PAGE BLANK NOT FILMED.





107-D

107-E



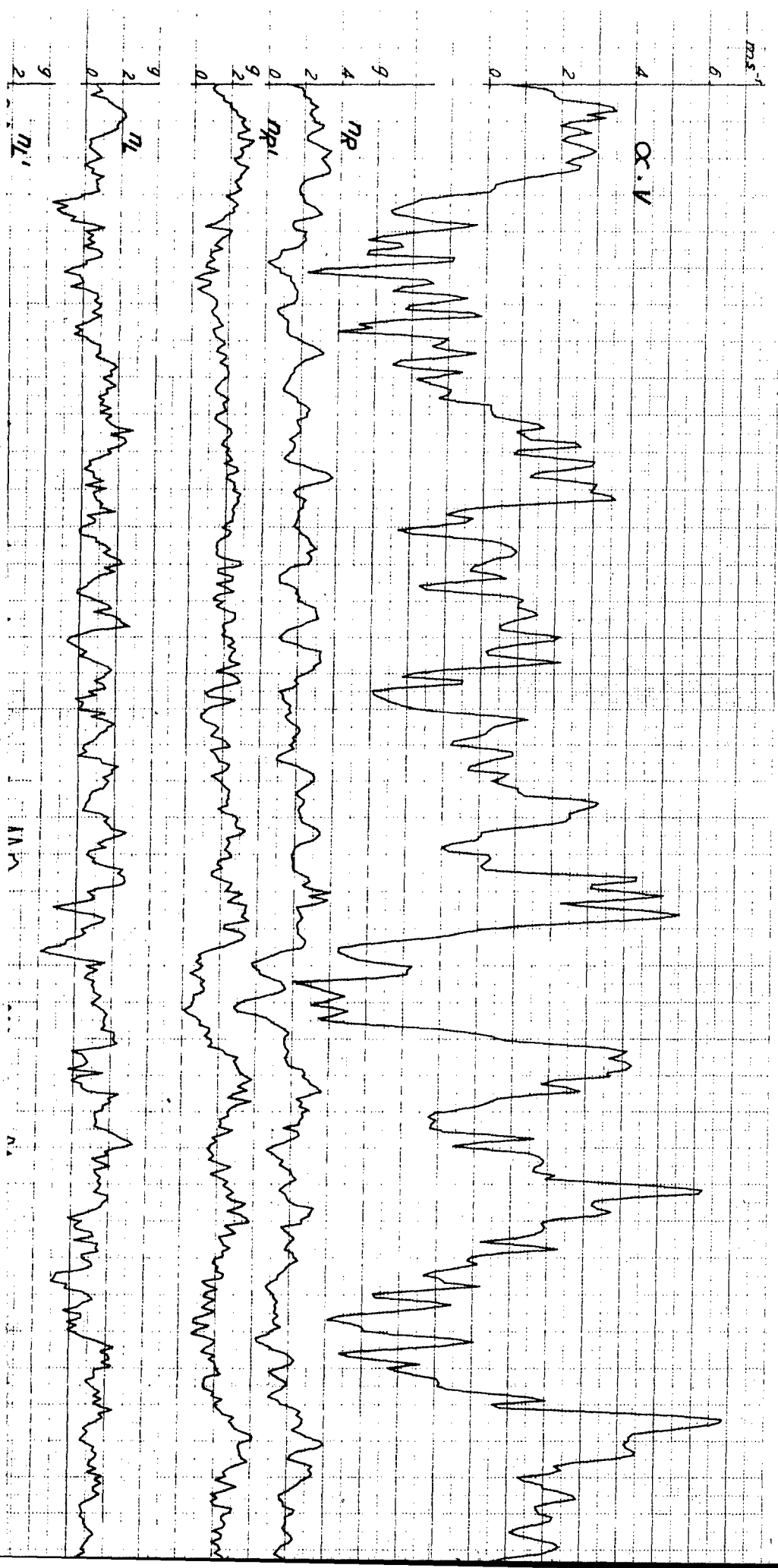
D

107 - E

107 - F

108-17

108-13

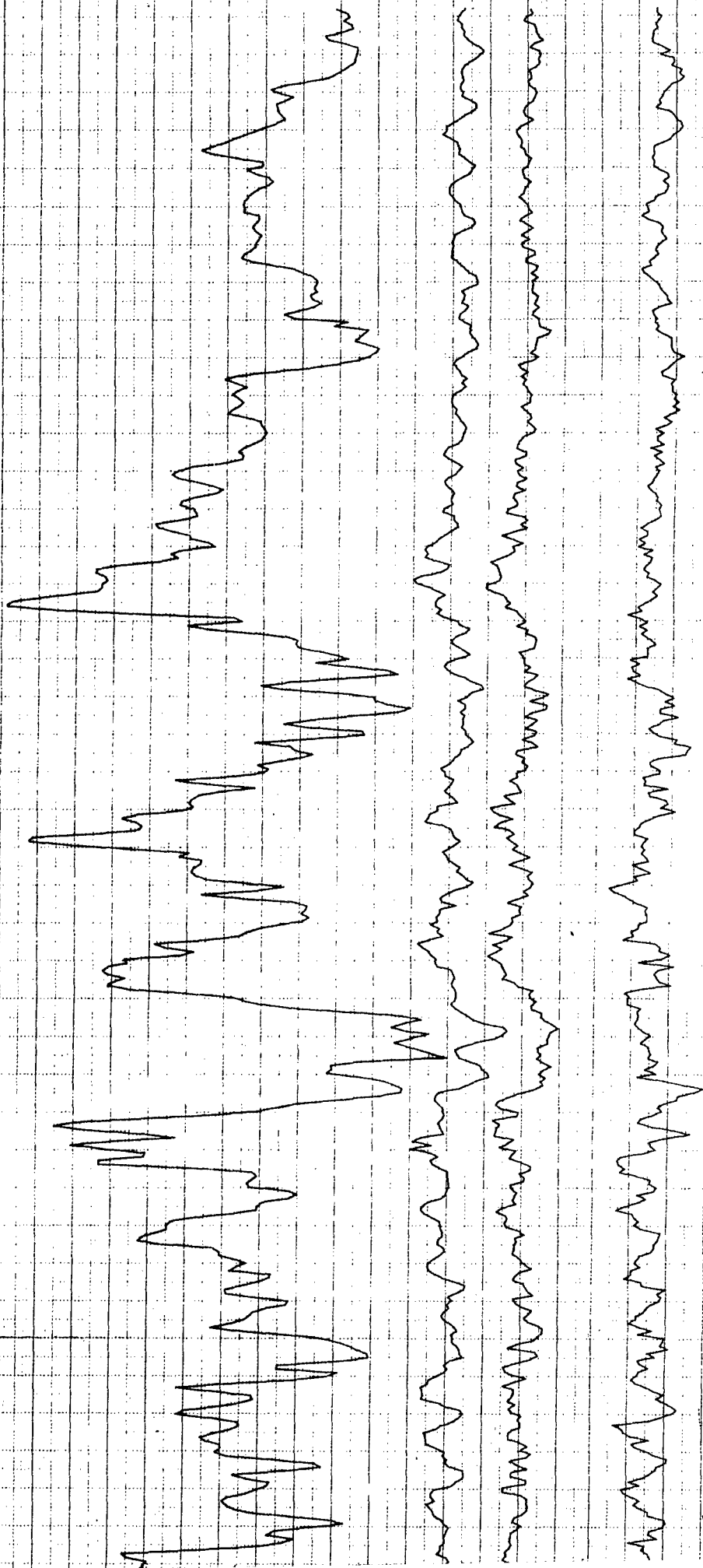


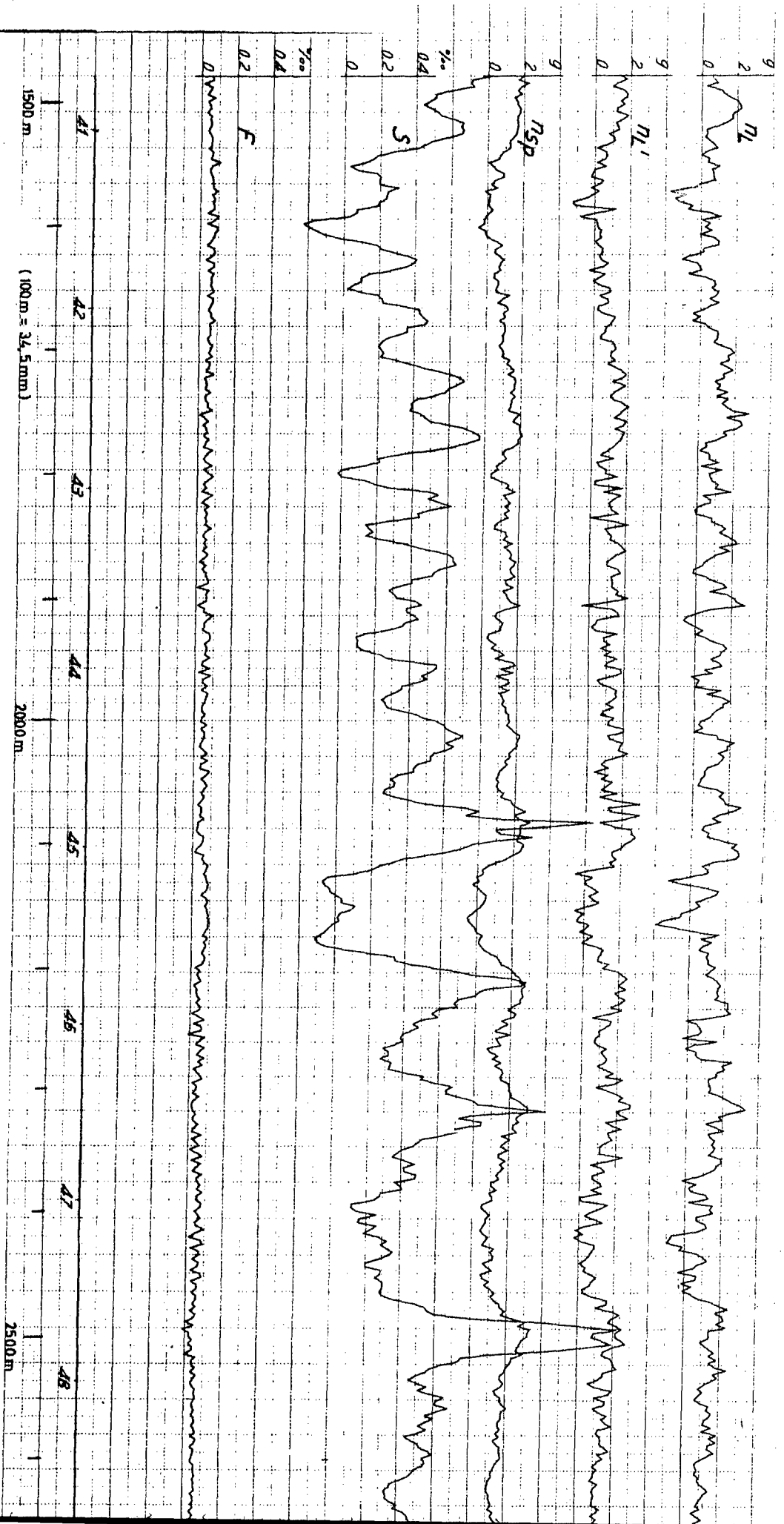
S-196

Fig. 1b

108 - C

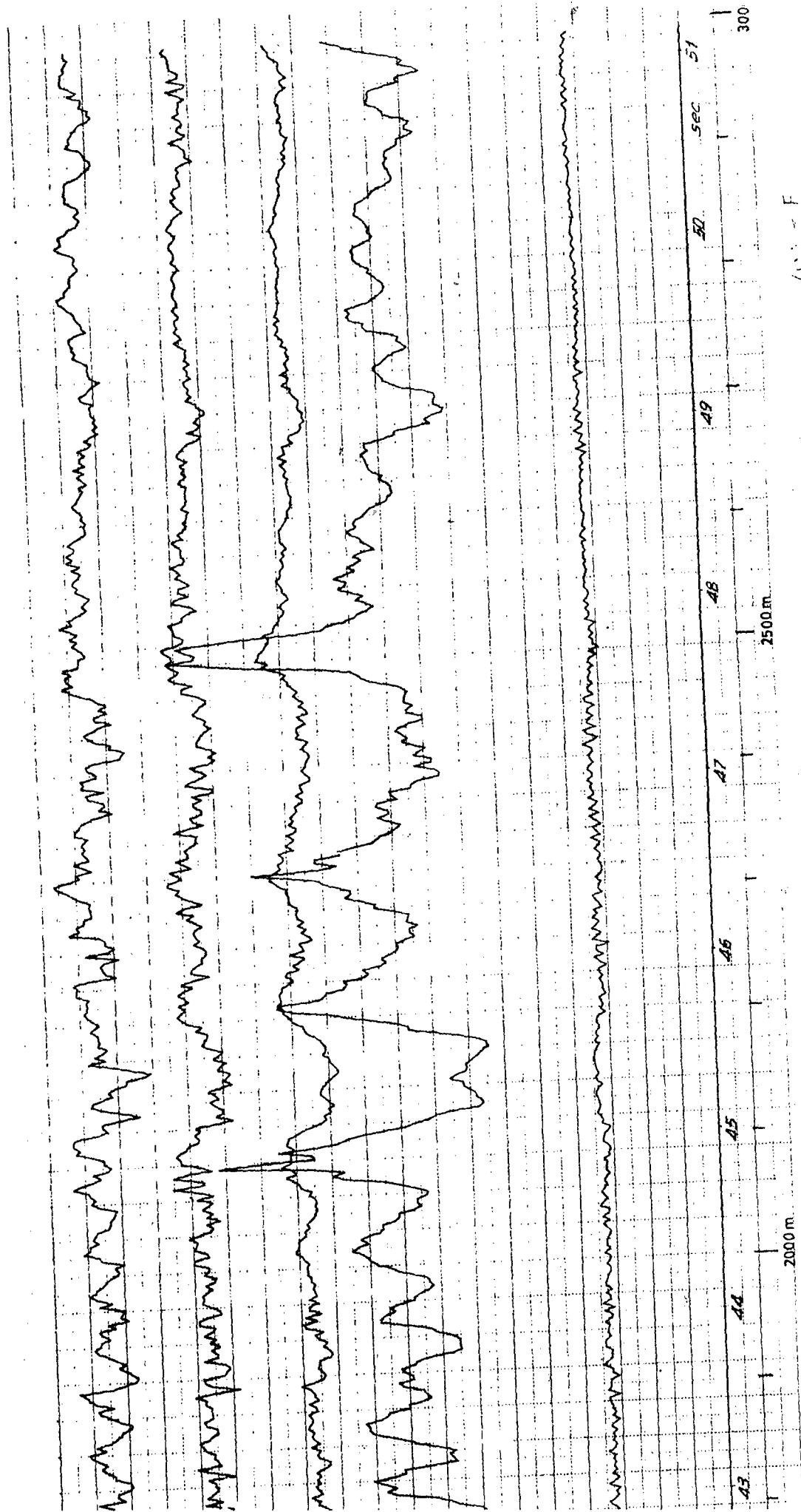
108 - B





108-D

108-E



1000 F

1000 F

1000 F

1 N 69-21587

A REVIEW OF RESEARCH ON AERONAUTICAL FATIGUE

IN THE UNITED STATES 1965 - 1967

Compiled by

Herbert F. Hardrath

NASA Langley Research Center

Langley Station, Hampton, Va. U.S.A.

CONTENTS

I.	NASA LANGLEY RESEARCH CENTER	247
	A. Supersonic Transport Considerations	247
	B. Fatigue Crack Propagation and Fracture	247
	C. Plastic Behavior at Notches	250
	D. Development of Test Facilities	250
	E. Contract Research	250
	F. Definition of Load Environment	251
II.	NASA LEWIS RESEARCH CENTER	252
	A. Crack Initiation and Propagation	252
	B. Cumulative Damage	252
	C. High-Temperature Low-Cycle Fatigue	252
III.	U.S. AIR FORCE FLIGHT DYNAMICS LABORATORY	252
	A. Fatigue Damage Indicator (S-N Gage)	252
	B. Optimization of Ordered Load Spectra in Full-Scale Structural Fatigue Tests	253
	C. Fracture Mechanics - Crack Propagation	253
	D. Time Compression in Elevated Temperature Fatigue Testing	253
	E. Fatigue Strength Design and Analysis of Aircraft Structures	254
	F. F-100 Fatigue Program	255
	G. Sonic Fatigue	267
IV.	U.S. AIR FORCE MATERIALS LABORATORY	255
	A. Mechanical-Metallurgical Aspects of the Fatigue Process	255
	B. Crack Propagation and Notch Effects	256
	C. Structural Reliability	258
	D. Mechanism of Stress Corrosion Cracking	259
	E. Work Hardening	260
	F. Surface Effects	261

V.	U.S. NAVY AERONAUTICAL STRUCTURES LABORATORY	262
	A. Structural Fatigue Research	262
	B. Environments Research	263
VI.	FEDERAL AVIATION AGENCY	264
VII.	INSTITUTE FOR THE STUDY OF FATIGUE AND RELIABILITY - Columbia University	265
VIII.	NORTHROP NORAIR	265
IX.	LOCKHEED-CALIFORNIA COMPANY	265

APPENDIX - FATIGUE OF STRUCTURAL MATERIALS SUITABLE FOR 275
THE SUPERSONIC TRANSPORT. By Herbert F.
Hardrath, NASA Langley Research Center,
Hampton, Virginia

A large number of investigators in the United States are actively studying fatigue problems. This report will summarize portions of this work. Because of its accessibility, the work conducted in Government Laboratories or under Government sponsorship will be emphasized. The review is organized according to the agency that sponsors the investigations.

I. NASA LANGLEY RESEARCH CENTER

A. Supersonic Transport Considerations

The evaluation of fatigue behavior in the environment of a supersonic transport has continued to occupy the attention of several investigators at Langley. More emphasis has been placed on the titanium alloy Ti-8Al-1Mo-1V than on other materials. However, the alloy Ti-6Al-4V is now favored for the SST, thus future projects are likely to be concerned with this material. A summary of results available at this time was presented at a recent meeting of the American Institute for Mining and Metallurgical Engineers. A copy of that presentation is appended to this review. More detailed descriptions of the investigations and results are available in the references to that paper.

B. Fatigue Crack Propagation and Fracture

A better understanding and analytical treatment of the rate of fatigue crack propagation and of the residual static strength of a member containing fatigue cracks or other damage is of interest for the estimation of both the fatigue life and the fail-safe characteristics of a structure. Since fatigue cracks can frequently be detected within the first small fraction of fatigue life, some investigators suggest that reasonable estimates of life may be obtained on the assumption that all of the fatigue life is spent propagating a crack from some small flaw inherent in the material. Whether this assumption will finally become the basis for fatigue life estimation is still in doubt. However, the number of cycles needed to propagate the crack must be considered to form a rational basis for analysis. Also, such crack propagation causes a progressive loss of strength such that the member can no longer support the loads encountered. Thus, life and fail-safe evaluations depend upon considerations of the residual static strength as well.

Langley research has been directed toward the systematic study of a number of parameters affecting these phenomena. Most of the recent results on fatigue crack propagation have been analyzed and correlated by stress intensity analysis procedures. Generally, the stress intensity at the tip of a

central crack is expressed by

$$k = S\sqrt{a} \alpha \quad (1)$$

where S is the applied stress computed on the gross cross section

a is the half-length of the crack

α is a correction factor for size or other geometrical considerations

The rate of fatigue crack propagation is found to be a consistent function of the range of the stress intensity, or Δk . Obviously, the relations among these parameters are also dependent upon other parameters such as temperature, material, and mean stress.

A relation proposed by Forman, et al, has been used to correlate the influence of mean stress on the rate of crack growth:

$$\frac{da}{dN} = \frac{C (\Delta k)^n}{(1-R) k_c - \Delta k} \quad (2)$$

where $\frac{da}{dN}$ is the increment of crack growth per cycle

R is the ratio S_{min}/S_{max}

k_c is the stress intensity at fracture

C and N are empirically-adjustable constants

A paper presenting the results of this study will be presented at a National Meeting on Fracture Mechanics at Lehigh University in June 1967 (ref. 1).

The effect of specimen width has been studied in specimens made of Ti-8Al-1Mo-1V. At a given stress level, the fatigue crack-growth curves for specimens having widths of 2-, 4-, 8-, and 20-inches (ref. 2) were very similar.

The effect of specimen length on rate of fatigue crack propagation and residual strength has been studied for 7075-T6 aluminum alloy sheet specimens 4 inches (100 mm) wide and from 0.5 (13 mm) to 24 inches (600 mm) long. The effect of length on rate of fatigue crack propagation was small but residual strength decreased appreciably for lengths less than 4 inches. These results did not correlate well with analysis, probably because the grips did not act in a rigid manner as assumed analytically.

Simple structural specimens incorporating unsymmetrical cracks, cracks growing from holes, simulated rivet forces, and combinations of these have also been studied. The appropriate stress-intensity factors have been taken from the literature or developed to account for the observed behavior. The preliminary results of this study were presented (ref. 3) at an ASTM Symposium on Fatigue Crack Propagation held last June in Atlantic City, New Jersey.

An analytical procedure has also been developed for computing stress intensity in large stiffened panels. The panel is assumed to be infinite in extent with uniformly-spaced stiffeners in the direction of the applied stress. Variable parameters in the analysis are: relative stiffness of sheet and stringers, spacing of stiffeners, spacing of rivets, efficiency of rivets, and the position of the crack relative to stiffeners. From this analysis, a designer should be able to anticipate the effectiveness of a given choice of these parameters. Experimental studies are underway to verify the trends indicated by the analysis and to provide data needed to assess the efficiency of rivets.

Experiments are being performed to study the effect of thickness on crack propagation. Plates up to $3/4$ inch (19 mm) thick and 3 feet (910 mm) wide and made of aluminum alloys are included. In addition, a group of special alloys in the zinc-bearing aluminum-alloy family is being studied to determine the role of alloying, heat treatment, and other metallurgical considerations on rates of fatigue crack propagation and fracture.

Many of the specimens used in the fatigue crack propagation studies are subsequently tested statically to study fracture characteristics. Generally, the stress at failure has been high relative to the yield strength of the material, so that allowance must be made for plastic action. The corrections for plasticity recommended by the ASTM Committee E-24 on Fracture are not always accurate, and in many cases the ASTM procedure disqualified itself because the net stress at failure exceeded the yield.

Mr. Paul Kuhn has devoted most of his time to further study of the fracture problem in order to provide an analytical procedure applicable over the full range of materials and configurations of interest. So far he has concentrated on the fracture of simple specimens with cracks through the thickness. Further use of the analysis he presented at the Third ICAF Symposium in Rome has shown certain deficiencies in attempting to "predict" failure strength from other material properties. Thus, he has modified the analysis, eliminating that feature and placing more reliance on tests of cracked specimens. He presented a discussion of these developments at the recent meeting of the AGARD Structures and Materials Panel in Turin, Italy (ref. 4). Mr. Kuhn made a survey trip of aircraft industry and government laboratories in Europe and Canada to review how extensively and by what methods fracture calculations were made. From this trip and from other contacts in the United States, he concluded that the application of materials data on residual strength is currently confined to cases where extensive experience is lacking for either the structure (missiles, hydrofoils) or the material and to quality control of materials. However, interest in wider application is growing rapidly.

In a separate development, the effect of plastic action at the crack tip is being treated by an extension of the procedure involving a model proposed by Dugdale. A preliminary report on this work will be presented at a National Meeting on Fracture Mechanics at Lehigh University in June 1967 (ref. 5).

C. Plastic Behavior at Notches

Studies of plastic action mentioned in the 1965 review are continuing. Emphasis has been on higher stress-concentration factors and on other materials. Thus far, the procedures for computing local stresses described in reference 6 have been successful for higher values of stress concentration.

In order to improve accuracy and efficiency of these tests, the testing equipment has been modified and expanded. A low-capacity (20,000 lb. or 89 kN) hydraulic loading device has been constructed to test the small unnotched specimen at the same time that a 120,000 pound (533 kN) capacity machine is applying load to the large notched specimen. Servo controls on the smaller machine maintain strains in the small unnotched specimens that are at all times equal to the strains measured at the base of the notch in the larger specimen. The system eliminates chances of human error involved in recording the strains in the larger specimen and in subsequently reproducing these strains in the smaller specimen. Further, it assures that exactly the same time scale is used for both tests and it improves efficiency by testing both specimens simultaneously.

D. Development of Test Facilities

A new fatigue test laboratory at Langley will be completed and occupied in May 1967. This laboratory will provide a large air-conditioned space for fatigue and static tests of material specimens and small structural components and a non air-conditioned space for tests of structural specimens at elevated temperature.

This laboratory will house the existing fatigue and static test equipment employed by the Fatigue Branch. One of the newest devices in this group is a high-speed tensile test machine with 1,000,000 pounds (4.45 MN) capacity. This device operates hydraulically and achieves loading rates up to 20,000,000 pounds per second (89 MN per second) by discharging hydraulic accumulators. The present pumping and valving system also facilitates cycling.

A large hydraulic fatigue testing machine is scheduled for delivery this summer. It is expected to produce loads up to 400,000 pounds (1.8 MN), deflections up to ± 1 inch (25 mm) and cyclic rates up to 1000 cpm (18 Hz) (not simultaneously).

Three fatigue test devices equipped with vacuum chambers are being installed. These devices have load capacities of 20,000 pounds (89 kN) and are expected to produce vacuum environment to 10^{-9} torr with temperature control.

E. Contract Research

A three-dimensional photoelasto-plastic stress analysis method was developed (ref. 7). This method was used to study experimentally the stress distributions in the vicinity of simulated cracks. The method utilizes the frozen stress and creep characteristics of plastic materials to simulate the

stress-strain behavior of aluminum alloys. Polymer materials are subjected to various thermal cycles, the maximum temperatures of which were significantly below the critical temperature, but high enough to promote creep. The strain and birefringence associated with this creep are frozen into the model which is subsequently sliced without relieving the frozen strain.

A material and thermal cycle were selected which exhibited an effective stress-strain curve similar to the uniaxial stress-strain behavior of 2024-T3 aluminum alloy. Models were machined from the selected material and subjected to constant tensile load and the appropriate thermal cycle to simulate 2024-T3 aluminum. The plate models contained centrally located holes 1/8 inch in diameter or simulated cracks with various ratios of crack length and of tip radius to thickness.

The stress-concentration factors determined for the plates with centrally-located holes are in very good agreement with theory. The stress-concentration factor for the thick plates was slightly higher at the midplane of the plates than at the surface. Due to the higher stresses at the midplane of the thick plates, there results a σ_z stress normal to the plane of the specimen. This σ_z stress is maximum at the midplane and surface of hole and diminishes to zero a short distance from the hole.

The elasto-plastic stress distributions determined for plates with centrally-located simulated cracks showed that all three stress components have maximum values a short distance from the crack tip. Apparently, the yield stress at each point in the specimen is influenced by the triaxial stress state.

F. Definition of Load Environment

During the past two years, NASA has continued its research aimed at defining the load environment for aircraft. This research has encompassed the repeated loads (due to gusts, maneuvers, landing impact, and ground operations) of commercial transports and general aviation airplanes, the atmospheric turbulence environment, the runway roughness environment, and loads on helicopters.

A summary of the repeated loads experienced by several types of commercial transports is given in reference 8. Reference 9 presents data on the loads experienced by several types of general aviation airplanes engaged in various categories of service. Runway roughness environmental data and airplane responses to the roughness are given in references 10 and 11. A summary of data on the atmospheric turbulence environment is given in reference 12. Structural loads measured on a hingeless-rotor helicopter are given in references 13, 14, and 15.

II. NASA LEWIS RESEARCH CENTER

A. Crack Initiation and Propagation

Empirical equations have been developed for predicting the number of cycles required to initiate a crack, and to propagate this crack to failure in a notched specimen knowing the fatigue behavior of unnotched specimens. This method is presently limited to estimates of the fatigue life of axially-loaded specimens containing notches and tested under completely-reversed constant strain conditions (ref. 16).

B. Cumulative Damage

A double linear cumulative damage rule (ref. 17) for predicting the fatigue life of unnotched specimens subjected to variable amplitude rotating bending or reversed axial strain has been developed. The fatigue process was originally considered to occur in two phases, crack initiation and crack propagation. It was proposed that fatigue damage accumulates at one rate during the first phase, and at a different rate during the second phase. A number of tests are required to establish the damage accumulation rates for the two phases. However, once these rates have been established, the hypothesis is that fatigue life can be predicted by linear accumulation of damage at the appropriate rates until the sum of the fractional damage equals 1 for each phase.

C. High-Temperature Low-Cycle Fatigue

A method has been developed whereby the low cycle fatigue in the life range from 10 to 10^7 cycles at temperatures above approximately half the melting point can be estimated from the tensile and creep properties measured in conventional static high-temperature tests. The method makes use of the universal-slopes equation (ref. 18) originally developed for low-cycle fatigue of materials at room temperature. In this method, the total strain range is separated into its elastic and plastic components which can be estimated from the tensile strength and reduction of area in the tensile tests. Corrections are introduced from the "creep effect" based on the concept that the micro cracks introduced by creep act as nuclei for fatigue. Good agreement has been obtained in correlating literature data from numerous sources. The research is described in a paper to be given at the Symposium on Thermal and High Strain Fatigue to be held in London in June 1967, and is to be published by the Institute of Metals, London, England (ref. 19).

III. U. S. AIR FORCE FLIGHT DYNAMICS LABORATORY

A. Fatigue Damage Indicator (S-N Gage)

Considerable work has been done within the U.S. technical community on the feasibility of utilizing an annealed foil strain gage as a fatigue damage indicator or S-N gage. Several of these gage configurations

are now on the commercial market in the U. S.

The Lockheed-Georgia Company recently completed a comprehensive feasibility investigation of this fatigue damage indicator concept under contract to the Air Force Flight Dynamics Laboratory (ref. 20). This effort was comprised of (1) evaluation of various gage concepts and configurations, (2) selection and optimization of sensor and integrated electronic systems, (3) determination of behavior characteristics and response on laboratory coupon fatigue tests, and (4) practical application tests on C-130E wing fatigue tests which were already in progress in the contractor's facility. From the results obtained, it appears the concept and use of these S-N gages show considerable promise as a means of directly determining the fatigue life status of a component. More work must be done in such areas as improving the threshold sensitivity of the gage (now limited to approximately 0.001 strain) and interpretation of the results. The Air Force Flight Dynamics Laboratory is continuing this S-N gage investigation in-house in its own Structures Laboratory.

B. Optimization of Ordered Load Spectra in Full-Scale Structural Fatigue Tests

This work, performed by the National Research Laboratories (Dr. Schijve) is the evaluation of random versus programmed (ordered) load sequences - with and without GAG cycles - utilizing the large F-27 wing skin panels as test specimens (ref. 21).

Supplemental work is underway by Dr. Schijve to continue the investigation of the optimum ordered spectra previously developed towards better definition of selection criteria for maximum and minimum load levels selected. Crack propagation phenomena will be used to define these limits.

C. Fracture Mechanics - Crack Propagation

An improved theory for the crack growth analysis of cyclic loaded structures is being developed in-house. The theory assumes that the crack-tip stress intensity-factor range, Δk , is the controlling variable for analyzing crack extension rates. The new theory, however, takes into account the load ratio, R , and the instability when the stress-intensity factor approaches the fracture toughness of the material, k_c . Excellent correlation is found between the theory and extensive experimental data. A computer program has been developed using the new theory to analyze the crack propagation and time to failure for cyclic loaded structures (ref. 22).

Current efforts are continuing in this area with attempts to apply this theory in work connected with crack propagation investigations associated with structure vulnerability to small arms fire of typical aircraft materials and configurations including residual fatigue life of damaged structure.

D. Time Compression in Elevated Temperature Fatigue Testing

Efforts are continuing in the AFFDL Structures Laboratory on a program of Experimental Verification of the Elevated Temperature Fatigue Test

Time Compression Theory as previously reported (ref. 23).

A general method is proposed for compressing the elevated temperature fatigue-test time for supersonic aircraft operating at Mach 2 to 5. For time-dependent processes, the test time can be compressed only by increasing the rate of damage accumulation in a controlled manner. The problem is approached by constructing interaction diagrams involving creep, fatigue, and thermal cycling. The fatigue test format for a particular mission is synthesized by combining appropriate portions of the interaction diagrams to achieve an adequate flight-damage simulation in minimum time.

Tests are in progress to construct the interaction diagrams for four regimes of the supersonic flight profile involving (1) moderate constant temperature, (2) moderate variable temperature, (3) elevated constant temperature, (4) elevated variable temperature. Two materials, Ti-8Al-1Mo-1V and AM 350 SCT 850, are being used.

Tests for the first regime are complete and indicate a maximum time compression ratio of 45 can be achieved by replacing a large number of low amplitude cycles with a smaller number of higher amplitude cycles. Thermal cycles in the second regime can be replaced by additional load cycles. Also, omission of creep time in the third regime may result in predicted lives which are too short.

Eventually, simulated mission tests on coupons and finally on component structures will be performed to substantiate the prediction method.

E. Fatigue Strength Design and Analysis of Aircraft Structures

Fatigue analysis and design of aircraft structures have been studied by the Air Force Flight Dynamics Laboratory (ref. 24). A computer program was generated to calculate fatigue damage in a structural element. Input data to the program basically consist of load spectra and fatigue strength data (S-N data). The program is oriented to an aircraft-mission flight-profile analysis. The Palmgren-Miner damage method is employed in the program.

As an aid to safe-life prediction, an investigation was conducted to establish applicable scatter factors to cover variations in fatigue allowables and loading environment. Basic scatter in fatigue life was derived statistically from fatigue test data representative of specimens and structures with various loading spectra. The assessment of load variations presented a more formidable problem. The approach to this aspect of life scatter was made through an operational life scatter factor. Operational life scatter factors were defined in terms of a joint probability distribution of applied load spectra variation in a fleet of aircraft and the basic fatigue scatter as established by fatigue test data. Several joint probability models were established. In an effort to check the concept of the joint probability model, a comparison was made with an actual C-124 aircraft service history failure. A good correlation was obtained between predicted and actual total number of failures.

Safe life of a structure can be estimated from the damage computed by the program and scatter factors associated with probabilities of failure can be derived. An additional utilization of this overall program is in the establishment of fatigue strength design charts.

F. F-100 Fatigue Program

The Air Force Logistic Command (Sacramento Air Material Area, SMAMA) has recently sponsored a structures investigation by North American Aviation to re-evaluate the service life of the F-100 series aircraft towards certifying the fleet for an extended service life of 5500 flight hours (ref. 25).

The program consists of three phases as follows:

- Phase I - In a "Lead the Fleet" accelerated flying program, 18 completely instrumented aircraft and 18 aircraft equipped with counting accelerometers were deployed at 5 bases. Standard useage was established from 100 aircraft equipped with counting accelerometers deployed at many bases.
- Phase II - "Analysis & Design - Fatigue Analysis," element fatigue tests, the re-design of any critical areas.
- Phase III - Full-Scale Fatigue Test - Two complete wings plus one complete fuselage and empennage were tested. One wing was in the current configuration. The second wing incorporated the modifications from Phase II - Analysis & Design.

IV. U. S. AIR FORCE MATERIALS LABORATORY

A. Mechanical-Metallurgical Aspects of the Fatigue Process

In one project (ref. 26), low-cycle axial fatigue tests were performed on high-purity aluminum and an Al-10% Zn alloy. Constant strain rates of 5 and 150% per minute were employed at a strain amplitude of 2% (+1%) over the temperature interval 20 to 482°C. Electron microscopy was applied utilizing improved replication techniques to study crack initiation, crack growth, and failure. A number of crack-growth curves were established. At temperatures above 260°C, where grain boundary sliding and migration become active, the one-to-one migration-cycle process (for fine-grained materials) yielded an activation energy of 18.5 K cal/mol, approximately equal to that for self-diffusion along boundaries. Double kinking in single crystals, orthogonal boundary diffusion and fracture at very high temperatures, and the role of strain rate are discussed in considerable detail.

In another research program, Weissmann (ref. 27) has studied the structural changes in bending fatigue of silver and aluminum crystals by metallographic, X-ray and electron microscope methods. The fatigue process may be

divided into three consecutive broad stages characterized by an increase in dislocation density, formation of substructure and fragmentation into cell structure, respectively. Strain and temperature are the two parameters controlling the development of the dislocation substructure. Both a decrease in strain or an increase in temperature cause growth of subgrains and cells, while variation of the parameters in the opposite direction has an inverse effect on the structure. The growth of subgrains and cells resulting from cycling with lowered strain amplitude is attributed to a mechanism involving dislocation climb. The life of single crystals of silver (low stacking fault energy, γ) was nearly two orders of magnitude greater than that of aluminum (high γ). The introduction of a grain boundary reduced the life for both to the same level, thus eliminating the beneficial effect of low stacking fault energy on fatigue life. The deleterious effect of boundaries introduced as stress-raisers was, however, eliminated by alternating the cycling between high and low strain amplitudes. The fatigue life of aluminum crystals could thus be extended fourfold. The technique of alternating cycling produced internal deformation of the areas with high internal stresses.

Grosskreutz is continuing his long-term research on fatigue mechanisms. Studies of the mechanism of long-life fatigue in notched 7075-T6 aluminum, by means of optical and electron microscopy, have just been reported (ref. 28). Cracks were observed to nucleate at inclusions on the notch surface as a result of highly localized plastic deformation. At least 65 percent of total life is expended before a crack greater than ~ 20 microns long can be detected. The final 20 percent of life is spent in propagating a dominant crack across the gauge section of the sample. The fracture surfaces so produced were studied by electron-microscope fractography. The dominant mechanism of crack propagation is striation formation. Striation spacings and surface crack lengths were used to calculate crack growth rates. No consistent power-law relationship between this rate and the crack tip stress-intensity factor could be found. Dislocation densities of $\sim 2 \times 10^{10}$ lines/cm² were observed near the crack tip by transmission electron microscopy. Comparison of the second-phase precipitate structure at the crack tip with the structure of uncycled material reveals evidence of overaging in the fatigued material.

B. Crack Propagation and Notch Effects

A room temperature, axial-loading low-cycle fatigue investigation on 2024-T4 and 7075-T6 aluminum alloys, using notched cylindrical specimens, was conducted at minimum-to-maximum stress ratios R of -2.5 , -2.0 , -1.5 , -1.0 , 0.0 and 0.6 . It was observed that the fracture mechanism of low-cycle fatigue involves "Stage II" fatigue crack growth which is characterized by the development of ductile striations and two essential types of secondary fracture surfaces. It is shown that ductile fatigue crack growth, which involves two types of ductile striations, is governed by the local irreversible plastic deformation at the crack tip in both alloys.

The most important mode of secondary crack growth in 2024-T4 aluminum is the brittle fracture or decohesion of the constituent particles ahead of the crack tip and the subsequent growth of the interior cracks toward the main crack. The size of the plastic zone at the crack tip appears to determine the

degree of influence of this mode of fracture on overall crack growth rate. In 7075-T6, the dominant mode of secondary crack growth is the quasi-cleavage fracture of the matrix. The frequency of occurrence of these two modes of secondary crack-growth increases with the stress ratio, i.e., with increasing mean stress. The change in the modes of crack growth due to a change from low to high mean stress contributes to the relative differences in fatigue strength of the two materials at various stress ratios (ref. 29).

The stress and strain in an elasto-plastic plate containing a crack have been obtained. The large deformations and general work-hardening have been taken into consideration. In addition, the results are used to predict a fracture stress as a function of the material's mechanical properties (ref. 30).

The three-dimensional stress distribution near the tip of a semi-infinite crack embedded in an infinite plate of arbitrary thickness has been investigated. The problem is formulated by means of three biharmonic functions in the classical theory of elasticity as developed by Galerkin. The eigenfunction expansion technique of Williams for solving two-dimensional crack problems is incorporated into the three-dimensional crack analysis. It is found that the stresses $\bar{r}\bar{r}$, $\bar{\theta}\bar{\theta}$, $\bar{z}\bar{z}$, $\bar{r}\bar{\theta}$ are singular of the order of $r^{-1/2}$, r being the distance measured from the crack point, but the transverse shear components $\bar{r}\bar{z}$, $\bar{\theta}\bar{z}$ are bounded everywhere in the plate. Determined in an approximate manner is the intensity of the crack-edge stress field which depends on the thickness coordinate of the plate. The results provide an improved understanding of the three-dimensional aspects of fracture theories, particularly on the effect of plate thickness (ref. 31).

Crack propagation experiments were conducted in polyester resin sheets containing a central crack. Uniaxial tension loading at several loading rates was applied perpendicular to the crack direction. Two types of experiments were conducted: (1) high loading rate tests at 24°C and -45°C, with a constant loading rate to study the acceleration characteristics of cracks running in a glassy material, and (2) high temperature low-loading rate tests to study slow crack propagation when appreciable viscous dissipation could occur. During crack propagation, full-frame photographs were taken of the photoviscoelastic isochromatic patterns and crack tip position at framing rates from 250 to 100,000 frames per second. Even at loading rates exceeding 10^5 psi per second, isochromatic patterns prior to crack propagation compared closely with static patterns. Constant crack velocities were achieved in the high loading-rate tests and the isochromatic patterns compared closely with the theoretical solution of Broberg. During the crack acceleration period, the experimental data could not be represented adequately by the Berry elastic theory. For the early phase of the slow (viscous) crack-growth period, the crack length could be predicted using a simple theory proposed by Schapery and Williams.

Several tests were conducted on silicon-iron metal sheets to show that the same testing technique can be applied to the study of crack growth in metals (ref. 32).

Neuber has developed a series of extensions to the notch stress theory which have been obtained in the last few years. In Part I an application of the leading-function hypothesis is checked by comparison with exact solutions of non-linear two-dimensional elastic problems. The first refers to the state of shear stress in sharp notches, the second to a symmetric state of plane stress in the neighborhood of a circular hole. Neuber treats problems of stress concentration in notches, loaded by single forces. As a typical example, the parabolic notch is explained in detail. Other problems given refer to the effect of couple stresses. Exact formulae are given for circular holes and spherical cavities in uniform tension fields by means of a new general solution derived by the author. A new interpolation formula for notches of any depth is established (ref. 33).

The effect of tensile stress fields due to holes, superimposed on the stress fields due to external notches, was investigated by means of photoelastic techniques and tensile fracture tests. A columbia-resin photoelastic material, CR-39, and the titanium alloy 2.5Al-16V, aged to a brittle condition, were used to construct simple model systems for these studies, as a first step to simulate a prototype ceramic material. For the model systems employed in the investigation, no significant degree of interaction occurred between the stress fields of holes and the stress field due to the notch. Although the holes produced considerable localized stress inhomogeneities, this effect did not extend to the root of the notch where the maximum stress was determined solely by the stress concentration factor of the notch. The results of the tensile fracture tests confirmed the stress field studies. Elastic stress-field equations of notches and holes provided a satisfactory means of estimating the earliest possible interaction of stress raisers. However, a more suitable ceramic-prototype should have an interaction of stress fields extending to locations of maximum stress. It is suggested that this may be achieved by closer spacing and increasing the severity of inhomogeneities (ref. 34).

The interaction effects of the stress fields of edge notches and holes or elongated slots have been studied by photoelasticity techniques, in an effort to obtain the basic information required for a fracture analysis of inhomogeneous brittle materials such as ceramics. Actual fracture tests on selected similar configurations were conducted on a brittle titanium alloy to provide an experimental check on the stress analysis and photoelastic work. Both one-sided and mutual interaction of the stress fields of the edge notches and holes were observed and their occurrence depends upon the configuration and proximity of the two stress concentrators. The photoelastic results revealed that a simplified uniaxial stress-distribution analysis predicts far larger interaction distances than were actually observed. Consideration of the stress field biaxiality together with a more accurate stress-distribution analysis is required for a quantitative prediction of the observed effects. A unified interpretation of the interaction effects can be obtained from a graph of stress-concentration factor increase versus the relative interflaw spacing ξ/r , where r is the root radius of the neighboring notch (ref. 35).

C. Structural Reliability

A new approach to structural reliability analysis based on order statistics is introduced by considering the expected time to the first

failure in a fleet of specified magnitude. Because in the design of large structural units, such as transport aircraft, failure of even a single unit must be prevented, reliability analysis and design for a "mean time to failure" seems to be an unjustified extension of the use of methods of reliability analysis developed for inexpensive mass-produced items of relatively short service lives to the reliability assessment of expensive, large units. A method for the estimate of the expected time to the first failure is outlined and the implications of the use of this time in reliability analysis and design are discussed (ref. 36).

General expressions were obtained for the probability that a simple redundant structure of material with a statistical yield point can sustain the applied load even when yielding occurs in some of its members. In fail-safe design, the conditional probability of survival of the structure, under the hypothesis that yielding has occurred in at least one of the members, is as significant as the expected life of the damaged structure. Numerical examples indicate that while the structure utilizing the yielding material is appreciably better, from the point of view of fail-safe design, than that using a brittle material, caution should be exercised to apply the notion of fail-safe design to redundant structures against failure due to yielding, since the conditional probability of survival is low (ref. 37).

The relationship between fleet size, earliest failures, and the reliability of the population based on non-parametric methods and on extremal statistics is examined. The use of extreme observations in the reconstruction of the distribution of "parent" populations is discussed, and is illustrated with data from fatigue and impact tests (ref. 38).

In the reliability analysis of large structures, usually only a very small sample can be tested. Hence, the expected time to first failure and possibly the expected value of the time interval between the first and the second failures are much more significant measures than the mean time to failure or any related measure of the central tendency of the distribution of times to failure. General expressions for these expected values and associated variances are derived and numerical computations are carried out using three types of distribution of the time to failure: (1) the logarithmic normal distribution, (2) the gamma distribution, and (3) the Third Asymptotic distribution of extreme (smallest) values (ref. 39).

D. Mechanism of Stress Corrosion Cracking

The mechanism of stress-corrosion cracking in 7079 aluminum alloy was investigated by analysis of microstructural changes that occur during exposure to 3.5 percent NaCl solution. During the corrosion reaction, dislocation networks were generated within the grains and along strain-contour bands. Grain-boundary voids occurred where several of these bands originated or terminated. This suggests that the intragranular structure develops as a result of hydrogen entering the alloy and that the voids are propagated under applied load to form grain-boundary cracks (ref. 40).

A review of the existing theories for the mechanism of stress-corrosion cracking indicated that the electrochemical-mechanical theory was most consistent with existing data for stress-corrosion cracking in high-strength aluminum alloys. However, experimental crack-kinetics studies did not reveal fast fracture steps which would be associated with such a mechanism. The cracking rates were well within the limits predicted by an electrochemical mechanism. A statistically-designed experiment to study the effects of metallurgical variables on stress-corrosion-cracking behavior of high-purity 7039- and 7079-type alloys has revealed several important facts. Stress-corrosion-cracking susceptibility is a function of the stress normal to the grain boundaries rather than a function of the applied stress on these materials in thin sheet and plate form. Compensation for this effect was necessary before the effects of other metallurgical variables could be determined. Chromium-alloy additions, silver additions, a more-severe-than-normal solution heat treatment, overaging, and the combination of silver and overaging or the combination of chromium and the more-severe-solution-heat treatment were all beneficial to the stress-corrosion-cracking resistance of these alloys. Copper additions were detrimental. The combined results of electrochemical, autoradiographic, electron-transmission, and electron-replica studies strengthen the belief that cathodically-produced hydrogen dissolved in strained grain boundaries is essential for the initiation of stress-corrosion cracking in these alloys. Based on these results a mechanism is proposed. This proposed mechanism involves the absorption of cathodically-produced hydrogen into tensile-strained, mechanically weak (alloy-depleted zones) grain boundaries. The hydrogen acts to reduce the activation energy for anodic dissolution of the metal and thus accelerates the localized corrosion at the grain boundaries perpendicular to applied tensile stresses (ref. 41).

E. Work Hardening

The influence of the work-hardening exponent on the fracture toughness of 4340, 18% nickel maraging, and AM-355 stainless steel was studied. In most cases, the effects produced by variations in work hardening were difficult to analyze due to accompanying changes in yield strength and microstructure. In this investigation, the transition in fracture mode induced by varying section size was used as a basic evaluation method since complicating effects due to yield strength changes were not introduced. The results indicated that the transition from flat to shear failures occurred in larger section sizes in the material with the lower work-hardening exponent. Once full shear failures were obtained, however, materials with higher work-hardening coefficients required greater energy to produce failure. The influence of work hardening on the transition behavior could be rationalized on the basis of the larger plastic zone present in the steel with the lower strain-hardening coefficient. Although useful correlations between the strain-hardening index and the fracture mode transition could be obtained, no quantitative relationship between the work-hardening exponent, as defined by strain to maximum load, and plane strain fracture toughness was evident (ref. 42).

The influence of the work-hardening exponent on the variation of fracture toughness with material thickness was studied for high-strength steel, aluminum, and titanium alloys. The results indicate that when materials are

compared at similar fracture toughness-yield strength ratios, the material with the lower work-hardening exponent undergoes the transition from flat to slant fracture at a larger thickness than material with a high work-hardening exponent. In the thickness range where complete slant fracture is obtained, the reverse is true and a lower work-hardening exponent results in a lower fracture toughness. The influence of work-hardening exponent on fracture toughness is, therefore, dependent on the particular fracture mode. In the transition region, a lower work-hardening exponent is beneficial for fracture toughness while in the 100% slant region it is detrimental. The influence of the work-hardening exponent on cyclically-induced crack-growth rates in AISI 4340 steel and 13V-11Cr-3Al titanium was also evaluated. In the steel the growth rate was slightly less for the material with the lower work-hardening exponent while the titanium exhibited no significant trend as a function of work-hardening characteristics. The specimen thickness had the greatest effect on the cyclically-induced crack growth with decreased growth rates present in the thicker specimens. Attempts were also made to control the process zone size by adding zirconia particles to a high-strength steel matrix through powder metallurgy techniques. Particle spacings between approximately 20 and 1700 microns produced no significant effect on the fracture behavior (ref. 43).

F. Surface Effects

Kramer (refs. 44, 45, 46) has demonstrated that a region of high-dislocation concentration exists in the region at the surface of a deformed metal. This dislocation-rich layer impedes the movement of mobile dislocations. Strain cycling tests of aluminum have shown that for a given applied stress, the average velocity of the dislocations is affected by the surface. It appears possible to explain the surface effects in terms of stress field associated with the surface layer, and the exponent m^* in the equation $V \propto \tau^{m^*}$, where V is the dislocation velocity and τ^* is the effective stress. For aluminum crystals, additional internal-dislocation barriers were not formed in Stage I and it was possible to show that Stage I ends when the difference between the applied stress and the surface stress on the secondary-slip system equals the critical resolved shear stress. The effect of the surface was found to be greater on polycrystalline specimens than on single crystals. For Armco iron, the surface stress was almost twice as great as that due to internal obstacles. The yield point in high-purity metals was associated with the surface layer.

The stress associated with the surface layer was determined for iron and molybdenum. These measurements show that the surface layer plays a very important role in the plastic deformation of b.c.c. metals. From the relationship between strain and the surface layer stress and the back stress imposed by the internal obstacles, it is proposed that the term

$$\sigma_1^0 \text{ of the Hall-Petch equation } (\sigma_f = \sigma_1^0 + K_d^{-1/2})$$

is related only to the surface stress while the term $K_d^{-1/2}$ is the stress required to move dislocations through internal obstacles. Further, it was possible to derive the well-known empirical equation $\bar{\sigma} = a \bar{\epsilon}^n$ and it is

shown that the term a is comprised of two terms: C_s associated with the surface layer stress and C_l related to internal dislocation obstacles.

The effect of specimen diameter, d , on the flow stress, $\bar{\sigma}_a$, of polycrystalline aluminum (99.997%) was studied. The increase in the flow stress could be accounted for by the increase in the surface layer stress with decreasing specimen size.

V. U. S. NAVY AERONAUTICAL STRUCTURES LABORATORY

A. Structural Fatigue Research

The fatigue investigations conducted by the Aeronautical Structures Laboratory (ASL) of the Naval Air Engineering Center are concerned primarily with the development and verification of (1) fatigue life prediction methods, and (2) statistical reliability methods applicable to structures. Laboratory structural-fatigue investigations and development work are also conducted in connection with specific structural problems arising in fleet aircraft. The laboratory facilities have been expanded by the addition of a 100-kip fatigue test machine and a multi-actuator structural-loading system, both of which are servo-controlled digitally-programmed systems capable of applying random loads.

The laboratory's investigation of cumulative damage and life estimation methods is continuing using both full-scale aircraft and simple beam structures. One of the major problems investigated is the effect of including negative loads in the positive load spectrum for fighter aircraft. A recently-completed program (ref. 47) using fighter wings made from 7075-T6 aluminum alloy demonstrated that the inclusion of negative loads in the spectrum for a fighter wing can reduce the fatigue life by as much as a factor of seven. This effect is being corroborated on current tests of simple beam structures of 7075-T6 but the life reduction factor has not exceeded four.

The life data obtained from these tests have been used to verify various cumulative-damage hypotheses. To date, the Smith method (ref. 48) is the only method that seems to produce good agreement with these test results. Although the Smith method appears to be based on cyclic-stress data, in reality it is a simplified cyclic-strain method of life prediction. The errors introduced in this simplified life prediction method may be caused by (1) the use of the monotonic stress-strain curve to estimate residual stresses instead of the cyclic stress-strain curve, (2) neglect of the Bauschinger effect, and (3) the assumption that the maximum residual stress that can be retained by the structure is equal to $0.9 F_{cy}$.

To overcome the errors in the Smith method and to investigate cyclic-strain methods of life estimation, an investigation is being conducted at the University of Illinois with Prof. J. D. Morrow as the principal investigator. The cyclic strain behavior of 2024-T4 and 7075-T6 aluminum alloys, SAE 4340 steel, and 8-1-1 titanium alloy is being studied. The first report (ref. 49) on this investigation covers the cyclic-strain life data for these materials. Subsequent work using two-step strain-controlled cycling indicates

that the strain approach to life estimation shows great promise for obtaining a valid cumulative damage theory.

In-house investigation of the cycle dependence of the strain field around open holes in a quasi-infinite plate under plane stress is providing substantiation for the cyclic-strain approach to damage accumulation.

B. Environments Research

A fleet-wide statistical survey of aircraft structural fatigue based on flight VGH recorder load-history data from operational aircraft is being conducted by the Aeronautical Structures Laboratory (ASL) of the Naval Air Engineering Center. Approximately 12,100 flight hours of oscillograph records of maneuver history from jet attack and fighter aircraft have been analyzed and reported. Results of these surveys are published in reference 50.

A study of helicopter flight-loads environment is being conducted in the SH-3A helicopter with recorders measuring rotor R.P.M., air temperature, and engine torque as well as VGH data. To date a total of 358 flight hours has been recorded. Since fatigue-sensitive components of helicopter structures are not always a function of maneuver loads, an additional parameter which may yield significant data on rotor loads will be recorded in a forthcoming survey with the CH-46 helicopter. This parameter is the periodic load fluctuation in the longitudinal cyclic links in the rotor control system.

A second aircraft survey is carried out by a counting accelerometer mounted at the center of gravity and an indicator which is read on a monthly basis. All first-line service aircraft will soon have a counting accelerometer as a permanent part of the aircraft equipment. As of January 1, 1967, 2400 aircraft were equipped with counter systems. Approximately 2,000,000 hours of counting-accelerometer data from 20 models of naval aircraft have been reported and analyzed to date (refs. 50 and 51). Statistical analysis of service aircraft-load histories reveals wide differences between the individual histories of such aircraft. Seasonal load-rate changes also have been observed. Change in weapon-system mission assignments of a given model aircraft often result in significantly different load histories. Knowledge of these changes in the flight-loads environment is an important consideration in the assignment and use of service aircraft.

It is expected that the VGH recorder data and counting accelerometer data combined with service experience and structural-fatigue test results can be combined to establish criteria for extending the useful life of an aircraft and to better predict airframe structural reliability.

The Laboratory collects approach and landing data of naval aircraft during field and carrier operations in order to obtain statistical data on the parameters that define this environment. The data are obtained through use of a specially-designed 70-mm camera system. The major parameters are: sinking speed for each gear, horizontal speed at touchdown, wing lift factor, airplane pitch and roll angles, off-center distance, glide-path angle, touchdown

distance from ramp, and flight-path, sideslip, and engagement angles.

These environmental data are used for both the solution of structural landing problems on operational aircraft and the formulation of requirements for the structural design and testing of new aircraft. In addition, these data have been used to evaluate various landing-aid systems and to develop improved carrier pilot techniques.

The photographic records are obtained without interference to field or carrier operations, and no installation of equipment on the observed aircraft is required. The photo measurements do not influence the landing process, because pilots are usually unaware of the presence of survey equipment. Results of these surveys are published in references 52 through 55.

Because of the increased hazards of night operations, the Laboratory is presently conducting research and development in an attempt to film night landings, and to compile statistical night approach and landing data.

VI. FEDERAL AVIATION AGENCY

The certification requirements and advisory materials for rotorcraft structural-fatigue certification have been revised completely. The revised requirements recognize the fail-safe concept and provide guidelines and requirements for its use. Also, the requirements were placed on a probabilistic rather than deterministic basis.

Revisions to the fatigue-certification requirements covering non-pressurized structure in light planes are also in the final phases of development. (The requirements for pressurized structures are already in effect.) According to present thinking, the fail-safe or safe-life characteristics of only the wing and attaching structure would need substantiation and previous satisfactory service experience could be used in such substantiation if applicable and sufficient to demonstrate adequate fatigue strength.

The fatigue requirements for supersonic transports are also being developed. The two principal features of these requirements are: (1) that fail-safe design is required where possible, and (2) that substantiation of the residual fatigue (in addition to residual static strength) strength after obvious partial failure would be required. A related activity concerns the development of certification requirements which would require additional redundancy and residual control in control systems after failure. Such requirements are being developed for the SST, subsonic transports and rotorcraft.

As is apparent from these activities, FAA is, in general, encouraging "damage tolerant" structure. In the proposed standards for the supersonic transport, this trend is emphasized by a requirement that cabin pressurization be maintained after cabin punctures, including those resulting from engine disintegration. Consideration of the effects of engine disintegration on structure and controls will also be required.

VII. INSTITUTE FOR THE STUDY OF FATIGUE AND RELIABILITY - Columbia University

Activity at this Institute continues under sponsorship of the U. S. Navy and the U. S. Air Force and under the direction of Prof. A. M. Freudenthal. Recent research has concentrated along three lines:

Fatigue mechanisms developing in cyclic torsion and in cyclic tension and tension were observed with the optical and electron microscope to study the state physics aspects of fatigue and damping in polycrystalline metals and in single crystals. Also, fractographic methods were employed to study the effect of micro-structure on crack-propagation under cyclic load; the observed similarity of the crack-propagation process in structurally dissimilar materials (such as metals and polymers) suggests that macroscopic fracture mechanics aspects overshadow the effects of microstructure. A new study is concerned with fatigue damage in composites, such as a tungsten-fibre reinforced-copper matrix.

The phenomenon of second-order strain accumulation in polycrystalline metals under cyclic torsion has been studied experimentally and theoretically to determine its relation to fatigue. The significance of this phenomenon on the continuum mechanics and on the micro-structural levels is of interest. The rate of second-order strain accumulation was found to increase with increasing temperature. The existence of the phenomenon has also been demonstrated in cyclic tension-compression tests.

The reliability of redundant structures was studied experimentally and theoretically. A rational procedure for assessing time to first failure was developed.

References 56 to 77 have been published by the Institute during the past two years.

VIII. NORTHROP NORAIR

A procedure was developed for analyzing the fracture of ductile sheets containing fatigue cracks. The procedure is designed to extend the usual Fracture Mechanics analysis of elastic restrained sheets to include the effects of buckling in unrestrained elastic panels and the effects of general yielding in restrained panels. Interactions among these influences were evaluated in tests of 2024-T3 aluminum alloy and Ti-8Al-1Mo-1V titanium alloy and in other data taken from the literature (ref. 78).

IX. LOCKHEED-CALIFORNIA COMPANY

Lockheed personnel have long favored fatigue tests with variable-amplitude loading under flight-by-flight schedules in preference to constant-amplitude tests. Their laboratories are equipped (refs. 79-81) with a large number of magnetic-tape controlled loading devices with capacities to 1,000,000 lbf. Equipment is available for tests of full-scale structural components with up

to 54 independent channels of load control.

They feel strongly that the higher initial cost of specimens and test apparatus and the higher skills required to conduct these more sophisticated tests are outweighed by many factors. For example, the relation of the structural details and load environment are preserved, less scatter is experienced, and the use of questionable cumulative damage analyses is eliminated. However, a need exists for simplifying the loading spectrum and for interpreting the life observed for one spectrum in terms of expected life under another. Lockheed is conducting systematic research to help supply solutions to these problems and thus to reduce the high cost of testing.

The "threshold" stress level below which the spectrum could be truncated without modifying test results is being evaluated. Use is made of Shanley's theories of fatigue (refs. 82-85) to guide the selection of the threshold stress. Spectrum tests are being conducted on simple specimens with and without stresses below the selected level. Once a threshold is established, significant time savings should be realized in full-scale tests by eliminating all stresses below that level.

In a related study, simplified crack propagation considerations are being employed to "adjust" the number of cycles of load applied at the lowest retained amplitude to compensate for cycles at lower amplitude that have been eliminated. Thus, a few cycles at one moderate stress level might be substituted for large numbers of cycles at lower levels. The resulting "trade-off" is being verified in systematic series of tests. Present indications and reasoning dictates that such "trading" be limited to low stress levels so as not to modify the effects of high loads.

A similar problem is related to tests of helicopter parts. For many parts a large number of cycles nearly-constant amplitude stress is superposed on a once-per-flight application of mean stress. If it could be shown that the large numbers of cyclic stress could be reduced systematically, a considerable saving in test time could be realized. Again, systematic tests are in progress to develop a reasonable adjustment procedure.

III. U. S. AIR FORCE FLIGHT DYNAMICS LABORATORY (Continued)

G. Sonic Fatigue

A method was developed (ref. 86) for including the beneficial influence of curvature in sonic fatigue design. The simultaneous application of heat and noise was much more severe than heat and noise alternately. Curved titanium-faced honeycomb sandwich panels were investigated to determine the effects of high-intensity sound, heat and low-frequency vibrating loads. A theory was developed for determining the natural frequency of curved, tapered-edge honeycomb panels.

Sonic fatigue curves have been developed from tests of three different configurations of glass fiber-reinforced structures which are applicable to flight vehicles. The fatigue behavior of each configuration was superior to that of aluminum-alloy skin-stringer panels with the same overall dimensions and surface weight. The program is continuing with emphasis on dynamic analysis and on tests of boron-reinforced structures.

The Sonic Fatigue Facility described in the 1965 Review is now operational and is being used to study fatigue behavior components of full-scale aircraft. A current project deals with the aft fuselage of the C-141.

An infrared inspection system for fatigue crack detection in metallic specimens has been developed for use in this facility. The device operates on a principle of focusing a small light beam on the surface of the specimen. The heat reradiated from the surface as the beam scans an area about one foot square is detected by a radiometer about 6 feet from the surface. Improvements are being made to eliminate ambiguous signals and to shield the instrument from the sonic environment.

REFERENCES

1. Hudson, C. Michael: Investigation of the Effect of Stress Ratio on Fatigue Crack Growth in 7075-T6 Aluminum Alloy. To be presented at Symposium on Fracture Mechanics, Lehigh University, June 1967.
2. Hudson, C. Michael: Investigation of Fatigue Crack Growth in Ti-8Al-1Mo-1V (Duplex Annealed) Specimens Having Various Widths. NASA TN D-3879, March 1967.
3. Figge, I.E. and Newman, J.C.: Fatigue Crack Propagation in Structures With Simulated Rivet Forces. Presented at Symposium on Fatigue Crack Propagation, American Society for Testing and Materials, June 1966. To be published in ASTM Special Technical Publication.
4. Kuhn, Paul: Residual Strength in the Presence of Fatigue Cracks (Part I). Presented to the Structures and Materials Panel - AGARD, Turin, Italy, April 17, 1967.
5. Newman, J.C.: Fracture of Cracked Plates Under Plane Stress. To be presented at Symposium on Fracture Mechanics, Lehigh University, June 1967.
6. Crews, J. H., Jr. and Hardrath, Herbert F.: A Study of Cyclic Plastic Stresses at a Notch Root. Presented at 1965 SESA Spring Meeting, Denver, Colorado, May 5-7, 1965.
7. Hunter, A.R. and Schwarz, M.E.: Development and Application of a Photo-elasto-Plastic Method to Study Stress Distributions in Vicinity of a Simulated Crack. Lockheed Missiles and Space Co., NASA CR 655, Dec. 1966.
8. Hunter, Paul A. and Walker, Walter G.: Operational Experiences of Turbine-Powered Commercial Transport Airplanes. NASA Conference on Aircraft Operating Problems, Langley Research Center, May 10-12, 1965, NASA SP-83.
9. Steiner, Roy: Summary of Atmospheric Turbulence Data. NASA Conference on Aircraft Operating Problems, Langley Research Center, May 10-12, 1965, NASA SP-83.
10. Morris, Garland J. and Hall, Albert W.: Recent Studies of Runway Roughness. NASA Conference on Aircraft Operating Problems, Langley Research Center, May 10-12, 1965, NASA SP-83.
11. Morris, Garland J.: Response of a Turbojet and a Piston-Engine Transport Airplanes to Runway Roughness. NASA TN D-3161, 1965.
12. Jewel, Joseph W., Jr. and Walker, Walter G.: Operation Experiences of General Aviation Aircraft. NASA Conference on Aircraft Operating Problems, Langley Research Center, May 10-12, 1965, NASA SP-83.

13. Ward, John F.: Exploratory Flight Investigation and Analysis of Structural Loads Encountered by a Helicopter Hingeless-Rotor System. NASA TN D-3676, 1966.
14. Ward, John F.: A Summary of Hingeless-Rotor Structural Loads and Dynamics Research - Symposium on the Noise and Loading Actions on Helicopter V/STOL Aircraft and Ground Effect Machines. Univ. of Southampton, Southampton, England, Aug. 30 - Sept. 3, 1965.
15. Huston, Robert J. and Ward, John F.: Handling Qualities and Structural Characteristics of the Hingeless-Rotor Helicopter. Conference on V/STOL and STOL Aircraft, NASA SP-116, 1966, pp. 1-16.
16. Manson, S. S. and Hirschberg, M.H.: Crack Initiation and Propagation in Notched Fatigue Specimens. NASA TM X-52126, 1965.
17. Manson, S.S.; Freche, J. C., and Ensign, C. R.: A Critical Evaluation of the Double Linear Damage Rule for Cumulative Fatigue. Presented at the ASTM Symposium on Fatigue Crack Propagation, Atlantic City, New Jersey, June 1966.
18. Manson, S. S.: Thermal Stress and Low-Cycle Fatigue. Published by McGraw Hill, New York, 1966.
19. Manson, S. S. and Halford, Gary: A Method of Estimating High Temperature Low-Cycle Fatigue Behavior of Materials. To be presented at Symposium on Thermal and High Strain Fatigue, London, England, June 1967. NASA TM X-52270.
20. Horne, Robert S.: A Feasibility Study for the Development of a Fatigue Damage Indicator. Air Force Technical Rept. AFFDL TR 66-113, Jan. 1967.
21. Schijve, J.; Broek, D.; De Rijk, P.; Nederveen, A.; Sevenhugsen, P. J.: Fatigue Tests With Random and Programmed Load Sequences, With and Without Ground-to-Air Cycles. A Comparative Study on Full-Scale Wing Center Sections. Air Force Flight Dynamics Laboratory Rept. TR 66-143, January 1967.
22. Forman, R. G.; Kearney, V. E. and Engle, R.M.: Numerical Analysis of Crack Propagation in Cyclic-Loaded Structures. Presented at 1966 Winter Annual Meeting of ASME.
23. Corten, Herbert T.; Finn, Joseph M. and Readey, William B.: Study to Determine the Suitability of Compressing the Time of Mission Profile During Elevated Temperature Fatigue Testing on Large or Full Scale Vehicles. Air Force Flight Dynamics Laboratory Tech. Rept. TDR-64-52, September 1964.
24. Abekis, P.R.; Bobovski, W.P.: Fatigue Strength Design and Analysis of Aircraft Structures, Parts I and II. Air Force Flight Dynamics Laboratory Rept. TR 66-197, in publication.

25. North American Aviation Report NA-65-607 and North American Aviation "Operation and Service News," vol. 22, no. 9, dated May 6, 1966.
26. Ritter, D.: Research on the Role of Strain Rate in Fatigue. Air Force Materials Laboratory TR 66-39, in publication.
27. Weissman, S.; Shrier, A., and Greenhut, V.: Fatigue of Metal Crystals Part I. Extension of Fatigue Life of Crystals Through Control of Substructure. Air Force Materials Laboratory TR 66-123, Part I, Aug. 1966.
28. Grosskreutz, J. C. and Shaw, G.G.: Mechanisms of Fatigue in 7075-T6 Aluminum. Air Force Materials Laboratory TR 66-96, May 1966.
29. Wang, D. Y.: Effect of Stress Ratio on Fatigue Crack Growth and Mode of Fracture in 2024-T4 and 7075-T6 Aluminum Alloys in the Low-Cycle Range. Air Force Materials Laboratory TR 66-216, Dec. 1966.
30. Swedlow, J. L.; Williams, M. L. and Yang, W. H.: Analyses of Elasto-Plastic Plates With Cracks. Air Force Materials Laboratory TR 66-248, Nov. 1966.
31. Sih, G. H.: Three Dimensional Stress Distribution Near a Sharp Crack in a Plate of Finite Thickness. Air Force Materials Laboratory TR 66-242, Nov. 1966.
32. Beebe, W. M.: An Experimental Investigation of Dynamic Crack Propagation in Plastic and Metals. Air Force Materials Laboratory TR 66-249, Nov. 1966.
33. Neuber, H.: Notch Stress Theory. Air Force Materials Laboratory TR 65-225, July 1965.
34. Weiss, V.; Takimoto, A., and Sessler, J.: A Study of the Effect of Super-imposed Stress Concentrations. Air Force Materials Laboratory TDR-64-144 April 1964.
35. Weiss, V.; Takimoto, A., and Sessler, J.: A Study of the Effect of Super-imposed Stress Concentrations. Air Force Materials Laboratory TR 65-168, October 1965.
36. Freudenthal, A.M.: The Expected Time to First Failure. Air Force Materials Laboratory TR 66-37, Feb. 1966.
37. Shinozuka, M. and Itagaki, H.: On the Reliability of Redundant Structures. Air Force Materials Laboratory TR 66-158, June 1966.
38. Heller, R. A. and Heller, A. S.: The Relationship of Earliest Failures to Fleet Size and "Parent" Population. Air Force Materials Laboratory TR 66-168, June 1966.
39. Freudenthal, A.M.; Itagaki, H. and Shinozuka, M.: Time to First Failure for Various Distributions of Time to Failure. Air Force Materials Laboratory TR 66-241, July 1966.

40. Haynie, F. H.; Vaughan, D. A.; Frost, P. D., and Boyd, W. K.: A Fundamental Investigation of the Nature of Stress-Corrosion Cracking in Aluminum Alloys. Air Force Materials Laboratory TR 65-258, Oct. 1965.
41. Haynie, F. H.; Vaughan, D. A.; Phalen, D. I.; Boyd, W. K., and Frost, P. D.: A Fundamental Investigation of the Nature of Stress-Corrosion Cracking in Aluminum Alloys. Air Force Materials Laboratory TR 66-267, June 1966.
42. Lauts, F. J. and Steigerwald, E. A.: Influence of Work Hardening Coefficient on Crack Propagation in High-Strength Steels. Air Force Materials Laboratory TR 65-31, May 1965.
43. Hanna, G. L. and Steigerwald, E. A.: Influence of Work Hardening Exponent on Crack Propagation in High-Strength Materials. Air Force Materials Laboratory TR 66-139, Oct. 1966.
44. Kramer, I. R.: Relationship of Surface Effects to the Mechanical Behavior of Metals. Air Force Materials Laboratory TR 66-2, Jan. 1966.
45. Kramer, I. R.: Effect of Surface on the Mechanical Properties of Metals. Air Force Materials Laboratory TR 66-4, Jan. 1966.
46. Kramer, I. R.: Surface Effects on Mechanical Properties of Metals. Air Force Materials Laboratory TR 67-75, in publication.
47. Berman, L.: The Effect of Including Negative Loading in the Flight Spectrum for a Typical Fighter Wing. Naval Air Engineering Center ASL-1107.
48. Smith, C. R.: A Method for Estimating the Fatigue Life of 7075-T6 Aluminum Alloy Aircraft Structures. Naval Air Engineering Center ASL-1096.
49. Endo, T. and Morrow, J.D.: Monotonic and Completely Reversed Cyclic Stress-Strain and Fatigue Behavior of Representative Aircraft Metals. Naval Air Engineering Center ASL-1105.
50. Survey of Flight-Load Parameters of Service Aircraft - Sixth Summary Report. Airtask 530/15, Naval Air Engineering Center ASL-1092 of Nov. 29, 1965.
51. Analysis of Counting Accelerometer Data - Fourth Summary Report. Airtask 530/13, Naval Air Engineering Center ASL-1091.
52. Statistical Presentation of Landing Parameters for Models F-4B, RF-8A, F-8E, A-6A, T-2A, T-28C, TS-2A, and C-1A Aircraft Aboard the USS F.D. Roosevelt (CVA-42). Naval Air Engineering Center ASL-1089 of Apr. 29, 1966.

53. Statistical Presentation of Landing Parameters for Models F-4B, F-8E, RF-8A, A-3B, A-4C, A-4E, C-1A, and E-1B Aircraft Aboard The USS F.D. Roosevelt (CVA-42) Operating Off the East Coast of Florida. Naval Air Engineering Center ASL-1090 of April 18, 1966.
54. Statistical Presentation of Landing Parameters for Models F-4B, A-4C, and RA-5C Aircraft Aboard the USS Independence (CVA-62) Operating in the North Atlantic. Naval Air Engineering Center ASL-1101 of July 26, 1966.
55. Statistical Presentation of Landing Parameters for Models F-4B, A-6A, A-4C, E-1B, and S-2D Aircraft During Field Mirror Landing Practice at NALF, Lentriss, Va. Naval Air Engineering Center ASL-1098 of Dec. 13, 1966.
56. Wood, W. A. and Reimann, W. H.: Extension of Copper and Brass Under Tension and Cyclic Torsion. Institute for the Study of Fatigue and Reliability, Columbia University, Rept. No. 18, April 1965.
57. Grosskreutz, J.C.; Reimann, W. H. and Wood, W.A.: Correlation of Optical and Electron-Optical Observations in Torsion Fatigue of Brass. Institute for the Study of Fatigue and Reliability, Columbia University, Rept. No. 19, April 1965.
58. Freudenthal, A. M. and Shinozuka, M.: On Fatigue Failure of a Multiple-Load-Path Redundant Structure. Institute for the Study of Fatigue and Reliability, Columbia University, Rept. No. 20, June 1965.
59. Shinozuka, M. and Yao, J. T. P.: On the Two-Sided Time-Dependent Barrier Problem. Institute for the Study of Fatigue and Reliability, Columbia University, Rept. No. 21, June 1965.
60. Ronay, M.: On Second Order Strain Accumulation in Aluminum in Reversed Cyclic Torsion at Elevated Temperatures. Institute for the Study of Fatigue and Reliability, Columbia University, Rept. No. 22, June 1965.
61. Freudenthal, A. M.: Second Order Effects on Plasticity. Institute for the Study of Fatigue and Reliability, Columbia University, Rept. No. 23, August 1965.
62. Wood, W. A.: Experimental Approach to Basic Study of Fatigue. Institute for the Study of Fatigue and Reliability, Columbia University, Rept. No. 24, August 1965.
63. Ronay, M.: Conditions of Interaction of Cyclic Torsion With Axial Loads. Institute for the Study of Fatigue and Reliability, Columbia University, Rept. No. 25, August 1965.
64. Heller, R. A. and Donat, R. C.: Experiments on the Fatigue Failure of a Redundant Structure. Institute for the Study of Fatigue and Reliability, Columbia University, Rept. No. 26, October 1965.

65. Shinozuka, M.; Yao, J. T. P. and Nishimura, A.: A Note on the Reliability of Redundant Structures. Institute for the Study of Fatigue and Reliability, Columbia University, Rept. No. 27, November 1965.
66. Mason, W. P.: Internal Friction Measurements and Their Uses in Determining the Interaction of Acoustic Waves With Phonons, Electrons and Dislocations. Institute for the Study of Fatigue and Reliability, Columbia University, Rept. No. 28, January 1966.
67. Shinozuka, M.; Hakuno, M. and Itagaki, H.: Response of a Multi-Story Frame Structure to Random Excitation. Institute for the Study of Fatigue and Reliability, Columbia University, Rept. No. 29, Feb. 1966.
68. Wood, W. A.: Suppression of Creep Induced by Cyclic Torsion in Copper Under Tension. Institute for the Study of Fatigue and Reliability, Columbia University, Rept. No. 30, April 1966.
69. Shinozuka, M. and Sato, Y.: On the Numerical Simulation of Nonstationary Random Processes. Institute for the Study of Fatigue and Reliability, Columbia University, Rept. No. 31, April 1966.
70. Mason, W. P.: Effect of Electron-Damped Dislocations on the Determination of the Superconducting Energy Gaps of Metals. Institute for the Study of Fatigue and Reliability, Columbia University, Rept. No. 32, May 1966.
71. Murro, R. P.: Creep Behavior of an Aluminum Alloy Under Transient Temperatures. Institute for the Study of Fatigue and Reliability, Columbia University, Rept. No. 33, June 1966.
72. Ronay, M.: On the Micro-Mechanism of Second-Order Extension of Aluminum in Reversed Cyclic Torsion. Institute for the Study of Fatigue and Reliability, Columbia University, Rept. No. 34, June 1966.
73. Wood, W. A.: Yield and Second-Order Effects Induced by Cyclic Torsion in Copper under Tension. Institute for the Study of Fatigue and Reliability, Columbia University, Rept. No. 35, June 1966.
74. Nine, H. D. and Wood, W.A.: On Improvement of Fatigue Life by Dispersal of Cyclic Strain. Institute for the Study of Fatigue and Reliability, Columbia University, Rept. No. 36, July 1966.
75. Jacoby, G.: Review of Fractographic Analysis Methods for Fatigue Fracture Surfaces. Institute for the Study of Fatigue and Reliability, Columbia University, Rept. No. 37, July 1966.
76. Donat, R. C. and Heller, R. A.: Experiment on a Fail Safe Structural Model. Institute for the Study of Fatigue and Reliability, Columbia University, Rept. No. 38, September 1966.
77. Freudenthal, A.M. and Gou, P.F.: Accumulation of Second Order Strain in Cyclic Loading of Viscous Bar. Institute for the Study of Fatigue and Reliability, Columbia University, Rept. No. 39, September, 1966.

78. Walker, E.K.: A Study of the Influence of Geometry on the Strength of Geometry on the Strength of Fatigue Cracked Panels. Air Force Flight Dynamics Laboratory Rept. TR 66-92, Oct. 1966.
79. Crichlow, W. J.; McCulloch, A. J.; Young, L., and Melcon, M.A.: An Engineering Evaluation of Methods for the Prediction of Fatigue Life in Airframe Structures. Air Force Aeronautical Systems Division Technical Rept. TR 61-434, March 1962.
80. McCulloch, A. M.; Melcon, M.A.; Crichlow, W. J.; Foster, H. W., and Rebman, R.: Investigation of the Representation of Aircraft Service Loadings in Fatigue Tests. Air Force Systems Division Technical Rept. TR 61-435, January 1962.
81. Ketola, R.N.: Full Scale Structural Fatigue Test Program. Jour. of Aircraft, vol. II, no. 5, Sept. - Oct. 1965.
82. Shanley, F. R.: A Theory of Fatigue Based on Unbonding During Reversed Slip. The Rand Corp., Rept. P-350, Nov. 11, 1952 and Supplement, May 1, 1953.
83. Shanley, F.R.: A Proposed Mechanism of Fatigue Failure. Proceedings I.U.T.A.M. Colloquium on Fatigue, Springer - Verlag, Berlin, 1956, pp. 251-259.
84. Shanley, F.R.: Strength of Materials. McGraw-Hill Book Co., New York, N.Y. 1957.
85. Shanley, F.R.: Discussion of Methods of Fatigue Analysis. Air Force Wright Air Development Center TR 59-507, Symposium on Fatigue of Aircraft Structures, Wright-Patterson Air Force Base, Ohio, 1959.
86. Ballentine, John R.; Plumblee, Harry E., and Schneider, Cecil W.: Sonic Fatigue in Combined Environment. Air Force Flight Dynamics Laboratory Rept. TR 66-7, May 1966.

FATIGUE OF STRUCTURAL MATERIALS
SUITABLE FOR THE SUPERSONIC TRANSPORT

By Herbert F. Hardrath
NASA Langley Research Center
Hampton, Virginia

Presented at Symposium on
Structural Materials in the Environment of the
Supersonic Transport

Sponsored by AIME
February 21-22, 1967
Los Angeles, California

ABSTRACT

The paper reviews some of the fatigue design considerations for the materials of the supersonic transport. Of particular interest are the effects of the load and temperature environments to be encountered during a desired life of 50,000 hours. Experimental work conducted at Langley to study behavior of candidate materials in fatigue tests, in crack propagation, in residual static strength, in outdoor corrosion-fatigue tests, in programmed-load tests and others are cited as necessary to develop an assessment of the important parameters of the problem. Most of the Langley work has included thermal environments ranging from -110°F to 550°F ; exposure times have ranged up to 3 years. While most of the data indicate that the effects of thermal exposure are negligible, some of the recent work indicates that beneficial effects of high load cycles on the subsequent fatigue behavior at lower loads can be decreased substantially by short-time exposure to elevated temperature. The need for continued research is indicated in order to allow a reliable design with a minimum of very costly testing.

INTRODUCTION

The loads induced mechanically in the primary structure of the wing of a supersonic transport during a typical flight are portrayed schematically on figure 1. The principal damage-inducing parameters in this environment are the following. For flight at Mach 3 (the original goal for the American SST), a representative temperature for external structural members is 550°F (561°K). This consideration alone requires that a material other than an aluminum alloy must be considered and titanium alloys are currently favored. Approximately 60 to 80% of the total flight time might be at speeds that produce elevated temperatures in the structure. Thus, behavior of materials during and after, say 30,000 hours, exposure to elevated temperature should be evaluated. The frequency and magnitude of loadings are greater during climb and cruise phases of flight when the material is at ambient temperature than they are during cruise when the material is at elevated temperature. The combined effects of loads, temperatures, and chemical environments are of interest.

The NASA Langley Research Center has conducted a variety of exploratory studies to identify the important facets of the fatigue problem in the design of a supersonic transport structure. It is the purpose of this paper to review some representative results of these studies and to develop from them some general conclusions. The elevated temperature used for most tests was 550°F (561°K). This temperature is higher than will be encountered at the presently-contemplated $M = 2.7$ cruise speed. However, the effects of lower temperature are expected to be less severe than those presented here. Most data are for the titanium alloy Ti-8Al-1Mo-1V in the duplex annealed condition, the material that became most favored about two years ago. The presently-favored Ti-6Al-4V material is expected to be superior in its resistance to corrosive effects. Although additional substantiating data are required, it is expected

that other trends exhibited in the data will be representative for both alloys.

Additional data and more complete descriptions of each investigation for these and other alloys are available from the references. Where appropriate, the data are compared with similar data for presently-used aluminum alloys.

Each of several considerations of interest to a designer is reviewed in turn.

DISCUSSION OF RESULTS

General Fatigue Properties

The S-N curves for notched ($K_T = 4$) sheet specimens of Ti-8Al-1Mo-1V are compared with a curve for 7075-T6 aluminum alloy in figure 2. The ordinate has been plotted on a scale of maximum stress divided by density to compare efficiencies of the two materials. The mean stresses for the two sets of data were 25 ksi (173 MN/m²) and 12 ksi (83 MN/m²), respectively. All data are for tests at room temperature. The basic S-N curve for the titanium alloy is seen to lie above the curve for 7075-T6, indicating a better efficiency. Even after 27,000 hours of unstressed exposure to 550°F (561°K), the S-N curve for the titanium was higher than that of aluminum (ref. 1). Fatigue properties of unnotched, fusion-welded and spot-welded specimens of titanium alloys were also essentially unaffected by the prolonged exposure to the elevated temperature. Other data (not shown) demonstrated that the fatigue lives of Ti-8Al-1Mo-1V specimens were reduced by a factor of 2 at a given stress level when the tests were conducted at 550°F (561°K). The fatigue notch-sensitivity of Ti-8Al-1Mo-1V also compared favorably with that of 7075-T6.

From these indications, one might conclude that from a fatigue point of view the use of the titanium alloy Ti-8Al-1Mo-1V should produce a structure at least as efficient as is achieved with current aluminum alloys.

Fatigue Crack Propagation

One of the most important considerations in evaluating the fatigue life and fail-safe characteristics of a structure is the rate at which a fatigue crack propagates through the material. Figure 3 shows a sample of data on the rates of fatigue crack propagation obtained in tests of simple sheet specimens of two aluminum and two titanium alloys (refs. 2 and 3). The sample was chosen for sheets 8 inches (203 mm) wide and a crack length of 0.8 inch (20 mm). The mean stress for all tests was approximately 20% of the ultimate tensile strength of each material. The abscissa is the ratio of the alternating stress to mean stress in each series of tests.

Both titanium alloys had lower rates of crack propagation than did the aluminum alloys, particularly at low alternating stresses. Similar data obtained at 550°F (561°K) and at -109°F (195°K) for titanium alloys indicated that the effects of these temperatures were moderate.

Thus, one might anticipate titanium alloy structures to compare favorably with current aluminum alloy structures from the crack propagation point of view.

Residual Static Strength of Cracked Sheet

Of considerable interest to the designer is the effect of cracks on residual static strength or conversely, the length of crack that produces failure at a given stress. Figure 4 presents sample data from static tests of sheet specimens made of two titanium and two aluminum alloys (refs. 4 and 5). The stress at failure, computed for the net section present before load was applied, has been divided by density of the material to facilitate comparisons. The abscissa for each of the three plots is the ratio of crack length to width of specimen for specimens 8 inches (203 mm) wide.

The strengths of both titanium alloys, Ti-8Al-1Mo-1V and Ti-6Al-4V, were higher than the room-temperature strength of 7075-T6 aluminum alloy throughout the temperature range investigated. The aluminum alloy RR-58 proposed for use on the Anglo-French Concorde had residual static strength properties reasonably like those of 7075-T6 over the temperature range of interest.

Again, these data indicate that titanium alloy structures might be expected to have residual static strengths higher than those of aluminum alloy structures of the same weight. Conversely, slightly longer crack lengths should be tolerable in the titanium alloy structure.

Effect of Aqueous Environment

Tests similar to those just discussed were also conducted in water or in salt water at room temperature. Loads were applied to cracked sheet specimens and maintained until failure occurred with the results shown in figure 5 (ref. 6). The data are portrayed on a plot of net section stress (computed for the net area existing before the load or water were applied) against the time to failure. Most of the data are for specimens 4 inches (102 mm) wide with cracks 1 inch (25 mm) long.

Very large reductions in strength were noted for aqueous exposures as short as 1 hour. The most deleterious effect was noted in mill-annealed Ti-8Al-1Mo-1V. Because the duplex-annealed form of this alloy was favored, this material was tested in several thicknesses. A very significant effect of thickness was noted with the thicker specimens much more seriously damaged. The alloy Ti-6Al-4V was found to be somewhat less susceptible to the aqueous environment than was Ti-8Al-1Mo-1V.

This consideration was the cause for much concern over the suitability of titanium alloys for use in the SST structure during the past two years. On the strength of data such as these, the Boeing Company chose the Ti-6Al-4V alloy as the primary material for its structure. The competing airframe companies, materials producers and other interested parties have worked most diligently to develop heat treatment procedures to improve the behaviors noted. As a result, current versions of these materials behave more satis-

factorily than indicated here. Research is continuing to improve the understanding of the basic mechanism of this mode of failure.

Incidentally, similar tests of the aluminum alloys 2024-T3 and 7075-T6 showed very little influence of the aqueous environment.

Combined Effect of Elevated Temperature and Outdoor Environment on Fatigue Behavior

In an effort to combine the effects investigated previously in the foregoing investigations, but in a somewhat more realistic manner, another set of fatigue tests was conducted out of doors. The apparatus used for these tests is shown in figure 6. The same apparatus had been used previously for tests of aluminum alloy specimens at ambient temperature (ref. 7). Basically, the machine is a table mounted on springs and constrained to vibrate in the vertical direction. Excitation of the table is provided by a slipping-clutch mechanism that moves the table at its natural frequency and at the desired amplitude. Sheet-bending cantilever specimens (66 in number) are clamped to the periphery of this table. Each specimen has a mass clamped to its free end to time the specimen to vibrate at the desired amplitude when the table is in motion (see figure 7). In addition, a second mass is suspended from the first by a soft spring in order to apply a desired mean stress in the specimen. Each specimen is heated to 550°F by quartz tube lamps mounted below the specimen. The temperature is controlled by a servo device responding to a thermistor sensor on each specimen.

In operation the temperature is maintained at 550°F for 20 hours each day with the specimens in a static position. The heating is interrupted for 4 hours each night (to allow dew to form), at any time that rain or snow is falling and for a short period twice each week during which time a few thousand cycles of stress are applied. Specimens of Ti-8Al-1Mo-1V with fusion welds or with central holes are currently under test in this device. The stress levels and the number of cycles of stress applied each week were chosen to produce failure in about one year if no deleterious influence of the outdoor-environment were found. The life was based on results of similar tests conducted without interruption in a laboratory at ambient temperature.

Preliminary results of these tests are displayed in figure 8. Only a few failures have been experienced but these occurred in approximately 1/2 as many cycles as were required to produce the earliest failures in the control tests. This effect is of about the same order of magnitude as that observed in ambient temperature tests of bare aluminum alloy specimens in the same apparatus earlier.

Effect of Preloading and Exposure to Elevated Temperature on Fatigue Behavior

Another factor which can influence fatigue behavior in service is the residual stress left when a part is subjected to loads high enough to produce local plastic deformations. Tests have been conducted in which notched ($K_T = 4$) sheet specimens were subjected to single cycles of axial load and then tested

in fatigue at a common amplitude of stress. The resulting test lives are indicated in figure 9. Tensile preloads produced improvements in life by factors up to 10; compression preloads reduced lives by smaller factors. Qualitatively, this effect is well known and has been demonstrated to occur in other materials. Although no specific advantage is usually taken of this effect in design, the effect is one of the reasons why some structures behave more favorably than is anticipated according to linear cumulative damage procedures.

When specimens preloaded in tension were exposed to 550°F (561°K) for periods as short as 30 seconds, the beneficial effect of the preload was all but eliminated. Fortunately, longer exposures (up to 30 days) caused no further reduction in fatigue life. This effect is a bit more disturbing than those discussed earlier, because each flight of the aircraft might introduce beneficial residual stresses, but the effect may be removed by any subsequent exposure to elevated temperature. Thus, a realistic fatigue evaluation is likely to require a flight-by-flight application of loads and temperatures.

Flight-by-flight Evaluation of Fatigue Behavior

In order to provide further insight into the fatigue behavior of a supersonic transport, tests are being conducted with flight-by-flight schedules of load and temperatures. The ten machines shown in figure 10 apply cyclic axial loads and heat cycles to sheet specimens containing six critical cross sections each. The loads are provided by servo-controlled hydraulic loading systems and the heat by quartz-tube heat lamps. Anti-buckling guides support the specimens laterally during compression loading. The elevated temperature is programmed to simulate heating in real time, but the ambient-temperature portions of the test are conducted at the speed achievable by the load apparatus (approximately 1 cps).

In companion machines similar tests are conducted on an accelerated time scale to develop methods for reducing the total time required to perform a test. (Unless the time scale is compressed significantly, an evaluation test could require twenty years.) Figure 11 shows that at ambient temperature the life of specimens changed by a factor of about 10 if the mean stress during level flight was changed in the range 25 to 35 ksi (173 to 238 MN/m²). Also, if the entire test was conducted at 550°F (561°K), the life was approximately one half the life at ambient temperature. At least some of the latter effect is thought to be attributable to the effect of elevated temperature on residual stresses discussed in connection with figure 9.

Other tests of a similar nature are underway to identify the influence of mechanically-simulated thermal stresses, taxi loads, the limits of the ground-air-ground cycle, corrosion, stress-concentration factor, exaggerated temperatures, and others. A large number of such tests will be required to provide guidance for future tests on complex components of the supersonic transport structure.

SUMMARY

Results of a variety of investigations have been presented to illustrate:

1. That the SST structure should be as fatigue resistant and efficient if built of titanium as are current aluminum alloy structures.
2. The effect of elevated temperature on fatigue properties is small.
3. The effect of prolonged exposure to elevated temperature on subsequent fatigue behavior of the material is also small.
4. Similarly, the fail-safe characteristics of titanium alloys, namely, crack propagation and residual static strength, compare favorably on a strength to density basis with those of aluminum alloys.
5. The effects of aqueous environment on residual static strength are significant.
6. The combined effects of exposure to elevated temperature and to outdoor environment are about the same as the effects of environment on behavior of aluminum alloys.
7. Brief exposure to elevated temperature can reduce the beneficial effects of high loadings.
8. Work is required to develop ways of evaluating fatigue behavior of SST structure without the extremely lengthy tests required under the current state of the art.

REFERENCES

1. Illg, W. and Castle, Claude B.: Effects of Exposure to 550°F on the Characteristics of 4 Steels and 3 Titanium Alloys. NASA TN D-2899, July 1965.
2. Hudson, C. Michael: Fatigue Crack Propagation in Several Titanium and Stainless-Steel Alloys and One Superalloy. NASA TN D-2331, Oct. 1964.
3. Hudson, C. Michael: Studies of Fatigue Crack Growth in Alloys Suitable for Elevated Temperature Applications. NASA TN D-2743, April 1965.
4. Figge, I.E.: Residual Static Strength of Several Titanium and Stainless-Steel Alloys and One Superalloy at -109°F, 70°F, and 550°F. NASA TN D-2045, December 1963.
5. Figge, I.E.: Residual Strength of Alloys Potentially Useful in Supersonic Aircraft. NASA TN D-2613, February 1965.
6. Figge, I.E. and Hudson, C. Michael: Crack Propagation, Delayed Failure and Residual Static Strength of Titanium, Aluminum, and Stainless-Steel Alloys in Aqueous Environments. NASA TN D-3825, February 1967.
7. Leybold, Herbert A.; Hardrath, Herbert F., and Moore, Robert L.: An Investigation of the Effects of Atmospheric Corrosion on the Fatigue Life of Aluminum Alloys. NACA TN 4331, September 1958.

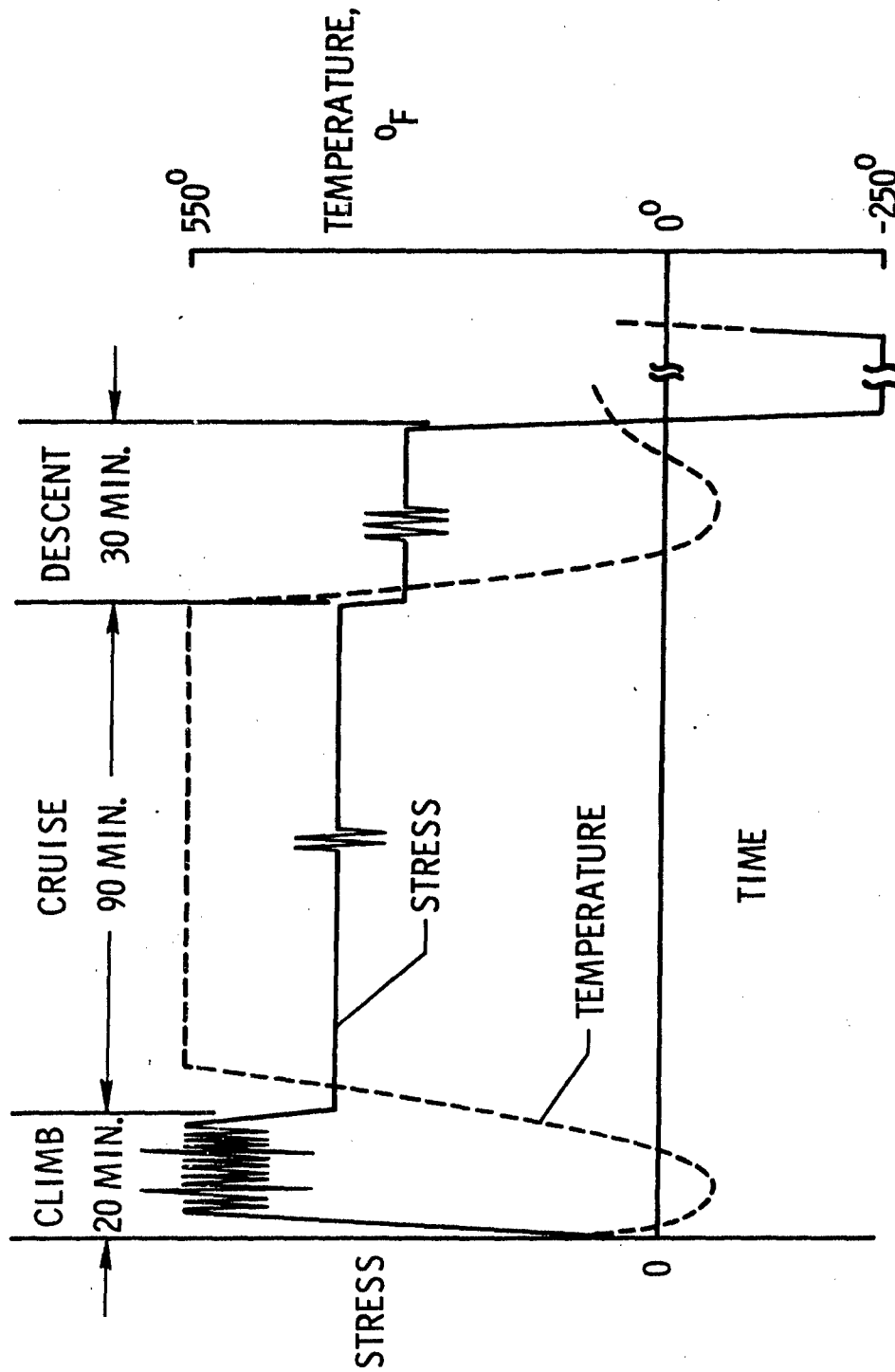


Figure 1.- Loads and temperatures in a typical flight of a supersonic transport.

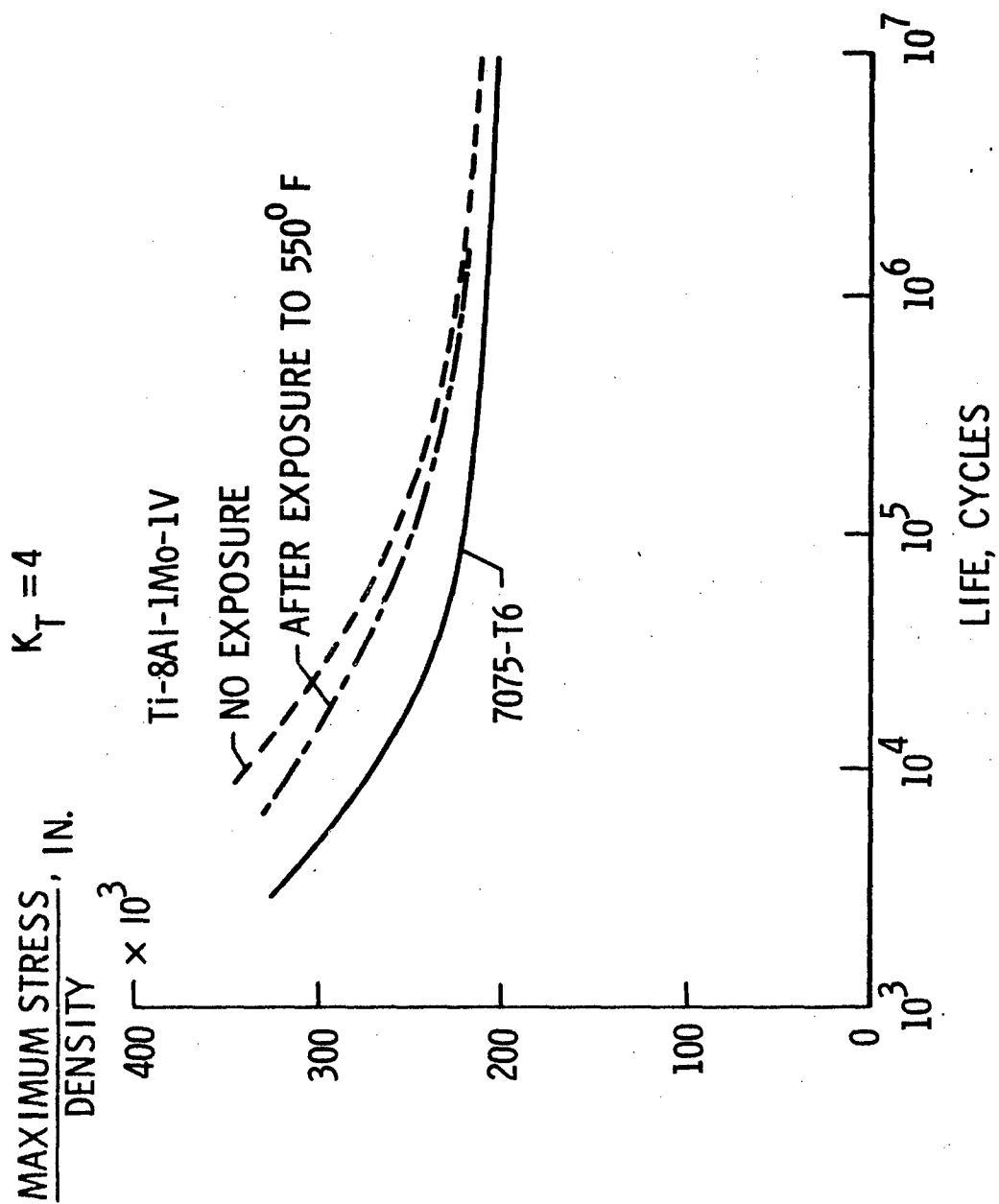


Figure 2.- Fatigue behavior at room temperature.

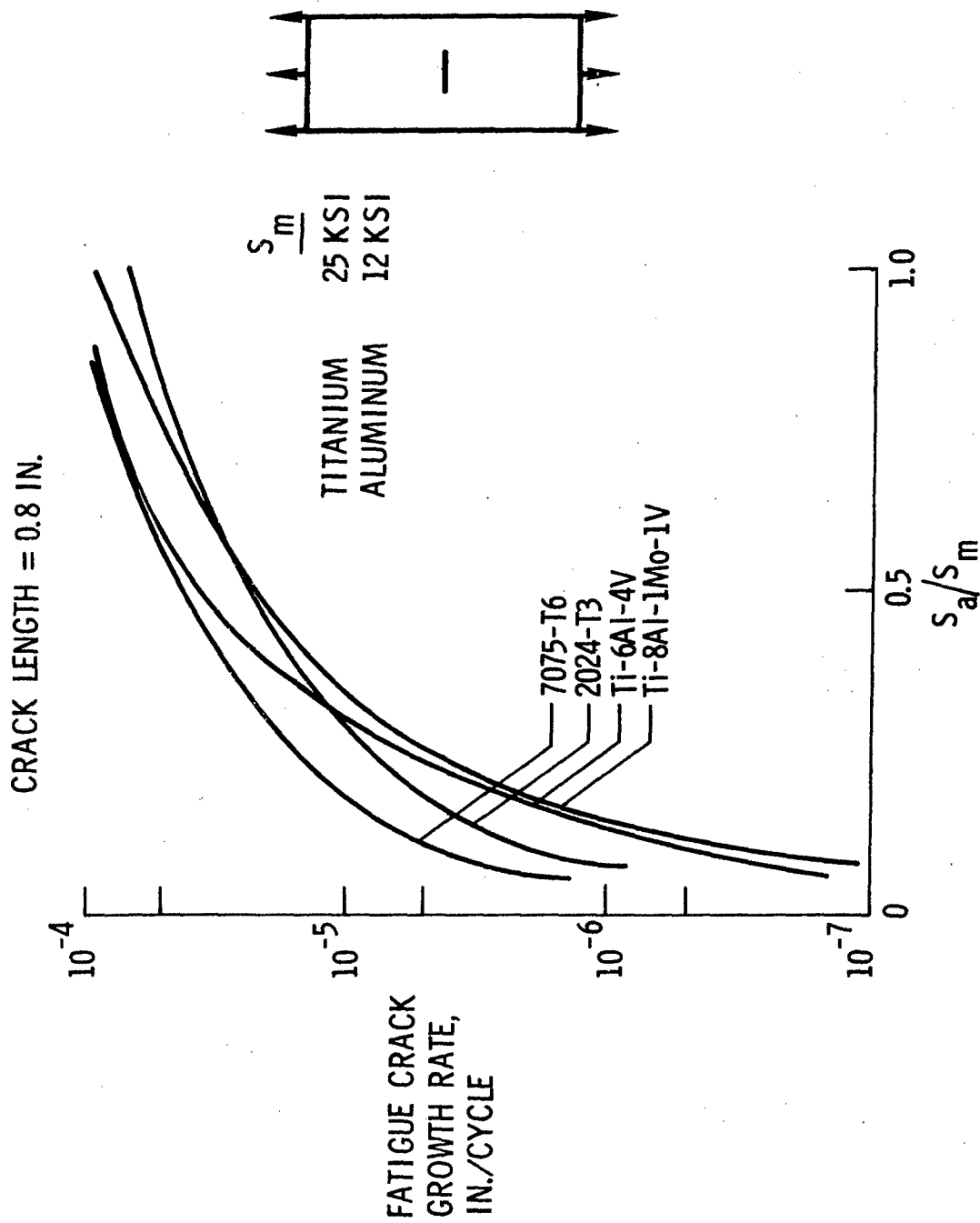
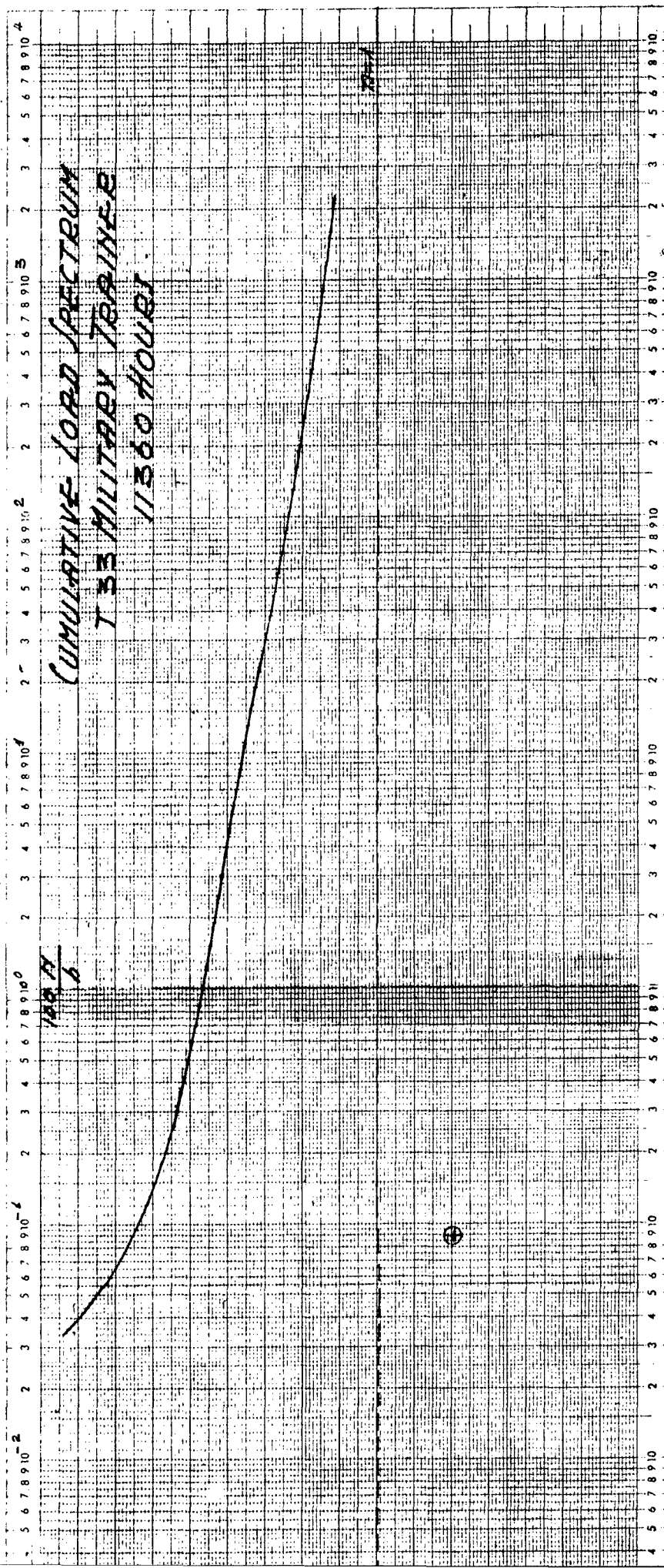
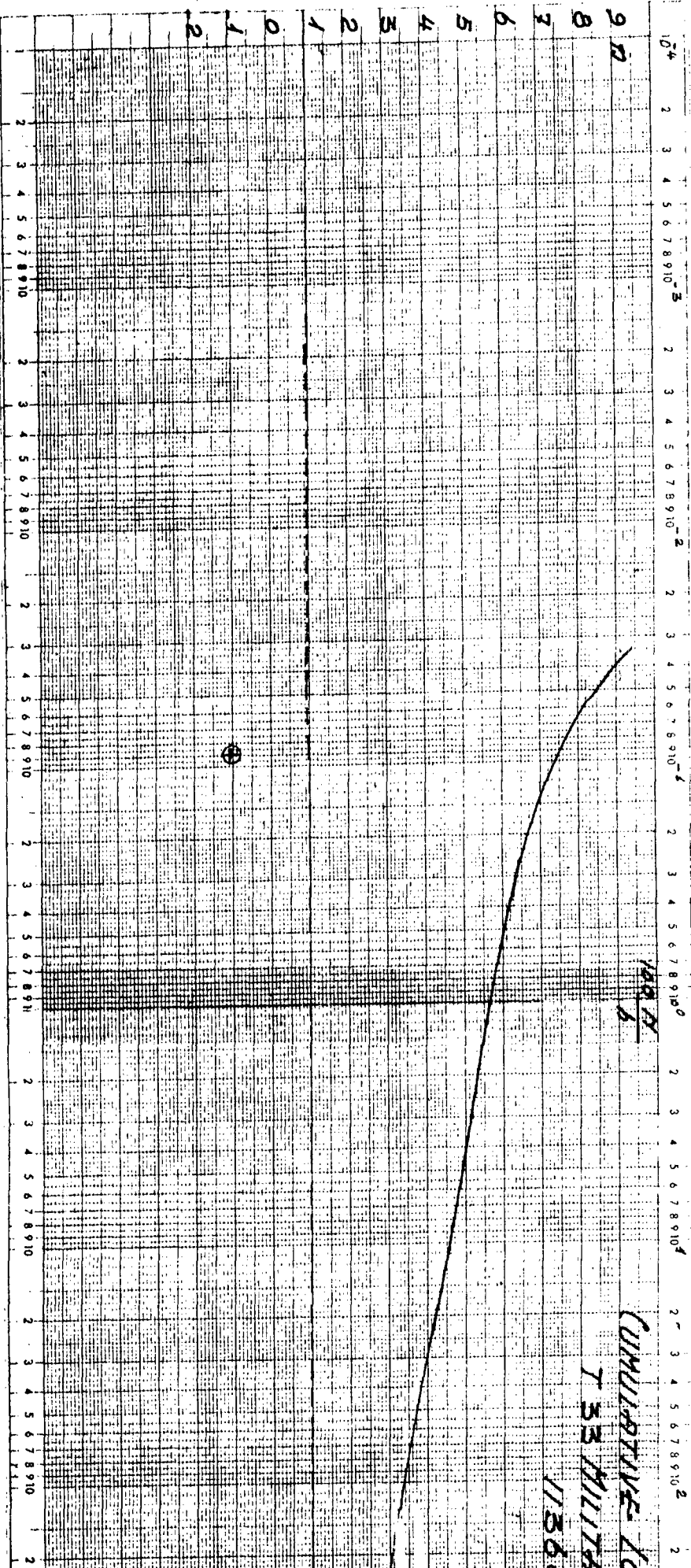


Figure 3.- Crack propagation in SST materials.

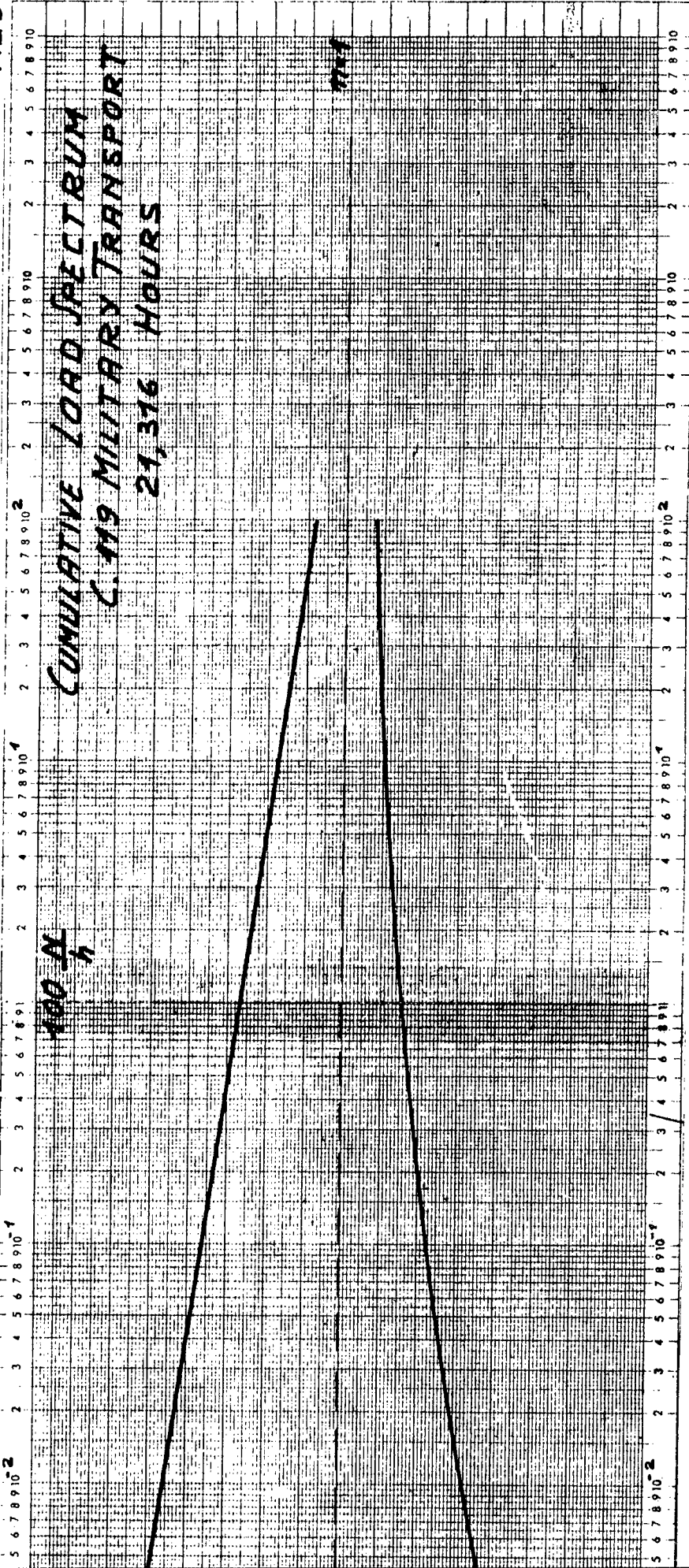
FIG. 2





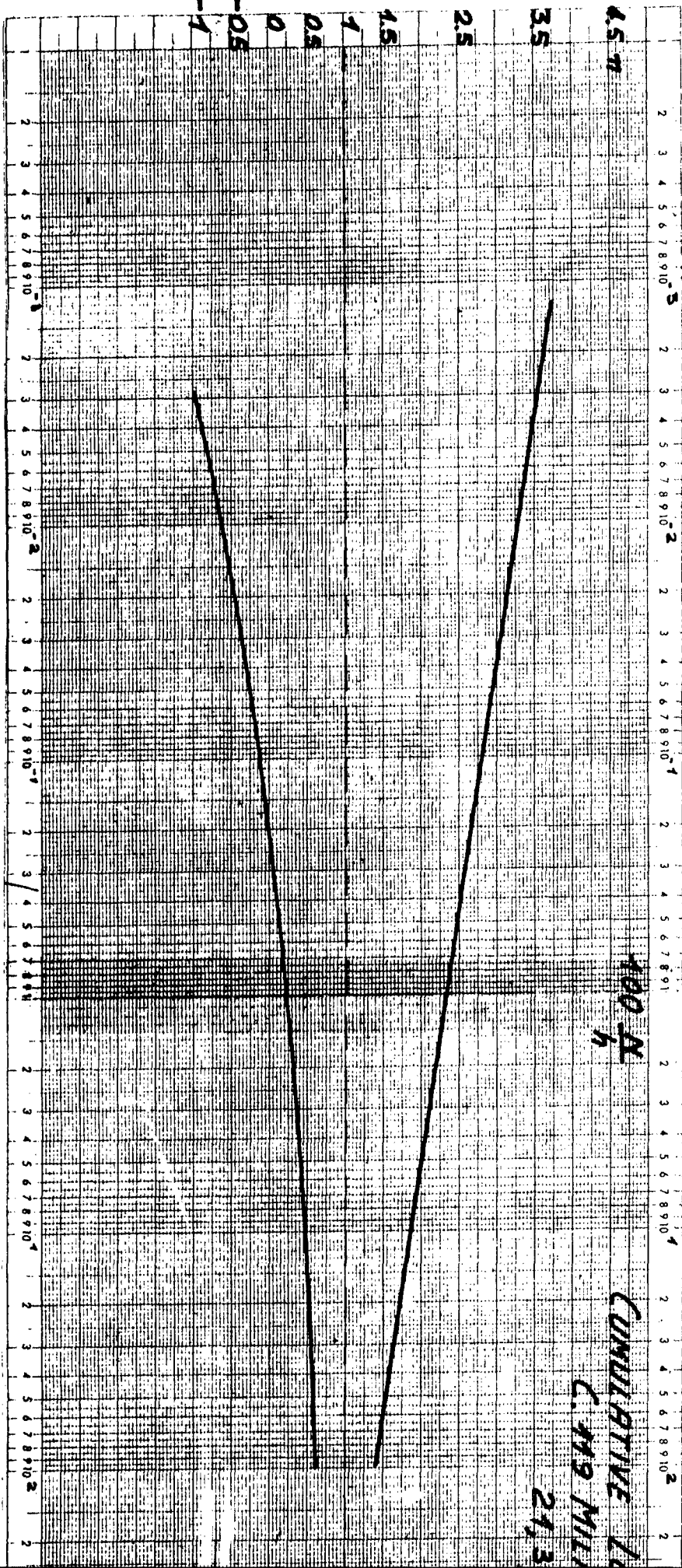
CUMULATIVE TO
T 33 MILITARY
1156

FIG 3



307-11

507-18



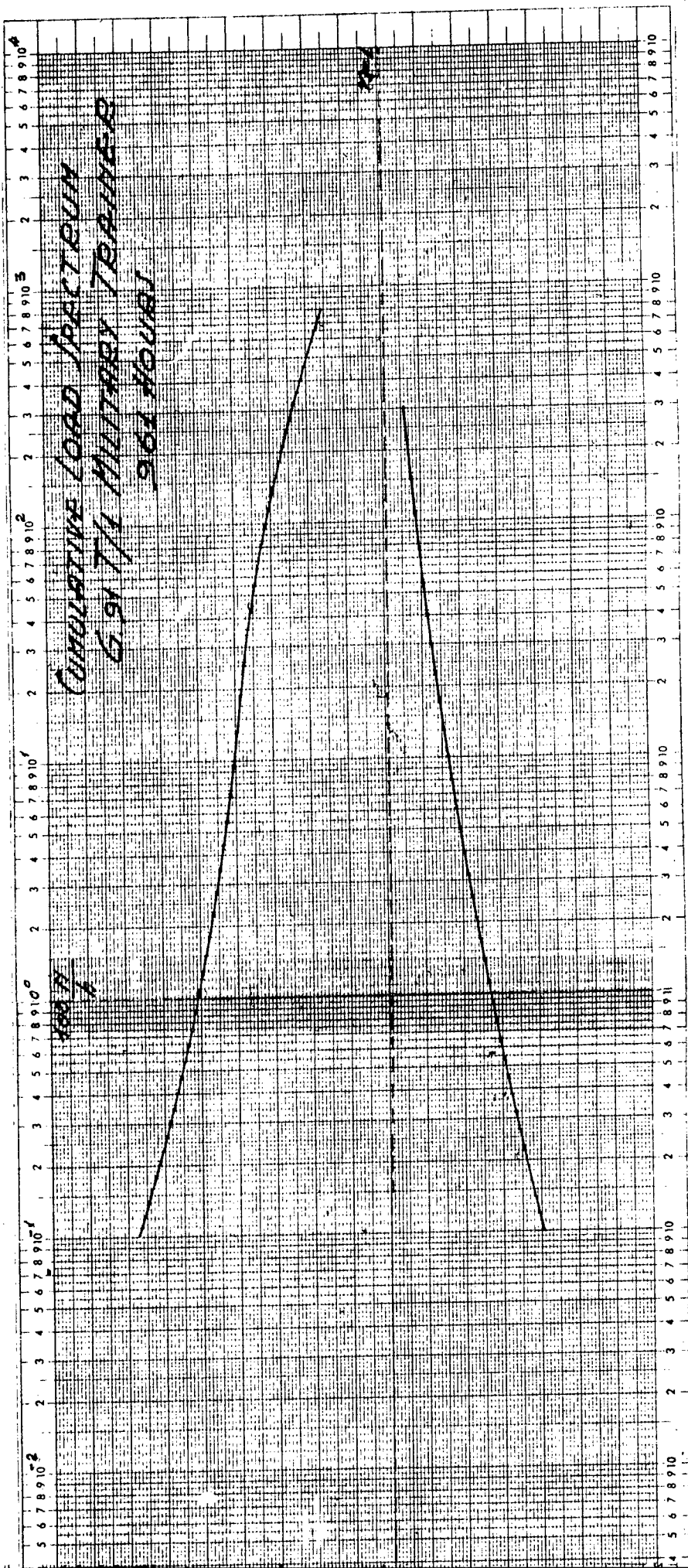
100 H

CUMULATIVE L

C. 119 MLL

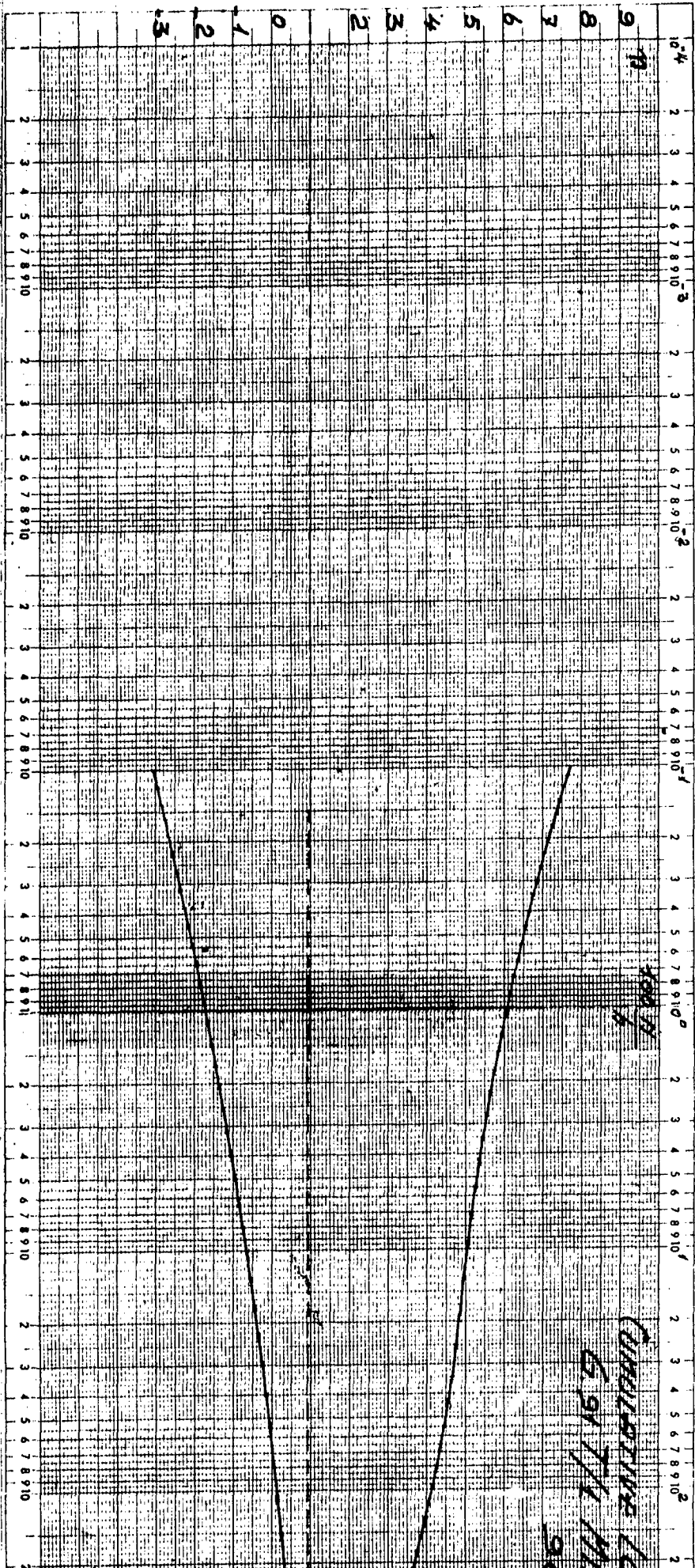
24.3

FIG. 4



308-A

308-B



APPENDIX 2 - RECENT ACTIVITIES IN THE FIELD OF FATIGUE
AT ISTITUTO SPERIMENTALE DEI METALLI LEGGERI,
Novara-Milano

ISML 1 THE CORROSION FATIGUE BEHAVIOUR OF Al-Mg AND
Al-Cu-Mg ALLOYS

In these studies of the corrosion-fatigue phenomena, confined to Al-Mg and Al-Cu-Mg alloys, an examination was made of the influence of some of the principal factors involved such as:

- magnesium content: Al-Mg alloys with the following Mg contents 2.5; 3.5; 4.4; 5%.
- structural state.
- corrosive media: the corrosive agents considered showed various stages of aggressiveness, for example, tap-water and solutions with sodium chloride content varying from 3 to 15%.
- stress frequency: the test rates used were 1000, 3000 and 11,500 cycles per minute (rotating bending stress).

In addition, pre-corrosion and the corrosion-fatigue damage have been considered.

The results (Figs. 5-8) have clearly shown that:

- there are no remarkable differences in the corrosion fatigue curves of the Al-Mg alloys with different Mg contents.
- the influence of test speed is noticeable.
- structural state of the alloys is of little influence.
- there are notable differences between the curves obtained with a moderately aggressive electrolyte and those obtained with a 3% NaCl solution, but there are no appreciable differences between 3% and higher sodium chloride concentrations.

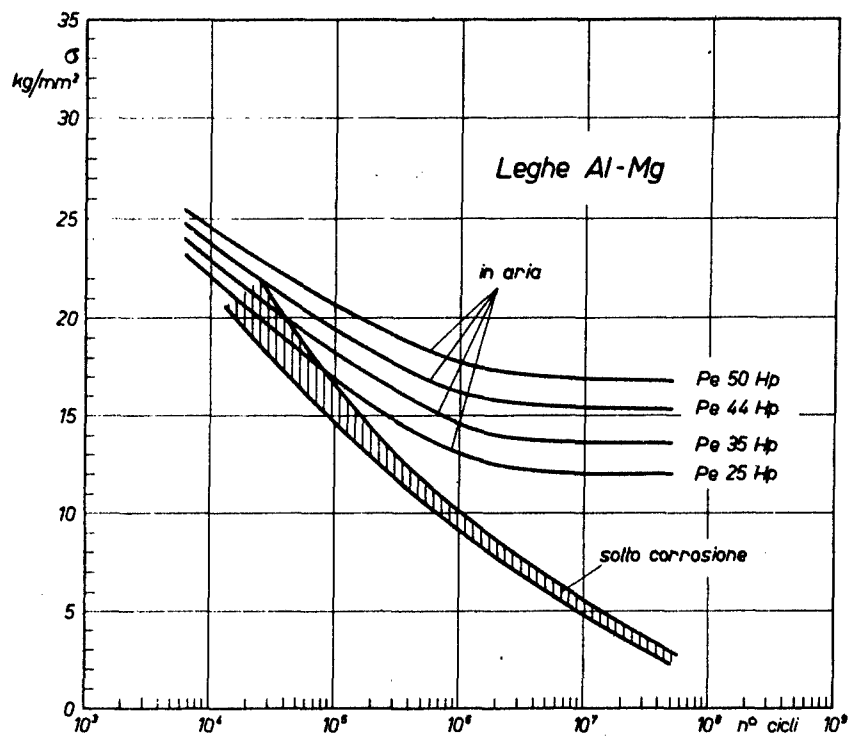


Fig. 5 Corrosion - fatigue behaviour of the extruded Al-Mg specimens tested in 3% salt solution.

in aria - in air

sotto corrosione - in salt solution.

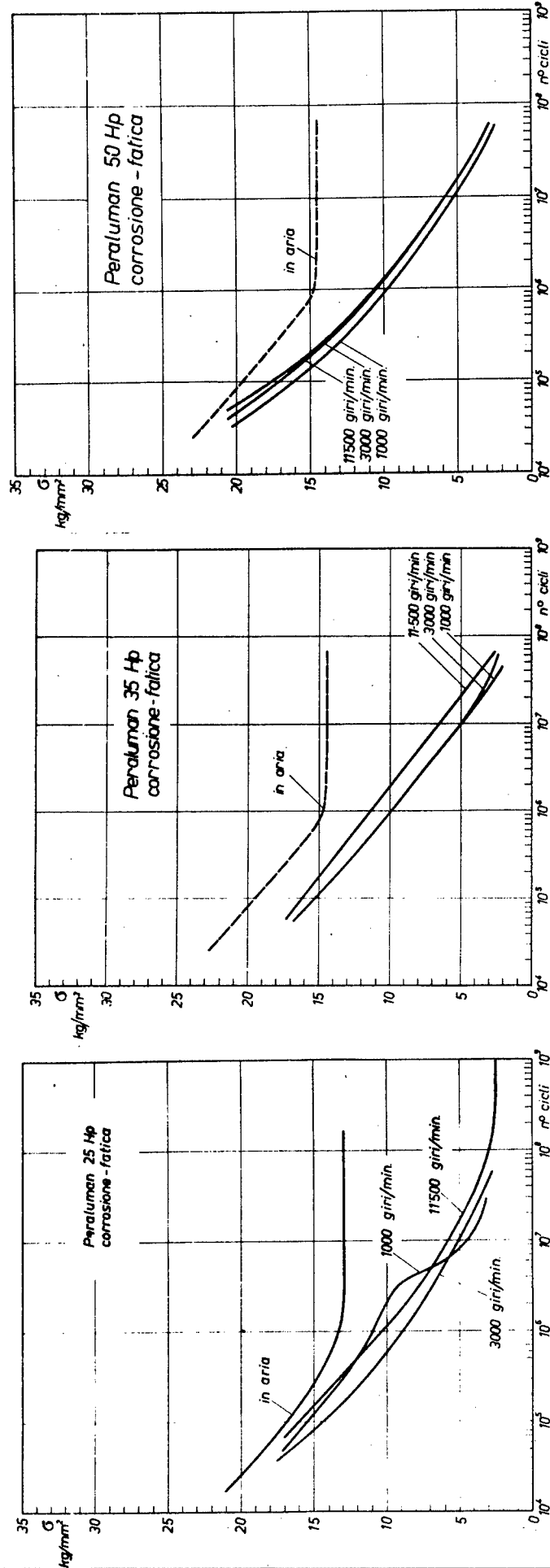


Fig. 6 Fatigue curves and corrosion-fatigue curves obtained for different frequencies and various Mg contents.

Peraluman 25 - Al-Mg 2.5
 Peraluman 35 - Al-Mg 3.5
 Peraluman 50 - Al-Mg 5.0

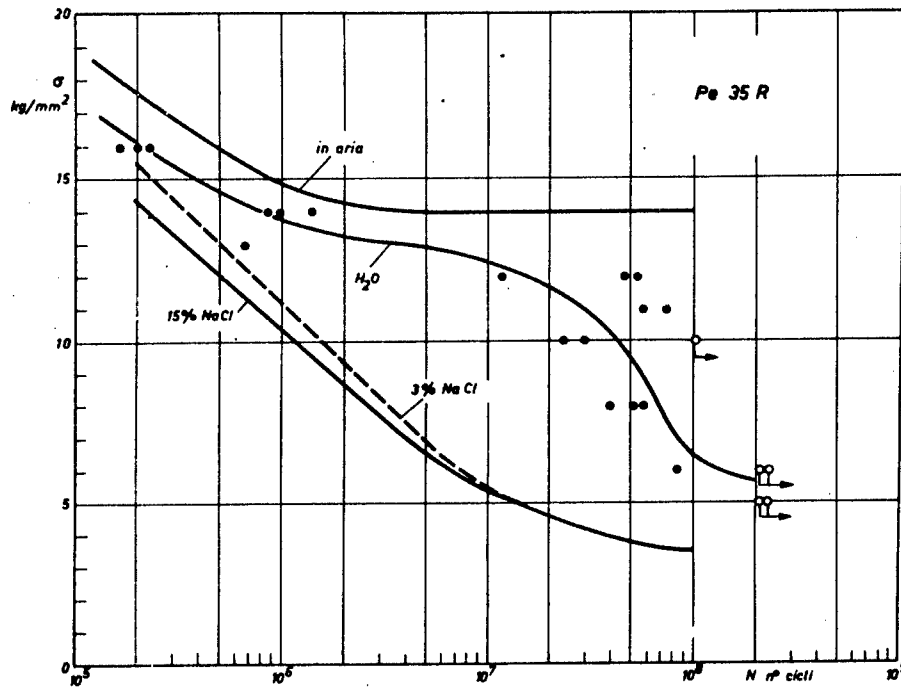


Fig. 7 Corrosion-fatigue curves obtained for Al-Mg 3.5 alloy specimens with different electrolytes at 11,500 cycles/min.

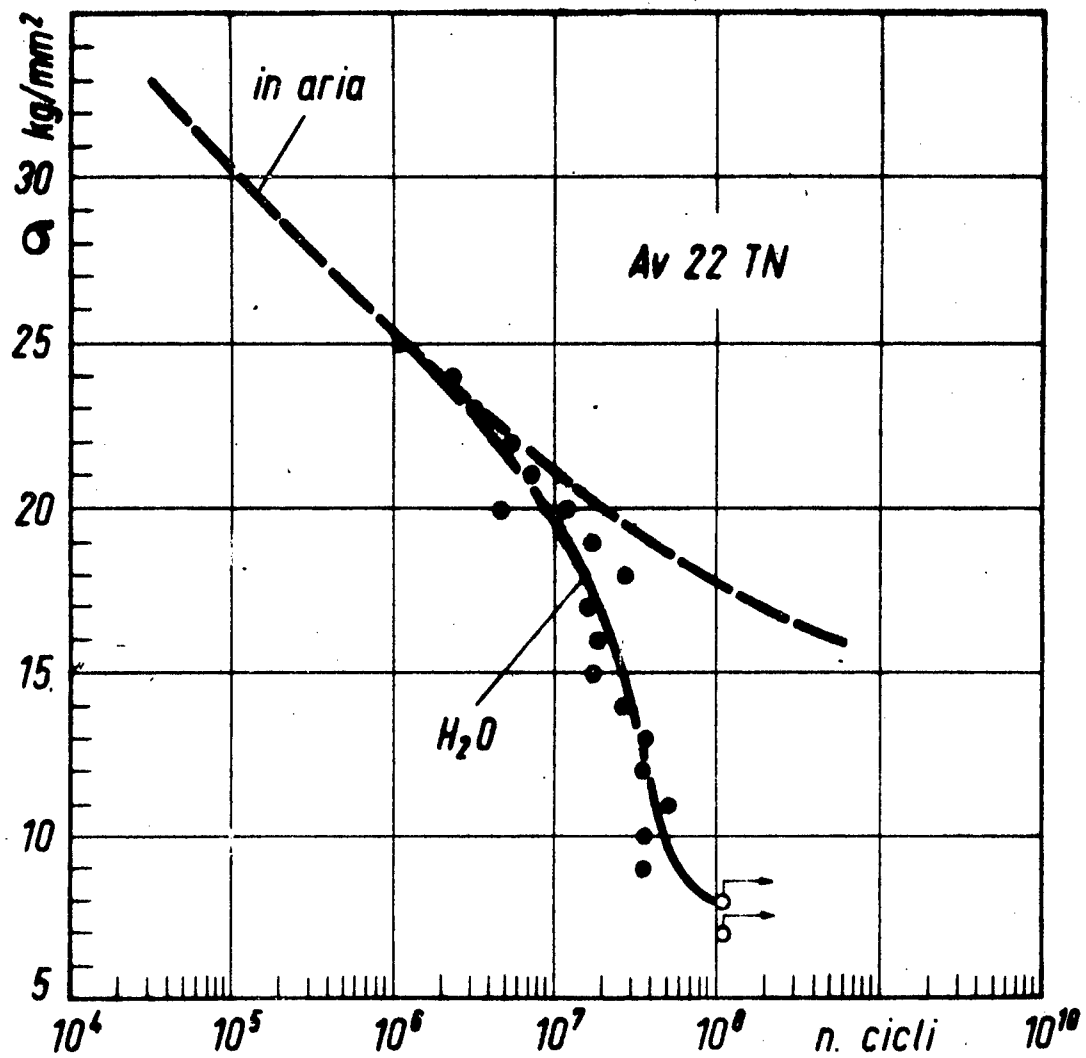


Fig. 8 Corrosion-fatigue curve for specimens of Al-Cu-Mg alloy tested in tap water.

- the pattern of the S-N curve obtained with tap-water is characteristic as there is a knee after about 10^7 cycles.
- hypotheses concerning corrosion-fatigue have been made.

ISML 2 THE NOTCH FACTOR IN THE FATIGUE BEHAVIOUR OF Al-Zn 5.8-Cu-Mg ALLOY AT LOW TEMPERATURES

The influence of the stress-concentration factor K_t and the test conditions on the fatigue behaviour of the Al-Zn 5.8-Cu-Mg alloy have been determined (Fig. 9), considering the following factors:

- stress-concentration factors of $K_t = 1; 1.2; 1.5; 2; 4.5$ and 9 .
- test temperatures: room temperature; -196°C and isothermal (cooled with water).

The correlations between K_t and K_f (strength-reduction factor) are shown in Fig. 10.

The K_t and K_f values are not proportional; the difference between K_f and K_t may be attributed to plastic deformation and it may be concluded that the ability of a material to deform plastically under alternating stress is an important factor in reducing its notch sensitivity.

ISML 3 THE FATIGUE BEHAVIOUR OF THE ALUMINIUM ALLOYS HARD ANODISED

Rotating and reversed bending fatigue tests have been carried out on the Al-Cu-Mg and Al-Zn 5.8-Cu-Mg alloys with the following oxide coating thicknesses: $20\mu; 30\mu; 40\mu; 80\mu$.

High decrease of the endurance limit in the case of hard anodising and a small decrease for a

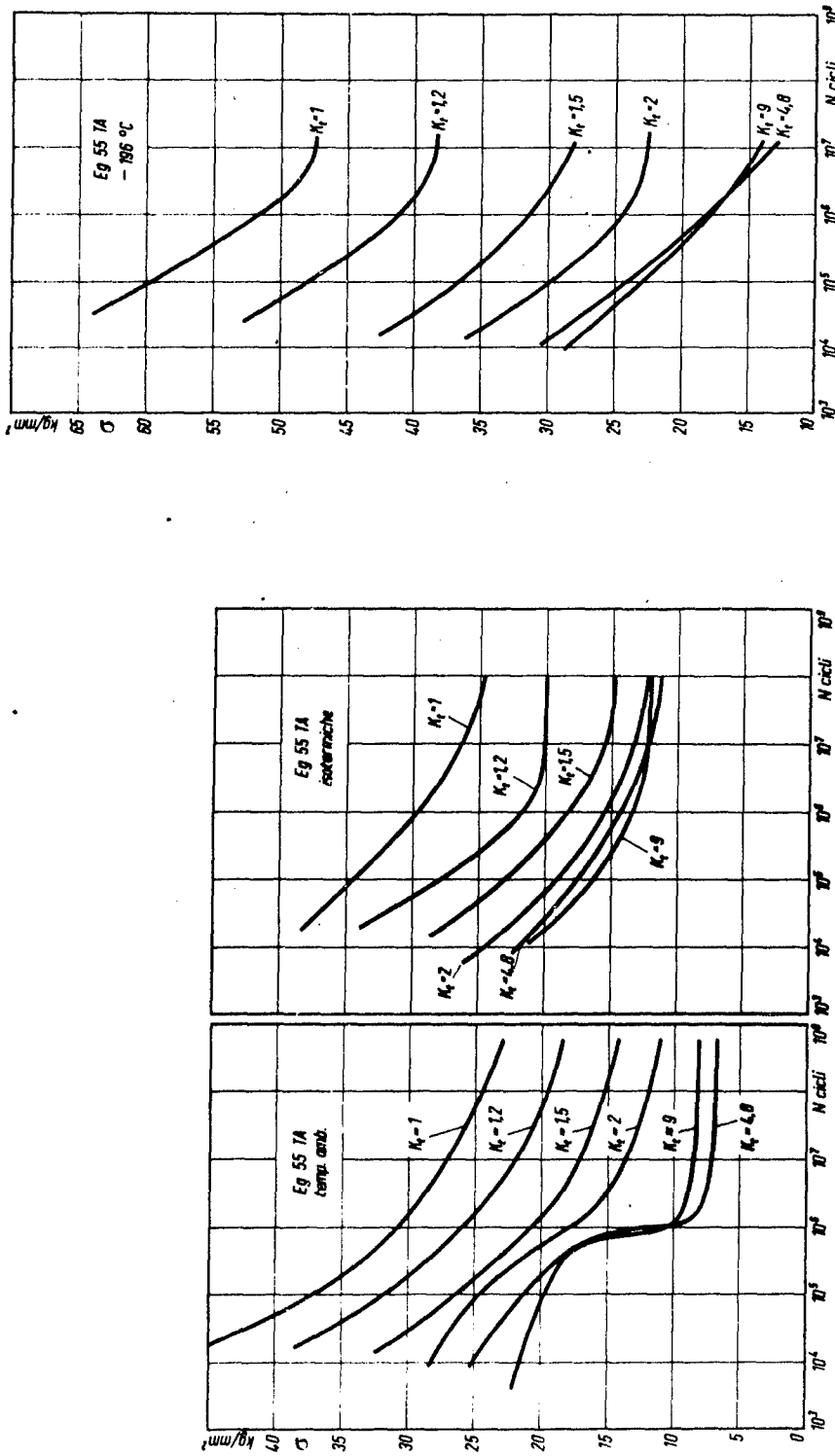


Fig. 9 S-N curves of Al-Zn 5.8-Cu-Mg alloy at different test temperatures and at different notch sensitivity.

temp. amb. - room temperature
isothermiche - water cooled at 18°C.

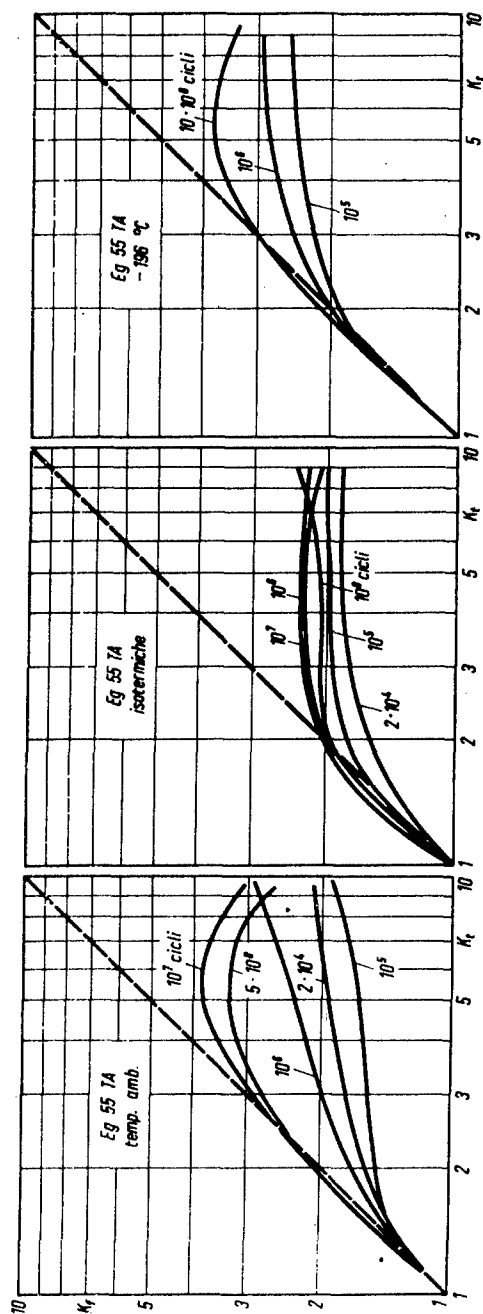


Fig. 10 K_t - K_f correlation of Al-Zn 5.8-Cu-Mg alloy at different test temperatures.

normal anodising process have been found (Fig. 11). The rate of decrease is connected with the thickness of the oxide coating and its surface irregularities (Centre Line Average). The oxide fracture causes a stress concentration factor on the metal. Moreover the oxide strength is connected with its characteristics and its surface irregularities.

Finally it has been ascertained that the fatigue curves of the hard anodised specimens show a knee shape at between 10^5 and 10^6 cycles, typical of notched specimens.

ISML 4 EFFECT OF TEMPERATURE ON THE FATIGUE BEHAVIOUR OF Al-Mg 5 ALLOY

This research was carried out both to estimate fatigue strength at high temperatures of the Al-Mg 5 alloy and to study temperature influence in the structural modifications.

The tests were carried out at 20°C; 130°C; 200°C and 250°C and the materials were employed in the following conditions: annealed; hardened by cold working and as extruded.

It has been observed that the S-N curve of the as extruded material at about 130°C (Fig. 13) loses the typical asymptotic endurance limit. This is connected with Mg precipitation which, in turn, depends on diffusion rate (controlled by vacancy concentration).

Hence, the endurance limit is present at 20°C since the diffusion rate is low, and above 200°C where the diffusion becomes appreciable.

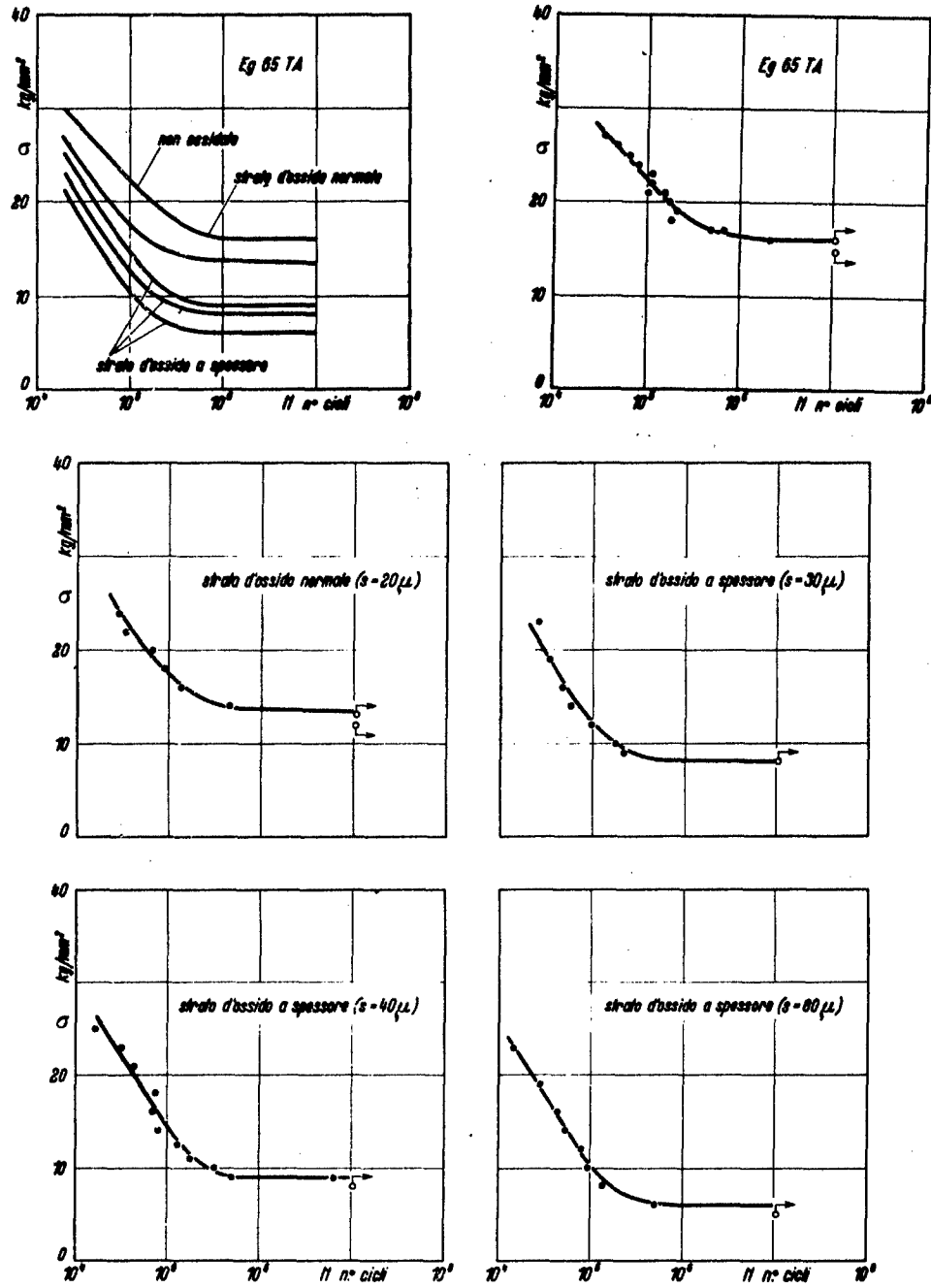


Fig. 11 Reversed bending fatigue curves of Al-Zn 5.8-Mg-Cu alloy specimens with different oxide thickness.

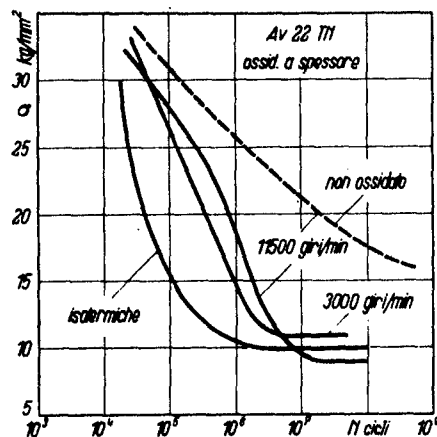


Fig. 12 S-N rotating bending curves of Al-Cu-Mg alloy hard anodized specimens for different frequencies.

non ossidato - non oxide coated
isotermiche - water cooled at 18°C.

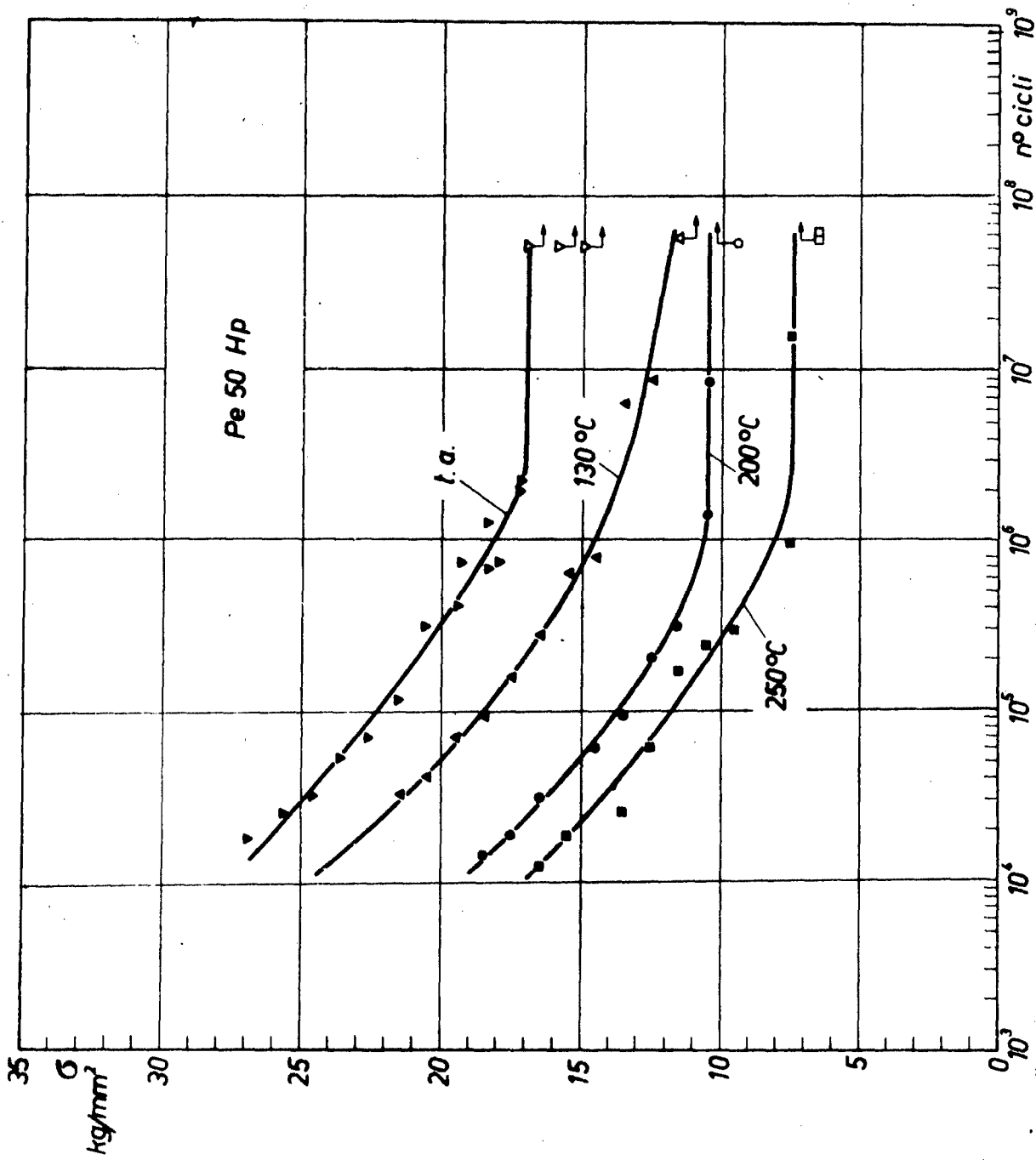


Fig. 13 S-N curves of Al-Mg 5% alloy (as extruded) at different temperatures.

ISML 5 THE FATIGUE BEHAVIOUR OF SPECIMENS WITH
SUPERFICIAL PROTECTION (VASELINE)

The fatigue tests have been carried out on the wrought aluminium alloys heat-treated and annealed specimens protected by vaseline.

The results (Fig. 14) showed a sensible increase in the failure-time, specially between 10^5 and 10^6 cycles, of the vaseline coated specimens compared with unprotected specimens.

It is possible to attribute this effect to the following factors:

- heat insulation.
- slower oxidation of the surface fatigue cracks.

ISML 6 THE EFFECT OF MEAN STRESS ON THE AXIAL FATIGUE
STRENGTH OF Al-Zn 5.8-Cu-Mg ALLOY

The effect of mean stress on the axial fatigue behaviour of Al-Zn 5.8-Cu-Mg alloy has been determined (Fig. 15) considering the following factors:

$R = \frac{\sigma_{\min}}{\sigma_{\max}} = +\frac{1}{2} ; 0 ; -\frac{1}{2} \text{ and } -1$; carried out on Amsler Vibrophores (150 Hz).

The reliability diagrams have been developed, according to the methods of Smith, Rös-Goodman (Fig. 16) and Gerber.

The curves obtained for the same materials in rotating bending tests are reported for comparison.

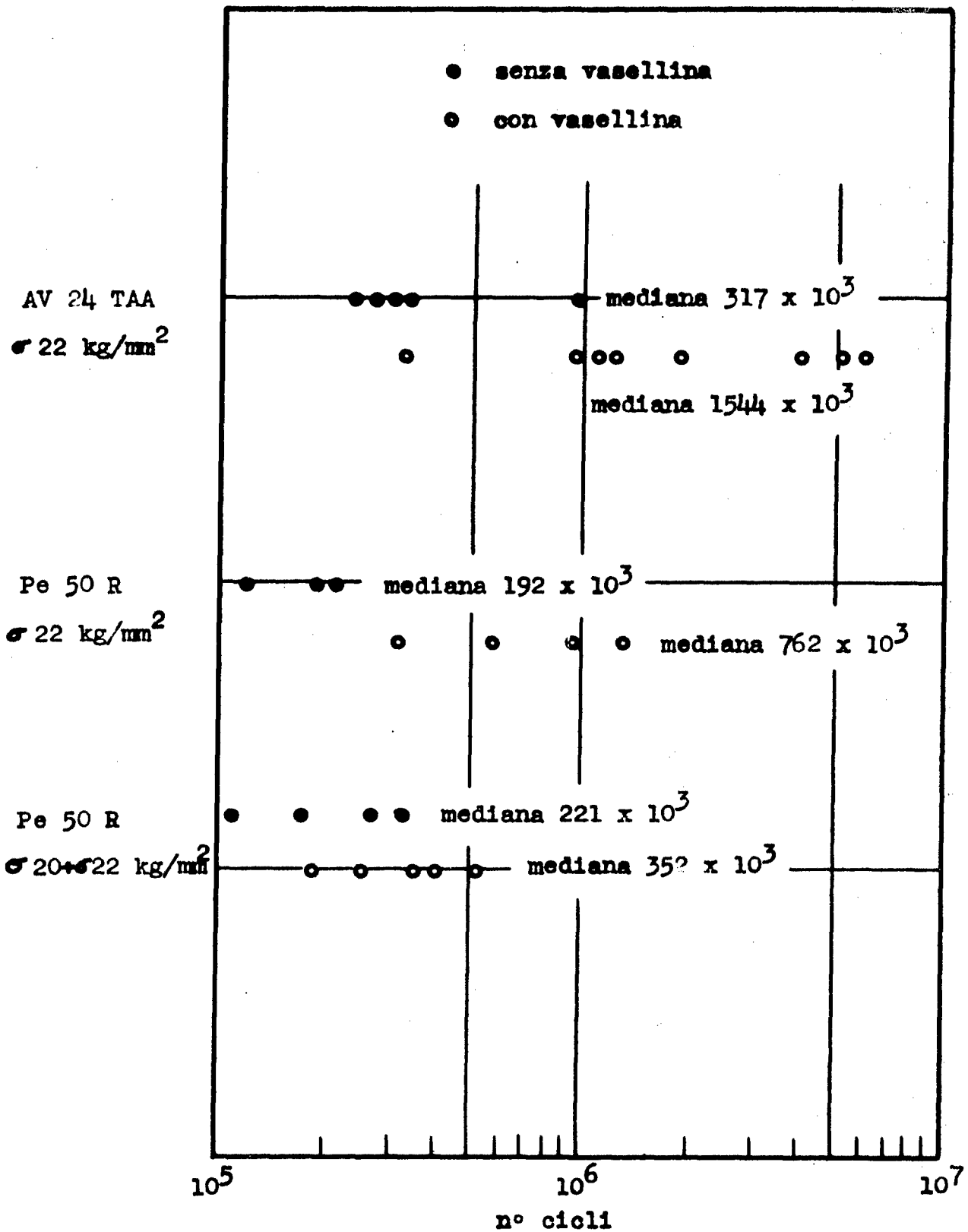


Fig. 14 Fatigue behaviour of aluminium alloy specimens protected and unprotected by Vaseline

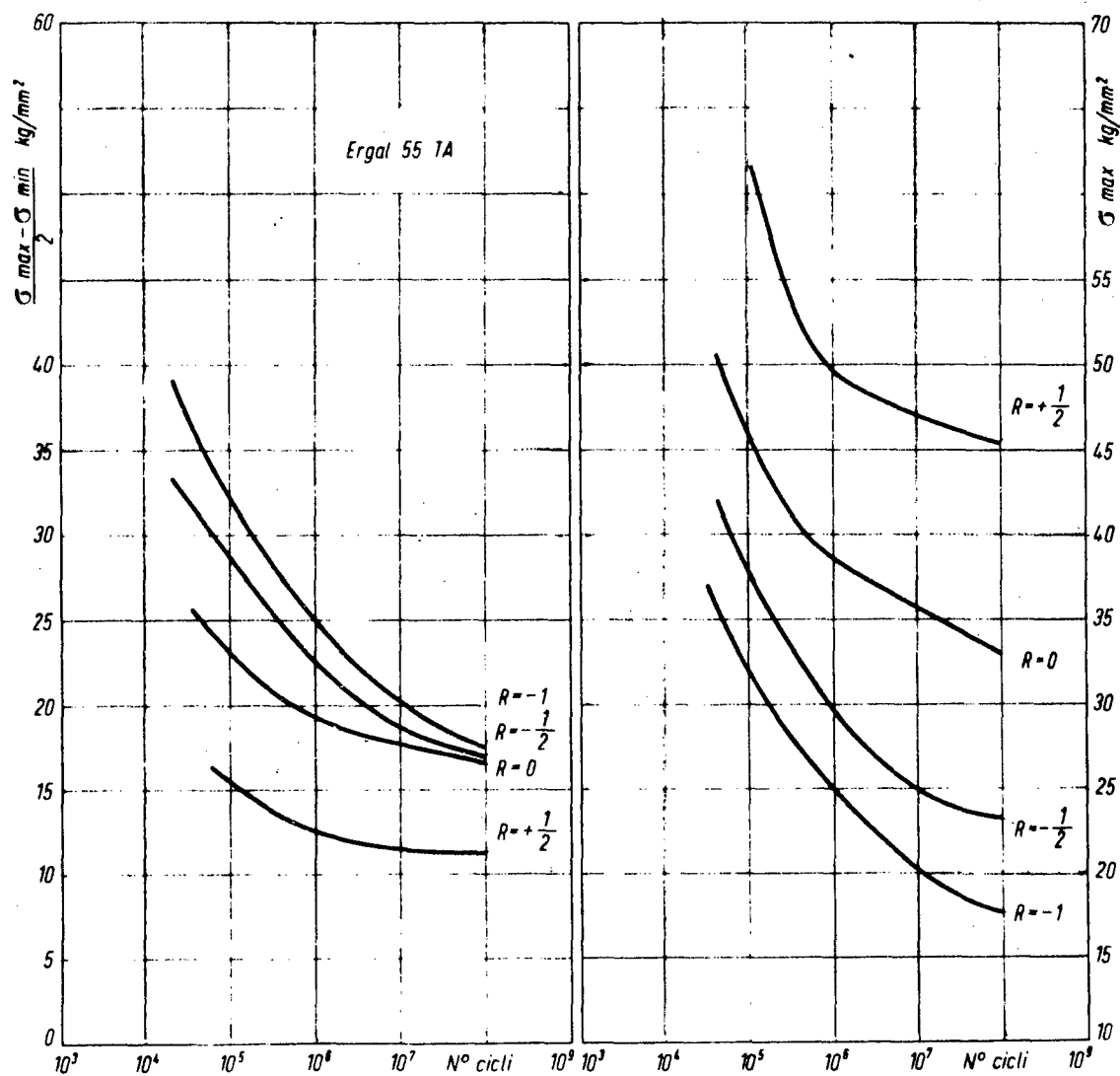


Fig. 15 S-N axial fatigue curves of Al-Zn 5.8-Cu-Mg alloy.

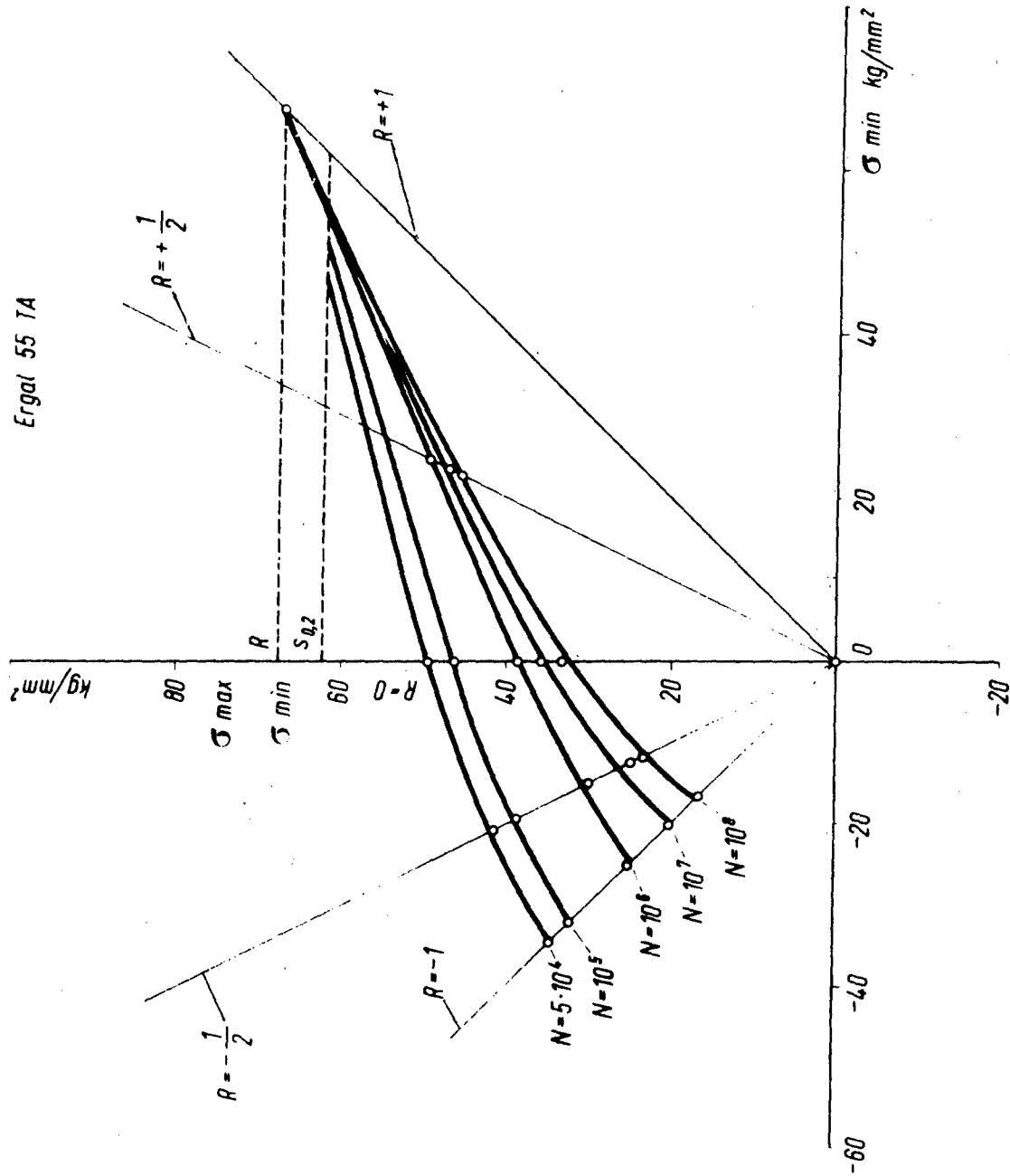


Fig. 16 Rös-Goodman diagram of Al-Zn 5.8-Cu-Mg alloy.

ISML 7 FATIGUE TESTS OF Al-Cu 6-Mn-Zr-V ALLOY AT HIGH TEMPERATURES

The tests were carried out in rotating bending machines at 3,000 r.p.m. at the following temperatures: 20°C; 150°C; 200°C and 250°C.

The fatigue properties at high temperatures appeared very satisfying (Figs. 17 and 18); considering both the absolute values and the ratio between static and dynamic characteristics.

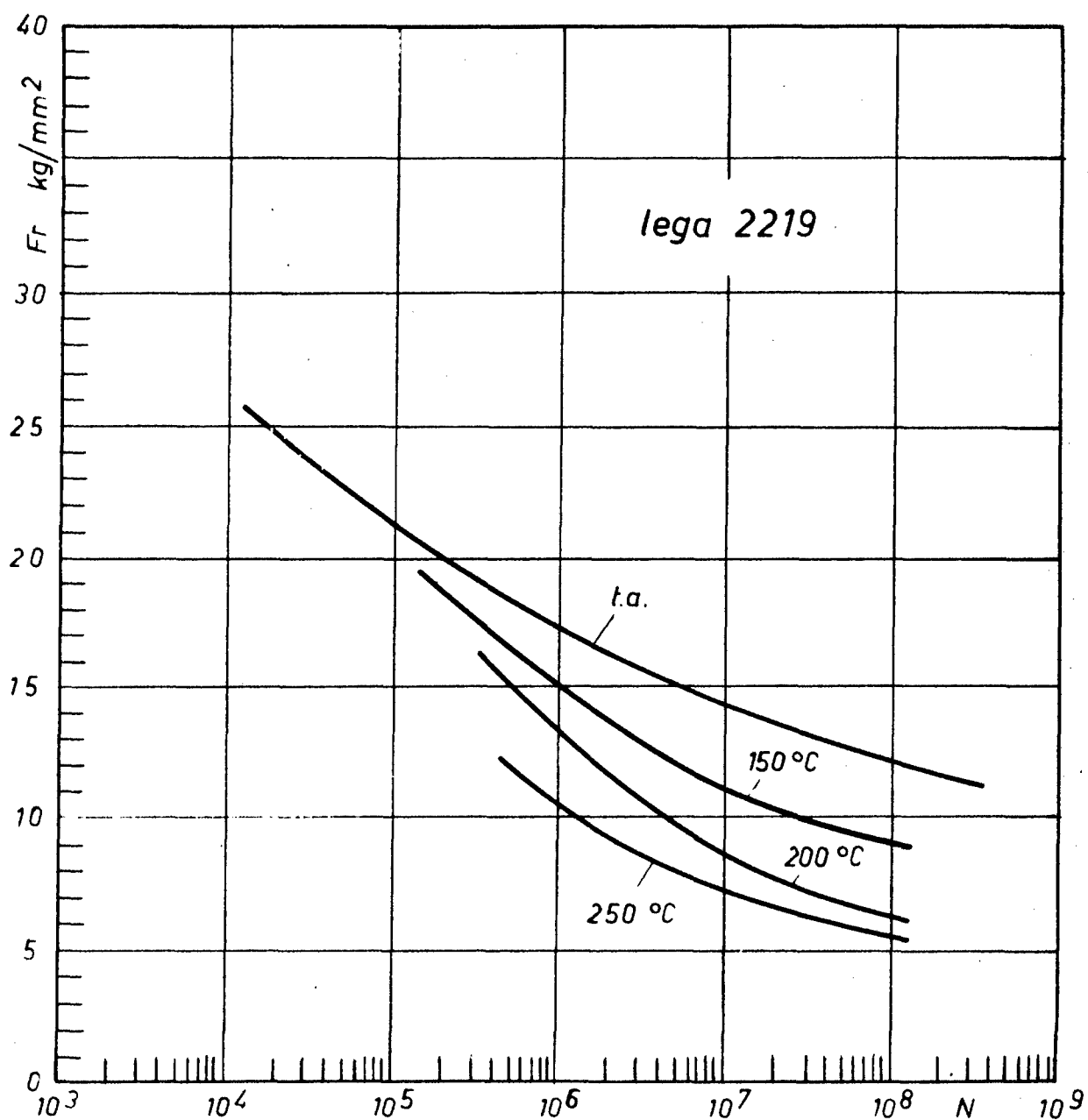


Fig. 17 S-N curves of Al-Cu 6-Mn-Zr-V alloy at different temperatures.

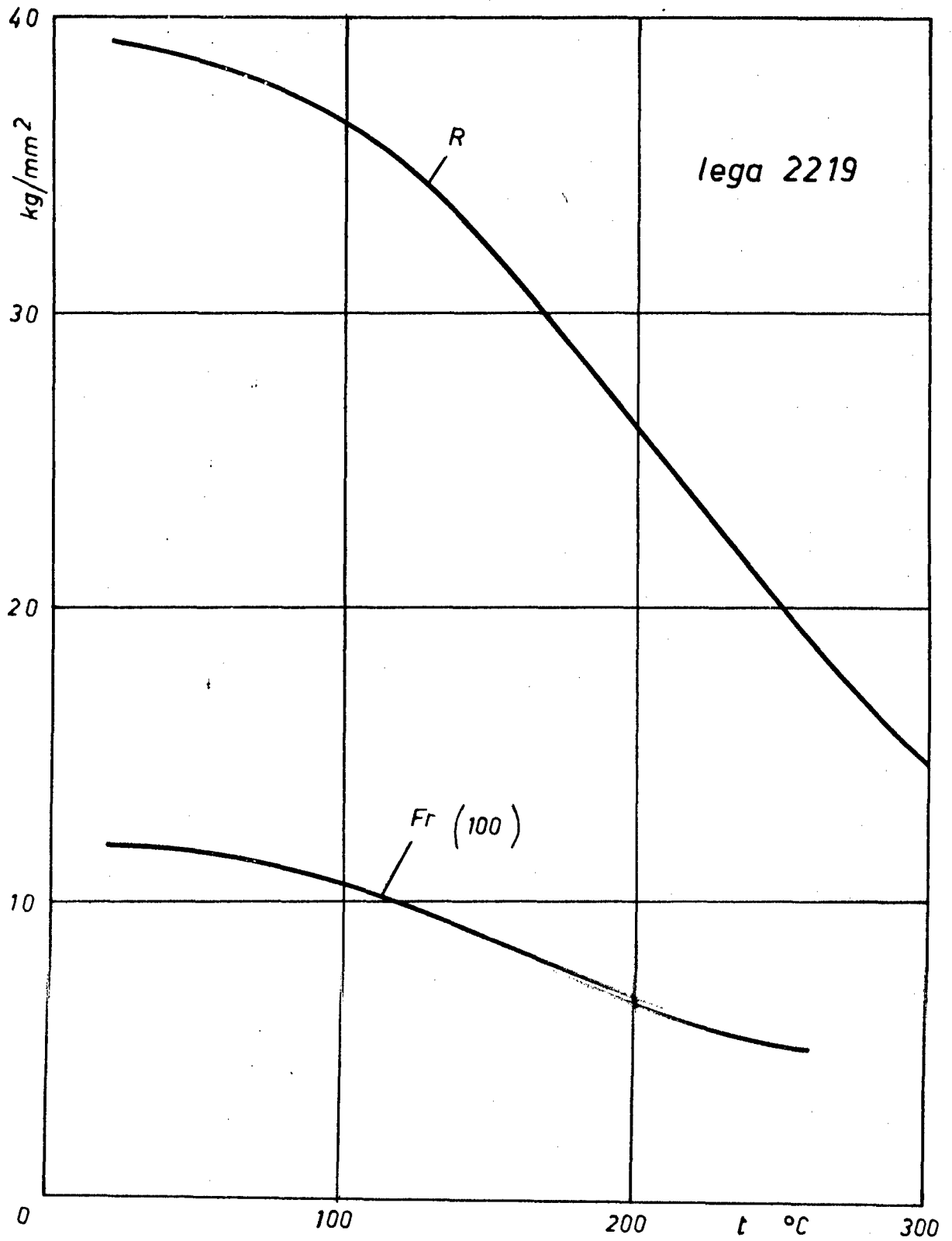


Fig. 18 Variations of static and dynamic characteristics at different temperatures.

APPENDIX 3 - REPORT ON FIAT ACTIVITIES IN THE
FATIGUE FIELD 1965 - 1967

FIAT activity in the fatigue field in the last two years has been devoted to the development of basic research, structural design development testing and short term research.

This activity can be summarised as follows :

AUTOMOTIVE - AERONAUTICAL RESEARCH LABORATORY (L. R. C. A. A.)

FIAT 1 BASIC RESEARCH ON FATIGUE

The Istituto Elettrotecnico G. Ferraris is conducting, under a FIAT contract, a study on the relationship between ageing and fatigue strength of a light alloy. Some structural evolution phenomena capable of changing the material strength if the ageing is continued beyond the optimum point, especially at temperatures greater than the room temperature, may be experienced in light alloys in which the mechanical properties are obtained by ageing. The RR 58 alloy, which is suitable for use in the hot conditions, is being considered and studied under various ageing conditions and with temperature ranges up to 270°C.

So far it has been found that this alloy shows a slight reduction (5%) of the fatigue limit at 200°C.

FIAT 2 CUMULATIVE DAMAGE

During the fatigue tests, on smooth and notched specimens under alternating and pulsating cycles, a comparison between the results obtained from the tests in the constant and programmed load cases

has been made using the data from the Laboratorium für Betriebsfestigkeit of Darmstadt for light alloys (2024) and from FIAT-L.R.C.A.A. for steel (38 NCD4).

The analysis of all the data obtained led to the conclusion that it is possible to estimate with a good approximation the results of a long programmed load test from a quicker conventional constant load test.

The correlation applies for an extended range of time regardless of the specimen shape. However, it is affected by the preload imposed during the test and, therefore, it is not possible to obtain a single correlation curve valid for alternating and pulsating cycle tests.

For the L.R.C.A.A. tests a new Schenck pulsator (6 tons) with load programme on punched tape has been used.

FIAT 3 FATIGUE-GAGES

A special type of fatigue gage (SN Fatigue Life Gage from Micro Measurements U.S.A.) has been experimented. This fatigue-gage should reveal, through resistance variations, the fatigue condition of the part to which it has been bonded, taking cumulatively into account the magnitudes of strains and number of cycles. The first results appear to be satisfactory with some limitations relative to the specimen shape (unnotched), cycle type (alternating) and sensitivity threshold ($\pm 8 \text{ Kg/mm}^2$ for light alloys and $\pm 25 \text{ Kg/mm}^2$ for steels).

At the same time some monitoring gages having a pre-established breaking section are being developed; they are made from aluminium sheet 0.1 mm thick, bonded

to 2024 specimens, fatigue tested under tension and bending loads, and are capable of operating like fatigue gages.

FIAT 4 FATIGUE STRENGTH OF SPECIMENS HAVING A SHARP EDGED CROSS-SECTION

The effect of edge sharpness on fatigue strength has been checked with a series of tests carried out on specimens having circular, rhombus and rhomboidal cross-sections. It has been found that the reduction of the fatigue limit, on steel specimens having very sharp edges, is 10% only.

FIAT 5 FATIGUE TESTS ON 7075 ALLOY AND NOTCH EFFECT

It is claimed that the 7075 light alloys, when subjected to fatigue tests, are more sensitive than 2024 alloys to the notch effect and have a higher rate of crack propagation.

In order to verify this assertion for Italian alloys, rotating bending tests are being conducted on PAZ 5.8 alloy (7075) in the range of 10^4 to 10^7 , on smooth and notched ($K \sim 3$) large diameter specimens (25 mm).

FIAT 6 SPOT-WELDED AND SEAM-WELDED JOINTS IN LIGHT ALLOY SHEETS

A comprehensive fatigue test programme of joints in light-alloy sheets, after having considered the welding from the point of view of the weld spots geometry, now takes into account the metallurgical aspects of the problem by tests on spot-welds and seam-welds having different penetration depths, on metal sheets of various thicknesses.

FIAT 7 FATIGUE TESTS ON BLADES IN THE HOT CONDITION

Fatigue tests carried out on light alloy blades (RR 58) have shown a reduction of the fatigue limit in the hot condition (155°C).

It was questioned (ICAF-AGARD Meeting in 1963) if this reduction had to be ascribed only to the direct effect of the test temperature or also to an in-direct effect due to the elimination of favourable superficial stresses during the ensuing machining operation. A series of further tests, conducted at different temperatures, on blades which had been annealed before being subjected to the fatigue stresses, showed that the second hypothesis is not true and that the reduction of the fatigue limit in the hot conditions is to be attributed to the direct effect of temperature only.

FIAT 8 HONEYCOMB STRUCTURE TESTING

Static and fatigue tests under torsion have been carried out on light alloy honeycomb panels, for which but a poor bibliography is available.

It has been found that the orientation of the honeycomb cells is very important (50% increase in the strength in the most favourable orientation as compared with the less favourable one).

Moreover, as regards the fatigue, the Miner's law on cumulative damage appears to be applicable.

FIAT 9 TESTS ON HEAT SHIELD STRUCTURAL PARTS

It is pointed out, although not in the field of fatigue, that particular tests have been carried out for heat shields (designed and built by FIAT) for ELDO A vehicle.

Some aspects of the separation of the heat shield from the 3rd stage have been studied through tests carried out on specimens simulating the base ring and its housing together with the junction line of shields, in order to have information about a possible stick-up due to self-adhesion or bonding phenomena of the parts subjected to a mutual compressive action (30 Kg/cm), in vacuum surroundings (10^{-5} mm Hg) and with a temperature up to 425°C. The test results have been satisfactory as no self-adhesion or bonding phenomena have been experienced under the specified operating conditions.

Other tests on sandwich honeycomb panels (glass fiber and phenolic resin) under extreme environmental conditions (2 mm Hg, 700°C) have been carried out to demonstrate the satisfactory behaviour of the structure.

AIRCRAFT EXPERIMENTAL LABORATORY

FIAT 10 In addition to the fatigue and residual strength tests carried out on structural details during the development of the G 91 Y, G222 and VAK 191 B projects, a short term research has been carried out on the fatigue strength of specimens cut in the three directions from 7075-T6 very thick prestressed plates and on the influence of chemical milling of various surface roughness.

FIAT 11 As for the full-scale tests, a preliminary fatigue test of the wing structure of the two engined G91 Y, successor of the G 91, is being prepared. This will be followed by a test on the wing-fuselage-empennage unit that will be carried out at three level loading blocks with the typical spectrum, already used for the G 91. It is pointed

out that this spectrum has been confirmed by the results obtained from the early production air-planes operated by the Italian Air Force: on five of these air-planes a typical crack, already observed during the full-scale fatigue tests, occurred with a 10% delay and a dispersion of $\pm 10\%$.

As for the tests on the ELDO heat shields, although not in the fatigue field, comprehensive tests have been developed to ascertain the influences of the polymerization of the phenolic laminates; mechanical and thermo-physical tests were performed. The bending of sandwich type structures has been widely tested under heat and load conditions. Finally, full-scale tests of the heat shields namely loading tests, heating (infra-red) test up to 900°K , combined heating and loading test and separation test, have been carried out.

Bibliography

Only the work on the fatigue-gages has been divulged outside :

- G. Bollani, "Functionality and possibility of using the cumulative damage fatigue-gages".

This Report was presented at the "Giornata dell' Estensimetria" - Turin, October 1966.

APPENDIX 4 - PIAGGIO ACTIVITY IN THE AERONAUTICAL
FATIGUE FIELD (years 1965 + 1967)

During the last two years, Piaggio activity in the aeronautical fatigue field has covered both testing and theoretical research.

PIA 1 Tests have been carried out mainly for the purpose of certification of the model PD-808 executive aircraft. Although its basic structure has been designed to be fail-safe, some areas such as pilot cockpit and engine mount have been fatigue tested to meet safe-life requirements.

The pilot cockpit has been tested in a water tank under the cyclic pressure load of 10 psi; derived by taking into account, in a conservative manner, cabin pressurization, aerodynamic suction and flight loads.

The engine mount has been tested under flight and ground loads in the Losenhausenwerk apparatus of the University of Pisa. Fatigue gages have been installed on the specimen in order to find residual fatigue life.

Regarding fail-safe strength of the model PD-808 aircraft, analysis and tests intended to demonstrate the ability of the airplane to withstand prescribed loads when fatigue failure occurs, are presented in a paper to be given at the 5th ICAF Symposium.

PIA 2 In the theoretical field, a computer program for the evaluation of the fatigue life of composite structures is now under way, together with an up-to-date library of the fatigue strength allowances for various structural elements.

Experimental correlation data will be provided by the planned fatigue testing of the P.166 aircraft wing and main landing gear.

Fatigue meter readings taken in P.166 aircraft operating in Australia under the MacRobertson-Miller Airlines will provide a good basis for these tests.

APPENDIX 5 - ACTIVITY OF THE SOCIETA' AERONAUTICA MACCHI
IN THE FIELD OF AERONAUTICAL FATIGUE DURING
THE PERIOD 1965/1967

MC 1 During the first part of this period the fatigue test of the full-scale structure of the Aircraft MB 326 was completed. During that test the behaviour of the structure versus the time was investigated under the combined action of aerodynamic, inertia and pressurization loads.

The applied loadings simulated 35,000 flying hours with 140,000 loadings and 280,000 complete pressurization cycles. The structural component with the highest fatigue sensitivity withstood not less than 15,000 flying hours.

MC 2 The test will possibly be renewed on the airframe of the derived prototype MB 326 G, which has an increased take-off weight, a higher thrust and some structural modifications.

N 69-21589

A REVIEW OF FRENCH WORK ON FATIGUE

FOR THE PERIOD 1964 - 1966

Compiled by

W. Barrois

Service Technique Aeronautique

Paris

CONTENTS

A.	<u>WORK AT THE "CENTRE D'ESSAIS AERONAUTIQUE DE TOULOUSE"</u>	342
A.1	SPECIFICATIONS OF CURRENT TESTS FOR CHARACTERIZATION OF METALS	342
A. 1. 1	- The development of thermal treatments	342
A. 1. 2	- Preliminary tests	342
A. 1. 3	- Fatigue tests (carried out by C.E.A.T.)	343
A. 1. 4	- Creep tests	344
A. 1. 5	- Toughness fracture tests on square bar specimens with fatigue crack	344
A. 1. 6	- Stress embrittlement tests	344
A. 1. 7	- Physic - chemical tests	344
A. 2	TOUGHNESS BENDING TESTS ON SQUARE BAR SPECIMENTS	345
A. 2. 1	- Interpretation of results	345
A. 2. 2	- Results on aluminium alloys	348
A. 2. 3	- Magnesium alloys	351
A. 2. 4	- Low alloy steels	351
A. 2. 5	- Precipitation hardening steels	359
A. 2. 6	- T-A6V titanium alloy	359
A. 3	FATIGUE TESTS ON SMOOTH AND NOTCHED SPECIMENS	360
A. 3. 1	- Aluminium alloys	360
A. 3. 2	- Artificial aging effect on fatigue strength of A-U4G1 aluminium alloy	365
A. 3. 3	- Effect of rounding sharp edges on the fatigue strength of the A-U4SG plates	365
A. 3. 4	- Fatigue tests at room and elevated temperatures on bars of T-A6V titanium alloy	367
A. 3. 5	- Fatigue tests on fiber glass-polyester panels	367
B.	<u>MISCELLANEOUS TESTS</u>	371
B. 1	TESTS BY AIRCRAFT MANUFACTURERS	371
B. 1. 1	- Fatigue behaviour of steel bushes cold-glued into aluminium alloy components	371
B. 1. 2	- Fatigue crack propagation in outer skin of a honeycomb sandwich fuselage	372
B. 2	O.E.C.D. WORK ON FATIGUE DAMAGE	376
	<u>REFERENCES</u>	378

A. WORK AT THE "CENTRE D'ESSAIS AERONAUTIQUE DE TOULOUSE"

The C.E.A.T. (formerly, E.A.T.) is carrying out tests on smooth and notched small specimens to define and characterize each use-condition of a metal or to study the effect of a manufacturing process. Other studies are carried out on joints and fittings on request of aircraft manufacturer to check particular points ; their description would be both difficult and incomplete so that I will not, in general, refer to them. Some certification tests are in progress on airframes and sub assemblies but these are not sufficiently complete to sustain a report. Some partial results will be mentioned by other authors during the I.C.A.F. Symposium. Here, I will restrict myself to works of the C.E.A.T. laboratory of materials reporting data provided by the laboratory's chief, Mr AUVINET.

A. 1 - SPECIFICATIONS OF CURRENT TESTS FOR CHARACTERIZATION OF METALS

The "Service Technique Aéronautique" (Materials section) and the C.E.A.T. have gradually worked out a program of systematic testing for metal characterization, which is preliminary to the fuller studies required before metal can be employed in mechanical engineering applications. It appears useful to give a full account of this program.

A. 1. 1 - The developement of thermal treatments

The metal manufacturer often points out the best treatment conditions but, sometimes, the C.E.A.T. studies some variants itself.

A. 1. 2 - Preliminary tests

These are carried out on all metals which must be fully studied, with the object of avoiding a loss of time on bad quality lots ; they include :

- i) macrographs : carried out on all elements of the lot (bars, sheets, ...) in the worked, large transverse and, if possible, short transverse directions.
- ii) Chemical analyses : several analyses are done for certain steels and some titanium alloys by lot ; absorbed gases are measured.
- iii) check of thermal treatment : the treatment recommended by the manufacturer is checked by carrying out tension, impact and hardness tests, micrographs, above and below recommended temperatures. Sometimes thermal expansion is measured.
- iv) measurements of mechanical strength properties : using two to ten specimens, they include the yield stresses $\sigma_{.05}$, $\sigma_{.1}$, $\sigma_{.2}$, for permanent strains .05 % , .1 % , .2 % , also the nominal ultimate tensile strength, σ_{ult} , the true fracture tensile strength σ_u^* , fracture elongation, A % , and the fracture reduction of area, Σ % . The proportionality limit stress, σ_p , is estimated.

Impact tests are sometimes executed on notched UF specimens.

A. 1. 3 - Fatigue tests (carried out by C.E.A.T.)

- a) Bars : for each level of tensile strength dependent upon thermal treatment, seven series of thirty specimens are used :

Tension - compression tests with notch factors, $K_t = 1.035$,

1.7, 3.3, and the mean stresses $\sigma_m = 0$ and $.5 \sigma_{ult}$, i.e.,

six specimen series, each including a static tensile test.

Rotation bending, that is, a test series in four - point loading with toric specimens.

The thirty specimens of each series are used to plot a mean

$\sigma - N$ curve between one and 3×10^7 cycles (twenty specimens)

and to determine the fatigue limit at 3×10^7 cycles (ten specimens).

- b) Thick plates : The same tests as for bars are carried out in longitudinal and large transverse directions ; in some cases only the large transverse is tested.

- c) Thin sheets : In place of $\sigma_m = 0$, fatigue tests are carried out in reversed tension, with $\sigma_m = \sigma_a$.
- d) Hot tests : Hot fatigue tests are carried out as room temperature tests ; however, two notch factors, $K_t = 1.035$ and 3.3 , and two loading patterns, $\sigma_m = 0$ and $\sigma_m = .5 \sigma_{ult.}$, only are used for each temperature.

NOTE : Some more extensive studies include the values :

$$K_t = 1.035 ; 1.7 ; 2.3 ; 3.3 ; 5 ;$$

$$\sigma_m = 0 ; .25\sigma_{ult.}; .5\sigma_{ult.}; -.25\sigma_{ult.}; -.5\sigma_{ult.}.$$

- A. 1. 4 - Creep tests. They are sometimes carried out in other laboratories on all metals used to be employed in aircraft, engines or rockets.
- A. 1. 5 - Toughness fracture tests on square bar specimens with fatigue crack.
- a) Bars : Tests about which I shall speak about later are carried out by C.E.A.T. on series of 15 to 30 square bar specimens of 20 x 20 x 150 mm in size.
In addition to these tests, impact tests are also carried out on IZOD specimens where the groove - notches were deepened by fatigue cracks. These tests are carried out on MANLABS machines using notched square bar specimens of 10 x 10 mm cross section.
- b) Thick plates : The same preceeding tests are carried out in longitudinal and large transverse directions with, if possible, the MANLABS program in short transverse.
- A. 1. 6 - Stress embrittlement tests. Carried out for titanium alloys and certain steels, in study of absorbed hydrogen effect as might occur, for instance, when cadmium coating is used.
- A. 1. 7 - Physic - chemical tests. They are :
- a) corrosion and stress-corrosion tests in several environments (salt water, elevated temperatures, ...).
- b) the protection method studies ; related to corrosion tests, the object of these studies is to define protection methods for each metal ; they include different tests such as, for instance, fatigue or stress embrittlement tests.

Note on manufacturing of specimens.

The manufacturing of specimens involves the following stages :

- cutting out
- rough machining
- thermal intermediate treatment
- intermediate machining
- prescribed thermal treatment
- final machining
- stress relief treatment, if necessary.

In all cases, each series of fatigue, toughness or creep specimens is machined and treated with three tensile specimens and three impact specimens.

A. 2 - TOUGHNESS BENDING TESTS ON SQUARE BAR SPECIMENS.

The full results of the numerous C.E.A.T. tests cannot be reported here. The analysis by the IRWIN method is in progress but final results are not yet available. I will present a digest of results interpreted by approximate method given in my paper MÜNCHEN Symposium of I.C.A.F., in 1965.

A. 2. 1 - Interpretation of results.

The principal features of the tests are : on square bars, 20 x 20 x 150 mm in size, a mark is made by means of an electric pencil, in the middle of a side surface. Then, a fatigue crack is developed from the crater-mark by reversed fatigue bending under electro-mechanical pulsed loading applied by a roll on the opposed side at the centre between the two supporting rolls, 120 mm apart. The static fracture is obtained with the same apparatus for several fatigue crack sizes.

During the fatigue crack developement and in the course of interspersed unloadings, the ratio, $M = \Delta P / \Delta f$, of the load variation to the deflection variation is measured ; the curve of M against the apparent sizes of cracks, plotted through experimental points, gives values of M for fractured specimens where each cracked area A of the cross-section is measured ; thus, it is possible to plot a mean curve⁽¹⁾

$$M = F (A).$$

By approximate derivation, it is obtained

$$G_c = \frac{1}{2} P^2 \frac{\partial \left(\frac{1}{M} \right)}{\partial A},$$

where G_c is the IRWIN parameter. In cases where this result is known, we have used the notation G_c "true" in tables of results.

We use an approximate method ⁽²⁾ with which there is only need to know the fracture load P and the superficial apparent length of crack at failure, $2a$.

The corresponding value of G_c correlates well with the former one : the deviations are smaller than the fracture load scatter effects or than the effects of crack size measurement errors.

We have using now, the notations

P = fracture load of the cracked bar,

$P_{ult.}$ = static failure load of the virgin bar,

$P_T = 44.4 \sigma_{ult.}$ = theoretical failure load of uncracked bar under the assumption of full elasticity.
 P_T is in daN if $\sigma_{ult.}$ is in daN/mm².

The plasticity effect in bending cannot give $P_{ult.} > 1.5 P_T$;

however, the ultimate bending strength is larger than the ultimate tensile strength because necking is partially prevented ; moreover, a part of the loading is balanced by the friction of the supporting rolls. The P/P_T ratio is larger than 1.6 in

aluminium alloys and 1.8 in steel and T - A6V titanium alloy.

With the P/P_T ratio as ordinate and $-\sqrt{2a/h}$ as abscissa,

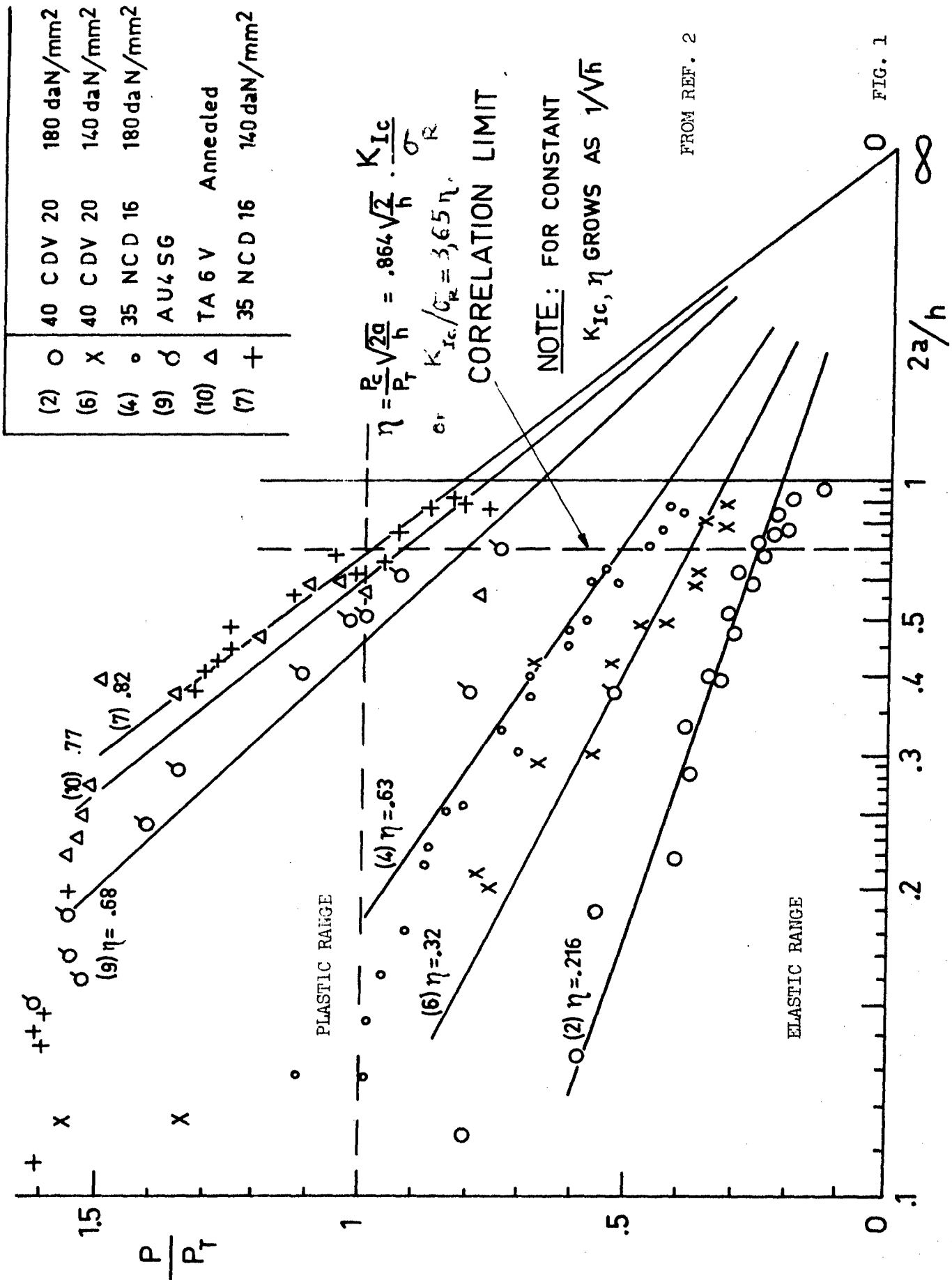
where $2a$ is the apparent crack length and $h = 20$ mm the width of the bar, figure 1 represents the relationship

$$\eta = \frac{P}{P_T} \sqrt{2a/h}$$

by a straight line plotted from the point 0 through test points corresponding to early results ⁽²⁾ :

$E G_c$ is computed from

$$E G_c = 10 \left(\frac{\eta \sigma_{ult.}}{.864} \right)^2,$$



where σ_{ult} is the ultimate tensile strength. Then, K_c is

obtained from $K_c = \sqrt{E G_c}$. K_c is also equal to $\frac{P \sqrt{a}}{39.2} \text{ daN/mm}^{3/2}$,

Remembering that 1 daN = 1.02 kg-weight = 2.25 lb ;
1 daN/mm² = 1.02 kg-weight per mm² = 1460 lb/in². In place
of daN/mm², the identical unity "hectobar", noted hbar is
sometimes used : 1 hbar = 1 daN/mm².

K_c represents the absolute residual static strength while η

represents the relative strength in terms of nominal theoretical
strength which is used in computations which do not account
of plasticity effects: $\eta = \frac{\sigma_{th}}{\sigma_{ult}}$.

If d is the specific weight, the strength to weight ratio
will be proportional to K_c/d .

The tables of results also include the relative dispersion
measured by the coefficient of variation, V , of η and K_c ,

defined as the ratio of the standard deviation to the median
value. In order to estimate V , it was supposed that deviations
of η from the median value are due to scatter ; the standard

deviation was estimated from the difference of quartiles. This
coarse estimate permits us only to say η is constant in

practice with $V \leq .05$. With larger values of V , we don't

known if the scatter is the only cause of the failure of the
assumption $\eta = \text{constant}$.

A. 2. 2 - Results on aluminium alloys.

The compositions and treatments of the studied alloys are given
in table A. 2. 2a. The table A. 2. 2b shows results of tensile,
impact and toughness fracture tests. With regard to 2014 and
A-U4SG specimens of near compositions, the correlations of K_c

and G_c with tensile properties are made only for area

reduction, $\Sigma \%$, and impact fracture energy, K_{UF} . However,

the reduction of area cannot permit comparison of A-U4SG with
A-U2GN, whereas $K_c - K_{UF}$ correlation is preserved for both
alloys.

There is a point of view, still accepted by certain metallurgists,

TABLE A.2.2a - ALUMINIUM ALLOYS

N°	NAME	FORM	COMPOSITION, PER CENT							TREATMENT
			Cu	Si	Mg	Mn	Fe	Ti	Ni	
1	2014	SPAR CAP	4.6	.82	.28	.81	.64	.03		UNKNOWN
2	A-U4SG	"	4.2	1.18	.49	.87	.35	.03		
3	"	BAR	4.3	.83	.39	.84	.39	.09		T6 (16h, 160°C)
4	"	THICK PLATE	4.25	.80	.63	.85	.44	.12		T651
5	A-U26N	"	2.50	.20	1.65		.98	.08	1.20	T651(20h, 190°C)

TABLE A.2.2b - TENSILE PROPERTIES AND FRACTURE TOUGHNESS
OF ALUMINIUM ALLOYS.

I. TENSILE PROPERTIES.

N°	NAME	VALUES IN daN/mm ²						E	A%	Σ%
		σ_p	$\sigma_{.05}$	$\sigma_{.1}$	$\sigma_{.2}$	σ_{ult}	σ_u^*			
1	2014	41.2	56.4	57.2	57.6	60.6	71.4	6,900	10.2	17
2	A-U4SG	33.6	42.1	43.4	44.4	49.5	58.1	7,300	9.8	18.2
3	" BARS	40	49	50	51	56	67.5	7,230	11.3	26
4	" SHEET, LONG	36.6	44.6	45.8	46.4	50.4	60.5	7,260	8.5	20.6
4	" " TRANSVERSE	34.7	42.6	44.2	45.2	49.5	56.3	7,350	7.6	13.4
5	A-U2GN, LONG	31.3	38.1	39	39.6	43.2	50.7	7,020	7.8	24.1
5	" TRANSVERSE	27.9	35.2	36.9	38.3	43.2	50.1	7,340	6.2	19.4

II. IMPACT AND FRACTURE PROPERTIES.

N°	K_{UF} J/cm ²	G_c^{TRUE} daN/mm	η	V	ESTIMATED		$\frac{P_{ult}}{P_T}$	$\frac{\sigma_u^*}{\sigma_{ult}}$	$\frac{\sigma_{ult}}{\sigma_{.2}}$
					K_c daN/3/2 mm ^{3/2}	G_c daN/mm			
1	6.5		.58	.09	130	2.44	>1.67	1.18	1.05
2	8		.63	.02	135	2.5	>1.5	1.18	1.12
3	13.2	4	.84	.05	175	4.2	>1.7	1.20	1.10
4	8.7	2	.71	.05	132	2.4	>1.6	1.20	1.09
4	3.9	1.4	.58	.07	106	1.54	>1.5	1.14	1.10
5	6	1.9	.78	.03	122	2.1	>1.7	1.17	1.09
5	5	1.3	.68	.05	109	1.6	>1.6	1.16	1.12

that a $\sigma_{ult.}/\sigma_y$ ratio near unity means brittleness. The table A. 2. 2b shows no such correlation of $\sigma_{ult.}/\sigma_y$ with K_c or K_{UF} .

A. 2. 3 - Magnesium alloys.

The studied alloys had the compositions, in per cent :
G-A 9 : 8.36 Al ; .62 Zn ; .31 Mn ; .20 Si ; .009 Fe ;
remainder Mg.

MSR : 2.25 Ag ; .56Zr ; .044 Fe ; remainder Mg.

The tensile and fracture toughness properties are given in table A. 2. 3. With regard the two treatments of G-A9 alloy, there is again no correlation between K_c and K_{UF} or K_c and $\sigma_{ult.}/\sigma_y$.

A. 2. 4 - Low alloy steels.

Their compositions are given in the table A. 2. 4a. The table A. 2. 4b gives some details of the treatments of specimens. The pre-treatments of bars by the supplier, or on specimens by C.E.A.T., are sometimes unknown or too complicated to be reported. The table A. 2. 4c gives the mechanical and fracture properties for the studied steels. The large values of η

indicate a good safety margin for fatigue cracked components. We obtain .97 and .95 in 25 CD4S and 15 CDV6 steels, which give few difficulties in service use, just as a 35 NCD16 steel treated for $\sigma_{ult} = 140 \text{ daN/mm}^2$ (200,000 lb/in²) and quoted in reference 2 ($A\% = 10$, $\eta = .82$, $K_c = 420 \text{ daN/mm}^{3/2}$).

With strengths $\sigma_{ult.}$ of 180 to 200 daN/mm² (260,000 to

290,000 lb/in²), the 35 NCD16 steel tempered at 220° C shows better toughness at room temperature than the 40 CDV20 steel tempered between 550° C and 580° C (this steel can serve at higher use temperatures). The vacuum second-melting improves, to a slight extent, the 35 NCD16 steel treated for 180 daN/mm² (+ 10 %) and for 195 daN/mm² (+ 20 %) whereas refrigeration before tempering gives no change (see 4K,2D and 4K,F2D).

As previously, there is no correlation between brittleness and the $\sigma_{ult.}/\sigma_y$ ratio. In the same order, for the 35 NCD16

steel, there is no correlation between K_c and K_{UF} or $A\%$,

$\Sigma\%$; this stresses the necessity of carrying out tests to obtain K_c to characterize the fatigue crack brittleness of

a metal. Figure 2 shows some fracture areas.

TABLE A.2.4a - COMPOSITIONS OF LOW ALLOY STEELS.

N°	NAME	FORM	C.E.A.T. REF. ORIGIN	2 TH MELTING	COMPOSITION, PER CENT									
					C	Cr	Ni	Mo	Mn	V	Si	S	P	
1	25CD4S	BARS $\phi 30$ mm	5C, FRANCE	AIR	.20	.99	.11	.20	.61			.047		
2	15CDV6	"	5D(VASCOJET, U.S. 90)	AIR	.16	1.28		.84	.74	.22		.10		
3	4340	"	4E, U.S.	AIR	.41	.82	1.67	.24	.66			.28		
4	35NCD16	"	4K, FRANCE	AIR	.39	1.56	3.80	.45	.35			.23		
5	"	"	5E "	VACUUM	.40	1.85	4.02	.45	.47			.28		
6a	"	BLOCKS	19298, FRANCE	AIR	.39	1.96	4.17	.47	.60			.36	.004	.009
6b	"	"	" "	VACUUM	.40	1.95	4.12	.45	.43			.30	.002	.004
7	40CDV20	BARS $\phi 30$ mm	9E, VASCOJET 1000, U.S.	AIR	.40	5	.24	1.21	.36	.40		.84	.004	
8	"	"	3C, FRANCE	AIR	.44	5.3		1.3	.26	.51		.92		
9	40NDV18	BARS $\phi 35$ mm	4M, FRANCE	AIR	.51	.52	4.8	1.26	.23	.48		.37		

TABLE A.2.4b - TREATMENTS OF LOW ALLOY STEELS.

N°	NAME	C.E.A.T REFER.	PRE- TREATED	AUSTENIZED	QUENCHED	REFRIGERATED	TEMPERED	STOP
1	25CD4S	5C		AIR, 40', 870°C	OIL	NO	1h, 525°C	OIL
2	15CDV6	5D		AIR, 1h, 970°C	"	"	1h15', 650°C	"
3	4340	4E	YES	SALT, 40', 840°C	"	"	2h, 280°C	"
4	35NCD16	4K, 2D	YES	SALT, 30', 875°C	AIR	"	1h, 220°C	AIR
	"	4K, F2D	"	"	"	4h, -76°C	"	"
5	"	5E	"	"	"	-10°C, 4h -76°C	"	"
6a	"	19298	"	AIR 1h30', 875°C	"	4h, -80°C	8h, 220°C	"
6b	"	" , Z187	"	"	"	"	"	"
7a	40CDV20	9E	"	SALT, 15', 1010°C	"	NO	1h, 625°C	"
7b	"	9E, 14	"	"	"	"	1h+1h, 610°C	"
7c	"	9E, 18	"	"	"	"	1h, 575°C	"
7d	"	9E, 18	"	"	"	"	1h+1h, 580°C	"
7e	"	9E, 20	"	"	"	"	1h+1h, 550°C	"
Note : for 7b and 7e : double tempering before fatigue cracking, for 7d : one tempering before and after fatigue cracking.								
8a	40CDV20	3C	YES	SALT, 15', 1010°C	AIR	NO	1h+1h, 640°C	AIR
8b	"	3C	"	"	"	"	1h+1h, 590°C	"
9	40NDV18	4M	NO	AIR, 30', 875°C	"	"	1h, 350°C	"

TABLE A.2.4c - TENSILE AND FRACTURE PROPERTIES
OF LOW ALLOY STEELS.

N°	NAME	C.E.A.T. REFER.	VALUES IN daN/mm ²										A%	Σ%	K _{UF} J/cm ²	η	V	ESTIMATED		$\frac{P_{ult}}{P_T}$	$\frac{\sigma_u^*}{\sigma_{ult}}$	$\frac{\sigma_{ult}}{\sigma_{1.2}}$
			σ_p	$\sigma_{0.05}$	$\sigma_{0.2}$	σ_{ult}	σ_u^*	σ_{true}	K_c daN/ mm ^{3/2}	G_c daN/mm												
1	25CD4S	5C	80	90	95	97	107	175	19500	14	62	114	.97	.09	380	7.4	>1.8	1.64	1.10			
2	15CDV6	5D	78.5	97.5	101	104	110	206	20500	17	67.5	107.5	.97		390	7.7	2	1.82	1.06			
3	4340	4E	134	142	144	146	178	235	19500	11.2	42.5	17	.22	.03	145	1.08	1.85	1.32	1.21			
4a	35NCD16	4K, 2D	94.5	119	128	140	178	280	19600	12	50	50	.41	.05	272	3.8	1.86	1.57	1.28			
4b	"	4K, F2D	89.4	119.4	130	141	181	248	18500	10.7	41.5	49.5	.41	.05	272	3.8	1.88	1.38	1.28			
5	"	5E	100	124	132	144	182	256		12	45	50	.45	.10	306	5.1	1.88	1.40	1.27			
6a	"	19298				160	196			9	34	36	.44	.06	320	5.4			1.23			
6b	"	" Z187				161	194			12.3	40	70	.55	.06	395	8.2			1.21			
7a	40CDV20	9E, 140				140			18100				.48		257	3.6	1.8					
7b	"	9E, 14				144			"	11	44		.28		152	1.3						
7c	"	9E, 18				180			"				.17		113	.7	1.9					
7d	"	9E, 18	92	120	136	151	190	241	"	10	35		.21	.07	148	1.2		1.26	1.25			
7e	"	9E, 20	92	120	136	153	203	244	"	7.5	24.5		.16	.04	120	.8		1.20	1.34			
8a	"	3C, 140	117						20000	14		56	.95	.05	450	10.5						
8b	"	3C, 180	127						"	11		43	.22	.06	144	1.05						
9	40NDV18	4M, 180	130	150	157	162	181	200	"	7	26	34	.39	.06	258	3.3	1.82	1.10	1.12			

TABLE A.2.3. - TENSILE AND FRACTURE PROPERTIES
OF MAGNESIUM CASTINGS.

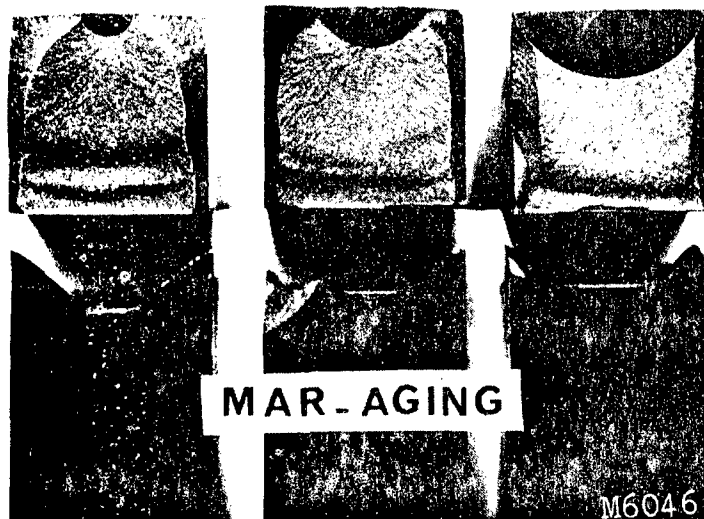
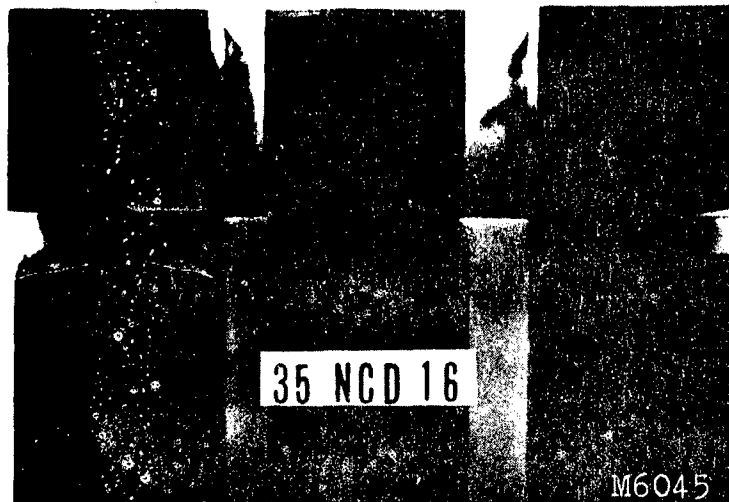
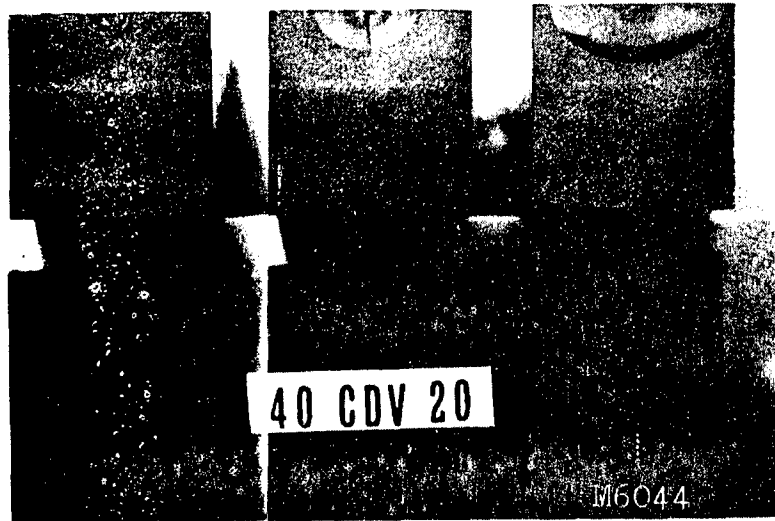
I. TENSILE PROPERTIES

NAME	VALUES IN daN/mm ²								
	σ_p	$\sigma_{.05}$	$\sigma_{.1}$	$\sigma_{.2}$	σ_{ult}	σ_u^*	E	A %	Σ %
G-A9-T	5.7	5.9	7.3	8.8	27.2	32.5	4,500	14.3	16.5
G-A9-TR	5.5	8.8	10.1	12.7	27.3	30	4,400	8.2	9
M S R	12.1	15	15.9	17.3	25.4	28.8	4,600	8.3	12

NOTE: σ_u^* is the true tensile strength; T and TR are two thermal treatment conditions.

II. FRACTURE PROPERTIES.

NAME	K_{Ic} J/cm ²	G_c True daN/mm	η	V	ESTIMATED		P_{ult} R_T	$\frac{\sigma_u^*}{\sigma_{ult}}$	$\frac{\sigma_{ult}}{\sigma_{.2}}$
					K_{Ic} daN ^{3/2} /mm	G_c daN/mm			
G-A9-T	4.8		.625	.03	63.5	.89	> 1.4	1.2	3.05
G-A9-TR	.4		.580	.09	58	.78	> 1.4	1.1	2.15
M S R	.65	.9	.625	.03	59	.75	> 1.35	1.14	1.48



SOME PATTERNS OF FRACTURE AFTER STATICAL FAILURE
OF FATIGUE CRACKED SPECIMENS

Fig. 2

TABLE A.2.5a - COMPOSITIONS OF PRECIPITATION
HARDENING STEELS.

No	NAME	C. & A. T. REFER.	FORM	2th	MEETING	C	Co	Mn	Mo	Al	Si	Ti	P
10 a			Bars	4P	AIR	.06	9.8	18.8	4.8	.12	.05	.06	
10 b			50 x 50 mm	4Q	VACUUM								
11	YN 18C		Bars	4J	AIR	.06	8.4	18.5	4.4	.30	.07	.72	
12	VASCOMAX 300N (U.S.)		"	2B	"	.03	9.1	18.3	4.7	.06	.09	.57	.006
13	"		"	4H	"	.07	9.1	18.7	4.4	.11	.05	.74	.004

No	C. & A. T. REFER	SOLUTION TREATING	QUENCHING	TEMPERING
10 a	4P	1 h, 820° C	AIR	3 h, 435° C
10 b	4Q	1 h, 820° C	"	"
11	4J	1 h 30, 870° C	"	4 h, 480° C
12	2B	1 h, 820° C	"	3 h, 480° C
13	4H	1 h 30, 670° C	"	4 h, 480° C

TABLE A.2.5a - TENSILE AND FRACTURE PROPERTIES
OF PRECIPITATION HARDENING STEELS.

		C.E.A.T.	VALUES IN dan/mm^2										ESTIMATED				*
REF.	NAME	σ_p	$\sigma_{.05}$	$\sigma_{.1}$	$\sigma_{.2}$	σ_{ult}	σ_u^*	$\Delta\%$	$\sum\%$	K_{IC}	η	V	L_0	G_0	Pult	σ_u	σ_{ult}
										$\frac{\text{J}}{\text{cm}^{3/2}}$			$\frac{\text{dan}}{\text{mm}}$	$\frac{\text{dan}}{\text{mm}^2}$			
10a	4 P	137	162	167	175	182	295	16600	8.7	41	30.5	26	175	1.86	1.83	1.63	1.04
10b	4 Q	148	165	174	180	188	300	17700	10.2	60	39.2	40	280	4.4	1.85	1.6	1.05
11	YN 18 C	4 J	116	146	160	167	175	232	17100	11.2	56	45	562	17.4	1.84	1.33	1.05
12	VASCOMAX 300	2 B	127	160	168	175	184	254	16500	9.5	54	46	500	15.4	> 1.8	1.38	1.05
13	"	4 H	141	160	167	173	184	237	16900	8.8	47	38	410	10	> 1.8	1.29	1.05

A. 2. 5 - Precipitation hardening steels.

The tables A. 2. 5a and A. 2. 5b give, respectively, the compositions and thermal treatments of the studied alloys. The mechanical and fracture properties are given in the table A. 2. 5c. It is noteworthy that, like usual steels, the "maraging" steels have a crack sensitivity dependent strongly upon treatment. With the french alloy YN18C, the safety even with fissuration is as good for 25 CD4S and 15 CDV6 steels tempered for 110 daN/mm², and for 40 CDV20 steel tempered for 130 daN/mm².

A. 2. 6 - T-A6V titanium alloy.

The composition was, in per cent :

6.3 Al ; 4.32 V ; .5Fe ; .04 C ; .18 N₂ ;

.057 H₂ ; .096 O₂ ; remainder Ti.

Treatment : annealed 1h in argon, air-cooled.

Tensile properties :

$\sigma_p = 68.7 \text{ daN/mm}^2$; $\sigma_{.05} = 96$; $\sigma_{.1} = 97.4$; $\sigma_{.2} = 98.2$;
 $\sigma_{ult.} = 102.1$; $\sigma_{u}^* = 133.3 \text{ daN/mm}^2$; $E = 10,550 \text{ daN/mm}^2$;
 $A\% = 14$; $\epsilon\% = 38$; $K_{UF} = 32 \text{ J/cm}^2$

The estimated fracture toughness properties are :

$\eta = .6$; $V(\eta) = .11$; $K_c = 225 \text{ daN/mm}^{3/2}$;

$q_c = 4.85 \text{ daN/mm}$.

On the other hand, q_c has been computed by means of IRWIN's method which gives :

$q_{c \text{ true}} = 6.5 \text{ daN/mm}$.

We have furthermore :

$\frac{P_{ult.}}{P_t} = 1.84$; $\frac{\sigma_u^*}{\sigma_{ult.}} = 1.31$; $\frac{\sigma_{ult.}}{\sigma_y} = 1.04$.

Like with "maraging" steels and 15 CDV6 steel at 110 daN/mm², the T-A6V titanium alloy has a $\sigma_{ult.}/\sigma_y$

ratio near unity. This demonstrates again that the view previously reported about the correlation between this fact and brittleness is false.

General remarks on the estimated values of K_c and q_c .

The IRWIN values of K_c and q_c are difficult to obtain and we did not know them in most of the previous cases.

We define q_c as the median value of fracture results $\frac{P^2 a}{1540 E}$,

where P is the failure load, and, a, the half of apparent crack length measured on the fractured specimen. Measuring a is not always easy and the preceding relationship is debatable with the large values of a which appear with ductile metals. Nevertheless, this relationship allows comparison of results without taking static crack propagation during failure into account. Moreover, on unfailed components, a is the only piece of information known. It seems impractical to complicate the state of affairs by making careful corrections to crude results in order to obtain a certain invariant parameter. It is very difficult to compare results of tests of various origins because of the different

types of tests. With a metal from a single casting, DOUILLET⁽³⁾ has shown a variation from 135 to 180 daN/mm^{3/2} for K_c in the case of the

40 CDV20 steel treated for $\sigma_{ult.} = 170 \text{ daN/mm}^2$, that is, extreme values

of q_c in a ratio of 1.8 between bending bar tests of C.E.A.T. and

tensile tests on flat specimens with a crack that has not crossed (STRAWLEY' method). Therefore, discussions about the "true" value of K_c remain rather academic.

A. 3 - Fatigue tests on smooth and notched specimens

A. 3. 1 - Aluminium alloys.

Figures 3 and 4, from a report by NOTTON and

AUVINET⁽⁴⁾, show results of axial fatigue tension - compression tests, carried out with zero mean stress and 12.5 daN/mm² mean stress on round smooth and notched specimens (D = 14 mm, d = 7.98 mm, radius of V-groove = 55 mm, 2 mm and .35 mm). The specimens were taken from A-U4SG aluminium alloy thick plate which had been used in tensile and fracture tests previously mentioned in mark 4 of the table A. 2. 2b.

Such plates have been used for the wing-boxes of Mystere 20 aircraft (Falcon) of which the upper and lower skin panels are mill-machined. This metal has been specially hot-forged in the three directions to obtain a good failure elongation in short transverse (about 3 %).

The table A. 3. 1a gives test results for A-U4SG extrusion bars (numbered 3 in table A. 2. 2b).

With A-U2GN thick plates, fatigue tests in longitudinal and transverse directions give results very near those of A-U4SG. The table A. 3. 1b shows results in axial fatigue tension-compression tests.

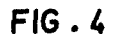


TABLE A.3.1a - A-U4SG EXTRUSION BARS, FATIGUE TESTS IN
AXIAL TENSION-COMPRESSION, values of σ_a in daN/mm²

	K_t	$N =$	10	10^3	10^5	10^7
$\sigma_m = 0$	1.035		57	48	27	17
	1.7		71	38	18	11.8
	3.3		62	30	12	6.6
$\sigma_m = 12,5$	1.035		44	41	21	15.4
	1.7		60	35	15	11.5
	3.3		55	25	6.5	4.7
VALUES IN daN/mm ²						

TABLE A.3.1b - A-U2GN THICK PLATES, FATIGUE TESTS IN
AXIAL TENSION-COMPRESSION, values of σ_a in daN/mm²

	K_t	$N =$	10	10^3	10^5	10^7
$\sigma_m = 0$	1.035		44	37	21	14.6
	1.7		59	31	12.5	7.8
	3.3		50	25	10	5
$\sigma_m = 12,5$	1.035		32.5	28	18	11.6
	1.7		48	30	11	7
	3.3		44	20	5	3
$\sigma_m = 25$	1.035		23	22.5	11	9
	1.7		37	25	8	5.4
	3.3		36	17	4	3

TABLE A.3.2a - A-U4G1 ALUMINIUM ALLOY, NATURALLY OR ARTIFICIALLY AGED, tensile properties (plates 30 mm Thick)

CONDITION	VALUES IN daN/mm^2					$\sigma_{U\text{ TRUE}}^*$	E	A%	$\Sigma\%$
	σ_p	$\sigma_{.05}$	$\sigma_{.1}$	$\sigma_{.2}$	σ_{ult}				
T351	16.4	27.1	30.1	32.6	47.4	56	7,175	15.6	16.6
T651	33.2	43.7	45.8	47.3	50.3	54.5	7,330	6.1	9.3

TABLE A.3.2b - A-U4G1 ALUMINIUM ALLOY IN PLATES, FATIGUE PROPERTIES IN AXIAL REVERSED LOADING,

Values of σ_{max} in daN/mm^2

	$N =$		1	10	10^3	10^5	10^7
$K_t = 1.035$	T351	T651	50	50	49	32.5	28
			52.4	52	51.5	32.5	27
$K_t = 3.3$	T351	T651	62.4	60	36	17	11.8
			58	56	32.5	15.5	13

TABLE A.3.4. EFFECTS OF SURFACE CONDITIONS ON FATIGUE

LIMIT OF T-A6V 25 mm BARS.

CONDITION OF SPECIMENS	K_t	FATIGUE LIMIT σ_a AT 3×10^7 CYCLES daN/mm ²
LATHE, ROUGHNESS 100 R.M.S.....	1.035	43
	3.3	16.5
60.....	1.035	47.6
	3.3	17.6
LATHE, ANNEALED 1 h, 750°C.....	1.035	36.3
	3.3	5.3
LATHE, ANN., SHOOT-PENED.....	1.035	46.5
LATHE, ANN., VAPOR-BLASTED.....	1.035	53.4
	3.3	9.8
ROUGH TURNED, CHEMICAL MILLED.....	1.035	41.5
	3.3	13.5
R. TURNED, CHEM. MILL., ...		
VAPOR-BLASTED.....	1.035	51.6
	3.3	17.5
MILL-MACHINED.....	1.035	56.4
	3.3	17

NOTE : These results were obtained with an early lot of titanium alloy ; recent results show larger values of fatigue strength.

Up to 10^5 cycles, the fatigue strength is something under that of A-U4SG. Between 10^6 and 10^7 cycles, they are comparable. The tests were carried out on an AMSLER Vibrophor of 100 kN

with a 110 Hz frequency for $10^4 \leq N \leq 10^7$, and on a SCHENCK pulsator at .3 Hz for $N < 5 \cdot 10^3$.

A. 3. 2 - Artificial aging effect on fatigue strength of A-U4G1 aluminium alloy.

For several years, the service behaviour of military aircraft employing A-U4G1 or 2024 extrusions in T351 quenched-stretched-naturally aged condition has drawn attention to the sensitivity of this condition to intergranular corrosion with exfoliations. It is known that an artificial aging for 12h at 190° C after quenching and stretching (T651 condition) greatly reduces this sensitivity, as also that to stress-corrosion.

The C.E.A.T. has carried out comparative fatigue tests on specimens taken out of thick (30 mm) A-U4G1 plates with in the two conditions :

T351 : water-quenched from 495° C, 1 % to 2 % stretched, naturally aged ;

T651 : water-quenched from 495° C, 1 % to 2 % stretched, artificially aged for 12 hours at 190° C.

The compositions was, in per cent :

4.4 Cu ; .20 Si ; .71 Mn ; .40 Fe ; 1.47 Mg ; remain Al.

The table A. 3. 2a gives the tensile properties. The smooth ($K_t = 1.035$) and notched ($K_t = 3.3$) specimens were machine-turned

with a small roughness (30 R.M.S.). The reversed fatigue tension tests ($\sigma_m = \sigma_a$) were carried out on an AMSLER Vibrophor at

110 Hz frequency in the range $10^4 \leq N \leq 10^7$, the results in table A. 3. 2b show no significant differences between T351 and T651 conditions.

Some others tests on extruded stringers showed a little decrease in fatigue strength, likely due to relief of cold-work hardening, dividing the fatigue life by a factor of two. Our inference is that the gain in safety obtained by the elimination of intergranular corrosion is well worth the small decrease in fatigue strength on an uncorroded component.

A. 3. 3 - Effect of rounding sharp edges on the fatigue strength of the A-U4SG plates.

In connection with the fatigue study of an executive aircraft,

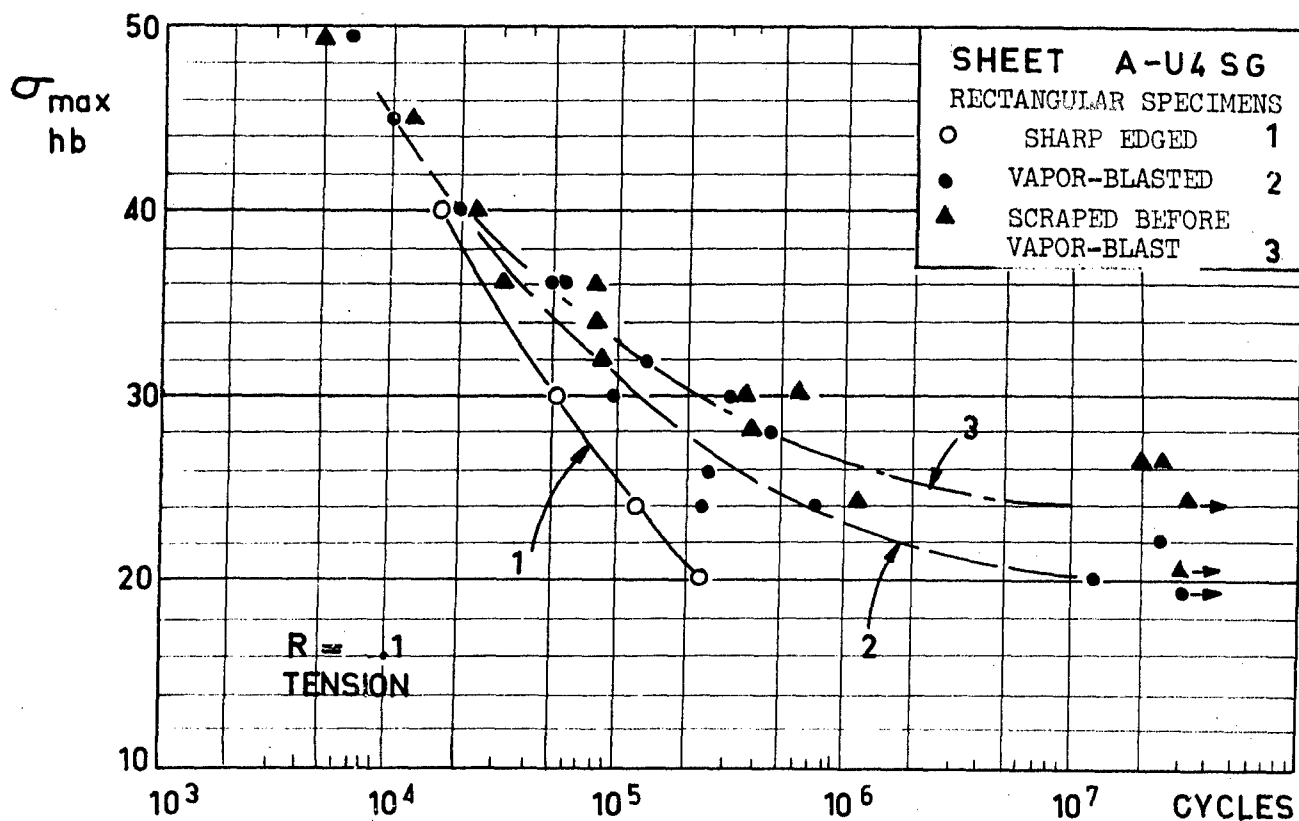


FIG. 5

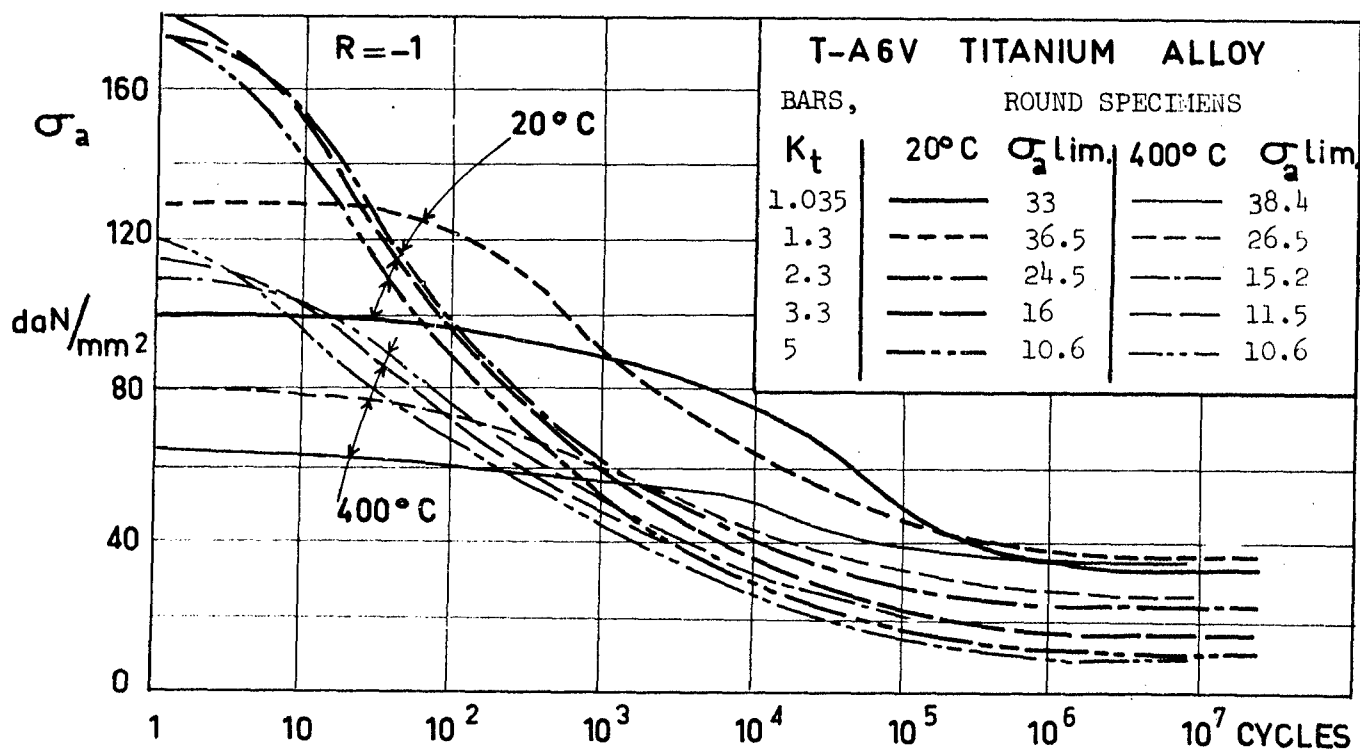


FIG. 6

the Mystère 20, the "Société des Avions Marcel Dassault" has placed an order with C.E.A.T. to carry out fatigue tests in reversed tension ($R = .1$) on rectangular flat specimens (30 x 4 mm in cross-section) machine-milled from A-U4SG sheets.

The three studied conditions were :

- 1 - as machined
- 2 - vapor-blasted
- 3 - scraped, before vapor-blasting.

Figure 5 shows the increase in life obtained by the rounding of sharp corners.

A. 3. 4 - Fatigue tests at room and elevated temperatures on bars of T-A6V titanium alloy.

These tests were carried out by the C.E.A.T. on the occasion of a study requested by the "Service Technique Aéronautique" and the "Société Messier". The metal's composition was :

.03C ; .10 Fe ; .02 Si ; 5.80 Al ; 3.90 V - remainder Ti.

The specimens were taken from bars 25 mm in diameter.

The mechanical properties were :

$$\sigma_{ult.} = 91 \text{ daN/mm}^2 ; \sigma_{y.2} = 88 \text{ daN/mm}^2 ; A \% = 14.5 ;$$

$$Z \% = 50 ; K_{UF} = 50 \text{ J/cm}^2.$$

Figure 6 shows fatigue test results ⁽⁶⁾ in alternating axial tension - compression at room temperature and at 400° C. The decrease of the fatigue strength at 400° C is significant with smooth specimens. With severely notched specimens in the range of high numbers of cycles, the hot fatigue strength is comparable to that at room temperature.

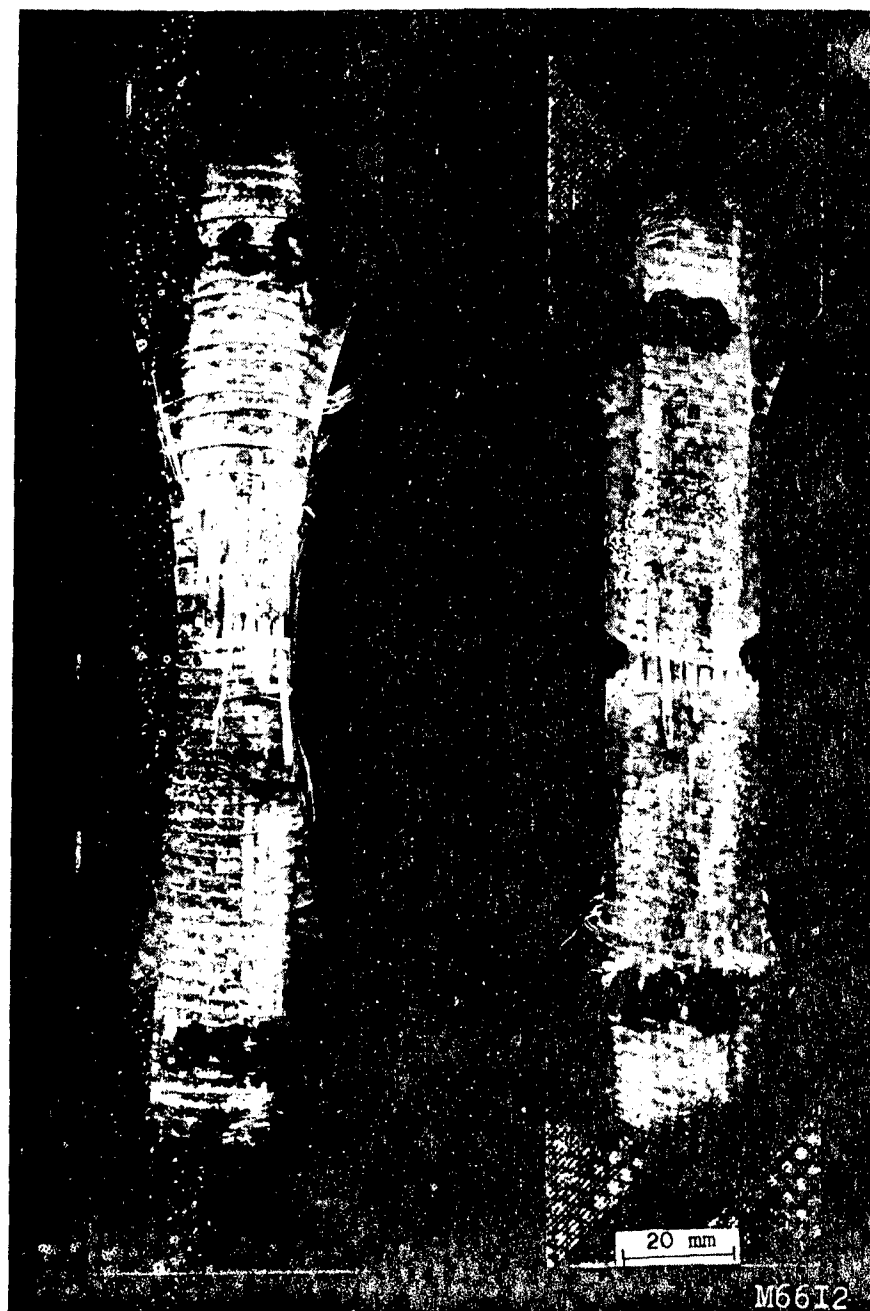
Another series of tests at room temperature was intended to study the effects of surface conditions. The table A. 3. 4 gives some of these results. The small values of σ_a , with

$K_t = 3.3$, after annealing, have been imputed to a "contamination"

during annealing. A complementary study ⁽⁷⁾ has shown that these small values were due to a hardened superficial layer of about .05 mm thickness on the annealed specimens.

A. 3. 5 - Fatigue tests on fiber glass-polyester panels.

The C.E.A.T. has carried out a study of the fatigue behaviour of smooth and notched flat specimens taken from panels made of polyester resin reinforced with fiber glass woven rovings.



$K_t = 1.035$

$K_t = 2.3$

FATIGUE TESTS ON FIBER-GLASS POLYESTER
NOTCH EFFECT IS LOW

Fig. 7

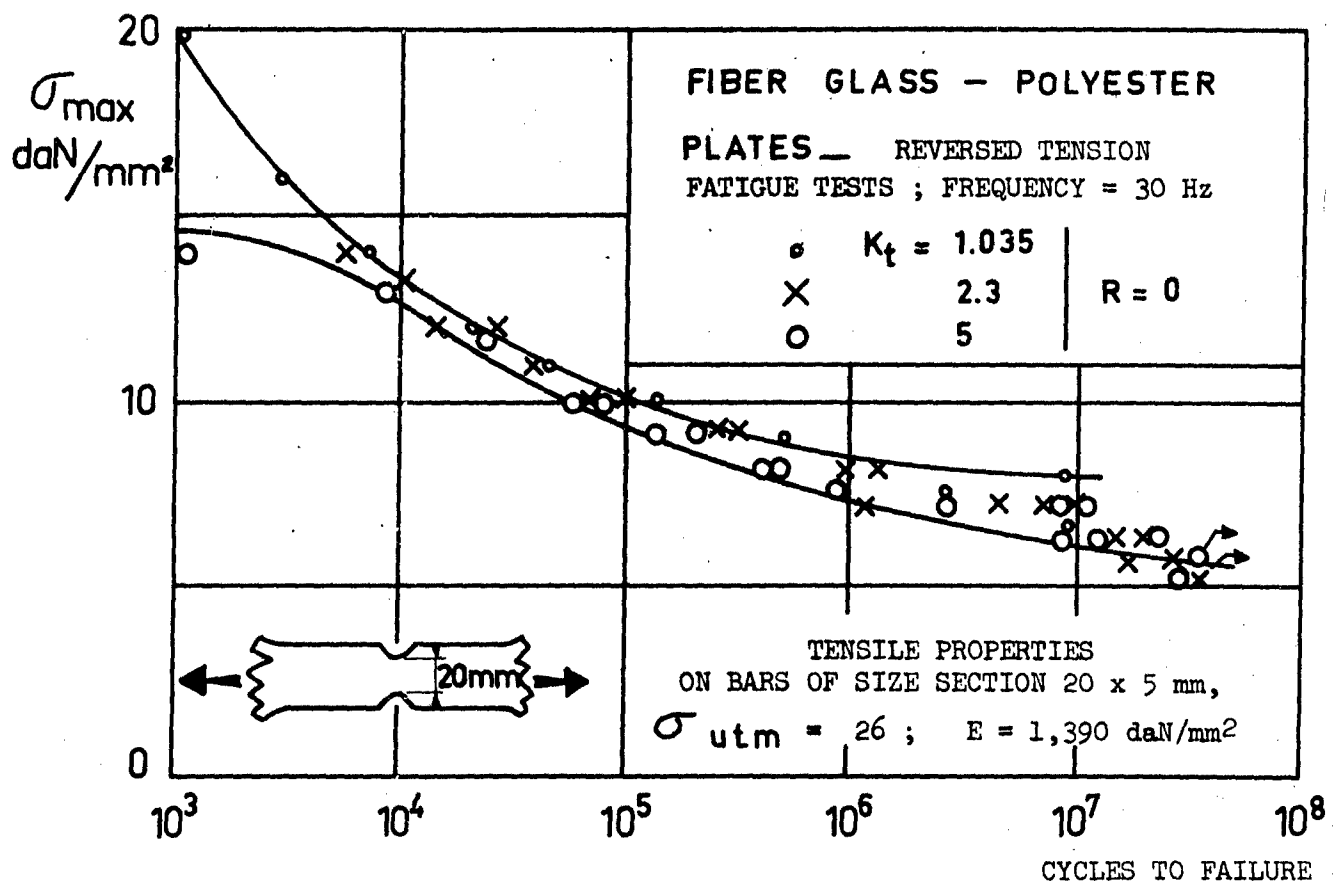
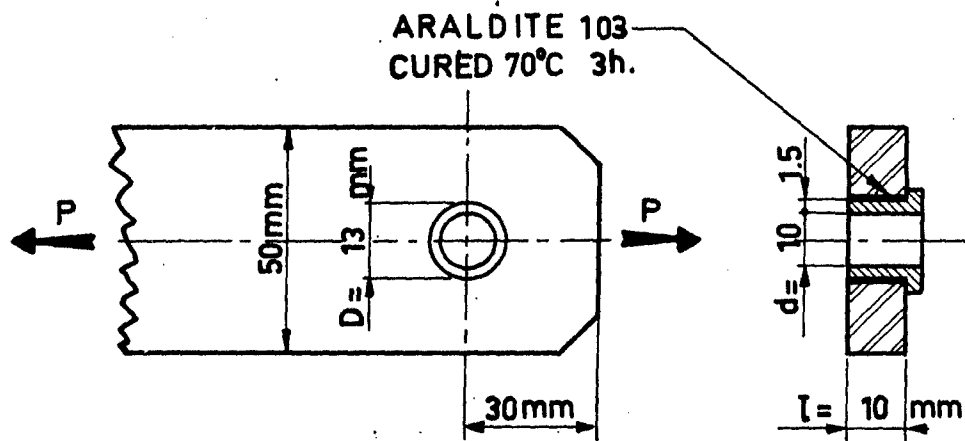


Fig. 8



GLUED BUSH

Fig. 9

TABLE B.1.1 - BEHAVIOUR OF GLUED BUSHES - SHEAR AXIAL STRENGTH AFTER BEARING FATIGUE.

DIAMETRICAL CLEARANCE mm	FATIGUE BEARING STRESS daN/mm^2	LOADING NUMBER OF CYCLES n	SHEAR AXIAL STRENGTH daN/mm^2
.07	0		3.1
	10 AND 20	100,000 20,000	2.15
	10	100,000	2.7
	20	20,000	2
	10	1,100,000	1.4
.10	0		3
	10 AND 20	100,000 20,000	1.68
	10	1,000,000	>1.2

Preliminary tests on Vibrophor have shown the damaging effect on resin of a temperature increase (140° C) due to internal friction. On BALDWIN and AMSLER pulsators, the results were

frequency = 30 Hz , $\Delta \theta$ = 20° C to 90° C

6 Hz , 5° C to 40° C

The conclusions was that, in regard to characterization tests, the frequency must be between 10 and 20 Hz and that, for checking actual parts, that it is of the highest importance tests be carried out at the service frequency.

The panels supplied by the "Société du Verre-Textile de Chambéry", under trade-mark "Verre-ester 49" contain 35 per cent of fiber glass. They received a post-baking of 15 hours at 60° C. Figure 7 shows a smooth specimen and a notched one, both of them damaged by fatigue. The lack of notch effect is noteworthy : the damage is limited to the glass fibers uninterrupted during the cutting out of the specimen. The $\sigma-N$ curves of figure 8 confirm this absence of notch effect which is also confirmed by static tensile failure tests with notched and fatigue cracked specimens. Fatigue tests, not reported here, at a frequency of 6 Hz for K_t values of 1.035 and 1.7 give results

indistinguishable from those of figure 8. Tests are now in progress on fiber-glass specimens reinforced with unidirectional roving. They concern partially the characterization of damage.

B. MISCELLANEOUS TESTS

B. 1 - TESTS BY AIRCRAFT MANUFACTURERS.

Like the C.E.A.T., the aircraft manufacturers carry out check tests on such elements as attachments, fittings, various components or partial assemblies. It is difficult to draw general conclusions from these check tests. Certain test series conceived by aircraft manufacturers include final tests in C.E.A.T. laboratories ; that was the case for the study formerly mentioned in paragraph A. 3. 3 of this paper. The following paragraph gives another example.

B. 1. 1 - Fatigue behaviour of steel bushes cold-glued into aluminium alloy components.

It is well known that the fatigue strength decrease, due to fretting between a steel axle and a light alloy component, can be avoided by interposition of a press-fitted steel bush. However, another failure risk arises from the tension stresses induced into the component by press-fitting, particularly in the cases of alloys sensitive to intergranular corrosion

or stress - corrosion, and/or brittle in short transverse direction. These circumstances have led the "Service Technique Aéronautique" to recommend avoidance of this kind of fitting in each case where the short transverse is under tensile stresses.

The "Société Breguet-Aviation" and the C.E.A.T. have carried out a study on the fitting of steel bushes by gluing. It is significant that warm-gluing is dangerous with curing temperatures in the range 120 to 170° C ; sometimes, this treatment sensitizes aluminium alloys to stress - corrosion. Because of this, it was decided to use a curing temperature of only 70° C. A recent

work (8) demonstrates a good behaviour of 30 NCD16 steel bushes glued into flat A-U4G aluminium alloy bar by means of Araldite 103 (with ten per cent of 930 hardener and 7.5 per cent of thiokol). The initial fit clearance was of .07 mm or .10 mm on diameter ; the curing temperature was 70° C.

Figure 9 shows the specimen. It was axially loaded by means of a fork fitted with a loaded specimen by a steel axle. The fatigue loading was carried out at a frequency of 6 Hz in reversed tension ($R = .1$). The loadings are shown in table B. 1. 1 in terms of

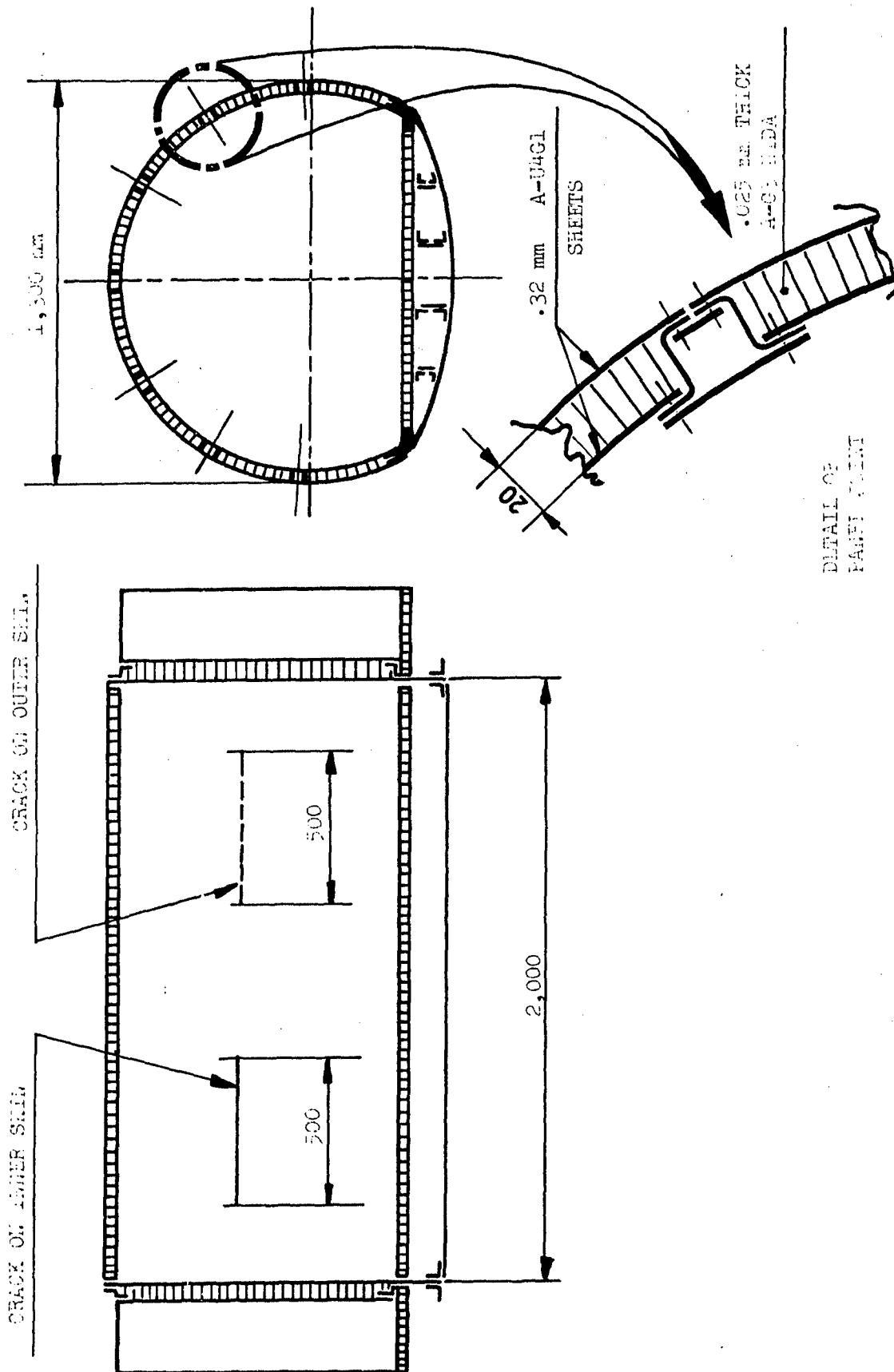
nominal bearing stresses, $p = \frac{P}{Dl}$, and of number of cycles, n .

After fatigue loading, during push out tests, the axial shear stresses applied to the glue and required for failure were measured. Table B. 1. 1 gives the results, i.e., the shear strength decrease with increase of initial clearance, level of fatigue loading, and number of cycles. It is evident that there remained an adequate shear strength to resist an accidental extraction of bush.

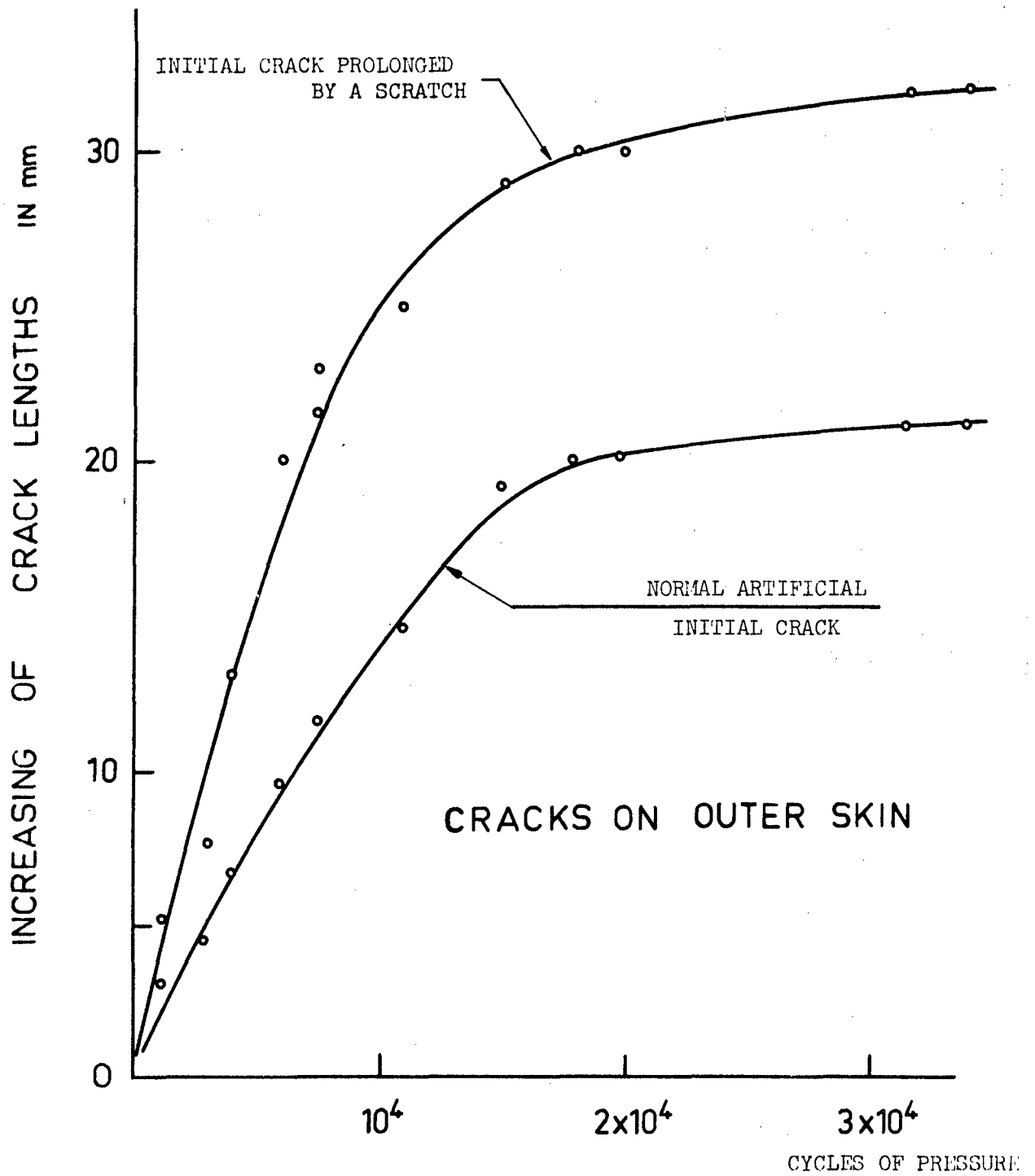
We put these results with previous test results obtained in 1949, on the fatigue strength of glued joints in control rods connecting A-U4SG tips and A-U4G1 tubes. The joints was made with Araldite powder cured 8 hours at 140° C. The fatigue loading, in axial alternating tension - compression by means of a SCHENCK pulsator, stopped automatically with the appearance of longitudinal relative movements due to slip on the glue surface. The fatigue shear limit was about 3 daN/mm². The "failed" specimens were found still able to resist half the loading of the original virgin specimens. A sectioning showed that the glue surface was severely fragmented : we imputed the residual static strength to friction arising from an expansion of the fragments from the glued joint.

B. 1. 2 - Fatigue crack propagation in outer skin of a honeycomb sandwich fuselage.

In connection with the "fail-safe" behaviour study of a pressurized fuselage of the navy patroller aircraft "Breguet 1150", the "Société Breguet-Aviation" has constructed a reduced model of a section of fuselage in order to carry out a preliminary study on rate of crack propagation during fatigue.



REDUCED MODEL OF AN AIRCRAFT FUSELAGE



LIMITED CRACK PROPAGATION ON HONEYCOMBE SKIN

Fig. 11

The primary aim of those tests is to prepare further large scale fail-safe tests for the actual aircraft fuselage, which will have been employed for classical fatigue tests.

The main function of a honeycomb core in sandwich structure is to stabilize the face sheets against local and general buckling. The shear stiffness of a metallic honeycomb core can also however transfer shear loads, thus diffusing into one of the skin sheets, a local load applied to the other. In case of a fatigue crack in one of the sheets, the initial tensile and shear stresses, cancelled by the crack are carried over into the other sheet. It follows, therefore, that the stress concentrations at the tips of the crack remain low and tend towards a limit value as the crack growth. Figure 10 shows the model. The inner radius of the upper section is 630 mm ; the panel, 20 mm thick, is made of two A-U4G1 sheets, .32 mm thick, and of a honeycomb core with hexagonal cells of 6 mm diameter and .025 mm thickness. The sheet-to-core and sheet-to-bordering extrusion joints are glued. The lower section has a radius of 1260 mm ; it is made with a sheet of 1 mm thickness. A honeycomb floor-plate carries the compression load resulting from the influence of the upper and lower sections.

A sawed artificial crack, 500 mm length, was made in the outer sheet of the upper section. The model was loaded by pressure and cycled between zero and $.6 \text{ daN/cm}^2$. About 30,000 cycles of pressure have been carried out, during which time, the crack length increases were measured. Figure 11 shows that the rate of crack propagation is constantly decreasing and is tending towards a very low limit value. At one of the tips, the initial saw-cut was stopped dead ; at the other one, where the sheet was scratched by the saw, a striation 10 mm in length caused a faster crack propagation. After 30,000 cycles of pressure, corresponding to fatigue tensile stresses reversed between zero and 5.9 daN/mm^2 , the crack has stopped dead. The total growth was 50 mm.

Honeycomb sandwich fullfills thus the two requirements of the fail-safe concept :

- a) that there is a second load path after partial failure.
- b) that a crack, sufficiently long to be really detectable, has a very low rate of propagation.

Nevertheless, I think that this kind of low-weight airframe construction, shown very safe in this particular case, is only fail-safe because the small values of stresses and stress concentration factors but is really safe-life. Since the total fatigue failure of a skin sheet would give a stress of 11.8 daN/mm^2 in the other one, it would not be able to create a crack in it ; therefore, it is fail-safe but only with this moderated stress. In effect, if one supposes a pressure of $.8 \text{ daN/cm}^2$ giving a tensile gross loop stress of 8 daN/mm^2 with the same sheet thicknesses, a long crack would give a 16 daN/mm^2 stress in the second sheet ; this stress value is able to develop a fast

growing fatigue crack in the sheet in the case where one had already some damage. If the inner sheet were the first failed for any cause, corrosion for instance, there is the risk that the outer sheet will experience some accidental damage such as to initiate a fast propagating fatigue crack. This is a reason to use sheet clad on both sides like is the case for the Breguet 1150 aircraft, and to authorize only moderate stresses, the sandwich core then having for single function the provision of stiffness against buckling.

B. 2 - O.E.C.D WORK ON FATIGUE DAMAGE

Though the object of this work is not aircraft fatigue nor only a french activity, we must mention this international co-operation carried out under O.E.C.D. (Organization of Economic Co-operation and Development) by several laboratories (R.F.A., Belgium, Canada, France, Italy, Netherlands, United Kingdom, Switzerland). The partial report on fatigue of a chrome-molybdenum steel under stresses of amplitude varying during the tests was edited in 1966 by BASTENAIRE, POMEY and SALKIN.

We cannot give an extensive summary of this enormous experimental study. The work deals with residual life and the new fatigue limit after the damaging effect of one or two fatigue pre-loadings at stress levels different from the final one which gave the failure.

The 35 CD4 steel studied had the composition, in per cent :

.35 C ; .32 Si ; .60 Mn ; .20 Ni ; 1.16 Cr ; .20 Mo ;
.006 S ; .016 P.

The 18 mm diameter bars had undergone the treatment : 45 min. at 850° C, oil quenching, tempering for 4 h at 590° C, air-cooling. Their mechanical properties were $\sigma_{ult.} = 100 \text{ daN/mm}^2$,

$\sigma_{y.2} = 87 \text{ daN/mm}^2$, A % = 15, Σ % = 57. The toric smooth

specimens (d = 6 mm, radius of groove = 40 mm) were polish-ground in the longitudinal direction from d = 6.05 mm to 6 mm in ten passes of .0025 on the radius.

A first series of simple tests under alternating tension-compression on the AMSLER Vibrophor, at a frequency of 185 Hz, with stress levels A = 55, B = 60 and C = 65 daN/mm², included 9 tests at each level.

Between the test results of the different laboratories the scatter was larger than for the test results of the laboratories involved : the ratio of the variance of the means to the mean of the variances had, respectively, the values 1.79, 3.4 and 9.5 for the levels A, B and C.

The reported fatigue limits at 10⁷ cycles varied from 48.5 to 53.3 daN/mm². The tensile strength was little modified (increase or decrease) by fatigue loading.

The reduction of area was not modified. After fatigue damage at any of the levels of loading, the scatter of fatigue limit remained unchanged. The variation of fatigue limit suggests no simple behaviour : the limit decreases or increases with the levels of damaging loads, without suggesting any obvious law.

Along with some other results, this particular result confirms me in opinion, held for about 13 years (10) (11), that fatigue damage is not describable by any single parameter but depends on several hidden parameters and their statistic distributions in intensities and locations.

REFERENCES

- 1 - DOUILLET, D., SERTOUR, G., AUVINET, J. ; Revue de Métallurgie, 61, N° 10, p. 877-883, Oct. 1964, PARIS.
- 2 - BARROIS, W. ; Symposium I.C.A.F., MUNCHEN, 1965.
- 3 - DOUILLET, D. ; Revue de Métallurgie, N° 9, p. 725-730, PARIS, Sept. 1966.
- 4 - NOTTON, AUVINET, J., Essai M3-7873, C.E.A.T., TOULOUSE, May 1965.
- 5 - OULIE, AUVINET, J., Essai M6-7325, C.E.A.T., TOULOUSE, Dec. 1966.
- 6 - NOTTON, AUVINET, J., Essai MO-7334, rapport partiel N° 2, C.E.A.T., TOULOUSE, August 1965.
- 7 - NOTTON, AUVINET, J., Rapport partiel N° 3, TOULOUSE, Dec. 1966.
- 8 - VIDAL, J., Essai M6-6000, C.E.A.T., TOULOUSE, March 1966.
- 9 - BASTENAIRE, F., POMEY, G., SALKIN, R. : Rupture par fatigue sous contrainte d'amplitude variable en cours d'essai. Cas d'un acier au chrome-molybdène. O.E.C.D., PARIS, 1966.
- 10 - BARROIS, W., Metaux - Corrosion - Industrie, N° 364, p. 497, PARIS, Dec. 1955.
- 11 - BARROIS, W., Revue de Métallurgie, LV, N° 8, p. 773, PARIS, 1958.

S
PRECEDING PAGE, BLANK NOT FILMED.

381

69-13 1590

REVIEW OF SOME SWEDISH INVESTIGATIONS ON FATIGUE

DURING THE PERIOD JUNE 1965 TO MARCH 1967

Compiled by

G. Wallgren

Flygtekniska Försöksanstalten

The Aeronautical Research Institute of Sweden
Stockholm

(FFA Technical Note No. HE-1203)

CONTENTS

1.	<u>Study of the fatigue properties of high-strength steels</u>	384
	- Vacuum melt 5.0% Cr-steel, type H-11 Mod.	384
	- 12% Cr-steel, type 420	385
	- Age hardening steel, type 17-4 PH	385
2.	<u>The effect of cold-working on the fatigue strength of high strength steels</u>	385
	2.1 Cold-working by rolling	385
	2.2 Cold-working by shot-peening	387
3.	<u>The effect of shot-peening on the fatigue strength of material Nimonic 90 at elevated temperatures</u>	387
4.	<u>Fatigue tests with riveted joints</u>	388
5.	<u>Fatigue strength of lugs</u>	389
	5.1 Constant load amplitude tests	389
	5.2 Programme tests	390
	<u>Reference</u>	391
	<u>Planned fatigue research for the near future</u>	392

Since last ICAF-meeting in Munich, our activities in the field of fatigue have been similar to those in earlier years. The work has been of experimental nature and has to a large extent been ad-hoc tests on materials and structural components. The fatigue investigations which have been carried out and which are of more general interest, deal with the following items.

1. Study of the fatigue properties of high-strength steels.

Since a few years, FFA and the SAAB Aircraft Company are conducting fatigue tests in order to study the fatigue properties of high-strength steels. At the previous conference, results were presented from tests on the following materials: Vacuum melt 5 % Cr-steel corresponding to AISI Type H-13, 18 % Maragingsteel and a Cr-Mo-Ni-steel similar to 4130. Results are now available from tests on vacuum-melt 5 % Cr-steel corresponding to AISI Type H-11 Modified, 12 % Cr-steel corresponding to AISI Type 420, and austenitic steel corresponding to 17-4PH. The chemical compositions and static properties for these materials are given in table 1.1.

The main portion of the tests was carried out with an alternating tensile-compressive loading with a mean stress of zero ($R = -1$), but in some cases fatigue tests also were performed with mean stresses of +40 and -40 kg/mm². Unnotched test specimens of circular cross section as well as notched specimens have been tested according to table 1.2. The test specimens were first rough turned. Then they were heat-treated to the required static ultimate strength, and fine turned. The notches were ground.

The results from the fatigue tests are reported in the following for each type of steel.

Vacuum melt 5.0 % Cr-steel, type H-11 Mod.

In order to study the effect of a small variation in ultimate strength on the fatigue strength, the material was heat-treated to two different values of the ultimate strength, viz. 170 and 180 kg/mm², (measured mean values were 168 and 179 kg/mm² respectively).

Results of S-N tests, conducted at a stress ratio of $R = -1$ are shown in Fig. 1.1. For unnotched specimens with $\sigma_{ult} = 180 \text{ kg/mm}^2$ the fatigue strength at $N = 10^6 - 10^7$ cycles is about 10 kg/mm² higher than the fatigue

strength of the specimens with $\sigma_{ult} = 170 \text{ kg/mm}^2$; i.e. the difference in fatigue strength is approximately the same as the difference in static strength. For the notched specimens with a stress concentration factor of 1.8, however, an increase in static strength from 170 to 180 kg/mm^2 has no significant influence on the fatigue strength. In Fig. 1.2, the relationship between stress amplitude and mean stress is given for different values of the life-time for the notched specimen ($K_t = 1.8$, $\sigma_{ult} = 170 \text{ kg/mm}^2$).

12% Cr-steel, type 420:

Unnotched test specimens were taken from a rolled bar of 60 mm diameter in both the longitudinal and transverse direction of the bar, while notched specimens were taken in the longitudinal direction only.

The results of the fatigue tests are presented in Fig. 1.3 showing the relationship between the stress amplitude and the mean stress for different values of N . The results show that the fatigue strength of unnotched specimens is considerably lower for specimens taken in the transverse direction of the bar compared with those taken in the longitudinal direction. The fracture surface of specimens taken in the longitudinal direction appeared to be quite normal, whereas the surface of the transverse specimens had a flaky structure.

Age hardening steel, type 17-4 PH.

This steel was also heat-treated to two different values of the ultimate tensile strength, viz. 110 and 143 kg/mm^2 . The results of the S-N-tests at $R = -1$ are compiled in Fig. 1.4. This figure shows that an increase in the ultimate strength from 110 to 143 kg/mm^2 , i.e. with 30 %, results in an increase in fatigue strength at $N = 10^7$ of 8 % for unnotched specimens, and of 5 % for notched specimens.

2. The effect of cold-working on the fatigue strength of high strength steels.

2.1. Cold-working by rolling.

An investigation was carried out in order to study the effect of cold-working by rolling and the influence of rolling pressure on the fatigue strength of two high-strength-steels. The materials investigated were a Cr-Mo-steel (corresponding to 4130) with a tensile strength of 100 kg/mm^2 , and a Hy-Tuf steel with a tensile strength of 170 kg/mm^2 . See table 2.1.

The specimens were taken from a 30 mm round rod and were manufactured as follows: First they were rough turned, leaving a 0.5 mm material layer for the final finishing process. After that, the specimens were heat-treated and fine ground to the required dimensions before rolling. The process of rolling was performed in a rolling machine manufactured by Hegenscheidt, and three different rolling pressures were used for each material; see table 2.2 where also the depth of the cold-worked layer are given.

Both unnotched and notched specimens ($K_t = 1.8$) according to Fig. 2.1, were fatigue tested in pulsating tension with the lower load limit equal to zero. ($R = 0$).

The results from the tests on specimens of Cr-Mo-steel are shown in Fig. 2.2. It is evident from this diagram that cold-working by rolling has little effect on the fatigue strength of unnotched specimens. The rolling procedure, however, gives a considerable increase in fatigue strength of notched specimens as can be seen if the two lower scatter bands are compared. The increase in fatigue strength is approximately 60 % at $N = 10^7$, independently of the magnitude of rolling pressure (90, 125 or 160 kg).

If a rolled notched specimen is statically pre-loaded to a high tensile stress immediately followed by a compressive stress of the same magnitude before fatigue testing, the increase in fatigue strength attained by rolling is completely lost. The squares in the diagram which lie within the scatter band for not rolled notched specimens, represent the fatigue life of rolled specimens which were pre-loaded to $\pm 70 \text{ kg/mm}^2$ (75 % of the yield strength).

The results from tests on the Hy-Tuf-steel are shown in Fig. 2.3. The rolling process had no effect on the fatigue strength of unnotched specimens. The testpoints for not rolled and for rolled test specimens fall within the same scatter band. The fatigue strength of the notched not rolled test specimens is comparatively high and it is only moderately increased (approximately 18 % at $N = 10^7$) by rolling. The highest rolling pressure, 200 kg, tends to raise the fatigue strength slightly more than the pressures 100 and 150 kg (4 % at $N = 10^7$). One preloading cycle to $\pm 115 \text{ kg/mm}^2$ (75 % of the yield strength) applied to rolled notched specimens results in a large reduction of the fatigue strength. The strength of rolled and pre-loaded specimens (squares in Fig. 2.3) becomes even lower than that of not rolled, notched specimens. A reason for this may be that the surface of the non-rolled test-specimens gained some cold-working when turned. If so, we have one explanation for the considerably smaller increase in fatigue strength gained by rolling of the Hy-Tuf steel, as compared with the Cr-Mo-steel.

2.2. Cold-working by shot-peening.

The effect of shot-peening on the fatigue strength has been studied for notched specimens of the 5 % Cr-steel mentioned in section 1. The ultimate tensile strength of the material was 170 and 180 kg/mm², and the stress concentration factor of the notch was 1.8, see table 1.2. In these tests the specimens were loaded in alternating tensile-compressive loading with a mean stress of zero ($R = -1$). The results from these tests showed that shot-peening had no influence at all on the fatigue strength.

3. The effect of shot-peening on the fatigue strength of material Nimonic 90 at elevated temperatures.

The possibility of increasing the fatigue strength of the root part of turbine blades by shot-peening has been investigated. The work was carried out at the Swedish Air Force Material Laboratory.

A metallographic investigation was first performed in order to study the influence of cold-working on the micro-structure of the material upon heating. Fatigue tests were then carried out at elevated temperatures on test specimens that had been cold-worked by shot-peening with glass bullets and also on unprepared specimens.

The purpose of the metallographic investigation was to find out whether recrystallization occurs at the working temperature of the turbine blade. If so, the effect of cold-working might very well be unfavourable and could result in a reduction of the fatigue strength. The investigation showed that recrystallization does not occur in cold-worked test specimens subjected to 400 and 600°C for 100 h. When heated to 800°C, a thin layer of recrystallized material appeared on the surface, but underneath, the effect of cold-working still remained. As the occurrence of temperatures in the root part of the blade in excess of 600°C has been deemed improbable, there should be no risk for recrystallization in service.

In the fatigue tests, notched specimens according to Fig. 3.1 were used. The radius of the specimen notch was the same as for the fir tree attachment part of the blade. The specimens were loaded in rotating bending at the temperatures 450 and 600°C. The loading frequency was about 3000 cycles per min. The results of these fatigue tests are presented in the form of S-N-curves in Fig. 3.1. It is evident from the diagram that shot-peening of the notch increases the fatigue strength at $N = 10^7$ cycles by approximately 40 per cent at 450°C, and by about 35 per cent at 600°C. Furthermore, the diagram shows that the fatigue strength of both unprepared and cold-worked specimens is

noticeably higher at 600°C than at 450°C. According to W. Belleridge ("The Nimonic Alloy") the tensile yield strength of Nimonic 90 is somewhat higher at 600°C than at 500°C. It is probable that the higher fatigue strength at 600°C is a consequence of this fact.

4. Fatigue tests with riveted joints.

The purpose of this investigation was to obtain more information on the fatigue properties of a riveted joint in Alclad 2024 sheet typical for aircraft structures.

The investigation comprises fatigue tests for the determination of the S-N-curves for different values of the mean stress and some programme tests. The fatigue lives obtained in the programme tests were compared with those predicted by means of the linear cumulative damage theory ($\sum \frac{n}{N} = 1$).

The test specimen, a triple row, single shear butt joint, is shown in Fig. 4.1. In order to simulate the normal stiffening effect of stringers in complete panels the splice plate of the joint was bent in the way indicated by the figure.

The results of the constant amplitude tests are compiled in Fig. 4.2, in the form of a Haigh-diagram. The stresses are based on the gross area of the test specimen, which averaged 99.3 mm². (The net-area at the first rivet row was 76.3 mm² and at the second row 64.8 mm²). The ultimate tensile strength of the joint was 30.5 kg/mm² and of the sheet material 45.3 kg/mm².

In the programme tests, the stresses were varied according to two different programmes, see Fig. 4.3. These programmes were derived from a cumulative load spectrum for a jet-trainer with a limit load factor, n_z , of about 7.3. Only the stress cycle minimums were different in the two load programmes A and B. In programme A the stress cycle minimums were varied. In programme B they were all the same and equal to zero. The fatigue life of the joint calculated according to the cumulative damage theory yielded practically the same value for the two spectra.

Programme tests were carried out at different stress levels. The stress level is defined as the highest stress within the programme block, $\bar{\sigma}_{\max}$, corresponding to 87 per cent of the stress at limit load σ_L . In the testing the number of loading cycles within a programme block was determined by means of the cumulative damage theory in such way that failure should occur after 10-30 programme blocks. In a few tests, however, the number of programme blocks exceeded 100 before failure. The results from the programme tests are shown in Fig. 4.4, which gives the relationship between $\bar{\sigma}_{\max}$ and the fatigue life

expressed in hours of flight. The diagramme also includes the calculated lives. It is evident that the experimentally obtained lives all exceed the calculated values, which means that the cumulative damage theory yields a conservative estimate of the fatigue life in these cases. Furthermore it is evident that the programme B tests, where the stress cycle minimum was zero, yield life times about twice as long as the programme A tests. This is in disagreement with the linear damage rule, which predicts the same life for the two load programmes. Thus, the present investigation confirms the experience gained in other works that compressive stresses in a load spectrum cause a decrease of the fatigue life in programme testing.

5. Fatigue strength of lugs.

At the last conference an account was given for an investigation, which had been commenced in order to study the fatigue strength of lugs and the possibility to increase the fatigue strength by fitting the lugs with interference fit steel bushes or by expanding the hole by pressing an oversize pin or ball through it. The investigation has been continued, and the effect of some different methods of increasing the fatigue strength of the lugs has been studied both at constant load amplitude tests and programme fatigue tests.

5.1. Constant load amplitude tests.

In these tests the influence of various degrees of cold-working on the fatigue strength was studied, as well as the influence of coating the bolts with Molycote Z106.

The cold-working was achieved by pressing an oversize ball through the hole. This operation results, however, in a hole with a diameter varying through the thickness of the lug, according to Fig. 5.1a. By pressing the ball once more through the hole, but in the opposite direction, a smaller variation in diameter is obtained, see Fig. 5.1b. The fact that the hole diameter becomes larger at the outer ends than in the middle of the thickness of the lug means that there will be difficulties to achieve a prescribed small clearance between hole and bolt. If, for example a clearance of g_6 is prescribed for a hole of 15.8 mm diameter, the deviation from this value is allowed to vary between 0 and +.018 mm. The process of cold-working yields in this particular case, according to Fig. 5.1b, a variation in the hole diameter of approximately .040 mm. In order to obtain the prescribed clearance, the hole has to be reamed, but then, of course, there is a risk that the effect of cold-working will diminish or

disappear completely. These circumstances were studied for different degrees of cold-working and for reaming to two different depths, .02 mm and .12 mm.

The specimen geometry is shown in Fig. 5.2. The material was cut from a forged bar of aluminium alloy 7079-T6 (140 mm in diameter and 500 mm in length) in such a way that the direction of loading was parallel to the length of the bar. In order to obtain as much information as possible from one test, different treatments were applied to the two holes of the test specimen. The tests, however, were interrupted when fracture occurred at one of the holes. Thus no information was obtained regarding the fatigue life of the other lug, apart from the knowledge that the treatment applied to that hole gave a higher fatigue strength. The different series of tests are defined in Fig. 5.2.

The test specimens were loaded in pulsating tension. The lower stress limit was constant and equal to 1.0 kg/mm^2 in all test series.

From the test results, see Fig. 5.3, the following conclusions can be drawn.

- a) A permanent plastic expansion of the hole yields an increase in fatigue strength of the lug. For the different levels of cold-working investigated, the fatigue strength seems to increase with an increase of the degree of expansion.
- b) A .02 mm reaming of a hole expanded 1.1 % yields a decrease in fatigue strength to the level obtained for an unreamed hole expanded 0.6 %. A .12 mm reaming applied to the first mentioned hole lowers the fatigue strength still further.
- c) Coating the bolt with Molycote yields an increase of the fatigue strength, but the magnitude of this increase has not been possible to determine because fracture always occurred at the hole where an untreated bolt was used.

5.2. Programme tests.

This investigation comprises lugs with the following variation in design.

- A. Lugs with steel bushes. The play between the lug and the bush was .11 %.
- B. Equal to series A, but the bushes were coated with Molycote X106.
- C. Lugs with interference fit steel bushes. The interference fit was 14 % of the hole diameter.
- D. Lugs with steel bushes and with expanded hole. The permanent expansion of the hole in the lug was 1.0 % and was obtained by pressing an oversized ball through the hole. The hole was not reamed after the expansion and therefore the play between the hole and the bush varied, as mentioned in section 5.1. The mean-value of the play was about .12 %.

Bushes were used in series A, B and D with the purpose of keeping the dimensions of lugs and bolts constant in all series to be able to compare directly the test results.

The dimensions of the lugs are shown in Fig. 5.4. The test specimens were taken from the same bar as the specimens used for the constant amplitude testing (section 5.1). The bushes, made of steel $\sigma_{ult} = 100 \text{ kg/mm}^2$, had an outer diameter of 19 mm and an inner diameter of 16 mm.

The testing has been carried out as a block-programme test. The relative values of the different stress levels and the number of stress cycles at each stress level within a block are given in table 5.1, valid for a constant lower stress limit equal to zero. Programme tests were carried out for different values of $\bar{\sigma}_{max}$ i.e. the maximum stress within a block.

This investigation is not yet finished but the results obtained up to now are presented in Fig. 5.5 which gives the relationships between $\bar{\sigma}_{max}$ and the fatigue life, expressed in total number of stress cycles N .

The results show that Molycote has a slightly improving effect on the fatigue life of the lug. The longest fatigue life has been obtained, however, for lugs with expanded holes and lugs with interference fit steel bushes, which is in agreement with the results of the constant amplitude tests carried out earlier. The difference in length of life between the latter two types of lug design is not so big, however, as could be expected from the testing at constant amplitudes, see Ref. [1].

When fatigue failure occurred at one of the holes of the test specimen fatigue cracks had usually been initiated, having propagated to various lengths, at the other hole. These lugs have been loaded statically in order to determine the residual strength. The results of the static tests are given in Fig. 5.6, which shows the ratio between the residual strength and the original ultimate strength versus the total area loss of the original net area due to cracks. In the diagram residual strengths obtained in the fatigue testing have also been included, assuming the ultimate residual strength to be equal to the load applied when the failure took place.

Reference.

- | | | |
|-----|--------------|--|
| [1] | Wällgren, G. | Review of some Swedish investigations on fatigue during the period April 1963 to May 1965. FFA TN No. HE-1063. |
|-----|--------------|--|

Planned fatigue research for the near future.

- a) The fatigue tests on lugs will be continued.
- b) Fatigue tests on specimens of aluminium alloy 7079-T6, taken from different forgings.
- c) Experimental study of riveted or bolted joints during fatigue cycling.
 - Determination of fastener deflections and its controlling parameters.
 - Determination of the fatigue strength of 2024-T3 joints expressed in terms of bypassing stress and fastener bearing stress. Constant amplitude tests will be performed at a stress ratio, $R = -0.2$.
 - A specimen with an open drilled hole will be used as a reference basis.
- d) Influence of length of service life and inspection intervals on probability of complete failure of fail-safe structure.
 - 1. Theoretical study of variable inspection intervals and cyclic inspection procedures.
 - 2. Experimental investigation of fatigue life until crack initiation, crack propagation and residual strength of wing panel under programme loading.

Table 2.2. Rolling pressure and depth of the cold-worked layer of test specimens.

Steel	Cr-Mo steel corresponding to 4130			Hy-Tuf		
Rolling pressure kg	90	125	160	100	150	160
Depth of cold-worked layer, μ mm						
plain specimens	- 1)	210	320	5	10	13
notched specimens	- 1)	140	150	10	15	20

1) Not measurable

Table 5.1. Loading programme for testing of lugs.

$$\bar{\sigma}_{\max} = 0,87 \sigma_L$$

σ_L = stress corresponding to limit load

$\sigma/\bar{\sigma}_{\max}$	σ/σ_L	n within a block
0,17	0,15	25625 · a
0,34	0,30	4250 · a
0,57	0,50	1219 · a
0,80	0,70	144 · a
1,00	0,87	25 · a
0,80	0,70	144 · a
0,57	0,50	1219 · a
0,34	0,30	4250 · a
0,17	0,15	25625 · a
Σn within a block		62501 · a

The value of a was either 1, 4 or 8 depending upon the expected life time.

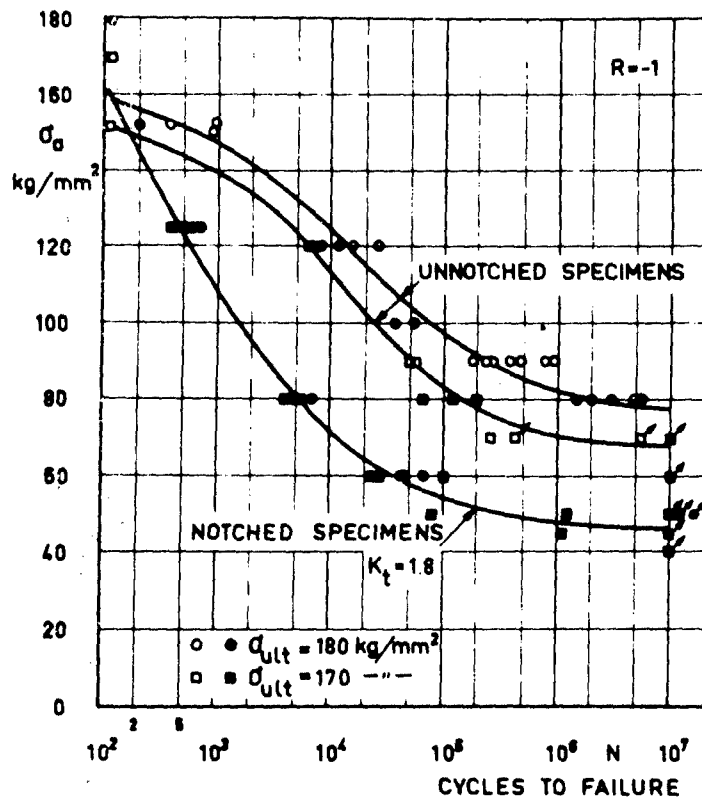


Fig. 1.1. Fatigue curves for 5 % Cr-steel.

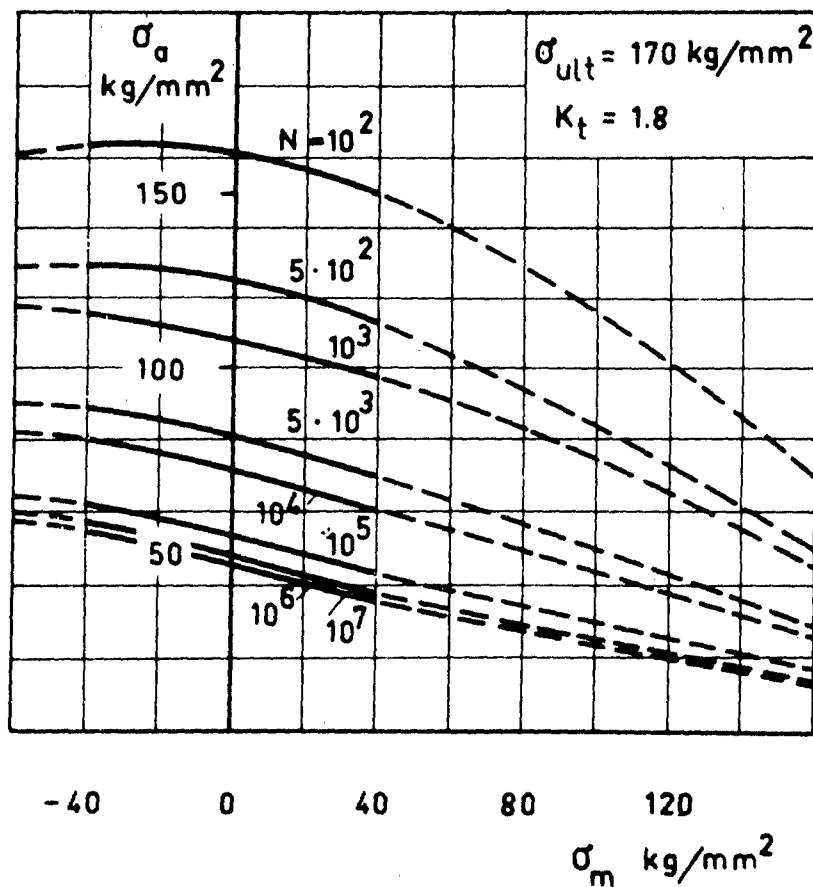


Fig. 1.2. The relationship between the stress amplitude, σ_a , and the mean-stress, σ_m , for notched specimens, $K_t = 1, 8$, of 5 % Cr-steel. $\sigma_{ult} = 170 \text{ kg/mm}^2$.

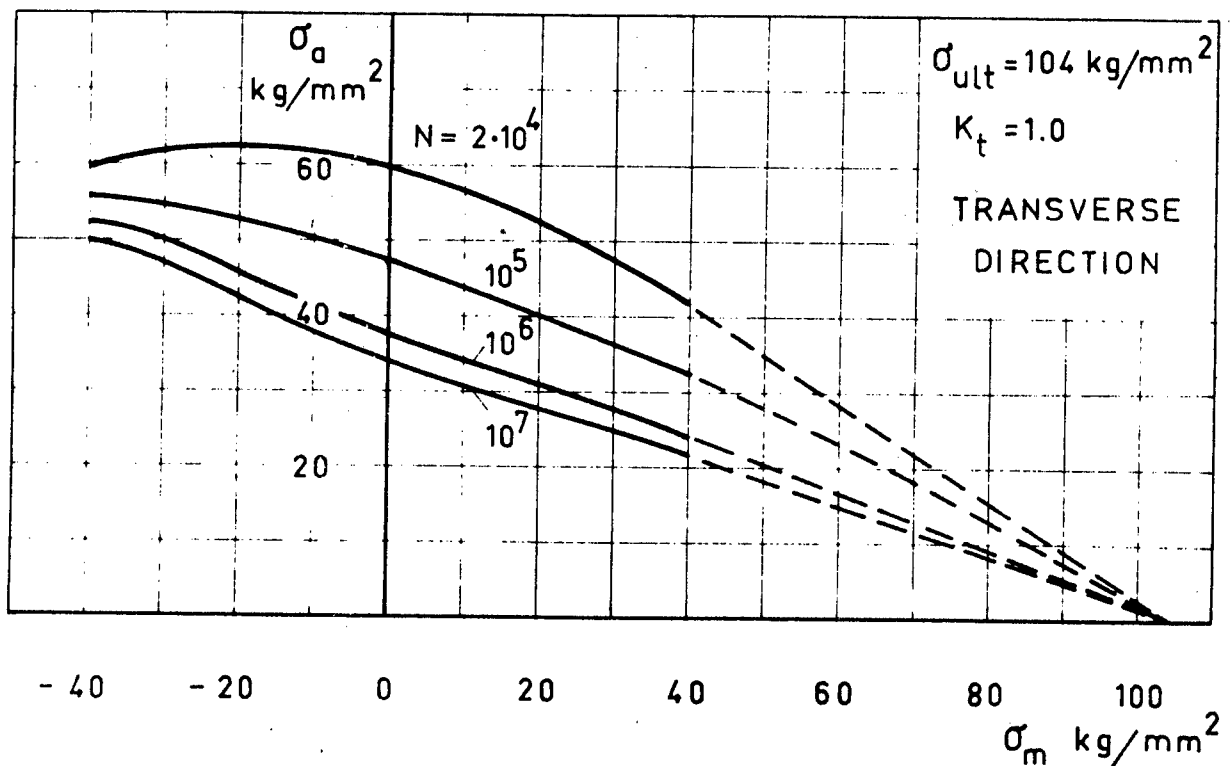
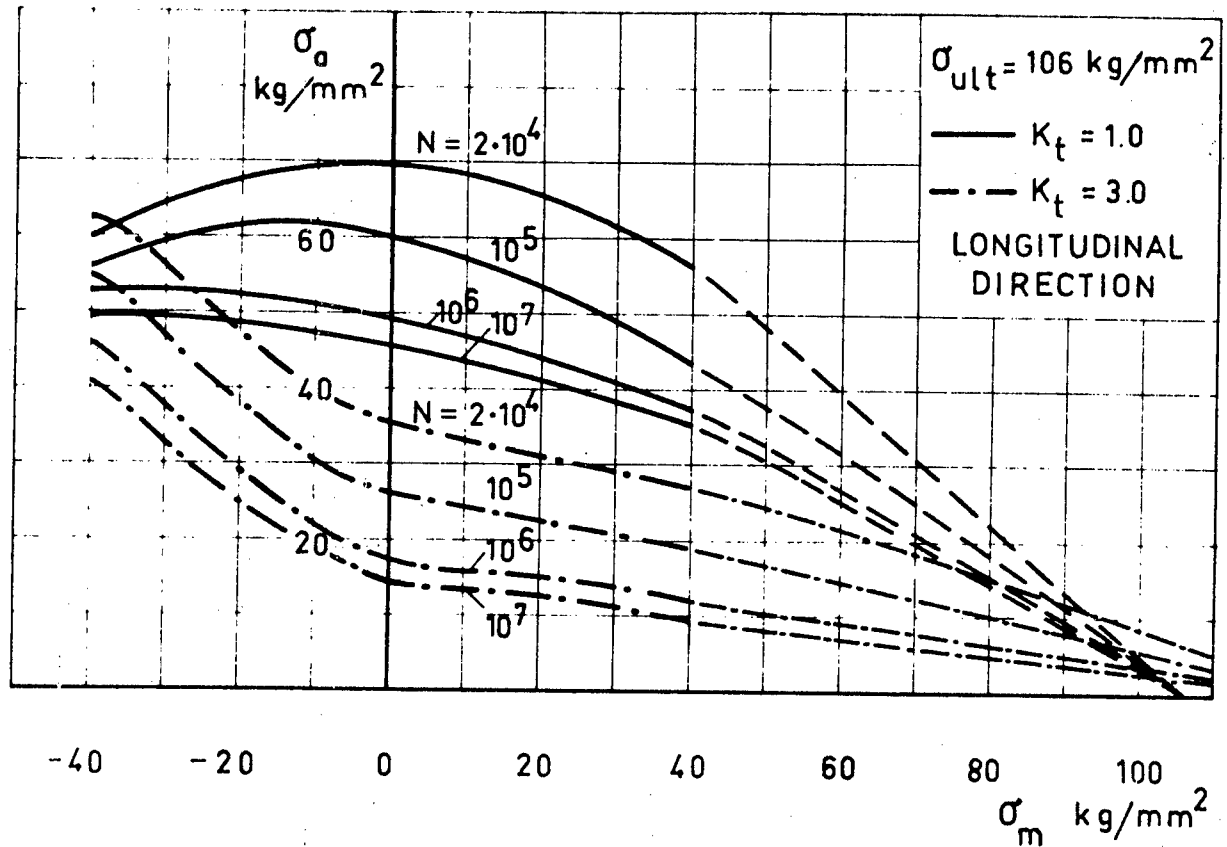


Fig. 1.3. The relationship between the stress amplitude, σ_a , and the mean-stress, σ_m , for plain and notched specimens of 12 % Cr-steel.

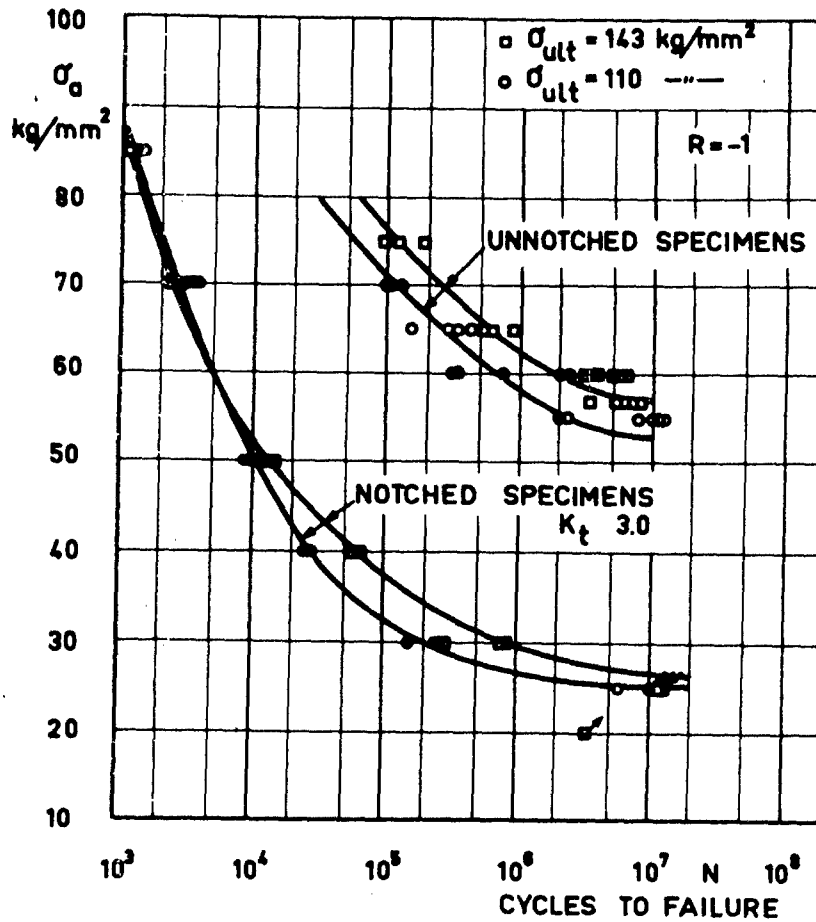


Fig. 1.4. Fatigue curves for steel 17-4 PH.

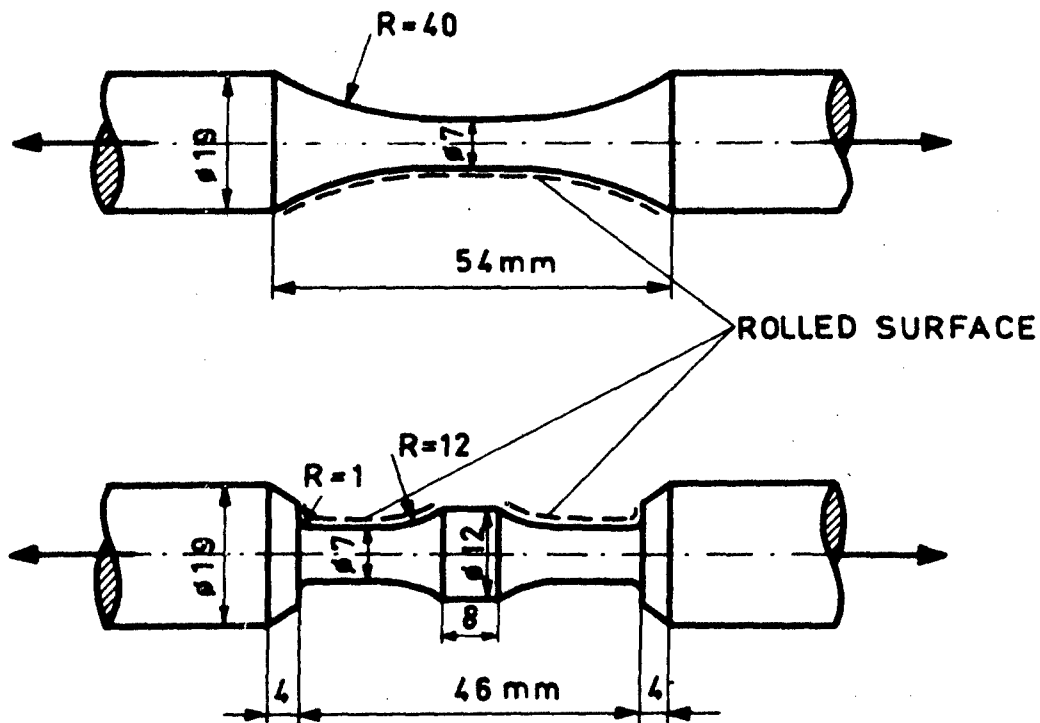


Fig. 2.1. Dimensions of test specimens.

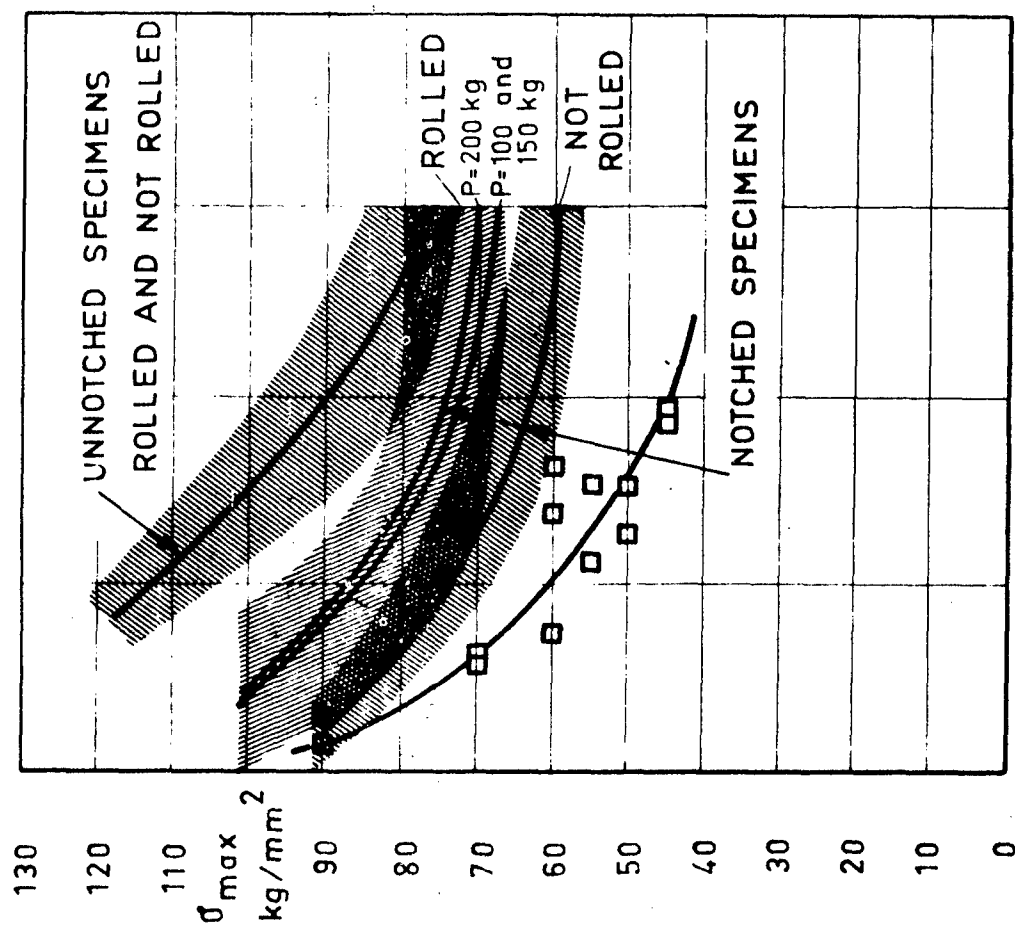


Fig. 2.3. Fatigue curves for specimens of Ry-Tuf steel.
 □ Notched, rolled specimens which have been pre loaded before fatigue-testing.

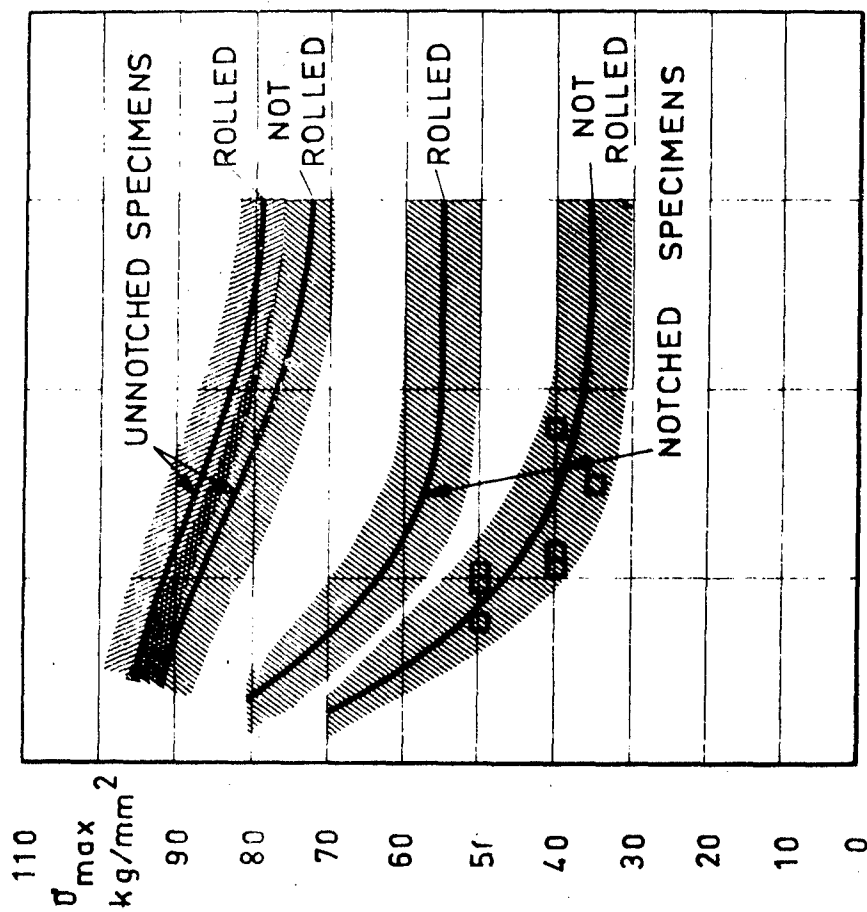


Fig. 2.2. Fatigue curves for specimens of Cr-Mo steel.
 □ Notched, rolled specimens which have been pre loaded before fatigue-testing.

10⁴ 10⁵ 10⁶ 10⁷ 10⁸
 CYCLES TO FAILURE

10⁴ 10⁵ 10⁶ 10⁷ 10⁸
 CYCLES TO FAILURE

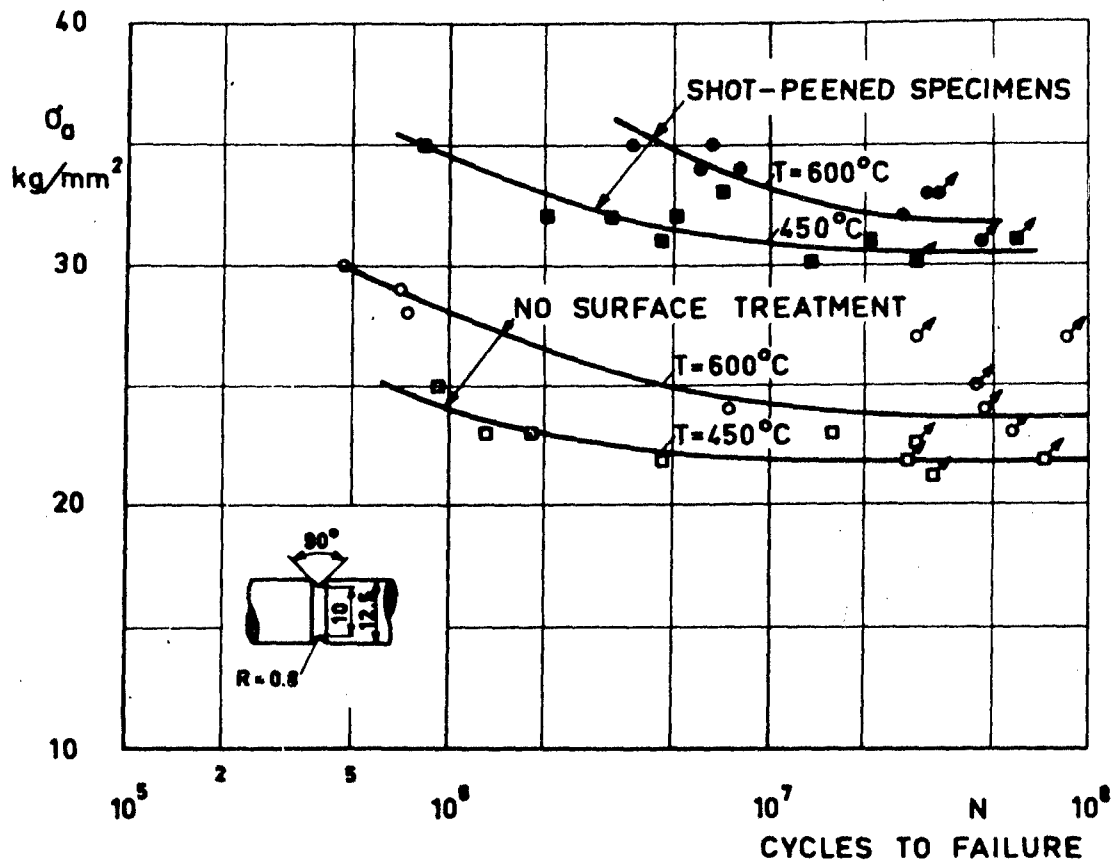


Fig. 3.1. Fatigue curves for notched specimens of Nimonic 90, loaded in rotating bending at 450 and 600°C. $R = -1$.

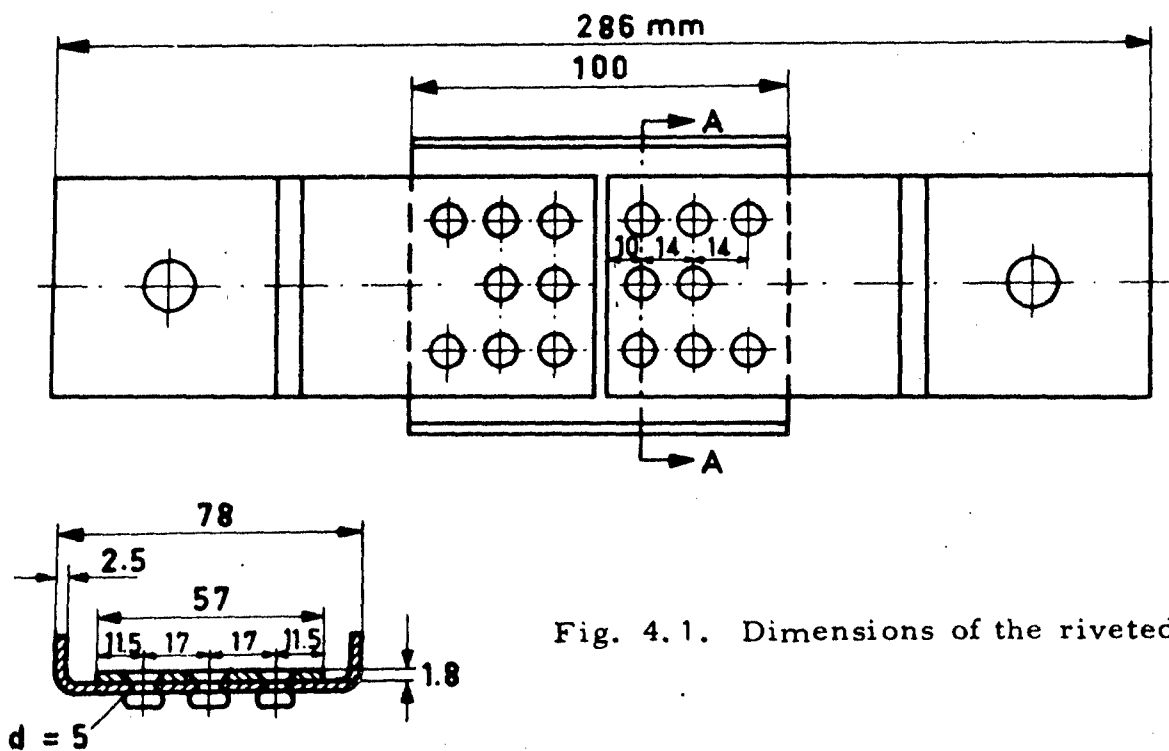


Fig. 4.1. Dimensions of the riveted joint.

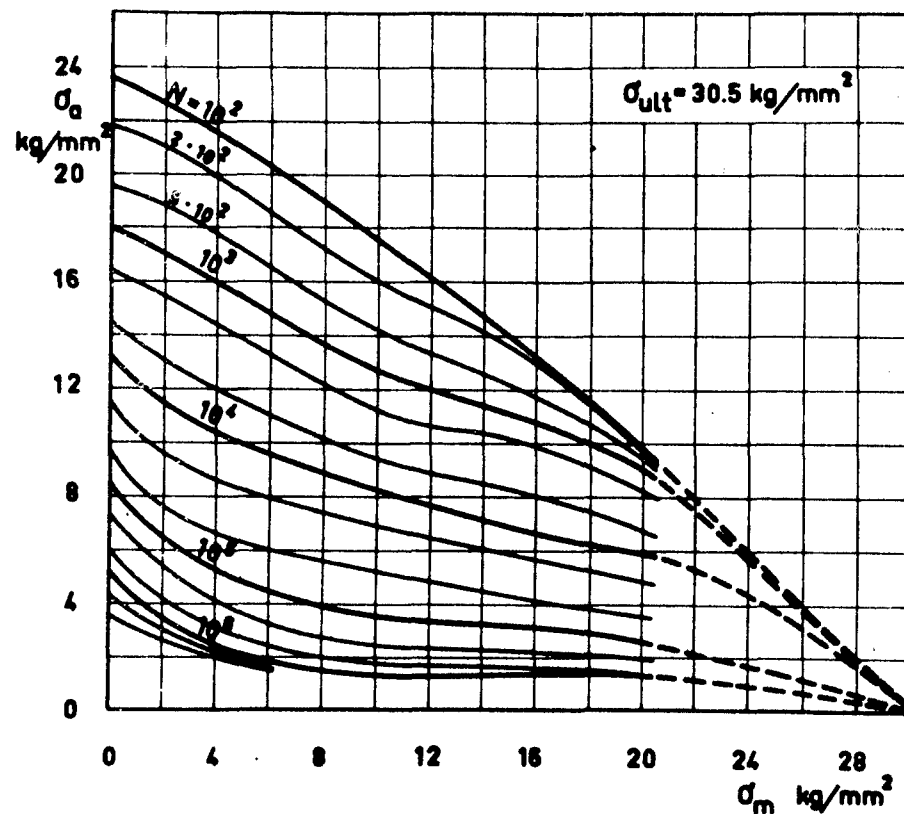


Fig. 4.2. The relationship between stress amplitude, σ_a , and the mean-stress, σ_m , for riveted joint shown in Fig. 4.1. The stresses are referred to the gross area.

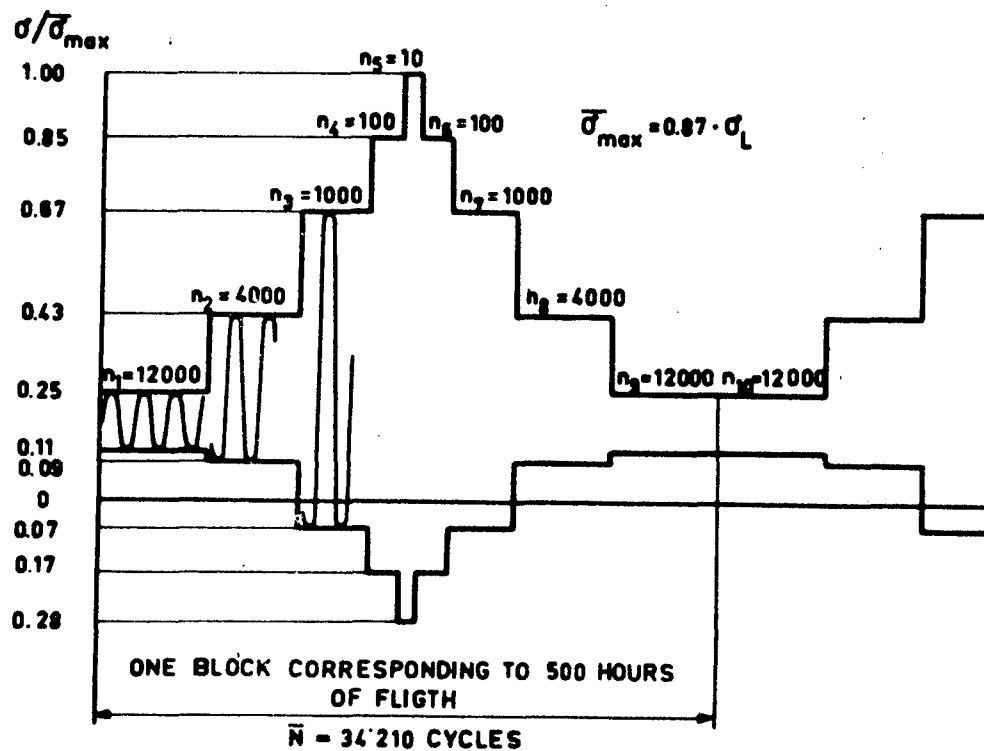


Fig. 4.3. Loading diagramme.. Programme A.
Programme B equal to A but the lower stress limit is constant and equal to zero.

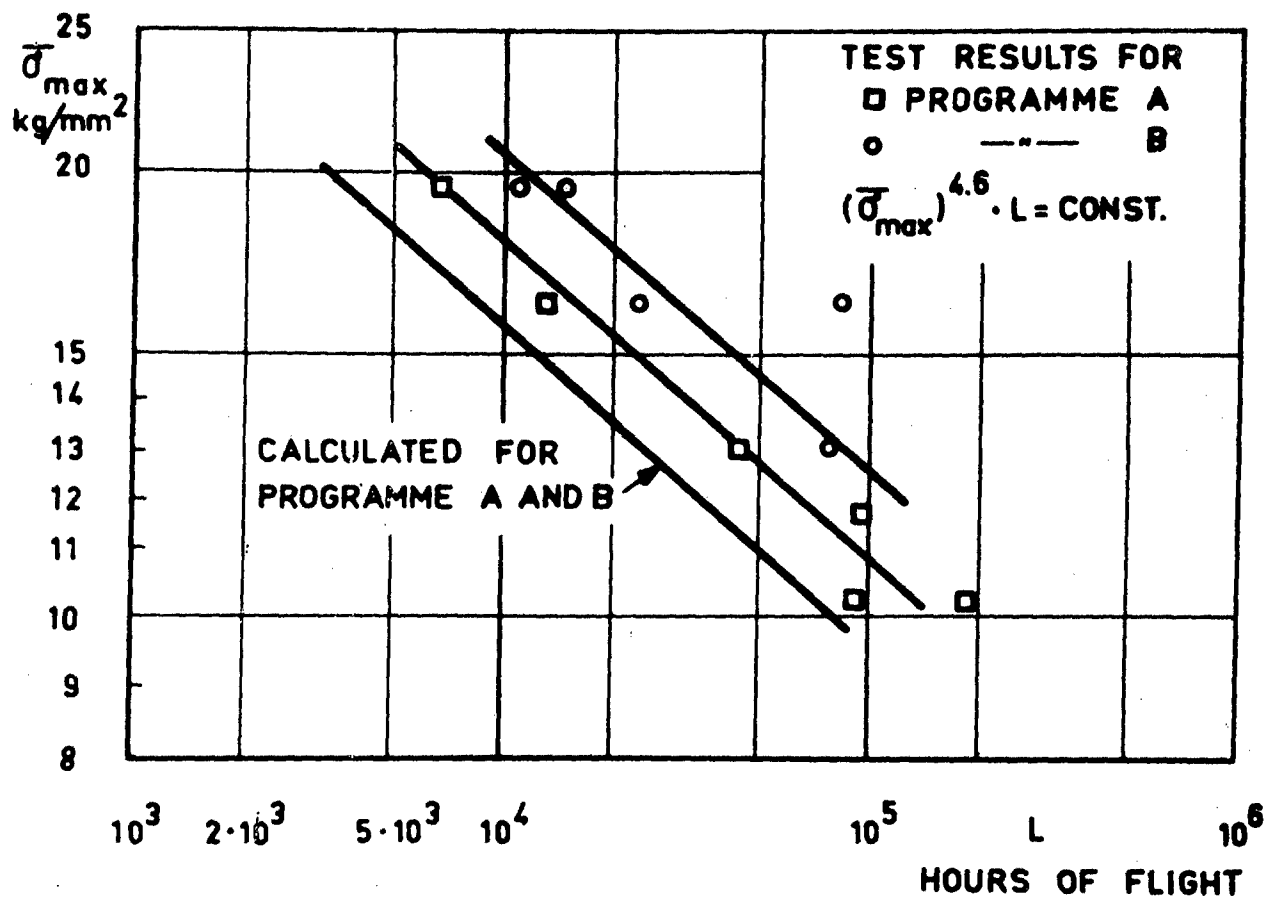


Fig. 4.4. Relationship between $\bar{\sigma}_{\max}$ and the life time for a riveted joint according to Fig. 4.1.

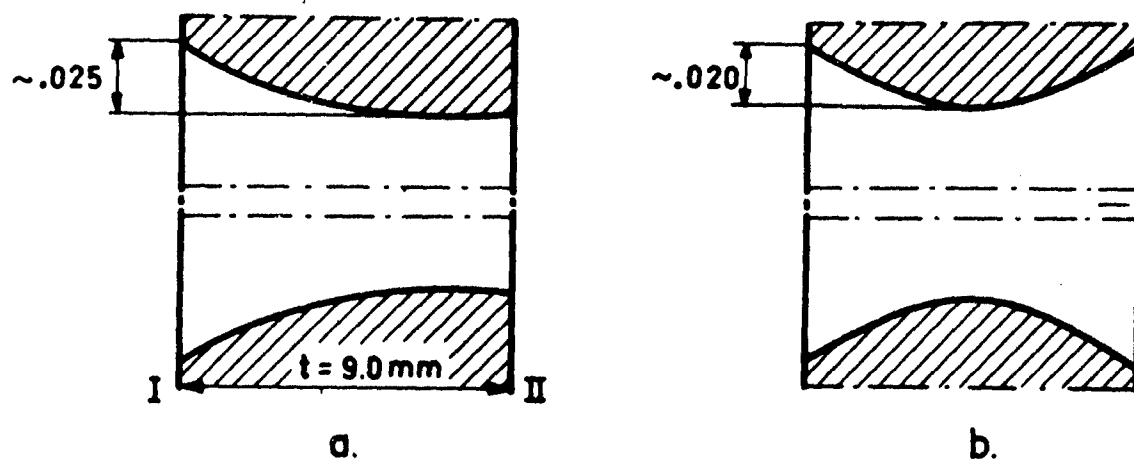
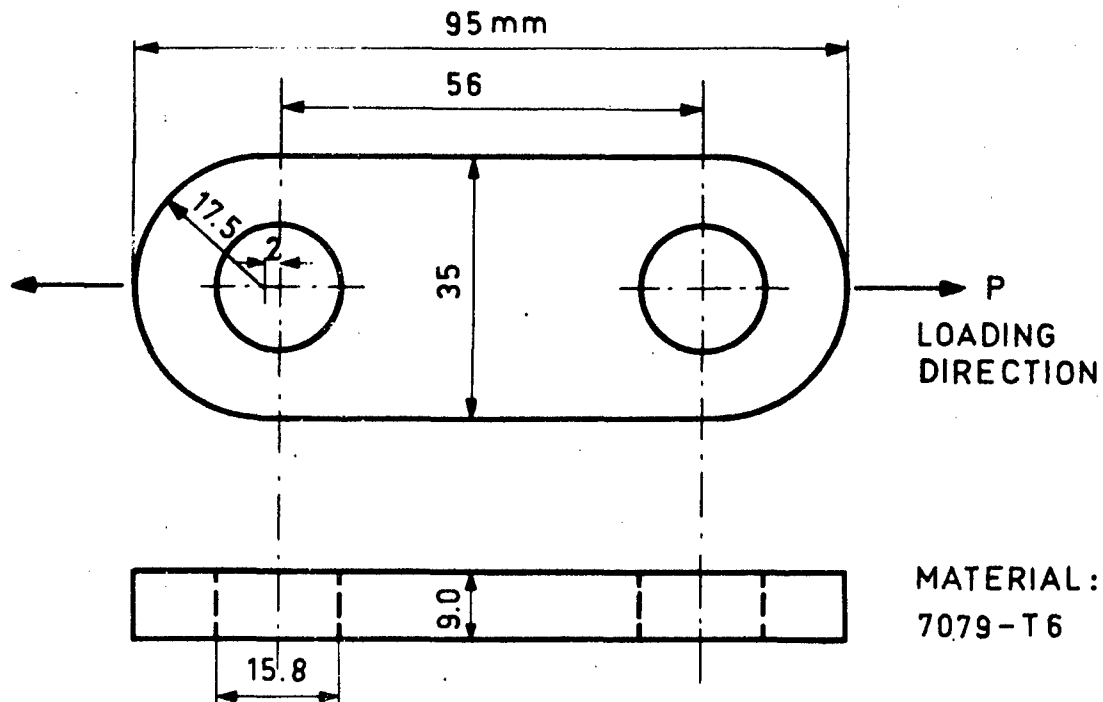


Fig. 5.1. Variation in hole diameter.

- The ball is pressed through the hole from side I.
- The ball is pressed through the hole from both sides.



Oversize of the ball %	Permanent expansion of the hole %	Number of lugs tested		
		Material thickness removed by reaming mm		
		0	.02	.12
1.2	0.6	[5 + 5 M ¹⁾]	-	-
1.7	1.1	[9 + 9]		4 + 4 M
2.5	1.8	-	[9 + 9 M]	-

¹⁾ M indicate that the bolt was coated with Molycote.

Fig. 5.2. Dimensions of test specimen and investigated combinations of cold-working and other treatments.

Clearance between pin and hole: .02 mm.

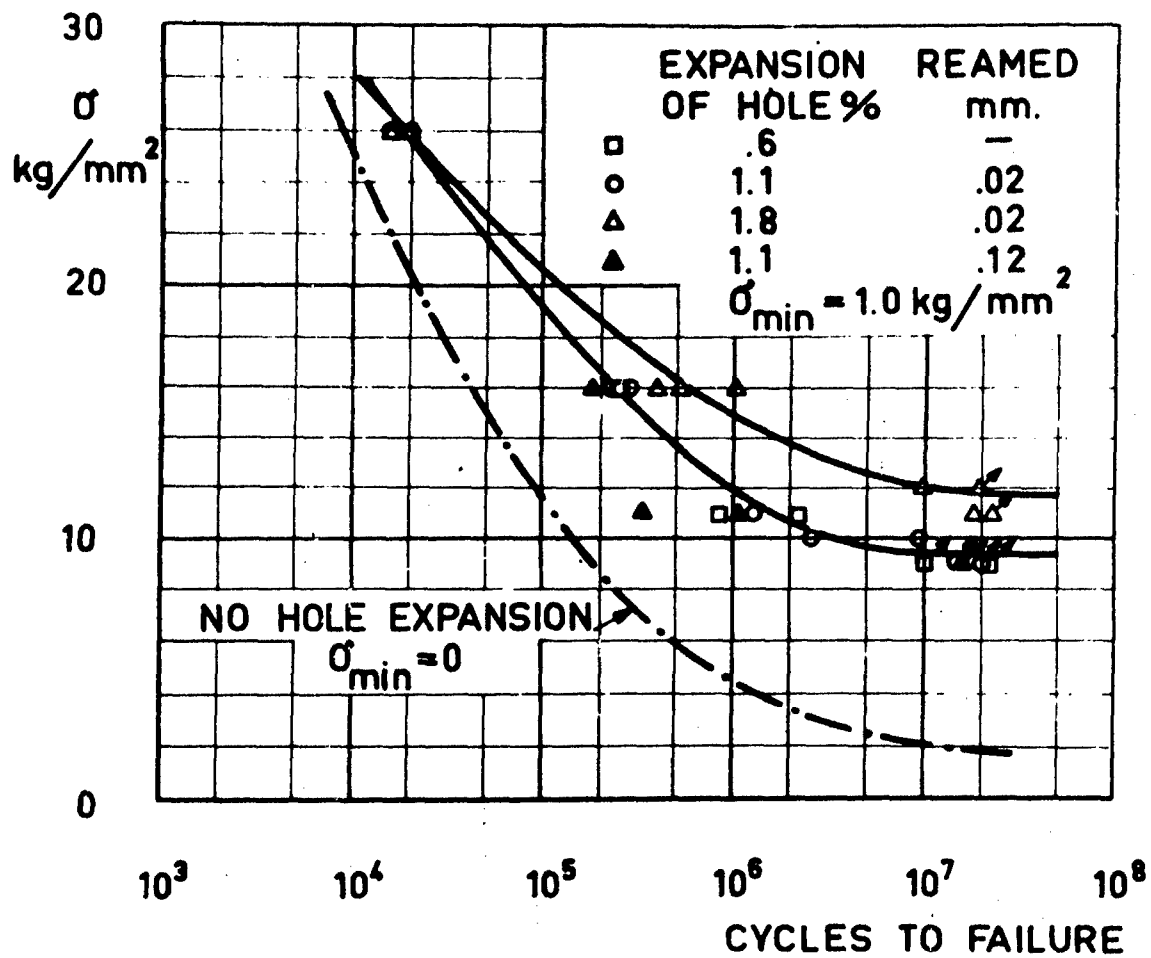


Fig. 5.3. Influence of expanded holes on the fatigue strength of lugs.

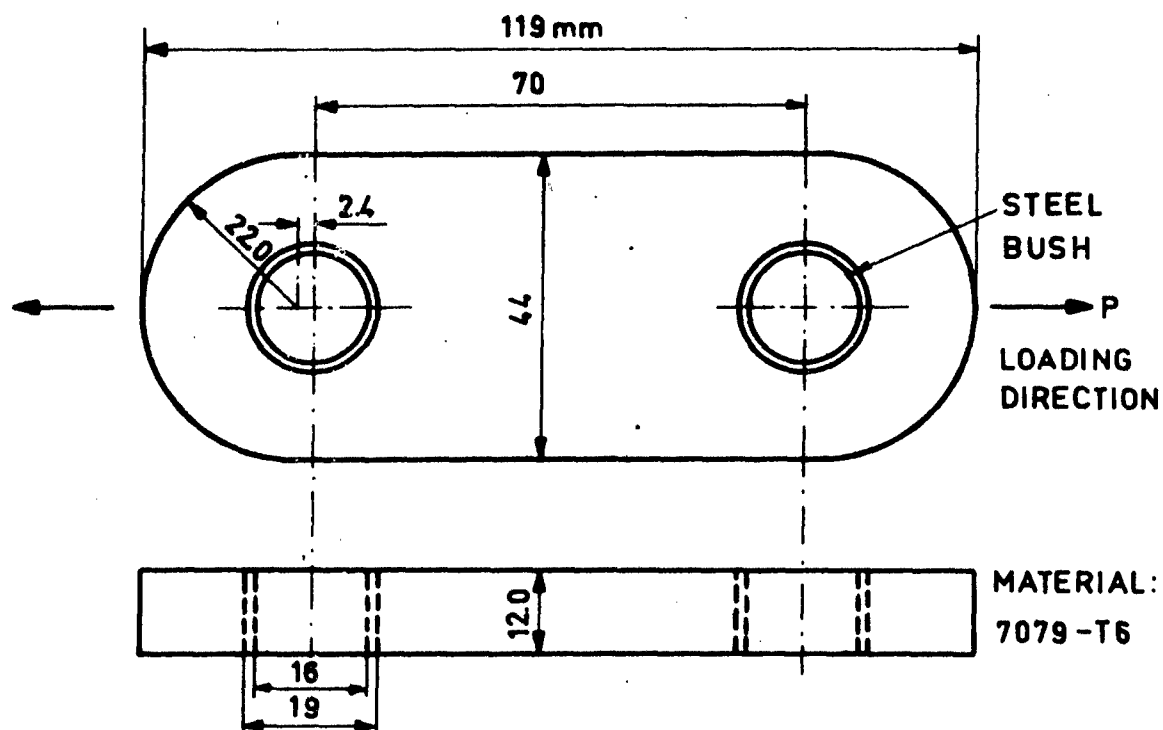


Fig. 5.4. Dimensions of testspecimen,

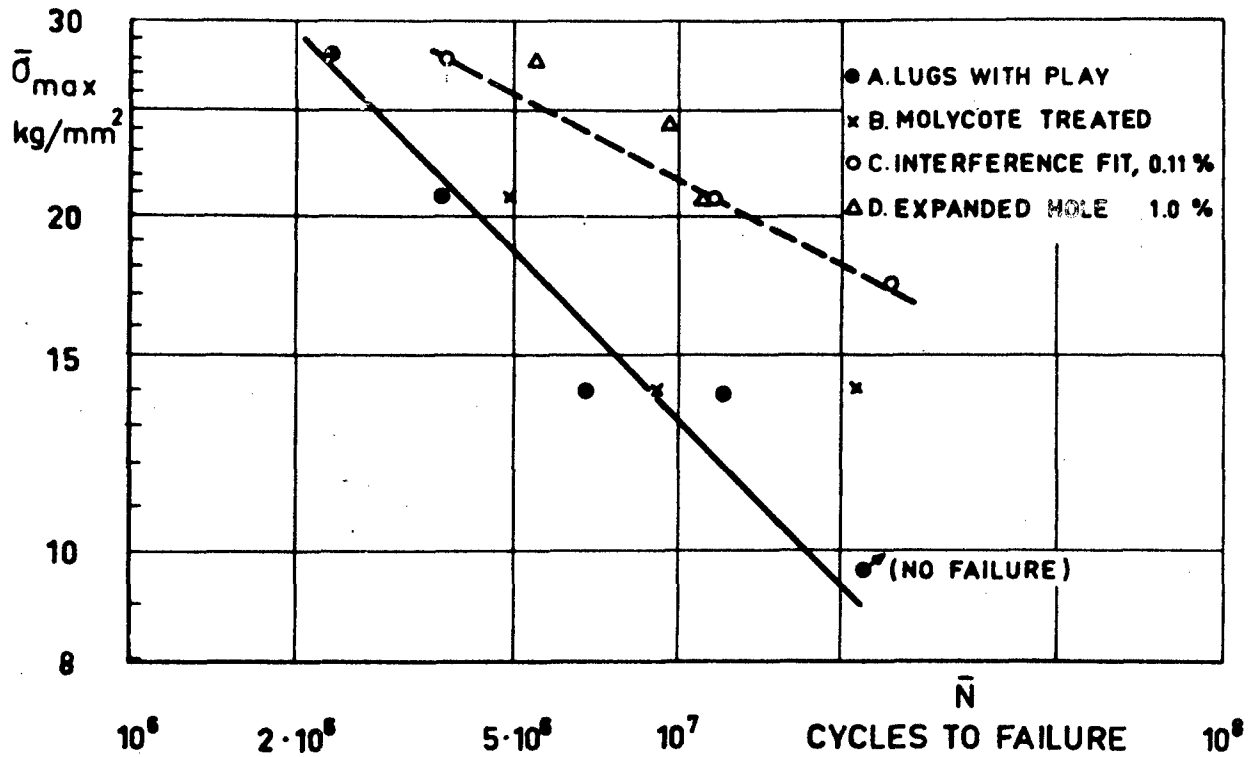


Fig. 5.5. Relationships between $\bar{\sigma}_{\max}$ and total number of cycles to failure for lugs according to Fig. 5.4.

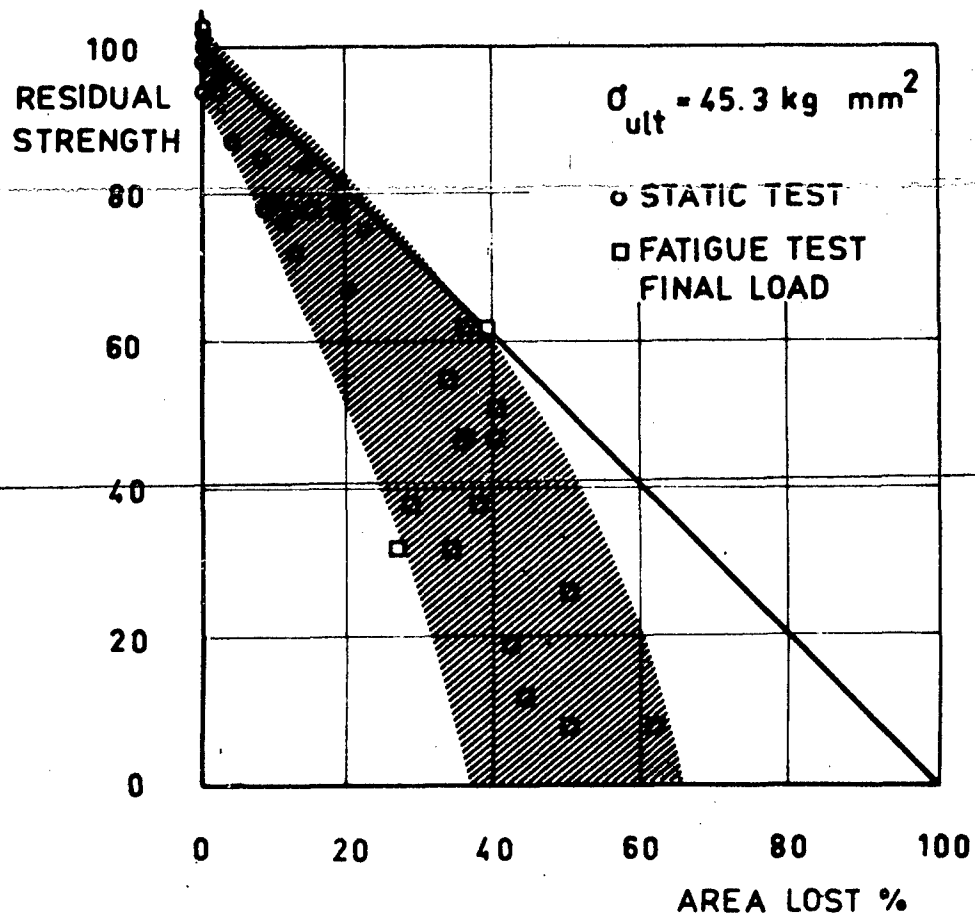


Fig. 5.6. The relationship between residual strength and area reduction for lugs according to Fig. 5.4

N 69-2159

A REVIEW OF AUSTRALIAN INVESTIGATIONS

ON AERONAUTICAL FATIGUE

DURING THE PERIOD APRIL 1965 TO MARCH 1967

Compiled by

J. Y. Mann

Aeronautical Research Laboratories

Department of Supply

Melbourne

CONTENTS

1.	INVESTIGATIONS ON MATERIALS	411
1.1	Silver-containing Al-Zn-Mg alloys	411
1.2	Relationship between fatigue behaviour and aged structure	411
1.3	The S/N curve discontinuity phenomenon	412
1.4	Axial load fatigue properties of extruded aluminium alloys	413
1.5	Batch to batch variation	413
1.6	Statistical properties of fatigue data	414
1.7	Cumulative damage	414
2.	FATIGUE OF JOINTS	415
2.1	Pin joints	415
2.2	Riveted joints	415
2.3	Welded S.A.E. 4130 Cr-Mo steel tubing	416
2.4	Skin-spar boom fastening methods	416
3.	FATIGUE OF COMPONENTS AND STRUCTURES	417
3.1	Airworthiness fatigue test of DH.104 'Dove' mainplane	417
3.2	Fatigue investigation of DH.115 'Vampire' wings	417
3.3	Fatigue investigation of Cessna 180 mainplane	417
3.4	Fatigue investigation of the Mirage IIIIO	418
4.	RELIABILITY AND RESIDUAL STRENGTH	418
4.1	Reliability study	418
4.2	Residual strength investigations	419
5.	KINETIC HEATING	419
5.1	Heat transfer in a fabricated structure	419
5.2	Investigations of shear webs under transient heating	420
6.	FLIGHT LOADS	420
6.1	Regular public transport aircraft	420
6.2	Agricultural and other light aircraft	420
6.3	Military aircraft	421
6.4	Atmospheric turbulence	421
6.5	Instrumentation	421
7.	FATIGUE LIFE ASSESSMENT	422
8.	FATIGUE PROBLEMS IN SERVICE	422
8.1	Fatigue of light aircraft	422
8.2	Aircraft control cables	423
8.3	'Sabre'	423
8.4	Economic aspects	423

CONTENTS (cont'd)

9.	MISCELLANEOUS, EQUIPMENT, TESTING TECHNIQUES, ETC.	424
9.1	Bibliography on the Fatigue of Materials, Components and Structures	424
9.2	Random noise fatigue machine	424
9.3	Rate of initial loading in fatigue tests	424
10.	PROPOSED FATIGUE RESEARCH	424
10.1	Crack propagation	424
10.2	Overheating of Al-Zn-Mg alloys during solution treatment	425
10.3	Directionality effects in aluminium alloy bar	425
10.4	Kinetic heating of full-scale structures	425
11.	ACKNOWLEDGEMENTS	425
12.	PUBLICATIONS	426
12.1	Referred to in the text	426
12.2	Other relevant publications	427

1. INVESTIGATIONS ON MATERIALS

1.1 Silver-containing Al-Zn-Mg alloys

The investigation of the influence of additions of 0.3 wt.% silver on the fatigue properties of the low-copper (0.45%) and high-copper (1.2%) versions of the aluminium-zinc-magnesium plate material D.T.D. 5060A has been continued. A summary of the most recent tests, on specimens taken from the longitudinal direction of the plates, is given in the following table.

Properties	DTD 5060A (0.45% Cu)		DTD 5060A (1.2% Cu)	
	No Silver	+0.3% Ag	No Silver	+0.3% Ag
T E N S I L E				
0.1% P.S. (psi)	68,800	69,300	72,500	74,000
U.T.S. (psi)	76,400	77,900	81,900	83,400
Elongation(%)	13	13	12.5	13
F A T I G U E				
Unnotched (psi)				
10 ⁶ cycles	27,000	27,000	25,000	25,000
	(17,000)	(17,000)	(17,000)	(17,000)
Notched (psi) - d=2				
10 ⁶ cycles	8,000	10,000	8,500	8,500
	(7,500)	(7,500)	(7,500)	(7,500)

x figures in parentheses are the short transverse properties.

Although the fatigue strengths of unnotched specimens taken from the longitudinal direction are significantly greater than those taken from the short transverse direction, there are only small differences in the fatigue strengths of notched specimens taken from the two directions.

1.2 Relationship between fatigue behaviour and aged structure

A study is being made of the fatigue processes in precipitation hardenable alloys in an attempt to optimise their metallurgical structure and fatigue behaviour. Two aspects are being investigated :

- (i) the effect of aged structure on fatigue strength;
- (ii) the effects of fatigue deformation on the aged structure.

Unnotched fatigue tests have been made on the ternary and commercial variants of RR.58 and 2L.65 aged to give particular structures. For the ternary alloys the zone structure resulted in the highest fatigue strength, the formation of intermediate and equilibrium precipitates being associated with progressively lower fatigue strengths. For the commercial alloys the zone and intermediate precipitate structures produced equally high fatigue strengths, but inferior properties were found in the overaged condition.

Surface deformation and fracture modes have been correlated with the fatigue properties and there are strong indications that slip band or shear mode fatigue is a slow fracturing process relative to the tensile mode fatigue fracture process. This has led to current experiments involving specimens in which a gradation in structure has been produced across the section, in such a way that the structure at the surface should have the maximum resistance to crack initiation and that in the interior maximum resistance to crack propagation.

Thin foil electron microscopy is also being carried out to establish, in more detail, the behaviour of the precipitates under the various fatigue deformation modes.

1.3 The S/N curve discontinuity phenomenon

A review of published work on this subject, supplemented by optical and electron microscopic examination of the fracture surfaces, has been completed (ref.1). Evidence has been found that the phenomenon is associated with differences in the mechanism of either fatigue crack initiation or propagation or both at different stress levels.

The discontinuity is apparent, to a marked degree, in S/N curves resulting from a rotating cantilever fatigue investigation on a number of cast, medium strength silver-containing aluminium alloys.

1.4 Axial load fatigue properties of extruded aluminium alloys

The investigation to determine comprehensive axial load fatigue data on 7178-T6 aluminium alloy has now been completed. It has involved a total of over 600 specimens tested under four tensile mean stresses (0, 12.5, 25 and 50% U.T.S.) and five different notch severities ($K_t = 1.6, 3.3, 5.2, 7.3$ and 10). More recent results support those reported in the last I.C.A.F. Review (ref.2) in showing that, under tensile mean stress conditions, notches can cause serious reductions in fatigue strength - much more so than under zero mean stress conditions. For example, at mean stresses of +12,500 and +25,000 p.s.i., the numerical values of K_f exceeded the relevant values of K_t in all cases. For a notch of $K_t = 5.2$, under a mean stress of 25,000 p.s.i. the value of K_f exceeded ten, while for the sharp notch it exceeded 30. No systematic correlation was found between the coefficient of variation of endurance and either the mean or alternating stresses. However, it was found that the coefficient of variation increased almost linearly with mean endurance, irrespective of mean stress and notch severity.

A similar investigation on 2L.65 aluminium alloy is nearing completion. For this alloy the absolute fatigue strengths in the unnotched conditions and for the notch of $K_t = 1.5$ are significantly less than for the 7178-T6 alloy, however for the other notches investigated there appears to be little difference in the fatigue strengths of the two alloys. The analysis of the data is not to the stage where any other comparisons are possible.

Unnotched fatigue tests on 2024-T4 aluminium alloy, the first phase of the investigation on this material, are now in progress.

1.5 Batch to batch variation

Eleven different batches of 2L.65 aluminium alloy have been manufactured into unnotched and notched (K_t values of about 2 and 4) rotating cantilever specimens. The determination of each S/N curve will involve approximately 50 specimens.

It is hoped to be able to isolate some of the sources of variability of fatigue properties and behaviour between batches of the same alloy.

1.6 Statistical properties of fatigue data

A survey of data on the variability in fatigue life of notched specimens and aluminium alloy structures has been carried out. This has enabled a comparison to be made of the standard deviation of the log-life under various types of loading sequences and under service conditions. The general conclusions are that :

- (i) there is a significant difference in variance under different types of load histories;
- (ii) there is a difference between the variance of notched specimens and structures under similar stress histories;
- (iii) although little data are available, there is an indication that the variance for service failures is significantly less than that obtained in relevant laboratory tests.

An investigation has now commenced into the probability distribution and variance of fatigue data under both constant amplitude and random loading sequences. The project involves the testing of a total of over 1000 notched specimens ($K_t = 3.1$) of 2L.65 aluminium alloy at a mean stress of 12,500 p.s.i. It is intended to examine theories for predicting the life distribution under programme and random loading from that under constant amplitude cycling.

1.7 Cumulative damage

A survey of the subject of cumulative fatigue damage is being made and the concepts of cumulative damage examined. A cumulative damage model has been enunciated having the damage capacity of a specimen or population defined by a single parameter. This model leads, in general, to a non-

linear cumulative damage theory though degenerating to the Palmgren-Miner linear hypothesis in some restricted and infrequent cases. It has been applied to predicting life distributions for two and three load level programme tests (ref.3).

2. FATIGUE OF JOINTS

2.1 Pin joints

The investigation on 2024 aluminium alloy pin joint specimens under axial loading at $R = +0.1$, reported in the last Review (ref.2), has been extended to cover tests on 2L65 aluminium alloy. Similar results have been obtained in that an 0.010 inch expansion on the 0.375 inch diameter hole has resulted in at least a 100 times increase in endurance.

In order to evaluate the influence of cyclic pre-stressing on subsequent fatigue endurance, a series of two load level tests was made on specimens with 'as reamed' holes. These were fatigue tested to different percentages of their mean endurances to failure at one stress level and then cycled to failure at either higher or lower stress levels. The results to date indicate that cyclic pre-stressing of up to 25% of the mean failure endurance has no influence on the subsequent endurance at lower or higher alternating stresses.

2.2 Riveted joints

A series of fatigue tests, under both constant amplitude and programme loading, has been carried out on small double row countersunk head riveted joints in 2024 alclad sheet. As a result of a number of failures in the pin joint within the 'grip' portion of specimens tested under programme loading, an investigation was made into the feasibility of several methods for increasing the fatigue strength of the end portions, including the bonding on of steel plates and expanding the hole by cold working. Initial tests have shown that both methods increase the fatigue strength of the ends by a sufficient margin to consistently result in failure along the rivet lines.

2.3 Welded S.A.E. 4130 Cr-Mo steel tubing

The main phase of this investigation, to determine basic information on the axial load fatigue properties of welded Cr-Mo steel tubing heat treated after welding to a U.T.S. of 180,000 p.s.i., is now in progress. It is apparent that the fatigue strength of the welded tube is low, the estimated fatigue limits (at 5×10^6 cycles) for the three mean stresses employed being :

Mean stress zero	: fatigue limit 9,000 p.s.i.
Mean stress 20,000 p.s.i.	: fatigue limit 7,000 p.s.i.
Mean stress 40,000 p.s.i.	: fatigue limit 5,000 p.s.i.

It is significant that one aircraft featuring a welded tubular steel structure was recently scrapped following the discovery of a large crack in the lower spar boom. The crack was well outside repair limits and the operator decided that the extensive re-build necessary was not warranted.

2.4 Skin-spar boom fastening methods

Basic S/N curves, at tensile mean stresses of 4,000 and 10,000 p.s.i. have been determined from tests on full-size section spar boom specimens with 'skin' fastened by means of either Parker-Kalon (P-K) self-tapping screws or by pinned Chobert blind rivets. Some fatigue tests have also been made on 'drilled' specimens, i.e. Chobert rivet type specimens in which the holes were unfilled.

Initial indications were that the P-K screw method of fastening resulted in longer endurances than those resulting from the Chobert rivet type fasteners, but later tests on specimens with over-size P-K screws suggest that the difference may, in part at least, be associated with a smaller edge-fastener distance in the case of the riveted specimens. There appears to be no significant difference between the fatigue strength of the 'drilled' specimens and the Chobert rivet specimens. As reported previously, in several cases the Chobert rivets were observed to loosen and pull out under the repeated loading of the boom section.

3. FATIGUE OF COMPONENTS AND STRUCTURES

3.1 Airworthiness fatigue test of DH.104 'Dove' mainplane

The five load range programme load fatigue test on this structure, referred to in previous Reviews, has now been completed. Following a recalibration to correct for the greater stiffness of the modified centre-section booms, the report on the booms is being drafted.

Two modified 'Drover' centre section spar booms were also tested in the 'Dove' rig. The results have been used to set a mandatory retirement life on these booms in service.

3.2 Fatigue investigation of DH.115 'Vampire' wings

The comprehensive investigation on 'Vampire' wings, which was partly reported at the 4th I.C.A.F. Symposium at Munich (ref.4), has now been completed and the final report is being drafted.

A comparison of tests under the six load range programme sequence and under a random load sequence indicated that the type of sequence had no significant effect on either the mean fatigue life or the types of fatigue failure which developed.

3.3 Fatigue investigation of Cessna 180 mainplane

The six load range programme load fatigue investigation, carried out on two wings of this type of aircraft, has been completed. It has enabled safe lives to be estimated for the Cessna 180 when operating in three different roles - civil charter, agricultural and army reconnaissance, and has provided data on crack propagation rates and the residual strength of a typical light aircraft wing structure.

In conjunction with the Defence Standards Laboratories. (D.S.L.) an X-ray inspection technique was developed to detect failures in the critical regions of the structure (ref.5). The fatigue cracks, which developed during initial testing to an advanced stage, were subsequently extended by saw cuts.

After further fatigue cycling the structure withstood proof load, thus satisfying the B.C.A.R. requirement for 'fail-safe'. By applying the fail-safe principle and adopting the recommended inspection procedure a considerable extension in life is possible.

The rear spar failure which had occurred in service under agricultural operations did not appear in the laboratory tests. Strain measurements taken both in the rig and in flight confirmed predictions that this particular failure could result from dynamic loads produced during landing and taxiing on unprepared runways (ref.6). These loads had not been included in the test spectrum.

3.4 Fatigue investigation of the Mirage IIIO

A preliminary fatigue analysis of the structure of the Mirage III, based on conditions representative of R.A.A.F. operations, indicated that in some areas of the structure the fatigue-life may be inadequate. It has been proposed that an airframe be instrumented, during fabrication, with both electric resistance strain gauges and temperature sensors; and that this particular aircraft be subjected to a flight programme whereby the temperature and strain spectra of the structure can be determined.

4. RELIABILITY AND RESIDUAL STRENGTH

4.1 Reliability study

In earlier work carried out in association with Professor Freudenthal of Columbia University, it was proposed that the acceptable life under fatigue loading could be defined as the life at which the risk of fatigue failure became equal to the risk of ultimate failure. This is a quantitative criterion which embraces both the fail-safe and safe-life philosophies and is capable of extension to other mechanisms of progressive deterioration such as creep (ref.7). This approach requires, however, that the risk of failure be predicted as a function of the life. Representative crack propagation and residual strength data from structures tested in fatigue are being utilized in order to investigate the correlation between the various parameters involved.

4.2 Residual strength investigations

Residual strength tests have been conducted on four 'Vampire' wings all of which had the same amount of prior damage resulting from the development of fatigue failures. The redistribution of tensile load around the failures involved multiple redundancies and it was considered that the data was, therefore, reasonably representative of the redundant type of construction. The coefficient of variation of the failing load was 4.2%, which is consistent with representative values for ultimate strength of undamaged structures. These results provide some valuable data on the variability in strength of structures cracked to the same extent, information which is essential for the reliability approach to airworthiness.

As indicated in section 3.3, the test on the Cessna 180 mainplane also provided further information on the residual strength of cracked structures.

5. KINETIC HEATING

5.1 Heat transfer in a fabricated structure

Some consideration has been given to predicting the temperature distribution in a fabricated structure subjected to transient heating and cooling. An electrical analogue has been used to investigate the heat conduction problem in a skin-spar web assembly.

A research project is now current on the question of heat diffusion by convection. This includes a theoretical study of convective heat transfer in a closed cell with heat absorbing walls, the upper and lower surfaces of the cell being maintained at a steady temperature. A thermodynamically similar model, using a suitable fluid in a rectangular cell, has been designed to experimentally investigate the theoretical analysis.

5.2 Investigations of shear webs under transient heating

An investigation has commenced on the relative efficiency of seven different types of aluminium alloy shear webs in box beams subjected to transient heating and cooling conditions. In the first stage of the investigation a plain web, a corrugated web and a web with lightening holes will be used. The programme includes shear loading at room temperature and under a temperature cycle from room to 130°C. The specimens will be instrumented with electric resistance strain gauges, temperature sensors and displacement transducers, and the web stresses and structural deflections compared with values predicted by theory. In initial tests the principal stresses obtained showed good agreement with those which were predicted.

6. FLIGHT LOADS

6.1 Regular public transport aircraft

The effects of route, altitude and time of year on the flight loads experienced by a type of regular civil transport aircraft have been investigated (ref.8).

The N.A.S.A. V-g-H Recorder is to be fitted to two of the Douglas DC-9 aircraft recently introduced on the Australian domestic services, following the successful programme of recording which involved the Boeing 727.

6.2 Agricultural and other light aircraft

A considerable amount of data have been collected from light aircraft in a variety of operational roles. Although a general body of usable gust load data for such operations as private, charter, flying training, and aerial survey are not yet available, in several cases valuable results have been obtained for specific aircraft.

As part of the Australian attack on the fatigue problem in agricultural aircraft, flight load data have been obtained for four aircraft types, including two manufactured

in Australia (refs.9-13). In one investigation it was subsequently shown that the frequent landings, occurring at five or six minute intervals, caused a very great reduction in fatigue life. In another study (ref.11), seven different pilots flew the same aircraft on nominally identical missions, but a large variation occurred in the frequency of loads of a given severity. As a result of these investigations, some suggested criteria for airworthiness have been proposed.

6.3 Military aircraft

Flight load data have been collected from Australian 'Sabre' fighter aircraft and from 'Winjeel' primary trainers, and safe life predictions made for critical regions of these aircraft.

6.4 Atmospheric turbulence

Australia is interested in the basic study of atmospheric turbulence, and particularly in clear air high altitude turbulence. Analysis of the experimental project - 'TOFCAT' - which was carried out in 1963 is continuing (refs.14-15).

In 1966 Australia collaborated with the United States in a project - 'HICAT' - in which a U2 aircraft searched for turbulence in the jet stream over Australia, at altitudes of from 50,000 to 70,000 feet. Turbulence was encountered on numerous occasions, and once at 67,000 feet it was so extensive and so severe that the U2 pilot was on the point of taking avoiding action. Australia has arranged with the United States to participate in the analysis of the results on aspects in which we are particularly interested.

6.5 Instrumentation

A study has been made of the precision and constancy of fatigue meters (ref.16). The variability included drifts of the threshold levels from one calibration to the next, and 'fuzziness' of the thresholds. As these appeared to be functions of time, it was recommended that meters be recalibrated at six monthly intervals.

An Australian civil transport aircraft is being used to test a memory gust recorder which has been developed in Canada. When activated above a selected threshold (by, for example an acceleration), the instrument will record the time history of several input signals from two minutes before the event until two minutes after or longer if the disturbance persists.

The instrumentation necessary for the magnetic tape flight data recording system, briefly referred to in the last Australian review, has now been procured and used for some preliminary trials. The equipment has the capacity, with time multiplexing, for recording some hundreds of input channels of data. Consideration is being given to data conversion to digital form before recording as a means of avoiding unnecessary degradation of the information in recording and replay.

7. FATIGUE LIFE ASSESSMENT

During the past two years the Aeronautical Research Laboratories and the Commonwealth Aircraft Corporation Pty. Ltd. have conjointly investigated the fatigue life of several military aircraft, including the 'Sabre', 'Neptune' and 'Hercules' operating under local service conditions.

8. FATIGUE PROBLEMS IN SERVICE

8.1 Fatigue of light aircraft

The problem of the fatigue substantiation of light aircraft continues to cause a great deal of concern to the Australian D.C.A. There are a large number of such aircraft operating in Australia which were not subjected to any real fatigue justification during their initial certification. In addition some of these aircraft are being utilized in roles for which they were not basically designed and are accumulating 'hours' at a rapid rate.

8.2 Aircraft control cables

The significance of the wear and fatigue problem in control cables was recently highlighted by the failure of a 'Chipmunk' rudder cable during a spin. The cable was found to be badly worn, with a pre-existing failure of the heart strand. A survey report, supplemented by static tests made at the Aeronautical Research Laboratories, is being prepared.

8.3 'Sabre'

Fatigue failures have occurred in several areas of the 'Sabre', including the main landing gear retraction cylinder support casting and eye bolt, resulting in the redesign of the defective parts. Fatigue cracks have also been detected in the unmodified centre section to outer wing joint structure, thus confirming American findings. This section is being rebuilt according to a manufacturer's modification.

8.4 Economic aspects

Airline operators are becoming increasingly sensitive to the quite severe economic penalties imposed by the sudden appearance of unexpected major fatigue cracks, stress corrosion defects, etc. The urgent fleet-wide inspections, followed by frequent repetitive inspections and possibly replacement or modification action, result in major disruptions to maintenance scheduling and availability of aircraft. The increasing seriousness of this aspect of fatigue is reflected in the steadily increasing number of cases where operators request an increase in a certain inspection interval or a short 'over-run' of a component retirement life in order to meet operational exigencies or to fit in with changed maintenance schedules. It is believed that airline operators will soon be requiring that manufacturers give a very convincing proof of a long crack-free life, and that this in itself may well lead to an increasing use of full-scale fatigue testing of airframes and major components for both heavy and light aircraft.

9. MISCELLANEOUS, EQUIPMENT, TESTING TECHNIQUES, ETC.

9.1 Bibliography on the Fatigue of Materials, Components and Structures

The manuscript of this work, covering published work on the subject up to and including the year 1950, is now complete and has been submitted to the Royal Aeronautical Society. It lists 4080 references and contains comprehensive subject and author indexes.

9.2 Random noise fatigue machine

The development of this machine is now almost complete, and preliminary tests under both constant amplitude cycling and a random noise sequence have been carried out. The alternating load is applied by an electro-magnetic vibrator coupled to the specimen through piezo-electric crystals which provide both load measurement and control. The other end of the specimen is connected to a seismic mass, thus eliminating resonances which would be introduced by a rigid machine frame. Frequency of cycling is 180 c.p.s.

9.3 Rate of initial loading in fatigue tests

Rotating cantilever tests have been carried out on unnotched and notched ($K_t = 1.5$ and 10) specimens made from 2024 aluminium alloy extruded bar. In each case initial rates of loading of 16 and 560 p.s.i. per cycle were used. It was found that in general, at a particular stress level, the initial rate of loading caused no significant differences in the endurances to failure.

10. PROPOSED FATIGUE RESEARCH

10.1 Crack propagation

In connection with the study of cumulative damage, an analogy has been drawn between damage and fatigue crack size. A proposed programme of further work, following from that referred to in the last Review, envisages tests on large prismatic material specimens and on actual structural components removed from aircraft in service. Some of the latter would be expected to contain small fatigue cracks.

10.2 Overheating of Al-Zn-Mg alloys during solution treatment

Evidence of 'overheating' has been observed in some failed components submitted for examination, and doubts have been expressed as to whether or not it could significantly influence fatigue properties. Some preliminary metallographic work and tensile testing has been carried out on specimens of D.T.D. 683 aluminium alloy extruded bar, solution treated at up to 100°C above the Specification limits. Blanks for fatigue specimens are being solution treated at the Specification temperature (465°C) and at 495, 525 and 555°C.

10.3 Directionality effects in aluminium alloy bar

It is proposed to investigate the fracture characteristics and endurance of specimens cut from three directions, relative to the direction of extrusion, in 2024 aluminium alloy rectangular section extruded bar. Both unnotched and notched fatigue tests will be included in this investigation.

10.4 Kinetic heating of full-scale structures

Consideration is being given to an investigation involving the repeated loading, concurrent with thermal cycling at moderate heating and cooling rates, of an aluminium alloy aircraft structure. These tests, which may involve 'Mustang' wings, will provide background information on the behaviour of such structures under kinetic heating conditions and allow a direct comparison with the behaviour of the particular structure at room temperature.

11. ACKNOWLEDGEMENTS

The co-operation of the Department of Civil Aviation, the Australian aircraft industry and my colleagues at the Aeronautical Research Laboratories in preparing this Review is gratefully acknowledged. It is published with the permission of the Chief Scientist, Department of Supply.

12. PUBLICATIONS12.1 Referred to in the text

1. Finney, J.M. A review of the discontinuity or hump phenomenon in fatigue S/N curves: theories and further results. Dept. Supply, Aero. Res. Labs., Report ARL/SM.314, March, 1967.
2. Mann, J.Y. A review of Australian investigations on aeronautical fatigue during the period April 1963 to March 1965. Dept. Supply, Aero. Res. Labs., Tech. Memo. ARL/SM.141, May, 1965.
3. Hooke, F.H. Some thoughts on cumulative fatigue damage theory. Dept. Supply, Aero. Res. Labs., Report ARL/SM.315, April, 1967.
4. Patching, C.A. and Mann, J.Y. Comparison of an aluminium alloy structure with notched specimens under programme and random fatigue loading sequences. Paper presented at the 4th I.C.A.F. Symposium, Munich, June, 1965.
5. Benoy, M.B. and Baxter, M.A. A radiographic inspection technique for Cessna 180 mainplanes. Dept. Supply, Aero. Res. Labs., Internal Tech. Memo. March, 1966.
6. Benoy, M.B. An investigation into the fatigue of Cessna wings at the rear spar root fillet. Dept. Supply, Aero. Res. Labs., Internal Tech. Memo. Dec., 1966.
7. Payne, A.O. Reliability approach to structural airworthiness. Aircraft, vol. 45, no. 1, Oct., 1965, pp.16-20.
8. Visick, J. Variability of flight loads on 'Viscount' aircraft as affected by route, month and altitude. Dept. Supply, Aero. Res. Labs., Report ARL/SM.308, Nov., 1965.
9. Patterson, A.K. Estimation of response parameters and confidence intervals in flight testing, with application to experiments on a 'Beaver' aircraft. Dept. Supply, Aero. Res. Labs., Report ARL/SM.309, Nov., 1965.
10. Visick, J. Loading actions on a 'Prospector' agricultural aircraft. Dept. Supply, Aero. Res. Labs., Note ARL/SM.309, Aug., 1966.

11. Foden, P.J. Flight load spectra for 'Beaver' aircraft on agricultural operations.
Dept. Supply, Aero. Res. Labs., Note ARL/SM.312, Sept., 1966.
12. Foden, P.J. Mean life estimates for wing strut of 'Beaver' aircraft on agricultural operations.
Dept. Supply, Aero. Res. Labs., Note ARL/SM.316, April, 1967.
13. Trayford, R.S. Flight load spectra and strain prediction equations for 'Ceres' aircraft.
Dept. Supply, Aero. Res. Labs., Note ARL/FL.41, March, 1967.
14. Burns, A. and Rider, C.K. Project Topcat - power spectral measurements of clear air turbulence in jet streams.
R.A.E. Tech. Rep. no. 65210, Sept., 1965.
15. Morgan, T.D. and Rider, C.K. Report on the conduct of clear air turbulence trials in Australia, July-October, 1963.
Dept. Supply, Weapons Res. Estab., Report TRD.18, Jan., 1966.
16. Nilsson, J. An examination of the precision and constancy of fatigue meters.
Dept. Supply, Aero. Res. Labs., Note ARL/SM.315, Dec., 1966.

12.2 Other relevant publications

1. Finney, J.M. and Vann, A. Axial load fatigue behaviour of 7178-T6 aluminium alloy notched specimens under three different loading spectra.
Dept. Supply, Aero. Res. Labs., Report ARL/SM.307, Nov., 1965.
2. Mann, J.Y. Fatigue of Metals - where it stands today.
Dept. Supply, Aero. Res. Labs., Note ARL/SM.305, March, 1966.
3. Finney, J.M. and Vann, A. Actual and predicted fatigue behaviour of 24 S-T and 2L.65 aluminium alloy notched specimens under both symmetric and asymmetric random loading spectra.
Dept. Supply, Aero. Res. Labs., Report ARL/SM.313, Nov., 1966.
4. Mann, J.Y. Fatigue of Materials - an introductory text.
Melbourne University Press, Carlton, 1967, pp.155.

CLOSED TECHNICAL MEETING

MELBOURNE

May 25 - 26, 1967

14.1 LIST OF PARTICIPANTS AT THE CLOSED TECHNICAL MEETING

The Closed Technical Meeting was held in the Theatrette of the National Mutual Centre, Collins Street, Melbourne on 25th - 26th May, 1967. It was attended by the following persons.

AUSTRALIA

<u>MANN, J.Y.</u>	Aeronautical Research Laboratories, Department of Supply, Melbourne (A.R.L.)
AXISA, R.	Trans-Australia Airlines, Melbourne
FINNEY, J.M.	A.R.L.
GORJANICYN, H.	Commonwealth Aircraft Corporation Pty. Ltd., Melbourne
GORNALL, W.J.	Commonwealth Aircraft Corporation Pty. Ltd., Melbourne
GRAFF, D.G.	Trans-Australia Airlines, Melbourne
HOOKE, F.H.	A.R.L.
HOOVER, D.R.	Government Aircraft Factories, Department of Supply, Melbourne
MACNAUGHTAN, J.	Department of Air, Canberra
MILLICER, H.K.	Vieta Aviation, Milperra, N.S.W.
MILLIGAN, I.S.	Department of Civil Aviation, Melbourne
O'BRIEN, K.R.A.	Department of Civil Aviation, Melbourne
PATCHING, C.A.	A.R.L.
PAYNE, A.O.	A.R.L.
SCOLES, B.A.J.	Department of Civil Aviation, Melbourne
STEVENS, R.H.	Qantas, Sydney
WOODGATE, B.G.	Trans-Australia Airlines, Melbourne

FRANCE

<u>BARROIS, W.</u>	Service Technique de l'Aeronautique, Paris
--------------------	---

GERMANY

<u>BUXBAUM, O.</u>	Laboratorium für Betriebsfestigkeit, Darmstadt-Eberstadt
" KRÄMER, D.E.	Lufthansa German Airlines, Hamburg- Fuhlsbüttel

NETHERLANDS

van BEEK, E.J. Royal Netherlands Aircraft Factories
"Fokker", Schiphol-Zuid

NEW ZEALAND

LABETT, E.T. Department of Civil Aviation,
Wellington

MILLER, N.A. Department of Scientific and Industrial
Research, Petone

SWEDEN

EGGWERTZ, S. Flytekniska Försöksanstalten (Aeronaut-
ical Research Institute of Sweden -
FFA), Bromma

JARFALL, L.E. Flytekniska Försöksanstalten, Bromma

SWITZERLAND

BRANGER, J. Eidgenössische Flugzeugwerk, Emmen

HUEPPI, H. Swissair, Kloten

WEIBEL, J.P. Eidgenössische Flugzeugwerk, Emmen

UNITED KINGDOM

RIPLEY, E.L. Royal Aircraft Establishment,
Farnborough

LAMBERT, J.A.B. Hawker Siddeley Aviation Ltd., Hatfield

PHILLIPS, C.E. National Engineering Laboratory, East
Kilbride

TROUGHTON, A.J. Hawker Siddeley Aviation Ltd.,
Woodford

UNITED STATES OF AMERICA

HARDRATH, H.F. NASA Langley Research Centre, Hampton

DONELY, P. NASA Langley Research Centre, Hampton

SWANSON, S.R. MTS Systems Corp., Minneapolis

14.2 REVIEW OF MUNICH RESEARCH RECOMMENDATIONS*

This part of the Meeting was chaired by Mr. J. Branger

1. Investigations on the correlation of component test results with complete airframe tests, as well as the correlation between fatigue strength of simple specimens and of components

Relevant investigations on complete structures, full-scale structural assemblies and components and more simple specimens were referred to in several National Reviews. However, no additional data relating to service experience were presented.

Several speakers expressed doubts as to whether tests on pieces of structure could provide a precise or even a good estimate of service life. In general such tests indicated longer lives than obtained from tests on a complete structure, and were more useful in providing qualitative information in the design or development stages.

It was also stressed that a representative full-scale fatigue test is the only way of ensuring where and when to inspect for cracks under service conditions. It was stated that the expense involved in a full-scale fatigue test could well be much less than that involved as a result of unnecessary maintenance and crack inspection schedules.

2. Investigations on the most suitable design of flight-by-flight tests (influence of the individual load levels and their frequencies on the test result)

There was general agreement as to the desirability

* Refer to "Minutes of the Ninth Conference of the International Committee on Aeronautical Fatigue", part II, p. 229.

of flight-by-flight testing. Several Delegates indicated that future tests in their countries would be based on more complex and sophisticated random loading sequences which would closely approximate the desired flight load spectra. Others indicated that suitable testing equipment for this purpose was being procured.

There was reluctance, however, to recommend a definite testing procedure applicable to all circumstances as important deviations could depend upon the type and mission of the aircraft.

3. Investigations on the possibilities of using one or more standardised load spectra for basic tests on the influence of materials and detail design

A standardised load spectrum for the comparative testing of materials and components has been proposed by Germany (see LBF Tech. Note TM15), and work is in hand in the U.K. to develop a standard programme-load fatigue test.

4. Statistical records containing data on fatigue life and on frequency of occurrence of service failures or cracks due to fatigue for individual types of aircraft; comparison with fatigue life as predicted from laboratory tests.

Current evidence still indicates that the life in service is less than that determined by a full-scale laboratory test. Although, in the early full-scale tests, with only very simple loading programmes, the two differed by a factor of four or five; with the current more complex and detailed structural test programmes the difference is becoming much less.

5. Influence of environmental conditions on the results of fatigue tests and on the representativeness of tests carried out in the laboratory

Several Delegates (Netherlands, U.S.A.) indicated that relevant investigations had been referred to in their National Reviews. It was generally agreed that atmospheric conditions were one of the major reasons for structural failures occurring earlier in service than in the laboratory test, and that they could account for a factor of at least two. It was suggested that full-scale fatigue certification tests on aircraft should be carried out in an outdoor environment and that indoor laboratory tests should be used for comparative testing only.

6. Theoretical studies of the probability of collapse of fail-safe structures of various designs and with various inspection procedures

Work on the reliability of fail-safe structures and the general reliability approach to airworthiness is in progress in Australia, Sweden, U.K. and U.S.A.

7. Establishment of fatigue critical load cases for landing gear and tail unit

It was generally agreed that, although limited investigations on these matters were in progress in most I.C.A.F. countries, a great deal more information was needed. It was also agreed that the undercarriage load case is much more complex than the air loads case and that it would be extremely difficult to formulate a generalised load spectrum for landing gear - the influence of impact, wheel spin-up, vertical, side and drag loads, braking, taxiing, etc. are dependent, to a large extent, on the characteristics and response of particular types of aircraft.

In general, the McBrearty spectrum is used for design and for the fatigue test schedule. Some doubts were expressed as to the adequacy of such a spectrum in view of uncertainties relating to the manner in which the different types of loading were actually combined in practice. Some countries tended to use the "most severe" condition as a basis with the peak loads of the spectra in each of the three directions (vertical, drag and side) applied simultaneously. Others attempted to exactly simulate the service loading conditions determined by load measurements on particular aircraft. It was pointed out that wide differences had been noted in operators' service experience with tyres and brakes, indicating large differences in load environment arising from operational practices.

Evidence was presented by several speakers which suggested that, in some aircraft types, fatigue failures in undercarriages and supporting structure were primarily associated with 'rebound' or 'springback'.

14.3 TOPICS PROPOSED FOR DISCUSSION AT THE MELBOURNE MEETING

This part of the Meeting was chaired by Mr. H.F. Hardrath

1. Reliability of safe-life estimates

Problem:

- (a) The estimates which are made of safe-lives, and the selection of inspection intervals, inevitably depend upon the input information available. Some is directly applicable to the structure and the load history of the aircraft in question, but much may be derived from data which are not strictly relevant. There are uncertainties in actual stresses, load spectra, reliability of fatigue test information, applicability of damage hypotheses, scatter, etc. and thus the degree of confidence in the preciseness of the estimated lives could be very low. How should one handle this problem in practice?
- (b) Inspection is necessary for both fail-safe and safe-life structures as one can never anticipate all the fatigue critical parts in a structure. How should one vary the inspection intervals during the life of the aircraft? Should sampling inspection be adopted for part of but not all of the fleet?

Discussion:

It was agreed that on most military and small aircraft there could be a marked 'pilot' effect on the load spectrum for a particular aircraft. Also, that for civil airliners both route and seasonal variations could occur. For a particular aircraft it is impossible to predict with certainty, from generalised data, its actual load and/or stress history; and therefore

recording for the entire life of the aircraft is the only way of determining the individual history. Even when an aircraft's load history is determined by fitting a Fatigue Meter or similar device, there will still remain uncertainties in the knowledge of actual stress levels at critical points in the structure. Furthermore, if individual load monitoring is not practicable one must consider sampling within the fleet on a statistical basis with the rotation of instruments, pilots, routes and perhaps missions. It was agreed that the safe-life of each individual structure could not be guaranteed with any reasonable degree of confidence, even if the individual load histories were known, and that regular inspections before the estimated 'safe-life' are still essential.

It was stated that for aircraft of a given class e.g. fighters, the gust load spectrum of each particular type, relative to their ultimate loads, was very similar. Other evidence suggested that the load history scatter factor of 1.5 for a particular type of aircraft, as specified in the British Av.P.970, was reasonable. For a fleet of one type of medium sized civil airliner in service with one operator it was reported that the scatter in load frequency was large for a small sample and, although it decreased with increasing sample size to a total of over 10,000 hours of records for individual aircraft, the minimum scatter between individual aircraft was in the order of two to three. It was thought that this suggested a genuine scatter in gust history but, on the other hand, it was further suggested that it might simply reflect drift or changes of calibration in the instruments.

Nevertheless, American experience was that, for gust loading conditions, the best for high altitude operations was a scatter of 2:1 while for low

altitudes (feeder line operations) it was 4:1.

For the medium size civil airliner it was thought that 60 - 70% of the fatigue damage was from the G-A-G cycle and thus, for a particular operator, one might expect relatively small scatter in fatigue life. For one particular type of aircraft 25 failures at a specific location in 18 individual aircraft of the fleet of one operator could be plotted as a straight line on log-life probability paper. On the question of the factor to be applied on mean test life for safe service life estimation it was stated that, for a fully inspectable structure, variations in material, processing and fabrication should be covered by a factor of two to three and that this should be increased to five to cover uncertainties in service loading history, etc.

There was general agreement that most of the current heavy civil aircraft (exceeding 12,500 lb.) had been subjected to some form of full-scale fatigue testing or evaluation by the manufacturer. However, a particular problem in Australia was the extensive usage of many types of light aircraft with annual utilizations approaching, in some cases, those of large transport aircraft on scheduled services. It was felt that, in many cases, the total flight times exceeded those envisaged when they were designed and constructed. In addition the majority of these aircraft were not required to have a full-scale fatigue test or even a realistic fatigue evaluation.

2. Fatigue load history recorders

Problem:

Is it satisfactory to determine the load history of individual aircraft by measurement of accelerations at their c.g., or should continuous records of strain measurements in the critical parts of the structure be made?

Discussion:

It was agreed that in order to make life estimates the basic requirement was knowledge of the strain or stress in particular locations. At the present time no simple, easily installed instrument for this purpose is available and the approach which has been followed, in most countries, is to fully instrument an aircraft with strain gauges and then subject it to a developmental flying programme. At the same time, calibration against accelerations at the c.g. provide a basis for the subsequent use of fatigue meters to establish the load history of individual aircraft.

Although this approach was considered reasonable - in the case of small rigid aircraft - for the measurement of loads caused by gusts and symmetric manoeuvres and perhaps ground loads, it was thought that for flexible aircraft (particularly under asymmetric manoeuvres) the measurement of vertical accelerations at the c.g. did not provide adequate information. This applies, even more particularly, in the case of landing and taxiing loads.

It was pointed out that to fully understand the structure would require the provision of quite elaborate instrumentation and it was suggested that, even if a satisfactory strain range counter or similar instrument was developed, it should be the task of a research organisation rather than that of the operator or even the manufacturer to monitor the strain history of individual aircraft. For an operator to carry additional flight loads instrumentation he must be convinced of the 'pay-off' in terms of either an increase in life or a more confident estimate of the life of individual aircraft. The difficulties in keeping complex instrumentation serviceable was also pointed out.

3. The laboratory test spectrum

Problem:

To what extent will truncation of the load spectrum at the low load high occurrence end affect the fatigue life under programme and random loading?

Discussion:

It was agreed that, after a fatigue crack had been initiated, it could be propagated at stresses much less than the original 'fatigue limit'. Also, that after a crack has initiated it is possible to predict the crack propagation rate in a structural element providing one knows how the load changes or redistributes in the element during the propagation process.

There was, however, uncertainty as to the influence of low loads during the pre-crack stage. Some work carried out in Switzerland on 7075 aluminium alloy test bars with $K_t = 4$ under random loading indicated a slightly longer life when the lower loads were not truncated from the spectrum. In this case the crack-propagation stage occupied approximately 80% of the total life. It was considered that the effect of truncation might be related to the proportion of the total life occupied by crack propagation.

4. Load spectra for T-tails

Problem:

What is the relationship between the intensities of vertical and horizontal gusts?

Discussion:

Reference was made to some American work during which a horizontal gust velocity of 90 f.p.s. had been measured. For 'normal flying practice' about

15% increase in intensity in vertical compared with horizontal gusts had been suggested, while for low level high speed flight a figure of 30% was quoted.

It was agreed that this was a necessary field for research in view of the increasing use of T-tails in modern aircraft.

14.4 RECOMMENDATION SESSION

This part of the Meeting was chaired by Mr. J. Branger

During this part of the Closed Technical Meeting a discussion was held as to the role and responsibility of I.C.A.F. in improving the fatigue safety of aircraft.

It was agreed that although I.C.A.F. had a moral responsibility in this regard, its function should primarily be one of an interchange of technical information; with individual Delegates acting as consultants to the various branches of the aircraft industry within their own countries. Although I.C.A.F. had no authority as a Committee to make recommendations on questions of airworthiness, it could nevertheless draw attention to problems or fields in which more information was required.

The two major technical matters discussed at the Recommendation Session were :

- (i) the necessity for full-scale structural fatigue tests;
 - (ii) the fitting of fatigue meters to all individual aircraft.
-
- (i) It was proposed that a comprehensive full-scale structural fatigue test on every aircraft type was highly desirable and that such a policy should be encouraged. Under some circumstances however it might be quite satisfactory to conduct extensive full-scale fatigue tests on selected major components under representative loading conditions.
 - (ii) The majority of the Delegates agreed that it was desirable for large civil aircraft to be fitted with fatigue meters or similar instruments for their entire operational life. The view was expressed

however that although it might be essential for such instruments to be fitted initially to a significant proportion of a new type of aircraft in each operator's fleet, the numbers could be reduced once the characteristics of the route, aircraft type, etc. had been established.

APPENDICIES

- I - PROGRAMME OF THE 5TH I.C.A.F. SYMPOSIUM
- II - LIST OF PARTICIPANTS AT THE 5TH I.C.A.F. SYMPOSIUM

APPENDIX IPROGRAMME OF THE 5TH I.C.A.F. SYMPOSIUM

"Aircraft Fatigue - Design, Operational and Economic Aspects"

Melbourne 22 -24 May, 1967

Monday, 22nd May, 1967

Morning Session (Chairmen: T.F.C. Lawrence, Australia;
H.F. Hardrath, U.S.A.; W.J. Gornall,
Australia)

- Opening address by Senator N.H.D. Henty, Commonwealth Minister for Supply
- A.M. Freudenthal: Reliability analysis based on time to first failure (presented by D.M. Forney)
- L.E. Jarfall: Optimum design of joints: the stress severity factor concept
- E.J. van Beek: Fatigue testing of the F.28 'Fellowship'

Afternoon Session (Chairmen: A.O. Payne, Australia;
O. Buxbaum, Germany)

- D. Lalli and G. Sergio: Design and certification for executive type aircraft (presented by D. Lalli)
- J. Besse and M. Peyrony: Fan jet Falcon - design and certification tests (presented by G.G. Douyere)
- E.T. Labett: The New Zealand light aircraft fatigue meter programme
- P.J. Foden: Agricultural aircraft flight loads: typical spectra and some observations on airworthiness

Tuesday, 23rd May, 1967

Morning Session (Chairmen: E.L. Ripley, U.K.; E.J. van Beek, Netherlands)

- P. Donely, J.W. Jewel and P.A. Hunter: An assessment of repeated loads on general aviation and transport aircraft (presented by P. Donely)
- O. Buxbaum and O. Svenson: Extreme value analysis of flight load measurements (presented by O. Buxbaum)
- J.P. Weibel: Undercarriage loadings of three aircraft: Porter PC6, Venom DH-112 and Mirage IIIS

- J.G. Wagner: Some considerations on acoustic fatigue (presented by J.L. Marchal)

Afternoon Session (Chairmen: D.R. Hooper, Australia;
S. Eggwertz, Sweden)

- H.T. Jensen: The application of Ti-6Al-4V titanium to helicopter fatigue loaded components
- W.J. Crichlow, C.J. Buzzetti and J. Fairchild: The fatigue and fail-safe programme for the certification of the Lockheed Model 286 rigid rotor helicopter (presented by W.J. Crichlow)
- J.A.B. Lambert and A.J. Troughton: The importance of service inspection in aircraft fatigue (presented by A.J. Troughton)

Wednesday, 24th May, 1967

Morning Session (Chairmen: I.S. Milligan, Australia;
P. Donely, U.S.A.)

- V.P. N'Guyen and E.L. Ripley: Design philosophy and fatigue testing of the Concorde (presented by E.L. Ripley)
- D.R. Donaldson and K.J. Kenworthy: Fatigue design and test programme for the American SST (presented by D.R. Donaldson)
- H. Rhomberg: Economic and operational aspects of fatigue: figures of a Swiss ground attack fighter (presented by J. Branger)
- P. Axisa and D.G. Graff: Economic aspects of fatigue in commercial airlines (presented by D.G. Graff)

Afternoon Session (Chairman: J.Y. Mann, Australia)

- R.C. Morgan: Some thoughts on the economics of fatigue
- D.M. McElhinney: Observations on designing to combat fatigue and its effects on the economics of civil transport aircraft
- Closing Session: Address by Mr. T.F.C. Lawrence

APPENDIX IILIST OF PARTICIPANTS AT THE 5TH I.C.A.F. SYMPOSIUM

The 5th ICAF Symposium was held in the Theatrette of the National Mutual Centre, Collins Street, Melbourne on 22nd - 24th May, 1967. It was attended by the following persons.

AUSTRALIA

MANN, J.Y.	A.R.L.
ANDERSON, J.B.	British Motor Corp. (Aust.) Pty. Ltd. Zetland, N.S.W.
AUSTIN, F.W.	T.A.A.
AVERY, N.L.	Department of Air, Canberra
AXISA, R.	T.A.A.
BARDEN, E.M.	D.C.A., Sydney
BARKER, R.E.	C.A.C.
BAXTER, R.G.	G.A.F.
BECKETT, R.C.	A.R.L.
BENNETT, A.S.	Department of Air, Melbourne
BENNETT, G.D.	G.A.F.
BIBO, J.H.	Ansett - ANA, Melbourne
BLACKLER, J.	Hawker de Havilland Aust. Pty. Ltd., Bankstown, N.S.W.
BOLONKIN, K.A.	D.C.A., Melbourne
BORCHARDT, H.A.	University of New South Wales, Kensington, N.S.W.
BROWN, B.	Hawker de Havilland Aust. Pty. Ltd., Bankstown, N.S.W.
BROWN, W.D.	Shell Company of Australia Ltd., Melbourne
BRUCE, G.P.	A.R.L.
CADWGAN, H.	Massey-Ferguson (Aust.) Ltd., Melbourne

A.R.L. - Aeronautical Research Laboratories, Department of Supply, Melbourne
 C.A.C. - Commonwealth Aircraft Corporation Pty. Ltd., Melbourne
 D.C.A. - Department of Civil Aviation
 G.A.F. - Government Aircraft Factories, Department of Supply, Melbourne
 T.A.A. - Trans-Australia Airlines, Melbourne

CARMICHAEL, A.J.	University of Newcastle, Newcastle, N.S.W.
CATERSON, J.	C.A.C.
CHRISTIE, J.B.	D.C.A., Sydney
CHAPLIN, P.E.	Army H/Q (DEME), Melbourne
CLARKE, J.D.	Hydro-Electric Commission, Hobart, Tasmania
CLARKE, R.J.	Dunlop Rubber Aust. Ltd., Bayswater, Victoria
COLLINS, W.M.	Department of Air, Canberra
COUSINS, F.A.	Department of Air, Canberra
DANCE, J.B.	A.R.L.
DINGLE, J.T.	Alcan Australia Ltd., Granville, N.S.W.
DODWELL, N.	Department of Main Roads, Sydney
DOIG, R.J.	Dunlop Rubber Aust. Ltd., Bayswater, Victoria
DOUYERE, G.G.	Avions Marcel Dassault, C/- G.A.F.
DOWNES, W.	Hawker de Havilland Aust. Pty. Ltd., Bankstown, N.S.W.
DRISCOLL, T.H.	Department of the Navy, Canberra
ELBER, W.	University of New South Wales, Kensington, N.S.W.
ELLIS, R.	A.R.L.
FAGGETTER, E.F.	Dunlop Rubber Aust. Ltd., Bayswater, Victoria
FAIRFIELD, E.	Department of Main Roads, Sydney
FINNEY, J.M.	A.R.L.
FODEN, P.J.	A.R.L.
FORD, D.G.	A.R.L.
GARDINER, L.M.	Hawker de Havilland Aust. Pty. Ltd., Bankstown, N.S.W.
GARE, J.	MacRobertson Miller Airlines Ltd., Perth
GERLACH, D.K.	C.A.C.
GORJANICYN, H.	C.A.C.
GORNALL, W.J.	C.A.C.
GRACE, W.G.	Repco Research Pty. Ltd., Dandenong, Victoria
GRAFF, D.G.	T.A.A.

GRANDAGE, J.M.	A.R.L.
HARRIS, F.G.	A.R.L.
HARRISON, P.	Comalco Industries Pty. Ltd., Sydney
HAYGOOD, A.J.	Alcoa of Australia Pty. Ltd., Melbourne
HOLLOWAY, E.	C.A.C.
HOOKE, F.H.	A.R.L.
HOOPER, D.R.	G.A.F.
HOSKIN, B.C.	A.R.L.
HOWARD, P.J.	A.R.L.
JOHNSTONE, W.W.	A.R.L.
JOYCE, N.B.	A.R.L.
KAHN, L.A.	The Boeing Company, North Essendon, Victoria
KANANEN, R.E.	Lockheed California Co., Melbourne
KELLY, J.R.	C.A.C.
KENTWELL, J.A.C.	C.A.C.
LALAS, M.	Qantas, Sydney
LAWRENCE, T.F.C.	A.R.L.
LLEWELLYN, D.J.	Hawker de Havilland Aust. Pty. Ltd., Bankstown, N.S.W.
MACNAUGHTAN, J.	Department of Air, Canberra
MARCHAL, J.L.	S.N.E.C.M.A., C/- C.A.C.
MARTIN, D.	C.A.C.
McARTHUR, I.D.	C.A.C.
McCOUBRIE, L.A.	C.A.C.
MILLAR, I.H.	T.A.A.
MILLICER, H.K.	Victa Aviation, Milperra, N.S.W.
MILLIGAN, I.S.	D.C.A., Melbourne
MIROVICS, I	I.C.I.A.N.Z., Melbourne
MITCHELL, L.H.	A.R.L.
MONKLEY, G.C.	Department of Air, Melbourne
MOUNTAIN, R.B.	Ansett - A.N.A., Melbourne
MUNDAY, M.	Department of Air, Highett, Victoria
NASH, A.	C.A.C.
NEWBIGIN, S.	Hawker de Havilland Aust. Pty. Ltd., Bankstown, N.S.W.
NICHOLAS, D.	Commonwealth Department of Works, Hawthorn, Victoria

O'BRIEN, K.R.A.	D.C.A., Melbourne
ODBERT, K.E.	Hawker de Havilland Aust. Pty. Ltd., Bankstown, N.S.W.
O'NEILL, M.J.	A.R.L.
PATCHING, C.A.	A.R.L.
PATTERSON, A.K.	A.R.L.
PAYNE, A.O.	A.R.L.
POULTER, A.F.	A.R.L.
RANKIN, C.McA.	C.A.C.
RICE, M.R.	D.C.A., Melbourne
RIDER, C.K.	A.R.L.
SAYERS, K.C.	G.A.F.
SCOLES, B.A.J.	D.C.A., Melbourne
SCALES, G.	Qantas, Sydney
SHAW, F.S.	University of New South Wales, Kensington, N.S.W.
SHEALES, P.J.	William Adams and Co. Ltd., Footscray, Victoria
SHELTON, T.L.	G.A.F.
SMITH, H.H.	Department of Air, Canberra
SMITH, W.R.	Department of Air, Canberra
SNOWDEN, K.	Broken Hill Smelters Pty. Ltd., Melbourne
SOLVEY, J.	A.R.L.
SPENCER, J.N.	R.A.A.F. Base, Richmond, N.S.W.
STAFFORD, C.P.	W. & T. Avery (Aust.) Pty. Ltd., Sydney
STEVENS, R.H.	Qantas, Sydney
STEWART, P.D.	Footscray Technical College, Melbourne
STUART, A.	Department of Air, Sydney
TORKINGTON, C.	D.C.A., Melbourne
WATKINS, J.L.	T.A.A.
WESTON, M.R.	D.C.A., Melbourne
WILLS, H.A.	Department of Supply, Melbourne
WILSON, J.H.	Executive Air Services Pty. Ltd., North Essendon, Victoria
WISDOM, J.C.	Department of Supply, Melbourne

WOOD, F.J.P.
 WOODBURY, S.P.
 WOODGATE, B.G.
 YOUNG, G.E.F.
 YUILLE, L.A.S.

Department of Air, Melbourne
 R.A.A.F. Base, Laverton, Victoria
 T.A.A.
 Ansett- A.N.A., Melbourne
 D.R. Johnston & Co. Pty. Ltd.,
 Melbourne

FRANCE

BARROIS, W.

Service Technique de l'Aeronautique,
 Paris

N'GUYEN, V.P.

Sud-Aviation, Toulouse-Blagnac

WAGNER, J.G.

Sud-Aviation, Toulouse-Blagnac

GERMANY

BUXBAUM, O.

Laboratorium für Betriebsfestigkeit,
 Darmstadt-Eberstadt

KRÄMER, D.E.

Lufthansa German Airlines, Hamburg-
 Fuhlsbüttel

INDIA

NINGAIAH

National Aeronautical Laboratory,
 Bangalore

ITALY

LALLI, D.

I.A.M. R.Piaggio S.p.A., Finale
 Ligure, Savona

NELLI, E.

Fiat Aircraft Division, Torino

JAPAN

KAWADA, Y.

Tokyo Metropolitan University, Tokyo

NETHERLANDS

van BEEK, E.J.

Royal Netherlands Aircraft Factories
 "Fokker", Schiphol-Zuid

NEW ZEALAND

CLAYTON, P.C.	New Zealand National Airways Corp., Christchurch
KEMP, T.D.	Air New Zealand Ltd., Auckland
LABETT, E.T.	Department of Civil Aviation, Wellington
MILLER, N.A.	Department of Scientific and Industrial Research, Petone
O'BRIEN, D.J.	Department of Scientific and Industrial Research, Petone

SWEDEN

EGGWERTZ, S.	Flytekaiska Försöksanstalten. Aeronautical Research Institute of Sweden (FFA), Bromma
JARFALL, L.E.	Aeronautical Research Institute of Sweden (FFA), Bromma

SWITZERLAND

BRANGER, J.	Eidgenössische Flugzeugwerk, Emmen
HUEPPI, H.	Swissair, Kloten
WEIBEL, J.P.	Eidgenössische Flugzeugwerk, Emmen

UNITED KINGDOM

RIPLEY, E.L.	Royal Aircraft Establishment, Farnborough
LAMBERT, J.A.B.	Hawker Siddeley Aviation Ltd., Hatfield
McELHINNEY, D.M.	British Aircraft Corporation (Operating) Ltd., Weybridge
MORGAN, R.C.	B.E.A. Helicopters Ltd., Hounslow
PHILLIPS, C.E.	National Engineering Laboratory, East Kilbride
TROUGHTON, A.J.	Hawker Siddeley Aviation Ltd., Woodford

UNITED STATES OF AMERICA

<u>HARDRATH, H.F.</u>	NASA Langley Research Centre, Hampton
CRICHLow, W.J.	Lockheed Aircraft Corporation, Burbank
DONALDSON, D.R.	The Boeing Company, Seattle
DONELY, P.	NASA Langley Research Centre, Hampton
FORNEY, D.M.	Air Force Material Laboratory (MAMD), Dayton
JENSEN, H.T.	Sikorsky Aircraft, Stratford
SWANSON, S.R.	MTS Systems Corp., Minneapolis